DISTILLATION

OPERATION AND APPLICATIONS

Edited by
Andrzej Górak and Hartmut Schoenmakers

Distillation: Operation and Applications

This page intentionally left blank

Distillation: Operation and Applications

Edited by

Andrzej Górak

Laboratory of Fluid Separations
Department of Biochemical and Chemical Engineering
TU Dortmund University
Emil-Figge-Str. 70
D-44227 Dortmund

Hartmut Schoenmakers

Laboratory of Fluid Separations
Department of Biochemical and Chemical Engineering
TU Dortmund University
Emil-Figge-Str. 70
D-44227 Dortmund

ELSEVIER

AMSTERDAM • BOSTON • HEIDELBERG • LONDON
NEW YORK • OXFORD • PARIS • SAN DIEGO
SAN FRANCISCO • SINGAPORE • SYDNEY • TOKYO
Academic Press is an imprint of Elsevier

Academic Press is an imprint of Elsevier
32 Jamestown Road, London NW1 7BY, UK
225 Wyman Street, Waltham, MA 02451, USA
525 B Street, Suite 1800, San Diego, CA 92101-4495, USA
The Boulevard, Langford Lane, Kidlington, Oxford OX5 1GB, UK

Library of Congress Cataloging-in-Publication Data
Application Submitted

British Library Cataloguing in Publication Data
A catalogue record for this book is available from the British Library

ISBN: 978-0-12-386876-3

Contents

This page intentionally left blank

Preface to the Distillation Collection

For more than 5,000 years distillation has been used as a method for separating binary and multicomponent liquid mixtures into pure components. Even today, it belongs to the most commonly applied separation technologies and is used at such a large scale worldwide that it is responsible for up to 50% of both capital and operating costs in industrial processes. It moreover absorbs about 50% of the total process energy used by the chemical and petroleum refining industries every year. Given that the chemical industry consumed 19% of the entire energy in Europe (2009), distillation is *the* big driver of overall energy consumption.

Although distillation is considered the most mature and best-understood separation technology, knowledge on its manifold aspects is distributed unevenly among different textbooks and manuals. Engineers, by contrast, often wish for just one reference book in which the most relevant information is presented in a condensed and accessible form. *Distillation* aims at filling this gap by offering a succinct overview of distillation fundamentals, equipment, and applications. Students, academics, and practitioners will find in *Distillation* a helpful summary of pertinent methods and techniques and will thus be able to quickly resolve any problems in the field of distillation.

This book provides a comprehensive and thorough introduction into all aspects of distillation, covering distillation history, fundamentals of thermodynamics, hydrodynamics, mass transfer, energy considerations, conceptual process design, modeling, optimization and control, different column internals, special cases of distillation, troubleshooting, and the most important applications in various industrial branches, including biotechnological processes.

Distillation forms part of the "Handbook of Separation Sciences" series and is available as a paper book and as an e-book, thus catering to the diverging needs of different readers. It is divided into three volumes: "Fundamentals and principles" (Editors A. Górak and E. Sorensen), "Equipment and processes" (Editors A. Górak and Ž. Olujić), and "Operation and applications" (Editors A. Górak and H. Schoenmakers). Each volume contains chapters written by individual authors with acclaimed expertise in their fields. In addition to that, readers will find cross-references to other chapters, which allow them to gain an extensive overview of state-of-the-art technologies and various research perspectives. Helpful suggestions for further reading conclude each chapter.

A comprehensive and complex publication such as *Distillation* is impossible to complete without the support of an entire team whose enduring help I wish to acknowledge. In particular, I wish to express my heartfelt gratitude to the 42 leading world experts from the academia and industry who contributed to the chapters of this book. I thank the co-editors of the three volumes of *Distillation*—Dr Eva Sorensen, UCL, Dr Žarko Olujić, Delft University of Technology, and Dr Hartmut

Schoenmakers, former member of BASF SE, Ludwigshafen—for their knowledgeable input and expertise, unremitting patience, and continuous encouragement. The invaluable editorial assistance of Dipl.-Ing. Johannes Holtbrügge during the entire editorial process is also greatly acknowledged.

Editorial assistance of Vera Krüger is also appreciated. I thank the Elsevier team Jill Cetel, Beth Campbell and Mohanambal Natarajan for their support and valuable help through the whole editing process.

Dr Andrzej Górak
TU Dortmund University

Preface to *Distillation: Operation and Applications*

This is the last of three books in a series covering all aspects of *Distillation*. This book on *Operation and Applications* provides an overview on all operational aspects and describes technologies in various application fields. It consists of 10 chapters of different authors. The approach to the content together with the choice of subjects and examples are the authors' choice but the book represents a comprehensive overview on the operational principles and the wide spread application range of distillation in general.

In Chapter 1 control and operation principles for columns including coupled mass and heat integrated configurations and plantwide control are described. The second chapter deals with column troobleshooting. Analysis of disturbances is introduced and methods to solve the problems are outlined. Strategies for understanding problems in connection with plant operation are given and special investigation techniques are explained in detail. Chapter 3 is on performance testing techniques for industrial scale columns with all types of internals. Instructions for running tests and procedures to evaluate the results are given.

The following four chapters describe in detail the configurations of distillation sequences used in different applications. The content of Chapter 4 is distillation in refining processes. Flowsheets of such processes are explained in detail and the improvement potentials even for well-established processes are shown including the choice of special and new column internals. Chapter 5 deals with distillation in bulk chemicals industry, in which columns of similar dimensions as in refining processes are used but physical properties of the separated components are quite different. Consequently new operational challanges like foaming, fouling, and design problems connected with column efficiencies arise. In Chapter 6 the aspects of distillation in small-scale plants for specialty chemicals that frequently need low-pressure conditions are discussed. Special aspects are low liquid loads in the columns, aqueous three phase systems, and reactions that may occur. In Chapter 7 very special application of air distillation is presented. The different process variants at the extreme conditions of pressure and temperature are explained and problems like maldistribution at the low liquid loads are adressed.

In the last part of the book future trends and developments are described. At first new distillation techniques like high-gravity equipment and microdistillation are shown in Chapter 8. Chapter 9 deals with application of distillation in biotechnology, especially with respect to the different demands connected with red, green, and white biotechnology. The last chapter explains the application of new separating agents like ionic liquids and hyperbranched polymers. Examples are given and the methods for thermodynamic description of these very special solvents are introduced.

At the end I would like to thank all the authors for their contributions.

Dr Hartmut Schoenmakers
BASF (emeritus)

This page intentionally left blank

List of Contributors

Wolfgang Arlt
University Erlangen-Nuremberg, Erlangen, Germany

Tony J. Cai
Fractionation Research, Inc., Stillwater, OK, USA

Stuart Fraser
Consultant. London, UK, Formerly Head of Separations Group, BP Oil

Henry Z. Kister
Fluor Corporation, Aliso Viejo, CA, USA

Hendrik A. Kooijman
Department of Chemical Engineering, Clarkson University, Potsdam, New York, USA

Koon Fung Lam
Department of Chemical Engineering, UCL, London, UK

Philip Lutze
Department of Biochemical and Chemical Engineering, Laboratory of Fluid Separations, TU Dortmund University, Dortmund, Germany

William L. Luyben
Department of Chemical Engineering, Lehigh University, Bethlehem, PA, USA

Anton Moll
Engineering Services, Linde Engineering Division, Pullach, Germany

Eva Sørensen
Department of Chemical Engineering, UCL, London, UK

Daniel Sudhoff
Department of Biochemical and Chemical Engineering, TU Dortmund University, Dortmund, Germany

Ross Taylor
Department of Chemical Engineering, Clarkson University, Potsdam, New York, USA

Gerit Niggemann
Evonik Industries AG, Hanau/Marl, Germany

Armin Rix
Evonik Industries AG, Hanau/Marl, Germany

Ralf Meier
Evonik Industries AG, Hanau/Marl, Germany

This page intentionally left blank

List of Symbols and Abbreviations

Latin Symbols

Symbol	Explanation	Unit	Chapter
A	Cross-sectional area	m^2	2, 6
A_b	Bubbling area	m^2	3
A_c	Column cross-sectional area	m^2	3
a	Specific surface area	m^2/m^3	6
a_{DC}	Relative downcomer area	m^2/m^2	5
a_e	Effective special interfacial area for mass transfer	m^2/m^3	7
a_P	Specific packing area	m^2/m^3	7
B	Molar bottoms flow-rate	kmol/s	1
B_{11}	Second virial coefficient	m^3/mol	10
Ca	Capillary number	–	7
C_{BA}	Ward tray capacity factor	m/s	5
C_D	Discharge coefficient	–	5
$C_{i,IL}^{\infty}$	Capacity of solvent *i* in IL	–	10
C_O	Orifice coefficient	–	7
C_L	Liquid capacity factor	m/s	3, 5
C_V	Vapor capacity factor	m/s	3, 5
CV	Coefficient of variation	–	3
c_p	Specific heat capacity	HJ/Kg °C	2
D	Overhead mass flow rate	Kg/H	2
D	Diameter	m	2
D	Molar distillate flow-rate	kmol/s	1
D_C	Column diameter	m	6
D_O	Orifice diameter	m	7
d	Diameter	m	6
d_h	Hole diameter	m	6, 7
d_P	Packing diameter	m	5
d_S	Sauter diameter	m	6
E	Energy	kJ	6
E_O	Overall tray efficiency	%	3
E_{OC}	Overall column efficiency	%	3, 5
F	F-factor	$Pa^{0.5}$	3, 7
F	Molar feed flow-rate	kmol/s	1
F_P	Packing factor	1/m	2, 5
f_i	Fugacity of component *i*	Pa	10
G^E	Free excess energy	J	10

(Continued)

—Cont'd

Symbol	Explanation	Unit	Chapter
G	Gravitational acceleration	m/s^2	6, 7
H	Enthalpy	MJ/kg	2
H^E	Excess enthalpie	J	10
H_i	Henry constant	Pa	10
h	Height/depth	m	2, 3, 7
h_{cl}	Clear liquid height on a tray	m	6, 7
h_{DC}	Downcomer backup	m	2, 3
h_f	Froth height	m	3
h_i	Specific enthalpy of stream/phase i	kJ/kg	2, 3
h_{LTU}	Height of liquid-side transfer unit	m	7
$\Delta h_{V,ref}$	Vapor enthalpy at the reference point	kJ/kg	3
h_{VTU}	Height of vapor-side transfer unit	m	7
h_W	Enthalpy of cooling water	kJ/kg	3
I	Radiation intensity of the detector	eV	2, 3
I_0	Radiation intensity of the source	eV	2, 3
K_C	Proportional gain, tuning parameter of a controller	–	1
K_i	Phase ratio	–	10
K_U	Ultimate gain, tuning parameter of a controller	–	1
k	Equilibrium factor	–	6
k_L	Liquid mass transfer coefficient	m/s	7
k_V	Vapor mass transfer coefficient	m/s	7
L	Liquid flow rate	kg/s, kmol/s	3, 5, 6, 7, 10
M	Mass flow rate	kg/h	2
$\dot{M}_i$	Mass flow rate of component or stream i	kg/s	2, 3
N_a	Number of actual stages/trays	–	3
N_{drip}	Number of drip points	$1/m^2$	7
N_t	Number of theoretical stages/trays	–	3, 6
$\dot{N}_i$	Mole flow rate of component or stream i	kmol/s	3
n_i	Number of moles	mol	10
P_U	Ultimate period	s	1
p	Pressure	Pa (bar)	1, 6, 7, 10
$p_{0,i}^{LV}$	Vapor pressure of component i	Pa	10
Δp	Pressure drop	Pa	2, 3, 6, 7
Δp_{flood}	Flood pressure drop, mm water per m of packing height	–	2
Δp_{dt}	Dry tray pressure drop	Pa	6
$\dot{Q}$	Duty	W or HW	1, 2, 3
R	Reflux mass flow rate	kg/h	2
R	Gas constant	J/mol k	10
R	Molar reflux flow-rate	kmol/s	1

—Cont'd

Symbol	Explanation	Unit	Chapter
RR	Reflux ratio (ratio of reflux to distillate)	–	1, 4
S	Stripping factor	–	3, 5, 6
S	Stream flow-rate	kmol/s	1
S^E	Excess entropy	J/K	10
SF	System Factor	–	5
T	Absolute temperature	K, (°C)	1, 7, 10
T	Temperature	°C	2
ΔT	Temperature difference	K	6
T_b	Boiling temperature, boiling point	K	
TS	Tray Spacing	m	2, 5, 6
u	Velocity	m/s	3, 5, 7
u_{DC}	Downcomer velocity	m/s	2, 5
u_h	Hole velocity	m/s	7
V	Vapor flow rate	kg/s, kmol/s	3, 5, 6, 7, 10
V_R	Retention volume	m^3	10
w_i	Mass fraction, weight fraction of component i	kg/kg	
x_i	Molar fraction of component i, liquid phase	mol/mol	1, 3, 7, 9, 10
y_i	Molar fraction of component i, vapor phase	mol/mol	1, 6, 10

Greek Symbols

Symbol	Explanation	Unit	Chapter
α	Relative volatility (10- > separation factor)	–	1, 3, 5, 7, 10
β	Separation efficiency	–	10
γ_i	Activity coefficient	–	10
ε	Porosity (void fraction)	m^3/m^3	6
η	Dynamic viscosity	Pa s	5, 7
θ	Contact angle	°	5, 7
μ	Effective mass absorption coefficient	1/cm	2, 3
μ	absorption coefficient	m^2/kg	2
χ	thickness	m	2
ρ	Density	kg/m^3	2, 3, 5, 6,7
$\overline{\rho}$	Average density	kg/m^3	3
$\Delta\rho$	Density difference	kg/m^3	5

(Continued)

—Cont'd

Symbol	Explanation	Unit	Chapter
ρ_W	Water density	kg/m^3	3
σ	Surface tension	N/m	5, 6, 7
τ_D	Derivative time constant of a controller	s	1
τ_I	Integrator time constant of a controller	s	1
ϕ	Volume fraction	–	3
φ	Flow parameter	–	5
φ_i	Fugacity coefficient of component *i*	–	10
ψ	Froth density	kg/m^3	3, 6
υ	Fraction of free area left for vapor flow	–	7
ξ_{dry}	Dry loss coefficient for contraction and expansion	–	7
χ	Thickness	m	2, 3

Subscripts

Symbol	Explanation	Chapter
C	Condenser	1, 3
L	Liquid	2, 3, 5, 6, 7
max	Maximum, maximal	7
min	Minimum, minimal	7
PA	Pump around	2
R	Reboiler	1, 3
V	Vapor	2, 3, 5, 6,7

Abbreviations

Abbreviation	Explanation	Chapter
AGMD	Air gap membrane distillation	9
AIChE	American Institute of Chemical Engineers	3, 5
API	Active pharmaceutical ingredients	8
ASU	Air separation unit	6
BAHX	Brazed aluminum heat exchanger	6

—Cont'd

Abbreviation	Explanation	Chapter
BAIM	Bubble-assisted interphase mass-transfer	9
BIP	Binary interaction parameter	5
CAD	Computer-aided design	7
Capex	Capital expenditures	5
CAT	Computer-aided tomography	2
CC	Composition controller	1
CDU	Crude distillation unit	4
CFD	Computational fluid dynamics	3, 7, 9
COK	Cokers	4
CPI	Chemical process industries	3
CSTR	Continuous stirred-tank reactor	
CT	Chimney tray	2
DC	Downcomer	2
DCAC	Direct contact air cooler	6
DCO	Decant oil (slurry)	4
DCMD	Direct contact membrane distillation	9
DPD	Drip point density	6
E	Entrainer	10
ECMD	Enhanced capacity multiple downcomer	5
EOS	Equation of state	5
EVC	Evaporation cooler	6
FC	Flow controller	1, 2
FCC	Fluid catalytic cracker	4
FI	Flow Indicator	2
FPL	Flow path length	5
FRI	Fractionation research inc.	3, 5, 7
FT	Flow transmitter	1
GAN	Gaseous nitrogen	6
GC	Gas chromatography	3, 10
GOX	Gaseous oxygen	6
GPDC	Generalized pressure drop correlation	5
HC	High capacity	5
HCK	Hydrocrackers	4
HCO	Heavy cycle oil	4
HDA	Hydrodealkylation	5
HETP	Height equivalent to a theoretical plate	3, 5, 6, 7, 9
HP	High pressure	6

(Continued)

—Cont'd

Abbreviation	Explanation	Chapter
HPC	High pressure column	1
HS-GC	Headspace gas chromatography	10
HSE	Health-safety-environment	3
HTU	Height of transfer unit	3
HyPol	Hyperbranched polymers	10
IGC	Inverse gas chromatography	10
IL	Ionic liquid	10
L	Liquid	10
LC	Liquid level controller	1, 2
LCO	Light cycle oil	4
LDA	Laser doppler anemometer	3
LDV	Laser doppler velocimeter	3
LIN	Liquid nitrogen	6
LiP	Linear program	4
LOX	Liquid oxygen	6
LP	Low pressure	6
LPC	Low pressure column	1, 6
LPG	Liquefied petroleum gas	4, 5
LTU	Liquid transfer unit	7
LVGO	Light vacuum gas oil	4
MHC	Maximum hydraulic capacity	3
MTC	Mass transfer correlation	5
MUC	Maximum useful capacity	3, 5
NMR	Nuclear magnetic resonance	2
OPEX	Operating costs	5
PC	Pressure controller	1
PFD	Process flow diagram	5
PFMD	Parallel flow multiple downcomer	5
PPE	Personal protective equipment	3
RD	Reactive distillation	8
RR	Reflux ratio	1, 5
RSO	Radiation safety officer	3
RTCDS	Reactive thermally coupled direct sequence	8
RTD	Resistance temperature detection	3
RZB	Rotating Zig-Zag Bed	9
SGP	Saturate gas plant	4
SGMD	Sweep gas membrane distillation	9
SP	Setpoint	1
SRK	Soave-Redlich–Kwong	5
SRP	Separation research program	3

—Cont'd

Abbreviation	Explanation	Chapter
TAN	Total acidity number	4
TBP	True boiling point	4
TC	Temperature controller	1, 2
TSGMD	Thermostatic sweeping gas membrane distillation	9
Unifac	Universal quasichemical functional group activity coefficients	10
V	Vapor	10
VDU	Crude vacuum unit	4
VLE	Vapor-liquid-equilibrium	2, 3, 5, 7, 10
VMD	Vacuum membrane distillation	9
V-MEMD	Vacuum-multi effect membrane distillation	9
VRC	Vapor recompression columns	5
VRU	Vapor recovery unit	4
VTU	Vapor transfer unit	7

Abbreviations of Chemical Compounds

Abbreviation	Explanation	Chapter
ABS	Acrylonitrile-butadiene-styrene	5
BD	Butadiene	5
CB	Chlorobenzene	3
DEA	Di-ethylene amine	5
DEG	Di-ethylene glycol	5
DHA	Docosahexaenoic acid	8
DME	Dimethylether	5
DMSO	Dimethyl sulfoxide	1
EB	Ethylbenzene	3, 5
EC	Ethylene carbonate	5
EDC	Ethylene di-chloride	5
EE	Ethylene-ethane	5
EG	Ethylene glycol	5
EO	Ethylene-oxide	5
EPA	Eicosapentaenoic acid	8
ETBE	Ethyl tert-buthyl ether	7
FAME	Fatty acid methyl ester	8

(Continued)

—Cont'd

Abbreviation	Explanation	Chapter
FDCA	2,5-Furan dicarboxylic acid	8
HMF	Hydroxyl-methyl-furfural	8
3-HPA	3-Hydroxypropionic acid	8
MA	Methyl-acetylene	5
MCH	Methylcyclohexane	10
MEA	Mono-ethylene amine	5
MEG	Mono-ethylene-glycol	5
MTBE	Methyl tert-butyl ether	7
PBT	Polybutylene terephthalate	8
PD	Propadiene	5
PDMS	Polydimethylsiloxane	5
PE	Polyethylene	5
PET	Polyethylene terephthalate	5, 8
PP	Polypropylene	5, 9
PS	Polystyrene	5
PTFE	Polytetrafluoroethylene	9
PVDF	Polyvinylidene fluoride	9
ST	Styrene	5
TAME	Tert-amyl methyl ether	7
TEA	Tri-ethylene amine	5
TEG	Tri-ethylene glycol	5
THF	Tetrahydrofuran	8
TMB	Tri-methyl benzene	5

Abbreviation	Explanation
C2	Ethane
C3	Propane
iC4	Isobutane
*n*C4	*n*-butane
iC5	Isopentane
cC6	Cyclo hexane
C7	*n*-heptane

Note: Used abbreviations of hydrocarbons on the basis of C atoms.

CHAPTER

Distillation Control 1

William L. Luyben
Department of Chemical Engineering, Lehigh University, Bethlehem, PA, USA

CHAPTER OUTLINE

Distillation: Operation and Applications. http://dx.doi.org/10.1016/B978-0-12-386876-3.00001-6

1.1 Introduction

Distillation control has been the subject of dozens of books and thousands of papers over the past half century. No other unit operation has received as much attention by both academic and industrial workers. A complete listing of all these references is impractical and of limited utility. A list of books that deal explicitly with distillation control is given in the Reference section [1–6]. The earliest reference dates back almost four decades [1], and the latest was published in 2013 [6].

Distillation columns come in many flavors, and no one control structure fits all columns. Differences in feed compositions, relative volatilities, product purities, and energy costs impact the selection of the "best" control structure for a given column in a given plant.

1.2 Basic control issues

Let us consider a plain vanilla distillation column with a single feed stream that produces a distillate product from a total condenser/reflux drum and a bottom product from a partial reboiler in the column base. Figure 1.1 sketches the flowsheet and gives the nomenclature used in this chapter. All flow rates are molar and all compositions are molar fractions. If the feed stream is set by an upstream unit, there are five control valves in this process (distillate, reflux, cooling water, reboiler steam, and bottoms), each of which must somehow be set. Thus the system is inherently a

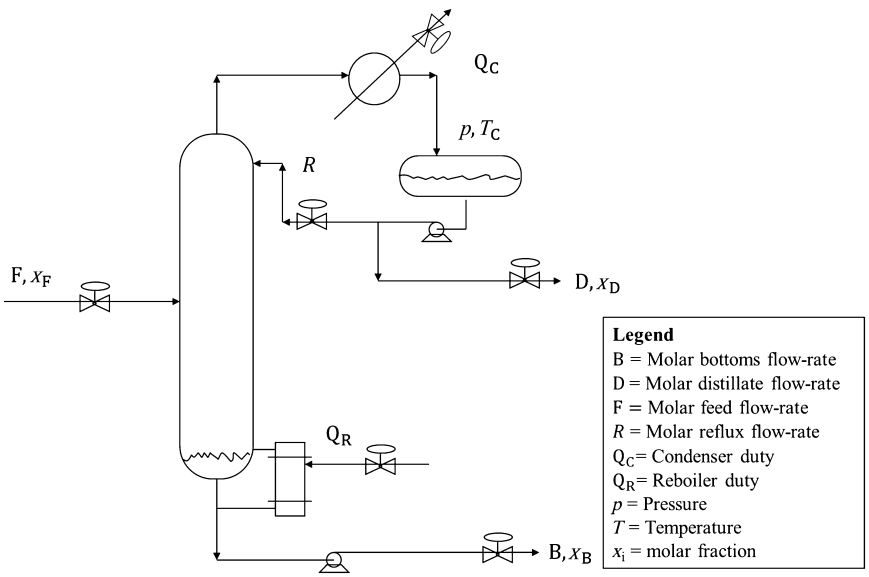

FIGURE 1.1 Flowsheet of a Basic Distillation Column

5×5 multivariable process. There are five-factorial possible combinations of variable pairings (120 possible control structures).

There are three variables that must be controlled: pressure, liquid level in the reflux drum, and liquid level in the base. A typical control structure would control pressure with condenser cooling water, reflux drum level with distillate, and base level with bottom stream. This leaves two control degrees of freedom available to control two variables.

In the design of a column, the normal design specifications are the purities (or impurities) of the two products. The amount of heavy key component in the distillate and the amount of light key component in the bottom stream are normally specified. In theory, these same specifications should be used to control the operating column. This "dual-composition control" structure is used in some columns, usually when separations are difficult (low relative volatilities) and energy is expensive. It requires, of course, two on-line composition measurements, which are sometimes expensive, require high maintenance, and introduce significant deadtimes in the loop. As a result, the vast majority of columns use a more simple control structure in which the two remaining control degrees of freedom hold the temperature on a suitable tray and control the ratio of reflux-to-feed, or reflux ratio (RR).

From a fundamental standpoint, the two parameters that affect product purities are material balance and fractionation. Material balance refers to how the feed stream to the column is split between the distillate and the bottom stream. This is sometimes called the cut point or product split. In an extreme case in which 100% of the feed stream is taken overhead as the distillate product, the composition of the distillate will obviously be equal to the feed composition. No amount of reflux will affect the distillate composition. The same is true if the entire feed stream goes out the bottom. It is clear that the product split has a major effect on the compositions of the products.

By fractionation we mean the energy put into the column to provide the work of "unmixing" of the components. It can be measured in terms of the RR or steam-to-feed ratio. Obviously, if there is no reflux or no steam, there is no separation. The higher the RR the more difference there is between the purity of the distillate and the purity of the bottom stream. But this difference in purities tends to approach some asymptotic limit. Even with an infinite RR (total reflux), the difference in the product purities is set by the number of trays and the relative volatilities.

Thus it is important to realize that manipulating the material balance (distillate-to-feed ratio or bottom-to-feed ratio) has a greater impact on product compositions than manipulating the fractionation. The first law of distillation control states:

> *You cannot fix the flow rate of either product (for a fixed feed flow rate) and still control a temperature or composition in the column.*

This law is a direct result of the fundamental concept of the dominant effect of the material balance on product compositions. Keep in mind that this manipulation of the material balance can be direct (using the distillate's flow rate to control a composition or temperature) or indirect (using the reflux flow rate for this purpose,

with the distillate maintaining the reflux drum level). Both structures are manipulating the material balance (the distillate is being changed).

In the following sections, some typical control structures are discussed and the rationale for their use in particular situations is presented. Once the control structure is selected we still need to tune the controller. This subject will be discussed in a later section.

The software and hardware that permit the use of dynamic simulations to quantitatively assess the effectiveness of various alternative control structures are now available. They provide an efficient means of comparing control structures and tuning methods. Of equal or more importance is their use in assessing the controllability of alternative process configurations. Simulations are much less expensive and less time consuming than trying to extract this type of information from plant tests.

1.3 Choosing a control structure

There is no single control structure that applies to all distillation columns. The control objectives differ from column to column, just as the economics and process conditions differ from plant to plant. There are two basic choices of the type of control structure to be selected. First, the engineer must choose between a conventional control structure (in which the feed stream to the column is set by the upstream unit) or an "on-demand" control structure. Second, the engineer must choose between a dual-end control structure and a single-end control structure.

1.3.1 Conventional vs on-demand control structure

One fundamental difference in control structures is the selection of what variable sets the throughput. In most columns the feed stream comes from some upstream unit and typically uses a liquid-level control (if the feed stream is a liquid) or a pressure control (if the feed stream is a vapor). In this case the product streams from the column depend on the feed flow rate and composition. The simple control structure shown in Figure 1.2 illustrates this conventional case. Liquid levels in the column set product flow rates.

However, in some plants the flow rate of one of the products is set by a downstream user. Now the feed stream must be manipulated to satisfy the material balance. This is called an on-demand structure. Figure 1.3 gives an example of an on-demand structure in which the flow rate of the bottom stream is flow controlled (and set by a downstream consumer) and the feed stream comes in to control the base level.

1.3.2 Dual-end vs single-end control structures

1.3.2.1 Dual-end control structures

As previously discussed, the theoretically ideal control structure is dual composition. Figure 1.4 shows this ideal, but fairly infrequently used, structure. The bottom composition is controlled by manipulating the reboiler, and the distillate

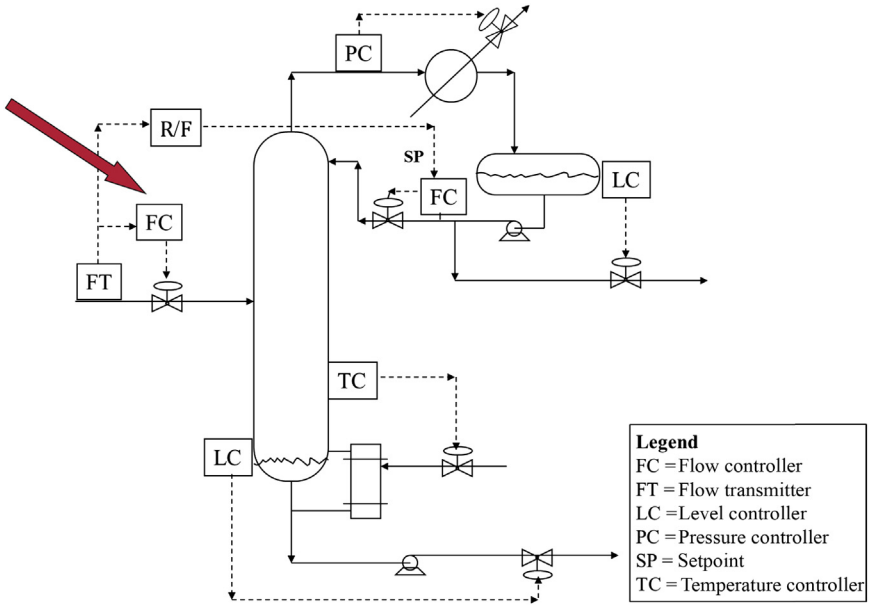

FIGURE 1.2 Basic Conventional Control Structure Using the Reflux-to-Feed Ratio (R/F)

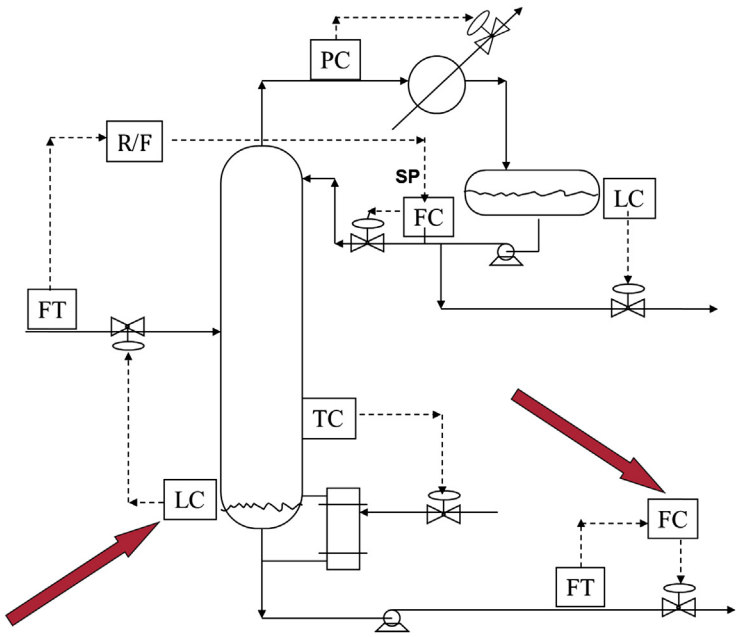

FIGURE 1.3 On-demand Control Structure with a Flow-Controlled Bottom Stream

FC, flow controller; FT, flow transmitter; LC, level controller; PC, pressure controller; R/F, reflux-to-feed ratio; TC, temperature controller.

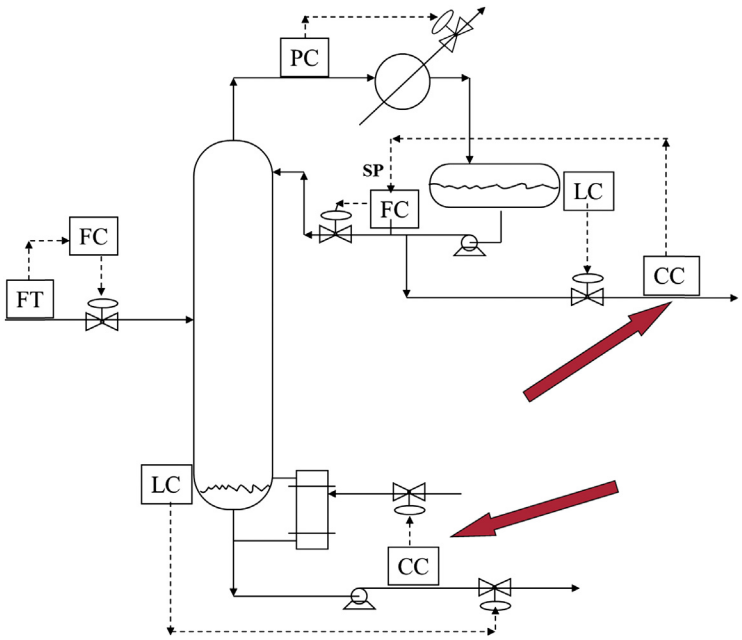

FIGURE 1.4 Dual-Composition Control Structure

The arrows indicate the composition controller (CC). FC, flow controller; FT, flow transmitter; LC, level controller; PC, pressure controller; SP, setpoint; TC, temperature controller.

composition is controlled by manipulating the reflux flow rate. This scheme holds both products at their specifications and uses the minimum amount of energy for any feed flow rate and feed composition.

However, it can present potential loop interaction problems because both reflux and vapor boil-up affect both product compositions. On-line composition measurements are often expensive, somewhat unreliable, require high maintenance, and introduce undesirable deadtimes in the loops.

It is sometimes possible to control two tray temperatures instead of two compositions, but this dual-temperature structure can be applied only when there are two locations in the column where temperatures accurately reflect compositions. Normally this means that there must be two temperature breaks in the temperature profile (temperature changes significantly from tray to tray). If there is only one temperature break, a dual-end control structure that controls one temperature and one composition can sometimes be used if indeed two-end control is required.

1.3.2.2 Single-end control structures

All dual-end control structures have the potential problems of loop interaction. It is often possible to use a more simple control structure that controls only one temperature or one composition.

We have already presented an example of this type of structure in Figure 1.2. An appropriate tray is selected whose temperature is controlled, usually by manipulating vapor boil-up. A later section addresses the issue of how we select this tray. Another feature in the structure shown in Figure 1.2 is the choice of a reflux-to-feed control structure. There are other alternatives that could be chosen. How do we know if the reflux-to-feed structure is the best? How do we decide if a single-end control structure will provide adequate control? One practical approach is to do a feed composition sensitivity analysis.

1.4 Feed composition sensitivity analysis

If the only disturbances that a distillation column has to contend with are changes in feed flow rate, a number of single-end control structures would be adequate to keep both the distillate and bottom products at their specified purities under steady-state conditions. Any control scheme that maintained any flow ratio (reflux-to-distillate or reflux-to-feed) and a single temperature (or composition) anywhere in the column would do the job.

One way to understand this concept is to remember that the McCabe–Thiele diagram is constructed using flow ratios. The tray compositions are the same for any feed flow rate. Therefore, simply keeping any ratio of flows constant as feed flow rate changes should give a steady-state condition with the same compositions throughout the column.

This principle applies only when feed composition does not change and there are no changes in pressures or tray efficiencies. In the face of feed composition disturbances, however, the composition profiles in the column will change if all we do is keep a constant flow ratio and a constant temperature on one tray. Product compositions will deviate from their specifications.

Our objective is to find a control structure that keeps the compositions of the two products at (or close to) their specified purities. How much will the column compositions change and how much must the flow ratios change as feed composition varies while keeping the two products at their specified purity?

To answer this question we perform a feed composition sensitivity analysis. A steady-state simulation of the column is used. We start at the design feed composition with the specified product purities and the design RR and reflux-to-feed ratio. The purities of both product streams are maintained at their specified values (in Aspen software this achieved using two *Design Spec/Vary* functions). The feed composition is varied over the expected range and the required changes in the ratios are examined.

Let us illustrate the method with a numerical example. A distillation column with a five-component hydrocarbon feed mixture has a feed of 100 kmol/h. At design conditions the feed composition is 1 mol% ethane (C2), 40 mol% propane (C3), 29 mol% isobutane (*i*C4), 29 mol% normal butane (*n*C4) and 1 mol% isopentane (*i*C5). The operating objective is to separate the light key component (propane) from the heavy key component (isobutane). Of course, the heavier-than-heavy key

components *n*C4 and *i*C5 go out the bottom with the *i*C4. The lighter-than-light key component C2 goes out the top with the propane. Column pressure is set at 16 atm to give a reflux drum temperature of 320 K so that cooling water can be used in the condenser. The column has 37 stages and is fed on stage 18 (using Aspen notation with the reflux drum being stage 1). Distillate impurity is specified as 2 mol% *i*C4. The impurity of the bottom stream is specified as 1 mol% C3. The RR required to achieve these purities is 2.364 at the design feed composition. Table 1.1 give results of the feed composition sensitivity analysis.

These results clearly show that in this system the required changes in reflux are very small. Therefore, a single-end control structure with a reflux-to-feed ratio has a good chance of providing effective control of both product purities.

So, the procedure to see whether a dual-end control structure is required is as follows:

1. If only feed flow rate disturbances occur (a rare situation), dual-end control is not required. Simply use either a RR or a reflux-to-feed ratio scheme and control one temperature anywhere in the column. This is not exactly true because an operating column will experience pressure drop changes when throughput varies that affect the temperature−composition relationships.
2. If the feed composition sensitivity analysis shows large changes in both ratios (>5 to 10%), dual-end control is required. Structures that control two compositions, two temperatures, or one composition and one temperature should be used to handle feed composition disturbances.
3. If the feed composition sensitivity analysis shows that one of the two ratios does not change much (<5%), single-end control may be adequate to keep both products near their specified purities in the face of both feed flow rate and feed composition disturbances. The single-end control structure may be able to use a tray temperature, depending on the shape of the temperature profile, but in some cases composition control may be required. We discuss in a later section the issues of selecting an appropriate tray for temperature control.

The control structure shown in Figure 1.2 uses single-end control with a reflux-to-feed ratio. Suppose the feed composition sensitivity analysis indicated that an RR

Table 1.1 Feed Composition Sensitivity Results

x_{C3} (mol/mol)	x_{iC4} (mol/mol)	R/F	Change from Design (%)	RR	Change from Design (%)
0.30	0.39	0.9560	−0.57	3.163	+33.8
0.35	0.34	0.9643	+0.29	2.721	+15/1
Design	0.29	0.9615	0	2.364	0
0.40					
0.45	0.24	0.9477	−1.43	2.065	−12.7
0.50	0.19	0.9208	−4.23	1.800	−23.9

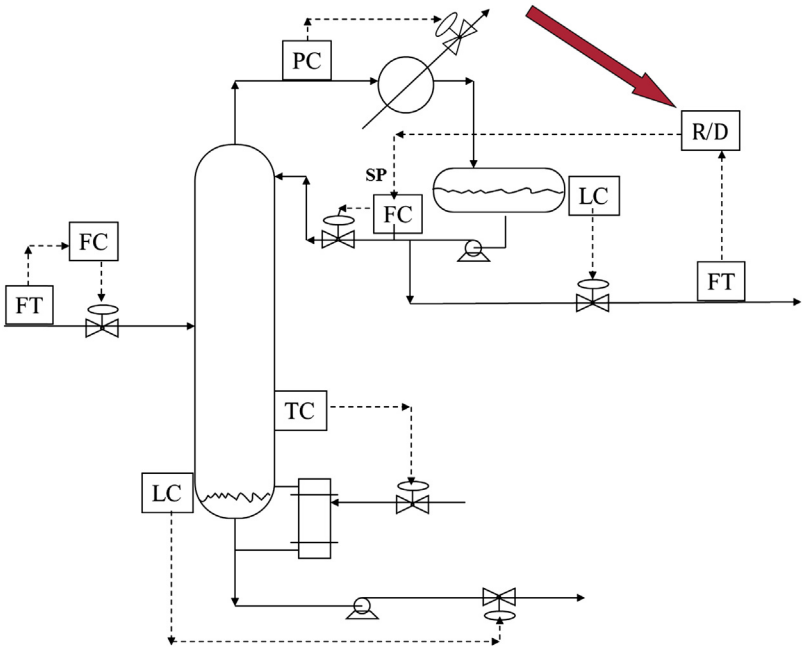

FIGURE 1.5 Basic Conventional Control Structure Using the Reflux Ratio (RR, Here, R/D, Arrow)

FC, flow controller; FT, flow transmitter; LC, level controller; PC, pressure controller; SP, setpoint; TC, temperature controller.

would be more effective. What would this control structure look like? Figure 1.5 shows a modified structure in which RR is controlled. Distillate flow rate is manipulated to control the reflux drum level. The distillate flow rate is measured and this signal is set to a multiplier whose other input is the desired RR. The output signal is the setpoint of the reflux flow controller.

There is another ratio that we have not mentioned: vapor boil-up-to-feed. In some columns this ratio is fairly constant as feed stream compositions vary. However, fixing this ratio precludes the use of reboiler heat input as a manipulated variable. Since vapor boil-up rates affect quite quickly all compositions and all temperatures throughout the column, reboiler heat input should usually be kept available for dynamic control performance.

1.5 High RR columns

The control structures shown in Figures 1.2 to 1.5 all control the reflux drum level by manipulating the distillate flow rate. This structure smooths the flow to downstream units and works well for a distillation column with low to moderate RRs. However, if the RR is large (>3), conventional distillation wisdom suggests that the reflux

drum level should be controlled by manipulating the reflux flow rate. The flow rate of the reflux is much larger than the flow rate of the distillate. Small changes in the overhead vapor will produce large changes in the distillate if it is controlling the level.

Figure 1.6 shows a modified dual-composition control scheme in which the reflux drum level is controlled by the reflux flow rate. Distillate composition is then controlled by manipulating the distillate flow rate. In this setup, the level loop is "nested" inside the composition loop, that is, the level controller must be on automatic for the composition loop to work. And if the level loop is tuned for slow averaging control, the composition loop will be slow.

Figure 1.7 shows a more effective modified structure for columns with a high RR. The reflux drum level is still controlled by manipulating the reflux flow rate. But now the reflux flow rate is measured and this signal is sent to a multiplier. The other input to the multiplier is the required distillate-to-reflux ratio that is the controller output signal from the distillate composition controller. The output signal of the multiplier is the setpoint signal of distillate flow controller. Now changes in the overhead vapor flow rate produce changes in both the reflux and distillate flow rates. The composition controller trims up the ratio to drive the distillate

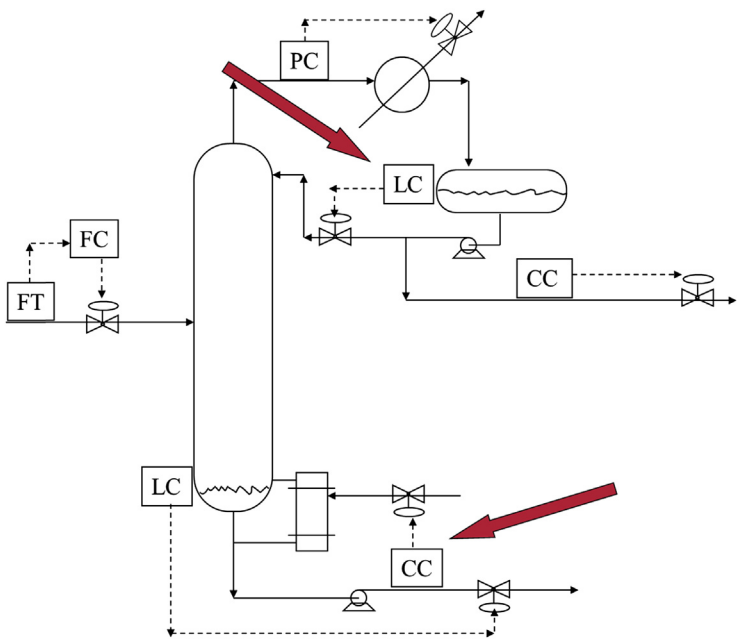

FIGURE 1.6 Dual-Composition Control (CC, Bottom Arrow) Structure for a Column with a Large Reflux Ratio

CC, composition controller; FC, flow controller; FT, flow transmitter; LC, level controller (top arrow); PC, pressure controller.

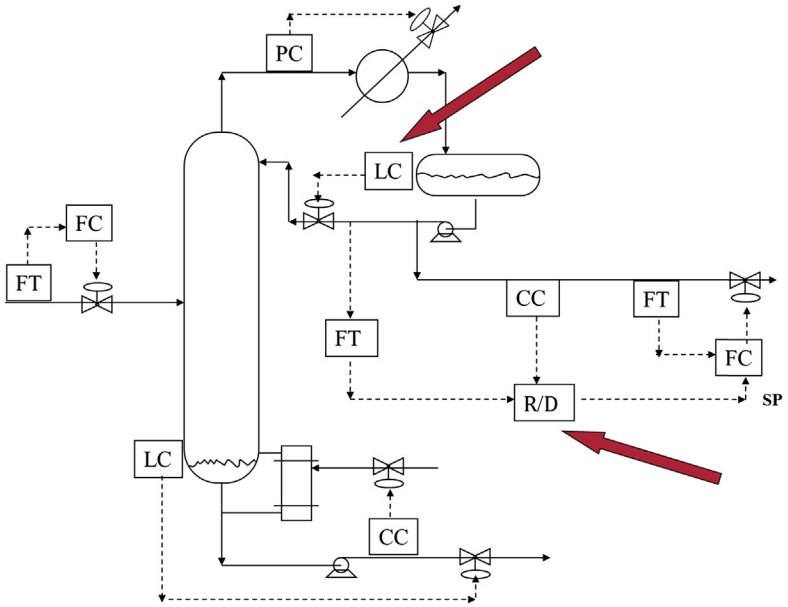

FIGURE 1.7 Modified Dual-Composition Control (CC) Structure for a Column with a Large Reflux Ratio (Bottom Arrow)

FC, flow controller; FT, flow transmitter; LC, level controller (top arrow); PC, pressure controller; SP, setpoint.

composition to its specification since different ratios will be required for different feed stream compositions.

1.6 Control tray selection

Temperature depends on both pressure and composition in vapor–liquid systems. Column temperature profiles depend on relative volatilities, product purities, RRs, the number of trays, and pressures on the trays (which depend on tray pressure decreases and the pressure in the reflux drum). If relative volatilities are large, there will be large temperature differences from tray to tray in the regions of the column where compositions are changing rapidly. These trays are usually good locations to infer composition from temperature. If relative volatilities are small, the temperature profile will be "flat" and the use of temperature to infer composition may be ineffective.

Many methods for selecting an appropriate temperature control tray have been proposed in the literature. They vary from the simple (pick a tray where the temperatures are changing rapidly from tray to tray) to the complex (use singular value decomposition to detect the sensitive trays). A detailed discussion is beyond the scope of this chapter. The interested reader is referred to Ref. [6].

1.7 Controller tuning

In this section common controller types are considered, including the proportional, proportional-integral, and proportional-integral-derivative controllers.

If a single-end control structure is used, there is one temperature or one composition controller to be tuned. If a dual-end control structure is required, there are two interacting controllers to be tuned. We discuss these situations below.

Besides these temperature or composition controllers, there are three (or four) other controllers that must also be set up. Simple heuristics can usually be used in these loops. All level controllers (reflux drum and column base) should normally use proportional-only controllers (controller's proportional gain, $K_C = 2$) to smooth the flow and attenuate flow disturbances moving down the sequence of units in the series. Flow controllers can use $K_C = 0.5$ and an integral time constant $\tau_I = 0.3$ min because of their fast dynamics. Column pressure controllers (manipulating condenser cooling) do not have to provide tight pressure control and can use the nominal settings of $K_C = 5$ and $\tau_I = 10$ min in most situations. We only want to avoid rapid changes in pressure, which can cause flooding or dumping if vapor flow rates change rapidly because of liquid flashing when pressure decreases or vapor condensing when pressure increases.

The temperature and composition controllers require the use of an effective tuning procedure. One simple and practical method is to experimentally determine the dynamic characteristics of the loop using the relay feedback test. This test gives the ultimate gain (K_U) and the ultimate period (P_U), which can then be used to find controller constants from tuning rules such as Ziegler–Nichols or Tyreus–Luyben (see Table 1.2). The latter are more conservative and more suitable for distillation columns in which rapid changes in manipulated variables are undesirable because they can cause hydraulic problems on the trays (flooding or dumping).

It should be pointed out that running the relay feedback test on a real column works quite well. Running it on a computer simulation requires that the measurement lags and deadtimes that are inevitably present in a real column be explicitly included in the simulation. If this is not done, the relay feedback test will provide useless results since a system must have a phase angle that drops lower than -180° to have an ultimate gain. If these dynamic lags are not included, the

Table 1.2 Ziegler–Nichols and Tyreus–Luyben Tuning Rules

		P	PI	PID
Ziegler–Nichols	K_C	$K_U/2$	$K_U/2.2$	$K_U/1.7$
	τ_I		$P_U/1.2$	$P_U/2$
	τ_D			$P_U/8$
Tyreus–Luyben	K_C		$K_U/3.2$	$K_U/2.2$
	τ_I		$2.2\ P_U$	$2.2\ P_U$
	τ_D			$P_U/6.3$

performance of the loop predicted in the simulation may be unrealistically better than what will be experienced in the real column.

Deadtime elements can be used to approximate typical measurement dynamics. A 1-min deadtime is suitable for temperature measurements. Composition measurements are typically slower, particularly if gas chromatographic measurement devices are used. Deadtimes of 3−10 min are common.

The discussion above is applicable to a single control loop with no interaction from another loop. The method can be used directly in single-end control structures. But what do we do in the case of a dual-end structure? A more complex column configuration can have three or more interacting temperature or composition loops. How do we handle them?

There are several approaches to the problem; some are quite elegant and require detailed dynamic identification of all the interaction parameters. The most simple and practical approach is to use sequential tuning. The idea is to put all the interacting controllers on manual. In the dual-composition control structure there would be two composition controllers. First, we select the "faster" of the two loops. This is normally the loop using reboiler duty (steam) as the manipulated variable because vapor boil-up affects all temperatures and compositions more quickly than reflux.

The other controller is left on manual (fixed reflux). The faster controller is tuned using the relay feedback test and an appropriate tuning rule. Then the faster controller is kept on automatic while the slower controller is tested and tuned in the same way. The resulting tuning constants implicitly account for any loop interaction that exists in the system.

1.8 Use of ratios and cascade control

We have already demonstrated several control structures that use ratios. The ratios use multipliers to give the desired flow ratios to handle feed composition disturbances.

But there are other applications of ratios. One of the most important is to achieve feedforward control for improved dynamic load rejection. Consider the basic control structure shown in Figure 1.2. Suppose the feed flow rate is increased. The temperature controller can only respond to the resulting decrease in temperature when it sees this decrease. Therefore, there may be a large dynamic transient drop in temperature, which could result in a similar increase in the light key impurity that drops down into the bottoms.

But we know that more feed flow will inevitably require more steam. So why not anticipate this action using feedforward control? Figure 1.8 shows a control structure in which a steam-to-feed ratio is used as the feedforward element. The feed flow rate signal goes to a multiplier (S/F) whose output signal is the setpoint of the steam flow controller. A change in the feed flow rate causes a change in the steam flow rate $\dot{S}$ before the temperature controller sees the disturbance. The other input signal to the multiplier is the desired steam-to-feed ratio, which is the controller output signal from the temperature controller.

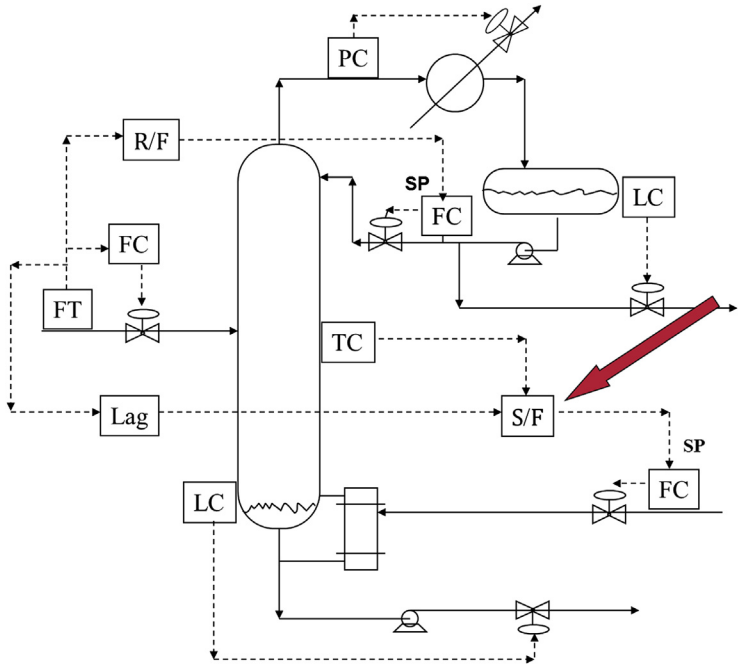

FIGURE 1.8 Steam-to-Feed Ratio (Arrow) to Provide Improved Load Rejection

FC, flow controller; FT, flow transmitter; LC, level controller; PC, pressure controller; R/F, reflux-to-feed ratio; SP, setpoint; TC, temperature controller.

Thus this structure is a combined feedforward/feedback system. Note that a dynamic lag is used on the feed stream flow rate signal so that the change in the steam flow rate is not instantaneous but is timed so that it matches the time it takes for the temperature sensor to recognize the disturbance.

Figure 1.9 demonstrates the significant dynamic advantage of using this ratio structure to reduce product quality deviations. The example is a depropanizer column separating propane from isobutane. The product specifications are 1 mol% propane in the bottoms (x_B) and 2 mol% isobutane in the distillate (x_D). Reboiler heat input (Q_R) is manipulated to control the temperature on stage 9 (T9). The control structure also includes a reflux-to-feed multiplier. The disturbance is a 20% step increase in feed flow rate. The solid lines indicate when only temperature control is used. The dashed lines indicate when a steam-to-feed feedforward multiplier is included.

The reductions in the peak dynamic transient deviations in both temperature and product compositions are striking. Without the ratio, the propane impurity of the bottoms hits a peak of 1.2 mol% from its specification of 1 mol%. With the ratio, the peak deviation is only down to 0.94 mol% propane. No dynamic lag was used on the feed flow rate signal, so the instantaneous increase in reboiler heat input caused

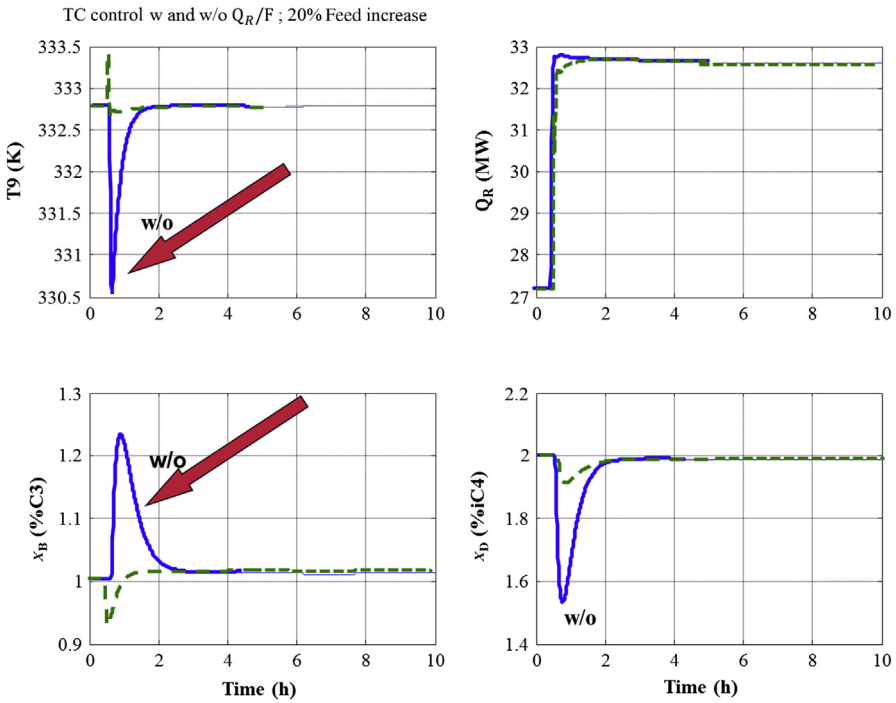

FIGURE 1.9

Temperature controller (TC) with (green dashed line) and without (w/o; blue solid line) a reboiler duty-to-molar feed flow rate (Q_R/F) ratio. Arrows indicate the transient responses.

some initial overpurification of the bottom product. This effect can also be observed in the temperature signal, which initially increases because of the immediate increase in reboiler heat input. These momentary moves in the wrong direction could be reduced by using a small dynamic lag on the feed flow rate signal.

It is important to remember that the tuning of the temperature controller changes as we move from a system where the controller output signal goes to a steam flow controller setpoint to a system where the controller output signal goes to a multiplier. In the former case, the temperature controller output is a flow rate. In the latter case, it is a ratio.

1.9 More complex columns

Up to this point we have considered a simple single-feed, two-product distillation column and presented several alternative control structures. The choice of the best control scheme depends on several factors. In this section we explore more complex

distillation systems, some with multiple columns and some with multiple product streams.

1.9.1 Partial condensers

Partial condensers, instead of total condensers, produce both a liquid stream that is removed from the bottom of the reflux drum and a vapor stream that is removed from the top of the reflux drum. There are two types of flowsheets. In the first, all of the distillate product is removed as a vapor stream. All of the condensed liquid is refluxed back to the column. In the second, the objective is to produce as little vapor distillate as possible. The control structures for these two situations are somewhat different.

1.9.1.1 All-vapor distillate

Figure 1.10 shows a control system for this type of column. Pressure is controlled by manipulating the flow rate of the vapor distillate. Reflux flow rate is ratioed to feed flow rate. A tray temperature is controlled by manipulating the flow rate of steam. The reflux drum level is controlled by manipulating cooling water flow rate to the condenser.

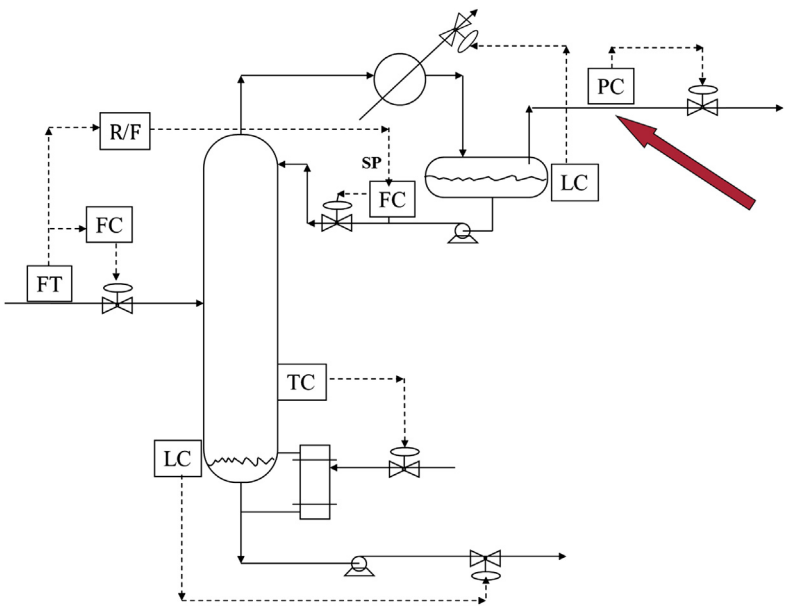

FIGURE 1.10 Partial Condenser (PC; Arrow) with Vapor Distillate

FC, flow controller; FT, flow transmitter; LC, level controller; R/F, reflux-to-feed ratio; SP, setpoint; TC, temperature controller.

1.9.1.2 Liquid and vapor distillate flowrates

Distillate streams: Partial condensers are most frequently used when the feed stream contains some lighter-than-light key components that would require a very low reflux drum temperature (refrigeration) or a very high column pressure to totally condense the overhead vapor. Since refrigeration is much more expensive than cooling water, reflux drum temperatures are typically designed for about 323 K so that cooling water at around 303 K can be used in the condenser. If this temperature is used and a reasonable pressure is specified, most of the overhead vapor will condense but not all. The objective is to minimize the amount of vapor distillate since this stream will often require expensive compression for further processing.

The consequence of this objective is that the cooling water flow rate should be maximized to do as much condensing as possible. Figure 1.11 shows a control structure that achieves this objective. The control valve on the cooling water line is fixed in its wide-open position. The flow rate of the vapor is therefore kept as small as possible.

1.9.2 Ternary sidestream column

Distillation columns can have more than two product streams. If the feed consists of a ternary mixture of light component *L*, intermediate component *I*, and heavy component *H*, a column with distillate, bottoms, and sidestream products can

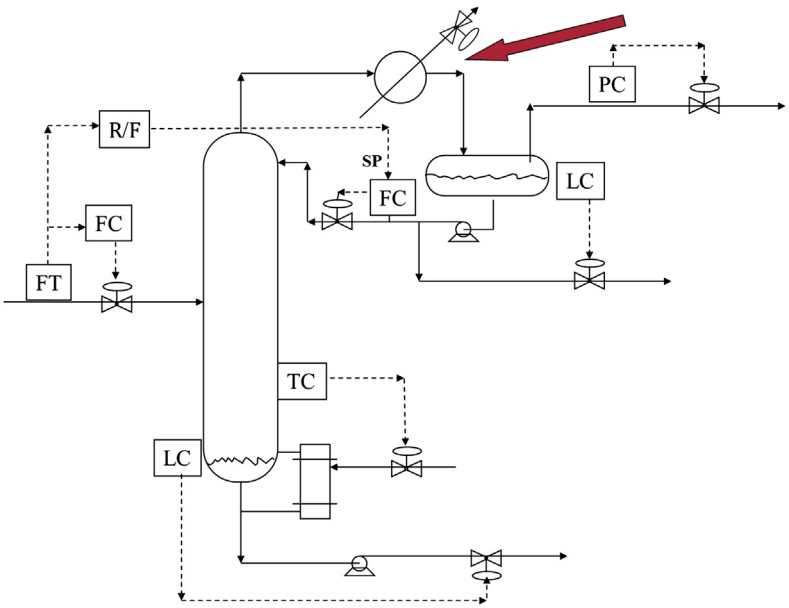

FIGURE 1.11 Partial Condenser (Arrow) with Liquid and Vapor Distillates

FC, flow controller; FT, flow transmitter; LC, level controller; PC, pressure controller; R/F, reflux-to-feed ratio; SP, setpoint; TC, temperature controller.

sometimes be used to achieve the desired separation. Figure 1.12 illustrates this process. A liquid sidestream that contains mostly the intermediate component *I* is withdrawn from a tray in the rectifying section.

The distillate contains mostly the light component *L* with some impurity of the intermediate component *I*. The sidestream contains impurities of both *L* and *H*. The bottom stream mostly consists of the heavy component *H* with small amounts of component *I* as an impurity.

The RR is typically large in this type of column, so we control reflux drum level with the reflux flow rate. The sidestream column has an additional degree of freedom compared to the two-product column. The three available variables that can be manipulated (after controlling pressure and the two liquid levels) are distillate flow rate *D*, reboiler heat input Q_R and sidestream flow rate *S*. Therefore, three variables can be controlled. The two obvious variables to control are the impurity of *I* in the distillate $x_{D(I)}$ and the impurity of *I* in the bottom stream $x_{B(I)}$. The third is not so obvious. Which of the impurities in the sidestream—*L* or *H*—should be controlled? We cannot control both.

In most sidestream columns of this type the impurity of the light component in the sidestream is predominantly fixed by the relative volatility between the light and

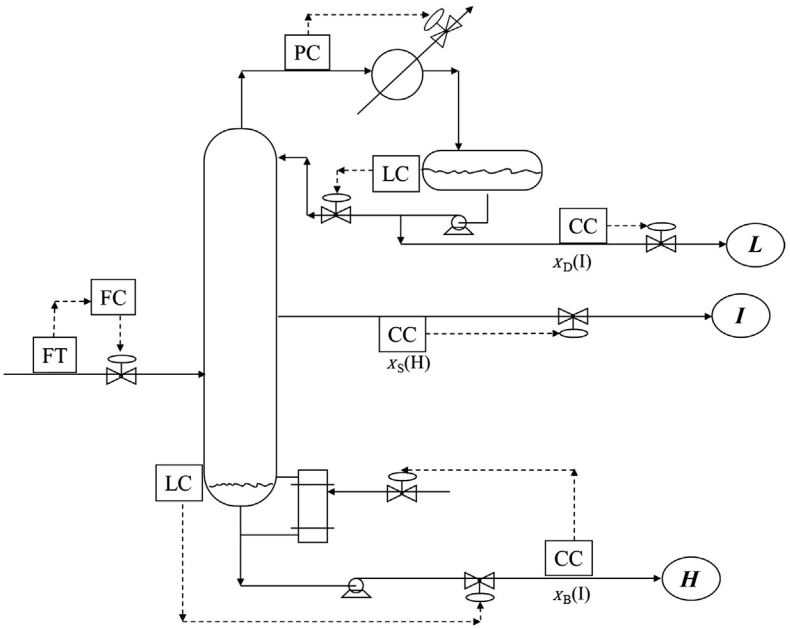

FIGURE 1.12 Ternary Liquid Sidestream Column; $x_S \rightarrow \dot{S}$

CC, composition controller; FC, flow controller; FT, flow transmitter; *H*, heavy component; *I*, intermediate component; *L*, light component; LC, level controller; PC, pressure controller; X_B(I), impurity of I in the bottoms; X_D(I), impurity of I in the distillate; X_S(H), impurity of heavy component in the sidestream.

the intermediate components. All of the light component must flow up the column in the vapor phase, so the vapor on the sidestream tray will inevitably contain some light component. The sidestream is withdrawn as a liquid in phase equilibrium with this vapor. If the relative volatility is large (or the amount of light component in the feed is small), there will be little intermediate impurity in the sidestream. The larger the relative volatility, the less impurity of the light component there will be in the sidestream. In any event, there is little we can do to control the light component's impurity. However, the impurity of the heavy component can be effectively controlled since it depends strongly on the sidestream flow rate and the vapor boil-up.

Figures 1.12 and 1.13 show two alternative "triple-composition" control structures in which the three manipulated variables are paired in different ways. In both control structures, the distillate flow rate is manipulated to control the impurity of the intermediate component in the distillate. In Figure 1.12 the sidestream flow rate is manipulated to control the heavy component's impurity in the sidestream. Increasing sidestream flow rates pulls more material into the sidestream and increases the concentration of the heavy component in the sidestream. So, this

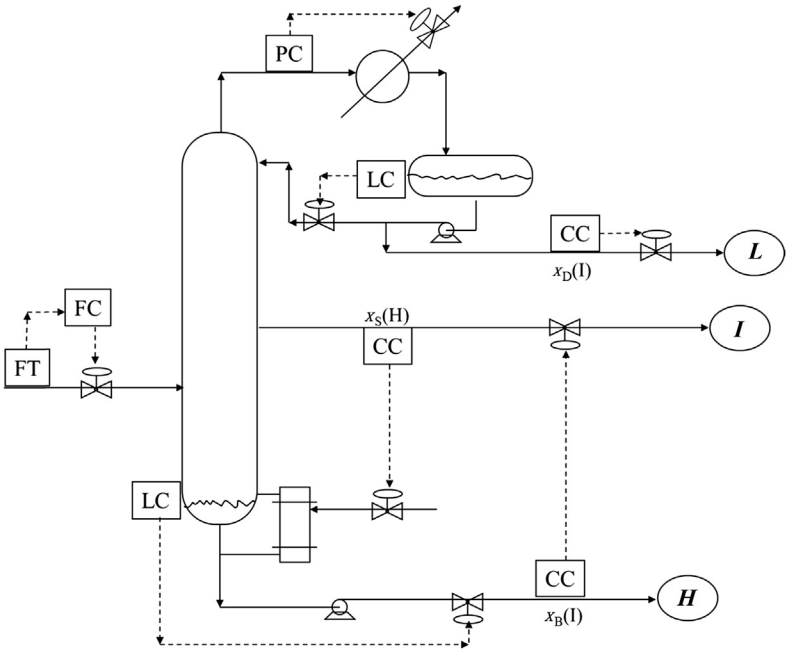

FIGURE 1.13 Ternary Liquid Sidestream Column; $x_S \rightarrow Q_R$

CC, composition controller; FC, flow controller; FT, flow transmitter; *H*, heavy component; *I*, intermediate component; *L*, light component; LC, level controller; PC, pressure controller; X_B(I), impurity of I in the bottoms; X_D(I), impurity of I in the distillate; X_S(H), impurity of heavy component in the sidestream.

composition controller is reverse acting. The reboiler duty is manipulated to control the impurity of the intermediate component in the bottoms. This composition controller is direct acting: more impurity requires more vapor boil-up to drive the intermediate component up the column.

In Figure 1.13 the two loops are switched. The sidestream flow rate is manipulated to control the intermediate component's impurity in the bottom stream. This composition controller is direct acting so that the sidestream flow rate is increased if too much intermediate component is dropping out the bottom. Reboiler duty is manipulated to control the heavy component's impurity in the sidestream. This composition controller is reverse acting so that less heavy component is sent up the column if there is too much impurity in the heavy component in the sidestream.

Both of these control structures have been used. There is no clear general understanding of which is better in what kind of system. Dynamic simulations can be used to decide this question in each specific case.

The sidestream column discussed in this section has a liquid sidestream, and the sidestream drawoff location is above the feed tray. In some cases the sidestream is withdrawn as a vapor and the sidestream drawoff location is below the feed tray since the concentration of the heavy component is higher in the liquid phase than in the vapor phase (see Figure 1.14). Control structure issues are similar to those

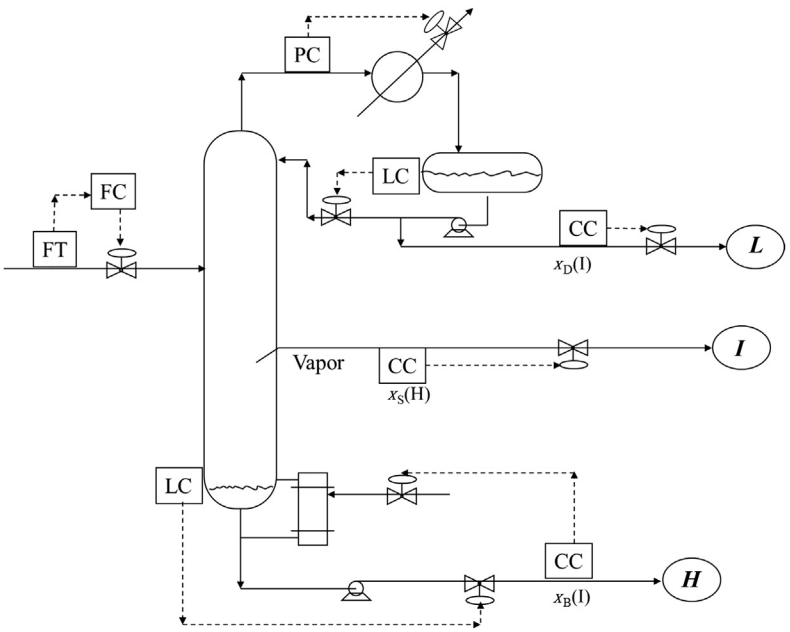

FIGURE 1.14 Ternary Vapor Sidestream Column

CC, composition controller; FC, flow controller; FT, flow transmitter; *H*, heavy component; *I*, intermediate component; *L*, light component; LC, level controller; PC, pressure controller; X_B(I), impurity of I in the bottoms; X_S(H), impurity of heavy component in the sidestream.

for a liquid sidestream except that now changing the sidestream flow rate changes the vapor going up the column above the drawoff tray. In the case of a liquid sidestream, changing the sidestream flow rate changes the liquid flowing down the column.

1.9.3 Sidestream column with stripper

As discussed above, the impurity of the light component in the sidestream is difficult to control in a sidestream column because the liquid on the sidestream drawoff tray is in phase equilibrium with the vapor passing up the column. Therefore highly pure sidestream products are seldom produced in a simple sidestream column. However, we can modify the process to achieve higher sidestream purities.

Figure 1.15 shows a flowsheet with a liquid sidestream column augmented by a stripper. Liquid from the column is withdrawn and fed to the top of the stripper. Heat is added in the stripper reboiler to drive the impurity light component back into the column. We have added an additional control degree of freedom, so now four variables can be controlled. Therefore, the impurities of both the light and the heavy components in the sidestream product can be controlled and high purities can be attained.

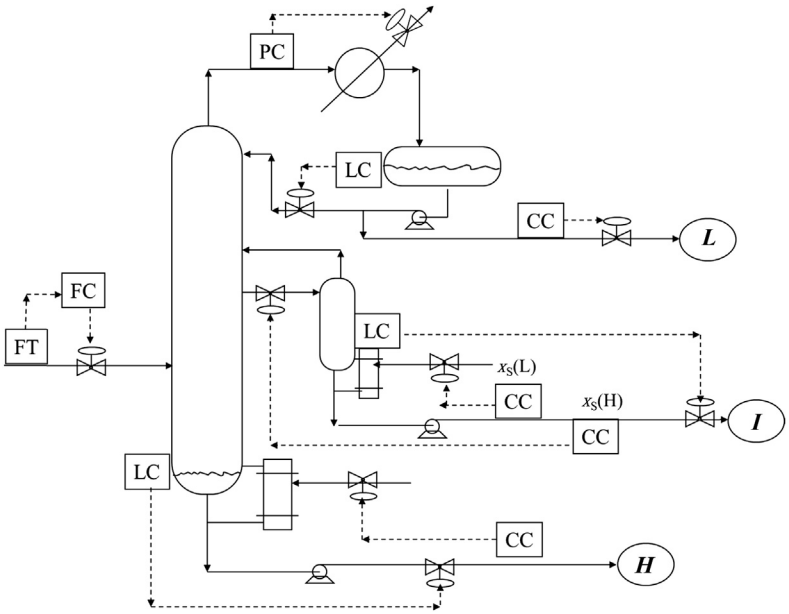

FIGURE 1.15 Ternary Sidestream Column with Stripper

CC, composition controller; FC, flow controller; FT, flow transmitter; *H*, heavy component; *I*, intermediate component; *L*, light component; LC, level controller; PC, pressure controller; X_S(L), impurity of light component in the sidestream.

The control structure shown in Figure 1.15 controls the impurity of the heavy component in the sidestream by manipulating the liquid withdrawn from the main column and sent to the top of the stripper. Withdrawing more liquid increases the impurity of the heavy component. The impurity of the light component in the sidestream is controlled by manipulating the stripper reboiler duty. Heat input is increased if too much light component is coming out the bottom of the stripper. The level in the base of the stripper is controlled by manipulating the liquid from the bottom of the stripper.

1.9.4 Sidestream column with rectifier

If a vapor sidestream is taken from the main column, a rectifier can be used to increase the purity of the intermediate product. As shown in Figure 1.16, the vapor sidestream is fed into the bottom of a small column. This column has its own condenser and reflux drum, which provide an additional control degree of freedom. The rectifier overhead vapor is condensed and a portion is refluxed back to the top of the rectifier. The rest is removed as product. The pressure in the rectifier is controlled by manipulating heat removal in the rectifier condenser. The rectifier base level is controlled by manipulating the flow rate of liquid from the base of the rectifier back to the main column.

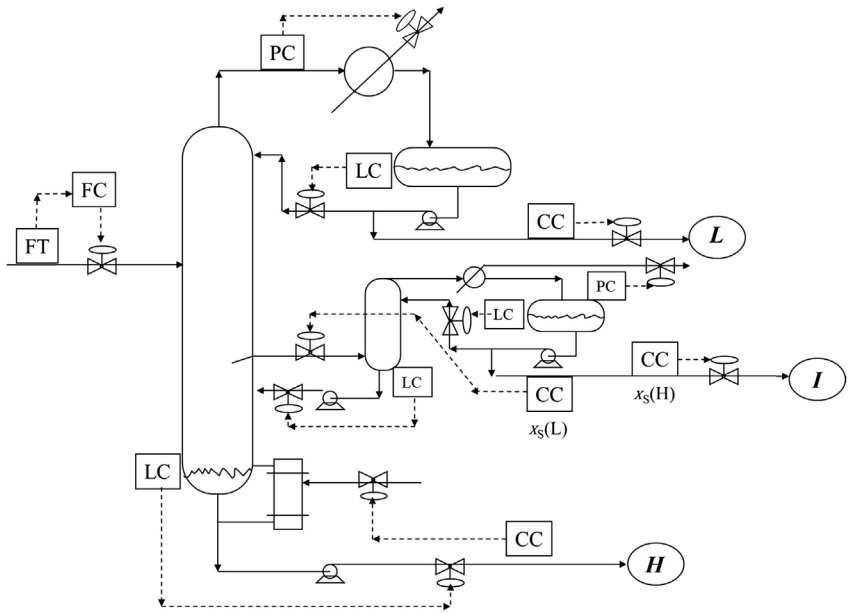

FIGURE 1.16 Ternary Sidestream Column with Rectifier

CC, composition controller; FC, flow controller; FT, flow transmitter; *H*, heavy component; *I*, intermediate component; *L*, light component; LC, level controller; PC, pressure controller.

Both the impurity of the light component and the impurity of the heavy component in the rectifier product can be controlled. Light component impurity is controlled by manipulating the flow rate of vapor fed to the base of the rectifier. Heavy component impurity is controlled by manipulating the flow rate of the distillate from the rectifier.

1.9.5 Sidestream column with prefractionator

Another two-column configuration uses an upstream column called a prefractionator to make an initial split of the ternary system. The idea is to keep essentially all of the heavy component from going overhead in the prefractionator and to keep essentially all of the light component from going out the bottoms. Some of the intermediate component goes out the top and some out the bottom. The prefractionator distillate is fed into a second column at an upper feed tray. The prefractionator bottom stream is fed lower into this column. A sidestream is withdrawn at a location between the two feed streams. Figure 1.17 shows the flowsheet.

This configuration keeps the heavy component from having to flow down in the liquid past the sidestream drawoff tray and keeps the light component from having to

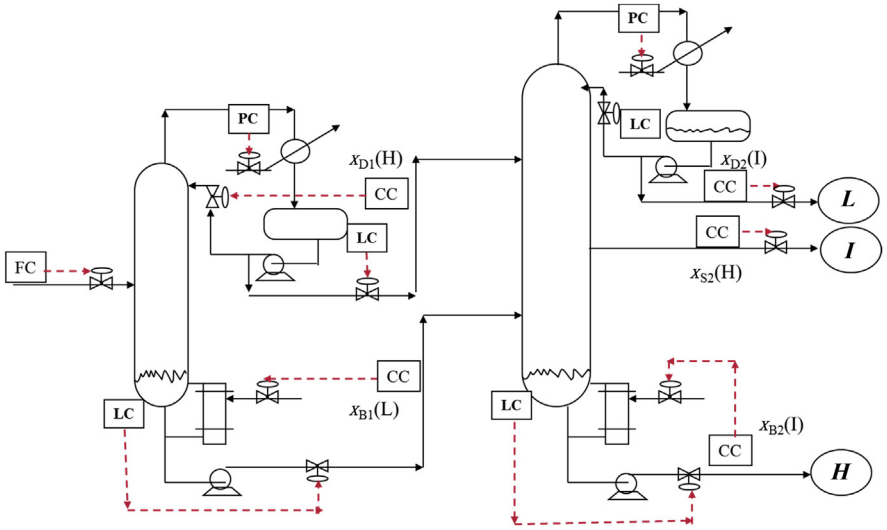

FIGURE 1.17 Prefractionator/Sidestream Column

Red dashed lines indicate control signals. CC, composition controller; FC, flow controller; FT, flow transmitter; *H*, heavy component; *I*, intermediate component; *L*, light component; LC, level controller; PC, pressure controller; X_{D1}(H), impurity of heavy component in the distillate from the first column; X_{D2}(I), impurity of intermediate component in the distillate from the second column; X_{B1}(L), impurity of light component in the bottoms from the second column; X_{B2}(I), impurity of intermediate component in the bottoms from the second column; X_{S2}(H), impurity of heavy component in the sidestream.

flow up in the vapor past the sidestream drawoff tray. This permits the production of a sidestream that contains very pure intermediate component. Note that each column has its own reboiler and condenser, so operating pressures can be different in the two vessels if there is an economic advantage in doing so.

The control structure shown in Figure 1.17 adjusts reflux and reboiler duty in the prefractionator to keep very low concentrations of the heavy component in the distillate and very low concentrations of the light component in the bottom stream. Then in the main sidestream column the concentrations of impurities in the three product streams are controlled by manipulating the three manipulated variables: distillate flow rate, sidestream flow rate, and reboiler duty.

1.9.6 Divided wall (Petlyuk) column

A fairly logical extension of the prefractionator configuration is to use only one vessel with one reboiler and one condenser. A vertical wall is constructed across some chord of the column circular cross-section (not necessarily in the middle). The vapor coming up from the stripping section splits between the two sides of the wall. At the top of the wall a total-liquid trapout tray collects all the liquid coming down from the rectifying section. A portion of the liquid is fed to the top of the prefractionator side of the wall. The rest is fed to the top of the sidestream side of the wall (see Figure 1.18).

Thus only one vessel and two heat exchangers are required, which lowers capital investment in some separations. Energy savings are sometimes also realized. The optimum economic design involves find the best vapor and liquid splits in addition to the number of trays in each of the four sections and the locations of the feed stream and the sidestream. Note that once the column is designed and built, the location of the wall is fixed. Therefore the vapor split is fixed.

This process has four control degrees of freedom: distillate flow rate, sidestream flow rate, reboiler heat input, and the liquid split. In the control structure shown in Figure 1.18 the impurities in the three product streams are controlled by manipulating the first three of these. The liquid split is manipulated to make sure that very little of the heavy component goes out in the vapor leaving the prefractionator side of the wall. This serves the very useful purpose of minimizing energy consumption when feed composition disturbances occur.

1.9.7 Heat-integrated columns

In the same way that multieffect evaporators function, multieffect distillation columns can be used in some systems to achieve very significant reductions in energy consumption. If the reflux drum temperature of one column is higher than the reboiler temperature of a second column, the two can be heat-integrated using a single heat exchanger that serves as a condenser in the high-temperature column and a reboiler in the low-temperature column.

There many types of heat-integrated columns. The example presented here considers the case in which a feed stream is split between two columns. Each column

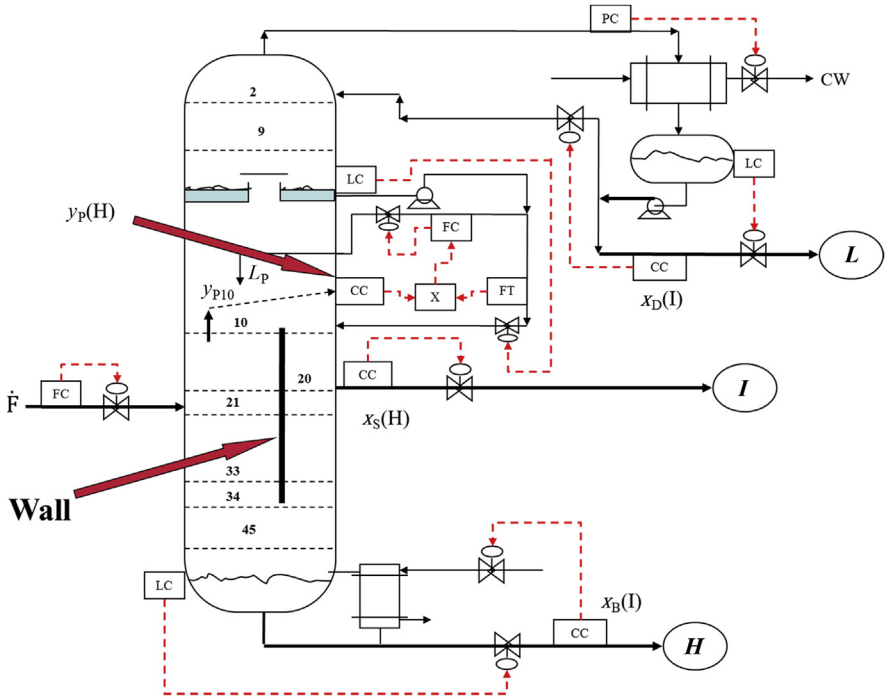

FIGURE 1.18 Column Divided with a Wall (Arrow)

CC, composition controller; CW, cooling water; FC, flow controller; FT, flow transmitter; *H*, heavy component; *I*, intermediate component; *L*, light component; LC, level controller; L_P, liquid fed to the top of prefactionator side of the wall; PC, pressure controller; Y_P(H), impurity of heavy component in the vapor leaving the top of the feed side of the wall; X_D(I), impurity of intermediate component in the distillate; X_B(I), impurity of intermediate component in the bottoms; X_S(H), impurity of heavy component in the sidestream.

produces distillate and bottom products that are at their specified purities. The pressure in one is set so that cooling water can be used in its condenser with the specified distillate composition (reflux-drum temperature of 323 K). This is the low-pressure column. The temperature in the base of this column is determined by the base pressure (reflux drum pressure plus total tray pressure drop) and the composition of the bottom product. Then the pressure in the second column (the high-pressure column (HPC)) is set so that the temperature in its reflux drum is higher than the temperature in the base of the low-pressure column (LPC). Figure 1.19 shows the flowsheet.

The smaller the difference between the two temperatures, the larger the area required for heat transfer will be. A rough economic heuristic is to design for a 20-K differential temperature. If the separation is favored by low pressure, the separation is more difficult in the HPC, so the optimum economic design will have an HPC with more trays than the low-pressure column.

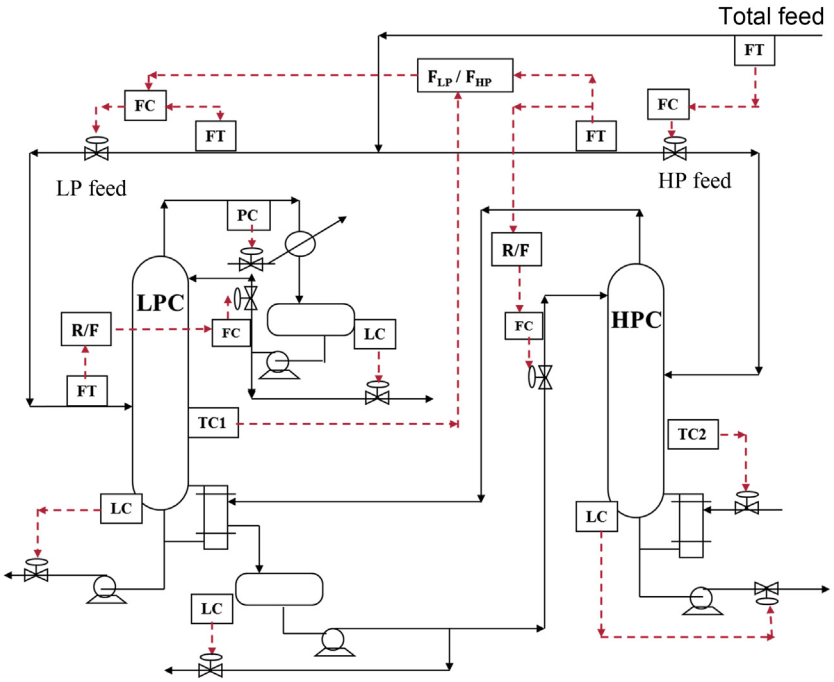

FIGURE 1.19 Heat-Integrated Columns

Red dashed lines indicate control signals. FC, flow controller; F_{LP}/F_{HP}, low-pressure feed-to-high-pressure feed ratio; FT, flow transmitter; HP, high pressure; HPC, high-pressure column; LC, level controller; LP, low pressure; LPC, low-pressure column; PC, pressure controller; R/F, reflux-to-feed ratio; TC, temperature controller.

The system shown in Figure 1.19 is designed for "neat" operation: all of the heat of condensation in the HPC is transferred as heat of vaporization in the low-pressure column. There is no auxiliary reboiler in the low-pressure column to generate additional vapor boil-up if needed. There is no auxiliary condenser in the HPC to provide additional vapor condensation if needed. In some systems one of these auxiliary heat exchangers is included in the design to provide some operation flexibility and to improve dynamic control. Of course, energy consumption is somewhat higher than in the neat configuration.

It might be useful to provide an economic comparison of a single-column system vs a heat-integrated two-column system, with both systems making exactly the same products. As a numerical example consider the binary methanol/water separation for a feed flow rate of 1 kmol/s of 60 mol% methanol and 40 mol% water in a column that produces a 99.9 mol% methanol distillate and a 99.9 mol% water bottom stream. We assume that in the single-column configuration, the column operates at 0.6 atm (so that cooling water can be used in the condenser) and that the column

has 32 stages. The temperature in the base is 367 K at the resulting base pressure and specified bottom stream composition. This column has a diameter of 5 m and consumes 35.6 MW of energy.

In the heat-integrated configuration we assume the low-pressure column also operates at 0.6 atm and has a base temperature of 367 K. The HPC operates at 5 atm, which gives a reflux drum temperature of 387 K. Thus the temperature differential is 20 K. For simplicity, we assume each column has 32 stages (note that this is not the economic optimum). The diameter of the low-pressure column is 3.5 m and that of the HPC is 2.6 m. Energy consumption in the reboiler at the base of the HPC is 21.8 MW. Thus there is a 39% reduction in energy consumption compared to the single-column design.

Of course, the temperature in the base of the HPC (428 K) is higher than the temperature in the base of the single-column design (367 K). Therefore, a higher-temperature, more expensive heat source must be used in the heat-integrated configuration than in the single column. The comparison should be on a monetary basis, not on the basis of energy consumption (megawatts). Assuming a low-pressure steam (433 K at $7.78 per gigajoule) can be used in the single-column configuration and a high-pressure steam (527 K at $9.88 per gigajoule) must be used in the heat-integrated configuration, the energy savings is still significant at 22%.

The capital cost of the two alternative configurations is also important. The total capital cost for the column shell and the two heat exchangers of the single-column configuration is $3,400,000. The total capital cost of the two vessels and the three heat exchangers in the heat-integrated configuration is $2,880,000. This somewhat surprising difference is a result of smaller-diameter columns and a smaller heat transfer area required because of the lower heat-transfer rates.

The control structure shown in Figure 1.19 controls a temperature in the HPC (TC2) by manipulating reboiler duty in the HPC. Vapor boil-up in the HPC, of course, determines the vapor boil-up in the low-pressure column. The low-pressure column does not have its own separate reboiler to use to control the temperature. We must find a manipulated variable to control the temperature in the low-pressure column. The control degree of freedom selected is the feed split (the fraction of the total feed that is fed to the low-pressure column).

The total feed to the process is flow-controlled by manipulating the feed to the HPC. A ratio is established between the feed to the low-pressure column and the feed to the HPC, so an increase in the setpoint to the total feed flow controller produces an increase in feeds to both columns. The ratio of the two feeds F_{LP}/F_{HP} is set by the temperature controller in the low-pressure column (TC1).

Note that these two temperature control loops interact strongly because both reboiler duty and feed split affect temperatures in both columns. Sequential controller tuning is certainly required to account for this interaction. Reflux-to-feed ratios are used in both columns. Distillate streams control reflux drum levels, and bottom streams control base levels. Pressure in the low-pressure column is controlled by manipulating cooling water to the condenser. The pressure in the HPC is *not* controlled. It floats up and down with changes in throughput and composition.

1.9.8 Extractive distillation process

Extractive distillation is one of several methods for achieving separations when a nonideal phase equilibrium results in the formation of azeotropes. Azeotropes produce distillation boundaries that prevent the separation of the components in a single distillation column. In extractive distillation a heavy solvent is used to alter the phase equilibrium so that the desired separation can be achieved in a two-column system.

A specific example to illustrate the extractive distillation process is considered in this section. The binary mixture of acetone (boiling point, 329 K) and methanol (boiling point, 338 K) form a homogeneous minimum-boiling azeotrope at 328 K with a composition of 77.6 mol% acetone. The binary feed stream is introduced into the first column near the middle. A heavy (high-boiling) solvent such as dimethyl sulfoxide (DMSO; boiling point, 463 K) is fed into a few trays from the top of the column. DMSO preferentially soaks up the methanol, so methanol and DMSO come out the bottom of the column. The distillate product is high purity acetone. Figure 1.20 shows the flowsheet.

The bottoms from the first "extractive" column is essentially a binary mixture of methanol and DMSO, which is easily separated in a second column with methanol going overhead and DMSO coming out in the bottoms to be recycled back to the first column.

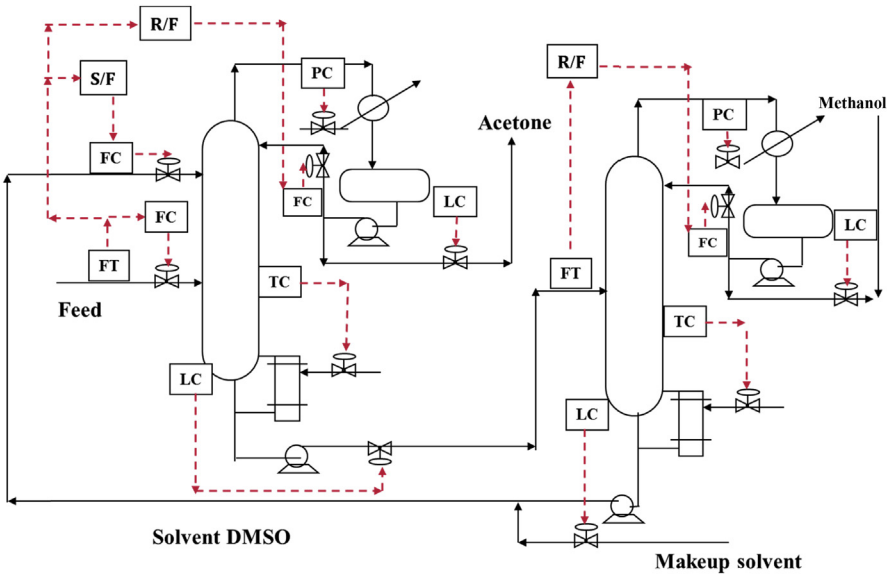

FIGURE 1.20 Extractive Distillation

Red dashed lines indicate control signals. DMSO, dimethyl sulfoxide; FC, flow controller; FT, flow transmitter; LC, level controller; PC, pressure controller; R/F, reflux-to-feed ratio; S/F, solvent-to-feed ratio; TC, temperature controller.

The design of an extractive distillation system requires economic optimization of both columns considered simultaneously. Major design optimization variables are the solvent-to-feed ratio and the RR in the extractive column. Higher solvent-to-feed ratios improve the separation between the key components but increase energy consumption in the solvent recovery column. An unusual nonmonotonic relationship exists between RR and product purity. Too much reflux dilutes the solvent and reduces the purity of the acetone product by letting some methanol go overhead. Too little reflux lets some solvent go overhead, which also reduces acetone purity.

The control structure shown in Figure 1.20 sets the solvent-to-feed ratio (S/F) and controls a tray temperature in each column by manipulating reboiler duty. Reflux-to-feed ratios are controlled. Distillate flow rates control reflux drum levels. The bottoms flow rate from the extractive column controls the base level. The base level in the second "solvent recovery" column is controlled by manipulating the flow rate of the makeup solvent since small amounts are lost in the two product streams. In the DMSO solvent system, these losses are very small, so the level in the base of the solvent recovery column must be sized to handle the transient changes that inevitably occur when throughput is changed. For example, suppose we increase the feed flow rate. The S/F ratio immediately increases the solvent flow rate. This drops the level in the base of the solvent recovery column. However, the increase in feed and solvent eventually work their way hydraulically down the extractive column and begin to increase the base level. The level controller increases the feed to the solvent recovery column, which eventually works its way hydraulically down the column and begins to drive the base level back up. The base of the solvent recovery column must be sized to handle these dynamic transients.

1.9.9 Heterogeneous azeotropic distillation process

Another method for separating azeotropes that involves distillation is heterogeneous azeotropic distillation. A component called a "light entrainer" is added; it has such great nonideal behavior with one of the key components that it greatly increases the volatility of that component and drives it overhead in the column. In addition, the nonideality is so great that when the overhead vapor is condensed, two liquid phases form. These "oil and water" partially miscible liquids separate in a decanter because of density differences. The aqueous phase is heavier than the organic phase.

To illustrate this type of process, we consider the dehydration of ethanol, using benzene as the light entrainer. Ethanol and water form a minimum-boiling homogeneous azeotrope at atmospheric pressure with a composition of 90 mol% ethanol and 10 mol% water at a temperature of 351 K. The boiling point of ethanol is 351.1 K and that of water is 273.2 K.

Most ethanol is produced in batch fermenters at low ethanol concentrations (4−6 mol%). A column is used to produce a more concentrated mixture (84 mol

%), which then is fed into a dehydration unit consisting of two distillation columns. In the first column a reflux stream rich in benzene is fed at the top. The benzene and water are so dissimilar that they are driven overhead. If enough benzene is fed, the bottom stream is highly pure ethanol at a concentration above the azeotrope. The overhead vapor has a composition that is close to the ternary azeotrope: 53.0 mol% benzene, 27.5 mol% ethanol, and 19.5 mol% water. After condensing, the steam splits into two liquid phases. The aqueous phase has a composition of 7.24 mol% benzene, 47.04 mol% ethanol, and 45.72 mol% water. The organic phase has a composition of 84.35 mol% benzene, 14.14 mol% ethanol, and 1.51 mol% water.

Figure 1.21 shows the flowsheet. The organic phase is refluxed to the first column. The aqueous phase is fed to a second column that takes the water out the bottom and produces an overhead distillate that is recycled back to the first column.

The design of this process is made tricky by the high degree of nonideality, which makes simulation studies difficult because of the occurrence of multiple steady-state solutions. Finding precisely the correct amount of organic reflux is critical. Too much benzene results in some of the benzene going out the bottom with the ethanol. Too little benzene lets the water go out the bottom. Obtaining the desired high-purity ethanol in the bottom stream requires a knife-edge balance.

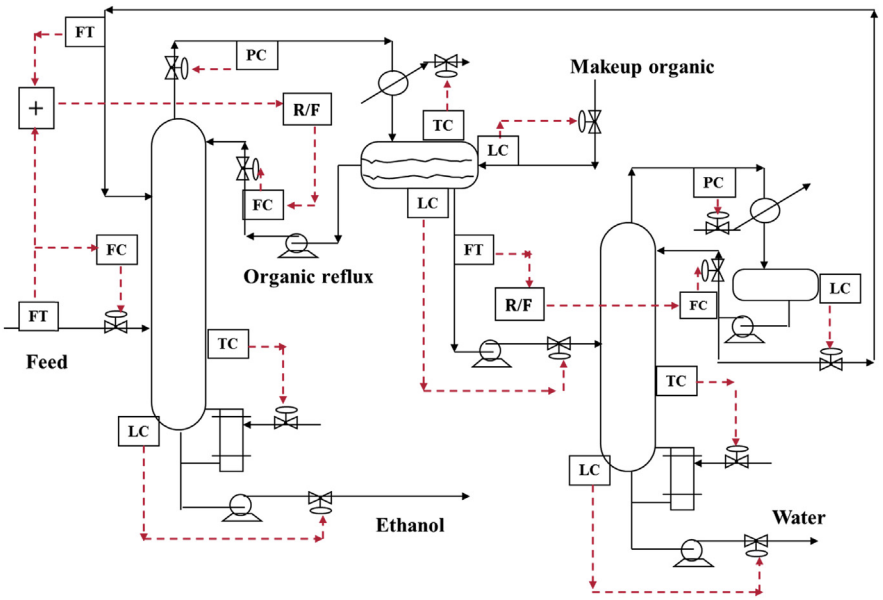

FIGURE 1.21 Heterogeneous Azeotropic Distillation

Red dashed lines indicate control signals. FC, flow controller; FT, flow transmitter; LC, level controller; PC, pressure controller; R/F, reflux-to-feed ratio; TC, temperature controller.

The control structure must maintain this fine balance in the face of disturbances in feed stream flow rate and composition. The control structure shown in Figure 1.21 has two important loops. The reboiler heat input in the first column controls a tray temperature such that the benzene cannot drop out the bottom. An adequate amount of benzene is fed to the column by maintaining a ratio of organic reflux to the sum of the two feed streams (fresh feed stream and distillate recycled from the second column).

1.9.10 Superfractionator control

Distillation columns that separate components with very low relative volatilities require a large number of trays (>100) and high RRs (>10). Common examples are the separation of propylene and propane in a C3 splitter and the separation of isomers (e.g. isopentane and normal pentane).

The high RR dictates that the reflux drum level should be controlled by manipulating the reflux flow rate since the distillate stream is so much smaller than the overhead vapor stream. To avoid valve saturation, the larger stream should be used to control the level. The same situation occurs in the column base. The bottom stream is much less than the liquid coming into the column base. This suggests that the base level should be controlled by manipulating the reboiler duty. Figure 1.22 shows the flowsheet and this control structure, which is called the DB structure.

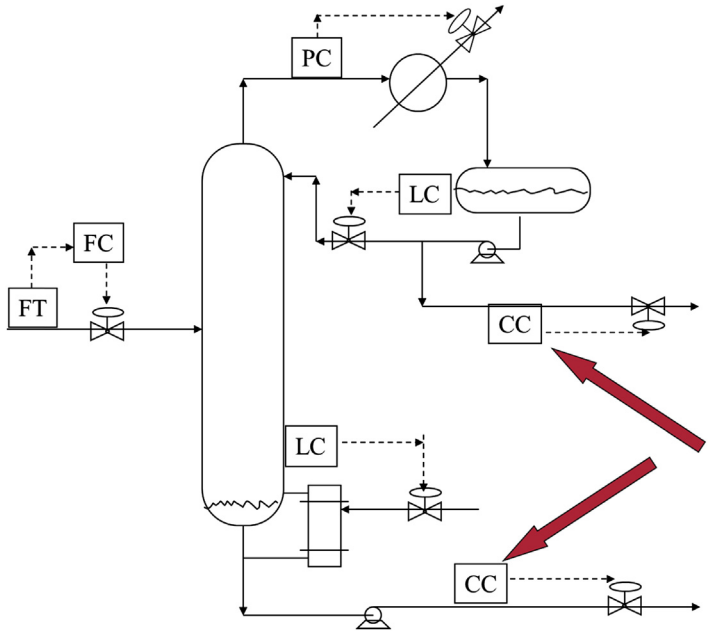

FIGURE 1.22 Superfractionator

CC, composition controller (arrows); FC, flow controller; FT, flow transmitter; LC, level controller; PC, pressure controller.

This setup seems strange because we cannot independently set the flow rates of both product streams since, under steady-state conditions, they must add up to the feed stream flow rate. However, this structure does work in columns with many trays because of the hydraulic dynamics. Two composition controllers set the flow rates of the two product streams. The reflux drum level is controlled by the reflux. The base level is controlled by steam.

The major problem with the DB structure is its fragility. If either of the composition loops is placed on manual, the structure will fail because one of the products will have a fixed flow rate. According to the first law of distillation control cited earlier, compositions cannot be controlled if the flow rate of the distillate or bottom stream is fixed. So, if one of the analyzers fails, the control structure must be modified.

1.10 Columns in a plant-wide environment

All of the distillation column control structures described so far in this chapter have considered the column in isolation. Control structures were developed to satisfy the control objectives of the column with little consideration of how the column fits into the rest of the plant. Plant-wide control structures often require column control structures that are significantly different than the structure that would be used if the column were a standalone unit.

An illustration of this is shown in Figure 1.23. The process has the typical multiunit flowsheet with a reaction section and a separation section. The reactor is an isothermal continuous stirred-tank reactor in which the reversible reaction $A + B \Leftrightarrow C$ takes place. The reactor effluent is a mixture of product C and unconverted reactants A and B, which must be separated. Two distillation columns are used since the volatilities are $\alpha_A > \alpha_C > \alpha_B$. An indirect separation sequence is used. The heaviest component B is taken out the bottom of the first column and recycled. The distillate of the first column is a mixture of A and C, which are separated in the second column into a bottoms of product C and a distillate of A for recycling back to the reactor.

The key plant-wide control issue is the management of the fresh feeds of reactants A and B. The temperature controllers in the two columns keep the losses of the reactants A and B at very low levels. Therefore, essentially all of each reactant must be consumed in the reactor. Flow measurement errors and changes in feed compositions make a simple fresh feeds ratio scheme ineffective. Some internal measurement of the accumulation or depletion of reactants must be used to provide feedback information to adjust the flow rates of the fresh feed streams.

Figure 1.23 presents one control structure that achieves this objective. The inventory of B in the system can be detected by the liquid level in the base of the first column. Likewise, the inventory of A in the system can be detected by the liquid level in the reflux drum of the second column. So, the two fresh feed streams are

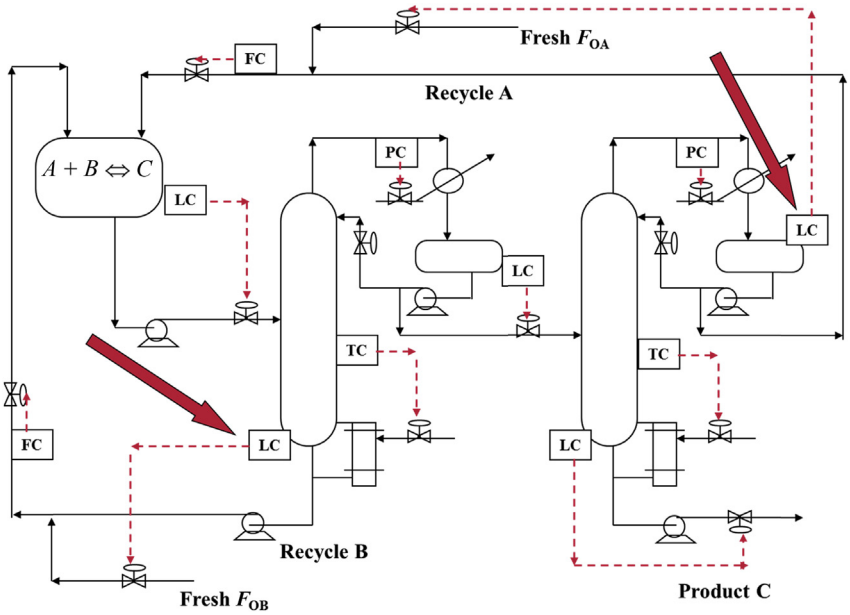

FIGURE 1.23 Column Control Structure in a Plant-Wide Environment

Red dashed lines indicate control signals. FC, flow controller; F_{OA}, flow rate of fresh feed of reactant A; F_{OB}, flow rate of fresh feed of reactant B; LC, level controller (arrows); PC, pressure controller.

manipulated to control these two liquid levels (using reverse-acting controllers). The flow rate of the stream after the fresh and recycle streams have been combined is flow controlled in each recycle loop. The production rate is changed by adjusting the setpoints of both of these two flow controllers.

At first glance, it may seem a poor idea to control the level in the reflux drum of the second column at the end of the process by manipulating the flow rate of the fresh feed of *A* at the beginning of the process. However, changing the fresh feed flow rate has an immediate effect on the reflux drum level. When the drum level drops, the reverse-acting level controller increases the fresh makeup flow rate. This immediately reduces the flow rate of liquid leaving the drum because the flow rate of the total stream is flow controlled. This has the desired effect of increasing the liquid level. Not shown in Figure 1.23 is how the reflux flow rates are set. Typically there would be a reflux-to-feed ratio on both columns.

The first law of plant-wide control is:

It is easy to find a plant-wide control structure that does **not** *work.*

What is also true is that are several plant-wide control structures that do work. Figure 1.23 shows one possibility. Figure 1.24 shows another. In this scheme the

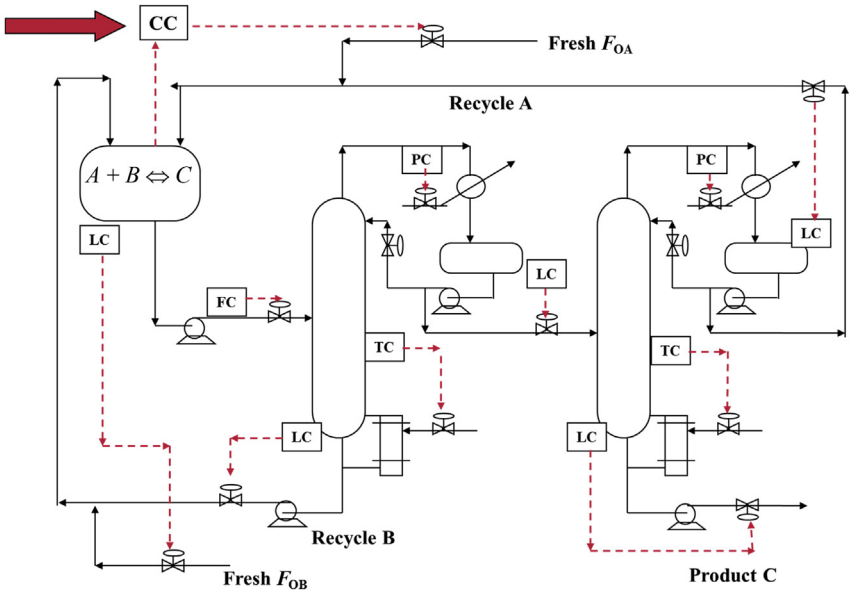

FIGURE 1.24 Alternative Plant-Wide Control Structure

Red dashed lines indicate control signals. CC, composition controller; FC, flow controller; F_{OA}, flow rate of fresh feed of reactant A; F_{OB}, flow rate of fresh feed of reactant B; LC, level controller; PC, pressure controller.

feedback of internal information depends on a composition measurement to detect whether reactant *A* is accumulating or being depleted in the system. The liquid level in the reactor is controlled by manipulating the fresh feed of *B*. The reactor effluent is flow controlled.

Both of these workable plant-wide control structures are based on the principle that feedback information about what is happening to the internal inventory of the reactants must be measured in some way so that appropriate adjustments can be made in the fresh feed streams. The stoichiometry of the reaction must eventually balanced "down to the last molecule."

1.11 Conclusion

A number of fundamental concepts of distillation column control have been discussed and illustrated in this chapter. It is hoped that this brief and basic introduction to the subject is useful and provides some practical guidelines for the development of effective distillation control structures.

References

[1] O. Rademaker, J.E. Rijnsdorp, Maarleveld, Dynamics and Control of Continuous Distillation Units, Elsevier, 1975.
[2] F.G. Shinskey, Distillation Control, McGraw-Hill, 1977.
[3] P.S. Buckley, W.L. Luyben, J.P. Shunta, Design of Distillation Column Control Systems, Instrument Society of America, 1985.
[4] P.B. Deshpande, Distillation Dynamics and Control, Instrument Society of America, 1985.
[5] W.L. Luyben (Ed.), Practical Distillation Control, van Nostrand Reinhold, 1992.
[6] W.L. Luyben, Distillation Design and Control Using Aspen Simulation, second ed., Wiley, 2013.

This page intentionally left blank

CHAPTER

Common Techniques for Distillation Troubleshooting

2

Henry Z. Kister
Fluor Corporation, Aliso Viejo, CA, USA

CHAPTER OUTLINE

Distillation: Operation and Applications. http://dx.doi.org/10.1016/B978-0-12-386876-3.00002-8

A well-known sales axiom states that 80% of the business is brought in by 20% of the customers. A sales strategy tailored for this axiom concentrates the effort on the 20% of the customers without neglecting the others. Distillation troubleshooting follows an analogous axiom. A person who is troubleshooting distillation columns must develop a good understanding of the factors that cause the vast majority of column malfunctions. For these factors, this person must be able to distinguish good practices from poor practices, then correctly evaluate the ill effects of the poor practices and their relevance to the assignment at hand. Although good knowledge and understanding of the broader field of distillation will be beneficial, the troubleshooter can often get by with a shallow knowledge of this broader field.

It is well accepted that troubleshooting is a primary job function of operating engineers, supervisors, and process operators. Far too few realize that distillation troubleshooting starts at the design phase. Any designer wishing to achieve a trouble-free column design must be as familiar with troubleshooting as the person running the column.

The two common troubleshooting practices are analogous to those in medicine. One common practice is to wait until an illness strikes before calling for help. This type of troubleshooting is practiced by operating engineers, supervisors, and process operators. A healthier practice is "preventive troubleshooting," which aims at eliminating the cause of an illness before it occurs. Although preventive troubleshooting is seldom perfect, it can go a long way toward reducing the chances, severity, and pain of potential ailments.

The vast majority of factors that cause column malfunctions have been described in detail elsewhere [1,2]. Many resources distinguish good from poor practices and propose guidelines for avoiding and overcoming troublesome design and operations (e.g. [3]). This chapter briefly surveys the prime causes of tower malfunctions and examines the tools available for uncovering malfunctions. It then looks at the basic troubleshooting techniques: the systematic strategy for troubleshooting distillation problems and the dos and don'ts for formulating and testing theories. Finally, it reviews the techniques for testing these theories and for focusing on the most likely root cause. Chapter 3 elaborates on the key measurement techniques, test procedures, and data processing.

2.1 Causes of column malfunctions

Close to 1500 case histories of malfunctioning columns were extracted from the literature and abstracted [2]. Most of these malfunctions were analyzed elsewhere [1] and classified according to their principal causes. Table 2.1 is a summary. If one assumes that these case histories make up a representative sample, then the analysis below has statistical significance. Accordingly, Table 2.1 can provide a useful guide to the factors most likely to cause column malfunctions and can direct troubleshooters toward the most likely problem areas.

The general guidelines in Table 2.1 often do not apply to a specific column or even plant. For instance, foaming is not high up in Table 2.1; however, in amine absorbers, foaming is a most common trouble spot. The author therefore warns against blindly applying the guides in Table 2.1 to any specific situation. The last three columns in the table show the split of the total cases according to industry category.

Table 2.1 Most Common Causes of Column Malfunctions

No.	Cause	No. of Cases	Refining Industry	Chemical Industry	Olefins/ Gas Plants
1	Plugging, coking	121	68	32	16
2	Tower base and reboiler return	103	51	22	11
3	Tower internals damage (excludes explosion, fire, implosion)	84	35	33	6
4	Abnormal operation incidents (startup, shutdown, commissioning)	84	35	31	12
5	Assembly mishaps	75	23	16	11
6	Packing liquid distributors	74	18	40	6
7	Intermediate draws (includes chimney trays)	68	50	10	3
8	Misleading measurements	64	31	9	13
9	Reboilers	62	28	13	15
10	Chemical explosions	53	11	34	9
11	Foaming	51	19	11	15
12	Simulations	47	13	28	6
13	Leaks	41	13	19	7
14	Composition control difficulties	33	11	17	5
15	Condensers that did not work	31	14	13	2
16	Control assembly	29	7	14	7
17	Pressure and condenser controls	29	18	3	2
18	Overpressure relief	24	10	7	2
19	Feed inlets to tray towers	18	11	3	3
20	Fires (no explosions)	18	11	3	4
21	Intermediate component accumulation	17	6	4	7
22	Chemicals release to atmosphere	17	6	10	1
23	Subcooling problems	16	8	5	1
24	Low liquid loads in tray towers	14	6	2	3
25	Reboiler and preheater controls	14	6	–	5
26	Tow liquid phases	13	3	9	1
27	Heat integration issues	13	5	2	6
28	Poor packing efficiency (excludes maldistribution/support/ hold-down)	12	4	3	2
29	Troublesome tray layouts	12	5	2	–
30	Tray weep	11	6	1	3
31	Packing supports and hold-downs	11	4	2	2

From Ref. [1]. Reprinted courtesy of the Institution of Chemical Engineers in the UK.

An analysis of Table 2.1 suggests the following:

- Plugging, tower base, tower internals damage, instrument and control problems, startup and/or shutdown difficulties, points of transition (tower base, packing distributors, intermediate draws, feeds), and assembly mishaps are the major causes of column malfunctions. Among them, they make up more than half of the reported incidents. Familiarity with these problems, therefore, constitutes the "bread and butter" of persons involved in the troubleshooting of distillation and absorption columns.
- Primary design is an extremely wide topic, encompassing vapor–liquid equilibrium, reflux-stages relationship, stage-to-stage calculations, unique features of multicomponent distillation, tray and packing efficiencies, scale-up, column diameter determination, flow patterns, type of tray, and size and material of packing. This topic occupies the bulk of most distillation texts (e.g. [4–7]), and perhaps represents the bulk of our present distillation know-how. While this topic is of prime importance for designing and optimizing distillation columns, it plays only a minor role when it comes to distillation operation and troubleshooting. Table 2.1 suggests that only one column malfunction in 14 is caused by problems incurred at the primary design stage. The actual figure is probably higher for a first-of-a-kind separation, but lower for an established separation. Due to the bulkiness of this topic in relation to its likelihood to cause malfunctions, and due to the coverage that the topic receives in several texts (e.g. [4–7]) and in this book, it was excluded from this chapter.
- The above statements must not be interpreted to suggest that troubleshooters need not be familiar with the primary design—quite the contrary. A good troubleshooter must have a solid understanding of primary design because it provides the foundation of our distillation know-how. However, the above statements do suggest that, in general, when a troubleshooter examines the primary design for the cause of a column malfunction, he or she has less than one chance out of 10 of finding it there.

PART A: COLUMN TROUBLESHOOTING: HOW TO INVESTIGATE

2.2 Column troubleshooting—a case history

In Sections 2.3 and 2.4, the systematic approach recommended for tackling distillation problems is mapped out. The recommended sequence of steps is illustrated with reference to the case history described below.[a]

[a]Reproduced from Norman P. Lieberman, *Troubleshooting Process Operations* (fourth ed., PennWell Books, Tulsa 2009). This case history is a classic example of how to perform a systematic troubleshooting investigation. The permission of PennWell Books and Norman P. Lieberman for reproducing this material is gratefully acknowledged.

The following story is not a myth; it really happened. One morning as I sat quietly at my desk in corporate headquarters, the boss dropped by to see me. He had some unpleasant news. One of the company's refinery managers was planning to visit our office to discuss the quality of some of the new plants that had been built in his refinery. As an example of how not to design a unit, he had chosen a new gas plant for which I had done the process design. The refinery manager had but one complaint: "The gas plant would not operate."

I was immediately dispatched to the refinery to determine which aspect of my design was at fault. If nothing else, I should learn what I did wrong so as not to repeat the error.

Upon arriving at the refinery, I met with the operating supervisors. They informed me that, while the process design was fine, the gas plant's operation was unstable because of faulty instrumentation. However, the refinery's lead instrument engineer would soon have the problem resolved.

Later, I met with unit operating personnel. They were more specific. They observed that the pumparound circulating pump (see Figure 2.1(a)) was defective. Whenever they raised hot oil flow to the debutanizer reboiler, the gas plant would become destabilized. Reboiler heat-duty and reflux rates would become erratic. Most noticeably, the hot-oil circulating pump's discharge pressure would fluctuate wildly. They felt that a new pump requiring less net positive suction head was needed.

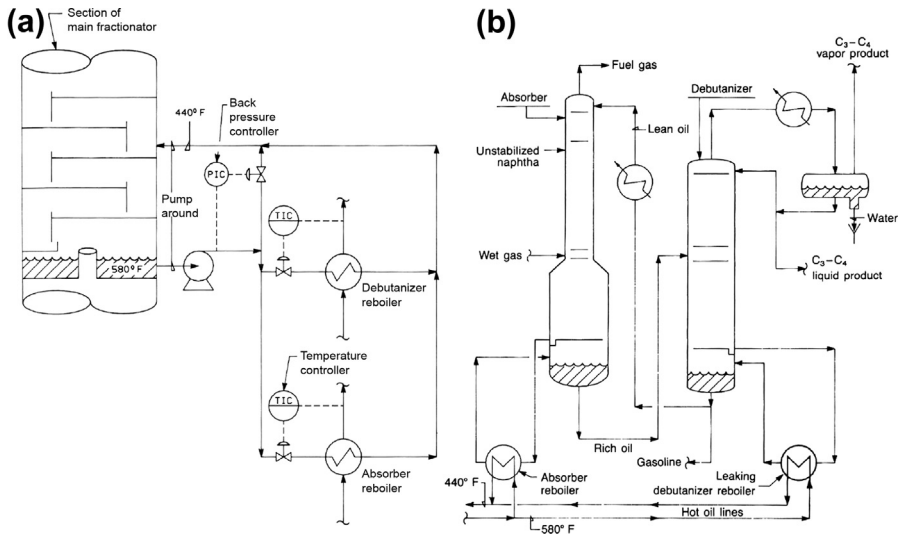

FIGURE 2.1 Column Troubleshooting Case History

(a) Hot oil from the fractionator supplies heat to gas-plant reboilers, (b) Leaking debutanizer reboiler upsets gas plant.

From Ref. [8] reprinted courtesy of PennWell Publishing Co.

Both these contradictory reports left me cold. Anyway, the key to successful troubleshooting is personal observation. So I decided to make a field test.

When I arrived at the gas plant, both the absorber and debutanizer towers were running smoothly but not well. Figure 2.1(b) shows the configuration of the gas plant. The debutanizer reflux rate was so low it precluded significant fractionation. Also, the debutanizer pressure was about 700 kPa below design. Only a small amount of vapor, but no liquid, was being produced from the reflux drum. Since the purpose of the gas plant was to recover propane and butane as a liquid, the refinery manager's statement that the gas plant would not operate was accurate.

As a first step, I introduced myself to the chief operator and explained the purpose of my visit. Having received permission to run my test, I switched all instruments on the gas-plant control panel from automatic over to local manual. In sequence, I then increased the lean oil flow to the absorber, the debutanizer reflux rate, and the hot-oil flow to the debutanizer reboiler.

The gas plant began to behave properly. The hot-oil circulating pump was putting out a steady flow and pressure. Still, the plant was only producing a vapor product from the debutanizer reflux drum. This was because the debutanizer operating pressure was too low to condense the C_3—C_4 product. By slowly closing the reflux drum vapor vent valve, I gradually increased the debutanizer pressure from 700 kPa gauge toward its design operating pressure of 1380 kPa gauge.

Suddenly, at 900 kPa gauge, the hot-oil flow to the debutanizer's reboiler began to waiver. At 930 kPa gauge, the debutanizer pressure and the hot-oil flow plummeted. This made absolutely no sense. How could the debutanizer pressure influence hot-oil flow?

To regain control of the gas plant, I cut reflux to the debutanizer and lean-oil flow to the absorber. I was now back where I started. The thought of impending failure loomed.

I repeated this sequence twice more. On each occasion, all went well until the debutanizer pressure increased. By this time, it was 3 a.m. Was it also time to give up and go home?

Just then, I noticed a commotion at the main fractionator control panel. The operators there stated that the fractionator was flooding again—for the third time that night. The naphtha production from the fractionator had just doubled for no apparent reason.

In every troubleshooting assignment, there always occurs that special moment—the moment of insight. All of the bits and pieces fall into place, and the truth is revealed in its stark simplicity.

I cut the debutanizer pressure back to 700 kPa gauge and immediately the flooding in the main fractionator subsided. The operators then closed the inlet block valve to the hot-oil side of the reboiler and opened up a drain. Naphtha poured out instead of gas oil. This showed that the debutanizer reboiler had a tube leak.

Whenever the debutanizer pressure reached 900 kPa gauge, the reboiler pressure exceeded the hot-oil pressure. The relatively low-boiling naphtha then flowed into the hot oil and flashed. This generated a large volume of vapor that then backed

hot oil out of the reboiler. The naphtha vapors passed on into the main fractionator and flooded this tower. Thus, the cause of the gas plant instability was neither a process design error, instrument malfunction, or pumping deficiency. It was a quite ordinary reboiler tube failure.

2.3 Strategy for troubleshooting distillation problems

In almost any troubleshooting assignment, it is desirable to solve a problem as rapidly as possible with the least amount of expenditure. In a surprisingly large number of cases, this objective is only partially achieved. One of the major obstacles to achieving this objective is a poor (often nonexistent) strategy for tackling the problem.

When devising a troubleshooting strategy, it is useful to think in terms of a "doctor and patient" analogy. The doctor's troubleshooting strategy in treating a patient is well established and easily understood by most people. Applying similar principles to solving distillation problems can often map out the most effective and least expensive course of action. The headings of the strategy outlined below are those applying to the medical analogy, while the discussion applies it to distillation troubleshooting.

The sequence of steps below is often considered optimum for tackling a troubleshooting problem. It is based on the author's experience as well as the experience of others [8–13] and makes reference to the doctor-and-patient analogy. Actions described in Lieberman's case history (see Section 2.2) are used to demonstrate the optimum sequence of steps. A good troubleshooting strategy always proceeds stepwise, starting with the simple and obvious.

1. *Save the patient and prevent the disease from spreading to others*
   Assess the safety or environmental hazard that the problem can create. If a hazard exists, an emergency action is required prior to any troubleshooting efforts. In terms of the medical analogy, measures to save the patient or prevent the patient's problem from affecting others have priority over investigating the cause of the problem.
2. *Temporary strategy: hospitalization, bed rest, special diet*
   Implement a temporary strategy for living with the problem. Problem identification, troubleshooting, and correction take time. Meanwhile, adverse effects on safety, the environment, and plant profitability must be minimized. The strategy also needs to be as conducive as practicable for troubleshooting. The strategy, and the adverse effects that are to be temporarily tolerated (e.g. instability, lost production, off-spec product), usually set the pace of the troubleshooting investigation.
   In the debutanizer case history, the short-term strategy was to run the column at a pressure low enough to eliminate instability and to tolerate an off-spec bottom product. In the medical analogy, the short-term strategy is hospitalization, bed rest, or just "taking it easy".

3. *Determine the urgency of treatment: is it life threatening or can it be tolerated?* The extent to which the temporary solution in step 2 above can be tolerated and, to a lesser degree, the estimated complexity of the problem and resources required and available, need next be considered and will set the pace of the troubleshooting investigation. "*Crisis*" urgency is often assigned when there is significant adverse safety or environmental impact, if the tower cannot make a valuable product, or if there is a major impact on plant profitability. "*Medium*" urgency is typical when the tower falls short of producing the desired capacity or product quality but can still operate and make acceptable products. "*Low*" urgency is usually assigned to instability, operating nuisance, or when the costs effects are not major. In the debutanizer example, the urgency was medium to crisis, as the plant could not make the overhead product and the bottom product was off-spec. In the medical analogy, a life threat sets a fast pace of treatment, while minor pain sets a slow pace.
4. *Doctor obtains problem definition (detailed symptoms) from the patient* Obtain a clear, factual definition of the symptoms. A poor definition of symptoms is one of the most common troubleshooting pitfalls. In the debutanizer case history above, the following definitions were used by different people to describe the symptoms of a reboiler tube leak problem.
   a. "The gas plant would not operate."
   b. "The gas plant's operation is unstable because of faulty instrumentation. However, the problem will soon be resolved by the instrument engineer."
   c. "The oil circulating pump is defective. Whenever the oil flow to the reboiler is raised, reboiler heat duty and reflux rate would become erratic, and the pump's discharge pressure would fluctuate wildly. A new pump requiring less net positive suction head is needed."
   d. "The column was running smoothly but not well. Reflux rate was too low, so it precluded significant fractionation. The column pressure was 700 kpa below design. Only a small amount of vapor, but no liquid, was being produced from the reflux drum, which should have produced mainly liquid. Other problems noticed by plant personnel are as described above."

   The above represents a typical spectrum of problem definitions. The last definition, supplied by a troubleshooting expert, can clearly be distinguished. The first two definitions were nonspecific and insufficiently detailed. The third described part of the story, but left out a major portion. The first three definitions also contained implied diagnoses of the problem, none of which turned out to be correct.

   Listening to the people involved helps one to reach a good definition. It is easy to miss or overlook details, some of which may be crucial. Different people focus on different details, and talking can bring out hidden details. In the debutanizer case, the observation by the plant personnel became part of the problem definition.

   The doctor-patient equivalents to the first three definitions are statements such as "I feel I am going to die," "I am feeling a bit off, but I will be ok soon," and

"I do have a sharp headache (without mentioning other pains and having a temperature as well)." It is apparent that these statements do not provide the doctor with the entire story.

5. *Doctor examines the patient*
   Examine the column behavior yourself. This is imperative if the problem definition is poor. In the debutanizer example above, the troubleshooter would have been oblivious to a major portion of the problem definition had he based his investigation entirely on other people's observations. Some communication gap always exists between people, and it is often hard to bridge. In a similar manner, a doctor always needs to examine the patient before starting treatment.
   In some circumstances, it may be impractical or too expensive for the troubleshooter to visit the site (e.g. a column located on another continent). In this case, the troubleshooter must be in direct (i.e. phone) communication with the operating person, who should be entirely familiar with the column, its operation, and its history. The problem definition in this case must be particularly sharp
6. *Doctor looks for swelling, rashes, or sounds*
   Walk around the column, looking for outside signs. Check all lines containing valves that cross-connect products and measure surface temperatures on each side of the valve. Valves often leak or are inadvertently left open. Filter baskets may have not been reinstalled after cleaning. This is the time to find them. Listen to sounds coming from the tower. These may indicate vibrations, eruptions, sloshing, loose nuts, or pump cavitation. Column sways may indicate a high base level.
7. *Doctor obtains health history of patient*
   Learn about the column history. The question, "What are we doing wrong now that we did right before?" is perhaps the most powerful troubleshooting tool available. If the column is new, closely examine any differences between the column and columns used for identical or at least similar services. In addition, examine any differences between the expected and the actual performance. Each difference can provide a major clue. Doctors always ask patients about their health histories, searching for similar clues. In the debutanizer example above, the troubleshooter included a comparison to design performance in the problem definition (he was working with a new column).
   Digging into the past may also reveal a recurring ("chronic") problem. If so, finding the correct link between the past and present circumstances can be very illuminating. Be cautious when identifying the link; a new problem may give the same symptoms as a past problem but be caused by an entirely different mechanism.
   A history search may also unveil a hidden flaw. In one case [10], a column modification caused a loss in column efficiency. The loss was unnoticed, and the reduced performance became the norm. The problem was noticed several years later.

8. *Doctor asks patient what hurt first*
   Search and scan events that occurred when the problem started. Carefully review operating charts, trends, computer records, and operator logs. Establish event timing in order to differentiate an initial problem from its consequences. Harrison and France [10] use a case history with actual operating charts to demonstrate the value of analyzing event timing. Their experience is discussed in Section 2.16. In terms of the medical analogy, doctors always ask patients if they did something different about the time when the trouble started, and what happened first.
   Include events that may appear completely unrelated, as these may be linked in an obscure manner to the problem. In the debutanizer example, it was the observation that flooding in the fractionator coincided with the debutanizer becoming unstable that gave the troubleshooter the vital clue. At first glance, the two appeared completely unrelated.
9. *Doctor learns about family health history*
   Do not restrict the investigation to the column. Often, column problems are initiated in upstream equipment. Doctors frequently look for clues by asking patients about people they have been in contact with or their family health history.
   Listen to shift operators and supervisors. Experienced people can often spot problems, even if they cannot fully explain or define them. Listening to those people can often provide a vital clue. In the debutanizer example, some of the key observations were supplied by these people.
10. *Doctor checks patient's responses ("take a deep breath")*
    Study the behavior of the column by making small, inexpensive changes. These are particularly important for refining the definition of symptoms, and they may contain a vital clue. Record all observations and collect data; these may also contain a major clue, which can easily be hidden and become forgotten as the investigation continues. In the debutanizer example, the troubleshooter increased column pressure and watched its behavior. This led him to the observation that the debutanizer pressure affected oil flow—a major step in refining the problem definition. In the doctor-and-patient analogy, this is similar to the doctor asking the patient to take a deep breath or momentarily stop breathing during a medical examination.
11. *Doctor obtains laboratory tests and blood work*
    Take out a good set of readings on the column and its auxiliaries, including laboratory analyses. Misleading information supplied by instruments, samples, and analyses is a common cause of column malfunctions. Always mistrust or suspect instrument or laboratory readings, and make as many crosschecks as possible to confirm their validity. Instruments may malfunction even when the instrument technician can swear they are correct. In one example [2,11], an incorrect pipe design caused an erroneous reading of a reflux flow meter. Survey the column piping for any unusual features, such as poor piping arrangement, leaking valves, "sticking" control valves, and valves

partially shut. Compile mass, component, and energy balances; these function as a check on the consistency of instrument readings and the possibility of leakage. This step is equivalent to laboratory tests taken by a doctor on the patient. Review the column drawings carefully for any unusual features. Check the column internals against good design practices and determine whether any have been violated. If so, examine the consequences of such a violation and its consistency with the information. Carry out a hydraulic calculation at test conditions to determine if any operating limits are approached or exceeded. If a separation problem is involved, carry out a computer simulation of the column; check against test samples, temperature readings, and exchanger heat loads.

12. *Doctor uses ultrasound, X-rays, and other noninvasive tests*
    If more information is needed, like looking inside the tower, there are a large number of noninvasive techniques, some of them high-tech, that can give good insights. These include gamma scans, neutron back scatter, surface temperature surveys, CAT scans, tracer injection, quantitative multichordal gamma scans, and others. These are equivalent to ultrasounds, X-rays, nuclear magnetic resonance, and CT scans used in medicine.
13. *Doctor critically reconciles results from different sources*
    The data obtained from one technique should be consistent with those of others. For instance, if testing for flood, check that alternative techniques such as gamma scan and differential pressure measurements both come up with the same results. Investigate any inconsistencies; these may provide a vital clue. Repeat measurements as necessary. Doctors check that the X-ray results are consistent with their examination results and with the blood work.

2.4 Dos and don'ts for formulating and testing theories

Following the previous steps, a good problem definition should now be available. In some cases (e.g. the debutanizer), the cause may be identified. If not, there will be sufficient information to narrow down the possible causes and to form a theory. In general, when problems emerge, everyone will have a theory. In the next phase of the investigation, these theories are tested by experimentation or by trial and error. The following guidelines apply to this phase:

1. *Get your facts right*
   Check and recheck the validity of your data until sure that they are correct. Never assume anything. See step 11 in Section 2.3 for typical validation checks. Incorrect data support the wrong theories and deny the correct ones. Look for independent ways of confirming or checking the validity of measurements and observations. Any theory must be consistent with adequately validated data. Adequately validated data form a strong basis for formulating theories.

2. *Theory vs data*
   Logic is wonderful as long as it is consistent with the facts and the information is good. Clearly distinguish facts from theories and interpretations. The pitfall to avoid is "Don't let the data get in the way of a good theory". Follow the data. There is no "impossible" data. If data appear "impossible," perform additional validation checks to confirm or deny. When you have conclusive data, adhere to them.
3. *Learn from past experiences*
   Distillation failures are repetitive (see Section 2.5). Therefore, learning from past experiences in similar systems is invaluable for formulating a good theory. Look for something that happened in the past rather than to large molecular-weight protein molecules wreaking havoc in your system. Talk to people that operate similar columns, or check experiences in the literature (see Section 2.5).
4. *Visualize what is happening*
   When formulating a theory, attempt to visualize what is happening inside the column. One useful technique is to imagine yourself as a pocket of liquid or vapor traveling inside the column. Keep in mind that this pocket will always look for the easiest path.
5. *Think of everyday analogies*
   Another useful technique is to think of everyday analogies. The processes that occur inside the column are no different from those that occur in the kitchen, the bathroom, or in the yard. For instance, blowing air into a straw while sipping a drink will make the drink splash all over; similarly, a reboiler return nozzle submerged in liquid will cause excessive entrainment and premature flooding.
6. *Do not overlook the obvious*
   In most cases, the simpler the theory, the more likely it is to be correct.
7. *Beware of the "obvious fault" pitfall*
   An obvious fault is not necessarily the cause of the problem. One of the most common troubleshooting pitfalls is discontinuing or retarding further troubleshooting efforts when an obvious fault is uncovered. Often, this fault fits in with most theories, and everyone is sure that the fault is the cause of the problem. The author is familiar with many situations where correcting an obvious fault neither solved the problem nor improved performance. Once an obvious fault is detected, it is best to regard it as another theory and treat it accordingly.
8. *Ask "why?"*
   In the debutanizer example, it was the troubleshooter's asking, "Why did the tower pressure influence the hot oil flow to the reboiler?" that was invaluable in connecting the dots.
9. *Calculation is better than speculation*
   Premises on which theories are based can often be easily supported or disproved by calculation. In one case it was argued that liquid entrainment was an

issue. A simple calculation showed that at the upward velocities involved, the rise of any liquid drops will be reversed by gravity within less than 25 mm. This totally invalidated the theory.

10. *Test theories effectively*
    Testing theories should begin with those that are easiest to prove or disprove, almost irrespective of how likely or unlikely these theories are. If shutting the tower down is expensive (which is almost always the case) and is required to test a leading theory, it is worthwhile to first cater to a number of theories that require less drastic actions to test even if they are longer shots. In the medical analogy, surgery should not be performed before performing a blood test that may identify a less likely cause.
11. *Use one-variable reversible changes to test theories*
    Test the response of the tower to changes in variables such as vapor flow-rate or liquid flow-rate. Compare the results to predictions from the various theories. For instance, if a tower flood responds to changes in vapor load but not in liquid load, every theory that argues that the flood is caused by excessive liquid load is denied. In one case [14], determining that the tower responded to changes in vapor load but not to changes in liquid load denied the leading theory and identified the correct root cause. Change one variable at the time. If several variables are allowed to change simultaneously, often the result will be inconclusive. See vapor and liquid sensitivity tests in Section 2.9. Refrain from making any permanent changes until all practical tests are done.
12. *Can the system be simplified?*
    Look for possibilities of simplifying the system. For instance, if it is uncertain whether an undesirable component enters the column from outside or is generated inside the column, consider operating at total reflux to check it out.
13. *Do not overlook human factors*
    Other people's reasoning is likely to differ from yours, and they will act based on their reasoning. The more thoroughly you question their design or operating philosophy, the closer you will be able to reconstruct the sequence of events leading to the problem. In many cases, you may also discover major considerations you are not aware of. Be cautious in your questioning. The attitude that you want to learn more about the system and what can be improved will win cooperation. Pointing fingers or implying that someone screwed up is a sure way of getting noncooperation [9].
14. *Ensure that management is supportive*
    Ensure that management is apprised of what is being done and is receptive to it [11,13]. Otherwise, some important nontechnical considerations may be overlooked. Further, management is far less likely to become frustrated with a slow-moving investigation when it is convinced that the best course of action is being followed.
    Often, management is by technical people with expertise who can contribute ideas. Moreover, such technical people often expect that their ideas are incorporated in the testing.

15. *Involve the supervisors and operators in each "fix"*
    Whenever possible, give them detailed guidelines of an attempted fix, and leave them with some freedom for making the system work. The author has experienced several cases where actions of a motivated operator made a fix work, and other cases where a correct fix was unsuccessful because of an unmotivated effort by the operators.
16. *Promote teamwork and prevent the "us against them" division*
    With different people having different ideas and theories, it is important to assemble all these ideas into a constructive teamwork and to suppress any confrontations. Some people will have stake in their theory being correct. They will feel that they win when their theory is pushed ahead and rejected when their theory is dismissed. Good troubleshooting leadership needs to encourage all ideas, treat all respectfully, recognize that even the ideas that are disproved contribute in the path to solving the problem, and acknowledge their initiators accordingly.
17. *Do not be afraid to admit when you are wrong*
    Admitting that you are wrong is inherently difficult to do. Nonetheless, recognize that the investigation is not about who is right and who is wrong, but about finding the correct technical solution. Everyone serves on the same team, and all will win when the correct solution is found. Accepting the truth, or accepting that other's ideas are superior to yours, sends the message of cooperation and the dominance of technical validity. This will promote ideas exchange, productivity and teamwork.
18. *Beware of poor communication while implementing a "Fix"*
    Verbal instruction, rush, and multidiscipline personnel involvement generate an atmosphere ripe for communication problems [10]. Ensure any instructions are concise and sufficiently detailed. If leaving a shift team to implement a fix by themselves, leave written instructions. Be reachable and encourage communication should problems arise. Call in at the beginning of the shift to check if the shift team understood your instructions.
19. *Recognize that modifications are hazardous*
    Many accidents have been caused by unforeseen side effects of even seemingly minor modifications. Ban "back of an envelope" modifications, as their side effects can be worse than the original problem. Properly document any planned modification, and have a team review it systematically with the aid of a checklist, such as a "hazop" checklist. Before completion, inspect to ensure the modification was implemented as intended.
20. *Properly document fixes*
    Document any fix that is being adopted, the reasons for it, and the results. This information will be useful for future fixes. In many cases, a sudden change in plant conditions lowers the priority of a troubleshooting endeavor, and it is discontinued. Some time later, the endeavor is renewed. Good documentation of the initial endeavor gives the renewed endeavor a much better starting point. At one time, we designed and built baffles to prevent vortexing near a feed

inlet, just to find that similar baffles had already existed, but they did not show on the drawings and no one knew about them.

2.5 Learning to troubleshoot

Troubleshooting is not magic, nor is it performed by magicians. It is a learned art. Unfortunately, not much of it is taught at school, although a few university courses on troubleshooting exist. It is learned in the school of hard knocks. You can avoid most of these hard knocks by learning from other peoples' experiences. The objective of Refs [1,2] was to put these experiences in the hands of every interested engineer, supervisor, or operator. Failures are repetitive, and learning from the past can solve today's problems and avoid tomorrow's.

There are many other resources. Talk to the experienced people in your plant and organization, to fellow workers in professional meetings, and attend their presentations. Get involved in startup, shutdown, and commissioning work. Get involved in incident investigations. Inspect equipment and participate in equipment testing.

PART B: COLUMN TROUBLESHOOTING—THE TOOLS

2.6 Classification of column problems

The problems experienced in distillation columns can usually be classified into the following types:

Capacity problems: Column cannot achieve the required feed or product throughput at the design reflux/boilup rates or incurs excessive pressure drop.

Efficiency problems: Column cannot achieve the required or design separation at the design reflux/boilup rates. In some cases, the column is unable to achieve product specs even when reflux and boilup are raised. In other cases, the column works well at maximum rates but unexpectedly loses efficiency upon turndown.

Pressure or temperature deviations: Column cannot attain the expected or design temperatures and pressures. Many times these reflect reboiler/condenser limitations or the existence/absence of a second liquid phase.

Startup/shutdown/commissioning problems: Column operates normally at steady state and turndown, but problems occur during abnormal operation.

Instability problems: Column cannot operate under stable conditions or is touchy and sensitive to small changes in operating conditions.

Often, an efficiency problem may show up as a capacity or instability problem. The reason is that due to poor efficiency, the operators increase reflux and boilup to maintain the product on-spec. This hydraulically loads up the column and the problem shows up as a capacity limit, or when operating right near the limit, as an instability. Conversely, a capacity problem may produce premature flood, which shows

up as poor efficiency or instability. Likewise, pressure or temperature deviations may be a reflection of premature flood or poor efficiency or may cause them.

The troubleshooter's challenge is to distinguish the cause from the result. The next sections will covers the prime techniques available to narrow the root cause down.

2.7 Flood point determination in the field: the symptoms

Flooding is the most common capacity limitation in distillation and absorption towers. Flooding is characterized by the accumulation of liquid in the column. This accumulation propagates from the lowest flooded region upward. Accumulating liquid backs up into the tray (or packed section) above, and so on, until the whole column fills with liquid or until an abrupt change in tray design or flow conditions (e.g. feed point) is reached. Flooding may or may not propagate above that point. Flooding can be recognized by one or more of the following symptoms:

1. Excessive column differential pressure
2. Sharp rise in column differential pressure
3. Reduction in bottom stream flow-rate
4. Rapid rise of entrainment from column top tray
5. Loss of separation (as can be detected by temperature profile or product analysis)

Pressure drop measurements across various column sections are the primary tool for flood point determination.

Excessive column pressure drop. The high pressure drop is caused by liquid accumulation which characterizes flooding. In general, a normal pressure drop per tray is 100−130 mm of liquid. With most organic and hydrocarbon systems whose specific gravity is around 0.7 to 0.8, this gives 0.7−0.9 kPa per tray. If the measured pressure drop per tray is double this amount, i.e. 1.5−2 kPa, and the measurements is good, flooding should be suspected.

With packed towers, the flood pressure drop is given by the following Kister and Gill equation [7,15−17]:

$$\Delta P_{\text{flood}} = 4.17 \ F_P^{0.7} \tag{2.1}$$

where

ΔP_{flood} = flood pressure drop, mm water per m of packing height
F_P = packing factor, m^{-1}

The values of packing factors to be used in Eqn (2.1) should be taken from the 8th edition of *Perry's Handbook* [17]. Packing factors originating from other sources can lead to inaccurate or even incorrect predictions. Measured pressure drops significantly higher than the value predicted from Eqn (2.1) indicate flooding.

While a high pressure drop (exceeding the values mentioned above) almost always signifies flooding, there are situations when a column floods yet the pressure

drop remains low. The high pressure drop indicates liquid accumulation. When the liquid accumulation is small, the pressure drop may not significantly rise. Typical scenarios include flooding near the top of the tower (only a few trays or a short packing length accumulate liquid), flooding in vacuum packed towers (accumulation is channeled and the vapor bypasses the accumulation region), and flooding at low liquid rates (slow liquid accumulation).

Sharp rate of rise of pressure drop. A sharp rate of rise of pressure drop with vapor rate may be an even more sensitive flooding indicator than the magnitude of pressure drop. As vapor loads are raised, so does the tray pressure drop. Upon flooding the pressure drop rise accelerates due to liquid accumulation. In many cases, once it starts, the pressure drop will keep rising even when vapor loads are no further raised.

The flood point can be inferred from a plot of pressure drop against vapor or liquid flow-rate, and is the point where the slope of the curve changes significantly (see Figures 2.2 and 2.3).

In tray columns, the slope change can be relatively mild (curve 1 in Figure 2.2), which is generally characteristic of entrainment flooding or a small number of flooded trays, or relatively steep (curve 2 in Figure 2.2), which is generally characteristic of downcomer (DC) flooding or flooding that propagates throughout several trays. It is not unusual to find a vertically rising pressure drop curve once the flood point is reached [18,19].

In packed columns, defining the flood point by use of a pressure drop vs load curve (Figure 2.3) is generally less satisfactory, because the slope begins changing at the loading point (point *B*), and the change may be continuous (curve *BCD*), rather than abrupt, in the vicinity of the flood point. Further, in many packed columns, a rapid drop in efficiency occurs well before the hydraulic flood point. Here,

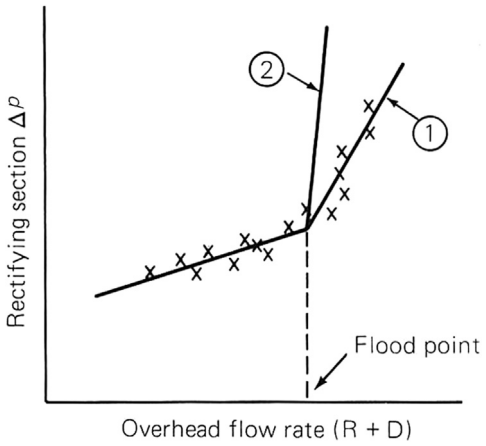

FIGURE 2.2 Plots of Pressure Drop vs Vapor Flow for Tray Columns

From Ref. [3] copyright © 1990 by McGraw-Hill, Inc.; reprinted by permission.

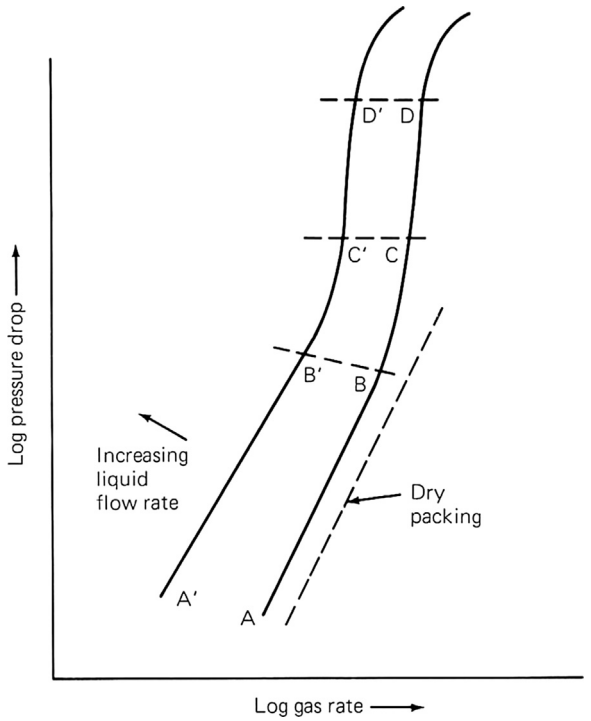

FIGURE 2.3 Typical Pressure Drop Characteristics of Packed Columns

From Ref. [3] copyright © 1990 by McGraw-Hill, Inc.; reprinted by permission.

throughput is limited by loss of separation and the hydraulic flood point may be of little practical value. There are some cases, especially in vacuum distillation, where flooding occurs but no point of inflection is observed [20].

Preferred techniques for pressure drop measurements are discussed in Chapter 3 and elsewhere [3,21]. It has been recommended [3,22,23] that, for best results, differential pressure recorders should be installed across each section of the tower prior to flood testing while troubleshooting. This technique can clearly identify the section of column where the flooding initiates. In one case, this technique was demonstrated to prevent misdiagnosis [24].

If it can be afforded, a multichannel pressure drop recorder has been highly recommended [22] and successfully applied [18,22] for flood tests. This instrument can trace the sequence of events, zero in on the location where flooding starts, the conditions when it takes place, how the flooding propagates, and which remedial action is working. This device may be particularly useful if flooding is caused by plugging of the top tray or downcomer (e.g. by corrosion products). In one case [25], conventional differential pressure devices failed to indicate this condition. Figure 2.4 [22] shows the type of information the multichannel pressure drop recorder can convey.

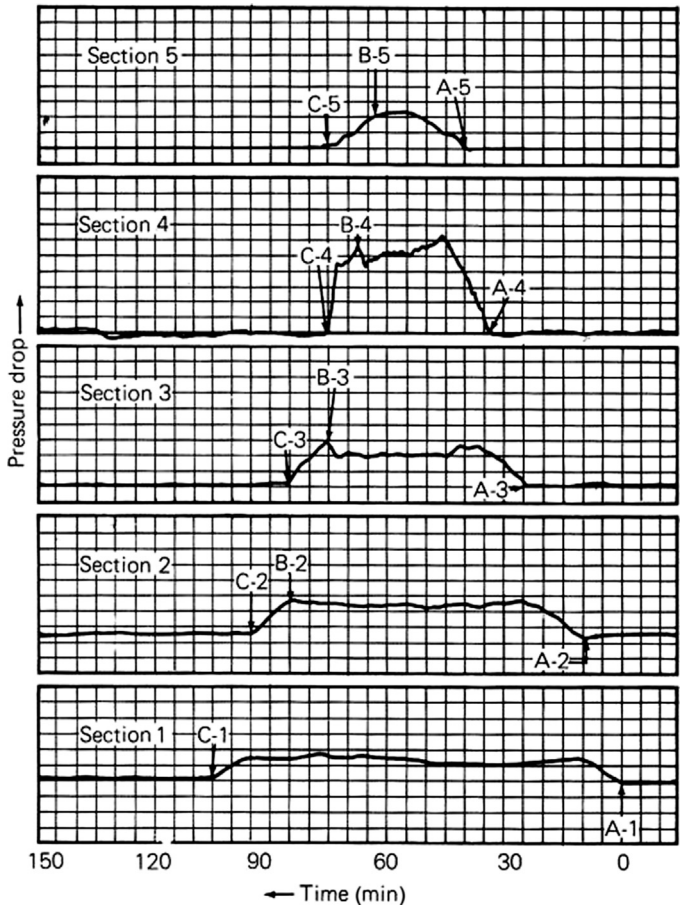

FIGURE 2.4 Pressure Drop Profile Obtained with High-Speed, Multichannel Strip-Chart Recorder

Ref. [22], reprinted by special permission from Chemical Engineering, copyright © 1970 by Access Intelligence, New York, NY.

Reduction in bottom stream flow rate. Reduction of bottom flow is a common indicator of flooding and is one of the main criteria to determine the flood point [3,26]. Upon flooding, liquid accumulates in the column so less of it reaches the bottom. This can be seen by a fall in the bottom level. Most frequently, the bottom level is controlled by manipulating the bottom flow-rate, so the level stays constant but the bottom flow-rate will decline.

While a reduction in bottom flow indicates flooding, many towers may flood without a significant decline in bottom flow. For instance, if flooding occurs in the rectifying section, while most of the feed is liquid, the bottom section may

continue to operate normally without a significant decline of bottom flow-rate. Also, if the flood point is well above the bottom, there may be a significant delay from the onset of flooding to the time the bottom flow is significantly reduced, which makes accurate measurements of the flooding conditions difficult.

Generally, reduction of bottom stream flow-rate is a good indicator of flooding in columns that flood near the bottom, and in columns that are relatively short [26], particularly if flooding occurs between the feed point and the bottom.

Rapid rise in entrainment. A rapid rise in entrainment is another common flooding indicator [3,21,25]. As liquid accumulates in the tower, it builds up to the top and is entrained in the tower overhead stream.

In towers whose overhead stream goes to a knockout drum or to the bottom of another tower, this entrainment can be recognized as buildup or rapid rise of a liquid level in the drum or bottom of the downstream column. In most distillation columns, the tower overhead goes to a condenser, and the condenser outlet stream continues to a reflux drum. The reflux drum usually has a level control that manipulates either the distillate rate (see Figure 2.5) or the reflux rate.

When the drum level controls the distillate rate, the entrainment rise is often indicated as a significant increase in distillate rate for no apparent reason. When the drum level controls the reflux rate, the entrainment is often indicated as a rise in reflux for no corresponding increase in boilup rate, and/or an increase in reflux flow-rate that does not result in an increase in heat input required to maintain the same bottom column temperatures. The increased reflux is unable to descend down the tower due to the flooding near the top, so it entrains back into the overhead, returns as more additional reflux, and never reaches the bottom of the column. The reflux valve often opens widely due to the recirculation of entrainment around the

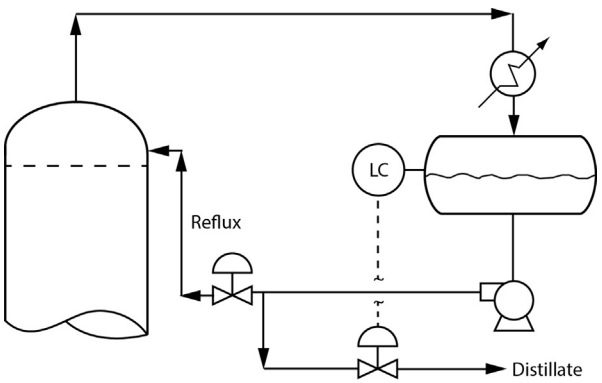

FIGURE 2.5 Typical Distillation Tower Overhead System

Reflux drum level control (LC) is connected either to distillate valve (shown connected) or to reflux valve (not connected in this diagram).

From H.Z. Kister, "Practical Distillation Technology," course manual, copyright © 2013; reprinted with permission.

tower overhead loop. Bleeders (see below) have also been used to detect this rise in entrainment [23].

This indicator is particularly useful when the pressure drop rise is not sharp. However, this indicator may fail to indicate a stripping section flood that does not propagate to the rectifying section.

Loss of separation. As flooding is approached, the rate of liquid entrained by the vapor sharply rises. At high pressures and/or high liquid rates, the quantity of vapor entrained in the downflowing liquid also rises. As either type of entrainment accelerates in the vicinity of the flood point, efficiency and separation plunge (see Figure 2.6).

The drop in efficiency tends to occur closer to the flood point with downcomer flooding than with entrainment flooding; in Figure 2.6, it is believed [27] that flooding was caused by a downcomer limitation in the butane system and by excessive entrainment in the cyclohexane-heptane system. In packed columns, the drop in efficiency occurs closer to the flood point with smaller packings. With large packings (e.g. 50-mm or larger random packings, and of surface area per unit volume below 200 m^2/m^3 for structured packings) and/or under vacuum or high pressure, the drop in efficiency may begin at rates well below the hydraulic flood point.

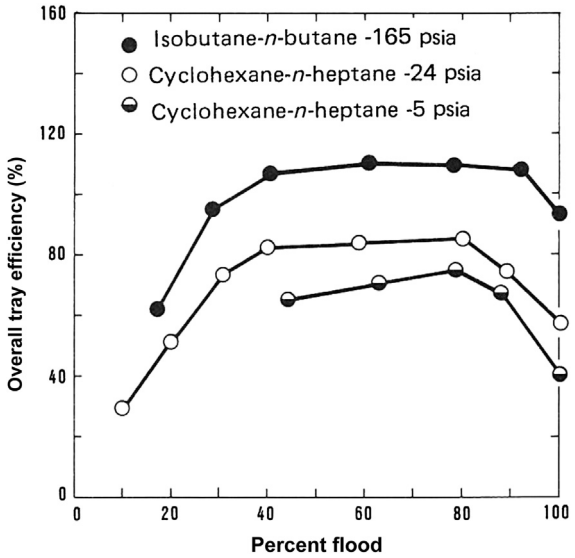

FIGURE 2.6 Overall Tray Efficiency, 1.2 m-ID Tower, at Total Reflux, Illustrating Drop of Efficiency near the Flood Point

Also shown is the little effect of vapor and liquid loads on efficiency in the normal operating range (between excessive weeping and excessive entrainment). Note: 165 psia = 1138 kPa; 24 psia = 165 kPa; and 5 psia = 34 kPa.

From Ref. [27], copyright © 1982, American Chemical Society; reprinted with permission.

Because the loss of separation begins before the column is fully flooded, using it as a flooding indicator can suggest a lower flood point than other indicators. This is hardly a disadvantage because the exact location of the hydraulic flood point is of lesser practical significance than the point where column efficiency starts to rapidly deteriorate. The latter point is often referred to as "the maximum operational capacity," or "maximum useful capacity", and usually occurs at flow-rates about 0–20% below the hydraulic flood point. In most atmospheric and superatmospheric tray columns, this point occurs at flow-rates of 5% or less below the hydraulic flood point.

The loss of separation is best recognized from laboratory analyses of column products. A plot of column efficiency (Figure 2.6) against flow-rate at a constant reflux ratio is commonly used to identify the point where loss of separation occurs.

Another good indicator of separation loss is the column temperature profile. Liquid accumulation is often indicated as a temperature rise above the flooded tray because the accumulating liquid is richer in heavies, and also because the flooded trays no longer achieve an efficient separation. A rise in temperature may also occur below the flooded section because the reduced downflow of liquid from the flooded section leads to heating up of this section and because the higher pressure drop increases the boiling point of the liquid.

For best results, application of this method requires a good knowledge of the normal and flooded temperature profiles under similar feed conditions. Figure 2.7 shows temperature profiles under normal and flooded conditions [28].

The column was uninsulated, and the points are pyrometer measurements of wall temperatures taken from the access ladder. The ladder was on the left of the column in Figure 2.7, so all the temperatures are for the even-numbered trays (the odd-numbered trays were obscured by the side downcomers descending from the even-numbered trays). The crosses map the normal temperature profile, showing a discrete reduction in temperature every two trays as one ascends the tower. The circles map the temperature profile when the bottom three to four trays were flooded. It shows that the temperature spread across the bottom four trays completely disappeared, indicating poor separation. It also shows hotter temperatures above, due to the heavier components moving further up the column due to the poor separation.

Caution must be exercised when curves of this type are interpreted because they may also indicate a "pinch" condition (i.e., poor separation due to insufficient reflux or reboil). To tell the difference, reflux and reboil can be raised. If separation improves, pinching is indicated. If it deteriorates or stays the same, flooding is indicated.

To reliably establish the column temperature profile, a large number of temperature measurement points is required. A multipoint temperature recorder with a short recording cycle is particularly suitable for obtaining a time record of temperature profiles. Alternatively, a vertical temperature survey can be conducted. Temperature surveys are discussed in detail in Section 2.13.

Temperature gradients are an effective, low-cost method of determining the flood point, but the method's success depends on the existence of a large-enough number of measurement points and on the existence of a sufficiently large temperature gradient under normal operating conditions. If the normal tray-to-tray temperature difference is small, as in close separations, the flooded temperature profile will not vary a great deal from the normal profile, and temperature profiles will be poor indicators of flooding.

Bleeders. One technique found effective for flood testing is the use of vapor bleeders [23]. Each bleeder is located in the vapor space above a tray and/or in the overhead line upstream of the condenser. If the bleeder is opened during normal operation, vapor will come out; if it is opened while the tray is flooded, liquid will spray out. When the tray liquid is above its atmospheric boiling point, it will flash

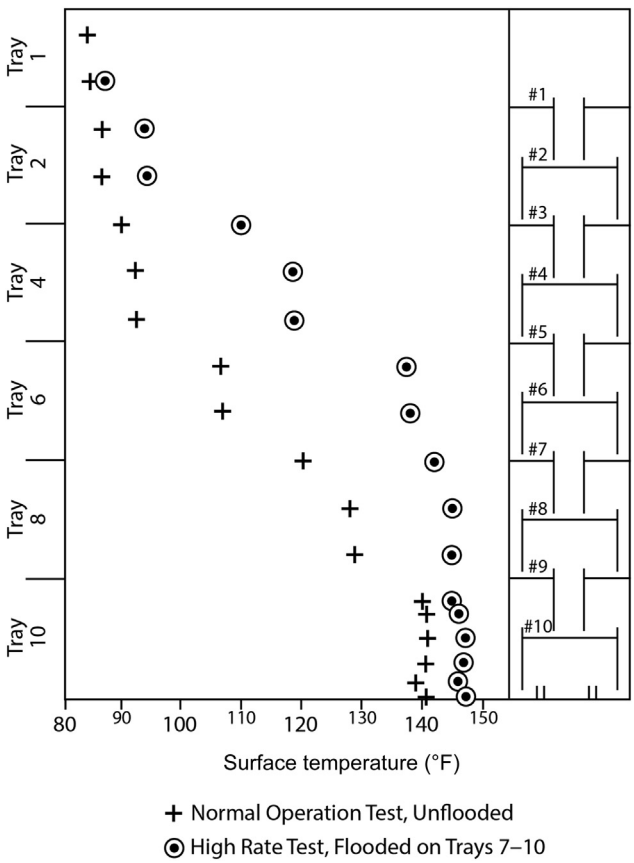

FIGURE 2.7 Flooded and Unflooded Temperature Profiles

From Ref. [28]; reprinted courtesy of the American Institute of Chemical Engineers.

and chill upon bleeding. The presence of liquid can thus be detected by a temperature recorder as a sharp temperature drop of gas issuing from the bleeder [23].

The bleeder technique is not very popular and can be hazardous or environmentally unacceptable. Other disadvantages are a need to know which trays are most likely to flood and lack of indication of an approaching flood condition.

Gamma scanning. Gamma scanning is one technique particularly suitable for flooding detection. It is powerful in diagnosing flooding, identifying the flooded regions, and often also providing insight into the nature of the flood. Detailed discussion is in Section 2.12.

Sight glasses. These have been used to give visual indication of flooding [3,23]. Sight glasses are expensive, increase the leakage potential, and may lead to a chemical release if the glass breaks. Supplying a light source that will permit observation can also be an issue. For these reasons, this technique is not commonly used in commercial columns. It is mainly used when the column processes nonhazardous material at near ambient pressure.

2.8 Flood point determination in the field: testing

To determine the flood point, either vapor or liquid flow-rate or both are raised. Most commonly, both are raised, because otherwise column material balance is affected and one product will have poor purity before flooding conditions are reached. The following techniques are commonly used for raising vapor and liquid rates during flood testing:

1. *Raising feed rate, while simultaneously increasing reflux and reboil in proportion or in a manner that keeps product composition constant*. This technique gives the most direct measurement of the maximum feed rate that can be processed through the column, but it can only be applied when upstream and downstream units have sufficient capacity to handle the additional feed.
2. *Raising reflux and reboil rate while keeping feed rate constant.* This is probably the most popular technique used. Only two variables (instead of three) need to be changed, product compositions will not change until actual flooding occurs, and it is independent of the capacities available in other units, making it simpler and easier to implement. In most cases, data provided by this technique can be easily extrapolated to predict the maximum column feed rate.
3. *Varying preheater or precooler duty while adjusting reflux and reboil*. This method, which can only be used if the feed is preheated or precooled, is often restricted by the exchanger capacity and is least popular. In some multicomponent distillations, it can give misleading results because it may induce accumulation of an intermediate impurity in one section of the column [3].

Using any of the above techniques, reflux and reboil rates are varied. The procedure of varying these rates is important and must take the column control system into account.

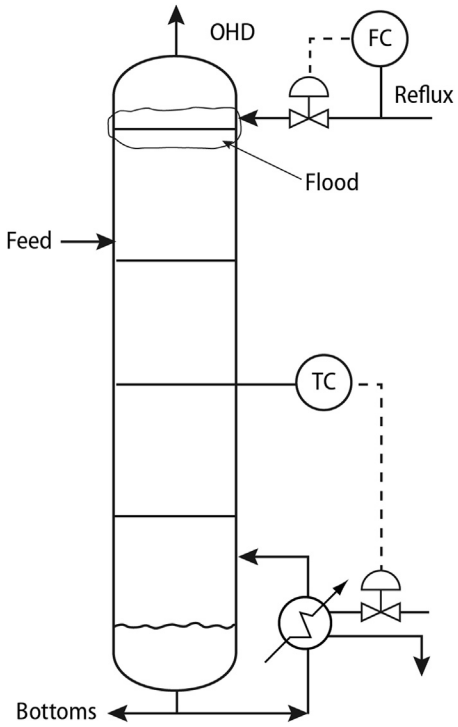

FIGURE 2.8 Simple Distillation Column with Temperature Control Manipulating Boilup and Reflux Entering on Flow Control

Flood is shown to initiate near the top in this example.

From H.Z. Kister, "Practical Distillation Technology," course manual, copyright © 2013; reprinted with permission.

Most column control schemes use the composition (or temperature) controller to manipulate either the reflux or reboil, directly or indirectly. The stream which is not controlled is commonly "free,"—that is, on flow control. This "free" stream is usually manipulated during flood testing, while the stream on temperature control will be automatically adjusted to maintain product composition. Figure 2.8 is an example in which the temperature control is on the boilup and the free stream is the reflux rate. In this case, flood testing is performed by raising the reflux rate. This cools the control tray. The temperature controller will call for more boilup, and the column will reach new stable conditions with both boilup and reflux increased.

This procedure may induce "overshooting" of the flood point. The column may look stable for quite some time following the change, even if the reflux and boilup rates that cause flooding have been exceeded, as it may take the liquid some time to reach the tray where flooding initiates. This is particularly true for tray columns containing a large number of trays. Also, it may take the liquid some time to fill up the

packing voids or tray decks and downcomers to an extent sufficient to initiate flooding that can be monitored, particularly in columns in which the volume is large and the internal liquid flow is small. In the meantime, vapor and liquid rates are raised further as the test progresses. When overshooting occurs, the flood point determined will be higher than the actual one.

The problem of "undershooting" the flood point is just as common. Its occurrence depends on the dynamics of the column. For instance, increasing boilup can increase the froth height and thus the inventory of liquid on the trays (or in the packings). This extra liquid holdup may take up enough of the void space in the packing or the disengagement space between the trays to cause the column to flood prematurely. When this occurs, the flood point determined will be lower than the actual one.

In order to avoid overshooting and undershooting, little can be offered as a substitute to raising vapor (or liquid) rates in extremely small steps and allowing long stabilization periods between steps. This is most important in columns containing a large number of trays. It may pay to carry out a preliminary flooding test, in which the steps are relatively large and fast. Typically, vapor (or liquid) rates are raised by 5−10% increments at 15- to 30-min intervals during the preliminary test [3]. Increments as small as 1−2% are preferable, even at the preliminary test. It was found [23] that frequent small increases in vapor (or liquid) rates are less likely to prematurely upset the column and generally require shorter stabilization periods [23].

Although results of the preliminary test may suffer from overshooting or undershooting, they are likely to determine the flood point within ±10%, and often within ±5%. The results of this test are used to determine a good starting point for the slow test. The preliminary test technique was found effective both for improving accuracy and reducing time requirements for flood point determination [23].

Accurate material and energy balances are important for flood point determination; these should close within 3% and 5%, respectively [21,23], and be checked prior to the test and during the test. There is generally no need for accurate component balances. Several of the key guidelines described in Section 2.11, particularly those pertaining to material and energy balances, are also useful for flood testing. Note, however, that flood tests are far less sensitive to analytical errors than efficiency tests and therefore require a much lower level of effort.

2.9 Flood mechanism determination: vapor and liquid sensitivity tests

In a troubleshooting investigation, there are usually many theories. The troubleshooter's challenge is to narrow down the number of theories to a manageable number that can be catered for. When flooding is involved, one of the best ways of narrowing down the theories is by performing vapor and liquid sensitivity tests.

Flood mechanisms. All floods are characterized by liquid accumulation. There are four different mechanisms that lead to this liquid accumulation in trays:

1. *Entrainment (jet) flood.* Froth or spray height on trays rises with vapor velocity. As the froth or spray approaches the tray above, some of the liquid is aspirated into the tray above as entrainment. Upon further increase in vapor flow-rate, massive entrainment of the froth or spray begins, causing liquid accumulation and flood on the tray above.
2. *Downcomer backup flood.* Aerated liquid backs up in the downcomer because of tray pressure drop, liquid height on the tray, and frictional losses in the downcomer apron. All of these increase with increasing liquid rate. Tray pressure drop also increases as the vapor rate rises. When the backup of aerated liquid exceeds the (tray spacing + weir height)—that is, fills up the downcomer—liquid accumulates on the tray above, causing downcomer backup flooding.
3. *Downcomer Choke Flood (also called downcomer entrance flood or downcomer velocity flood*). A downcomer must be sufficiently large to transport all of the liquid downflow. Excessive friction losses in the downcomer entrance, and/or excessive flow-rate of vapor venting from the downcomer in counter-flow, will impede liquid downflow, initiating liquid accumulation (termed downcomer choke flooding) on the tray above.
4. *System limit flood (also called ultimate capacity flood).* This is an ultimate jet flood, which takes place when the vapor momentum force acting to lift the large liquid drops above the tray exceeds the gravity force. This flood is independent of tray geometry and tray spacing.

In packed towers, there are three flood mechanisms:

1. *Flood in the vapor-rich region.* As vapor loads are raised, a point is reached where the vapor rate interferes with the free drainage of liquid. The bed starts loading up with liquid. Upon further increase in vapor rate, large liquid accumulation takes place and floods initiates.
2. *Flood in the liquid-rich region.* At high liquid loads and high vapor densities, liquid holdup in packed beds becomes much higher and frothiness increases, making liquid drainage more difficult. As vapor or liquid loads are raised, a point is reached where the drainage of liquid is impeded. The bed starts accumulating liquid. Floods initiates when the accumulation becomes large.
3. *System limit flood (also called ultimate capacity flood)*. This is the same as in tray towers.

From the above discussion, it can be seen that entrainment (jet) floods, packing vapor-rich floods, and system limit floods are induced by excessive vapor loads and are therefore highly vapor-sensitive. If there is any sensitivity to liquid loads with

these floods, it is minor and very secondary. On the other hand, downcomer choke floods, packing liquid-rich floods, and floods due to packing distributor overflows are caused by excessive liquid loads and are therefore highly liquid-sensitive. If there is any sensitivity to vapor loads, it is very secondary. Downcomer backup flood can be induced by either excessive vapor load or excessive liquid load, depending on the dominant term in the downcomer backup equation [4–7,17], and can be sensitive to either or both.

When troubleshooting a flood problem, there are usually many theories: some argue excessive vapor loads, others argue excessive liquid loads, and some argue both. Testing the sensitivity of a flood to step changes in vapor load and step changes in liquid load is a powerful means of narrowing down the number of theories. Typically, these sensitivity tests result in invalidating about half the theories.

Figure 2.8 is a sketch of a simple distillation column with its controls. For flood testing using technique 2 in Section 2.8 (raising reflux and boilup), the reflux is gradually raised until symptoms of flood (Section 2.7) are observed. This test determines at which vapor and liquid loads the flood occurs, but it cannot tell whether the flood is vapor-sensitive, liquid-sensitive, or both. The increase in reflux rate increases the liquid load, but the higher reflux rate also cools down the tower and lowers the control temperature. The lower control temperature increases the boilup, which increases the tower vapor load. From this test, one cannot tell whether the flood was due to the initial increase in reflux (therefore, a liquid-sensitive flood), or due to the subsequent increase in boilup (therefore, a vapor-sensitive flood), or due to both (a vapor- and liquid- sensitive flood).

To determine whether the flood is liquid-sensitive, the temperature control needs to be disconnected, and the boilup kept constant (on flow control or in manual). The reflux is now raised. If the tower floods, then the flood is liquid-sensitive. The drawback of this test is that since reflux is raised without a matching increase in boilup, lights are induced into the bottom product, making it off-spec. Similarly, a vapor-sensitivity test can also be performed. For this test, the reflux is kept constant (in Figure 2.8 it already is constant as it enters on flow control) and the boilup is raised. In this test, the temperature controller can remain in auto and the temperature set point is raised. Flooding in this test indicates a vapor-sensitive flood. The drawback of this test is that it induces heavies into the distillate and gets it off-spec. The good news is that these are usually quick tests; if correctly performed each test will yield the answer within 2–3 h. Once these two tests are performed, all the theories that did not predict the observed sensitivities are invalidated. Reference [14] describes a case in which these tests invalidated a leading theory and paved the way for a second theory that until then was considered far less likely. The second theory was later proven correct and led to a successful fix.

Overall, the trick here is to test the response of the tower to one variable at a time.

2.10 Flood and flood mechanism determination: hydraulic analysis

Hydraulic calculation procedures are available in most distillation texts (e.g. [4–7,17]) to calculate the proximity of each tray or packed bed in the tower to the points of initiation of the various flood types. Updated published procedures are in the latest version of *Perry's Handbook* [17]. In addition, hydraulic calculation software is available from technology suppliers, such as Fractionation Research Inc. (FRI) and from equipment vendors. First, the tower is simulated to give the internal vapor and liquid loads and physical properties for each stage in the tower at the desired conditions, typically at the highest throughput before the tower runs into trouble. The highest internal vapor and liquid loads in each section of tower are then used together with the relevant physical properties in the hydraulic equations.

Calculating the proximity of flood limits is invaluable in diagnosing the root cause of a tower capacity problem. Table 2.2 [29] shows a case in which the hydraulic analysis was sufficient to diagnose the root cause of a tower flood problem. This tower was 1.83 m in diameter at the bottom, swaging to 0.91 m at the top. Upon feed rate increase, flooding was observed just above the swage. The tower was simulated at the maximum throughput. Based on the simulation and tray/DC geometry, the capacity limits were calculated using the FRI software.

Table 2.2 first lists the geometrical parameters, followed by calculated characteristic hydraulic parameters. Below these, Table 2.2 lists "Jet flood, %", "Froth in the downcomer, %", and "Downcomer choke velocity, %," which describe the proximity of the main capacity limits. A value exceeding or approaching 100% for one of these parameters indicates flooding by this mechanism.

Table 2.2 shows that all the trays operated a comfortable margin away from jet and downcomer choke floods. Above the swage (top section), froths in the downcomers were also a large margin away from flood. In contrast, froth heights in the downcomers immediately below the swage (trays 15–25) exceeded 100%, indicating a likely flood due to excessive downcomer froth heights. The froth heights in the downcomers on trays 26 to 73 approached flood but did not get there yet. This analysis led to the conclusion that the observed flood most likely originated just below the swage and not above it as was previously thought, even though the symptoms appeared above the swage.

The hydraulic analysis permitted focusing in on the root cause. Below the flood limits, Table 2.2 lists the various calculated hydraulic factors that contribute to the downcomer backup. The downcomer backup is the sum of the tray pressure drop, inlet clear liquid height, and head loss under the downcomer [4–7,17]. Table 2.2 shows that below the swage, the dominant term is the pressure drop, particularly the dry pressure drop. The dry pressure drop is the friction head through the tray openings when no liquid is present. A high dry tray pressure drop means a small open area. Therefore, the hydraulic analysis pointed out to insufficient open area as the root cause. Indeed,

Table 2.2 Demethanizer Hydraulic Analysis that Diagnosed Tower Problem

	Top Section		Bottom Section		
	Trays 1–6	**Trays 7–14**	**Trays 15–25**	**Trays 26–28**	**Trays 29–73**
D_{tower} (m)	0.91	0.91	1.83	1.83	1.83
Tray spacing (mm)	457	457	457	533	584
A_{hole} (% of A_{active})	6.5	6.5	3.2	5.6	7
$A_{DC,inlet}$ (% of A_{tower})	14	14	30	30	30
Downcomer (DC) clearance (mm)	33	33	38	71	71
$h_{outlet\ weir}$ (mm)	38	38	38	51	51
Vapor C-factor, based on net area (m/s)	0.043	0.040	0.024	0.034	0.043
Liquid load [(m^3/h)/(m of outlet weir)]	19	25	56	98	121
$u_{DC\ inlet}$ (m/s)	0.040	0.055	0.034	0.061	0.073
% Jet flood	47	46	62	65	70
% Froth in DC	58	53	106	94	87
% DC choke velocity	51	53	38	65	78
Total DC backup (mm liquid)	152	152	300	312	312
Tray inlet clear liquid height (mm)	61	64	79	112	112
Head loss under DC (mm liquid)	5	8	30	28	43
Tray pressure drop (mm liquid)	86	81	191	173	157
Tray dry pressure drop (mm liquid)	58	48	163	119	94

From Ref. [29], reprinted courtesy of the Oil & Gas Journal.

the hole areas below the swage were 3.2% of the tray active area, compared to typical values of about 8–10%. Retraying the sections below the swage with trays containing more hole area eliminated the flood and debottlenecked the tower.

2.11 Efficiency testing

2.11.1 Purpose and strategy of efficiency testing for troubleshooting

The incentive for efficiency-testing a malfunctioning column is obvious. The simulation with the expected efficiency shows how the tower should perform. The simulation based on plant data provides the real efficiency. In the absence of flooding, a real efficiency below the expected signifies poor separation and root causes such as maldistribution or channeling in trays and packings, poor hydraulic design, corrosion, or damage. In many cases (e.g. [30–33]) a mismatch between simulation and plant data, or a low efficiency obtained from good plant data, was the key for correct diagnosis and an effective solution to an operating problem.

An efficiency test is essential even for a well-performing unit, for the following reasons:

1. When the unit malfunctions at a future date, availability of good operation test data tremendously reduces the troubleshooting effort.
2. A unit may appear to perform well, even while it is running at nonoptimum conditions; for instance, energy usage may be excessive. Because of overdesign, these factors may be hidden. Yarborough et al. [34] presented several case histories (not all distillation-related) where performance testing directly led to major improvements in profitability.
3. Simulations used to determine best running conditions and to assess the effectiveness of proposed modifications may be misleading unless tested against reliable data.
4. A discrepancy between the simulation and the tower performance (e.g. differences between simulated and measured temperature profile) may identify a hidden problem.

Good efficiency testing is rigorous, effort consuming, and time consuming. The cost effectiveness of the rigorous procedure is often questioned, and a shortcut version is sought. A suitable shortcut procedure can be derived from the rigorous procedure outlined in Refs [3] and [21] by skipping over guidelines that are considered less important.

The best procedure to adopt depends on the objective of the test. A shortcut test is best suited for detecting gross abnormalities and is often performed as a part of a troubleshooting effort. When investigating a gross malfunction, rigorous testing may seriously delay identification and rectification of the fault. When a column appears to perform well, a shortcut test can provide a useful, albeit unreliable, set of data for future reference.

A shortcut test is unsuitable and often misleading for detecting subtle abnormalities, for determining column efficiency, for checking the design, for optimization, and as a basis for performance improvement or debottlenecking modifications. The author is familiar with many cases where shortcut tests applied for these purposes needed repeating several times, yielded conflicting data, provided inconclusive results, and led to ineffective modifications. In most of these cases, the test objectives were not met even though the total time, effort, and expense spent were several fold those that would have been spent had single rigorous test been performed. The author therefore strongly warns against applying a shortcut procedure for these purposes. This recommendation is shared by others [34].

Shortcut tests range from those that do little more than take a set of readings and samples from the column to those that incorporate checks of material, component, and energy balances and key instrumentation. Even for shortcut tests, the author recommends incorporating the above checks and spending time on preparations to ensure that key indicators are working. These checks will permit at least identification of major problem areas and enable a rough assessment of data reliability. These key items can be extracted from the list of preparations and checks recommended in Refs [3] and [21] for rigorous tasks.

2.11.2 Planning and execution of efficiency testing for troubleshooting

General. It is best to carry out a performance test engulfing the whole unit. Individual testing of columns, one at a time, increases the total effort and time consumed and reduces the reliability of measurements. Testing the entire unit provides several material balance cross-checks and enables better identification of erroneous meters and lab analyses. For instance, if the column feed analysis is off, the column component balance may not be sufficient to point out which analysis is suspect; however, if data from a component balance on upstream and downstream equipment are also available, the incorrect analysis can easily be identified.

A shortcut to the above recommendation may be acceptable when the plant inlet rate and compositions have not significantly changed since the last plant test and the problem areas are well-known. In such cases, it may suffice to test only the specific column area [3,34].

Another shortcut is often acceptable when the column is near the end of a processing train which yields reasonably pure products. Product analysis and metering tend to be far more reliable than intermediate stream measurements, and there is usually more to be gained from cross-checks with downstream measurements than with upstream measurements. In such cases, it may suffice to restrict the testing to the column area and the downstream equipment.

Duration. It is best to carry out a performance test over a 2- to 3-day period [3,21]. If shorter periods are used, variations in plant conditions may introduce

serious errors. Over a period of 2 days, errors are averaged out. Further, column control problems may make it difficult to obtain a sufficiently long period of stable operation if the test is short. Over a 2-day period, the column should be running under stable conditions at least for some of the time.

Timing. The best time to carry out a performance test is when the plant is stable. In most plant situations, weekends are ideal, as changes due to fluctuations in upstream units are minimized.

Safety and environment. Test procedures must conform to all statutory and company safety and environmental regulations. The test plan should be reviewed with persons familiar with safety and environmental requirements and amended as necessary to fully conform to these.

Preparations. Adequate preparations ahead of the test are critical to the success of a performance test. A malfunctioning meter, a leaking block valve, or a poor laboratory analysis during the performance test can dramatically reduce the reliability of the results and defeat the purpose of the test. This is the time to sort out all potential bottlenecks.

Detailed considerations are important and were formulated into a detailed procedure that is spelled out in length in Refs [3] and [21] (much the same procedure in both). This procedure is based on the author's experience supplemented by Refs [8,22], and [34–36]. Since Refs [3] and [21] have the detailed procedure spelled out, it will not be repeated here. However, it is most important that the preparations are implemented correctly, and the reader is encouraged to review these references prior to embarking on a performance test.

2.11.3 Processing the results

The first step is compiling material, energy, and component balances for the unit. A good way to tackle this is to fill a blank process flow diagram with the test data. The performance of each piece of equipment can then be determined. Check laboratory analyses using dew point and bubble point calculations. Some flows and compositions may need readjustment to satisfy the balance equations. Any inconsistencies must be resolved before proceeding with result processing.

Column efficiency determination. To determine column efficiency, the steps below are often followed:

1. Make an initial guess of the column efficiency and assume it is uniform throughout the column. This initial guess need not be accurate. From knowledge of the actual number of trays and the guessed tray efficiency, estimate the number of theoretical stages.
2. Using the test material balance and the estimated theoretical number of stages, run a computer simulation for the test conditions. Adjust the number of stages in the column to give the measured product purities.
3. Check that simulated exchanger duties match measured values. If they do not, carefully investigate the cause. Pay attention to latent heat data used in the simulation.

4. Compare the simulated temperature profile with the profile measured during the test. If significant discrepancies exist, alter the number of stages in the relevant section to improve the match. Similarly, if internal column samples were obtained, check them against stage compositions predicted by the simulation and adjust the number of stages accordingly.
5. If the number of stages in one column section was significantly altered in step 4 above, the total number of stages in the column may also need adjustment. Repeat steps 2 and 4 until the simulation matches both the component balance and the temperature or internal composition profile.
6. Apply the simulation to examine the sensitivity of product purity to changes in the number of stages. This is perhaps the most critical step in processing test data; overlooking it has been a prime source of grossly misinterpreted test data. It is not uncommon to find that column efficiency was overestimated by a factor of 2, and even more, in columns where product purity is insensitive to the number of stages. Scale-up of such misinterpreted data has proved disastrous on many occasions.
7. When a column operates near minimum reflux, contains an "excess" of trays, or operates under other pinched conditions, product purity is often insensitive to the number of stages. The author is familiar with one tower operating close to minimum reflux where product purity remained practically unchanged when the number of stages was halved. When the column was simulated with less than three stages, product purity was sensitive to the number of stages. In the same column, changing the number of stages between 5 and 15 yielded product purity changes far smaller than those that could be detected by the lab analysis. A similar experience was reported in the top section of the column tested in Ref. [37]. Pinching (either due to a mislocated feed, proximity to minimum reflux, or a tangent pinch) is commonly implicated by the above insensitivity. A McCabe–Thiele diagram and a key ratio plot can help identify the cause; application of these techniques for this purpose is described elsewhere [7,33].
8. Similar to step 6 above, check the sensitivity of the number of stages to errors in the reflux rate. Prepare a stages vs reflux plot around the measured reflux rate. Near minimum reflux or a pinched condition, minor changes (equivalent to typical flow meter errors) can have a greater effect on product purity than doubling (or halving) the number of stages in the column. In contrast, near the minimum number of stages, it is possible to get reliable efficiency determination even when there is a poor closure of the energy balances [37].
9. Check the sensitivity of the simulation to a reduction in the number of stages in each section. In multicomponent distillation, examine the effect of reducing the number of stages on the key component ratios (ratios of light key to heavy key concentration) in the top and bottom products. The author experienced one case where using an efficiency ranging from 40% to 60% in the stripping section matched test data quite well; in that case, the key component ratios gave a closer estimate.

10. Allow for stages contributed by reboiler, condenser, interreboiler, and intercondenser. Common rules of thumb include the following:
    - A single stage is allowed for a once-through reboiler, a kettle reboiler, or when the bottom draw compartment is separated by a preferential baffle from the reboiler compartment [3]. Half or zero theoretical stages are allowed for an unbaffled recirculating reboiler arrangement.
    - A single stage is allowed for a partial condenser and none for a total condenser. Note, however, that most computer simulations count a total condenser as a stage.
    - Determine whether an interreboiler or an intercondenser approximates a theoretical stage. If so, allow for it.

    Subtract the total number of stages contributed by these devices from the number of stages calculated by the simulation. The difference is the number of stages in the column.
11. Compare test run efficiency with the design efficiency or the efficiency of other towers in the same service. Efficiency comparison can be misleading when relative volatility is low (<1.5, and especially <1.2), unless identical vapor-liquid-equilibrium (VLE) data are used. At low relative volatility, differences in VLE values are reflected as differences in column efficiency. A 2% difference in the relative volatility of a low-volatility (1.1) system is sufficient to account for a difference of 50% in the determined efficiency value [38]. Unless the design or operating conditions of the top and bottom section are widely different, column efficiency should be reasonably uniform throughout the column. If the simulation indicates wide variation from top to bottom, it may suggest an error in the simulation or an actual performance problem.

2.12 Gamma-ray absorption and other radioactive techniques

Gamma scanning of distillation columns employs radioactive sources in the 500- to 2500-keV range [39]. Compton scattering is the chief process responsible for the attenuation of these rays. The radioactive sources used are normally cobalt-60 and cesium-137. A summary of the principles of this technique follows; a detailed description is available elsewhere [39].

When a gamma ray passes through a medium from a radioactive source to a detector, some of its radiation is absorbed by the medium. The amount of radiation that is not absorbed is given by the following equation [39–41]:

$$I = I_0 e^{-\mu\rho\chi} \tag{2.2}$$

where I is the radiation intensity in keV, as seen by the detector; I_0 is the radiation intensity of the source, in keV; ρ is the density of the medium; χ is the thickness of the medium; and μ is the absorption coefficient, which depends on the γ-ray source and the medium material.

When the energy of the gamma ray exceeds 200 keV, μ becomes independent of the chemical composition of the medium, and the absorption becomes a function of the product of the density and thickness of the medium [39,40]. For a horizontal chord of fixed length (Figure 2.9(a)), the intensity of radiation received at the detector is therefore a function of the density of the medium. If the gamma ray passes through metal (very high density) or liquid (high density), the intensity received by the detector is relatively low, but if the ray passes through a vapor space (low density), the detector reading is high.

The source and detector are lined up on the same horizontal plane, and a reading is taken either across the tray or across the downcomer (as desired). Both source and detector are then simultaneously moved to the next lower vertical position, where the next reading is taken. The source and detector are thus simultaneously moved vertically down the column, and radiation intensity reaching the detector is recorded at each vertical position. High recorded intensities indicate vapor spaces along the ray's path; low recorded intensities are interpreted as passage through liquid or solid.

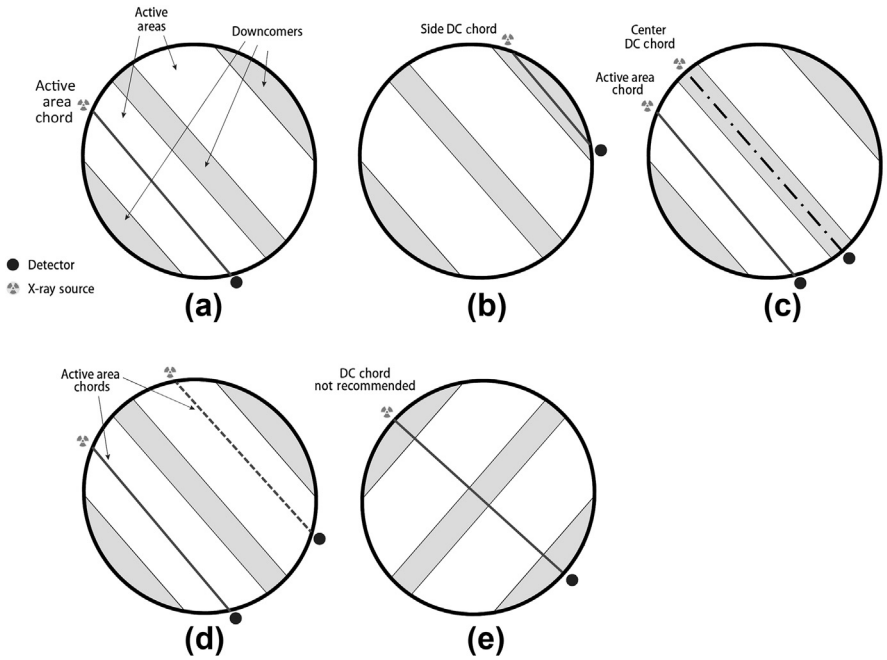

FIGURE 2.9 Gamma Chords in Tray Towers, Shown for a Tower with Two-pass Trays

(a) Active area scan. (b) Side downcomer scan. (c) Active area and center downcomer scans. (d) Scans through active areas on both sides, looking for channeling. (e) Poor practice of a scan chord that passes both through active areas and downcomers.

From H.Z. Kister, "Practical Distillation Technology," course manual, copyright © 2013; reprinted with permission.

The vertical intensity profile thus obtained provides information on column behavior and identifies the location and nature of column irregularities.

2.12.1 Regular qualitative gamma scans

This is the most common and least expensive gamma-scanning application technique and accounts for over 80% of the applications of the gamma scans. In tray towers, it involves shooting a single chord through the trays active areas (Figure 2.9(a)) and moving this chord down the tower, taking shots typically every 50 mm of vertical height. After the completion of the scan, additional chords can be shot. Often a second chord is shot through the downcomers (Figure 2.9(b) or Figure 2.9(c)) or through another pass of the tray to look for channeling (Figure 2.9(d)).

Figure 2.10(a) [39,40,43] and Figure 2.10(b) [43] are fault−condition diagrams illustrating how different types of irregularities show up on a gamma scan.

For normal operation, a tray active area scan will show a high-density (or low-detector-reading) region just above the floor of each tray (due to the presence of liquid) followed by a low-density (or high-detector-reading) region in the vapor space between the trays. A high-density region between trays implies flooding; a region of uniform intermediate density between trays implies foaming; whereas a low-density region where a tray is expected implies a missing or damaged tray. In a packed column, a packed bed will show up as a medium-density region (medium detector reading), a collapsed bed as a low-density region (high detector reading), and plugging or flooding as a high-density region.

Figure 2.11 is an active area scan illustrating a typical evaluation of tray active areas. Tray locations and sources of external interference (e.g. welds, supports, nozzles, insulation rings) are marked on the plot. The actual scan data, which are the connected dots from the measurements taken every 50 mm, form the solid plot. The right side of the plot shows the "clear vapor" line, which is a reference line showing the transmission of gamma rays through clear vapor. This line can be determined reliably if the scan passes through a region where clear vapor exists (typically above the top tray or above the reboiler return inlet in the absence of flooding in this region). The line labeled "froth height intensity" is used to determine froth heights. This line is an empirical measure of froth heights by averaging the radiation counts of vapor and liquid. On Figure 2.11, the vapor radiation count is 4000, the liquid radiation count is 200, so the froth line is at a radiation count of their average (2100). The froth height is determined by measuring the physical distance from deck to spray as shown for tray 2 in Figure 2.11. For this tray, the froth height is 9 in (225 mm). A more accurate method for determining froth densities was presented by Harrison [45].

In Figure 2.11, all the vapor space peaks reach clear vapor, indicating little or no entrainment. When some of the spray approaches the tray above, the vapor space peak falls short of the clear vapor line. This condition is reported as "entrainment". The degree of entrainment can be determined from the proximity of the top of the

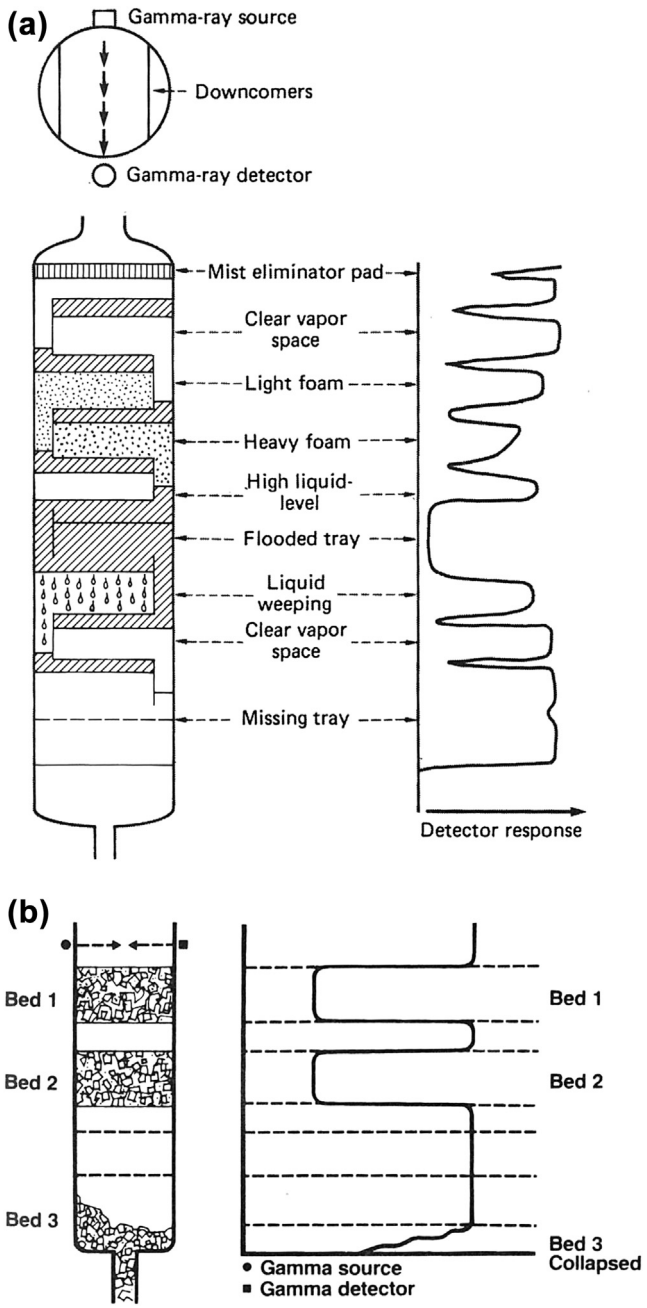

FIGURE 2.10 Illustrative Gamma Scans, Depicting Various Types of Column Irregularities

(a) Tray column (b) Packed column.

Part (a) from Ref. [40], reprinted by special permission from Chemical Engineering, copyright © 1983 by Access Intelligence, New York, NY. Part (b) from Ref. [42] reproduced courtesy of the American Institute of Chemical Engineers.

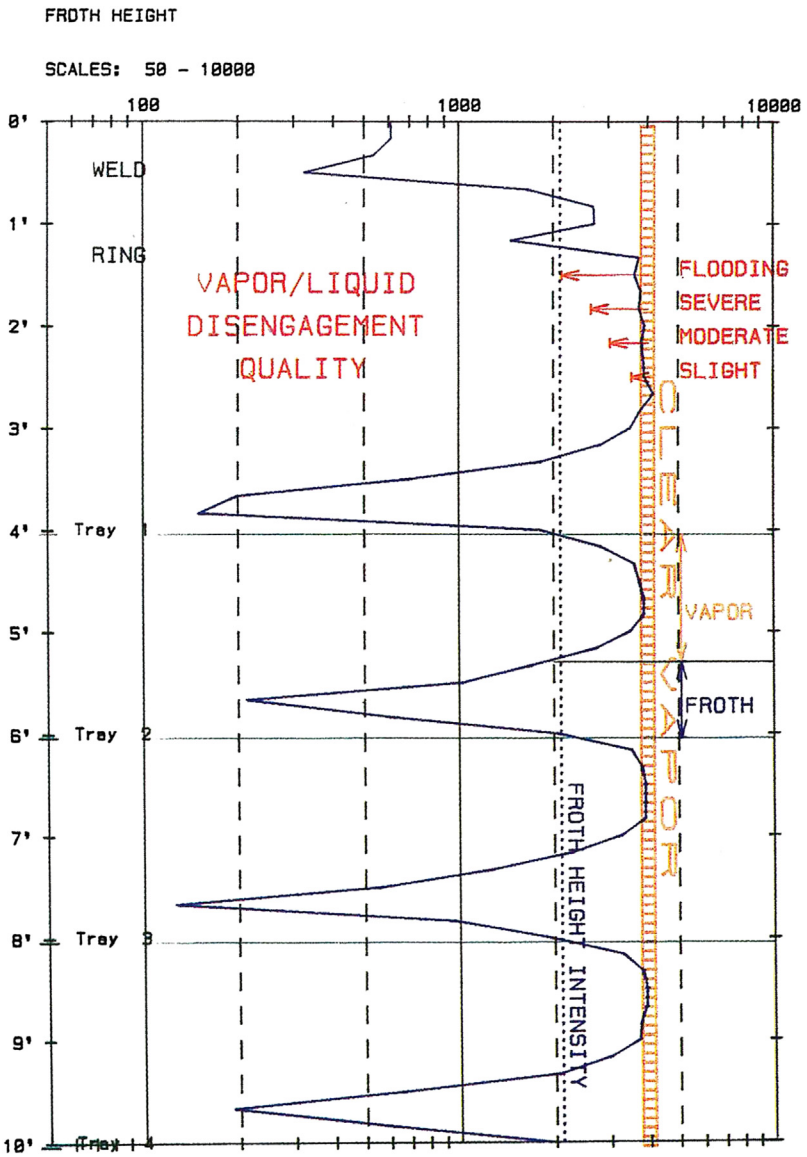

FIGURE 2.11 A Gamma Scan Illustrating Typical Evaluation of Tray Active Areas

From Ref. [44]; reproduced courtesy of the American Institute of Chemical Engineers.

peak to the clear vapor line. The arrows above tray 1 show the terms commonly used, ranging from "slight" to "heavy" entrainment and finally "flooding". Note that the entrainment referred to in the scans does not measure the amount of liquid entrained into the tray above; rather, it refers to the amount of liquid drops near the top of the

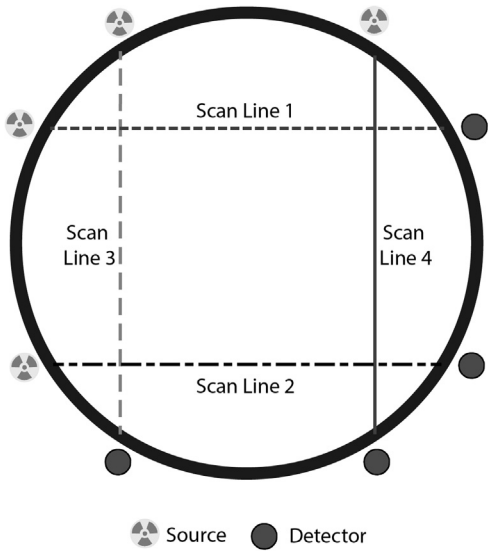

FIGURE 2.12 Typical Packing Grid Scan

From H.Z. Kister, "Practical Distillation Technology," course manual, copyright © 2013; reprinted with permission.

spray. One case was presented [46] in which a column performed well despite severe entrainment from many of its trays.

Gamma scans can readily detect gross abnormalities such as missing trays, collapsed trays, flooding, or heavy foaming. This technique can also detect more subtle abnormalities such as high or low tray loadings, foaming, excessive entrainment, excessive weeping, blockage, and multipass liquid maldistribution. Gamma scans performed on a routine basis can also be used to monitor deterioration in column performance due to fouling, corrosion, and other factors.

In packed towers, four equal chords are often shot, one after the other (Figure 2.12).

Each chord has the source and detector moving simultaneously down the bed in the same manner that the chord moves down a tray column. This "grid" gamma scan looks for maldistribution and channeling, which is by far the main culprit for packed tower efficiency loss [1]. When liquid distribution is good, the scan of the four chords look the same (bed 1 in Figure 2.13).

Differences between the chords are interpreted as bed maldistribution. For instance, one of the chords in bed 2 of Figure 2.13 shows more radiation transmission than the other three, indicating less liquid flowing through the bed along this chord. The higher transmission begins immediately below the distributor, indicating less liquid issues from the distributor along this chord and therefore a distributor problem.

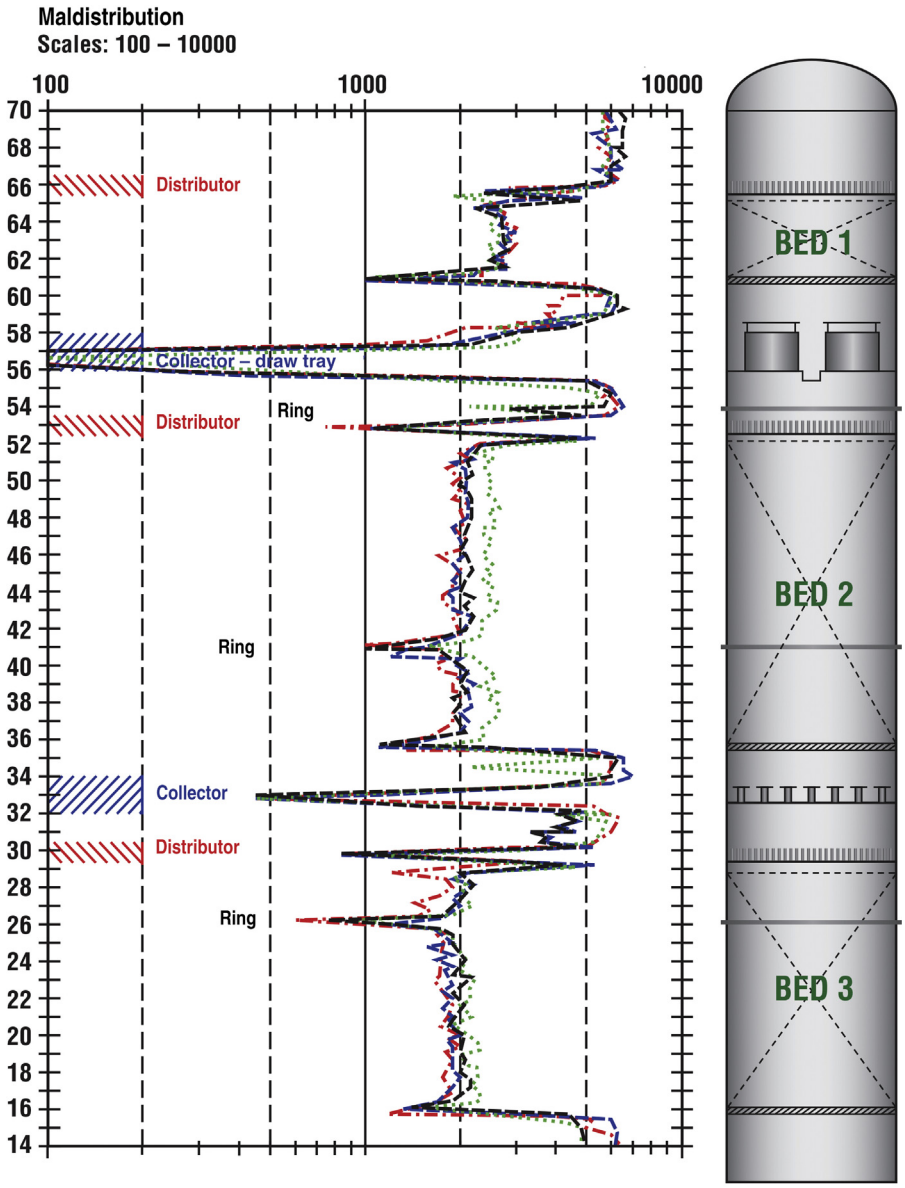

FIGURE 2.13 Packed Bed Grid Scan Showing Good Liquid Distribution in Bed 1 and Maldistribution Originating at the Distributor in Bed 2

Reprinted courtesy of Tracerco.

The packing chords are selected to run through the bed such that two intersect the other two at an angle of 90°. This arrangement allows the verification of the presence of liquid distributors and collectors. With judicious setting of the chords, this arrangement can also provide a measurement of liquid height and frothiness of the liquid contained in collectors and distributors, and hence determine whether the hardware is working correctly, is overflowing, or is angled causing liquid maldistribution. In addition, this strategy is normally able to detect the position of the bed, the disappearance of some of the packings (e.g. by being corroded away), significant blockages, and local flooded regions.

Vidrine and Hewitt [47] outlined some limitations that constrain the accuracy of the liquid maldistribution diagnostics. They noted that with a 2.5 m tower with packing density of 240 kg/m^3 and low liquid wetting, the wetting measured accounts for only 24 kg/m^3. In this case, a 50% maldistribution gives a radiation variation similar to that produced by a 30-mm shift in both source and detector positions (e.g. due to a platform disturbance or by wind). Also, the statistical error in radiation counting varies the density calculation by typically twice the square root of the count rate, which in the cited example gives the same radiation variation as a 50% liquid maldistribution. Finally, Vidrine and Hewitt pointed out that the error rapidly escalates with reduced source strength and with wider towers. In large diameter towers (>5−6 m), the source needed to get a reliable liquid maldistribution diagnostics may be too strong to be practical.

One application of gamma scans is to perform "time studies". Stationary gamma ray sources are placed in the vapor spaces at strategic elevations in the unflooded condition. The rates (feed, reflux, boilup, or whatever variable is studied) are raised until the amount of radiation transmitted sharply falls in one of the vapor spaces, indicating liquid accumulation and therefore flooding. The location where the radiation initially drops off is where flooding initiates and the rates at which it occurs are the flood rates. One limitation is that the vertical positions for the stationary sources cannot be too close to each other (typically about 2 m apart) to avoid radiation interference.

To correctly detect subtle abnormalities, it is important to have a reference ("baseline") gamma scan, usually when the column operates satisfactorily, or an empty column scan—or ideally both. The reference scan enables distinguishing the subtle abnormalities from interferences from column internals, lagging, flanges, piping, platforms, and the like. Accurate positioning of the source and detector is required and is taken care of by the scanning contractors. Metal guides attached to the column, as well as mechanized systems that move the detector and source synchronously up and down the guides, are used for this purpose.

Some pitfalls. Column gamma scans can be of little value, even misleading, unless scanning pitfalls are avoided. The author had experience with the following pitfalls that adversely affect the quality of information supplied by gamma scans:

1. It is important to supply the scanners with good drawings of the column and with good data on tray location and column shell thickness. This information is essential for good planning and interpretation of the scans.

2. Interpretation of gamma scans may at times be difficult and requires good knowledge of both scanning technology and column operation. In many cases, a gamma scan contractor is brought into the plant, shoots a scan, and then writes a report. The author has seen many such reports containing interpretations that were way off the mark. To avoid this, it is important to have a person or persons who are familiar with the tower design and operating history communicate closely with the contractor both when the column is being scanned and when the scans are being interpreted.
3. It is important to ensure stable plant operation while scanning. Otherwise, variations due to instability may be misinterpreted as column abnormalities.
4. Avoid shooting gamma scans in extreme weather conditions. These often lead to column instability while slowing down the gamma scans. Both may lead to variations that can be misinterpreted.
5. When troubleshooting for flood or other capacity limits, always perform a flooded and an unflooded scan. The flooded scan can give a good indication of the location of the flood, but does not give much information on what causes it. The unflooded scan should be shot at loads just below the flood point, and is invaluable in providing information on what is likely and what is unlikely to be the cause.
6. Some commercial scanners prefer to shoot downcomer scans perpendicular or angled to the outlet weir (e.g. Figure 2.9(e)) instead of parallel to the weir as shown in Figure 2.9(a). The author has had very few satisfactory experiences with downcomer scanning perpendicular or angled to the weirs. Such scans are very difficult—often impossible—to correctly interpret due to the coupling between the tray and downcomer dispersions, making them breeding ground for misleading diagnostics. The problem is aggravated when the downcomers are sloped. Further, the gamma rays used in scanning the top of every downcomer travel through support beams, which may be quite thick; their presence shows up in the same manner as extra liquid. For these reasons, the author recommends always performing downcomer scans parallel to the weir (Figure 2.9(a), or 2.9(c)) and not perpendicular or angled to it (Figure 2.9(e)).
7. Scanning downcomers parallel to the weir (Figure 2.9(a)) also has pitfalls. If the scan chord is shallow, scattering and reflection may lower its accuracy. When the column shell is thick (e.g. high-pressure services), the metal can absorb a larger portion of the radiation than the fluid. Consider a scan along a 300-mm chord in a downcomer containing liquid of 0.5 specific gravity at 50% aeration. If the column shell is 25-mm thick, it will absorb approximately five times more of the radiation than the process fluid. For this reason, in high-pressure columns it is best to scan center rather than side downcomers (Figure 2.9(c)).
8. It is important to combine the information provided by the scans with information from other troubleshooting techniques such as flood tests, vapor liquid sensitivity tests, and hydraulic analysis. Questions such “Are the gamma scans show flood where the hydraulic analysis predicts flood?” or “Has there been

foaming experience in the service where the gamma scans interpreted the trays to foam?" can go a long way to eliminate "lying gamma scans".

9. With the gamma scans shot every 50 mm and the tray thickness being about 2−3 mm, it is difficult for gamma scans to distinguish dry trays from missing trays. Gamma scans do not see trays; they see the liquid sitting on the trays. This can be a major issue in low-liquid-load and low-vapor-load trays. It is important to check using the hydraulic analysis whether there are low liquid and/or vapor loads, and if so, to repeat the scan at higher values. If the rescan at the higher vapor or liquid loads still sees no liquid on the tray, then the missing tray diagnosis is supported.
10. With packed towers, it is useful to measure liquid levels in collectors and distributors whenever possible. Overflowing collectors and distributor troughs is one of the most common malfunctions reported in packed towers, but it may require extra scans to avoid interference from the trough metal.

Applications. Several case histories involving gamma-ray scanning have been reported [40−54]. These sources illustrate, with the aid of detector intensity diagrams, the application of gamma-ray scanning to diagnose the following abnormalities:

1. Flooded trays [41,45,46,48,51]
2. Rate of flooding a tray [45]
3. Time study to determine exact rate or location of flooding [45,46]
4. Indication of tray froth height [45]
5. Plugged trays [45,51,52]
6. Plugging causing maldistribution in two-pass or multipass trays [51]
7. Identifying and bypassing a downcomer restriction [47]
8. Monitoring tray plugging [39,45]
9. Foaming [39,54]
10. Dry tray panels [48]
11. Missing trays [40]
12. Damaged trays [40,41,48,51]
13. Maldistribution in packed beds [45,46,49,50,53,54]
14. Packing gas distributor problem [54]
15. Flooded packing [46,54]
16. Packing distributor fouling [46,54]
17. Collapsed packed beds [42,53]
18. Damaged packed beds [50]
19. Damage to liquid collector or distributor in packed tower [53]
20. Packing damage or crushing [46]
21. Base liquid level above reboiler return or bottom vapor feed [45,46]
22. Bottom liquid level [39]
23. No abnormality where one was expected [41,48]
24. Two different types of abnormalities in one column [40]
25. Plugging in a sidestream line [43]

2.12.2 CAT scans

This technique is used primarily to identify the nature of maldistribution in packed beds. While the grid scan (Figure 2.12) is capable of identifying maldistribution and often provides clues for the nature of this maldistribution, the CAT scan is invaluable in closely examining the liquid profile in the bed. It is also invaluable in showing a center-to-periphery liquid maldistribution that grid scans cannot identify.

Figure 2.14(a) shows how a CAT scan is shot. A gamma-scan source is placed and a number of detectors (typically about nine; for simplicity and clarity, Figure 2.14(a) only shows three) are set around the bed at evenly spread marked radial positions, all at the same elevation. Once done, the source is moved to the position of the nearest detector, the detector to the position of the source, and the scan is repeated. This continues until the source is placed in all the radial positions around the bed. The profiles obtained in all positions are then integrated to give the two-dimensional absorption density profile at the elevation. This density profile identifies liquid-rich regions (high density) and drier regions (low density). If desired, the CAT scan can be repeated at additional elevations along the bed.

Figure 2.14(b) is a CAT scan through a packed bed [49b]. The liquid density increases as one moves from the center of the bed to the peripheral regions. There is a circle right in the center of the bed that approaches total dryness. This circle occupied about 15% of the tower cross-section area. The normal grid scan showed maldistribution, but it took the CAT scan to give a good definition of the nature of maldistribution that led to the diagnosis of the tower problem.

CAT scans are expensive. Also, they may have difficulty getting a good measure of the liquid density near the periphery. Before performing the CAT scan, it is a good idea to perform the normal grid scans. The grid scans often show the region where the problem is intensified, which guides the optimum selection of the CAT scan elevation(s). A detailed discussion of the technique is in Ref. [49a].

2.12.3 Quantitative analysis of gamma scans

Towers containing either conventional or high-capacity trays, especially those with larger diameters, occasionally experience liquid and/or vapor maldistribution. Such maldistribution lowers tray efficiencies, upping the reflux, reboil and energy requirement, and bottlenecking tower capacity. Vapor and liquid maldistribution is difficult, often impossible, to diagnose using conventional troubleshooting techniques such as vendor software, ΔP measurement, and conventional single-chord qualitative gamma scans. Judicious multichordal gamma scans with quantitative analysis are the best tool for diagnosing maldistribution on trays.

With this method, several parallel chords, typically three to six, are shot along the flow path (Figure 2.15(a)). Froth heights, froth densities, liquid heads, and entrainment index data are determined for each tray at each chord using high-accuracy methods as described in Refs [24] and [45]. From the data, the profiles of these variables along the flow path are mapped and are plotted using a Kistergram, which

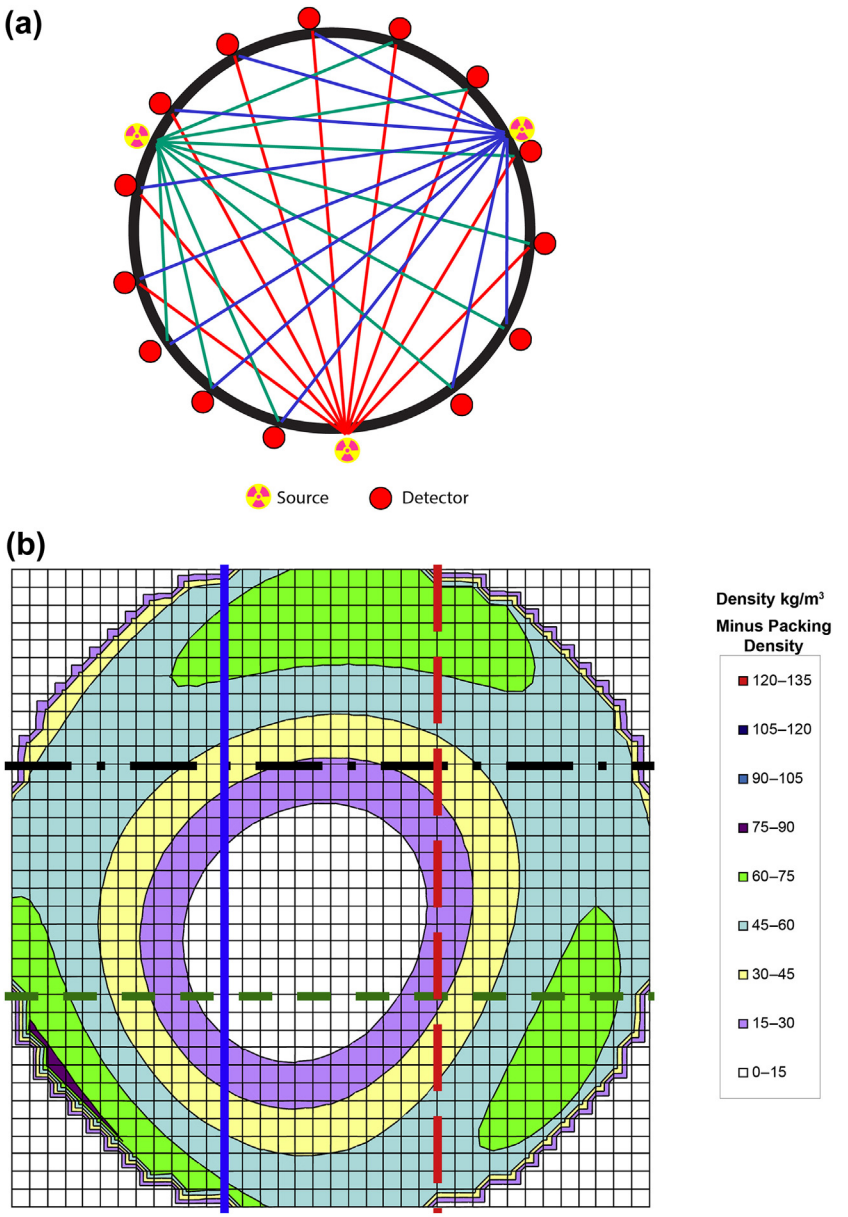

FIGURE 2.14 Computer-Aided Tomography (CAT) Scanning

(a) CAT scan chords (b) CAT scan profile showing little liquid near the center of the bed and most liquid around the periphery.

Part (a) from H.Z. Kister, "Practical Distillation Technology," course manual, copyright © 2013, reprinted with permission. Part (b) from Ref. [49b]; reprinted courtesy of IChemE.

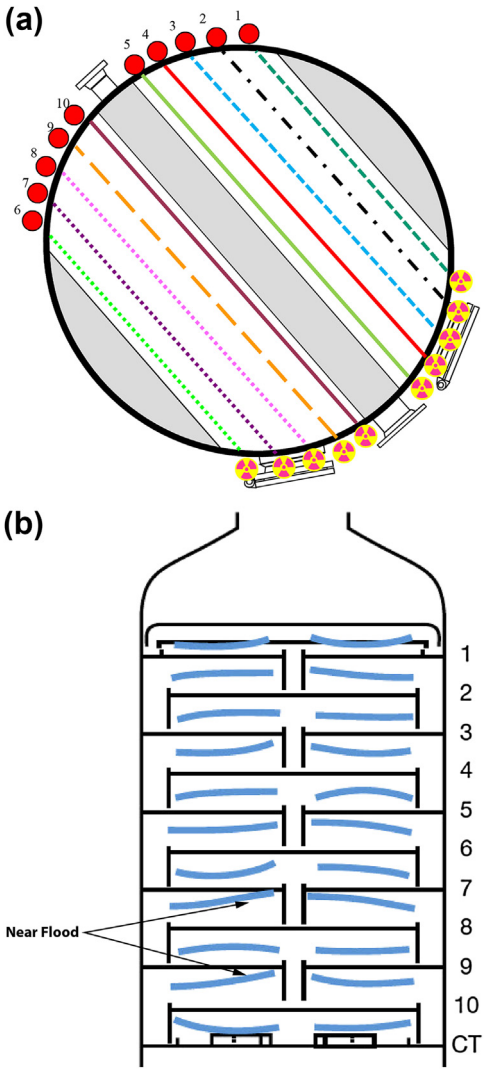

FIGURE 2.15 Multichordal Channeling Scans Used for Quantitative Gamma Scan Analysis

(a) Scan chords (b) Kistergram showing to-scale graphic of spray heights profiles from multichordal channeling scans with quantitative analysis.

Part (a) from H.Z. Kister, "Practical Distillation Technology," course manual, copyright © 2013; reprinted with permission. Part (b) reprinted with permission from Ref. [28]; reprinted courtesy of the American Institute of Chemical Engineers.

shows the variable to-scale on a tray diagram. Figure 2.15(b) is a Kistergram showing froth height profiles along the flow paths in a 10-tray tower as measured by multichordal gamma scans. Froth heights reaching the tray above indicate flooding or proximity to flood. The diagram indicates tall froths, approaching the tray above, near

the centers of trays 6, 8, and 10. Because tall froths are induced by high vapor loads, vapor preferably channels through the center of the tower. The chimney tray (tray CT beneath tray 10) had froth heights exceeding the chimneys (these too are drawn to scale), especially near the sides, suggesting liquid overflowing the chimneys near the sides, which would route the vapor to channel preferentially towards the middle. Therefore, the scans attributed the channeling to chimney tray overflow, which propagated due to excessive tray open area of the trays above. Modifying the chimney tray and reducing the trays open areas solved the tower problem [24,28].

Multichordal quantitative analysis of gamma scans has been invaluable for troubleshooting conventional and high-capacity trays. One application in which previous gamma-scanning techniques had limited success is trays containing multiple truncated downcomers. This includes towers in which successive trays are rotated at 90° to each other and those in which each tray is a mirror image of the tray below. As pointed out, the quantitative scanning technique has made it possible to study the hydraulics of these trays [55].

2.12.4 Neutron backscatter techniques

Neutrons are high-energy particles that are capable of penetrating a substantial thickness of metal. These fast neutrons, however, are slowed down by collision with hydrogen nuclei. These collisions transfer energy to the hydrogen atoms, and slow neutrons are reflected back toward the source. This is analogous to rebound of balls on a pool table. The intensity of the rebounded neutrons is proportional to the concentration of hydrogen atoms in the medium adjacent to the source and can be measured by a detector. A more detailed description of this technique is provided elsewhere [39,43].

Neutron backscatter techniques are suitable for locating the interface between two materials that have different hydrogen atom concentrations. Figure 2.16(a) shows a typical device. The source and detector are mounted on the same handheld sweeper. The sweeper is positioned near the wall of the vessel and is moved up and down along the surface. The intensity of reflected radiation changes at the interface. Figure 2.16(b) is an illustrative scan showing low reflected radiation intensity from the vapor space, where the molecules are far apart and concentration of hydrogen atoms is therefore low. The reflected radiation intensity is much higher for hydrogen-containing liquids, where the molecules are close together. The step change in hydrogen atoms concentration in an oil-water interface makes this technique suitable for detecting a liquid−liquid interface.

The most common applications of this technique in distillation and absorption columns is for liquid level and liquid level interface detection, especially when normal level-measuring techniques suffer from plugging. Neutron backscatter is also commonly used for downcomer froth height measurements and for detecting near-dry or plugged downcomers. One case history has been described [39] where downcomer froth height measurements using neutron backscatter led to a detection of downcomer deposits that caused premature flooding of the column. Neutron

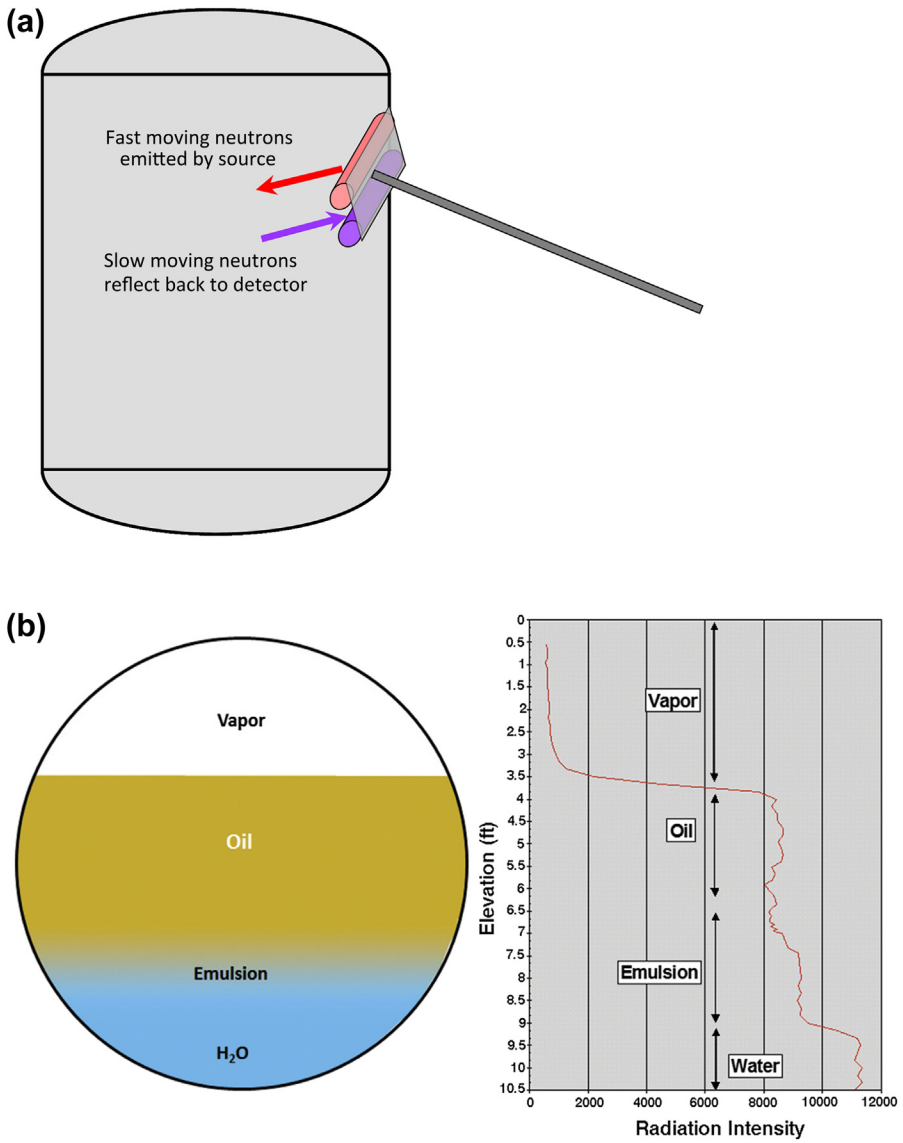

FIGURE 2.16 Neutron Backscatter Technique

(a) A schematic of the hand-held sweeper that houses both the source and the detector. (b) An illustrative neutron backscatter scan showing low reflection from vapor, and different reflections from different liquids.

Reprinted courtesy of Tracerco.

backscatter is invaluable for detecting overflows from chimney trays, collectors, and distributors, but can only be applied when the liquid is near the tower wall. Neutron backscatter can detect a liquid interface far more effectively than gamma scans, particularly in large-diameter columns and when the densities of the two liquids are similar.

Neutron backscatter also enables level measurements from one side of the vessel only, which is invaluable for measuring liquid levels in reboilers [56], where gamma rays transmission is obscured by the tubes.

Neutron backscatter is difficult to apply through wall thicknesses exceeding 40 mm or through insulation. Wet or icy insulation can lead to misleading measurement due to significant concentration of hydrogen atoms in the insulation. Neutron backscatter cannot be applied where hydrogen atoms are absent (e.g. carbon tetrachloride).

2.12.5 Tracer techniques

These involve injection of a radioactive tracer into sections of the plant and monitoring its movement with the aid of radiation detectors. Depending on the application, the tracer may be injected either as a pulse or at a constant rate. To minimize contamination, the vast majority of applications use pulses.

Tracer techniques are often applied for leak detection, flow measurement, and packing maldistribution studies. For instance, a tracer can be injected into the reboiler steam line, and a detector on the process side will determine whether any of it found its way into the process fluid. A case where this technique successfully diagnosed a reboiler leak and measured the rate of leakage has been reported [39]. Tracer techniques are discussed in detail elsewhere [39,40,42,43].

2.13 Wall temperature surveys

Holes can be cut in the insulation around the tower, and wall temperatures measured by a surface pyrometer, a contact pyrometer, or a thermal camera. These wall temperatures are invaluable for validating simulations, testing theories, detecting packed tower maldistribution, flood determination, and for identifying the presence or absence of a second liquid phase.

In tray towers, wall temperatures can provide a detailed tray-by-tray temperature profile that often can lead to identification of the root cause of a problem. In one hydrocarbon separation tower, increasing the rates under some conditions led to a step increase in heavies in the top product. A tray-by-tray temperature survey showed that the step increase was accompanied by a shift of the temperature profile, as shown in Figure 2.17.

While the on-spec temperature profile showed a normal temperature decline as one ascended the tower, the off-spec profile had an unexpected temperature inversion. Ascending from the feed point, temperatures declined, to about 65−70 °C, then rose by about 10 °C, and finally declined again. This behavior suggested the

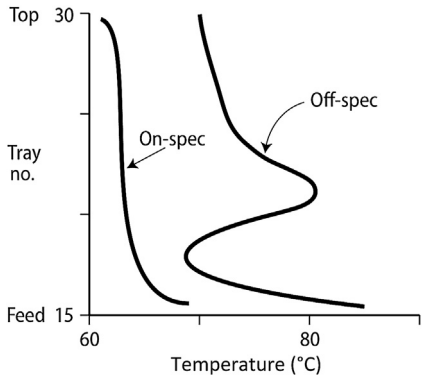

FIGURE 2.17 Temperature Inversion Measured by a Pyrometer

From H.Z. Kister, "Practical Distillation Technology," course manual, copyright © 2013; reprinted with permission.

presence of an unexpected second liquid phase—water. Presence of water not near the top of the tower, but just above the feed, suggested accumulation, possibly with the help of a higher boiler like caustic or salt. In another tower [57], wall temperature measurements identified another inversion due to unexpected mixing of a cold pumparound stream with the product stream. In this tower, a time study of changes in the wall temperature identified the root cause of this unexpected behavior. In both towers, the temperature inversions could not be seen on the normal temperature instruments on the tower. The use of temperature surveys to identify flood during a test was also described [28] and is depicted in Figure 2.7.

Probably the most common application of temperature surveys is to troubleshoot for maldistribution in packed beds. Six to eight holes are cut in the insulation at the same radial plane (Figure 2.18(a)), and wall temperatures are measured. If liquid distribution is good, all these temperatures will be the same. Temperature differences between different points at the same elevation (more than 10−15 °C) indicate maldistribution. This technique can only be applied where temperatures vary greatly along the tower height. When the maldistribution is solely between the center of the tower and the circumference, wall temperatures at a given elevation may not vary much, but the wall may be either colder than expected (excess liquid near the wall) or hotter than expected (liquid deficiency near the wall).

For maximum effectiveness, the temperature survey should be applied at three different elevations: near the top of the bed, near the bottom of the bed, and near the middle of the bed [49b,50]. This procedure tracks the variation of the maldistribution pattern along the bed height. Also, measurements at one elevation provide a consistency check for those above or below.

Figures 2.18(b) shows the results of temperature surveys for one packed bed at four elevations [49b]. To the three recommended elevations, a fourth, above the reflux inlet, was added. The survey shows a cold spot on the northwest that persisted

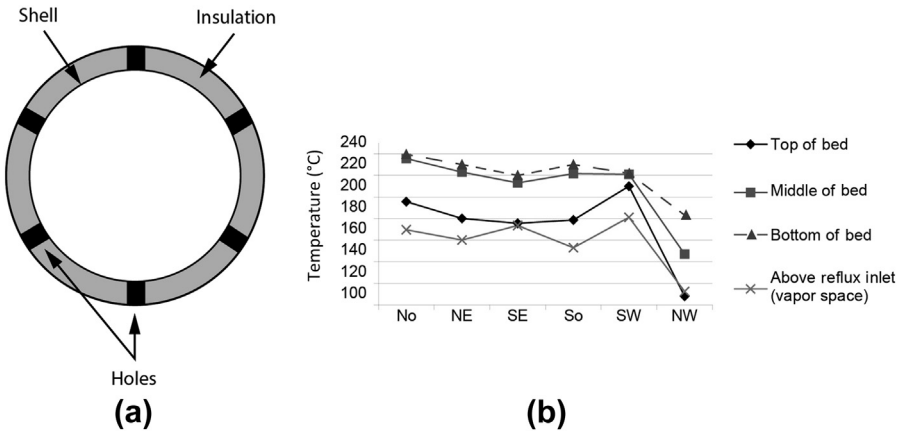

FIGURE 2.18 Circumferential Temperature Survey of a Packed Bed

(a) Holes cut in the insulation for wall temperature measurements (b) Measurements at four different elevations point.

Part (a) from H.Z. Kister, "Practical Distillation Technology," course manual, copyright © 2013; reprinted with permission. Part (b) from Ref. [49b]; reprinted courtesy of IChemE.

throughout the upper bed. That cold spot even extended to near the tangent line above the bed (above the elevation of the reflux inlet and distributor). Temperatures at the northwest near the top of the bed and above it were much closer to the reflux temperature of 87 °C than to the tower overhead temperature of 195 °C.

Besides the maldistributed profile, the temperature survey provided the major clue in the investigation. It showed cold, maldistributed temperatures near the top tangent line, as much as 80 °C colder than the overhead vapor temperature. This is very unusual and suggests that the apparently subcooled reflux is likely to have been sprayed upwards, with vengeance. This spraying led to the diagnosis of flashing of the reflux. Prior to the temperature survey, there was no basis to suspect flashing of the reflux.

In the cases described above, the success of the surveys is attributed to the validity and reliability of the measurements, as verified by many consistency checks. In contrast, unreliable temperature measurements lead to incorrect diagnostics. In one case, variations of more than 60 °C along the circumference of a crude tower wash bed, which were interpreted as maldistribution, were caused by incorrect surface temperature measurements. It is therefore critical to ensure the validity and reliability of the surface measurements. The key to a successful temperature survey is reliability, repeatability, and consistency. Here are some ideas for achieving these:

1. Check the expected temperature profile in the tower. If the temperature does not change much (less than 10−15 °C or so) over a section of tower, the inaccuracies in temperature measurement may be large compared to the temperature changes and a temperature survey will often be of limited benefits.

2. Check if there are any features that may preclude the use of temperature surveys. For instance, check if the section of tower is glass-lined or cladded with corrosion-protective material on the inside that may not conduct heat well. In cryogenic columns, holes cut in the insulation ice up rapidly and often do not permit reliable measurement.
3. Check for safety or environmental limitations on cutting holes in the tower insulation. If the tower has asbestos insulation, cutting the insulation is not permitted or requires major special procedures. In this case, the temperature survey may need to be abandoned. Confirm with your safety personnel that holes in the insulation can be safely cut and whether there are any special requirements.
4. It is important to avoid water ingress into the insulation. Such water ingress can lead to severe corrosion with both carbon steel and stainless steel columns (e.g. [59]). Holes cut in the insulation should have tight-fitting caps that close them and positively prevent water ingress when not in use.
5. Steady tower operation at the desired operating conditions is imperative for the success of a temperature survey. Process temperature changes during the survey are a common cause of temperature profile misinterpretation. The one exception here is when temperature surveys are used to study temperature variation at a given point as a function of time ("time studies"). This technique can be applied to study the source and nature of an instability, as has been demonstrated in one case study [57].
6. Calibrate your temperature measurement device. This is done by measuring surface temperatures next to every thermocouple in the tower. The thermocouple gives the fluid temperature inside the tower. It is anticipated that the inside temperature is somewhat higher than the wall temperature. Typically, when the inside temperature is 100 °C, the wall temperature is about 85−95 °C. A plot of wall temperatures next to all the thermocouples vs the thermocouples temperatures should be a smooth curve. This smooth curve will permit converting any measured wall temperature into an inside fluid temperature. Caution is required where the thermocouples stick some distance into a packed bed and may therefore read a temperature that this different from that at the wall. Check the thermocouple specs and do not include in the calibration if there is a reason to suspect that the wall and inside temperatures are different. There is often a discussion on what emissitivity to set the pyrometer at. Usually a high value, between 0.9 and 1.0 is selected. In the author's experience the value does not make much difference as the calibration will make up for any emissitivity errors.
7. Perform a preliminary temperature survey, proceeding in one direction. Then repeat, without looking at the previous results. Assuming the tower is stable, differences between temperature measurements at any given spot should not exceed about 3 °C. If they do, it suggests that there are some unresolved measurement issues. Keep repeating until your measurements are fully repeatable.

8. Another useful consistency check is to go up the tower in a team of three (or at least two). Involve an operator if possible. Each member of the team takes a reading without telling the others. Compare notes only after all members are done. The differences should be less than 1−2 °C.
9. Temperatures should consistently decline as one ascends the tower. Check this by measuring temperatures along the tower height in the region of interest. The temperatures should smoothly change with elevation. Investigate any "bumps" or "inversions" by a thorough study of the region where they are observed.
10. People often debate whether wind, rain, and sunlight affect wall temperature measurements. In the author's experience, when the insulation holes are not larger than about 80 mm in diameter, the impact of sun, wind, and light rain (which is not blown into the hole) has been minimal. Temperature surveys should be avoided during strong rain or other extreme weather conditions. Not only can the measurements be affected, but towers often become less steady (see items 4 and 5 above).
11. There are several other consistency checks. The more consistency checks are conducted, the greater confidence one has in the validity of the data.
12. In packed towers, circumferential temperature surveys should be conducted along at least two, and preferably three, elevations in the investigated bed. The case study in Figure 2.18 is an excellent demonstration of this procedure. This procedure provides excellent consistency checks of the measurements (data collected at one elevation needs to be consistent with those at the other elevations, as shown in Figure 2.18(b)). This procedure also yields the trends of the propagation of maldistribution, which give invaluable insights into the cause of maldistribution, as it did in that case study.
13. To perform an adequate packed tower temperature survey (per item 12 above), scaffolding is usually necessary. Scaffolding is expensive and requires special safety precautions, yet in the author's experience, necessary for obtaining reliable data. It has been the author's experience that short-cut procedures such as measuring fewer points or using a crane to access inaccessible spots leads to misleading data. Do not proceed with a packed tower temperature survey without adequate scaffolding and access.
14. When using infrared pyrometers, it is important to keep in mind that surface temperature is not uniform. Point-to-point temperature variations of more than 10−20 °C in the same insulation hole occur due to variations in surface texture and emissivity. It is recommended to take a multitude of measurements in each insulation hole and pick the highest consistent temperature measurement as the true wall temperature.
15. With infrared pyrometer surveys, it is important that each point reading focuses on a small point in the hole rather than spreads over an area containing higher and lower temperatures. For this reason, the measurements should be performed with a pyrometer that has a focusing mechanism, such as laser guidance or camera focusing.

Even though the pyrometer laser spot focuses on one point, the pyrometer averages the wall temperatures over a circle centered at that point. The pyrometer specs list the diameter of the circle. Circles 40 mm in diameter are unsuitable for tower wall temperature measurements. Standard pyrometers draw circles that are 20 mm in diameter and are suitable. High-accuracy pyrometers draw circles as small as 6 mm in diameters and are recommended. The circle diameter varies with the distance between the pyrometer and the tower wall. Generally, the pyrometer is held 150–300 mm from the tower wall. Some pyrometers actually show a light ring around the focal point to show the circle drawn on the tower wall.

16. With infrared pyrometer surveys, shiny surfaces have high reflectivity. Spray-paint the insulation holes with dull (nonshiny) black paint before the survey. If the wall is fabricated of stainless steel, make sure the paint is low in chlorides.
17. Watch out for changes of tower wall metallurgy. If such a change takes place, each section of tower needs to be calibrated separately because the emissivity changes with the metallurgy.
18. The limited experience available with temperature surveys on plastic-walled towers has not been good. The wall temperature of such towers tends to be much lower than the inside fluid temperature. For instance, when the tower temperature is 100 °C, the wall temperature is typically 50–70 °C due to the good insulation qualities of the plastic. We expect a similar argument to extend to glass columns.

2.14 Energy balance troubleshooting

Energy balances are particularly useful for identifying leaks, including internal leaks, entrainment, and insufficient reboil or reflux.

If the measured reflux rate is higher than the actual, the condenser duty based on this measured reflux rate is higher than the actual. An energy balance will show that the condenser duty and reflux are lower than inferred from the measured reflux rate. This may identify a reflux measurement issue where insufficient reflux is the root cause of a separation problem, such as in case studies 2.6 and 25.2 in Ref. [2]. Alternatively, if the reflux measurement is correct and the reflux is returned to the tower on level control from the reflux drum, the energy balance can identify flooding, with excessive liquid circulation in the reflux loop due to carryover from the tower top.

In direct contact cooling services, such as most refinery main fractionators, olefins, sulfur plant quench towers, and many other services, energy balances are the prime tool for identifying internal leaks or overflows. The example in Figure 2.19 demonstrates such application to the upper section of a refinery fuels vacuum tower. This section contains a pumparound, which is a direct contact total condenser (negligible vapor product) consisting of a packed bed and a total

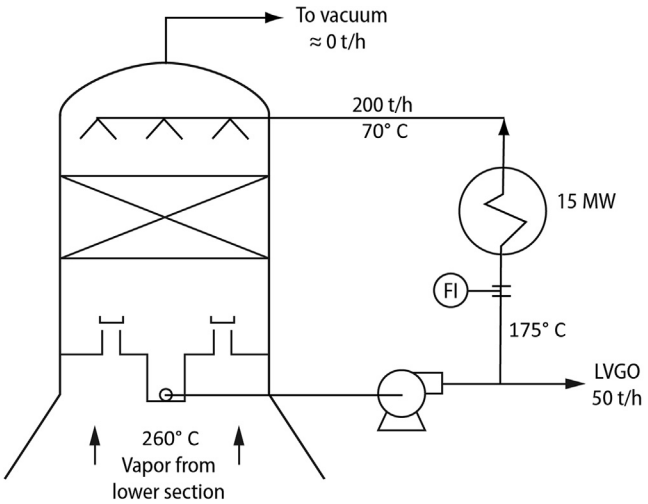

FIGURE 2.19 Energy Balance Application to the Top Section of a Refinery Vacuum Tower

From H.Z. Kister, "Practical Distillation Technology," course manual, copyright © 2013; reprinted with permission.

draw chimney tray underneath. Part of the liquid from the chimney tray becomes the light vacuum gas oil (LVGO) product, the rest is cooled and returned to the top of the packed bed where it cools and condenses the ascending vapor.

During troubleshooting, an energy balance was compiled on the upper section. Because it is a total condenser (the chimney tray is a total draw tray), the flow-rate of vapor in equals the flow-rate of LVGO product out. The LVGO section heat duty is therefore

$$Q_{\mathrm{LVGO}} = \left(H_{\mathrm{V},\,260^{\circ}C} - H_{\mathrm{L},175^{\circ}\mathrm{C}}\right)\cdot M_{\mathrm{LVGO}} = 0.43\,\frac{\mathrm{MJ}}{\mathrm{kg}}\cdot\frac{50,000\,\frac{\mathrm{kg}}{\mathrm{h}}}{3600\,\frac{\mathrm{s}}{\mathrm{h}}} \approx 6\ \mathrm{MW}$$

where Q_{LVGO} is the heat duty in MW; H_{V} and H_{L} are vapor and liquid enthalpies in MJ/kg; and M_{LVGO} is the LVGO product flow-rate in kg/h. Altogether, 6 MW were removed from the vapor in this section. The LVGO section heat duty can also be calculated from the heat removed in the coolers.

$$Q_{\mathrm{LVGO}} = M_{\mathrm{PA}}\cdot c_{\mathrm{p}}\cdot(T_2 - T_1) = \frac{200,000\,\frac{\mathrm{kg}}{\mathrm{h}}}{3600\,\frac{\mathrm{s}}{\mathrm{h}}}\cdot 0.0025\,\frac{\mathrm{MJ}}{\mathrm{kg}\cdot{}^{\circ}\mathrm{C}}\cdot(175-70)\ {}^{\circ}\mathrm{C} \approx 15\ \mathrm{MW}$$

where M_{PA} is the pumparound flow-rate (as measured on the flowmeter, Figure 2.19) in kg/h, c_{p} is the specific heat capacity in MJ/kg °C, and T_1 and T_2 are the pump-around return and pumparound draw temperatures, respectively, °C.

The heat removed by the coolers was much larger than that required to condense the LVGO product flow-rate. Instrument checks verified that none of the measured numbers was in gross error.

The energy balance is based on the assumption that all the vapor entering the LVGO section exits as LVGO product. This assumption is valid only if condensed liquid is not escaping some alternate route. There are two plausible alternate routes: entrainment from the top of the tower or leakage/overflow from the chimney tray. In this tower, entrainment from the top can readily be detected as liquid product ("slop") in the ejector steam condensate. In this tower, little slop was produced. This leaves leakage/overflow from the chimney tray as the only plausible explanation. The energy balance permits calculation of the leakage/overflow. At 0.43 MJ/kg, enthalpy difference between entering vapor and condensate (above), and a heat duty of 15 MW, the total amount of liquid condensed in the LVGO section is

$$M_{\text{condensate}} = \frac{15\ \text{MW}}{0.43\ \text{MJ/kg}} \cdot 3600 \frac{\text{s}}{\text{h}} \approx 125,000 \frac{\text{kg}}{\text{h}}$$

Therefore, a total 125,000 kg/h LVGO was condensed. Of this, 50,000 kg/h became the LVGO product. The balance leaked or overflowed down from the chimney tray. In this tower, the leaking or overflowing LVGO ended up in the lower section, where it lowered the bubble point, causing a bottleneck in the coolers of the lower section. Seal-welding of the chimney tray at the next turnaround solved the problem.

2.15 Drawing to-scale sketches at points of transition

Our tower malfunction survey [1], as summarized in Table 2.1, lists points of transition (tower base, packing distributors, intermediate draws, feeds) as one of the major causes of column malfunctions. In any troubleshooting investigation, it is imperative to closely review the relevant points of transition for a possible root cause of the problem.

The best technique for troubleshooting points of transition is to generate a sketch to-scale that will give a clear picture of how this point of transition is supposed to work. Then, draw the likely vapor and liquid patterns on the sketch and address the question, "Is it working like it should?".

Note that the author does not recommend just looking at the tower drawings. The tower drawings contain a multitude of details, many of which are not relevant to the functionality of the point of transition and to the troubleshooting assignment in question. Worse, the relevant details are usually scattered among several tower drawings and it is difficult to put together a clear picture. Clear sketches permit troubleshooters to take out the irrelevant details and focus on the important details. It is important that the sketches are drawn to scale. There is no need for high accuracy, but it is important to see the proximity of items to each other. Out-of-scale sketches may mislead. The sketches may include elevation and plan sketches, side views, whatever is needed to get a good definition of how the point of transition is supposed to work and what are the obstacles in the path of the vapor and/or liquid.

In the case study below [58], a sketch such as advocated here made the difference between the success and failure of a revamp. As part of the revamp to maximize capacity of a fluid catalytic cracker main fractionator, the two side product draw off-take trays were replaced by total-draw chimney trays. The purpose was to minimize reflux to the sections below.

The reflux was minimized by careful monitoring and control while eliminating any fluctuating leakage or overflow from the chimney tray above. It was most important to ensure that the chimney tray is a total draw. Any leakage or overflow would turn into liquid recycle that would be vaporized underneath and load up the tower. The tower capacity at the revamp conditions was extremely tight, and any vaporized recycle would have led to a capacity shortfall compared to design. To positively prevent leakage, the chimney tray was to be fully seal-welded.

The new chimney trays were designed as shown in Figure 2.20(a). Liquid, from the two-pass tray above, descended via side downcomers, which terminated in seal pans. All liquid from the chimney tray was drawn from a sump (not shown) located right beneath the chimney tray. The old downcomers from the take-off tray to the section below were converted to overflows by raising outlet weir heights from approximately 350 mm to 610 mm. Normal liquid level on the chimney trays was about 300 mm and the overflow downcomers were to be inactive. However, should an upset occur and the chimney tray liquid level exceed 610 mm, the liquid would overflow into the downcomers.

At the design stage, the seal pans and the chimney tray were on different drawings, which had been approved for fabrication. A last-minute drawing review put together the sketch on Figure 2.20(b), which revealed a major flaw. The gas issuing from the outside chimneys and blowing towards the tower wall would blow liquid descending from the seal pan directly into the overflow downcomers. Thus, despite the seal welding of the chimney tray, liquid would bypass it.

Figure 2.20(c) shows how the problem was circumvented. The openings of the outside chimneys that would blow gas towards the wall were closed. A 25-mm vertical drain lip was installed at the bottom of each seal pan to prevent the issuing liquid from crawling underneath and ending in the overflow downcomers.

The moral of this story: when it comes to troubleshooting points of transition (feeds, drawoffs, bottom sumps, chimney trays), you do not need an expert. You need a sketch.

2.16 Event timing analysis and reviewing operating charts

Item 7 in Section 2.3 highlights the importance of learning about the column and/or event history. The question, “What are we doing wrong now that we did right before?” is perhaps the most powerful troubleshooting tool available.

The most common technique is identifying the time when the problem initiated and simply plotting synchronized operating charts for key variables at around that time on a single plot. With the aid of this plot, carefully review the sequence of

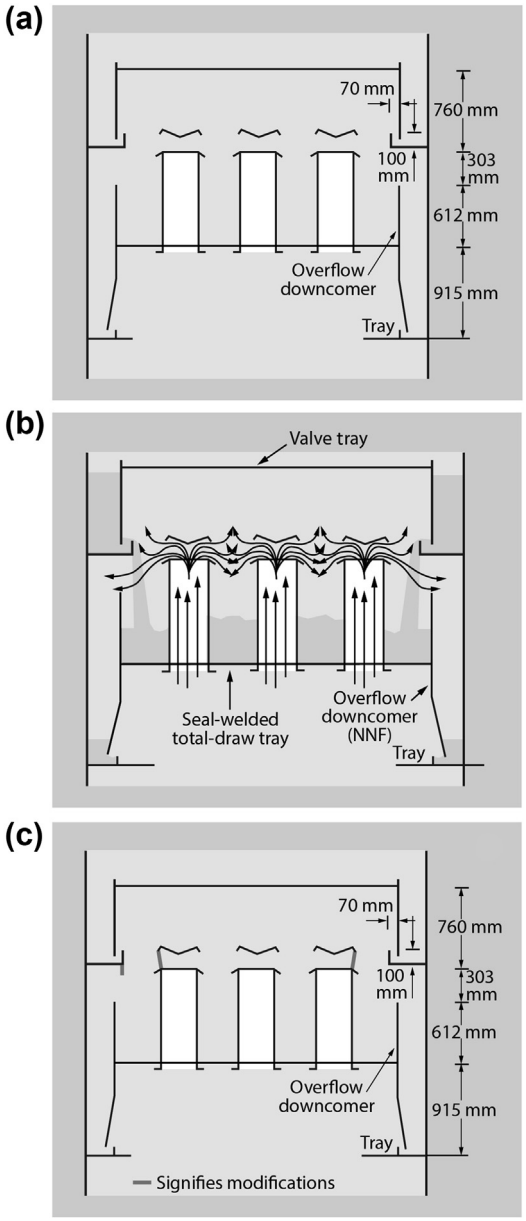

FIGURE 2.20 Total-Draw Chimney Tray Failing to Achieve Total Liquid Draw

(a) Initial design. (b) Expected flow pattern. (c) Modifications to circumvent liquid bypassing around the chimney tray.

From Ref. [58]; reprinted courtesy of Hydrocarbon Processing.

events. This type of analysis can reveal not only what the problem is but also what initiated it and how it progressed to give the apparent symptoms. This is illustrated by Case 8.3 in *Distillation Troubleshooting* [2], contributed by Mark Harrison.

The troubleshooter was called in to the control room because "the tower did not make on-spec products." A look at the operating charts (Figure 2.21(a)) showed that the tower was flooded. This is evidenced both by the ΔP rise and the reduction in bottom flow.

The operating team was aware that the tower was flooded. They stated that the tower products were off-spec even before the column flooded. Figure 2.21(a) shows the reflux coming up even before the tower flooded, obviously with the intent to improve product purity.

Rolling back the charts to the beginning of the reflux rise (Figure 2.21(b)) indicates that at that point the tower again was flooded. This is evidenced by the high ΔP, but this time the base level and bottom flow-rate were also high. With an ordinary flood, the bottom flow-rate and base level tend to decline as liquid accumulates in the tower.

Figure 2.21(c) shows the initial event. There was a temporary loss of the bottom pump. As a result, the base liquid level went up. The bottom level indicator initially showed a level increase, but then leveled off as it reached the maximum of its range. The liquid level kept on rising, now into the trays, as evidenced by the rise in the tower ΔP.

Some time later, the pump came back online and intensely pumped out the base liquid. The liquid accumulation in the tower ceased and the ΔP first leveled off, then started to decrease (Figure 2.21(b)). Soon after, the bottom level came back to normal. However, the ΔP did not fall back to normal; rather, it fell to a value below normal, suggesting some trays collapsed or were damaged during the high-liquid level event. At the same time, the reflux started increasing in order to meet the reduced purity with the reduced number of trays. Further increases in reflux and boilup brought the tower to flood (Figure 2.21(a)), still without getting the product back on-spec.

This case provides a classic illustration of the importance of studying the history of an event (or the tower) and the sequence of events.

2.17 Inspection: you get what you inspect

Assembly mishaps are in the fifth spot among distillation malfunctions [1]. In 1997, an earlier distillation malfunction survey [60] singled out assembly mishaps as the fastest growing malfunction, with the number of malfunctions reported between 1990 and 1997 more than double the number of malfunctions between 1950 and 1990. The good news is that this growth has leveled off. It appears that the industry took corrective action after noticing the alarming rise in assembly mishaps. Many major organizations have initiated systematic and thorough tower process inspection programs, and these are paying good dividends.

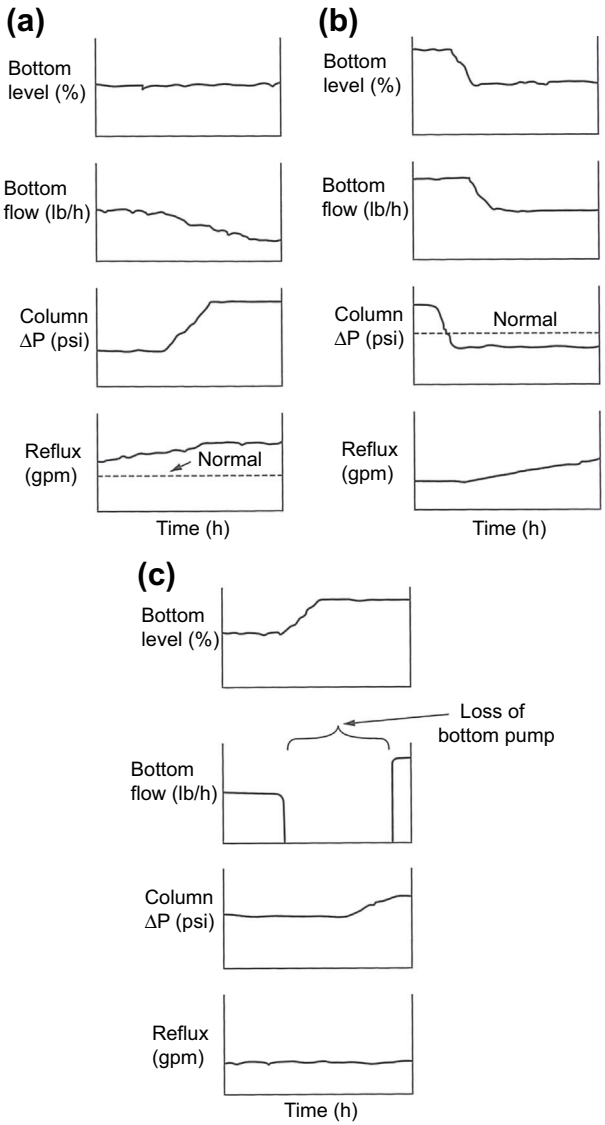

FIGURE 2.21 Operating Charts for High Liquid-Level Damage Incident

(a) Final charts, showing flood in tower. (b) Intermediate charts, showing rise of reflux following a flood incident. (c) Initial charts, showing high liquid level that caused tray collapse.

Table 2.3 Most Common Assembly Mishaps

No.	Cause	Cases
1	Assembly mishaps in packing liquid distributors	13
2	Incorrect packing assembly	13
3	Improperly tightened nuts, bolts, clamps	9
4	Incorrect assembly of tray panels	8
5	Flow passage obstruction and internal misorientation at tray tower feeds and draws	7
6	Leaking collectors and low liquid rate trays	7
7	Downcomer clearance and inlet weir misinstallation	5
8	Debris left in column	5
9	Tray manways, hatchways left unbolted	4
10	Materials of construction inferior to those specified	4

From Ref. [1]. Reprinted courtesy of the Institution of Chemical Engineers in the UK.

Assembly mishaps lead to poor separation, instability, lost capacity, and higher energy consumption, all with negative economic impact. In some cases, a tower may cease to work forcing a premature outage. Proper inspection following construction and during turnarounds is the best tool to identify installation mishaps, design oversights, fouling, and damage and to correct them before they turn into malfunctions. An ounce of prevention is better than tons of cures. Preventive troubleshooting emphasizes thorough process inspections.

Table 2.3 lists the most common assembly mishaps per our malfunctions survey [1]. The largest number of reported assembly mishaps is for packing liquid distributors. Most of these cases are recent. This is one area where inspections can be improved. Incorrect packing assembly is another major issue; it is more troublesome in some less common packing assemblies (e.g. breakage of ceramic random packing, collapse of poorly assembled grid beds, unsupervised installation of structured packings). Therefore, these should not reflect negatively on the majority of packing assemblies. The lesson is that the good practice is to have the supplier supervise structured packing installation (including the distributors), and to exercise special caution in specific situations like dumping ceramic packings, fastening grid, and when deciding whether to leave the tray support rings in the towers.

Improper tightening of nuts, bolts and clamps, and incorrect assembly of tray panels, are near the top of the assembly mishaps, and deserve to be on the checklist of every tower inspector. Debris left in the column, and incorrect materials of construction also belong on the same checklist. Other items that have been frequently encountered, and that process inspectors should focus on, include: flow passage obstruction and internals misorientation in feed and draw areas; leakage from "leak-proof" and "leak resistant" collector trays (these should be water-tested at turnarounds); downcomer clearances improperly set; and tray manways left unbolted.

Several recent papers (e.g. [61–64]) present several case histories of towers where inspection and turnaround testing identified potential and actual bottlenecks caused by improper internals installation, inadequate past inspection, fouling, and internal damage. In each case, the inspection led to problem identification followed by a simple, low-cost solution. The papers demonstrate that thorough and well-thought-out inspections often prevent major malfunctions in operation. When it comes to towers, you get what you inspect—not always what you expect.

References

[1] H.Z. Kister, What caused tower malfunctions in the last 50 years? Trans. IChemE 81 (Part A) (January 2003) 5.
[2] H.Z. Kister, Distillation Troubleshooting, John Wiley and Sons, NJ, 2006.
[3] H.Z. Kister, Distillation Operation, McGraw-Hill, NY, 1990.
[4] B.D. Smith, Design of Equilibrium Stage Processes, McGraw-Hill, 1963.
[5] M. Van Winkle, Distillation, McGraw-Hill, 1967.
[6] R. Billet, Distillation Engineering, Chemical Publishing Company, New York, 1979.
[7] H.Z. Kister, Distillation Design, McGraw-Hill, New York, 1992.
[8] N.P. Lieberman, Troubleshooting Process Operations, fourth ed., PennWell Books, Tulsa, OK, 2009.
[9] R. Sands, Thoughts on troubleshooting: tips from those who do it best, in: Distillation 2011: The Dr. James Fair Heritage Distillation Symposium, Topical Conference Proceedings, AIChE Spring National Meeting, Chicago, IL, March 13–17, 2011, p. 315.
[10] M.E. Harrison, J.J. France, Distillation column troubleshooting, Chem. Eng. (March 1989) 116. April 1989, p. 121; May 1989, p. 126; and June 1989, p. 139.
[11] C.S. Wallsgrove, J.C. Butler, Process Plant Startup, Continuing Education Seminar, The Center for Professional Advancement, East Brunswick, New Jersey.
[12] M. Gans, S.A. Kiorpes, F.A. Fitzgerald, Plant startup—step by step, Chem. Eng. (October 3, 1983) 74.
[13] A. Sofronas, Case 70: twenty rules for troubleshooting, Hydroc. Proc. (September 2012) 35.
[14] J. Ponting, H.Z. Kister, R.B. Nielsen, Troubleshooting and solving a sour-water stripper problem, Chem. Eng. (November 2013) 28.
[15] H.Z. Kister, D.R. Gill, Flooding and pressure drop in structured packings, Distillation and Absorption 1992, IChemE Symposium Series 128, p. A109, IChemE/EFCE, 1992.
[16] R.F. Strigle Jr., Random Packings and Packed Tower, second ed., Gulf Publishing, Houston, TX, 1994.
[17] H.Z. Kister, P. Mathias, D.E. Steinmeyer, W.R. Penney, J.R. Fair, Equipment for Distillation, Gas Absorption, Phase Dispersion, and Phase Separation, Section 14, in R. H. Perry and D. Green "Chemical Engineers' Handbook", eighth ed., 2008.
[18] R.G. Garvin, E.R. Norton, Sieve tray performance under GS process conditions, Chem. Eng. Prog. 64 (3) (1968) 99.
[19] D.W. Jones, J.B. Jones, Tray performance evaluation, Chem. Eng. Prog. 71 (6) (1975) 65.
[20] H.Z. Kister, R. Rhoad, K.A. Hoyt, Improve vacuum-tower performance, Chem. Eng. Prog. (September 1996).

[21] AIChE Equipment Testing Procedure, Trayed and Packed Columns: A Guide to Performance Evaluation, third ed., AICHE, January 2014.
[22] D.B. McLaren, J.C. Upchurch, Guide to trouble-free distillation, Chem. Eng. (June 1, 1970) 139.
[23] R.E. Kelley, T.W. Pickel, G.W. Wilson, How to test fractionators, Pet. Ref. 34 (1) (1955) p. 110, and 34 (2) (1955) p. 159.
[24] H.Z. Kister, Use quantitative gamma scans to troubleshoot maldistribution on trays, Chem. Eng. Prog. (February 2013) 33.
[25] N.P. Lieberman, Troubleshooting Natural Gas Processing, PennWell Publishing, Tulsa, Oklahoma, 1987.
[26] F.C. Silvey, G.J. Keller, Testing on a commercial scale, Chem. Eng. Prog. 62 (1) (1966) 68.
[27] T. Yanagi, M. Sakata, Performance of a commercial scale 14% hole area sieve tray, Ind. Eng. Chem. Proc. Des. Dev. 21 (1982) 712.
[28] H.Z. Kister, K.F. Larson, J.M. Burke, R.J. Callejas, F. Dunbar, "Troubleshooting a water quench tower", Proceedings of the 7th Annual Ethylene Producers Conference, Houston, Texas, March 1995.
[29] S.P. Bellner, W. Ege, H.Z. Kister, Hydraulic analysis is key to effective, low-cost demethanizer debottleneck, Oil Gas J. (November 22, 2004).
[30] H.Z. Kister, Can we believe the simulation results, Chem. Eng. Prog. (October 2002).
[31] H.Z. Kister, S. Bello Neves, R.C. Siles, R. da Costa Lima, Does your distillation simulation reflect the real world? Hydrocarbon Process. (August 1997).
[32] S. Opong, D.R. Short, "Troubleshooting columns using steady state models", in: Distillation: Horizons for the New Millennium, Topical Conference Preprints, AIChE Spring National Meeting, Houston, TX, March 14−18, 1999, p. 129.
[33] H.Z. Kister, Troubleshooting distillation simulations, Chem. Eng. Prog. (June 1995).
[34] L. Yarborough, L.E. Petty, R.H. Wilson, Using performance data to improve plant operations, in: Proc. 59th Annual Convention of the Gas Processors Associations, Houston, March 17−19, 1980, p. 86.
[35] G.J. Gibson, Efficient test runs, Chem. Eng. (May 11, 1987) 75.
[36] C. Branan, The Fractionator Analysis Pocket Handbook, Gulf Publishing, Houston, Texas, 1978.
[37] H.Z. Kister, E. Brown, K. Sorensen, Sensitivity analysis key to successful DC_5 simulation, Hydrocarbon Process. (October 1998).
[38] H.Z. Kister, Effect of design on tray efficiency in commercial columns, Chem. Eng. Prog. (June, 2008) 39.
[39] J.S. Charlton (Ed.), Radioisotope Techniques for Problem Solving in Industrial Process Plants, Gulf Publishing, Houston, Texas, 1986.
[40] J.S. Charlton, M. Polarski, Radioisotope techniques solve CPI problems, Chem. Eng. (January 24, 1983) 125 and February 21, p. 93, 1983.
[41] W.A.N. Severance, Advances in radiation scanning of distillation columns, Chem. Eng. Prog. 77 (9) (1981) 38.
[42] V.J. Leslie, D. Ferguson, Radioactive techniques for solving ammonia plant problems, Plant/Operations Prog. 4 (3) (1985) 144.
[43] R.L. White, On-line troubleshooting of chemical plants, Chem. Eng. Prog. 83 (5) (1987) 33.
[44] J.D. Bowman, Use column scanning for predictive maintenance, Chem. Eng. Prog. (February 1991) 25.

[45] M.E. Harrison, Gamma scan evaluation for distillation column debottlenecking, Chem. Eng. Prog. (March 1990) 37.
[46] S.X. Xu, L. Pless, Distillation tower flooding—more complex than you think, Chem. Eng. (June 2002) 60.
[47] S. Vidrine, P. Hewitt, Radioisotope Technology—Benefits and Limitations in Packed Bed Tower Diagnostics, Paper Presented at the AIChE Spring Meeting, New Orleans, Louisiana, April 25−29, 2004.
[48] W.A.N. Severance, Differential radiation scanning improves the visibility of liquid distribution, Chem. Eng. Prog. 81 (4) (1985) 48.
[49] [a] W. Mixon, S.X. Xu, Identify liquid maldistribution in packed distillation towers by CAT-scan technology, in: Distillation 2005: Learning from the Past and Advancing the Future, Topical Conference Proceedings, AIChE Spring National Meeting, Atlanta, GA, April 10−13, 2005, p. 375;
[b] H.Z. Kister, W.J. Stupin, J.E. Oude Lenferink, S.W. Stupin, Troubleshooting a packing maldistribution upset, Trans. IChemE 85 (Part A) (January 2007).
[50] R. Duarte, M. Perez Pereira, H.Z. Kister, Combine temperature surveys, field tests and gamma scans for effective troubleshooting, Hydrocarbon Process. (April 2003).
[51] F.J. Sattler, Nondestructive testing methods can aid plant operation, Chem. Eng. (October 1990) 177.
[52] D. Ferguson, Radioisotope techniques for troubleshooting olefins plants, in: 7th Annual Ethylene Producers Conference Proceedings, AIChE, 1995.
[53] J. Bowman, Troubleshoot packed towers with radioisotopes, Chem. Eng. Prog. (September 1993) 34.
[54] M.M. Naklie, L. Pless, T.P. Gurning, M. Ilyasak, Radiation scanning aids tower diagnosis at Arun LNG plant, Oil Gas J. (March 26, 1990).
[55] H.Z. Kister, Apply quantitative gamma scanning to high-capacity trays, Chem. Eng. Prog. (April 2013) 45.
[56] H.Z. Kister, H. Pathak, M. Korst, D. Strangmeier, R. Carlson, Troubleshoot reboilers by neutron backscatter, Chem. Eng. (September 1995) 145.
[57] H.Z. Kister, D.W. Hanson, T. Morrison, California refiner identifies crude tower instability using root cause analysis, Oil Gas J. (February 18, 2002).
[58] H.Z. Kister, B. Blum, T. Rosenzweig, Troubleshoot chimney trays effectively, Hydrocarbon Process. (April 2001).
[59] A.D. Jain, Avoid stress corrosion cracking of stainless steel, Hydroc. Proc. (March 2012) 39.
[60] H.Z. Kister, Are column malfunctions becoming extinct—or will they persist in the 21st century, Trans. IChemE 75 (Part A) (September 1997).
[61] R. Cardoso, H.Z. Kister, Refinery tower inspections: discovering problems and solving malfunctions, in: Proceedings of at the Topical Conference on Distillation, the AIChE National Spring Meeting, San Antonio, TX, April−May 2013.
[62] J.M. Sanchez, A. Valverde, C. Di Marco, E. Carosio, Inspecting fractionation towers, Chem. Eng. (July, 2011) 44.
[63] G.A. Cantley, "Inspection War Stories—Part 1", Presented at the Distillation Topical Conference, AIChE Spring National Meeting, Houston, April 1−5, 2012.
[64] E. Grave, P. Tanaka, The final step to success—tower internals inspection, in: Part 1 and Part 2, Proceedings of at the Topical Conference on Distillation, the AIChE National Spring Meeting, Houston, TX, April 22−26, 2007, pp. 533−547.

This page intentionally left blank

CHAPTER

Column Performance Testing Procedures

3

Tony J. Cai
Fractionation Research, Inc., Stillwater, OK, USA

CHAPTER OUTLINE

Distillation: Operation and Applications. http://dx.doi.org/10.1016/B978-0-12-386876-3.00003-X

3.1 Introduction

Distillation is a dominant separation process in chemical process industries, especially for mixtures that are usually processed as liquids [1]. It is expected that distillation will continue to dominate separations because it often has a distinct economic advantage at large throughputs. Over the years, researchers and engineers have learned a great deal about distillation that is well supported by a huge database of vapor and liquid equilibriums (VLEs).

Although significant progress has been made in computational fluid dynamics (CFD) as a useful design and development tool for improving distillation internals, for example, trays and packings, CFD must still be regarded as a tool that requires validation. The day when molecular modeling and CFD simulation will make experimental work unnecessary is still in the distant future. Until people can confidently simulate multiphase, turbulent fluid dynamics coupled with mass transfer, performance measurements of a distillation column will be necessary and important.

Though the general techniques and principles outlined here could be applied to a plant test, a large-scale experimental test, a pilot test, and a laboratory-size column test, it is not intended to cover the actual procedures and steps for testing and

troubleshooting an industrial column. For an industrial column performance testing and/or troubleshooting, the recently updated American Institute of Chemical Engineers Equipment Testing Procedure-Trayed and Packed Columns [2] thoroughly discusses the proper testing procedures and contains a wealth of information related to plant testing. Kister [3], Liberman [4], Hasbrouck et al. [5], and France [6] also presented useful information, ideas, and insights on the troubleshooting and testing of an industrial column.

Testing of distillation internals, trays and packings, remains the best and most reliable way of evaluating the performance of distillation equipment. Performance testing plays an important role in understanding distillation fundamentals, advancing distillation technologies, developing new internals, providing basic data for new designs, identifying column bottleneck(s), accumulating consistent and reliable data, and developing new advanced performance models. Testing is also the best tool for troubleshooting performance problems and validating computational simulations.

Performance tests provide consistent and reliable hydraulic and mass transfer experimental data. For a tray test, the hydraulic test data include tray hydraulic flood capacity, tray pressure drops, downcomer backup, tray liquid holdup, weeping rate, and entrainment; the mass transfer data include the maximum useful capacity (MUC) and tray efficiency. Similarly, for a packing test, the hydraulic data provide hydraulic flood capacity, pressure drops, and liquid holdup inside the packing; the mass transfer data include the MUC and the mass transfer efficiency. For packings, the mass transfer efficiency is usually represented by height equivalent to a theoretical plate (HETP). HETP and separation efficiency have an inverse relationship.

A performance test should be properly planned and executed. The execution of successful testing starts with planning, preparing, and choosing correct column configurations. Careful planning ensures that the testing objectives are met and maximizes the amount of useful information obtained. Choosing a proper test system is important in evaluating the performance of distillation internals. Since different internals have their most suitable applications, their performance needs to be tested and evaluated using different test systems. Once the test systems are chosen, the validated and consistent physical properties of the test systems are crucial for correctly interpreting test results.

Trays or packings and other hardware must be correctly installed and thoroughly inspected according to the test procedures and specifications. To evaluate the hydraulic and mass transfer performance of distillation internals, choosing the right instrumentation is critical to successfully measuring temperatures, pressure, compositions, and pressure drops. Locations and configurations of those instruments need to be correctly specified and designed before testing. The quality and accuracy of the data need to be analyzed. Test data need to be evaluated, interpreted, and presented using a consistent method and procedure.

This chapter provides general approaches, procedures, and guidelines for conducting, interpreting, and reporting performance tests of trays and packings. The main focus is to provide a collection of experimental techniques and principles

for conducting performance tests. The approaches, procedures, and guidelines in the chapter should not be used as a substitute for an equipment manufacturer's acceptance test.

3.2 Existing test facilities

There are several distillation test facilities around the world that are used to conduct distillation studies and performance tests. Those facilities, which are described in the given references, can be grouped into four different categories:

- Research facilities [7,8]
- Distillation equipment manufacturers' testing facilities [9,10]
- Production companies' testing facilities [11,12]
- University-based testing facilities [13,14]

For each of these facilities, no complete details on equipment parameters, test procedures, test systems, physical properties, and so on, have been published. Each testing facility has different test configurations and follows different testing procedures to conduct performance testing. Most facilities are operated only at total reflux mode, so the effect of liquid loadings on tray or packing performance for a given testing system cannot be measured. Furthermore, no complete details on instrumentation and column setup were reported.

Not having a consistent testing procedure or standard and a lack of consistent definitions or criteria for performance results make it difficult to compare the performance of different distillation internals [15].

3.3 Definition and terminology

To measure and report the performance of distillation equipment, it is necessary to have consistent definitions of terms associated with performance measurements, such as capacity, efficiency, pressure drop, and turndown ratio, among others.

3.3.1 Flooding

Flooding or flood of a distillation column is generally defined as the condition of column inoperability due to excessive retention of liquid inside the column. When a column is at the flood condition, there are multiple symptoms, such as the changes of the liquid level at the feed tank and at the bottom of the column, as well as a markedly increase of the pressure drop.

It is noted that the flooding definition of an air/water simulator may be different from that of a distillation column. With the air/water simulator, the flooding condition is usually defined by the amount of liquid entrained by the vapor, or percent of liquid entrained by the vapor.

3.3.2 Incipient flooding or maximum hydraulic capacity

Flooding is an inherently unstable condition. Once the column reaches the flood condition, continued steady operation becomes impossible. To collect experimental data, once the column approaches the flooding condition, the operator usually needs to reduce the column vapor/liquid loading slightly until the column can be operated without losing control. This condition is normally called the incipient flooding condition, or the maximum hydraulic capacity (MHC). All flooding data are actually logged when the column is at the incipient flood condition. Therefore, the MHC of a tray or packing is measured and reported as a point beyond which the column operation cannot be controlled or the column is inoperable.

3.3.3 Maximum useful capacity

The MUC is defined as the point where mass transfer efficiency starts to deteriorate because of the onset of the flooding condition. Sometimes it is also defined as the highest loading where the column can still be operated stably with acceptable overall column efficiency. The MUC can usually be determined from efficiency data. Therefore, it may be somewhat subjective.

The characteristic points indicating the MHC and the MUC of a trayed column and a packed column are illustrated in Figures 3.1 and 3.2, respectively. These figures show the typical pattern of measured efficiencies as a function of the vapor load, expressed as the socalled capacity factor C_V, which is defined later (Section 3.15.4.2).

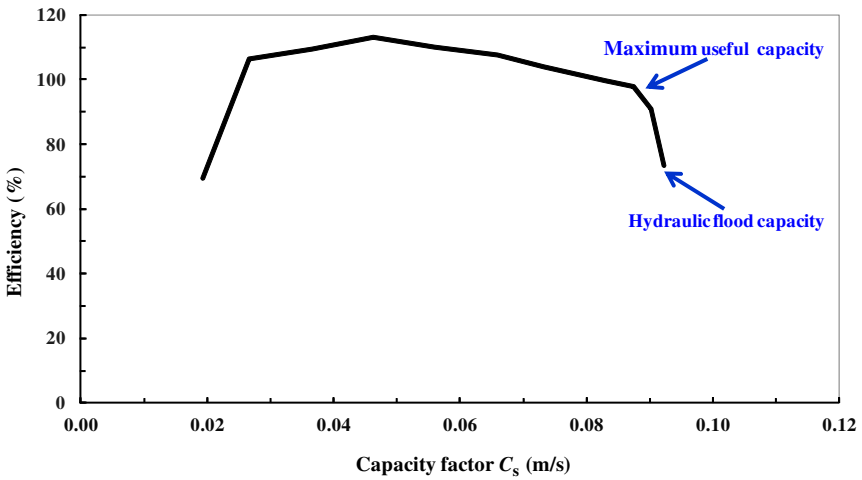

FIGURE 3.1 Hydraulic and Maximum Useful Capacities of a Trayed Column

(For a color version of this figure, the reader is referred to the online version of this book.)

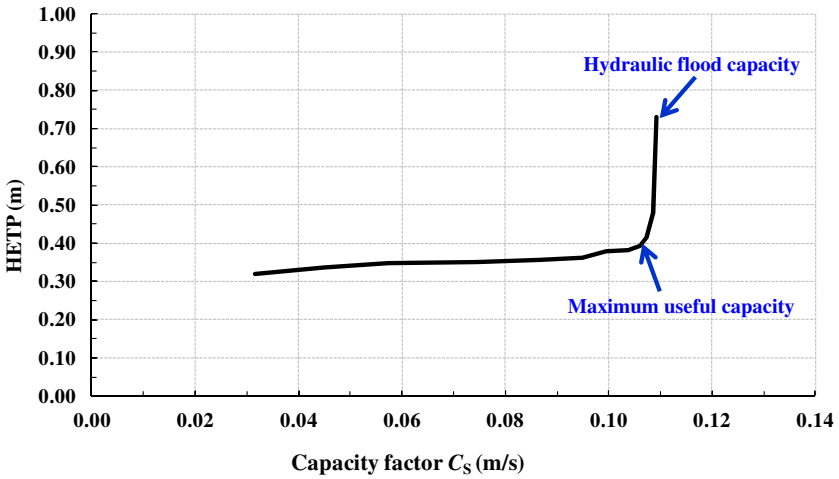

FIGURE 3.2 Hydraulic and Maximum Useful Capacities of a Packed Column

HETP, height equivalent to a theoretical plate. (For a color version of this figure, the reader is referred to the online version of this book.)

Depending on the test systems, the mass transfer efficiency may deteriorate long before the MHC is reached. At low liquid rates or low operating pressures, the MHC might be substantially higher than the MUC, which makes the MHC less reliable and less useable for column designs.

3.3.4 Efficiencies

For a trayed column, there are various definitions of efficiency.

Overall tray (column) efficiency, E_o (%), is defined as the ratio of the number of theoretical stages (N_t) to the number of actual stages or trays (N_a).

If the overall tray efficiency is similar for all sections of a distillation column, it is called the overall column efficiency E_{CO}. The overall tray efficiency is usually measured from column performance testing.

Apparent Murphree tray efficiency refers to the efficiency of a single tray. It can be measured by withdrawing samples of liquid or vapor entering and exiting the tray.

Murphree point efficiency is the Murphree efficiency at a single point on the tray.

The relationships among these various efficiencies can be found in Refs. [16,17].

3.3.5 Height equivalent to a theoretical plate

For a packed column, the HETP is normally used to evaluate the mass transfer performance of a packing. HETP is defined as a bed height where the mole fraction of vapor leaving the top of the bed is in equilibrium with the mole fraction of liquid leaving the bottom of the bed. HETP can be directly measured from performance tests.

3.3.6 Height of a transfer unit

Height of a transfer unit (HTU) is the height of packing required to obtain one mass transfer unit. It is a measure of the mass transfer efficiency. The relationship between the HETP and HTU is discussed in Section 3.15.4.4.

3.3.7 Hydraulics

Tray pressure drop is the head loss of vapor passing through a tray. The tray pressure drop is an important parameter for a trayed column design. It is usually expressed in terms of the unit of millimeters of hot liquid per tray.

Tray deck liquid holdup, or liquid head, is a measure of the liquid level on a tray. It is an important parameter when measuring tray performance because it affects tray efficiency, pressure drop, flooding, weeping, downcomer backup, and entrainment.

Tray downcomer backup measures the clear liquid head inside the downcomer.

Tray downcomer froth height is the height of froth inside the downcomer. The ratio of backup to froth height is normally called the average froth density inside the downcomer.

Weeping and weeping rate refer to the amount of the liquid flowing/weeping through the tray deck. If the pressured drop of the tray deck is insufficient to support the liquid head on the tray deck, some liquid on the tray will flow through the perforations on the deck to the next tray below without entering into the downcomer.

Entrainment refers to the liquid, usually liquid droplets, carried by vapor upward to the tray above or to the top of the packed bed. Entrainment is caused by high vapor velocity. It is detrimental to tray or packing efficiency. Excessive entrainment can result in column flooding.

Packed bed pressure drop is the head loss of vapor passing through a packed bed. It is an important parameter for packed column designs. Packed bed pressure drop is usually expressed in terms of millimeters of water or millibar per unit length of the packing.

Packed bed liquid holdup is the volume of liquid per volume of packing that drains out of the bed after the gas and liquid flows to the column are stopped. It is usually expressed in terms of liquid volume fraction inside the packed bed.

3.4 Test design and planning

A properly designed and prepared test program, as opposed to the "jump in and try something" approach, can lead to a more efficient test program, less overall cost, and better quality and more reliable test results.

3.4.1 Health safety and environmental considerations

A performance test must be conducted in a manner that protects public and occupational health, ensures environmental and employee safety, and strives to eliminate

all accidents and environmental incidents. Before any test, health safety and environmental (HSE) considerations should be a high priority when designing and planning tests. It should ensure that test complies with all HSE laws and regulations.

3.4.2 Test facility capacity vs tray or packing flooding capacity

With the advance of distillation technologies, distillation equipment now has higher flooding capacities. To test high-capacity trays or packings [18–20], the capacity of a test facility needs to be checked so that devices to be tested can be flooded. The boiling capacity of a reboiler, the cooling capacity of a condenser and a cooling tower, and the capacities of pump(s) must be adequate to flood the testing devices. If the facility capacity is not high enough to flood the equipment being tested for a particular system, an alternate test system may be considered.

3.4.3 Number of testing trays

The number of testing trays can be affected by various factors, such as the column height, the tray spacings, and the test systems. In general, 6 to 10 testing trays are required to avoid any possible end effects in conjunction with a hydrocarbon test system. However, for a system with very high relative volatility, fewer trays may be considered to avoid composition pitch problems and analytical difficulties.

3.4.4 Packed bed depth

The bed depth of a packed testing column is normally shorter than that of an actual industrial column. The bed depth needs to be carefully chosen to obtain consistent performance data.

In conjunction with a hydrocarbon test system, the bed depth for a test system with high relative volatilities will be shorter than that with low relative volatilities. During the test planning stage, the number of theoretical stages needs to be estimated based on the specific geometric area of the packing and physical properties of the test system. It is suggested that the number of theoretical stages of a packed bed be between 10 and 15 stages. However, if the test system has a high relative volatility, fewer theoretical stages need to be used to avoid having extreme purities at the top and bottom of the packed bed. A packing with a larger specific area will require less bed height to accommodate the same number of theoretical stages than a packing with a less specific area.

3.5 Mode of operations

Efficiencies and pressure drop of tested devices, as shown in the general form of trays and packings in Figures 3.1 and 3.2, are usually measured over the whole operating range. As shown in Figure 3.3, the performance diagram of a trayed column

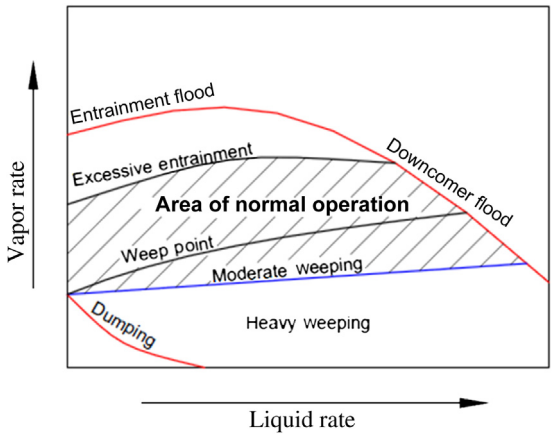

FIGURE 3.3 Typical Tray Performance Diagram

(For a color version of this figure, the reader is referred to the online version of this book.)

includes tray flood capacities, entrainment, weep point, weeping rate, and dump point. More details on tray performance diagrams can be found in Chapter 2 of (Book on Distillation, Book 2).

For a packed column, the performance diagram does not have any weeping or dumping curves. Figures 3.4 and 3.5 is a typical performance diagram of a packed column. Solid symbols in the diagram represent the flooding points at various liquid loadings. The mass transfer performance of a packed column is usually presented by HETPs at various vapor loadings, as shown in Figure 3.2. A lower HETP means higher mass transfer efficiency.

Most efficiency results of a distillation column are measured at the total reflux mode. Figure 3.6 shows the configuration of a column operating at total reflux conditions. The actual process diagrams can vary among test facilities, but they are operated with similar principles. In the total reflux mode, all condensate from the condenser is routed back to the top of the column as the reflux flow, that is, $L/V = 1$. The mass transfer efficiency of the distillation equipment depends on the ratio of liquid to vapor flow, L/V, inside the column. Operating a column at the total reflux mode avoids potential composition pinches and eliminates any possibility of error in the L/V ratio.

Since the amount of liquid holdup in the column increases while the column approaches the flood condition, the feed tank and the accumulator in Figure 3.6 provide the required surge capacities. If an oversized kettle reboiler is available, the reboiler can be used to provide extra surging capacities. If so, the feed tank in the figure may not be needed.

Pilot plants and testing facilities normally operate as closed systems that do not have net overhead and bottom streams. They usually do not operate with the feed in the middle of the column.

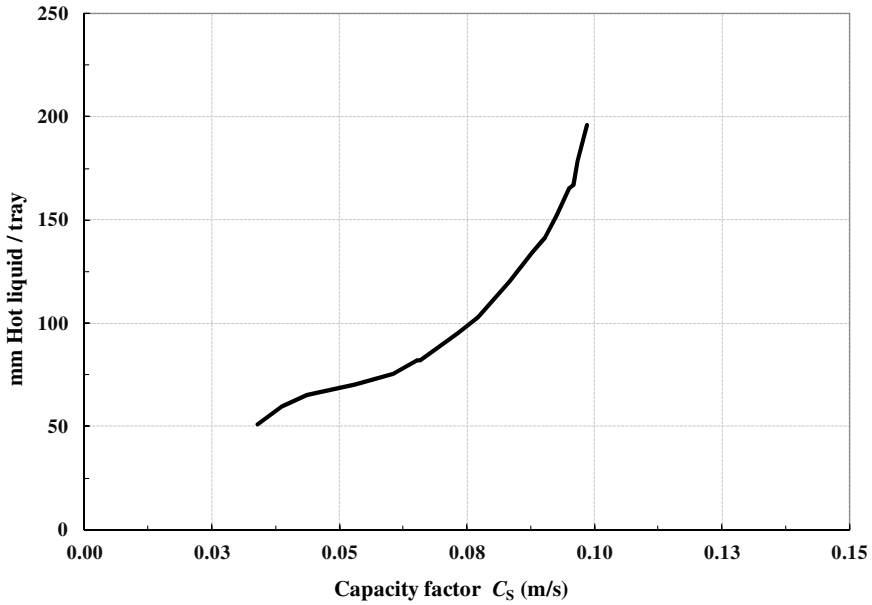

FIGURE 3.4 A Typical Tray Pressure Drop Curve

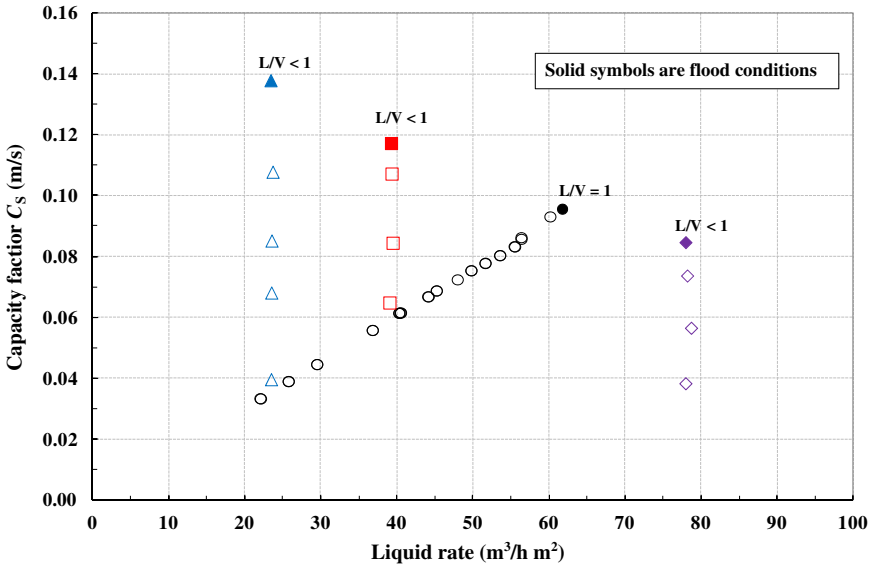

FIGURE 3.5 Typical Operational Diagram for a Packed Column

Solid symbols indicate flood conditions. L/V, ratio of liquid to vapor flow. (For a color version of this figure, the reader is referred to the online version of this book.)

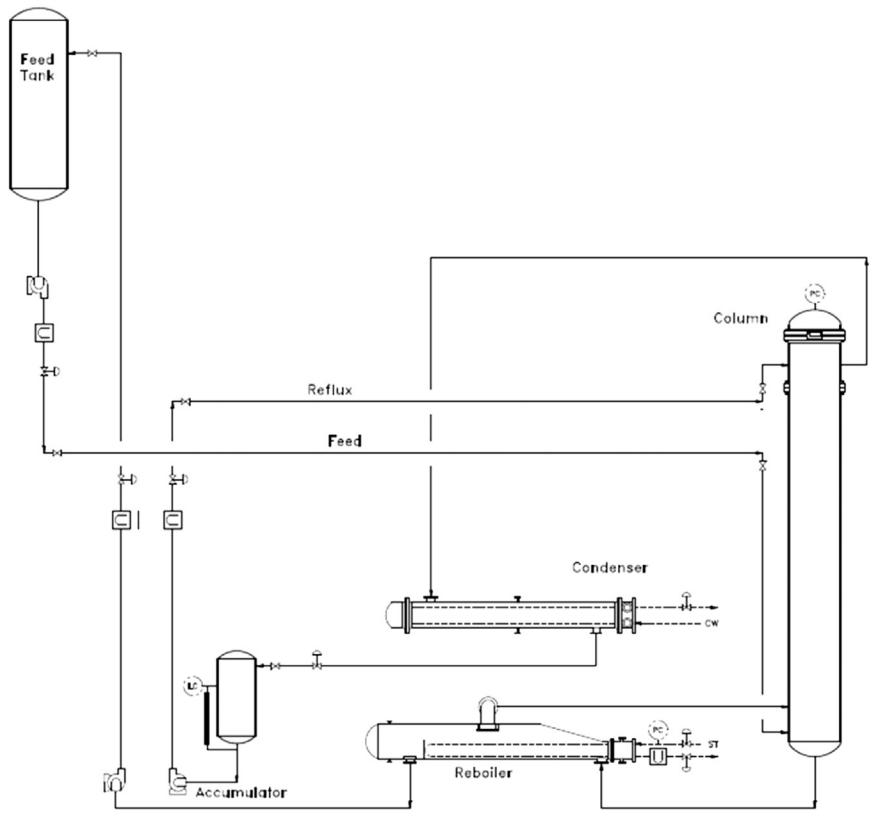

FIGURE 3.6 Distillation Column and Auxiliary Equipment at Total Reflux Mode

As a prominent distillation equipment testing and research consortium, Fractionation Research Inc. (FRI) has two industrial-scale distillation columns that can be operated at the total reflux ratio, as well as lower (L/V < 1) and higher (L/V > 1) liquid-to-vapor loading ratios (operating modes) with hydrocarbon and other distillation systems at pressures ranging from deep vacuum to 35×10^5 Pa [21].

To measure and evaluate the performances of trays or packings at different liquid-to-vapor ratios, it is necessary for a test column to simulate the operation of a rectifying section or a stripping section. The rectifying section is referred to as the section with an L/V < 1. Conversely, the stripping section is referred to as the section with L/V > 1.

At the rectifying operation mode, a portion of the overhead condensate is routed to the feed tank, and the rest of the condensate is returned to the top of the column as reflux. So, inside the column in this configuration, L/V < 1.

In the stripping operation mode, some of the liquid from the feed tank is pumped to the top of the column. The liquid from the feed tank combines with the condensate

from the condenser before they are all fed into the top of the column. Therefore, inside the column L/V > 1.

Non−total reflux operation modes are usually used for hydraulic studies to measure the flood capacities and pressure drops of a distillation column at constant liquid rates. There are very few non−total reflux test results available in the literature. Most of them were published by FRI [21−25].

3.6 Test column and auxiliary equipment

As shown in Figure 3.6, a distillation testing facility consists of a column, heat exchangers, vessels, pumps, piping, valves, and instruments. If a column is used for tray and packing testing, a column with a clean inner wall allows either trays or packings to be installed at any location inside the column. Sight windows strategically located along the column allow visual observations inside the column. Several column openings or nozzles are usually required along the column shell to allow access for sensors so that temperatures and pressures to be measured and liquid/vapor samples to be withdrawn.

The column height depends on the space occupied by testing trays and packings, liquid and vapor distributing devices, and the space at the top and bottom of the column. Extra space at the top, typically an additional 1.0−2.0 m, is required to allow for vapor and liquid disengagement. The bottom of the column must be high enough to serve as a liquid reservoir and provide adequate space for vapor inlet and vapor distribution. If the weeping rate and entrainment rate are measured, additional spaces are needed to install the necessary equipment. For a packed column, the vapor distributor or liquid collector below the packed bed may be needed. A packed bed also needs a liquid distributor to provide initial uniform liquid distribution. If a predistribution device is used at the top of the liquid distributor, additional space is required.

A reboiler is used to provide the necessary vaporization for the distillation process. A condenser is utilized to condense the vapor from the top of the column. An accumulator, or a reflux drum, is used to store the condensate/reflux so the liquid reflux can be recycled back to the column. The accumulator also provides the required surge volume. Most reboilers use high-pressure steam as a heating source. Other heat transfer fluids, such as hot oils, may also be used as the heating source.

It is important to size the reboiler and condenser according to the design capacity of a testing facility. A reboiler circuit has to be properly designed; the malfunction of the reboiler circuit is one of the main causes of operational problems in columns [26]. If a kettle reboiler is used as the surge volume of a distillation test column, it has to be oversized accordingly to accommodate the significant increase of liquid holdup in the column when the column approaches the flooding condition.

3.7 Reflux heating

Similar to industrial columns, the reflux in a distillation testing column is usually subcooled when it is fed into the column. Compared to the reflux at bubble point, the effect of the subcooled reflux on distillation performance may not be conclusive. The consensus among distillation researchers is that the subcooled reflux has little effect on separation efficiencies and capacities. However, the subcooled reflux does reduce the reflux flow rate feeding into the column. For a packed bed, that means the amount of liquid entering the liquid distributor will be less than the column's internal liquid rate. Therefore, the liquid distributor should be properly designed to ensure good liquid distribution at low liquid rates.

3.8 Test systems and physical properties

The physical properties of a system have a significant effect on the performance of trays and packings. One test system would ideally cover a wide range of process conditions and system properties. Unfortunately, it is difficult, if not impossible, to find such a system. In practice, several systems are required to test different types of distillation devices at operating pressures as close as possible to the actual ones.

3.8.1 Air/water system

An air-water system at ambient conditions is widely used for collecting hydraulic performance data for trays and packings, such as liquid holdup, pressure drops, entrainment, and capacities. One of the main problems with air−water systems is that it is difficult to collect efficiency data. To measure the efficiencies and the MUCs of packed and trayed columns, a distillation column test has to be conducted. This chapter mainly discusses performance tests with distillation systems.

3.8.2 Hydrocarbon systems

Binary hydrocarbon systems are test systems that are commonly used for distillation column performance testing. Various hydrocarbon systems can easily cover a wide range of physical properties and process conditions. The pure compound of a hydrocarbon system is available at a reasonable cost. Hydrocarbon systems are mostly noncorrosive, so they are ideal test systems for carbon steel equipment.

Para/ortho xylene (p/o xylene) is a good system for testing distillation internals at low pressures or low liquid rate conditions, such as structured packing testing. This system has been used often by FRI [27,28]. In Europe, a system with physical properties to similar those of p/o xylene, chlorobenzene/ethylbenzene (CB/EB), is widely used for testing structured packings. Using p/o xylene or CB/EB as the test system, physical properties and liquid/vapor loadings are similar along the test column [15].

Cyclohexane/normal heptane (C_6/C_7) is widely used for performance testing system operation at low to moderate pressures. Using this system, the liquid loading can be reached up to 50 $m^3/h\ m^2$ at 1.65×10^5 Pa operating pressure. The C_6/C_7 system has been adopted by both FRI [29,30] and the Separation Research Program [31]. This system can be used for testing trays and packings.

Testing tray performance requires a system that can be operated at high pressure and high liquid loading conditions. The ideal hydrocarbon system for this type of testing is iso/normal butane, iC_4/nC_4. This system is often used by FRI [32]. With the iC_4/nC_4 system, physical properties and liquid/vapor loadings at the top of the column and those at the bottom of the column are similar.

3.8.3 Aqueous systems

In addition to the hydrocarbon systems discussed above, aqueous systems also are used for testing the performance of trays and packings. The most commonly used aqueous test system is methanol−water. Other aqueous systems, such as acetic acid−water and propylene glycol−water, are sometimes used by distillation researchers. For aqueous systems, the boiling temperatures of the two components are generally very different, so the liquid and vapor loadings change significantly along the column. The relative volatilities of the aqueous systems are usually very high and are sensitive to composition. Compared to typical hydrocarbon systems, fewer theoretical stages are required for aqueous systems to achieve the same purities at the top and bottom of the column. To avoid having extreme purities at the overhead and the bottom flows in the column, fewer trays or short bed depths are required when testing aqueous systems.

3.8.4 Physical properties

To process and interpret performance test data, it is important to have validated and consistent physical properties of the test systems over the whole range of column operation conditions. Densities, viscosities, and surface tensions are needed for hydraulic calculations. Latent heat and heat capacities are required for heat transfer calculations. VLE data and diffusivities are required for column simulation and efficiency calculations. Accurate and reliable VLE data or correlations are a prerequisite for meaningful determination of theoretical stages. Tables 3.1−3.4 list the physical properties of commonly used test systems: p/o xylene, CB/EB, C_6/C_7, and iC_4/nC_4.

3.8.5 Composition range

For testing with a binary system, having a 50/50% mixture of the test fluid is a good practice. To obtain consistent results from different performance tests, it is necessary to maintain similar composition ranges from the overhead to the bottom flow streams. To avoid having extreme purities that may cause larger errors in composition analyses and VLE data, maintaining compositions of the more volatile

Table 3.1 Physical Properties of ortho/para Xylene

Items	Unit	Properties	Properties
Pressure	10^5 Pa	0.1	1
Liquid density	kg/m^3	821.76	761.43
Vapor density	kg/m^3	0.442	3.284
Relative volatility		1.235	1.165
Liquid viscosity	Pa s	3.86 E-4	2.42 E-4
Surface tension	N/m	0.023	0.017
Liquid diffusivity	m^2/s	0.363 E-8	0.687 E-8
Vapor viscosity	Pa s	6.98 E-6	9.10 E-6
Vapor diffusivity	m^2/s	0.219 E-4	0.036 E-4

Table 3.2 Physical Properties of Chlorobenzene/Ethylbenzene

Items	Unit	Properties	Properties
Pressure	10^5 Pa	0.1	1
Liquid density	kg/m^3	930.00	870.00
Vapor density	kg/m^3	0.409	3.233
Relative volatility		1.180	1.130
Liquid viscosity	Pa s	5.0 E-4	3.0 E-4
Surface tension	N/m	0.025	0.020
Liquid diffusivity	m^2/s	0.340 E-8	0.640 E-8
Vapor viscosity	Pa s	8.0 E-6	10.0 E-6
Vapor diffusivity	m^2/s	0.40 E-4	0.042 E-4

Table 3.3 Physical Properties of Cyclohexane/N-heptane

Items	Unit	Properties	Properties
Pressure	10^5 Pa	0.31	1.62
Liquid density	kg/m^3	680.64	641.02
Vapor density	kg/m^3	1.101	4.971
Relative volatility		1.1871	1.578
Liquid viscosity	Pa s	3.58 E-4	2.27 E-4
Surface tension	N/m	0.018	0.013
Liquid diffusivity	m^2/s	0.359 E-8	0.619 E-8
Vapor viscosity	Pa s	6.98 E-6	8.21 E-6
Vapor diffusivity	m^2/s	8.722 E-4	2.184 E-6

Table 3.4 Physical Properties of Isobutane/Normal Butane

Items	Unit	Properties	Properties
Pressure	10^5 Pa	6.9	11.4
Liquid density	kg/m^3	520.80	487.36
Vapor density	kg/m^3	15.910	28.689
Relative volatility		1.300	1.232
Liquid viscosity	Pa s	1.14 E-4	0.89 E-4
Surface tension	N/m	0.008	0.005
Liquid diffusivity	m^2/s	0.296 E-8	1.767 E-8
Vapor viscosity	Pa s	8.8 E-6	9.6 E-6
Vapor diffusivity	m^2/s	0.63 E-4	0.41 E-6

compound at bottom flow and overhead flow above 10% and below 90%, respectively, is suggested. If this is not the case, the number of theoretical stages needs to be reduced accordingly.

3.9 Preparing for installation

Preparation and installation are the important phases of a performance test. Trays or packings must be installed safely in a column. The process of installation must follow the test plan and column layout. Every step of the installation process should follow the procedure and meet specific requirements. Despite whether it is a packed or a trayed column, it is equally important to have the liquid and vapor uniformly distributed.

3.9.1 Vapor inlet

The pressure drops of a packed column are much lower than those of a trayed column. When testing the performance of a packed column, it is necessary to check whether the entering vapor inlet is adequate for proper vapor distribution. If a vapor nozzle is too close to the bottom of the packed bed, or if the vapor velocity in the return line is too high, a vapor distributor should be used to ensure uniform vapor distribution below the packed bed.

3.9.2 Vapor distributor and liquid collector

A vapor distributor below a packed bed is normally designed as the liquid collector as well. When the vapor distributor is used in a performance test, it needs to be designed to have a higher capacity than the packed bed so the vapor distributor will not limit the column's capacity. It is also important to make sure that the vapor will not entrain the liquid exiting from the bottom of the packed bed.

3.9.3 Packing amount

The amount of random packing is commonly measured by volume. Since material packs differently in a small shipping box or a large shipping container with square sides, ordering 10–20% more packings than the packed bed volume is recommended [33].

3.9.4 Liquid distributor and water test

Poor liquid distribution is the most common cause of unexpected poor separation efficiency in packed columns [34,35]. Researchers, academia, and industry have made a great effort to study the effect of liquid distribution on packing performances. Packing efficiencies vary greatly with the quality of liquid distribution. FRI and other independent testing groups have shown that both the number and the layout of distribution points are important for packing separation efficiencies. To consistently measure the true performance of a packing, a high-quality distributor should always be used to ensure that liquid is evenly distributed across the top of the packed bed.

A liquid distributor should never be installed in a packed column before it is water tested. If the distribution quality does not meet the quality specification, the distributor should not be used. The results of distributor water tests should be kept and documented in the test report.

3.9.5 Distribution quality

Various criteria have been used by researchers [27,36–38] to define the distribution quality of a liquid distributor. The coefficient of variation (CV) is commonly used. The CV is the dimensionless statistical analysis of point-to-point rate comparisons based on random selection and the measurement of drip point rates or groups of drip points. It measures the overall performance of a liquid distributor, including a predistributor, a liquid momentum breaker, and metering orifices. A liquid distributor is required to have a CV below 5%.

3.9.6 Drip point density

Pour point density is defined as drip or pour points per square meter. Pour point density requirements are related to the size and type of packing. A distributor with a pour point density of 100–150 drip points/m^2 is generally adequate for a distillation column.

3.9.7 Distributor open area for vapor flow

A liquid distributor needs to be designed to have an adequate open area for vapor flow. Otherwise, the distributor may limit the column flood capacity. Depending on the test systems, it is recommended that the distributor have 25–45% of the

column's cross-sectional area for vapor flow. In general, low-pressure test systems require a large open area.

3.10 Packed column installation

Before installing packings, care should be taken to ensure that the vessel is clean. The elevations of the different hardware need to be clearly marked and frequently checked during the installation process to ensure the correct depth of packing is installed and to ensure all hardware is correctly placed. Actual installation procedures vary with different packing types, but all procedures should aim for the same objective: achieving and measuring the true performance of the packings.

3.10.1 Installation of packing support grid

The packing support grid needs to be placed in the correct orientation to the vapor return nozzle. The grid needs to be leveled using either a carpenter level or a laser level.

3.10.2 Installation of liquid distributor

Correctly installing a properly designed liquid distributor is critical to obtaining the best performance from a packed column. Installation of liquid distributors greatly affects the performance of a packed bed. A distributor water test does not guarantee the distributor's performance in the column. The distributor must be carefully leveled during installation to ensure that the liquid uniformly spreads on the top of the packed bed. Water leveling is the preferred method for leveling the distributor. It's good practice to design a liquid distributor that has a built-in mechanism to adjust the level. The spacing between the bottom of the distributor and the top of the packing has to meet the specification.

3.10.3 Random packing

Random packing can be either dry packed or wet packed. Wet packing has been largely superseded except for ceramic packing, in which case it is necessary to avoid breakage. When a packing is packed wet, the packing is floated down through the column of water.

It is not necessary to pack metal packings wet. Test results of a wet packed bed and a dry packed bed showed little effect on packing separation efficiencies [34]. Methods of packing the test column should be established and applied consistently when a packing test is conducted.

The first half meter of packing should be installed by lowering the box or container into the column and emptying it from a distance close to the packing

support grid. Care should be taken to spread the packing elements uniformly around the support grids and over the column cross-section.

The bed limiter, or antimigration screens, must be used to keep the random packing elements from moving into the distributor during flooding or upset conditions. The bed limiter should not interfere with the liquid distribution.

3.10.4 Structured packing

Metal structured packing is generally installed in multiple layers. Each layer consists of several blocks that are sized to fit through a manhole. Before installing the packing inside the column, it is good practice to lay out at least one complete layer of the structured packing outside the column to ensure that the configuration is correctly understood and to check that the layer has the correct dimensions. The first layer on the support grid must be correctly oriented according to the vendor's specifications. Subsequent layers should be rotated according to the vendor's instructions. The orientation from one layer to the next is usually 90°. Most structured packings, if not all, have wall-wipers that are tack welded to the packing blocks. The wall-wipers should touch the column wall so that any liquid flows along the wall will be collected and directed into the packings.

The bed depth and elevations of the different hardware need to be clearly marked before being installed. The bed depth should be checked occasionally as the bed is packed to ensure that the height is consistent with the number of layers installed.

During installation, the installer should never walk directly on the structured packing. A metal plate or plywood should be used to spread the weight of the installer, as shown in Figure 3.7.

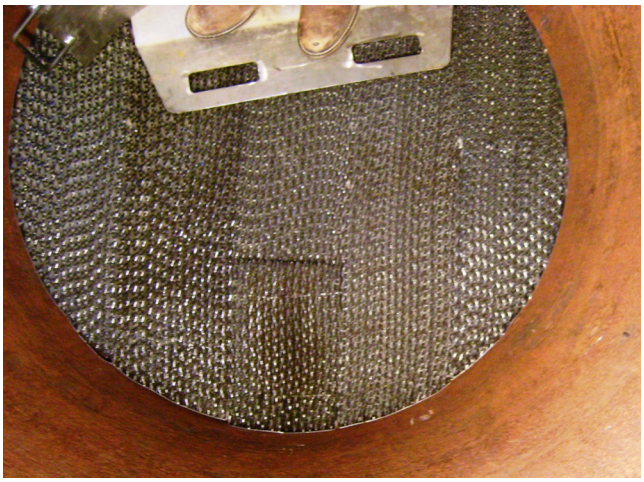

FIGURE 3.7 Metal Plate Used to Spread the Weight of the Installer

(For a color version of this figure, the reader is referred to the online version of this book.)

A packing retainer should be applied on the top of the packed bed so the structured packing remains in place during upset or flood conditions.

3.11 Trayed column installation

The same principles used when installing a packed bed should also be applied to tray installation. For tray installation, tray rings are normally used. It is critical to make sure tray rings are leveled and sealed with gaskets against the column wall so that liquid will not leak through the gaps between the ring and column wall. Otherwise, the tray efficiency and capacity will suffer.

It is good practice always to mock up the trays outside the column before actual installation to ensure that all parts fit together well. A tray mock-up helps to visualize how the trays are to be assembled together, identify potential problems, and fix any problems before installation. It also gives the installer the opportunity to check all tray parameters and find any potential discrepancies.

When trays are installed, tray decks need to be carefully leveled because distillation trays that are not level will not function properly. It is critical that the downcomer width, downcomer clearance, and the outlet weir height meet the design specifications. Like the tray decks, the downcomers, outlet weirs, and the inlet weirs need to be carefully leveled. For a tray with movable valves, all of the valves on the tray deck must move freely.

Trays are generally assembled from components of such size that they can be brought in and removed through a manway. Therefore, a trayed column contains trays assembled from panels. Where these panels join together, regions of possible leakage exist. To prevent leakage, joints may be gasketed.

In summary, installation is one of the most important and critical steps for a successful performance test. If trays or a packings are not correctly installed, the true performance of the devices will not be measured. In addition to correctly installed trays or packings, other auxiliary equipment, such as the feed pipe, liquid and vapor inlets, liquid and vapor distributors, and false downcomers, must also be designed and installed correctly.

3.12 Operation and measurements

3.12.1 Operations control

The effective and smooth operation of a distillation column is important for collecting accurate, consistent, and reliable performance data. Effective operation is determined by the control of many variables. General control principles and configurations are beyond the scope of this chapter and can be found in Chapter 1 [39].

The controlled variables, manipulated variables, and disturbance variables of a distillation test column may be different from those of a distillation production

column [40,41]. The typical controlled variables for a testing column are column pressure, accumulator level, reboiler level, and feed level. The manipulated variables are reboiler and condenser duties and sometimes condenser levels. The disturbance variables are changes in test conditions, condenser cooling water supply, and weather. Liquid level controls ensure the material balances of the test column. The pressure control ensures energy balance and mass transfer equilibrium. Pressure is usually regulated and controlled using the rate of water flow to the condenser. Increasing or decreasing the water flow rate alters the temperature of the condensing liquid and hence the amount of vapor in the column. This, in turn, changes the pressure in the column. The column pressure can also be controlled by manipulating the surface area of heat transfer, such as changing the condenser level or injecting inert gas to reduce the effective heat transfer rate of the condenser.

3.12.2 Hydraulic steady state

A hydraulic steady state refers to the condition where hydraulic parameters at any single point of a distillation column do not change over time. The hydraulic parameters include column pressures, pressure drops, liquid holdups, and flow velocities.

For a column performance test, operating conditions can be varied from flooding to less than 20% of the flooding. Whenever the operating condition changes, it takes time for the column to reach a hydraulic steady state. The time to steady state depends on the column operating pressure, type of testing devices, the amount of inventory inside the column, and the magnitude of the condition change.

Various parameters can be used to identify the hydraulic steady state. Pressure drops across the trays or the packed bed usually take longer to reach a steady state than other flow parameters do. For a distillation column, the most reliable and commonly used parameter of identifying steady state is the pressure drop across overall testing trays or the pressure drop across the overall packed bed. Once the column is set on a specified condition, it usually takes about 30−60 min to reach a hydraulic steady state. It could take less time to reach a hydraulic steady state if the testing column has a small diameter or a small amount of inventory.

3.12.3 Mass transfer steady state

The performance of a distillation column includes both the hydraulic and mass transfer performance. The hydraulic performance has to be measured after the column reaches a hydraulic steady state. Similarly, the mass transfer performance must be measured after the column reaches a mass transfer steady state, which refers to the condition at which the liquid and vapor at any point in the column reaches mass transfer equilibrium. Once the column is at a mass transfer steady state, the composition at any location in the column will be unchanged.

In general, it takes longer for a distillation column to reach a mass transfer steady state than a hydraulic steady state. The time to reach a mass transfer steady state

varies with the test system, operating pressure, testing device, column size, and amount of inventory.

3.12.4 Determining time to steady state

Before taking any performance data, the time to hydraulic steady state and the time to mass transfer steady state must first be determined. Since the time to steady state varies with the operating pressure and test system, it has to be determined experimentally. The time to hydraulic steady state can be determined from the pressure drop measurement. Plots of trends of pressure drops from the control system are normally used to identify the hydraulic steady state.

Although temperatures are sometimes used as the parameters for identifying the mass transfer steady state, they are generally not very reliable indicators, especially for test systems with close boiling points. The most reliable way to identify the mass transfer steady state is composition analysis data. Once the column is set on a specific condition and after it reaches a hydraulic steady state, liquid samples, preferably from the reflux and the bottom of the reboiler, can be analyzed at a specific time interval. Once the compositions do not change significantly between two consecutive samplings, the time to reach the steady state can be determined.

For a commercial-size column, it can take a long as 2−3 h to reach the mass transfer steady state. However, smaller columns may reach the mass transfer steady state more quickly.

3.13 Measurements

Reliable and consistent performance data depend greatly on flow rate, temperature, pressure, pressure drop, and composition measurements. The success or failure of a performance test is directly related to the accuracy and reproducibility of the measurement data, all of which can only be obtained after the column has reached a steady state condition. This section briefly discusses the general principles of those measurements and their corresponding instruments and provides basic guidelines for using those instruments. More details on the instruments can be found elsewhere [42].

3.13.1 Flow rate measurements

Flow rate measurements are crucial in determining the liquid and vapor loadings and the heat and mass balances of a distillation testing column. Determining the column throughput and capacity requires very accurate and reproducible flow measurements. Instruments to measure flow should introduce small flow resistances. Most flow instruments require straight sections of piping before and after the instrument to ensure a steady and fully developed flow. The flow meters discussed in this section are for clean fluid services.

There are various types of flow meters. Commonly used flow meters in a distillation column are pressure-based, electromagnetic, ultrasonic, and Coriolis flow meters, as well as laser Doppler flow meters.

3.13.1.1 Pressure-based meters

Pressure-based flow meters rely on Bernoulli's principle, deriving the dynamic pressure by measuring either the differential pressure within a constriction or the static and stagnation pressures. The relationship between flow rate and pressure difference is determined by the Bernoulli equation, assuming that changes in elevation and heat transfer are negligible. Venturi meters, orifice plates, and Pitot tubes are some of the commonly used pressure-based flow meters.

3.13.1.2 Electromagnetic, vortex, and ultrasonic flow meters

Electromagnetic flow meters, often called mag meters, use a magnetic field applied to the metering tube/pipe, which results in a potential difference proportional to the flow velocity perpendicular to the magnetic flux lines. The potential difference is sensed by electrodes aligned perpendicular to the flow and the applied magnetic field. Magnetic flow meters require a conducting fluid and generally do not work with hydrocarbon systems.

Vortex flow meters are based on the vortex shedding phenomenon. Within the flow meter, as flowing liquid moves across a tiny cylinder, vortices are shed but on a smaller scale. The frequency at which those vortices alternate sides is proportional to the flow rate of the fluid. Vortex flow meters transmit an ultrasonic beam through the vortex pattern downstream of the cylinder. As vortices are shed, the carrier wave of the ultrasonic signal is modified. This change in the carrier wave is measurable. Digital processing allows the vortex frequencies to be counted and converted into a flow velocity. A volumetric flow rate can be obtained using the measured flow velocity and the cross-sectional area of the pipe where the meter is installed.

Ultrasonic flow meters use sound waves to determine the velocity of a fluid flowing in a pipe. At no flow conditions, the frequencies of an ultrasonic wave transmitted into a pipe and its reflections from the fluid are the same. Under flowing conditions, the frequency of the reflected wave is different from that of the transmitted wave because of the Doppler effect. When the fluid moves faster, the frequency shift/difference increases linearly. The flow transmitter processes signals from the transmitted wave and its reflections to determine the flow rate. By using absolute transit times both the averaged fluid velocity and the speed of sound can be calculated.

3.13.1.3 Coriolis flow meters

Using the Coriolis effect that causes a laterally vibrating tube to distort, direct measurements of mass flow rate and fluid density can be obtained using a Coriolis flow meter (shown in Figure 3.8). Since mass is unaffected by variations in pressure, temperature, viscosity, and density, reasonable fluctuations of those parameters in the system will

FIGURE 3.8 Coriolis Flow Meter

(For a color version of this figure, the reader is referred to the online version of this book.)

not affect the accuracy of the flow meter. Coriolis measurements can be very accurate (0.05% of mass flow rate) irrespective of the type of gas or liquid that is measured. The same flow meter can be used for hydrogen gas and bitumen without recalibration.

3.13.1.4 Laser Doppler flow meter

Laser Doppler flow meters are a noninvasive method of measuring flow velocity. The meter is based on the Doppler effect [43]. A laser Doppler velocimeter, also called a laser Doppler anemometer, focuses a laser beam into a small volume of the flowing fluid that contains small particles (naturally occurring or induced). The particles scatter the light with a Doppler shift. Analysis of this shifted wavelength can be used to determine directly, and with great accuracy, the speed of the particle and thus a close approximation of the flow velocity.

In a distillation performance testing column, Coriolis flow meters, vortex flow meters, and orifice plate flow meters are commonly used. The Coriolis flow meter has the highest accuracy but is relatively expensive and causes large pressure drops. Coriolis flow meters have been used more often to measure the mass flow rate of a distillation testing column, especially for critical measurements such as the steam condensate and reflux flow. The orifice flow meter has a lower accuracy than the vortex meter but is very reliable since it has no moving parts that can wear out.

3.13.2 Temperature measurements

3.13.2.1 Types of temperature sensors

Process conditions and physical properties of a distillation column are directly related to temperatures that change with locations and operating conditions.

Temperatures must be accurately measured to obtain reliable process and performance data. Temperatures should be maintained within certain limits to ensure reliable, steady, and consistent operation.

In most cases, temperature sensors should be protected from process materials to prevent them from pressure and flow-induced forces and from the chemical effects of the process fluid. They should also be protected from interference in proper sensing and damage. Therefore, some physically strong and chemically resistant barriers are put between the process fluid and the temperature sensors. A commonly used barrier is a sheath or a thermowell. A thermowell is usually made from metal tubing. With the thermowell a temperature sensor can be removed, replaced, and calibrated as necessary without disrupting the process operation. When the sensor is removed or replaced during operation, caution needs to be taken and proper safety procedures have to be followed.

Thermocouples and resistance temperature detectors (RTDs) are the temperature sensors preferred for use in distillation columns because of their ruggedness and availability. Regardless of the type of temperature sensors, they must be checked and calibrated before taking any measurements.

Thermocouples provide a good balance of accuracy, reliability, and cost and so are one of the most widely used temperature sensors in process industries and pilot plants. Thermocouples are available in different combinations of metals. The four most commonly used types are J, K, T, and E, which are composed of nickel alloys [44]. Each type has its own measurement range, so the proper thermocouple needs to be selected for a specific application. RTDs are usually more accurate than the thermocouples but also are more expensive.

3.13.2.2 Temperature measurements in a distillation column

For a packed column, multiple thermowells usually are placed at different elevations inside the packed bed so the temperature distribution along the packed bed can be measured. If the column has a large diameter, or if the liquid distribution across the column cross section is a concern, multiply thermowells can be applied at the same elevation around the perimeter of the column to measure the radial temperature distribution. The degree of the temperature variations across the column cross section may give a good indication of the quality of the liquid distribution. Similarly, the temperature changes at various vertical locations are directly related to the mass transfer efficiencies.

For a trayed column, temperatures are usually measured in downcomers and tray decks. The downcomers are preferred locations for measuring liquid temperatures. If a conventional tray is tested, a receiving pan or seal pan under the downcomer is the ideal location of measuring the temperature because the thermowells are fully submerged at those locations. However, if a testing tray uses a truncated downcomer, the thermowell needs to be placed in the bottom of the downcomer, where a layer of clear liquid exists. Whenever the temperature is needed to calculate physical properties, the locations where the temperatures are measured should be close to where liquid or vapor samples are taken.

3.13.2.3 Temperatures at other auxiliary equipment

In addition to temperatures from the packings and trays, temperatures around the reboiler, condenser, feed flow, and reflux flow should also be accurately measured to determine the material and enthalpy balances, to calculate liquid and vapor loadings, and to determine the efficiencies and capacities of a packed or trayed column.

3.13.2.4 Liquid and vapor temperatures

Liquid temperatures are commonly measured in trays, packings, and other process streams. For a trayed or packed column, vapor temperatures are more difficult to measure accurately because of probable interference of the liquid phase. So the vapor temperature measurements are usually avoided. If the vapor temperature has to be measured, for example, in heat transfer studies, the thermowell needs to be specially designed to prevent liquid impingement. Figure 3.9 shows some of the possible designs for measuring vapor temperatures.

Those designs have been successfully used by FRI [45] in its extensive heat transfer studies of trays and packings. Measurements of vapor temperatures in the top of the column and the vapor return line are generally more accurate since no liquid interferences exist in those locations.

3.13.3 Accuracy and calibrations

All thermowells need to be inspected and calibrated before they are put into service. If it is not possible to calibrate the thermowell over the range of temperatures to be measured, the calibrations should be done against a controlled temperature source, such as an ice bath.

The accuracy of a thermowell depends on the type of sensor and the range of the temperature measured. When testing a typical distillation column, the accuracy of a thermocouple is about ± 1 K. The accuracy of an RTD can be as high as ± 0.1 K.

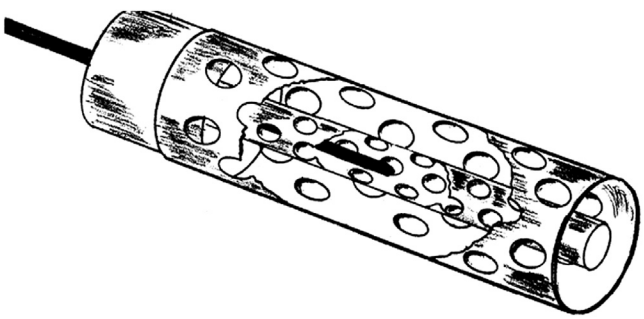

FIGURE 3.9 Thermocouple Shield for Vapor Temperature Measurements

3.13.4 Column pressure and pressure drop measurements

3.13.4.1 Column pressure

Pressure of a distillation column is normally measured at the top of the column. Fluctuations of the column pressure alter column vapor loadings and temperature and composition profiles. Therefore the column pressure should be accurately measured and closely controlled because its variations affect the column's performance. Details on effectively controlling column pressure can be found in Chapter 1 [39] and in the literature [40,41,46].

3.13.4.2 Pressure drops

Distillation applications require packings or trays with small pressure drops and high capacities and efficiencies, especially for vacuum applications. Pressure drops across trays and packings are one of the most crucial factors when evaluating the column's performance. Pressure drop measurements also play an important role in troubleshooting distillation columns since misleading or incorrect measurements are among the top 10 causes of column malfunctions [47].

To collect accurate and reproducible pressure drop data, it is necessary to carefully design the measurement system, including pressure taps, lines connecting to pressure transmitters, locations of the tap and transmitters, and calibrations. Various factors may affect the pressure drop results [48]. Selecting pressure transmitters and calibrations is the first and most important step but is beyond the scope of this chapter, which focuses on how to correctly measure, interpret, and use pressure drop results.

Causes of incorrect pressure drop measurements include the effects of column diameters, pressure tap sizes, locations, and vapor condensation. The static vapor head also affects the pressure drop data and column pressures.

3.13.4.3 Tray pressure drops and packed bed pressure drops

Figures 3.10 and 3.11 are typical column set-ups for tray and packing pressure drop measurements, respectively.

As shown in Figure 3.10, in addition to the overall pressure drop, the sectional tray pressure drops also are measured. When a column approaches the flooding condition, the pressure drop in the top half of the trays generally tends to be higher than that of the bottom half of the trays. Separation between those two sectional pressure drops, which occur at high vapor loads, as shown in Figure 3.12, is a good indicator for detecting the column flooding condition.

3.13.4.4 Instrument types and their accuracy

Although manometers are the most convenient and economic instrument for measuring pressures and pressure drops, differential pressure transmitters are recommended for distillation performance tests.

Various differential pressure transmitters are available. When choosing a pressure transmitter for performance testing, the accuracy, stability, reliability, safety, and range of the transmitters need to be considered and compared. Users should

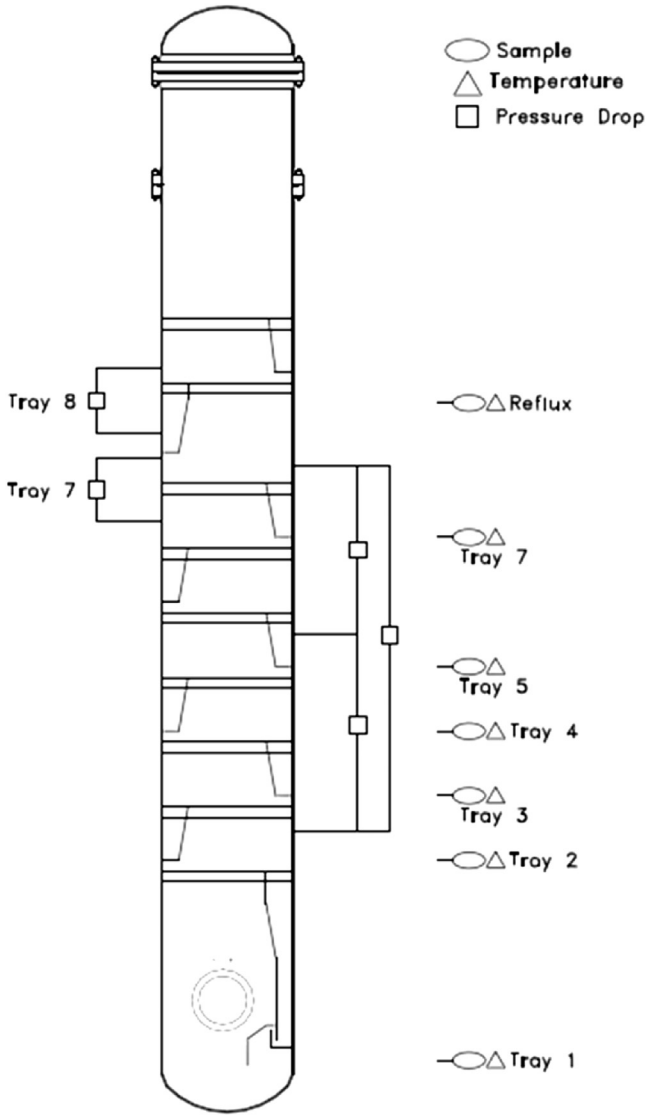

FIGURE 3.10 Typical Test Set-up for a Trayed Column

also consider the product quality and operational and maintenance costs. Most transmitters can be used in a variety of hazardous environments, so any potential safety problems need to be fully addressed.

The column pressure transmitter and differential pressure transmitters should be calibrated before they are installed and put into service. Modern pressure transmitters generally have an accuracy of $\pm 0.04\%$ of the range of the measurement, with

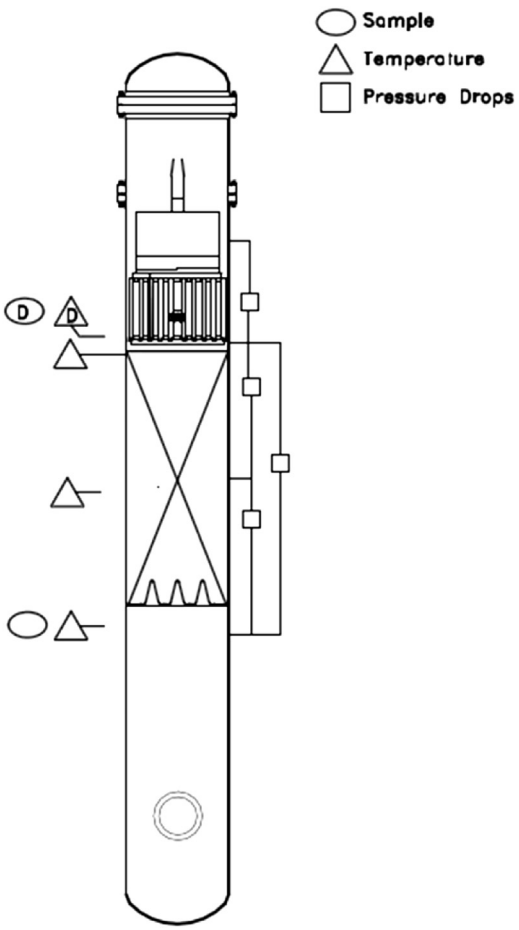

FIGURE 3.11 Typical Test Set-up for a Packed Column

high stability. Therefore, the actual accuracy of the column pressure and pressure drop results is most likely determined by other factors, such as pressure taps, column diameters, vapor condensations, and gas purges.

3.13.4.5 Pressure taps

Pressure drops are generally obtained using differential pressure transmitters that measure the difference of static pressures at two different locations. To accurately measure static pressure in a flowing vapor/liquid, static pressure taps on the column wall are typically used. The static pressure tap consists of a small hole drilled in the column wall, which is connected to a pressure transmitter via independent tubing. Errors in static pressure measurements caused by the tap will directly affect the column's pressure drop data [48].

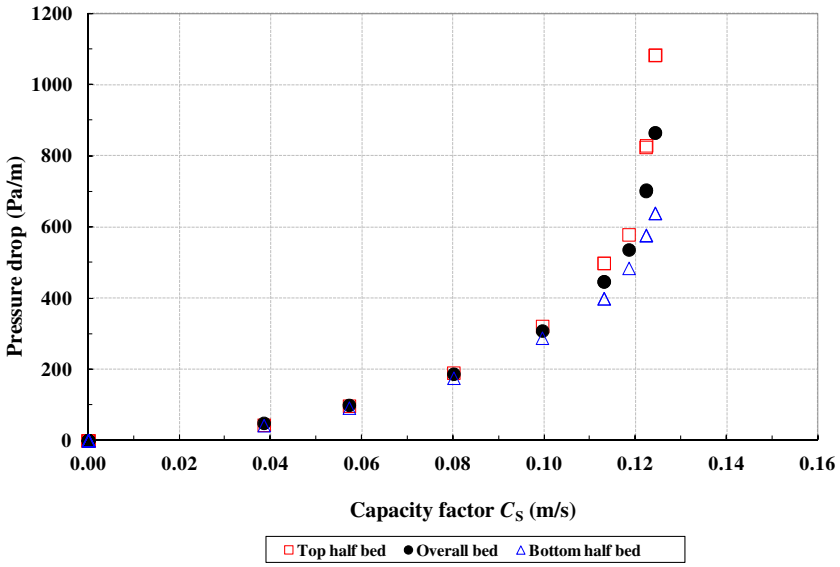

FIGURE 3.12 Sectional Pressure Drops of a Packed Column

(For a color version of this figure, the reader is referred to the online version of this book.)

As a practical guide, it is recommended [49] that taps used for the static pressure measurement have the following characteristics:

1. large and constant tap depth (h_{tap})-to-tap diameter (d_{tap}) ratio (at least h_{tap}: $d_{tap} > 2$) to make sure that the flow within the cavity (tap) is fully developed;
2. a small d_{tap}-to-pipe/column diameter (D_c) ratio to minimize the effect of tapping on flow stream;
3. for taps with a small h_{tap}-to-d_{tap} ratio (<2), a wide cavity behind the tapping is suggested to minimize the error.

The second type of error occurs if the static pressure tap is not flush with the wall or protrudes into the column. This may happen if, for example, the pressure taps are mounted incorrectly or the surface of the column wall is eroding or ablating. The larger the protruding length is, the bigger the error will be. Therefore, protruding taps should be avoided for column pressure drop measurements.

3.13.4.6 Column diameter

Researchers [34,50] found that column size affects pressure drops across a packed bed, but the effect is dependent on the packing. For random packings and small columns (<0.9 m), the smaller-diameter column presents lower bed pressure drops. This is most probably due to the effect of column wall, that is, a higher packing porosity in the wall zone than in the bulk of packing. Compared to

larger-diameter columns, small columns have a higher ratio of wall surface area to packing surface area. This may explain why pressure drops in small columns seem smaller than those in large columns. However, for structured packings, the effect of column size on pressure drops is opposite. Limited pressure drop data for structured packings [50] indicate that pressure drops measured in smaller columns are higher than those from larger columns. This may be caused by the relatively higher number of bends in vapor flow in a small column. I believes that wall-wipers with structured packings may also play a significant role, resulting in higher measured pressure drops in small columns.

3.13.4.7 Vapor static head and column pressure

The measured differential pressure between two pressure taps in a distillation column has two parts: The first is the static vapor head due to the weight of the vapor between the taps, and the second is the dynamic pressure drop due to the resistance of internals to the flow. The vapor static head needs to be corrected in pressure drop measurements. The static head is usually insignificant in a trayed column because of the relatively large pressure drop in the tray. However, the static head may cause serious errors for a packed column, especially for structured packings with a small pressure drop. When the operation pressure increases, the static head becomes a significant portion of the dynamic pressure drops. Thus it is necessary to correct the static head.

The column pressure is mostly measured at the top of the column. The existence of static vapor head in the column and pressure drops across the testing device will make the pressure at the bottom of the column significantly higher, especially for high-pressure trayed columns or for very tall columns. To calculate the local pressure, the pressure drop and the static vapor head need to be added to the pressure measured at the top of the column.

3.13.4.8 Vapor static correction and inert gas purge

Figure 3.13 shows a sketch of typical set-up for pressure drop measurements. No static head correction is needed if both legs of a pressure transmitter are filled by process vapor in the column. However, for a majority of distillation applications, the vapor condenses at ambient temperatures. The pressure lines are purged with a noncondensable inert gas, for example, nitrogen (N_2), so static vapor head correction is needed to get correct pressure drop results.

For a column set-up like that shown in Figure 3.13, the dynamic pressure drop in millimeters of water is given by

$$\Delta p_{\text{dynamic}} = \Delta p_{\text{meter}} - \left(\frac{\rho_{\text{v}} - \rho_{\text{N}_2\text{Amb}}}{\rho_{\text{w}}}\right) \cdot h_{\text{PL}} \tag{3.1}$$

where Δp_{meter} (millimeters of water) is the meter reading of the output of the pressure transmitter; ρ_{v} (kilograms per meter cubed) is the average vapor density over the section of pressure drop measurement, $\rho_{\text{N}_2\text{Amb}}$ (kilograms per meter cubed) is the density of N_2 at ambient pressure, ρ_{w} (kilograms per meter cubed) is the density

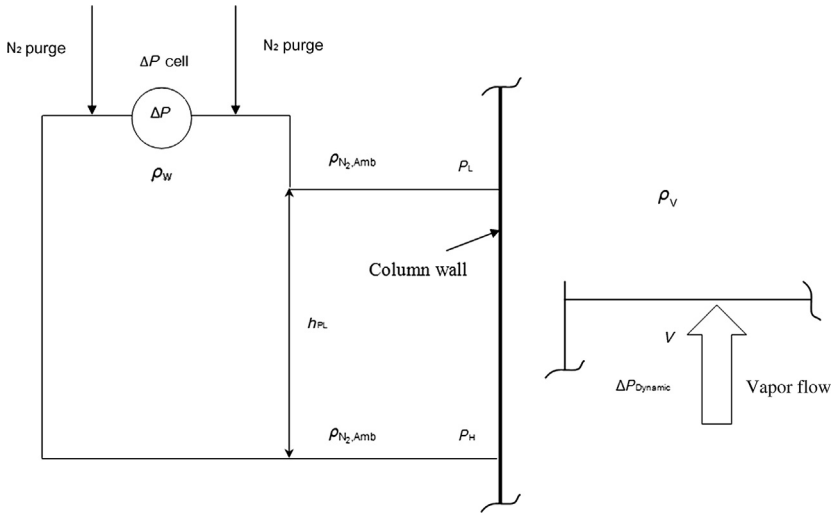

FIGURE 3.13 A Set-up for Measurement of Pressure Drops

h_{PL}, the distance between two taps (m); P_L, low static pressure tap; P_H, high static pressure tap; V, vapor flow.

of water, and h_{PL} (millimeters) is the distance between two taps of a pressure transmitter.

3.13.4.9 Tap locations

Pressure taps should be correctly placed to accurately measure pressure drops. Pressure taps preferably should not be placed too close to vapor inlets or outlets. It is important to make sure that any vapor condensation in the line flows back to the column to avoid its effect on pressure drop measurements. In practice, all pressure taps need to be placed below the pressure transmitter. It is suggested that an inert gas, such as N_2, be used to equally purge each line to make sure there is no vapor condensation inside the line. A picture of a differential pressure transmitter and N_2 purge lines can be seen in Figure 3.14.

Any changes in local flow profiles will affect the static pressure. If pressure taps are placed at locations with very different local velocities, the measured pressure drops need to be corrected according to the vapor velocity changes. Column diameter change, vapor side-draw, hardware below or above the pressure taps, among other properties, will affect the local flow profile.

3.13.4.10 Checking for leakage of lines and fittings

Pressure drop results will be impaired if there are any leakages on the lines and fittings. Pressure taps, tubings between the taps and pressure transmitters, adapters, and other fasteners must be checked for leaks before they are put into service.

FIGURE 3.14 Differential Pressure Transmitter and Nitrogen Gas Purge Lines

(For a color version of this figure, the reader is referred to the online version of this book.)

Photo courtesy of Fractionation Research, Inc.

3.13.5 Composition measurements

A successful distillation performance test is directly related to and greatly depends on the accuracy of the composition measurements. It is definitely necessary, if not imperative, that each sample be completely representative of the stream from which it is taken. The sample must be delivered to the analyst or analyzer without any loss or contamination. Since proper sampling requires great care, the proper procedure should be followed and be carried out under the direct supervision of the engineer responsible for the performance test.

Samples should be withdrawn from the test column during a single phase. Vapor samples are rarely taken for composition analysis because it is difficult to take a good representative sample of vapor. Vapor samples usually condense in the sampling line and sampling device. Vapor samples also are difficult to handle and analyze. Therefore, liquid samples are normally withdrawn and analyzed in distillation performance tests. If a vapor sample must be used, it works best if the vapor sample is routed directly to the composition analyzer via sampling tubing, such as an online sampling system.

Proper sampling techniques are required when taking representative liquid samples. As with temperature measurements, liquid samples should be withdrawn in the well-mixed part of the distillation process. Gas chromatography (GC) is usually used to analyze the composition of liquid samples. GC should be calibrated with known test mixtures (standards) using the fluids used in the performance tests.

It is suggested that duplicate samples be taken under the same process conditions to verify the sampling and analytical technique and steady state. When samples are taken from the column's internal or liquid stream, care should be taken so that the

sampling process does not alter or upset the steady state of the mass transfer process in the column. It is important that sampling does not upset the process material balance and phase ratios. This is even more important if the performance test is conducted in a small column that has a small amount of inventory in the system.

Liquid or vapor samples may be under pressure and hot, or they may flash. The samples may be toxic or react with air or water. Therefore, sampling should be done only by trained personnel with the proper personal protective equipment.

3.13.5.1 Sampling locations and samplers

Selecting proper sampling locations is crucial for obtaining representative liquid samples. Pump outlets, the bottom of the column, the reboiler, and the feed tank, as well as the reflux line, are preferred locations for collecting well-mixed and representative liquid samples. To measure tray and packing efficiencies, liquid samples in a distillation column should also be taken.

For a packed column, if a liquid collector is used, the samples of liquid exiting the packed bed can be taken from the collector. If not, samples of liquid exiting the packed bed can be collected from samplers directly under the packing support grid. A cross-sampler, as shown in Figure 3.15, is usually installed right below the support grid to catch the liquid sample [51].

The cross sampler has four arms that slightly slope toward the center. Liquid collected by the four arms is mixed and withdrawn from the center of the sampler. For a packed bed with random packings, this type of sampler can also be used to collect liquid samples inside the bed. For a packed bed with structured packings, bayonet samplers can be inserted into the packed bed to withdraw the liquid samples inside the bed. The best place for collecting liquid samples entering the packed bed is from the liquid distributor or predistributor.

For a trayed column, the liquid samples should be taken where clear liquid exists. For a conventional tray with a receiving pan or a seal pan, a sample of well-mixed liquid can be obtained from the bottom of the receiving pan or seal pan. For trays

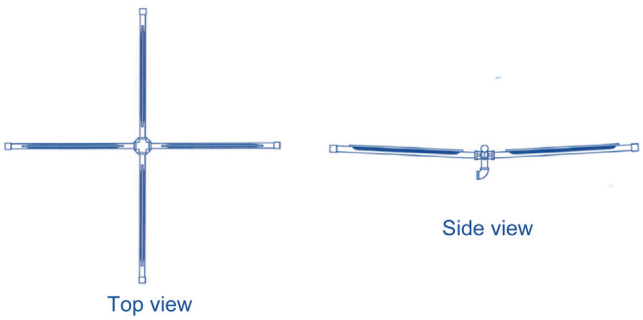

FIGURE 3.15 Cross Sampler

(For a color version of this figure, the reader is referred to the online version of this book.)

Image courtesy of Fractionation Research, Inc.

with truncated downcomers, the liquid sample can be taken from the bottom of the downcomer, where a layer of clear liquid exists. For trays without downcomers, such as a dual-flow tray, samples of liquid from the tray deck can be withdrawn and collected using a sampling cup attached to the bottom of the tray deck. The cup should be deep and large enough to provide a vapor-liquid disengaging volume.

Composition and temperature are needed to calculate the physical properties, enthalpies, and VLE of the test system. Therefore, it is important to measure the temperature and composition at the same location. The temperature should be measured at the same location from which the liquid sample is taken. If it is not possible to do that, the temperature sensor should be placed as close as possible to the sampling location.

3.13.5.2 Sampling techniques

Before taking any liquid samples, sampling bombs, sampling lines, fittings, and other auxiliaries related to sampling need to be closely checked for leaks. Any leaks in the sampling system will impair the composition measurements. To obtain a well-mixed and fresh liquid sample, it is necessary to purge the sampling line and sample bomb with fresh liquid. To reduce the need for purging large amounts of material, small sample lines, preferably 3−6 mm in diameter, should be used. The sampling line should also be as short as possible. If the permanent block valve at the sample outlet is too large to give the necessary control during withdrawal of the sample, a small valve should be installed downstream from the block valve. This will be subsequently used as the sample valve. A cooling coil, usually 6-mm tubing in an open container filled with coolant, is used to avoid liquid flashing during the sampling process. The cooling coil should be placed between the block valve and the sampling valve.

3.13.5.3 Composition analysis

Samples should be analyzed as soon as possible to minimize any composition changes due to potential leakage and/or evaporation. If the liquid sample is not under pressure, it will usually be transferred to a small sample vial for composition analysis. If the sample is under pressure, a special sample injection system needs to be used. Details of composition analyses are beyond the scope of this chapter. They can found from various publications or from GC vendors [52,53].

After samples are analyzed, it is good practice to store them in a refrigerator for probable further review. It is suggested that all liquid samples be kept until the performance test is completed and test report is issued.

3.13.6 Holdup and backup measurements

3.13.6.1 Packed column liquid holdup

Liquid holdup is one of the key parameters for hydraulics and mass transfer calculations in packed columns. It is defined as the volume of liquid held per volume of the packed bed under operating conditions. The residual fraction of the liquid in the

packing, after liquid drainage has stopped, is referred to as static liquid holdup. The liquid held in the packing during the operation is called total liquid holdup. The difference between the total holdup and the static holdup is referred to as the dynamic holdup. The total liquid holdup is usually measured during the performance test.

The liquid holdup in the packing is measured either by volumetric or gravimetric measurements and, in recent years, by gamma ray absorption measurements. For volumetric measurements, all feed lines are shut off simultaneously after reaching a hydraulic steady state condition and the amount of liquid draining from the packing is collected. This technique is simple to handle and very reliable. This technique works well with air/water systems. Using this technique, the amount of liquid volume in the liquid distributor has to be known and subtracted from the total amount of liquid collected. However, it is difficult—practically impossible—to conduct this type of measurement in a distillation column.

Similar situation is found with gravimetric measurements, where a scale is attached to the packing or the column section. This technique can measure the total liquid volume of the packing as well as the static liquid holdup. Again, it may be used only for air/water testing.

Gamma ray absorption is well known as a diagnostic and troubleshooting tool in the analysis of distillation column performance [54–56]. As experienced in recent years at FRI, with a stronger gamma ray source, it is also a very useful and powerful tool to measure the liquid holdup in a packed bed. A more detailed overview is given later, in the section "Gamma Ray Scanning".

3.13.6.2 Froth density, liquid head, downcomer backup measurements in trayed columns

Froth density, or liquid volume fraction, is an important parameter for determining downcomer backup and tray holdup. In the past, forth density has been determined from the combination of manometer readings and visual observations. Figure 3.16 is a schematic diagram illustrating the measurement of the clear liquid backup, h_{DC}, inside a downcomer.

A similar configuration can be used to measure the liquid head on tray decks. The froth height, h_f, in a downcomer or on a tray deck is usually measured/estimated by visual observations. The froth density or liquid volume fraction, Ψ, can be calculated from the liquid head and froth height, as follows:

$$\Psi = \frac{h_{DC}}{h_f} \tag{3.2}$$

Gamma ray scanning recently has been used more in distillation performance tests, such as measuring the froth density, liquid holdup, and downcomer backup.

3.13.6.3 Gamma ray scanning

Gamma scanning is not intrusive so it does not affect the hydraulics and mass transfers inside the column. When troubleshooting a column, compared to gamma

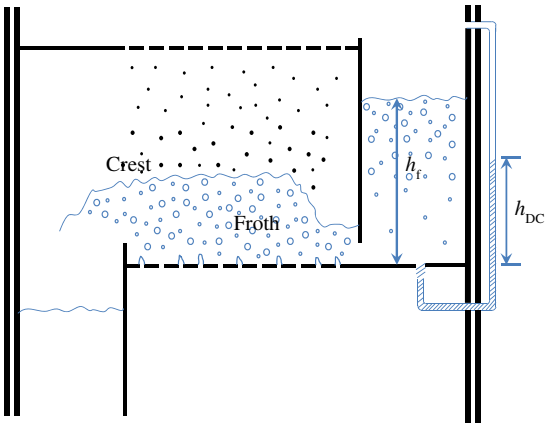

FIGURE 3.16 Schematic of Downcomer Backup Measurements

h_f, froth height; h_{DC}, height of the distillation column. (For a color version of this figure, the reader is referred to the online version of this book.)

scanning, scanning during column performance testing requires a more powerful source and a more precise positioning mechanism to accurately measure the liquid holdup and backup.

A special license and permit are required to use gamma ray sources during performance tests. Sometimes it takes considerable time and effort to apply for or renew a license. An organization licensed by the Nuclear Regulatory Commission to use radioactive materials must designate a person as a radiation safety officer (RSO). The RSO within the organization is responsible for the safe use of radioactive materials as well as regulatory compliance.

The absorption of gamma rays by a homogeneous material can be described by the following equation:

$$I = I_o e^{-\mu\rho\chi} \tag{3.3}$$

where χ (meters) is the thickness of the material, ρ (kilograms/meters cubed) is the material density, μ (−) is the effective mass absorption coefficient of the material, and I_o (kiloelectron volts) is the gamma ray intensity from the source (see also Chapter 2). Two commonly used gamma ray sources are cesium 137 and cobalt 60.

When the process density inside the column changes from ρ_1 to ρ_2, the corresponding intensities measured by the detector have the following relationship:

$$\frac{I_2}{I_1} = e^{(-\mu\chi\rho_2 + \mu\chi\rho_1)} \tag{3.4}$$

For given densities of ρ_1 to ρ_2 and measured $\frac{I_2}{I_1}$, the term $\mu\chi$ and I_o can be solved from Eqns (3.3) and (3.4) as follows:

$$\mu\chi = \frac{\ln \frac{I_2}{I_1}}{\rho_1 - \rho_2} \tag{3.5}$$

$$I_o = I_1 e^{\mu\chi\rho_1} \tag{3.6}$$

Combining Eqns (3.3), (3.4), and (3.6), the unknown process density ρ can be calculated from the measured intensity I as follows:

$$\rho = \rho_1 + \ln\frac{I_1}{I}\frac{\rho_1 - \rho_2}{\ln \frac{I_2}{I_1}} \tag{3.7}$$

Equation (3.7) indicates that calibration has to be conducted before using the gamma ray scan to measure process densities. In theory, any vapor or liquid with a known density can be used for calibration. In practice, air is usually used for vapor phase calibrations and the actual test liquid for the liquid phase calibrations.

The measured process density obtained from Eqn (3.7) is usually converted to liquid volume fraction as follows:

$$\phi = \frac{\rho - \rho_V}{\rho_L - \rho_V} \tag{3.8}$$

Figures 3.17 and 3.18 are the typical liquid volume fraction profiles in the tray deck and in the downcomer at various column loadings, respectively.

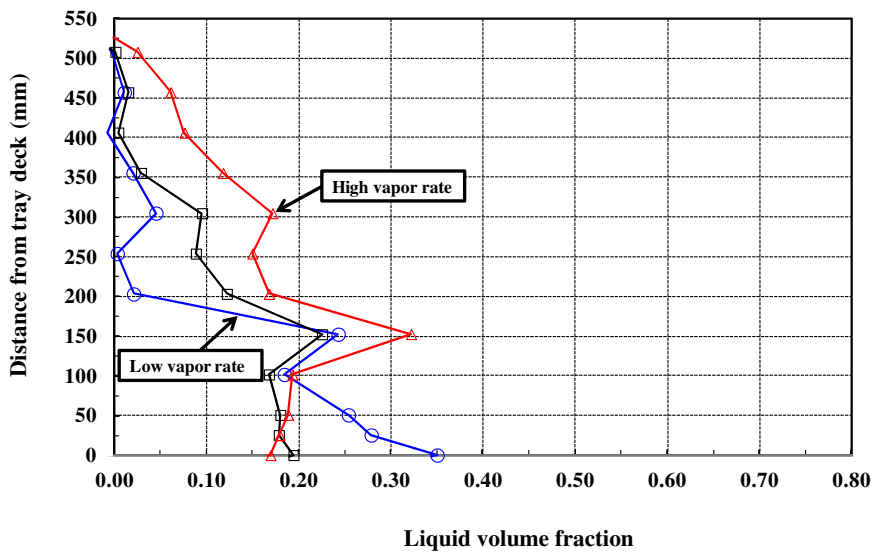

FIGURE 3.17 Typical Liquid Volume Fraction Profiles on a Tray Deck

(For a color version of this figure, the reader is referred to the online version of this book.)

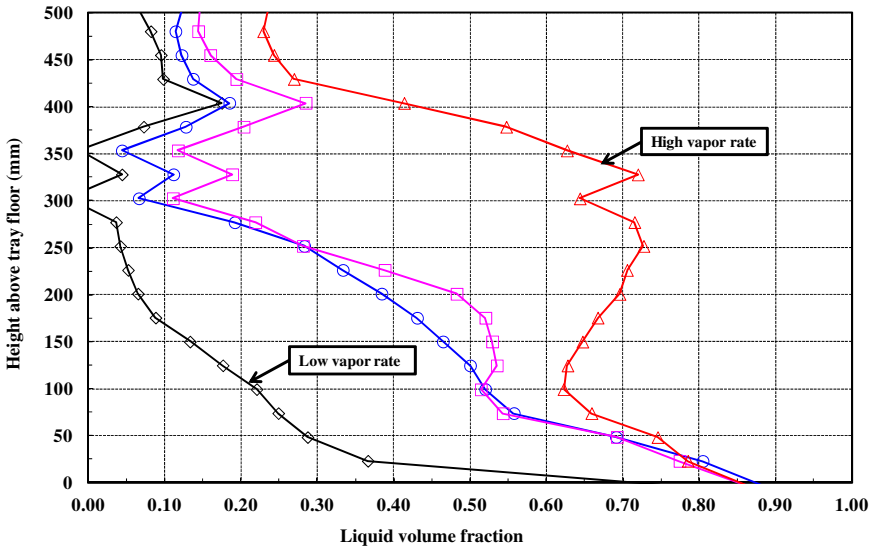

FIGURE 3.18 Typical Liquid Volume Fraction Profiles in a Downcomer

(For a color version of this figure, the reader is referred to the online version of this book.)

As shown in Figure 3.18, with the increase of vapor loadings, C_V, the froth height and the liquid volume fraction inside the downcomer increase. Once the liquid volume fractions are measured for various locations, the liquid head on the deck or downcomer backup can be found by numerical integrations.

For a packed column, the process densities measured from the gamma ray scanning are usually converted to liquid volume fractions. The gamma scan data, liquid volume fractions, at various locations inside the packed column yield the important liquid distributions.

3.14 Test procedure

Before conducting performance testing, it is necessary to have a proper test procedure ready. The procedure needs to be followed accordingly.

3.14.1 Preliminary test preparation

Before performance testing, the test plan should be reviewed with engineers and operations staff. All test procedures must comply with safety and environmental regulations.

Modern test facilities are generally well equipped with an advanced control and data acquisition system, which needs to be configured according to the test plan. All

instruments and composition analyzers need to be calibrated and configured before the test begins.

After trays or packings are installed in the distillation column, the entire test facility, including column, piping, valves, instrumentation, and auxiliary equipment, must be checked for leaks and evacuated according to the test procedure.

3.14.2 Test conditions and procedure

Most efficiency tests are performed at total reflux conditions. The flood point of the test column is usually determined first. After that, the vapor loading in the column is reduced to low rates to find the turndown ratio of the testing device.

As the column approaches the flooding condition, heat input into the column, or vapor loading, should be done in small increments to avoid premature flooding. Once the column shows the symptoms of flooding, the column loadings should be reduced slightly until the column can be held at a stable condition to log the process data.

Mass transfer efficiency changes with vapor and liquid loadings. A rigorous efficiency test requires measuring the separation efficiencies at various operating conditions. Once the flood capacity is determined, efficiencies are usually measured at the conditions of 20%, 40%, 60%, 80%, 90%, and 95% of the flooding. If efficiencies change significantly between two neighboring conditions, fill-in conditions are required to complete the efficiency measurements. In the efficiency test, the column must be at the mass transfer equilibrium (steady state) before logging the efficiency data. If necessary, a duplicate set of liquid samples can be taken to verify the existence of the steady state.

In addition to flood capacity at total reflux, the flood capacities at constant liquid rates also are measured. To do this, the test facility needs to be configured and equipped to operate at non-total reflux mode. Once the flood capacity at a constant liquid rate is measured, by keeping the same liquid rate, the pressure drops at various vapor loadings should be measured.

3.15 Data reduction

Most control and data acquisition systems are capable of collecting a large quantity of raw process data, including fluid flow rates, column pressures, pressure drops, levels, and temperature profiles at a specific period. Those raw data are very useful in identifying and verifying the steady state condition. All of those data make possible a rigorous analysis of material and heat balances.

3.15.1 Material balance

Overall material balance and individual component material balance should be verified before collecting performance data. A test facility, or a pilot plant,

is usually well equipped with accurate instruments and well insulated from heat losses. The error of overall and individual material balances should be within ±2%.

3.15.2 Heat balance

In addition to the material balance, before any performance data can be taken and calculated the heat balance and consistency around the column must also be checked. Reboiler duty, condenser duty, and heat loss have to be estimated accurately for a test column to obtain reliable and consistent performance data. It is feasible and realistic for a test column to have a heat balance with a ±5% deviation. If a reflux preheater is used, the amount of heat input to the preheater has to be accounted for in the heat balance calculation.

Systematic error analysis of heat input and output needs to be conducted. Factors affecting heat duty calculations should be investigated. The accuracy of heat duties needs to be studied. The most accurate duty should be used to calculate the column loadings. Reboiler duty is usually more reliable and consistent than condenser duty because the latter is affected more by weather conditions, the accuracy of the temperature measurement, the subcooled reflux, and so on. Furthermore, the temperature changes of the cooling water around the condenser, especially at low heat fluxes, are often quite small—less than 5−10 K. The inherent accuracy of the thermocouple, ±1 K, results in a greater possibility of error in the condenser duty. Therefore, reboiler duty is normally more reliable and usually used for vapor and liquid loading calculations.

3.15.3 Determination of reboiler and condenser duties

Reboiler duty is the amount of heat removed from the heating medium, such as high-pressure steam. Conversely, condenser duty is the amount of heat gained by the cooling medium, usually cooling water. The reboiler duty is calculated as follows:

$$\dot{Q}_{\mathrm{R}} = \dot{M}_{\mathrm{SC}}(h_{\mathrm{V}} - h_{\mathrm{L}}) \tag{3.9}$$

where $\dot{Q}_{\mathrm{R}}$ (kilowatts) is the reboiler duty, $\dot{M}_{\mathrm{SC}}$ (kilograms/second) is the mass flow rate of steam condensate, h_{v} (kilojoules/kilogram) is the steam enthalpy, and h_{L} (kilojoules/kilogram) is the steam condensate enthalpy.

Similarly, the condenser duty can be calculated as follows:

$$\dot{Q}_{\mathrm{C}} = \dot{M}_{\mathrm{W}}(h_{\mathrm{WO}} - h_{\mathrm{WI}}) \tag{3.10}$$

where $\dot{Q}_{\mathrm{C}}$ (kilowatts) is the condenser duty, $\dot{M}_{\mathrm{W}}$ (kilograms/second) is the mass flow rate of cooling water, h_{WO} (kilowatts/kilogram) is the enthalpy of cooling water return, and h_{WI} (kilowatts/kilogram) is the enthalpy of the cooling water supply.

3.15.4 Hydraulic performance calculations

Most important hydraulic parameters of a distillation column are vapor and liquid loadings in the column, flood capacities, and pressure drops. All of them are directly or indirectly related to heat duties and physical properties.

3.15.4.1 Determining liquid and vapor loadings

Liquid and vapor loadings in a distillation column are usually determined by the heat and material balances around the top or the bottom of the column or at a reference location inside the column. They are normally calculated using the reboiler duty and the latent heat of vaporization at the reference location. For a total reflux operation, the internal vapor rate is determined by the following expression:

$$\dot{M}_{\mathrm{V}} = \frac{\dot{Q}_{\mathrm{R}} - \dot{Q}_{\mathrm{loss}}}{\Delta h_{\mathrm{V,ref}}} \tag{3.11}$$

where $\dot{M}_{\mathrm{V}}$ (kilograms/second) is the vapor rate at the reference point, $\dot{Q}_{\mathrm{R}}$ (kilowatts) is the reboiler duty, $\dot{Q}_{\mathrm{loss}}$ (kilowatts) is heat loss, $\Delta h_{\mathrm{v,ref}}$ (kilojoules/kilogram) is the latent heat of vaporization at the reference point.

The latent heat of vaporization varies with composition and temperature, so the vapor rate inside the column changes with the reference point. The bottom tray, middle tray, top tray below the bed, the middle of the bed, and the top of the bed, respectively, are usually chosen as reference points.

For total reflux operations, the internal liquid rate is the same as the internal vapor rate as the entire overhead vapor stream is condensed and returned to the column as liquid reflux.

If the operation mode is not total reflux, the internal vapor will be different from Eqn (3.11). The internal vapor and liquid rates in the column are different and should be determined from the material and heat balances.

3.15.4.2 Determination of F-factor and capacity factor

The capacity of a tray or a packing is commonly presented by the F-factor and capacity factor C_{V}. The F-factor and capacity factor C_{V} usually are based on the physical properties at the middle tray or the middle of the packed bed. For test systems operating in a deep vacuum condition or that have very different boiling points, the physical properties undergo significant changes from the top of the column to the bottom of the column. Consequently, the F-factor and capacity factor C_{V} at the top and bottom of the column, respectively, should be determined.

The F-factor is based on the superficial vapor velocity; F is defined as follows:

$$F = u_{\mathrm{V}}\sqrt{\rho_{\mathrm{V}}} \tag{3.12}$$

$$u_{\mathrm{V}} = \frac{\dot{M}_{\mathrm{V}}}{\rho_{\mathrm{V}} A_{\mathrm{C}}} \tag{3.13}$$

where u_{v} (meters/second) is the superficial vapor velocity based on the column's cross sectional area A_{C}, F ($\mathrm{Pa}^{0.5}$) is the superficial F-factor, ρ_{v} (kilograms/meters

cubed) is the vapor density at reference point, A_C (meters squared) is the column's cross sectional area, and $\dot{M}_V$ (kilograms/second) is the vapor rate at reference point.

Capacity factor, C_V, based on the column's cross sectional area, can be obtained from Eqn (3.14):

$$C_V = u_V\sqrt{\frac{\rho_V}{\rho_L - \rho_V}} = \frac{F}{\sqrt{\rho_L - \rho_V}} \tag{3.14}$$

where ρ_L (kilograms/meters cubed) is the liquid density at the reference point.

For a trayed column, the capacity factor also is calculated based on the tray bubbling area, A_b (meters squared).

3.15.4.3 Pressure drops

The pressure drop reading from a differential pressure transmitter is usually presented in millimeters of water. As mentioned in Section 3.13.4.8, the reading from the pressure transmitter includes the vapor static head. The dynamic pressure drop should be calculated using Eqn (3.1).

For a trayed column, the pressure drop is customarily expressed in terms of pressure drop per tray (millimeters of hot liquid/tray). So, the pressure drop calculated in Eqn (3.1) should be simply converted into the millimeters of hot liquid per tray as follows:

$$\Delta p(\text{mm hot liquid}) = \Delta p(\text{mm } H_2O)\frac{\rho_w}{\overline{\rho_L}} \tag{3.15}$$

where ρ_w (kilograms/meters cubed) is the water density and $\overline{\rho_L}$ (kilograms/meters cubed) is the averaged liquid density across the specific column section.

For a packed column, the pressure drop is usually presented in terms of pressure drop per unit length. So, the pressure drop from Eqn (3.1) needs to be divided by the height of the packed bed.

3.15.4.4 Efficiency calculation

As previously mentioned, a majority of efficiency data on fractionators have been collected under total reflux conditions. For trayed columns, the efficiency results are expressed in terms of overall tray efficiency E_o. When the composition of all testing trays are available, tray efficiency across a section of trays can also be calculated. The overall tray efficiency E_o is defined as the ratio of the number of theoretical stages (N_t) required to meet the given separation to the number of actual trays (N_a) needed to achieve the same separation (see Eqn (3.16)).

$$E_o = \frac{N_t}{N_a}\cdot 100\% \tag{3.16}$$

At the total reflux condition, the number of theoretical stages for both trays and packings is calculated from the Fenske equation [57]:

$$N_t = \ln\frac{\left[\left(\frac{x}{1-x}\right)_T\right] - \ln\left[\left(\frac{x}{1-x}\right)_B\right]}{\ln\,\alpha_{avg}} \tag{3.17}$$

where x (−) is the mole fraction of the most volatile component in the liquid, T represents the location of liquid entering the top tray or the top of the packed bed, B represents the location of liquid leaving the bottom tray or the bottom of the packed bed, and α_{avg} (−) is the geometric relative volatility:

$$\alpha_{avg} = \sqrt{\alpha_T \alpha_B} \tag{3.18}$$

Combining Eqns (3.16−3.18), the efficiency of all testing trays or a section of testing trays can be found:

$$E_o = \frac{\ln\left[\left(\frac{x}{1-x}\right)_T\right] - \ln\left[\left(\frac{x}{1-x}\right)_B\right]}{N_a \ln\left(\sqrt{\alpha_T \alpha_B}\right)} \cdot 100\% \tag{3.19}$$

For packings, the mass transfer efficiency is usually represented by the HETP, that is, the ratio of the bed height and the number of theoretical plates contained in given bed height:

$$\text{HETP} = \frac{h_{PB}}{N_t} = \frac{h_{PB}\ln\left(\sqrt{\alpha_T \alpha_B}\right)}{\ln\left[\left(\frac{x}{1-x}\right)_T\right] - \ln\left[\left(\frac{x}{1-x}\right)_B\right]} \tag{3.20}$$

For systems with relative volatilities that are significantly different from the top of the bed and the bottom of the bed, HETPs along the packed bed will be substantially different. In this case, to minimize the effect of relative volatilities on the packing performance, the HTU is a closer representative of the packing efficiency than the HETP.

The HETP of the packing is related to the HTU and stripping factor S, as follows:

$$\text{HETP} = \text{HTU}_{OG}\frac{\ln(S)}{S-1} \tag{3.21}$$

and

$$\text{HTU}_{OG} = \text{HTU}_G + S \cdot \text{HTU}_L \tag{3.22}$$

where HTU_G (meters) is the height of a gas phase transfer unit, HTU_L (meters) is the height of a liquid phase transfer unit, HTU_{OG} (meters) is the height of an overall gas phase−related transfer unit, and S (−) is the stripping factor.

The stripping factor is calculated with the following equation:

$$S = m\frac{\dot{N}_V}{\dot{N}_L} \tag{3.23}$$

with

$$m = \frac{\alpha}{[1 + (\alpha - 1) \cdot x]^2}$$

where x is the mole fraction of the light component in the liquid phase, α $(-)$ is the relative volatility of the light component, m $(-)$ is the slope of the equilibrium curve expressed in mole fraction, $\dot{N}_V$ (kilomoles/second) is the molar flow rate of vapor, and $\dot{N}_L$ (kilomoles/second) is the molar flow rate of liquid.

3.15.4.5 Maximum useful capacity

The tray efficiency curve and packing HETP curve are presented in Figures 3.1 and 3.2, respectively. The MUC can be determined from those curves.

3.16 Experimental errors and test troubleshooting

Compared to industrial columns, the testing columns at research facilities and laboratories generally involve much smaller errors because the equipment and instrumentation at those facilities are specifically designed and configured for testing purposes and conditions.

Potential errors of a test column may be caused by the following factors:

1. Instrumentation
2. Sampling
3. Composition analysis
4. Heat losses
5. Unsteady state condition

Errors caused by instrumentation problems can be due to wrong flow rates and temperatures or wrong calibrations or pressure drop readings. Poor connections in the thermowell may cause wrong temperature readings. Leaks in the lines connecting to pressure transmitters will cause incorrect pressure drop results. To minimize potential errors, all instruments should be calibrated and checked regularly. Temperature sensors need to be calibrated properly with ice slurry or/and boiling water. Flow meters should be regularly calibrated or sent out for recertification. Pressure transmitters should be calibrated before each test. All tap lines and connections should be checked for leaks. The lines should be purged using inert gas to avoid any condensation on the lines.

The accurate measurement of compositions is crucial for performance measurements. Errors in the compositions will yield wrong physical properties and incorrect capacity and efficiency results. Wrong compositions could be due to sampling or analysis problems. Sampling lines, connections, and valves should be checked for leaks. Sample line needs to be adequately purged until fresh hot process liquid flows through the line. For composition analysis, the analytical equipment, for example,

GC equipment should be frequently checked against sample standards to ensure analytical accuracy.

To minimize heat losses, the test column and auxiliary equipment should be properly insulated. The amount of heat loss should be accurately estimated and accounted for in the data reduction.

No performance data should be collected until the column reaches a steady state. Various factors can cause unsteady state operations, such as control problems, water accumulation in the system, changes in steam pressure, and changes in cooling water temperature.

More details on operating column troubleshooting can be found in Chapter 2 in this volume.

3.17 Documentation and reporting

A distillation performance test should be documented using a consistent and concise approach. The document needs to contain all pertinent test information. A complete testing document may include the following items:

1. Test objectives
2. Hardware information
3. Column setup and installation
4. Instrumentation
5. Test systems
6. Test sequence
7. Data analysis
8. Experimental results
9. Conclusions and recommendations

It is not necessary for a test report to include all of these items. The following sections discuss general guidelines for test reporting.

3.17.1 Test objectives

A distillation performance test can have several objectives, such as capacity and efficiency measurements, performance validation testing, and fundamental studies. The test objectives need to be clearly stated in the test document.

Capacity and efficiency testing may be used to test a distillation internal that is still at the developmental stage. Test results will help researchers identify any problems and improve the product. Performance validation testing is considered the best way to verify whether the distillation internals are performing as promised by vendors.

At a testing facility a lot of performance tests are carried out to study the basics and fundamentals of distillation, for example, studying the effect of physical

properties on tray efficiencies or studying the effect of packing geometries on packing performance. Performance tests are useful to accumulate experimental results for developing predictive models or validating models.

3.17.2 Hardware information

The hardware information should be included in the performance test report. The hardware information is important so other people can understand and interpret the test results, validate the performance of testing devices, and develop performance models.

Tray parameters and packing geometries in particular should be included in the test report. The list of tray parameters includes, but is not limited to, downcomer type, downcomer area, bubbling area, deck type, open area, downcomer clearance, outlet weir height, and downcomer clearance.

For packings, the specific surface area, void fraction, and packing materials need to be included in the report. For structured packing tests, the number of layers, block height, crimple angle, and surface treatment should also be reported.

3.17.3 Column setup and installation

Column setup should include the type and number of testing trays, tray spacing, tray elevations, and liquid and vapor inlets. If entrainment and weeping rates are measured, the setup should document how the entrainment and weeping data are measured. For a packed column, details on the bed depth, liquid distributor, vapor distributor (if used), packing support grid, and bed limiter need to be included in the report.

Liquid or vapor samplers are an important part of the installation. How and where the liquid or vapor samples are taken should be detailed in the test report.

3.17.4 Instrumentation

All instruments, including temperature sensors, column pressure transmitters, and differential pressure transmitters, used in the performance test should be documented. The locations where the temperatures and pressure drops were measured need to be clearly stated in the report. The report should include how the temperature sensors and pressure transmitters are calibrated.

3.17.5 Test systems

Distillation internals often are tested using different test systems. The main physical properties and VLE data need to be included in the report so other people can check and duplicate the performance calculations, such as capacity and efficiency calculations. Information about the test system is also important for the development of performance models.

3.17.6 Test procedure and test sequence

The test procedure and test sequence are important for collecting reliable and consistent performance data. They should be followed for all phases of performance testing and documented in the test report. Sometimes the exact procedure or sequence may not be followed for various reasons. If this is the case, the actual test sequence needs to be clearly stated and included in the report.

3.17.7 Data analysis

Data analyses include how liquid samples are analyzed and how raw experimental data are processed. The data reduction of a tray test may be different from that of a packing test. For example, for a packed column test, the bed depth used to calculate HETP needs to be clearly specified. For a trayed column test, the number of trays used to calculate tray efficiency should be clearly stated in the report. Similarly, for a trayed column test, the bubbling area used to calculate the capacity factor should be included in the test document.

3.17.8 Results and conclusions

All experimental results should be tabulated. If more than one test system was used in the test, the results of each test system need to be included in a separate table. Important test results, such as capacity, mass transfer efficiency, and pressure drop, need to be plotted in terms of vapor or liquid loadings.

The last part of the report is the conclusions and recommendations. The conclusions are basically the final comments on the test results. They summarize the main findings or main discoveries from the performance tests. Recommendations can make suggestions for further improvement and speculate on future directions.

References

[1] J.G. Kunesh, H.Z. Kister, M.J. Lockett, J.R. Fair, Distillation: still towering over other options, Chem. Eng. Prog. (October 1995) 43–54.
[2] AIChE Equipment Testing Procedure, Trayed & Packed Columns, American Institute of Chemical Engineers, 2013.
[3] H.Z. Kister, Distillation Operation, McGraw-Hill, New York, 1990.
[4] N.P. Lieberman, Troubleshooting Process Operations, second ed., Penn Well, Tulsa, 1985.
[5] J.F. Hasbrouck, J.G. Kunesh, V.C. Smith, Successfully troubleshoot distillation columns, Chem. Eng. Prog. 89 (1993) 63–71.
[6] J.J. France, Troubleshooting Distillation Columns, Presented in AIChE Spring Meeting, Houston, March 1993.
[7] T.J. Cai, G.X. Chen, C.W. Fitz, J.G. Kunesh, Effect of bed length and vapor maldistribution on structured packing performance, Chem. Eng. Res. Des. 81 (2003) 85–92.

[8] Z. Olujic, A.F. Seibert, B. Kaibel, H. Jansen, T. Rietfort, E. Zich, Performance characteristics of a new high capacity structured packing, Chem. Eng. Process. 42 (2003) 55–60.
[9] T.D. Koshy, F. Rukovena, Distillation Columns Containing Structured Packings, Presented at the AIChE Spring Meeting, March 28–April 1, 1993.
[10] L. Spiegel, W. Meier, Distillation columns with structured packings in the next decade, Trans. IChemE 81 (Part A) (2003) 39–47.
[11] Z. Olujic, B. Kaibel, H. Jansen, T. Rietfort, E. Zich, Experimental characterization and modeling of high performance structured packings, Ind. Eng. Chem. Res. 51 (2012) 4414–4423.
[12] J.F. Billingham, M.J. Lockett, Development of a new generation of structured packing for distillation, Trans. IChemE, Chem. Eng. Res. Des. 77 (Part A) (1998) 583–587.
[13] Z. Olujic, M. Behrens, L. Spiegel, Experimental characterization and modeling of the performance of a large-specific-area high-capacity structured packing, Ind. Eng. Chem. Res. 46 (2007) 883–893.
[14] Z.P. Xu, A. Afacan, K.T. Chuang, Predicting mass transfer in packed columns containing structured packings, Chem. Eng. Res. Des. 78 (2000) 91–98.
[15] M. Ottenbacher, Z. Olujic, T. Adrian, M. Jodecke, Structured packing efficiency–vital information for the chemical industry, Chem. Eng. Res. Des. 89 (2011) 1427–1433.
[16] H.Z. Kister, Distillation Design, first ed., McGraw-Hill, New York, 1992.
[17] M.J. Lockett, Distillation Tray Fundamentals, Cambridge University Press, 1986.
[18] R. Weiland, J. DeGarmo, I. Nieuwouldt, Converting a commercial distillation column into a research tower, Chem. Eng. Prog. 101 (7) (2005) 41–46.
[19] J.L. Bravo, K.A. Kusters, Tray technology for the new millennium, Chem. Eng. Prog. 96 (12) (2000) 33–37.
[20] Z.P. Xu, B.J. Nowark, K.J. Richardson, R. Miller, Simulflow device capacity beyond system limit, in: Presented in the Distillation Topical Conference of the 2007 Spring AIChE Meeting, Houston, Texas, April 22–26, 2007.
[21] C.W. Fitz, J.G. Kunesh, A. Shariat, Performance of structured packing in a commercial scale column at pressures of 0.02 to 27.6 bar, Ind. Eng. Chem. Res. 38 (1999) 512–518.
[22] T.J. Cai, C.W. Fitz, J.G. Kunesh, Vapor Maldistribution Studies on Structured and Random Packings, AIChE Annual Meeting, Reno, Nevada, November 2001.
[23] C.W. Fitz, D.W. King, J.G. Kunesh, Controlled liquid maldistribution studies on structured packing, Chem. Eng. Res. Des. 77 (1999) 482–486.
[24] T.J. Cai, G.X. Chen, Liquid back-mixing on distillation trays, Ind. Eng. Chem. Res. 43 (2004) 2590–2596.
[25] A. Shariat, T.J. Cai, The Effect of Outlet Weir Height on Sieve Tray Performance, AIChE 2008 Annual Meeting, Philadelphia, Pennsylvania, November 16–21, 2008.
[26] T.J. Cai, M.R. Resetarits, A. Shariat, Hydraulics of Kettle Reboiler Circuit, AIChE Annual Meeting, Salt Lake City, Utah, November 7–12, 2010.
[27] J.G. Kunesh, L. Lahm, T. Yanagi, Commercial scale experiments that provide insight on packed tower distributors, Ind. Eng. Chem. Res. 26 (1987) 1846–1856.
[28] J.G. Kunesh, L. Lahm, T. Yanagi, Controlled maldistribution studies on random packing at a commercial scale, Distillation and Absorption (1987). IChemE Symp. Ser.No. 104, P. A233l.

[29] T.J. Cai, G.X. Chen, A. Shariat, Entrainment Particle Size from Commercial Scale Distillation Trays, AIChE Annual Meeting, San Francisco, California, November 16–21, 2003.
[30] T.J. Cai, G.X. Chen, Control of Liquid Flow on Fractionating Trays, AIChE Spring Meeting, Atlanta, Georgia, April 10–14, 2005.
[31] Z. Olujic, A.F. Seibert, J.R. Fair, Influence of corrugation geometry on hydraulics and mass transfer performance of structured packings: an experimental study, Chem. Eng. Proc. 39 (2000) 335–342.
[32] C.W. Fitz, A. Shariat, J.G. Kunesh, Performance of Mellapak Structured Packing Using the Butane System at Pressures of 7 to 28 Bar, Gvc, Luzern, Switzerland, April 29–30, 1996.
[33] J.G. Kunesh, Practical tips on tower packing, Chem. Eng. (December 1987) 101–105.
[34] R. Billet, Distillation Engineering, Chem. Pub. Co, New York, 1979.
[35] F. Rukovena, T.J. Cai, Achieve good packed tower efficiency, Chem. Proc. (November 2008) 22–31.
[36] T.J. Cai, G.X. Chen, Structured packing performance, in: First China-USA Joint Conference on Distillation Technology, Tianjin, China, June 15–18, 2004.
[37] F. Moore, F. Rukovena, Liquid and gas distribution in commercial packed towers, in: CPP Edition Europe, August 1987, p. 11.
[38] J.F. Billingham, D.P. Bonaquist, M.J. Lockett, Characterization of the Performance of Packed Distillations Column Liquid Distributors, Distillation and Absorption Symposium, Maastricht, The Netherlands, 1997, 841–851.
[39] L.W. Luyben, Control of distillation process, in: A. Gorak, H. Schoenmakers (Eds.), Distillation Book, vol. III, Elsevier, Amsterdam, 2014.
[40] L.W. Luyben, Process Modeling, Simulation, and Control for Chemical Engineers, McGraw-Hill, New York, 1990.
[41] F.G. Shinskey, Process Control Systems: Application, Design, and Tuning, fourth ed., McGraw-Hill, Inc, New York, 1996.
[42] R.H. Perry, Perry's Chemical Engineer's Handbook, seventh ed., McGraw-Hill, Inc, New York, 1998.
[43] Y. Yea, Z. Cummings, Localized fluid flow measurements with an He-Ne laser spectrometer, Appl. Phys. Lett. 4 (1964) 176–178.
[44] Manual on the Use of Thermocouples in Temperature Measurement, fourth ed., ASTM, 1993, 48–51.
[45] T.J. Cai, J.G. Kunesh, Heat Transfer Performance of Large Structured Packing, AIChE. Spring Meeting, Houston, Texas, March 1999.
[46] A.W. Sloley, Effectively control column pressure, Chem. Eng. Prog. (January 2001).
[47] H.Z. Kister, Distillation Troubleshooting, Wiley-Interscience, Hoboken, New Jersey, 2005.
[48] T.J. Cai, M.R. Resetarits, Pressure drop measurements on distillation columns, Chin. J. Chem. Eng. 19 (2011) 779–783.
[49] B.J. Mckeon, A.J. Smith, Static pressure correction in high Reynolds number fully developed turbulent pipe flow, Meas. Sci. Technol. 13 (2002) 1608–1614.
[50] Z. Olujic, Effect of column diameter on pressure drop of corrugated sheet structured packing, Chem. Eng. Res. Des. 77 (1999) 505–510.
[51] F.C. Silvey, G.J. Keller, Chem. Eng. Prog. (1966) 62–68.
[52] D.L. Pavia, G.M. Lampman, G.S. Kritz, R.G. Engel, Introduction to Organic Laboratory Techniques, fourth ed., Thomson Brooks/Cole, 2006, 797–817.

[53] C. Daniel, "Gas Chromatography, fifth ed, W. H. Freeman and Company, 1999. Quantitative Chemical Analysis (chapter), 675−712.
[54] J.G. Kunesh, D.W. .King, C.W. Fitz, Use of gamma scanning to obtain quantitative hydraulic data on a commercial scale, Distillation and Absorption (1992). IChemE Symp. Ser., No. 128, P. A211.
[55] T.J. Cai, M.R. Resetarits, L. Pless, R. Carlson, A. Ogundeji, Gamma Scanning of FRI Kettle Reboiler Vapor Return Lines, 2010 AIChE Spring Meeting, San Antonio, TX, March 2010.
[56] M.E. Harrison, Gammas scan evaluation for distillation column debottlenecking, CEP (March 1990).
[57] M.R. Fenske, Ind. Eng. Chem. 24 (1932) 482−487.

CHAPTER

Distillation in Refining

4

Stuart Fraser

Consultant. London, UK, Formerly Head of Separations Group, BP Oil

CHAPTER OUTLINE

4.1 Scale of the operation

Distillation is the main separation process in crude oil refining. Depending on the size and complexity of the refinery, typically there could be 30 or more large distillation columns ranging from 2 to 14 m diameter. Figure 4.1 shows that the refinery landscape is dominated by many distillation columns.

In addition to the primary crude oil fractionation of raw crude oil into different petroleum distillates (naphtha, kerosene, diesel, etc.), all of the refinery conversion and upgrading processes utilize distillation units to separate the reactor effluents into the various refining product distillates. These conversion units (discussed in Section 4.10) typically require complex distillation unit flow schemes of several large columns.

Distillation is an energy-intensive process, and despite best efforts to heat-integrate these units, typical energy usage is on the order 10–200 MW per

Distillation: Operation and Applications. http://dx.doi.org/10.1016/B978-0-12-386876-3.00004-1

FIGURE 4.1 Refinery Landscape Dominated by Distillation Columns (Encircled by Dotted Ovals)

distillation unit (depending on the unit throughput and separation quality required). The heights of these distillation columns largely depend on the separation quality specifications required and the difficulty of the separation (this is discussed later). The diameter of these columns largely depends on the unit throughput and the reflux requirements.

The main and most important separation process in refining is the crude unit complex. This is located at the beginning of the refinery flow scheme (see Figure 4.2). The crude unit processes all of the raw crude, and this unit is likely to be the oldest and largest unit on site. A large-scale crude unit would process 250 Mbpd (approximately 40,000 m^3/day). For a unit of this capacity, the crude unit size would be around 8−9 m in diameter and typically around 50 m high. The main crude unit, often referred to as the atmospheric column, typically operates at close to atmospheric pressure (0.5−2 barg), and the products generated are called atmospheric distillates. Separation of the distillates is carried out by boiling range with the lightest distillate drawn from the top of the column. Progressively heavier distillates are drawn as side draws off the atmospheric column. The heaviest residue is taken off the bottom of the column. It is important to recognize that only hydrocarbons that can be vaporized in the feed heater can be recovered as atmospheric distillates. In order to maximize the recovery of atmospheric distillates, the crude unit operates at a relatively high inlet feed temperature of typically 360−370 °C. Consequently, these units use large fired heaters to heat the raw crude from a heater inlet of around 250 °C to a heater outlet of 370 °C. The energy usage of a crude unit heater for a 250 Mbpd atmospheric unit would be around 200 MW, depending on the type of crude processed and percentage of vaporization of the feed.

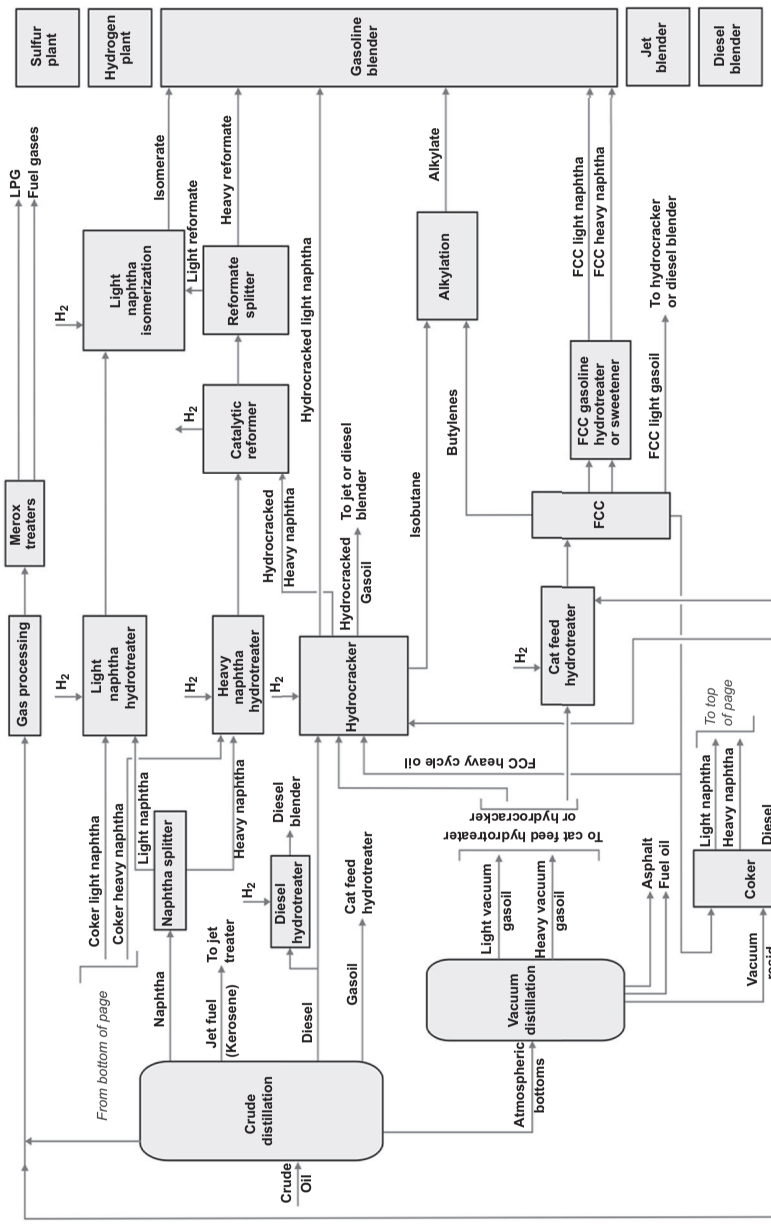

FIGURE 4.2 Typical Modern, Single-Train Refinery Flow Scheme

Hydrocarbon components that are too heavy to vaporize in the atmospheric unit fall into the residue stream drawn at the bottom of the column (atmospheric residue). This stream is then routed to the crude vacuum unit, where a second attempt is made to recover distillates (vacuum distillates). The operating principle of the crude vacuum unit is similar to that of the atmospheric unit except that the column operates in a deep vacuum of typically 10−50 mBara pressure. The lower operating pressure for the vacuum unit allows a greater degree of vaporization of the atmospheric residue, which is recovered as vacuum distillates. However, the lower operating pressure for the vacuum unit requires even larger vessel sizes compared to the crude unit. Refinery crude vacuum columns are often 12−14 m in diameter. The photographs shown in Figure 4.3(a) and (b) give an indication of the scale of crude vacuum units. It is interesting to note that since these units operate at such a low absolute pressure, this not only requires large vessel diameters to handle the vapor/liquid loads but also very large feed inlet lines to handle the high inlet velocities. The feed inlet is a mix of vapor and liquid, and the vapor velocity should not exceed the sonic velocity (around 100−130 m/s). The photograph shown in Figure 4.3 (taken during a maintenance outage) shows a person working on the inlet feed line. This line for this particular unit is 2.24 m in diameter.

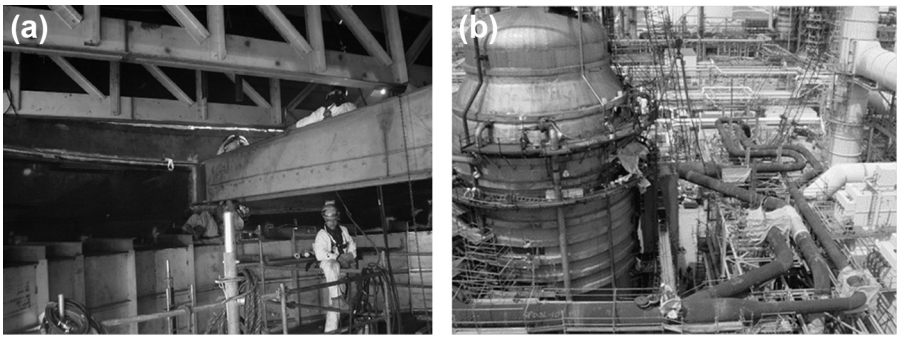

FIGURE 4.3 Typical Refinery Crude Vacuum Distillation Unit

(a) Inside the vacuum unit vessel. (b) Vacuum unit feed transfer inlet lines.

4.2 Refinery flow schemes

Refineries evolve to meet changing feedstock supply and varying commercial demands. Older refineries may have two or three crude unit trains of varying sizes, probably added at different stages to meet expansion plans. Newer refineries ideally would have a larger single train (as shown in the refinery flow scheme in Figure 4.2), and this allows for operation at a lower fixed cost. The main downside of a single train configuration is that the entire operation is dependent on the high availability of the crude unit complex. However, crude units can be designed and operated for

5 years with typical unit availabilities around 98%, so a single train would normally be preferred for a new refinery design.

Nowadays, there are no finished products from the crude and vacuum units, and all distillates are processed in downstream conversion or treatment units. Therefore, the operation and fractionation quality of the crude/vacuum unit has a very significant domino effect on the downstream refinery operations. The optimization of the crude/vacuum unit is a key objective for all refineries. Generally, a more aggressive (higher) operating temperature for the crude and vacuum unit results in an improved unit profitability. However, it is essential to ensure that these units operate safely and reliably for the full planned operating period, which is typically 4–5 years.

4.3 Crude oil characterization

Crude oils contain thousands of pure components, and therefore it is not possible to characterize these by pure component speciation. Crude oil laboratory distillations or assays are used to characterize the raw crude. These are shortcut batch distillations carried out under laboratory conditions using standardized equipment and processes (e.g. ASTM D2892, shown in Figure 4.4). A batch sample of crude oil is

FIGURE 4.4 ASTM D2892 STILL

distilled and the percentage of distillate collected is correlated against the still head temperature, corrected to atmospheric pressure.

These assays tend to be carried out in specialized laboratories and typically take 2−3 weeks to complete and report. An important outcome of the assay test is the presentation of the crude oil true boiling point data (TBP), which shows the crude TBP temperature vs the percentage of cumulative weight or volume distilled (see Figure 4.5). The TBP data can be used to determine the yield (percentage weight) of refinery distillates that potentially could be recovered and processed in the refinery units.

The TBP data are therefore an important property in valuing the crude. However, there are many other assay properties that are also important in valuing the crude, and these are determined by analyzing the various distillates collected during the assay process. Property distillation curves can then be developed by regression of the laboratory property analyses from the standard assay cuts. Some key properties of particular interest to refiners would include:

- the distribution of sulfur species in the crude (indicates potential yield and difficulty of producing clean low sulfur products).
- the pour point or cloud point distribution (this may dictate the maximum yield of diesel fuel achievable).
- distribution of metals and asphaltenes (indication of suitability of processing in downstream catalytic conversion units).

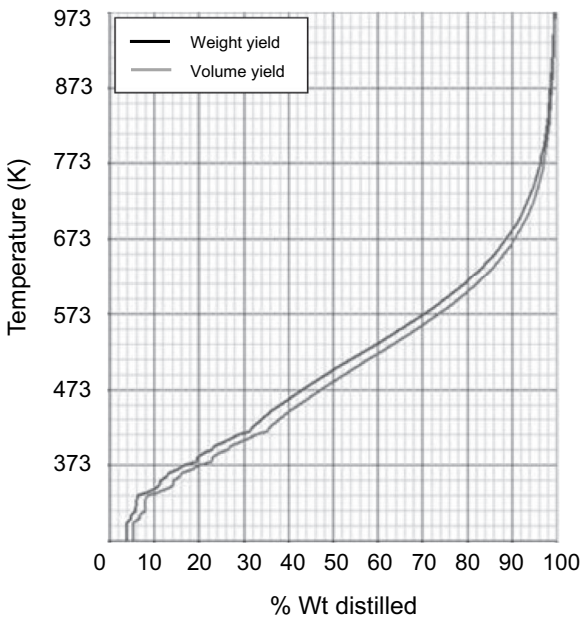

FIGURE 4.5 Crude Oil True Boiling Point Curve

- Conradson carbon distribution (indication of coke yield potential for residues).
- any specific crude quality that could potentially constrain the refinery operation in some way. For example, depending on the metallurgy design of the units, naphthenic acid content (often referred to as the crude total acidity number (TAN)) of the crude oil will restrict the quantities of crudes with a high TAN that may be processed.

Given a detailed knowledge of the crudes likely to be processed, the resulting product yields of the refinery distillates can be estimated from knowledge of the crude TBP curve and the distillate qualities.

For the example shown in Figure 4.6, the yield of atmospheric distillates (gasoil and lighter distillates) is 57%. The atmospheric residue yield is therefore 43% on feed, and ideally the downstream vacuum distillation unit that processes the atmospheric residue should be large enough to handle this rate (assuming that the refinery is operating at maximum throughput).

Refineries often run blends of crudes (typically a blend of three to four crudes), and this blend is selected to optimize the refinery's profitability. The optimization process involves a planning process that typically uses some form of a linear program (LiP) to optimize profitability. The LiP would include a comprehensive representation of the key unit and product quality constraints (e.g. throughput limits,

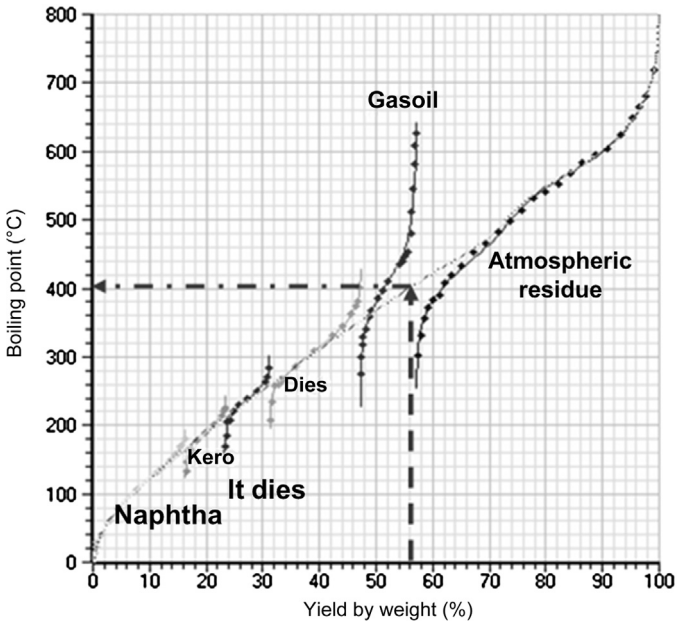

FIGURE 4.6 True Boiling Point's Cumulative Product Yield

Dies, diesel; kero, kerosene.

capacity of product draws on the unit, quality specifications). The objective function of the LiP is to optimize the overall profitability of the refinery.

The overlaps between the crude oil distillates (shown as the dotted ovals in Figure 4.7) are an indication of the separation quality between the various distillates. The larger the overlaps, the poorer the separation quality. In the example in Figure 4.7, the separation that has been achieved (on the crude unit) between kerosene and diesel is better than that between diesel and gasoil.

Refinery products such as gasoline, kerosene, and diesel also contain many hundreds of pure components and they also are characterized by laboratory shortcut distillations.

The laboratory distillation tests used to characterize products are similar to the crude oil assay distillation tests described above, but not as detailed. The ASTM D86 test is generally used to characterize lighter distillates such as gasoline and kerosene, and the ASTM D2882 test is generally used to characterize heavier distillates such as gasoils and vacuum distillates. Both tests are automated, take 30−60 min to complete, and generate a distillate curve similar to a crude TBP curve. The ASTM D86 test generates a D86 boiling point plot correlated against the percentage volume of distillate collected (see also Figure 4.8), whereas the D2882

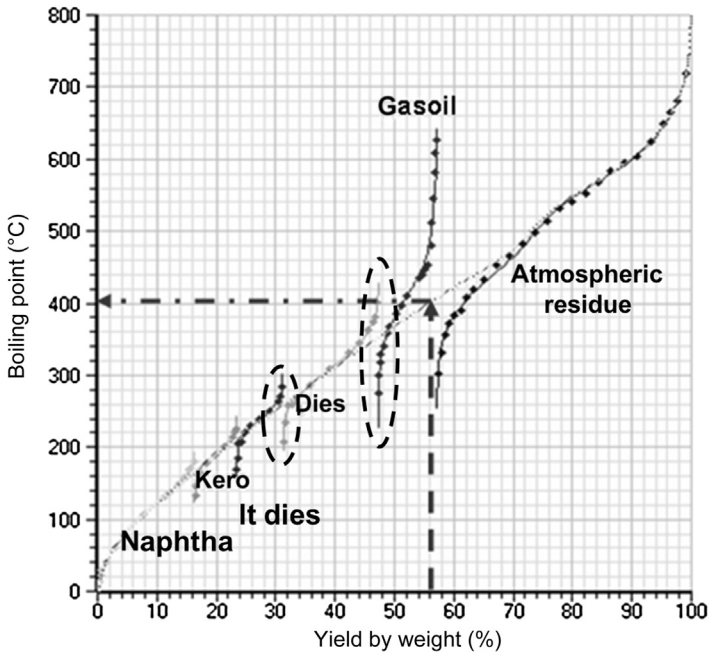

FIGURE 4.7 Product Distillations Showing Fractionation Overlaps (Encircled by Dotted Ovals)

Dies, diesel; kero, kerosene.

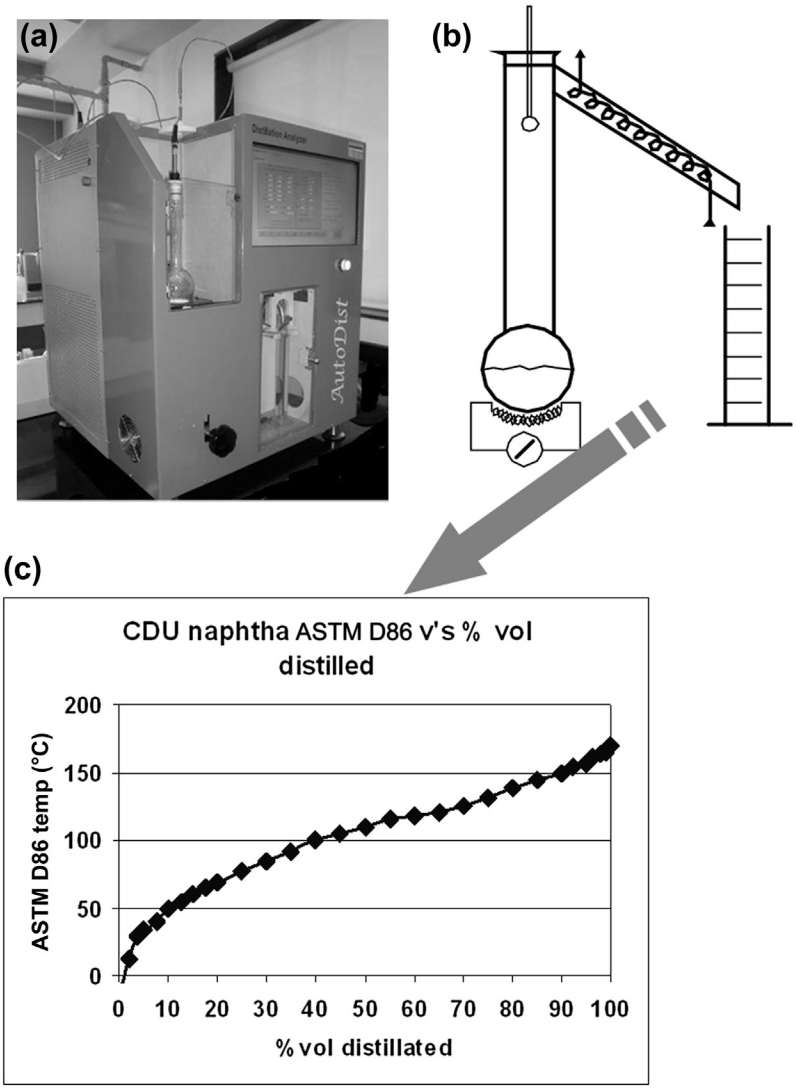

FIGURE 4.8

(a) ASTM D86 laboratory test unit for products. (b) Its distillation still. (c) The main output from this unit is a distillation boiling point curve for refining products.

(SimDis) is a chromatographic technique that is calibrated to generate a TBP curve correlated against the percentage weight recovered. Most refinery liquid distillates will have product specifications that include at least one distillation specification specifying a minimum and/or a maximum boiling point. These distillation

specifications will likely are based on either the ASTM D86 or SimDis test methods. For example, naphtha D86(95) should be less than 180 °C. Copies of these ASTM standards can be purchased online [1]. The translation of ASTM curves into groups of pure petroleum components is usually carried out using software simulation packages such as Aspentech [2] and Invensys SimSci [3].

Whereas distillation specifications are important quality specifications, there are many other product specifications that are also equally important. Some of these include:

- *Product flash point*: indication of ignition temperature in the presence of a flame and related to the front end of the distillation curve. Most products will have a minimum flash point specification, which is important for safe storage in tankage.
- *Product cloud and pour point*: important for diesel fuels and indicates risk of forming wax in vehicle tanks and distribution systems. This is related to the back end of the distillation curve for the product (and the crude type).
- *Product freeze point*: important for kerosene/jet fuels and indicates risk of forming freeze crystals. This is also related to the back end of the product distillation curve and the crude type.
- *Cetane properties*: an important parameter for combustion of diesel fuels and indicates detonation properties. This is related to crude type and the conversion process used in the refinery.
- *Reid vapor pressure*: indicates product vapor pressure and is important for fuels that are stored in atmospheric tanks. This is related to the front end of the distillation curve.

All of these properties can be estimated based on the crude assay data and the product distillation curves. There are several other quality specifications that could be more or less critical depending on the disposition of the intermediate products. For example, distillates processed in a downstream catalytic conversion unit may be constrained by levels (parts per million) of impurities that may poison the catalyst. Consequently, it would be important to know the corresponding boiling point concentration of metals in the crude versus the percentage weight distilled.

For a refinery crude unit, most of the distillate draws will have preferred quality specifications of some form, but the number of distillate draws and quality specifications will vary depending on the refinery configuration and the disposition of the distillate draws. As an example, a set of product specifications for a crude unit are shown in Figure 4.9. It is important to understand the product specifications and ensure that they are feasible.

For example, the naphtha back end distillation specification shown in Figure 4.9 (naphtha d86(95), less than 180 °C) will also impact the front end distillation curve for the kerosene. The kerosene flash point specification is largely dictated by its own front end distillation curve. So, these two specifications will be competing specifications and may or may not be feasible depending on the separation efficiency that can be achieved between these two products in the unit.

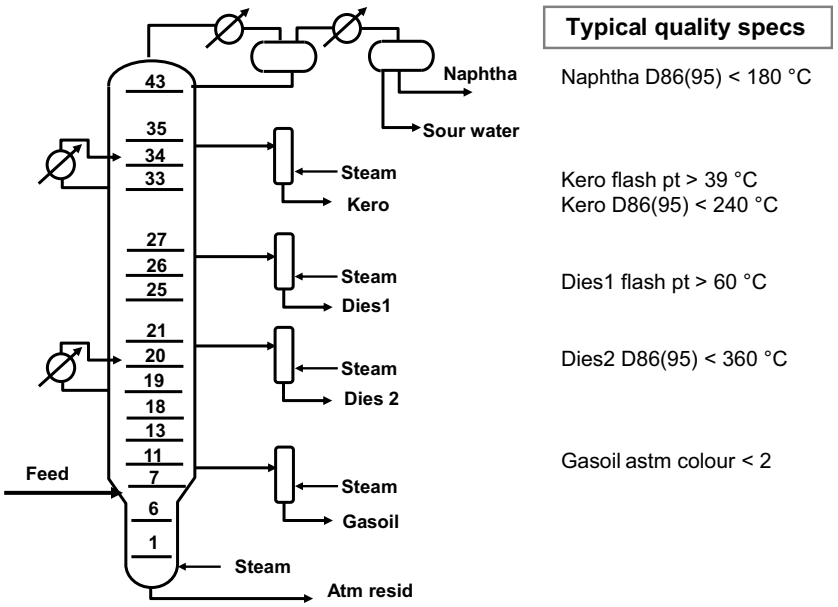

FIGURE 4.9 Typical Quality Specifications for a Crude Unit

Atm resid, atmospheric residue; dies, diesel; kero, kerosene.

4.4 Refinery crude and vacuum units

The crude distillation unit (CDU) is at the start of the refining processes, and, since it processes all of the raw crude, relatively modest changes in operation can have a major impact on the downstream operations. If the site has a single crude unit, then clearly any impact on throughput or unit availability will have a profound impact on downstream units. Most of the downstream conversion and treatment units are catalytic units, and as a consequence poor fractionation quality from the crude unit can potentially reduce the catalyst life. The crude unit is likely to be the oldest and most heavily modified unit on the site. It is likely that the original configuration would have been a two-column arrangement integrated with the vacuum unit, similar to that shown in Figure 4.10. More information about vacuum distillation is to be found in Volume 2, Chapter 9.

Many crude unit configurations with different draw arrangements and different flow schemes may have evolved along with the expansion of the refinery. The example in Figure 4.11(a) shows a CDU with a preflash column. The preflash column typically prefractionates and recovers around 60−70% of the naphtha boiling range distillates before the CDU.

The preflash unit essentially removes bottlenecks from the crude unit, the hot preheat train, and the CDU heater [4]. This flow scheme is often added as a revamp project to allow the refinery to process lighter crudes (and also condensate feeds). An

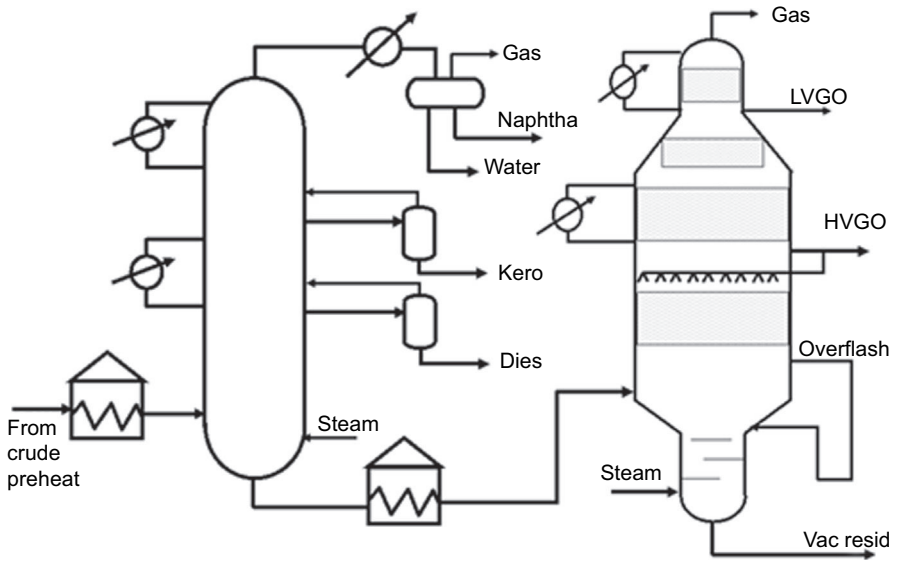

FIGURE 4.10 Typical Crude and Vacuum Configuration

Dies, diesel; HVGO, heavy vacuum gasoil; kero, kerosene; LVGO, light vacuum gasoil; vac resid, vacuum residue.

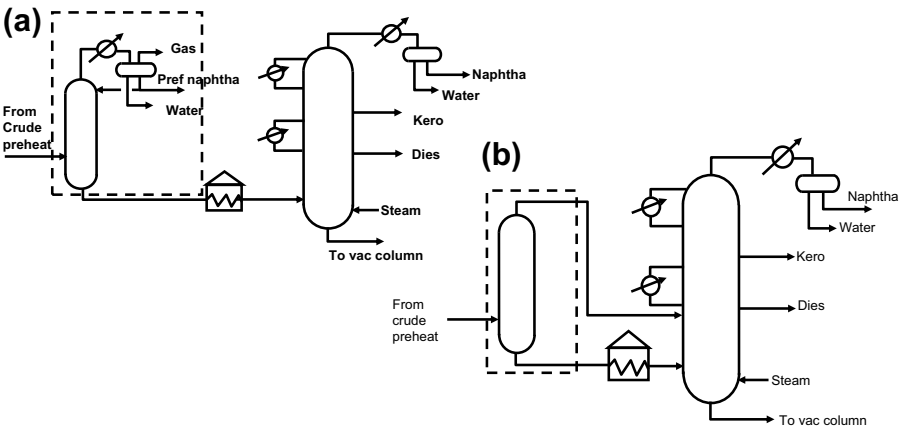

FIGURE 4.11

Crude unit with preflash column (a) and preflash drum (b). Dies, diesel; kero, kerosene; vac, vacuum.

alternate lower-cost revamp option is to use a preflash drum rather than a preflash column, as shown in Figure 4.11(b). This unloads the CDU heater and the hot preheat train and, to a limited extent, the lower section of the CDU column.

The number of distillate product draws and the draw locations also vary from site to site. The optimal fractionation quality normally is achieved by minimizing the number of side products. However, depending on the design and number of downstream hydrotreating units, there may be an incentive to draw additional side products. In general, lighter boiling range distillates are easier to desulfurize; higher boiling range distillates may require a more severe (higher operating pressure) hydrotreatment process to fully desulfurize the product. The main unit operations associated with the crude and vacuum units are shown in Figure 4.12.

4.4.1 Crude preheat

The crude cold and hot preheat trains are a collection of shell and tube heat exchangers (Figure 4.13) designed to maximize heat recovery between the cold incoming crude and the hot distillate products. The raw crude inlet temperature is typically ambient (5−20 °C).

Furnace inlet temperatures of 280 °C (the temperature out of the hot preheat train) can be achieved, but more typically this is usually 240−260 °C, depending on the design of the heat exchanger network. These preheat systems are very complex and difficult to design [5]. They need to be designed to allow adequate flexibility to process a range of different crude types of varying product yields. Often,

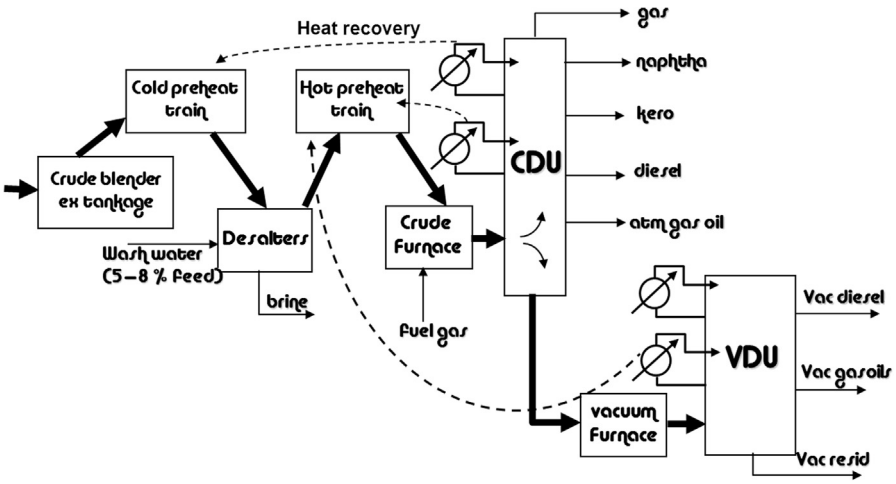

FIGURE 4.12 Main Unit Operations for a Crude Distillation Unit (CDU) and a Vacuum Distillation Units (VDU)

Atm, atmospheric; dies, diesel; kero, kerosene; vac, vacuum.

FIGURE 4.13 Photo of Crude Preheat Exchangers

the crude unit heat is integrated with other refinery units, and this adds to the design's complexity. Preheat units of 20−30 exchanger bundles are fairly typical, and total preheat surface areas on the order 5000−10,000 m^2 are common. The thermal and hydraulic performance of these preheats systems can greatly constrain the crude unit's operation. Depending on the crudes processed, crude preheat systems may be susceptible to fouling. This results in an increased pressure drop and a lower heat recovery. Ultimately, preheat fouling can easily restrict the crude throughput. Once fouled, usually the most effective means to clean these exchangers is to isolate them, bypass the bundle, and manually clean them offline (with high-pressure water jets). However, many refineries may not have the capability to isolate exchangers and clean "on the run".

4.4.2 Crude desalting

Crude oil is usually contaminated with salt (sodium, calcium, and magnesium chlorides), and some of these salts will hydrolyze in the hot crude preheat to form hydrogen chloride (HCl).

$$MgCl_2 + 2H_2O \rightarrow Mg(OH)_2 + 2HCl$$

$$CaCl_2 + 2H_2O \rightarrow Ca(OH)_2 + 2HCl$$

The HCl will be absorbed into any free water in the crude unit and can cause severe corrosion in the colder sections of the main crude unit (top section of the column). Therefore, most crude units include a single or double desalting process (see Figure 4.14), where a wash water stream is mixed into the crude. The total wash water rate is typically 4−8% of the raw crude rate. The fresh water dissolves and dilutes the salts and the resulting effluent brine is routed to the effluent treatment process.

To allow good separation of the crude and resulting brine, desalter vessels are usually quite large horizontal vessels with a controlled interface of oil and water.

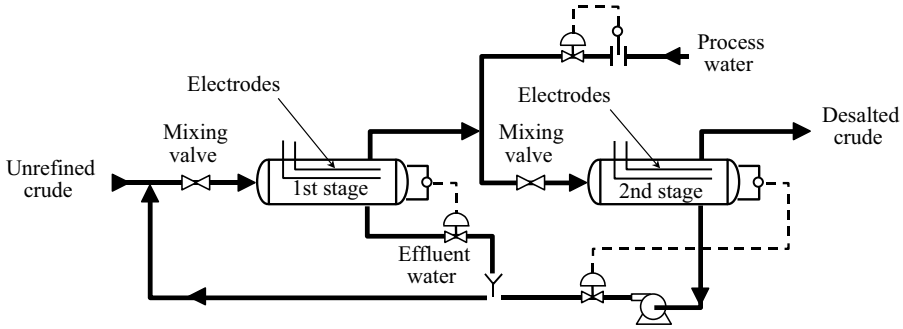

FIGURE 4.14 General Arrangement of the Desalting Process

The vessels are sized to allow high residence times for effective separation of the brine from the oil. Oil and water residence times of 30 and 60 min, respectively, are typical. In addition, an electric field is used to further promote improved separation of the brine from the oil. A well-performing two-stage desalter would achieve desalted crude salt contents of 1−2 ppm and water contents of 0.2−0.3%wt. The key performance indicator of the desalter is the level of chlorides observed in the water phase drawn from the CDU overhead reflux receiver [6].

4.4.3 Crude unit fired heaters

Crude units require large fired heaters (see Figure 4.15) to generate high-grade heat. The recovery of atmospheric distillates from the crude unit requires that those distillates be vaporized in the feed heater.

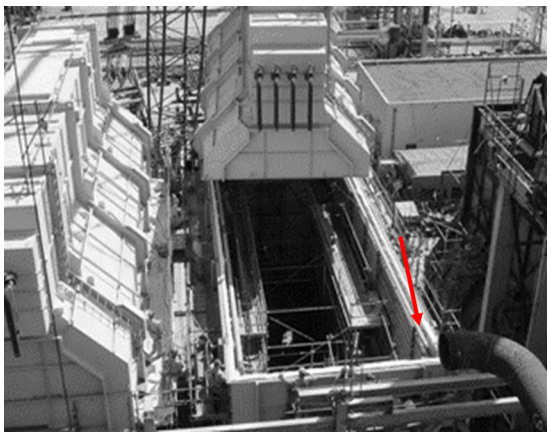

FIGURE 4.15 Crude Unit Heater in Construction; the Arrow Indicates the Radiant Section Tubes

The crude unit heater outlet temperature is maximized but not above a temperature at which thermal cracking and coke formation occur on the insides of the heater tubes. For atmospheric crude units, in practice that means operating crude unit heaters with a heater coil outlet temperature of around 360−380 °C. For vacuum unit heaters, it is possible to operate at higher heater outlet temperatures up to 415−425 °C. This is mainly due to the higher velocity and shorter residence times in vacuum heaters. Typical crude and vacuum unit heaters are directly fired (with usually fuel gas burners) with radiant and convective sections. Figure 4.15 shows a horizontal cabin-type heater under construction, where the convective roof section is about to be lowered into position. The radiant tubes are located on the sides of the heater. Tube sizes are usually 150 or 200 mm in diameter, and normally the heater is designed with multiple passes (four or eight) to control the tube flow regime. The design of these heaters is a specialist task requiring a detailed thermal analysis of the firebox, tube flow regime, and tube wall temperatures. Regular process monitoring, including monitoring of tube wall skin temperatures, firebox temperature, excess oxygen in the flue, thermal efficiency, and absorbed heat, is carried out to ensure that these heaters operate reliably and within design limits. As a backup and calibration check of tube skin thermocouple readings, infrared thermography checks are regularly carried out through firebox viewing port holes. The maximum wall temperature permissible will depend on the tube metallurgy, but if the heater tube becomes coked, the coke acts as an insulating layer and wall temperatures gradually increase with time. The only recourse for the operator is to reduce the heater firing and ultimately shutdown the heater for a manual decoke. The flow regime of the heater tubes is an important parameter that impacts the oil film wall temperature. Excessive oil film wall temperatures will result in coking of the heater tubes. For that reason, these heaters have a limited operating range and often cannot be easily operated at crude feed rates less than 50% of design. For some unit designs, a higher operating range may be permissible by adding steam into the heater tubes. The steam increases the tube side velocity and promotes hydrocarbon vaporization by reducing the hydrocarbon partial pressure. This is discussed later in the text. Usually, the coil outlet operating temperature of the heater is a key optimization parameter for the crude unit and particularly the vacuum unit. Small changes (increases) to the coil outlet temperature can result in potential yield benefits of several million dollars per year for a typical crude unit. On the downside, excessive heater coil temperatures carry a higher risk of coking the heater.

4.5 Basic principles of crude units

A CDU is essentially similar to all other distillation units but has some unusual operating features (refer to Figure 4.16).

Hot vapor (shown by the gray arrows in Figure 4.16) is generated in the feed heater and flows up the column. Hydrocarbons that cannot be vaporized (shown by the black arrows) in the feed heater drop into the atmospheric residue. As the hot vapor

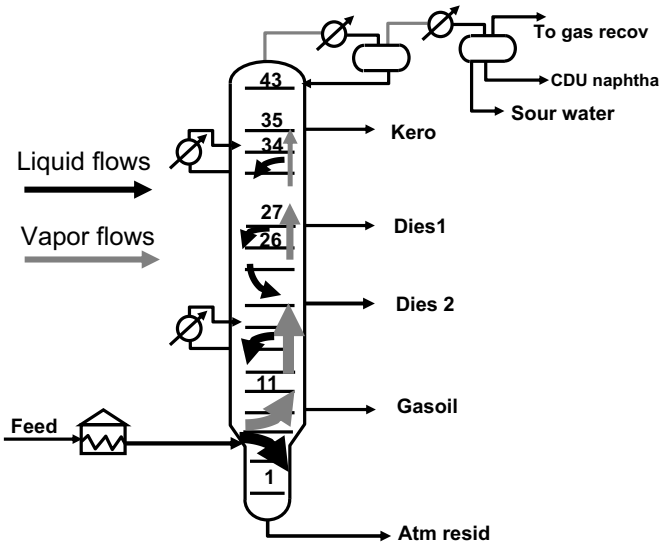

FIGURE 4.16 Basic Principles of a Crude Distillation Unit

Atm resid, atmospheric residue; dies, diesel; kero, kerosene.

passes up the column, the less volatile components in the hot vapor are condensed by contact with the colder reflux flowing down the column. The more volatile component in the colder reflux vaporizes and flows up the column. This is the same principle used by any binary fractionation process in hundreds of distillation processes. As with conventional distillation processes, the higher the reflux rate or, more accurately, the liquid-to-vapor (L/V) ratio, the better the quality of fractionation.

Crude units utilize side strippers to improve the separation quality between the side draw and the distillate above the side draw. Vapor generation in the side stripper is generated by adding stripping steam (discussed later) or, alternatively, by reboiling the side stripper (refer to Figure 4.17). The side stripper is therefore referred to as either a reboiled stripper or a steam-stripped stripper. The main function of the side stripper is to selectively improve fractionation between the side distillate and the distillate drawn from above.

The side stripper operating severity (measured by the reboiler duty or the strip steam rate) progressively strips more and more of the lighter components out of the liquid phase in the side stripper and returns them back into the main column. Side strippers largely improve the separation of the front end of the distillate draw. For the example in Figure 4.17, increasing the kerosene side stripper duty will improve the separation sharpness between kerosene and naphtha and potentially allow the operator to maximize the separation and ultimately the recovery of kerosene from naphtha. Varying the kerosene side stripper duty will have no impact on the lower side distillate qualities. Side strippers are usually designed with 6–10 distillation trays.

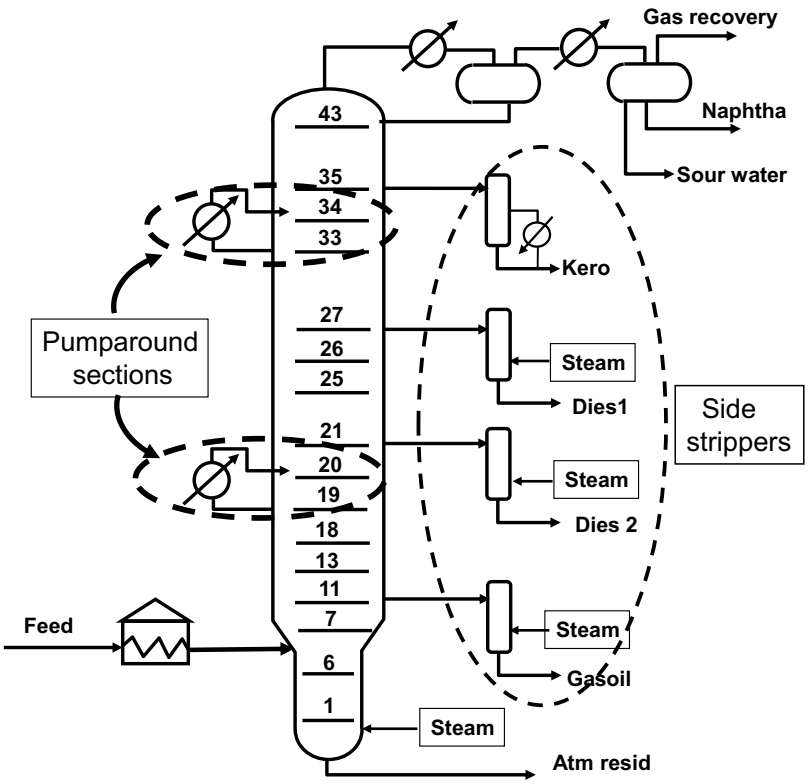

FIGURE 4.17 Crude Unit Pumparounds and Side Strippers

Atm resid, atmospheric residue; dies, diesel; kero, kerosene.

An unusual feature of crude units is that *pumparound* zones are used to generate some of the internal reflux. These can be considered as direct heat exchangers inside the column. A liquid stream is drawn from the column, subcooled in an external heat exchanger circuit, and then returned to the column two to four stages above the pumparound draw (refer to Figure 4.17). Pumparound zones do not directly contribute to fractionation but serve to generate internal reflux, which does have a huge impact on the separation quality. Pumparound rates and heat duties can be significant. A typical pumparound circulation rate could be 50−100% of the crude feed rate, and the pumparound duty could be several megawatts. The location and the number of pumparounds have a significant impact on the L/V ratio in that section of the column, and as a consequence they have a major impact on the fractionation efficiency in that section of the column. In the example shown in Figure 4.17, if we assume that we wish to achieve the best possible separation between kerosene and diesel 1, then we would want to maximize the upper pumparound duty in order to maximize the L/V ratio in trays 32−27. To achieve the best possible L/V ratio in

this section of the column, we also would want to minimize the pumparound duty in the lower pumparound (trays 19−20). In practice, the flexibility to vary the pumparound duties will depend on the unit design and the impact on crude preheat. To extend the above example, if we minimize the lower pumparound duty, then this will impact the crude preheat recovery and also will increase the vapor loads into trays 21−33. Therefore, the optimum pumparound operation is a complex optimization issue and is often a tradeoff between fractionation quality against preheat recovery. Regular use of simulation tools can be used to predict yield and energy effects by varying the pumparound heat distributions. In practice, because of unit constraints there is often restricted flexibility to significantly vary the pumparound heat distribution. Nevertheless, optimization of the pumparound duty is an important operating parameter.

Crude units sometimes also generate reflux via a condenser similar to that in simple binary distillation columns. This also contributes to generating the L/V ratio in that section of the column. For the example shown in Figure 4.18, reducing the top pumparound duty and increase the crude unit reflux will generate a higher L/V ratio in that section of the column (between trays 43−35) and will improve the separation quality between the naphtha and kerosene.

However, the main disadvantage of increasing the top reflux at the expense of top pumparound duty is that it is more difficult to recover the heat from the overhead condenser since it is a lower grade of heat (it is at a lower temperature).

Steam is extensively used in refinery crude and vacuum units to increase vaporization (refer to Figure 4.17). The addition of steam into the bottom of the column (residue section) reduces the hydrocarbon partial pressure (according to Dalton's Law) and significantly increases the percentage vaporization at the inlet to the column. The addition of so-called partial pressure steam significantly improves the achievable yield of the heaviest atmospheric distillate (gasoil stream in the example shown in Figure 4.17). The stripping steam rates are significant and several tonnes of steam per hour are often used. In general, typical stripping steam rates added are

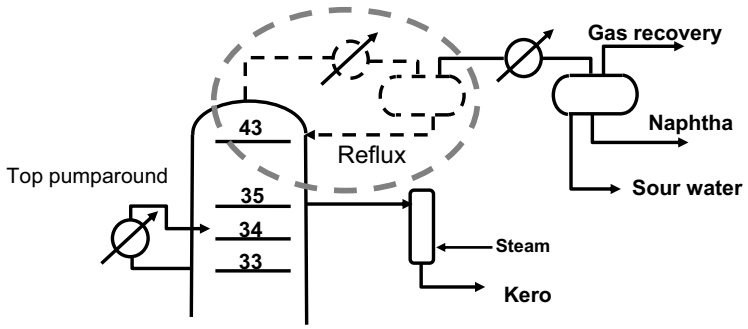

FIGURE 4.18 Crude Unit Reflux Arrangement

Kero, kerosene.

around 20–40 kg steam/m^3 atmospheric residue (for the residue zone) and 10–20 kg steam/m^3 atmospheric residue for the atmospheric side distillates. However, there are problems with too much strip steam addition, such as:

- potential to generate a free water phase at the top (colder) section of the column. This could result in severe corrosion problems for the internals and the vessel walls.
- excessive vapor loads. The low molecular weight of the steam will significantly increase vapor velocities, possibly to a point where the column internals are overloaded.
- all of the strip steam added has to be condensed and recovered and the water treated. This increases energy requirements for the unit and the size of the CDU overhead condenser. Nevertheless, strip steam is an important optimization parameter for both crude and vacuum units.

4.6 Crude vacuum units

Crude vacuum units (VDUs) have essentially the same basic principles as those for crude units.

- Large fuel-fired feed heaters are used to heat the atmospheric residue feed to achieve typical vaporization rates (depending on crude type) of around 40–80%. The VDU heater temperature is usually significantly higher than that on the crude unit (due to the shorter residence times and hence lower coking tendency).
- Pumparounds are used to generate reflux (similar to the crude unit).
- Steam is often used in the heater tubes and in the column to reduce the hydrocarbon partial pressure and increase hydrocarbon vaporization (discussed later).
- Side strippers are used where sharp fractionation of the side distillates is required (e.g. in refinery vacuum units generating lube oil distillates).

Vacuum units differ from crude units in that:

- The unit pressure is maintained by a vacuum generation system (as shown in Figure 4.19). The target operating pressures (at the top of the VDU vessel) are typically 10–40 mBara. Steam ejectors (three stages) are usually used to generate a vacuum. A typical ejector scheme is shown in Figure 4.19. The sour gas (generated by thermal cracking of the feed) is compressed via the ejectors and either recovered or burned in the crude unit heater. The sour gas rate is quite small and on the order 0.1–0.2%wt of the VDU feed. Nevertheless, it is important to estimate this rate carefully in order to properly size the vacuum ejectors.
- The overhead distillate flow rate from the vacuum unit (slop oil plus cracked gas product) is relatively low compared to the VDU feed rate, and therefore VDUs

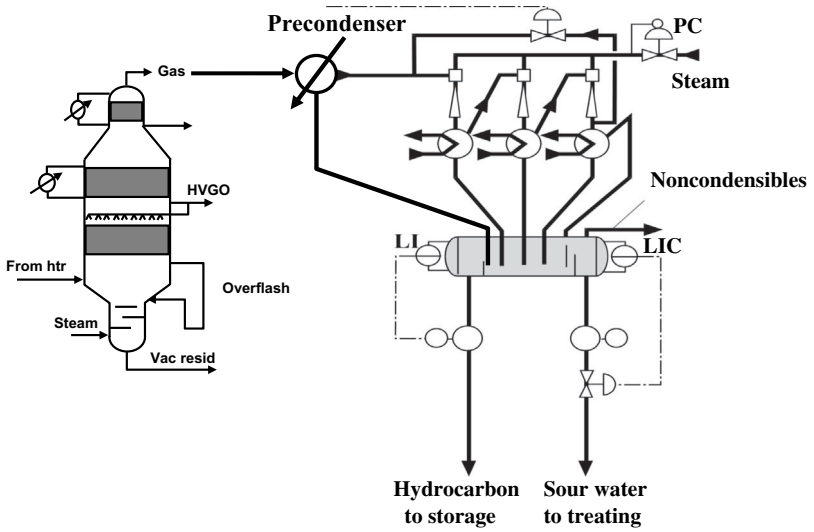

FIGURE 4.19 Typical Ejector Arrangement for a Vacuum Distillation Unit

HVGO, heavy vacuum gasoil; htr, heater; LI, level indicator; LIC, level indicator and controller; PC, pressure controller; vac resid, vacuum residue.

are generally operated without cold reflux from the overhead condenser (unlike CDUs).

- The flash zone conditions essentially set the yield of the heaviest vacuum distillate possible (the heavy vacuum distillate in Figure 4.20), and this is set by the hydrocarbon partial pressure at the flash zone inlet. As with crude units, it is possible to recover only vacuum distillates that can be vaporized at the flash zone inlet. To minimize the hydrocarbon partial pressure (and maximize vaporization at the flash zone inlet), it is important to operate the VDU at the lowest flash zone pressure possible. This is set by the VDU top pressure plus the pressure drop across the column internals. Consequently, there is a large incentive to minimize the pressure drop across the VDU column internals, and for that reason the internals for VDUs almost exclusively use packed internals (whereas CDUs are more typically trayed internals).

The pressure drop for packed column internals (such as random, grid, and structured packed internals) is typically 25% of a corresponding trayed unit. For the example in Figure 4.20, if we are able to reduce the flash zone pressure by, say, 10 mbar for a modest-size vacuum unit, the additional heavy distillate recovered would be worth in excess of $1 million/year. Depending on the refinery's complexity, the price delta between heavy vacuum distillate and the vacuum residue is usually the largest margin of any the refinery intermediate products, and consequently there is a strong incentive to maximize the yield of heavy vacuum distillate.

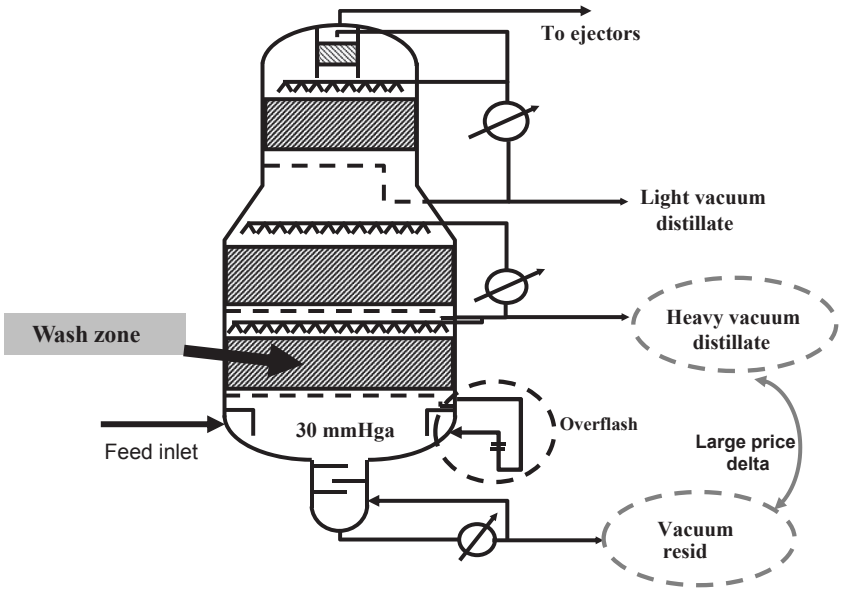

FIGURE 4.20 Vacuum Unit Showing Liquid Overflash Arrangement

Vac resid, vacuum residue.

- Due to the large commercial incentive to maximize the heavy vacuum distillate yield, VDU heaters are usually operated at significantly higher heater outlet temperatures compared to CDUs. Heater coil outlet temperatures up to 425 °C are possible for vacuum units. It is possible to operate VDU heaters at these higher temperatures and avoid coking since the liquid film residence time is shorter in VDUs compared to those in CDUs. Also, steam is often added into the VDU furnace tubes, and this has the dual benefit of reducing the hydrocarbon partial pressure and also increasing tube side velocity and further reducing oil film residence times.
- Due to their higher operating temperatures, refinery crude vacuum units are more troublesome to operate and have a greater coking risk than CDUs. The hottest zone in the vacuum unit, called the wash zone, is the zone that is most susceptible to coking, and it is very important that this zone is properly refluxed and never operated in a dried out condition. The liquid rate leaving the underside of the wash bed is called the *overflash rate* (see Figure 4.20). This rate should be controlled to maintain a minimum liquid load. This minimum liquid rate is subject to unit operating conditions and crude types being processed. With a flash zone diameter of possibly 14 m, it can be a challenge to ensure that the wash zone is properly distributed and controlled to achieve the minimum wetting rate across the entire area of the bed. An excessive overflash rate could easily result in a financial yield loss of several million dollars per year (by

downgrading heavy vacuum distillate into vacuum residue). However, inadequate overflash will result in bed coking and an unscheduled shutdown of the unit. If the wash bed becomes coked, there is no recovery option other than to shut the unit down, remove the coked bed, and then replace it. Careful operation and monitoring of the wash zone is a must for any unit engineer to ensure successful operation over the VDU planned operating cycle. An added complexity for the unit engineer is understanding the true overflash rate. This is a key issue since the measured overflash will likely include some liquid entrainment from the feed (which has a very high inlet velocity).

- Due to their higher operating temperatures of VDUs compared to crude units, the lower sump section for vacuum units is usually quenched with subcooled vacuum residue, as shown in Figure 4.20. The lower quench temperature reduces the likelihood of thermal cracking in the sump and this reduces the quantities of cracked gas, which has to be handled via the ejectors.
- Vacuum units also utilize side strippers (like CDUs), where product separation between the side distillates is important. This is the case where VDUs are used to generate base oils for lubricants, and good fractionation between the lube base oil distillates is required (refer to Figure 4.21(a)). However, most vacuum units are so-called fuels units, where the side distillates are processed in a

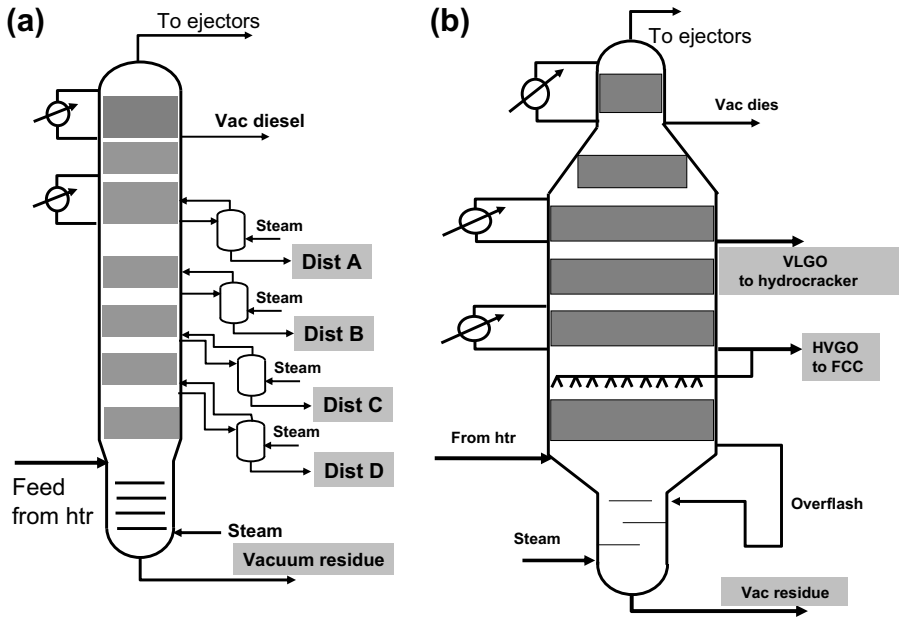

FIGURE 4.21

Vacuum unit for (a) lube oils and (b) for fuels production. HVGO, heavy vacuum gasoil; FCC, fluid catalytic cracker; htr, heater; vac dies, vacuum diesel; VLGO, vacuum light gasoil.

conversion unit such as a fluid catalytic cracker (FCC) or a hydrocracker. In these cases, side strippers are not generally required. However, steam stripping of the residue section is common, and this also has a significant impact on the heavy vacuum distillate recovery possible (see Figure 4.21(b)).

4.7 Key factors affecting the fractionation quality

There are relatively few parameters that affect the quality of separation of product distillates, and these are summarized here. Most of these parameters apply to all distillation separations; however, some of these are more specifically applicable to refinery crude and vacuum units.

1. L/V ratio (or reflux ratio)
2. Operating pressure
3. Heater operating temperature
4. Cut widths of side distillates
5. Stripping steam ratio
6. Efficiency of the column internals

The *reflux ratio (L/V ratio)* is probably the most important parameter influencing the separation efficiency. Consider the basic principles of a distillation column: hot vapor generated in the heater passes up the column and is cooled by colder reflux (refer to Figure 4.22).

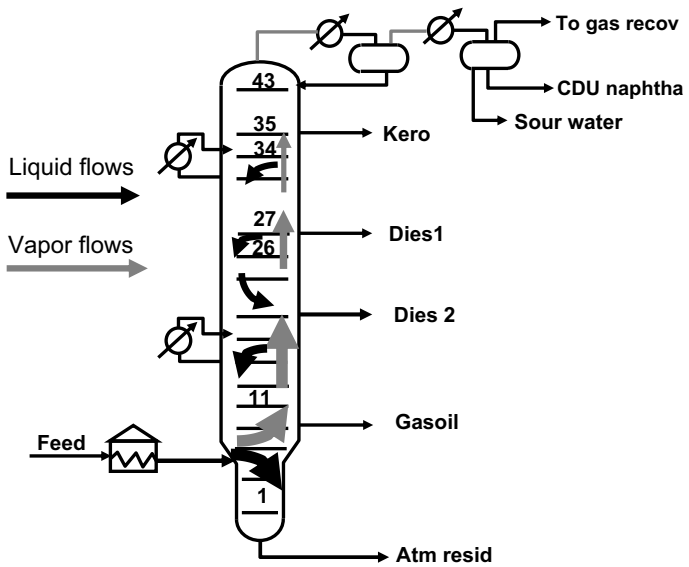

FIGURE 4.22 Vapor/Liquid Flows in a Crude Units

Atm resid, atmospheric residue; CDU, crude distillation unit; dies, diesel; kero, kerosene.

Where the hot vapor is cooled by the reflux, heat transfer occurs, followed by mass transfer. The less volatile component from the vapor phase condenses and the more volatile component from the liquid vaporizes. Clearly, more or less heat transfer and mass transfer occur depending on the L/V ratio in that section of the column. Nowadays, the L/V ratio in various sections of complex fractionators like crude units can easily be determined by process simulation of the unit. Based on the operational duties of the pumparound sections, the simulation will show the predicted L/V ratio throughout the column.

For each section of the column, the higher the L/V ratio in that section the better the separation efficiency.

The L/V ratio for the various sections in the column can be manipulated by varying the pumparound duties. This is quite a complex issue, but the simulation tools are of great assistance in understanding the relationship between L/V ratio, pumparound duties, and the corresponding impact on distillate yields.

Operating pressure impacts the separation efficiency, but only to a modest extent since in practice there is usually little flexibility to vary the column operating pressure.

The lower the operating pressure the higher the relative volatility and the easier the separation.

However, for most refinery distillation columns, the operating pressure is essentially set by the condensing temperature (which is usually ambient air or cooling water). Therefore, if the overhead distillate product is a light distillate it may be necessary to operate the column at an elevated pressure in order to condense this distillate at the available condensing temperature. It is, however, important to understand the benefits of lowering the column pressure where possible. For example, it may be possible to operate the unit at a lower pressure in the winter months when a lower condensing temperature may be achievable. Energy savings by exploiting day/night and summer/winter variations in the condensing temperature can be significant: on the order 1−2 MW in some units.

The *heater outlet temperature* is a very important parameter for crude and vacuum units. The higher the heater temperature, the higher the percentage vaporization at the heater outlet. A key separation in any crude unit is the recovery of atmospheric distillates out of atmospheric residue and, in order to maximize distillate recovery, we need to maximize the L/V ratio in the zone immediately above the flash zone. For crude and vacuum units, this is called the wash zone. The rate of liquid leaving the section immediately above the feed inlet flash zone (tray 7 in the example shown in Figure 4.23) is called the overflash rate, and this is usually expressed as a percentage of liquid rate relative to the crude feed rate. The higher the overflash rate, the higher the L/V ratio in that section of the column and the better the recovery of gasoil from atmospheric residue. However, we should recognize that in order to generate a higher liquid overflash rate, we first need to increase the percentage of vaporization at the heater outlet. That requires a higher heater outlet temperature, a lower operating pressure, or a reduced hydrocarbon partial pressure.

Typical heater temperatures for CDUs are 360−380 °C the maximum heater temperature is set by the heater design and the types of crude processed. For refinery

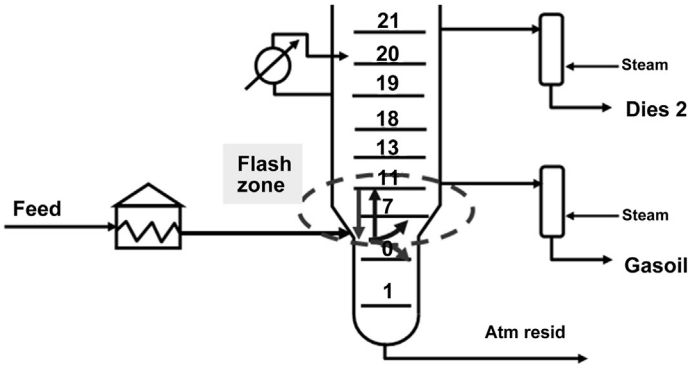

FIGURE 4.23 Liquid from Tray 7 is Crude Overflash

Atm resid, atmospheric residue; dies, diesel.

vacuum columns, heater temperatures up to 425 °C are possible, but careful design and operation of the heater is required to understand the heater coking risks.

The *number and the cut width of side distillates* have a significant impact on the separation efficiency. Narrow cuts are more difficult to separate from wider cuts and, when possible, the number of side distillates should be minimized to achieve the best possible separation. If we consider the example shown in Figure 4.24, crude unit A has four side distillate draws, but some of these are blended outside the column. Crude unit B has only two side distillate draws.

From a fractionation viewpoint, crude unit B is a better design, and this flow scheme will allow easier separation and a higher distillate yield for whatever product specifications are set. For example, if the most valuable product is kerosene, then the yield achievable for crude unit B could be typically 5% higher than that of crude unit

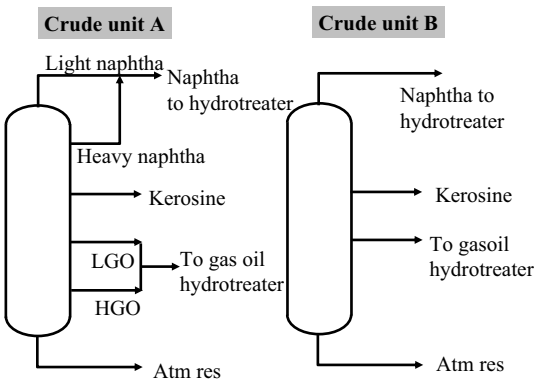

FIGURE 4.24 Impact of Cut Widths on Fractionation Quality

Atm res, atmospheric residue; HGO, heavy gasoil; LGO, light gasoil.

A. In general, for optimum fractionation, always attempt to minimize the number of side draws from a column and avoid drawing multiple draws and then reblending these outside the column.

The *fractionation quality between side distillates* can be tracked by reviewing the distillation overlaps between adjacent distillates (refer to Figure 4.7). In a CDU, the overlaps for the lighter distillates are usually lower (better fractionation) compared to those of the heavier distillates. This is mainly because of the higher L/V ratios in the upper section of the crude unit.

Stripping steam in crude and vacuum units has a significant impact on the L/V ratio, particularly in the wash section of the column, and therefore this has a pronounced impact on the recovery of the heaviest distillate. Steam reduces the hydrocarbon partial pressure and allows a higher vaporization at the flash zone inlet and, consequently, a higher heavy distillate recovery. Stripping steam, along with the heater outlet temperature, is a key optimization parameter for crude and vacuum units. For vacuum units, depending on the heaviest vacuum distillate quality specification, there is an incentive to maximize both heater and stripping steam limits. This is illustrated in the VDU example shown in Figure 4.25 (for a feed rate of 250 t/h). In general, optimizing the heater is more beneficial than stripping steam, but both are beneficial and can significantly impact the yields of the heaviest distillate (HVGO (heavy vacuum gasoil) in the example shown in Figure 4.25).

When optimizing the stripping steam for vacuum units, it is likely that increasing the stripping steam will adversely affect the performance of the vacuum ejectors (particularly if there is no precondenser before the ejectors). In that case, it is necessary to factor in any potential change in column vacuum as a result of more or less stripping steam.

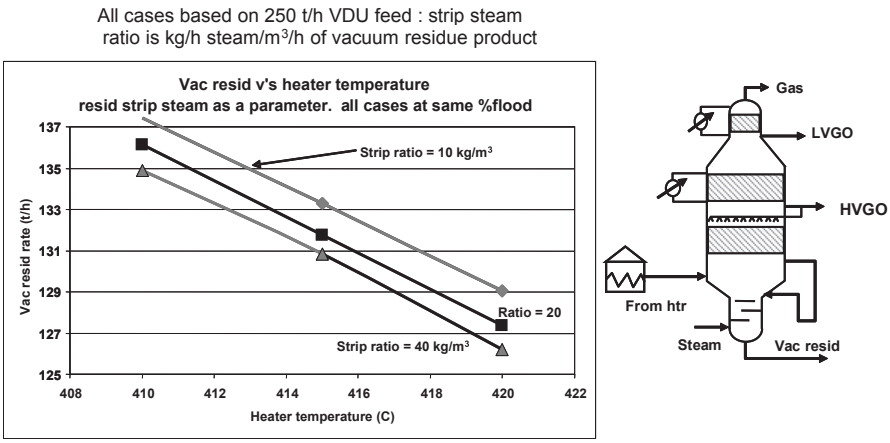

FIGURE 4.25 Impact of Heater Temperature and Stripping Steam on Distillate Yield

Htr, heater; HVGO, heavy vacuum gasoil; LVGO, light vacuum gasoil; vac resid, vacuum residue.

The efficiency of the column internals will impact the separation efficiency but only insofar as there is an adequate L/V ratio in that section of the column. Clearly, if the L/V ratio in a particular zone of the column is zero, then it won't matter if we have 100 theoretical stages—the fractionation levels will simply be poor because of insufficient reflux.

4.8 Column internals for refining applications

Trayed column internals are generally preferred for crude units and other refinery atmospheric and higher pressure units. The main reason is that they are more reliable than packed internals, more robust, easier to clean, and easier to access during column inspections. There are many different types of tray decks used that offer higher or lower operating flexibility, but in general trayed designs are fairly well understood, with modest technical risk. Tray metallurgy used in refining is generally stainless with tray decks 2−3 mm thick. Tray spacing is usually 610 mm. Fixed (nonmoving) valve designs are becoming more commonly used since most refinery column designs do not usually require a high operating turndown. Also, fixed valves are more robust and more easily cleaned during column turnarounds compared to the older style moving valves.

Packed column internals are universally preferred for vacuum column applications and a few other refining applications. This is because there is a large operational benefit afforded by the lower pressure drop that packed internals offer over trays. In general, the pressure drop for packed internals is around 2−3 mbar/m of packing. Trayed internals would be typically 4 times the equivalent figure. For vacuum column applications, the gains yield resulting from a lower pressure drop make a compelling case for the use of packed internals over trays. However, all designers of vacuum columns know that there are a number of critical design issues that need careful consideration when specifying packed internals, not least of which is the design and turndown of the distribution systems.

The packing vendors manufacture several grades or sizes of these packings, but generally the higher the packing surface area/unit volume, the better the fractionation efficiency. However, packings with a large surface area have a lower vapor liquid handling capacity and, therefore, fractionation efficiency is a tradeoff against unit capacity. When refineries are looking to debottleneck a unit for greater throughput, then this may be possible by installing a packing with a smaller surface area (or a higher voidage).

4.9 Hazards of pyrophoric scale

In many refining services, sulfides are present in the crude, and during normal operations thin layers of iron sulfides can form inside the vessel and then collect on the

internals. Iron sulfide is pyrophoric in the presence of air, and during shutdown outages, when the vessel is open to the air, there is a serious risk of internal fires:

$$2FeS + 2O_2 = 2FeO + 2SO_2 + \text{Heat}$$

There are many examples within the industry of spontaneous fires in distillation columns due to pyrophoric scale [7]. Some of these have been very damaging, particularly where exotic metallurgies (which are partially reactive) have been used.

Pyrophoric scale fires are more of an issue with structured packings than any other packing type (but they can still be an issue with other packing types), and this is because structured packings have a relatively small thermal mass (due to the very thin sheet metal elements). Consequently, pyrophoric scale trapped inside structured packings can heat up in the presence of air and achieve relatively high local temperatures.

The solution for dealing with pyrophoric scale is to keep the packing thoroughly wetted with water, particularly during the early stages of the shutdown. But this can be a challenge for large-diameter vessels, especially if the distribution systems are not designed to handle very high wetting rates. There are also specialist vendor chemical treatments for neutralizing pyrophoric scale. Suffice it to say that this is a serious safety issue that the industry has to deal with, particularly if structured packed internals are used. In refining, the main units where pyrophoric scale has been an issue during turnarounds are:

- crude vacuum units
- FCC main fractionator units
- coker main fractionator units.

4.10 Other distillation units in refining

There are many other distillation units used throughout the refinery, and these are mainly associated with the many conversion units used to upgrade intermediate products. Most of these conversion units are thermal and catalytic units that operate at relatively high temperatures and pressures and essentially convert hydrocarbons with a heavier boiling range into a range of lighter more valuable refining distillates. Separation of the reactor effluents into saleable refined products is carried out by distillation processes. The distillation units associated with these processes often comprise four to six different distillation columns. Some of the main refinery conversion units are as summarized in Table 4.1.

In addition to the conversion processes, there are also a significant number of distillation units associated with the recovery and treatment of gases and products from across the refinery (although some of these processes are absorption processes). Commonly used gas recovery and treatment units are summarized in Table 4.2.

Some of the flow schemes and key performance indicators for the distillation operations for these units are discussed below.

Table 4.1 Summary of Main Distillation Units in Refinery Conversion Units

Conversion Unit	Feed Components	Products	Distillation Columns
Fluid catalytic cracker	Heavy gasoils, TBP: 360–600 °C	Gas, LPG, gasoline, diesel, fuel oil, and coke	Main fractionator, absorber, stripper, secondary absorber, debutanizer, gasoline splitter
Hydrocracker	Heavy gasoils, TBP: 360–500 °C and H_2	Gas, LPG, gasoline, diesel, and fuel oil	Feed stripper, main fractionator, debutanizer, absorber, depropanizer
Catalytic reformer	Naphtha, TBP: 80–180 °C	Increased octane gasoline, H_2	Gasoline stabilizer and reformate splitter
Isomerization unit	C5s and C6s and H_2	Light gasoline, LPG	Isomerization stabilizer, deisohexanizer
Alkylation unit	Butylenes and *i*C4	C8 gasoline, C3, *n*C4, and acid-soluble oil	Alkylation main fractionator, depropanizer, propane stripper, gasoline debutanizer
Coker unit	Vacuum residues: 600–1200 °C	Coke, gas, LPG, gasoline, diesel, and fuel oil	Coker main fractionator, absorber, debutanizer
Naphtha desulfurization units	Naphtha, TBP: 0–180 °C and H_2	Naphtha and H_2S, LPG	Stabilizer, naphtha splitter
Distillate desulfurization unit	Distillates, TBP: 240–360 °C And H_2	Diesel and H_2S, LPG	Stabilizer

H_2, hydrogen; H_2S, hydrogen sulfide; iC4, isobutane; LPG, liquefied petroleum gases; nC4, normal butane; TBP, true boiling point.

4.10.1 Saturated gas plant

Typically, saturated gas plants (SGPs; see Figure 4.26) process and fractionate most of the lightends fractions (C1s−C6s, H_2, and H_2S) in the refinery. These lightends partly come from the raw crude, but they are also formed by thermal cracking in most of the refinery conversion processes. H_2S is generated from the product hydrotreaters, and a small proportion of the hydrotreater feed is cracked into C1s−C4s and so-called wild naphtha. The main function of the SGP is to separate and recover the heavier hydrocarbon components from the feed gas (C3s and heavier). The lighter

Table 4.2 Distillation and Absorption Units Used in Refinery Treatment Units

Refinery Unit	Feed Components	Products	Distillation Columns
Saturate gas plant	All refinery gases (hydrogen, C1, C2, C3, C4, and C5s)	Fuel gas, propane, butane, and C5+	Absorber, stripper, depropanizer, and debutanizer
Sour water stripper	Refinery water streams	H_2S, NH_3 and clean water	Stripper column
Fuel gas absorbers	Refinery fuel gas streams and amine	H_2S and treated fuel gas	Amine absorber and stripper column
LPG absorber	LPG and amine	Treated LPG and rich amine	Liq–liq amine absorber

LPG, liquefied petroleum gases.

components (C1s, C2s, H_2S) are rejected into the refinery fuel gas stream (after absorption to remove the H_2S).

The SGP uses an absorber and naphtha boiling range stream, usually called lean oil, to absorb the heavier components in the feed gas. The absorption process is carried out at relatively high pressure (10−20 Bar) and at low temperature (20−30 °C) in order to maximize the absorption. The most difficult component to recover is propane (methane and ethane recovery are not targeted here), and a key performance

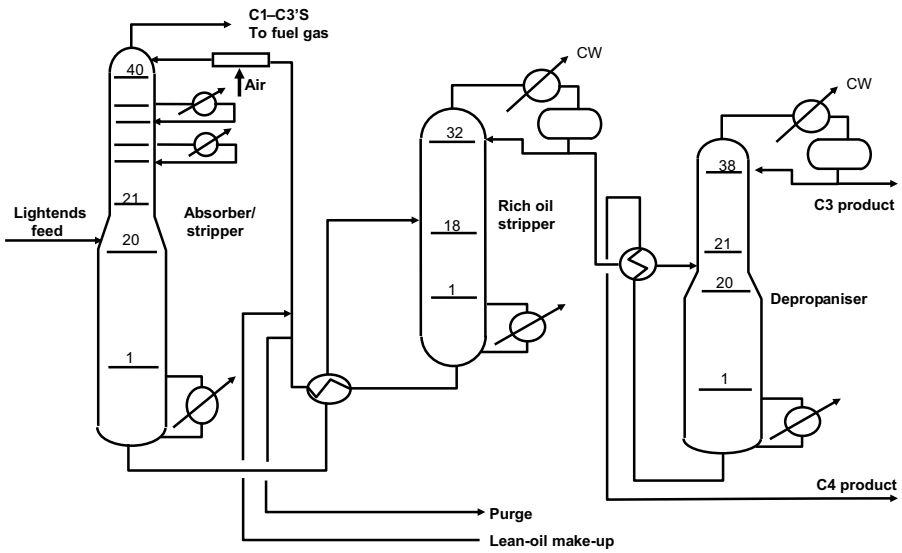

FIGURE 4.26 Saturated Gas Plant

CW, cooling water.

indicator of this unit is the overall recovery of propane. Typical propane recoveries of greater than 90% would be targeted.

Process parameters that help recover C3 from the absorber include:

- high operating pressure (usually set by the feed gas pressure).
- low operating temperature; many units add pumparound coolers in the absorber to maintain a low temperature (as shown in the example in Figure 4.26).
- high lean oil rates, although this is a compromise between energy costs and equipment size required for the downstream rich oil stripper column.
- good lean oil quality (low levels of C3 and C4 content in the lean oil).

During the absorption process, some quantities of C1s and C2s are also absorbed into the lean oil. Therefore, a stripper column is added after the absorber to strip (and remove) the C1s and C2s. For some SGP flow schemes, the stripper column may be a separate vessel located after the absorber, but in others it is combined with the absorber into a single vessel, as shown in the example in Figure 4.26. The stripper column is operated with a targeted reboiler temperature in order to remove (strip out) ethane from the bottom stripper product. The normal sales specification for propane allows around 2% ethane in the propane product; therefore, the stripper column would be operated with varying reboiler duties in order to control the C2-to-C3 ratio in the bottom stripper stream to 2% or less. Overstripping is a common cause of poor recovery of C3 from SGPs since overstripping also strips out some propane in addition to ethane. The SGP process engineer monitoring this unit would typically look at the propane content in the fuel gas and also the ethane content in the propane. Zero ethane content in the saleable propane is an indication that the stripper is being over-reboiled, and it is likely that this would cost the refinery a loss of propane into fuel gas (this would be confirmed by higher than expected C3 content in the fuel gas). Poor operation of the SGP can easily result in lost opportunity costs of $1−3 million/year.

The SGP flow scheme shown in Figure 4.26 uses a lean oil that is purged and partly recycled with a make-up lean oil stream. The rich oil from the absorber-stripper is stripped to recover C3 and C4s, which are separated in the downstream fractionator. The rich oil stripper is operated with a varying reboiler duty to strip out C4s from the rich oil. The C4 product sales specification allows typically 2.5% C5s in the C4 product; therefore, the key quality specification for the rich oil stripper column is the C5-to-C4 ratio in the overhead distillate of the rich oil stripper. This column would be operated at the maximum permissible reflux rate with a varying distillate draw rate set to control the C5-to-C4 ratio to no higher than 2.5%. The maximum permissible reflux rate is dependent on the column design (vessel size, internals capacity, and reboiler capacity). The operating pressure of the rich oil stripper should be minimized as far as possible, but this would be set by the condensing temperature of the C3/C4 overhead distillate (overhead pressure is usually around 6−7 Barg). C5s and C6s recovered in the SGP are recovered by the lean oil purge. This is purged (and recovered) to the crude naphtha units.

4.10.2 Fractionation flow schemes for heavy oil conversion units

The three main heavy oil conversion units in refineries are fluid catalytic crackers (FCC), hydrocrackers (HCK), and cokers (COK). For each of these processes, the reactor effluent is a mix of C1−C5 lightends and refinery distillates such as gasoline, diesel, fuel oil, coke, and unconverted oil. The catalyst selectivity and process operating conditions can be tailored to target a high yield of specific products (such as diesel), but nevertheless the reactor products are somewhat similar to a synthetic crude oil and consequently the fractionation unit design required is similar to that of a crude unit. A typical flow scheme for a hydrocracker unit is shown in Figure 4.27.

The hydrocracker effluent is first stripped to remove liquid petroleum gases, light naphtha, and H_2S, and then the stripper's bottom product is fractionated in a main fractionator, which is very similar in design and operation to that of a crude unit. The lighter distillates (recovered from the feed stripper's overhead product) are separated and recovered in a gas plant similar in concept to the previously described SGP. The key performance indicator from this unit would be to maximize diesel recovery out of unconverted oil. Maximum diesel recovery could be achieved by:

- minimum main fractionator operating pressure
- maximum heater temperature
- maximum base stripping steam
- optimum design of trays between diesel and unconverted oil.

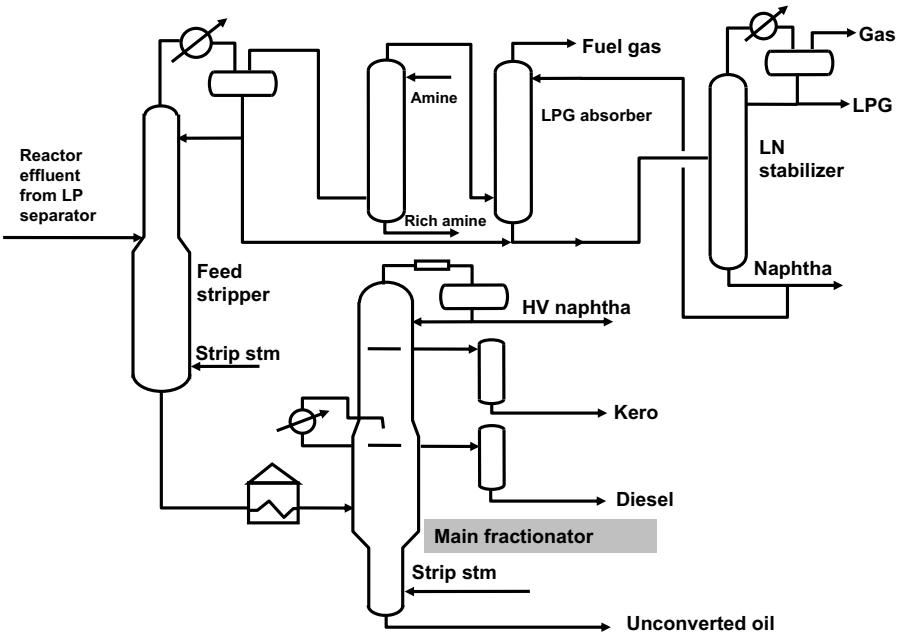

FIGURE 4.27 Hydrocracker Gas Plant

HV naphtha, heavy naphtha, kero, kerosene; LN, light naphtha; LP, low pressure; LPG, liquid petroleum gas; stm, steam.

Product separation between the various distillate products would be monitored by tracking ASTM product overlaps (in a way similar to that used to monitor a crude unit).

The FCC main fractionator unit configuration is shown for a trayed unit in Figure 4.28(a) and for a packed unit in Figure 4.28(b). The reactor effluent enters the main fractionator at the base of the column. All of the reactor effluent is vaporized (since the reactor outlet temperature is around 500 °C). The FCC main fractionator looks like, operates like, and is often a similar size to the refinery's main crude unit. Typical FCC main fractionator intermediate products are shown in Figure 4.28(a) and (b):

- naphtha (gasoline) and lightends, particularly propylene, would be routed to the gas plant for recovery;
- heavy cracked naphtha (HCN) and light cycle oil (LCO) have a diesel boiling range that is routed to a hydrotreater for desulfurization and then into the diesel pool;
- heavy cycle oil (HCO) is heavier than diesel and will go either to a fuel oil pool or to a coker unit feed; and
- decant oil (DCO, sometimes called slurry) is routed to fuel oil or to a coker feed.

The operating pressure of the FCC main fractionator is low, typically around 1 Barg. The reactor yield of lightend gases can be relatively high, and consequently the wet gas compressor (which compresses the main fractionator condenser offgas) is often a key capacity constraint for the unit. In this case, there is usually a good incentive to revamp the main fractionator internals from trayed internals to packed

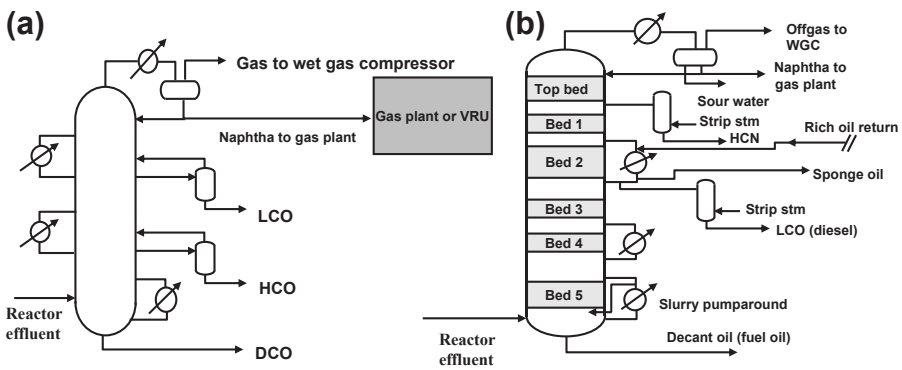

FIGURE 4.28

Typical fluid catalytic cracker main fractionator units with trayed internals (a) and packed internals (b). DCO, decant oil; HCN, heavy cracked naphtha; HCO, heavy cycle oil; LCO, light cycle oil; stm, steam; VRU, vapor recovery unit; WGC, wet gas compressor.

internals. The smaller pressure drop for the packed column internals may debottleneck the wet gas compressor.

The FCC gas plant or vapor recovery unit is shown in Figure 4.29. This is quite similar to the SGP previously described. The lightends from the fractionator are compressed to around 12−15 Barg in the wet gas compressor and then absorbed in an absorber/stripper unit. The absorption oil is naphtha (cooled) from the main fractionator. A second absorber (secondary absorber) is commonly used in FCC gas plants to recover the equilibrium C4s and C5s in the primary absorber offgas (since the primary absorber lean oil has fairly high levels of C4s and C5s).

Key performance indicators for FCC fractionators and gas plant are:

- maximize LCO recovery out of DCO (diesel from fuel oil).
- maximize C3 and, more specifically, propylene recovery from the gas plant (typically can achieve 90−95% recovery). Some units refrigerate their lean oil to achieve higher recoveries or alternatively use a secondary lean oil recycle from the debutanizer bottoms to the primary absorber. The unit engineer will track C3 levels in the absorber offgas and C2 levels in the C3 product (to avoid overstripping).
- main fractionator pressure drop is monitored, including the pressure drop of the overhead condenser.

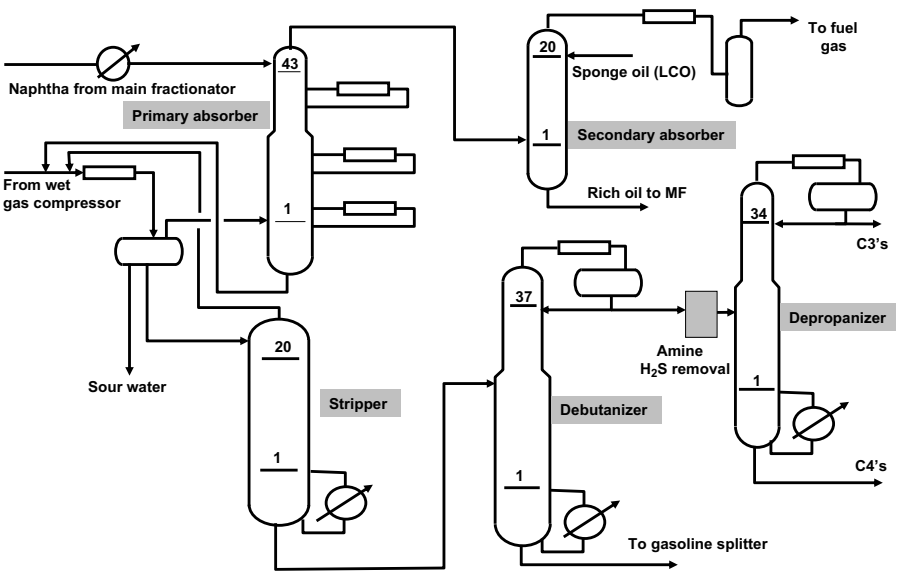

FIGURE 4.29 Typical Fluid Catalytic Cracker Gas Plant

LCO, light cycle oil; MF, main fractionator.

Acknowledgment

Most of the illustrations, photos and examples within the text are shown with permission from BP Refining.

References

[1] http://www.astm.org/Standard/index.shtml?complete.
[2] Aspentech Hysys Simulation Software, http://www.aspentech.com/hysys/.
[3] Invensys SimSci Simulation Software, http://iom.invensys.com/UK/Pages/SimSci-Esscor.aspx.
[4] M. Errico, G. Tola, M. Mascia, Energy saving in a crude distillation unit by a preflash implementation, Appl. Therm. Eng. (July 28, 2008).
[5] B. Linhoff, E. Hindmarsh, The pinch design method for heat exchanger networks, Chem. Eng. Sci. 38 (1983) 745−763.
[6] J. Gutzeit, Controlling Crude Unit Overhead Corrosion − Rules of Thumb for Better Crude Desalting, Nace International Document 07567, March 2007.
[7] M.S. Mannan, Best Practices in Prevention and Suppression of Metal Packing Fires, Texas A&M University System, August 2008. http://kolmetz.com/pdf/articles/MetalFires.pdf.

CHAPTER

Distillation of Bulk Chemicals

5

Hendrik A. Kooijman, Ross Taylor

Department of Chemical Engineering, Clarkson University, Potsdam, New York, USA

CHAPTER OUTLINE

Distillation: Operation and Applications. http://dx.doi.org/10.1016/B978-0-12-386876-3.00005-3

5.1 General industrial separations

This chapter discusses various aspects of the distillation of bulk chemical processes—that is, distillation columns with diameters of 6 ft (2 m) and larger. These large columns form the basis of all separations in state-of-the-art industrial (petro-) chemical plants. Competitive world-scale plants require hydraulically balanced (high-capacity) column internals that can be reliably scaled over several orders of magnitude in capacity. The design of such industrial columns requires attention to negative performance factors that are less well defined, such as foaming, wetting, polymerization/fouling, scaling, or entrainment. These factors often change over time and relate to catalyst aging or the handling of different feedstocks. Chemical distillation processes must account for high turndown or complicated chemical interactions stemming from the nonideality of the components to separate, such as the presence of salts. The removal of trace components to produce high-purity products also requires nonstraightforward distillation process configurations. These topics are illustrated by means of distillation column internals layouts in actual industrial process plants. The first part of this chapter describes generic issues related to the design of distillation column internals in chemical process plants. In the second part, it will be shown how these translate to specific design aspects for the column internals of existing industrial processes; issues relating to unit operation lineup, column operation, configuration, integration, and design will be considered.

5.1.1 Separation systems in chemical plants

Chemical plants center around the reactor, which is usually fed with two reactants and optional inerts from which one mixed stream is obtained containing products, potentially several side products, the inerts, and some unreacted feedstock [1]. Usually, reactor feeds must be preheated to increase the chemical reaction rates to obtain reasonable conversion. If the reaction occurs in the gas phase, (part of) the feed may need to first be vaporized. Reactor effluents are then often cooled to slow or stop subsequent reactions. Sometimes, this must be done quickly by means of quenching in order to prevent formation of undesired byproducts. Typically, the reactor product is then separated relatively crudely between products and reactants, where the reactants are recycled back to the reactor system to increase the overall conversion of the process.

Most of the time, this crude separation is a simple vapor–liquid flash sending components to a vapor and to a liquid recovery system; sometimes, this separation is done directly by a distillation column. In some special (and until recently rare) cases, the reactor and the first separation unit can be combined with the recycle into one unit, the reactive distillation column, resulting in a very compact chemical plant (see Volume 2, Chapter 8). However, in many processes, this early separation is done by means of a set of quench and/or wash columns followed by a primary fractionation. Such quench columns often consist of simple one- or two-bed columns

with a pump-around zone of cooled water or oil. Example of such a line-up are the quench columns for processing of pygas (pyrolysis gas from a Naphtha cracker).

Generally, the vapor recovery system can recover products or reactants by means of

- Condensation (often requiring refrigeration)
- Absorption (with subsequent stripping)
- Adsorption
- Membranes
- Reactors

The selection of the best method depends on the location of the system, either in a purge stream (to prevent loss of reactants and/or products), in the gas recycle stream (to prevent recycling of products), or in the vapor stream from the preseparation unit. Sometimes, it is just cheaper to have no recovery system at all, particularly when just a small purge suffices and the purge can be safely disposed off [1].

In general, multiple separations are used for the individual constituents of the vapor stream, such as in the production of ethylene oxide (EO), where the product itself is first removed from the gas recycle stream, as recycled EO would oxidize and be lost mostly as CO_2. The EO is removed from the gas by absorption in water to concentrations of 100 ppm or less. This step is followed by the selective removal of CO_2 by another absorption, using a potassium carbonate solution. The gas is then recycled back to the reactor via a compressor. Absorption is not the focus of this book, so the reader is referred elsewhere [2–6] for further information.

A typical application for a membrane separation is the purification of hydrogen-containing streams that selectively permeate through the membranes. Water can be effectively be removed from gas streams by condensation and (pressure of temperature swing) adsorption. High-purity argon used to be an example for reacting away the impurities: close-boiling oxygen was reacted away catalytically using an excess of hydrogen. The subsequent distillation was much easier because of the much lower boiling point of hydrogen.

The recovery system for the liquid stream typically uses fractionation on the basis of volatility of the products and reactants because it is still one of the easiest of separation methods (despite its high energy requirements). As such, many of the decisions in synthesizing "reactor workup sections" center on what type and order of distillation separations will be used, which of course depend on the nature of the mixtures produced—namely, whether they are zeotropic or azeotropic in nature. For example, the energy spend on splitting azeotropic mixtures can sometimes be saved by recycling them back to the reactor directly.

When we use distillation, it must be decided how to remove the light-end products. This can be done by employing the following (see also Figure 5.1):

- Phase splitting after reducing pressure or increasing the temperature
- A partial condenser on the product column
- A pasteurization section on the product column
- A stabilization column before a product column

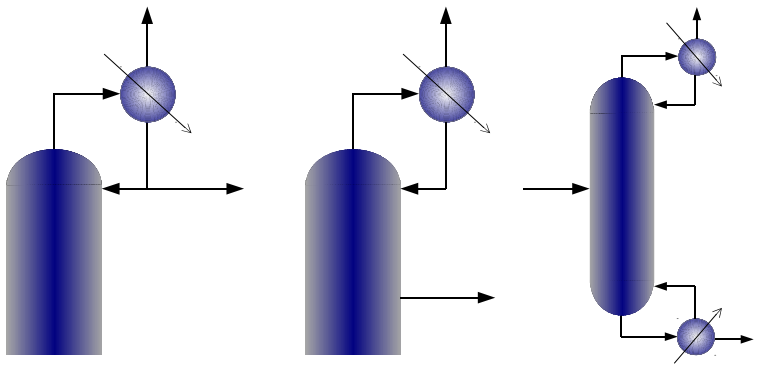

FIGURE 5.1

Light-ends distillation solutions: partial condenser (left), pasteurization section (middle), and stabilizer (right).

It is possible that the light-ends can be vented, sent to a flare or fuel, or recycled to the vapor recovery system. An example of the latter is formaldehyde formed in the production of dimethylether (DME) from methanol. It is separated in a partial condenser from the product DME and then sent to an absorption column operated with cooled methanol from the subsequent methanol recovery column. This will also capture valuable DME that is not recovered in the partial condenser. The DME containing methanol is recycled back to the reactor. Pasteurization sections are often used to remove trace components and create very pure products, such as in propylene-propane splitters to obtain a polymer-grade product, free of light (acetylene) and heavy (methylacetylene (MA) and propadiene (PD)) impurities. Of course, a pasteurization section requires a (small) vapor product to be taken from the condenser. This stream represents a (small) loss of product unless the product can be absorbed in a reactant and recycled to the reactor such as in the case of DME. Such recycles only make sense when the reaction product does not react with one of the reactants to form a byproduct. Recycling can also cause buildups of specific undesired light-ends that would contaminate the product. Examples of pasteurization sections are shown in Section 5.2 for ethylene and propylene as well as ethylene-glycol production.

Nonazeotropic mixtures can be fractionated directly (by distilling off the lightest components, one at a time) or by means of indirect separations (by distilling only the highest boiling component over the bottom). General heuristics that apply to this kind of column sequence include removing corrosive or reactive (unstable) components as soon as possible in a direct sequence to keep distillate products free from salts, solids, and particulates. Similarly, it is preferable to recover recycle streams as distillate streams to prevent solids from being recycled, particularly to reactors containing packed beds. In general, it is most advantageous first to separate the most plentiful component in order to reduce the size of the remaining fractionation columns (and hence the total energy required) and to favor equimolar splits (creating balanced

hydraulic loadings in the column and hence equal column diameters for sections below and above the feed). Side rectifiers can be used to combine two columns operated at the same pressure in a direct sequence, and side strippers to combine two columns in an indirect column sequence. Because the operation is done at the same pressure, the condensing or reboiling has to be done at a less favorable temperature and internal traffic increases in part of the column. Nevertheless, side columns can save energy when they remove components that are (much) less plentiful in the feed. An industrial example is the removal of the less than 1% argon from air. Significant capital savings can be achieved when the side columns are combined within the same column shell by use of a dividing wall.

Similarly, interconnected prefractionators, with a main fractionator with multiple products taken as side draws can have significant energy savings, as patented by Brugma [7] and now used by Stone & Webster in the preseparation of methane, ethane, ethylene, propane, and propylene. When operated at one column pressure, they are called Petlyuk arrangements. When combined into one column shell by using a dividing wall, significant capital benefits can be obtained. Dividing wall technology can also be favorable for extractive or azeotropic distillation column arrangements (see Volume 2, Chapter 5). Detailed discussions of optimal zeotropic and azeotropic column sequencing can be found in Volume 2, Chapter 8 and in Ref. [8], which includes a good discussion of when to draw products with sidestreams, when to apply side strippers/rectifiers, and when to use a divided wall column arrangement. Recently, even more heat-integrated configurations have been published for the separation of three or more products that benefit from significant energy and capital savings [9,10].

Separation of azeotropic mixtures is described in Volume 2, Chapters 6 and 7. In this chapter (Section 5.2), we discuss special types of distillation processes, such as multiple-effect distillation, to remove solvents and diluents (e.g. water), which can also be a reactant as in the production of ethylene-glycol. Distillation can also be used to remove salts that are used as homogeneous catalysts or as an alternative form of salting out specific compounds. These topics are not discussed in detail here.

5.1.2 Distillation constraints (feasible column sizes, internals, temperatures and pressures)

Industrial process plants are shaped by the product purity specifications, economical conditions, and environmental constraints prevalent during their design as well as during the occasion of their revamping. For example, the separation of air in its constituents was commonly done by means of cryogenic distillation with trayed columns until around 1990, when structured packings were introduced in the low-pressure oxygen and argon columns. The low pressure drop per theoretical stage of these packings allowed the direct distillation of high-purity argon, which typically requires 150 equilibrium stages in the side stripper to separate argon from the higher boiling oxygen. This marked an improvement over the older process designs that

first separated the argon to 97−99% purity to catalytically react the remainder of the oxygen with hydrogen; this required additional heat exchangers to heat and cool the argon, as well as an additional separation equipment to remove the produced water and the excess hydrogen. Furthermore, the low height equivalent to a theoretical plate (HETP) of structured packing enabled the stacking of heat-integrated columns without having to split them because of the prevalent practical height constraint of 50−60 m of industrial plants. Note there are exceptions to this constraint as some propylene-propane columns have been erected as single columns with heights over 80 m).

Structured packings also enabled sharper separations in the production of styrene monomer (ST) produced via the dehydrogenation of ethylbenzene (EB), where product and reactant are separated by means of vacuum distillation in which the temperature must be maintained below 100−110 °C to prevent polymerization of styrene. To reach the desired purity for ST polymerization of 2000 wt ppm of EB in ST, 70−80 trays were required and reflux ratios of 6. The first process plants erected during World War II used a heat-integrated split column design to alleviate the 0.47 bar total pressure drop over the bubble-cap trays [2]. The advent of improved low-pressure drop trays from Linde allowed a single-column operation with a total pressure drop of 0.23 bar, eliminating a column shell and its associated heat exchangers. The introduction of Sulzer Mellapak™ [11] allowed such low pressure drops, 0.10 bar or less, that it became possible to use more theoretical stages (90) in a single column shell, thereby enabling the production of styrene at much higher purities (150 ppm of EB). The advent of high-capacity Mellapak packing in 1999 allowed the use of even more stages (100−140), providing a 30−40% reduction in energy requirements.

Similar progressions in technology occurred in catalysts, improving the conversion and selectivity of the reactions, which changed the feed conditions such that different separation lineups become feasible or more energy efficient. For example, the conversion of EB to ST changed from an initial 40% to 60% nowadays! Progress in heat exchanger technology enabled revamping of columns with high-capacity internals without requiring replacement of heat exchanger shells or the improvement of process plants efficiencies. Also, the introduction of new types, such as brazed aluminum, plate-frame, or printed circuit designs, allow much tighter heat integrations and thus new process lineups to be developed.

Most practical limits on industrial process operating temperature and pressure are imposed by the equipment materials as well as the cost and availability of heating or cooling mediums. Because most equipment is made from carbon steel, common temperature limits range from −45 °C to 450 °C. The temperature limits of (stainless) steel can also influenced by the process medium; for example, hydrogen has a strong effect on the embrittlement of stainless steel and chlorides can induce stress corrosion.

The thermal stability of the reactants, products, and raw materials is another important factor that determines operating conditions. Some compounds are not stable at their normal boiling points. For example, in the refining of crude oil, the main atmospheric fractionator inlet temperature is determined by the thermal stability of

Table 5.1 Types of Maximum Temperature Limits in Industrial Distillation Processes

Limitation	Process/ Substance	Typical Maximum Temperature (°C)	Typical Operating Pressure (bar)
Thermal cracking	Crude oil	350–370	2
	Long residue	390–420	0.02
	Tall oil	260	0.005
Auto ignition	H_2O_2	60–80	1 (formation of SO_3)
Chemical reaction	H_2SO_4	170	(Formation of NO_x)
	HNO_3	$<T_b$	
Polymerization	Styrene	100–110	0.03
	Acrylic acid	130	
Heating medium	Steam (bar)		Relative cost
	Exhaust (1)	90	50%
	Low pressure (7)	145	100%
	Medium pressure (15)	180	130%
	High pressure (30)	210	150%
	High pressure (80)	270	
	Hot oil	400	
	Flue gas	450	
	Molten salt	700	

Adapted from [8].

the heavier hydrocarbons in the feed that limit the feed furnace outlet temperature typically to 370 °C, depending on the residence time of the crude in the furnace (as some limited cracking can be allowed). These heavier fractions can only be separated without cracking in a vacuum distillation column. Table 5.1 lists the various types of temperature limits imposed on industrial distillation processes. For condensing steam services, an economic temperature difference of 20 °C is used and relative costs are listed. Of course, the temperature approach can be chosen over a range, but values less than 10 °C are not very practical. Except for very small columns, electrical heating is not practical.

Minimum temperatures in distillation columns are set by the melting points of the compounds in the process flows. Even when such compounds are present in small amounts, distillation becomes infeasible unless these compounds are removed first, often by means of some other type of separation process, such as temperature or pressure swing adsorption. The most common factor determining the minimum column temperature is the available cooling medium (see Table 5.2). The cheapest coolant is air and, as such, it is gaining popularity over cooling water. Because energy costs are much higher for the coolants below ambient temperatures, the economic

Table 5.2 Typical Minimum Product-Side Temperatures and Relative Costs of Commonly Used Cooling Media

Cooling Medium	Temperature (°C)	Relative Cost (%)
Air	40–70	60
Cooling water	40–50	100
Chilled water/sea water	20–30	150
Ammonia	10	300
	−5	400
	−30	500
Propane/propylene	−30	
Ethane/ethylene	−75	
Methane	−150	
Nitrogen	−190	

Adapted from [8].

temperature approach for heat exchangers is much smaller, often 10 °C, and for the deep cryogenic exchangers in air separation it can be as little as 1 °C!

Constraints on temperature implicitly determine the range of feasible operating pressures. As already discussed, often the operating pressure has to be lowered to decrease the operating temperatures. Industrial applications with a single-stage vacuum pump can operate down to 100 mbar or, with a double-stage vacuum system, down to 20 mbar. Minimum operating pressures of 2−5 mbar require a three-stage system. Often, these systems consist of a combination of ejectors and ring pumps. As motive fluids for the ejectors, either steam, water, or oil are used; the selection depends on the ease of separation with the compounds being distilled. An alternative to operating under vacuum is to add a low-boiling compound, such as nitrogen or steam, to decrease the boiling temperature of the mixture.

A column operating at elevated pressures can distill low-boiling compounds, such as light hydrocarbons. This can significantly lower the operating cost (OPEX) for a given separation when this avoids the use of refrigeration. However, when doing so, power must be consumed to compress vapor feeds. If compression can be done in the liquid phase, this is much preferred because it requires two or three orders of magnitude less power (and is a direct result of the difference in density between the phases). Furthermore, the relative volatility will also decrease with increasing pressure, resulting in more stages being needed to perform the same separation and hence more capital expenditures (CAPEX).

The critical pressure of the components that are to be separated form an upper limit for the operating pressure. The closer to the critical pressure we operate, the smaller the relative volatility will be; hence, the balance will shift to larger CAPEX. Typically, substances are not separated with distillation at pressures that exceeds 50% of their critical pressure. One of the exceptions is methane, as demethanizers can run at pressures of up to 33 bar, or 70% of its critical pressure.

Energy and capital cost drive the further integration of process columns and heat exchangers, such as vapor recompression columns (VRCs) or multieffect distillation column trains. Such heat integration links the operating pressures of two, three, and sometimes up to four columns, posing significant limits on the selection of heating and/or coolant media as well as the column operating pressures. This is also the case when the columns are in fact integrated in one single column shell, as is the case in a divided wall column. These integrations, however, can bring such large operating and capital savings that they warrant the use of cooling/heating media at slightly less attractive temperature levels (see Volume 1, Chapters 7–10).

Finally, columns are constrained in their size by the efficiency and capacity of their internals and the column shell materials. Most often, pressure vessels are manufactured from steel cylinders. Economies of scale of columns operating at high pressure are diminished by the thickness of the column shell, which must increase with increasing diameter; the increased difficulty of welding and of column heads are increasing cost. Large columns also require larger internals and piping and, thus, larger manholes. However, on thick-walled high-pressure vessels, these tend to become costly. Similarly, manholes on vacuum towers are to be kept to a minimum to avoid air ingress. This can be often mitigated by the use of multiple feed and product draw piping as well as I- or H-shaped pipe spiders inside. The largest industrial distillation columns are vacuum columns, typically found in refineries; not withstanding the fact that they are equipped with high-capacity internals in order to obtain the smallest possible diameter, they can be as large as 15 m in diameter with feed pipes up to 5 m. They require special (vane-type) inlet devices to handle the high inlet vapor velocities, which exceed 100 m/s, and to prevent liquid from entraining upwards with the vapor.

The packed bed height for industrial distillation columns is determined either by mechanical constrains (operational and static weight) or by the decrease in separation efficiency induced by liquid (or vapor) maldistribution. When the liquid flowing down a packed column is unevenly distributed, the liquid-to-vapor (L/V) ratio will vary across the column cross-section. The L/V ratio influences the stripping factor and, hence, the local packing efficiency. The net effect will be a lowering of the separation efficiency of the bed as a whole. The extent of this loss depends on the type of packing, the quality of the liquid distributors, and how close to a pinch the bed is operated, but it easily can amount to 20% or more [12].

With proper design and good-quality liquid distributors (with less than 5% variation in the liquid distribution), beds can be designed with up to 15–20 equilibrium stages of random packing or up to 20–30 stages of structured packing. In doing so, a certain loss in bed efficiency must be accounted for by the designer. Because the liquid holdup for random packings can easily amount to 10–20% of the bed volume and there is no structural strength in the bed, the packing material must be strong enough to handle the bed weight in order to not collapse (and cause local flooding). Metal thickness also is dependent on the required corrosion resistance; for 50-mm rings, it ranges from 0.4 to 0.8 mm. This contrasts with

structured packings, where the typical sheet thickness is only 0.1−0.2 mm (depending on packing materials and density). Consequently, randomly packed beds with common packings that have nominal diameters of 25−50 mm are limited to less than 7 m in height. This compares to up to 9-m high beds in the pure argon columns of air separation plants.

Table 5.3 lists the typical number of equilibrium stages and sizes of some common (petro-) chemical industrial distillation columns. The second part of this chapter discusses some of these separations in more detail. Note that the number of stages required depends on feedstock, reactor technology, and product specifications. For example, specifications for monomer purity become more stringent over time, either because of desired structural improvements to the final polymer or because of toxicity of the intermediates. Sometimes developments in distillation allowed companies to create higher value products that over time became also the market standard.

Columns can become out of round if they were improperly fabricated or erected. For random packings, this is generally not a problem; however, if left unaddressed, it can lead to gaps for structured packing that promote increased liquid or vapor flow, which can bypass a complete layer of packing and lead to severe under performance. Care must be taken that trays cover the complete tray ring in columns that are out of round; otherwise, significant leakage results through tray bypassing. Although columns equipped with trays normally do not suffer from liquid distribution issues, tray tilt can be detrimental for trays without weirs, such as the low tray spacing columns in high pressure air columns. Columns can be tilted when they were improperly erected, when they have a bad foundation, or when tray rings are uneven. Uneven tray rings can be corrected with use of shims, but care must be taken to avoid creating (large enough) gaps through which liquid can bypass the tray. Therefore, tray ring tolerance for trays without weirs are as tight as 1−2 mm per meter column diameter, whereas for trays with weirs this tolerance is twice as high. At low liquid loading, the tray tilt issues can be avoided by using higher weirs and/or by enforcing a minimum height of liquid over the weir, through the use of picketed or serrated weirs. Nevertheless, the loss in efficiency from tilt problem increases when the column diameter increases.

For trays with segmental downcomer with low liquid loadings, this problem can be mitigated by splitting the tray decks into multiple decks at different levels, with intermediate weirs to ensure even flow over each deck. This requires split panels, extra beams, split-level tray rings, as well as a higher overall tray spacing. Another way to mitigate the tilt problem is the use of a higher number of smaller downcomers, such as by using MD™ trays from UOP or Calming Section™/HiFi™ trays from Shell. Nevertheless, tray ring tolerances should always be less than 6−8 mm in total, depending on the tray type. Distillation column heights are limited by height over diameter ratio and zoning restrictions. Column heights in industrial plants can extend up to 50−60 m. Columns heights higher than 70 m are rare but a few exist. Some of the tallest type of columns erected are propylene-propane (PP) splitters (see Section 5.2.1.3) that can reach 100 m in height.

Table 5.3 Industrial Distillation Processes and Typical Internals and Sizes

Component	Typical Number of Equilibrium Stages / *Type and Number of Internals*	Typical Column Diameter (m)
Industrial Gases		
Nitrogen/oxygen	100 / *20-m structured packings, 350 m^2 / m^3*	4–5
Argon/oxygen	150 / *30-m structured packings, 750 m^2 / m^3*	2–3
Petroleum and Aromatics		
Crude oil (atmospheric)	35 / *50–60 trays*	6–10
Long residue (vacuum)	5 / *grids and structured packings*	8–15
Ethane/ethylene	60 / *100–120 low tray spacing HC trays*	4–7
Propane/propylene	120–150 / *150–350 low tray spacing HC trays*	4–8
Benzene/toluene	34	
Toluene/ethylbenzene	30	
Toluene/xylenes	45	
Orthoxylene/metaxylene	130	
Ethylbenzene/styrene	90–140 / *28-m structured packing 250 m^2 / m^3*	7–9
Organic Chemicals		
Methanol/formaldehyde	23	
Dichloroethane/Trichloroethane		
Ethylene glycol/diethylene glycol	16	4–5
Cumene/phenol	40	
Phenol/acetophenone	40	
Aqueous Systems		
Hydrogen cyanide/water	15	
Acetic acid/water	40	
Methanol/water	60	
Ethanol/water	60	
Isopropanol/water	12	
Vinyl acetate/water	35	
Ethylene oxide/water	50	
Ethylene glycol/water	16	4–5

HC, high capacity.
Adapted from [8].

5.1.3 Hydraulic constraints and foaming

It is the task of the industrial distillation expert to find a robust design point for each section in a distillation column such that there is a maximum overlap in the operating ranges for all the sections in the column. This will consist of a compromise between largest capacity, widest turn-down and turn-up range, and an acceptable internal efficiency. In revamps it is common that turn-down is sacrificed in exchange for extra capacity (and often, some tray efficiency). Chapter 3 in Volume 1 contains a detailed discussion of the hydrodynamics of distillation columns, with further detail on tray design and operation in Chapter 2 of Volume 2. Here we focus on how practical operational limits are applied in industrial columns to high-capacity internals that use gravity for disengagement of the phases (i.e., not using centrifugal forces as in ultrahigh capacity tray technology).

5.1.3.1 Trays

The major hydraulic limits on the operation of high-capacity trays are as follows:

- Minimum vapor loading to keep the liquid on the trays and prevent the liquid from weeping (which will reduce tray efficiency by 10−20%) or dumping (where control of any separation can be lost), which is set by the tray open area, weir height, and type of bubbling devices (e.g. bubble-caps do not weep).
- Minimum liquid loading, which prevents the vapor from unsealing and bypassing the trays (where control of separation is lost) but also of the liquid height on the trays being less than that required to accomplish the desired separation, mainly determined by the downcomer design and sealing.
- Maximum vapor, which will entrain liquid to the tray above, mainly set by operating at low flow parameters.
- Maximum vapor to jet-flood bed expansion, set by the available bubbling area, the type of bubbling devices, and the liquid residence time on the tray as determined by the tray layout and resulting liquid flow pattern.
- Maximum vapor loading, which will cause so much pressure drop that liquid backs up one of the downcomers; this is influenced mainly by the tray open area, amount of pressure drop generated by the bubbling devices, the height of the weir and presence of liquid push valves, as well as the height available for backup in the downcomers and the liquid density in the downcomer.
- Maximum liquid loading, where the downcomer entrance becomes chocked; i.e., where the froth flowing over the weir is unable to enter the downcomer. It is determined by the downcomer's top width, shape, and the presence of anti-jump baffles/column wall.
- Maximum downcomer velocity (roughly equivalent to a residence criterion for froth collapse).

Some of these limits depend on the type of bubbling device employed, whereas others are determined by the shape and size of the downcomers. Further complicating the design is the influence of foaming on the maximum tray limits. This is captured by

means of foaming or system factors, which are a measure of the maximum fractional capacity that can be obtain for a certain chemical system in comparison with a non-foaming system. Table 5.4 lists some values for ordinary conventional sieve trays and most common applications. It is important that these factors often are derived from the jet-flood capacity limit, and as such, should be applied to that limit.

Typical industrial trays are designed for 70−85% of flood, dependent on the experience with the particular system and client demands on plant flexibility and capacity revamp. The plant owner will expect that over the lifespan of the chemical plant, minimally 10 but often 30 years or more, there will be catalyst improvements that increase the reactor conversion and add more production capacity. Therefore, the separation train must be able to grow along with the reactor to make maximal use of the invested capital. Only if there is sufficient scope left for such improvements will a design of columns with regular column internals make sense, as otherwise plant cost can be lowered by using available high-capacity (HC) internals. Hence, mature chemical processes with conversions that are already high (i.e. >80%), will see more use of HC internals, unless plants contain recycle loops that can still be debottlenecked, or reactor capacity can be added at low cost. Of course, the auxilary equipment of the column must also be able to handle the extra capacity. As auxiliaries such as heat exchangers and distributors are typically over-designed with a 10−20% margin, it is not surprising that most HC equipment is designed to add about 20% extra capacity, and that technology that adds more spare capacity experiences less market penetration.

For regular trays, the Ward tray capacity factor correlation (in m/s) is useful (see Eqn (5.1)):

$$C_{\mathrm{BA}} = \left[\frac{0.26\cdot \mathrm{TS} - 0.095\cdot \mathrm{TS}^2}{(1-a_{\mathrm{DC}})\sqrt{1+14.6\cdot \mathrm{TS}^{0.75}\cdot\varphi^2}}\right] \mathrm{MAX}\left[1, \frac{1+f}{1+f\cdot\varphi}\right] \times \mathrm{MIN}[1, 0.56+23\cdot\varphi]\mathrm{MIN}\left[1, \left(\frac{\sigma}{3}\right)^{0.2}\right] \tag{5.1}$$

where TS is tray spacing in meters, φ is the flow parameter, a_{DC} is the relative downcomer area with respect to the cross-sectional tray area, and σ is the surface tension in dyn/cm. The second term is a correction for high-capacity bubbling devices, such as the MVG of Sulzer or VG-0 of Koch-Glitsch where f varies from 0.1 to 0.2. The third term is a simple de-rating term for the low-flow parameter region where entrainment limits the capacity. The last term is a de-rating for low surface tension as observed by Summers [15]. For high-capacity trays, the constant 14.6 should be lowered to values of 8−10, depending on the type of tray. The first estimate for the required downcomer area may be computed from the maximum downcomer velocity with:

$$a_{\mathrm{DC}} = \frac{\varphi\cdot C}{u_{\mathrm{DC,max}}}\sqrt{\frac{\Delta\rho}{\rho_{\mathrm{L}}}} \tag{5.2}$$

Table 5.4 System Factors (SF) for Trayed Columns According to Lockett [13], Recommended Design Pressure Drops are from Kister [14], and the Derived Packing System Factors are from Both of These Sources

Type Column	SF Trays Lockett	Design dp in.H_20/ft Kister	SF Packing	Ln* SF packing / Ln SF trays
Light forming				
Depropanizers	0.9	0.9	0.95	0.5
Hot carbonate strippers	0.9	0.4	0.93	0.7
Freons	0.9			
H_2S Strippers	0.9			
Hot carbonate strippers	0.9			
Moderate foaming				
High pressure $2.94/\rho_G^{0.32}$	0.84			
De-methanizers top	0.85	0.8	0.88	0.8
De-menthanizers bottom	1		1	
Oil absorbers	0.85	0.6	0.90	0.6
Amine strippers	0.85			
Glycol strippers	0.85			
Sulpholane systems	0.85			
Crude towers	0.85	0.35	0.88	0.8
Hot carbonate absorbers	0.85	0.3	0.88	0.8
Furfural refining	0.8			
Heavy foaming				
Amine absorbers	0.75	0.25	0.840	0.6
Oil reclaimer	0.7			
Glycol contactors	0.65			
Methyl ethyl ketone	0.6			
Sour water strippers	0.6			
Stable foam				
Alcohol synthesis abs	0.35			
Caustic regenerators	0.3			
			Average	0.7
			St.Dev.	0.1

System Factor (SF) for packings computed from given design pressure drop and flood pressure drop of 1.8″ hot process liquid by scaling vapor and liquid rates for 1.5 Pall rings using Ludwig (1979) pressure drop model and a design fraction of flood of 80%.
**Ln is the mathematical natural logarithmic operator.*

For some high-capacity trays, the Glitsch maximum downcomer velocity (see Eqn (5.3)) can be

$$u_{\mathrm{DC,max,Glitsch}} = \mathrm{MIN}\left[0.17, 0.0081\sqrt{\mathrm{TS}}\sqrt{\Delta\rho}\right] \tag{5.3}$$

whereas for other high-capacity trays, the Nutter design rule matches best when used without any tray spacing dependency (as long as tray spacings are not too small):

$$u_{\mathrm{DC,max,Nutter}} = 0.15\,\mathrm{MIN}\left[1, \sqrt{\frac{\Delta\rho}{400}}\right] \tag{5.4}$$

Downcomer area's should be limited to a practical maximum (e.g. 30%). With the initial guess for the downcomer area, the weir length can be determined. Using this length and the liquid and vapor loadings, the froth height can be computed. For trays with straight flow paths, the fraction of downcomer entrance choking can be computed by dividing the froth height minus the weir height by a fraction of the downcomer width (for a multi-downcomer tray, normally 40%). When the downcomer fraction exceeds the desired fraction of flood, the downcomer area must be increased until the criterion is satisfied. On trays equipped with an anti-jump/splash plate, a 5% advantage can be assigned to the downcomer width fraction. On regular segmental downcomer trays, the total tray area consists of the bubbling area plus two times the downcomer area. For high-capacity trays with truncated downcomers, the total area equals the bubbling area plus the area of only *one* downcomer. For truncated trays, the downcomer backup is computed from the dry and wet pressure drop using normal methods. When the truncated downcomers are equipped with seal pans, for example on Shell CS trays, the normal clearance loss correlations can be used. The hydraulic loss of dynamically sealed slots depends on the slot open area, shape, and number. As there is no open literature correlation, specific vendors must be consulted. To compute actual backup height in the downcomer, the average liquid density is required. Figure 5.10 in Lockett [13] for UOP MD trays without slash plates can be approximated by Eqn (5.5)

$$a_{\mathrm{DC}} = 0.8\,\mathrm{MIN}\left[1 - \frac{0.25}{SF}, \frac{\Delta\rho}{1000}\right] \tag{5.5}$$

where the first part computes the fraction of the downcomer available for backup. On trays with splash plates, collapse is faster and the factor 0.25 can be reduced to 0.15 to 0.1. To determine the stability and weep point limits for high-capacity trays, the regular correlations can be used (see Volume 2, Chapter 2).

5.1.3.2 Packings

Detailed information on random and structured packings can be found in Chapters 3 and 4 of Volume 2. Here we focus on how practical designs of packed distillation columns are made for industrial bulk chemical processes, especially for the application of high capacity packings. Column design builds on capacity correlations for these packings. Early capacity correlations are mostly variations on the generalized

pressure drop correlation (GPDC), which correlates the vapor capacity factor (C_V) as a function of the flow parameter using a packing specific "packing factor", F_P. Wallis [16] defined a liquid capacity C_L (Eqn (5.6)) in a manner analogous to that of the definition of the vapor capacity (Eqn (5.7)):

$$C_L = u_L \sqrt{\frac{\rho_L}{\Delta\rho}} \tag{5.6}$$

$$C_V = u_V \sqrt{\frac{\rho_V}{\Delta\rho}} \tag{5.7}$$

where $\varphi = \frac{L}{V}\sqrt{\frac{\rho_V}{\rho_L}} = \frac{C_L}{C_V}$.

He observed that $\sqrt{C_V}$ is a linear function of $\sqrt{C_L}$ that is $\sqrt{C_V} = a + a\sqrt{C_L}$ and that this relationship can be converted into one (see Eqn (5.8)) that provides vapor capacity as function of the flow parameter.

$$C_V = \frac{a}{1 - 2b\sqrt{\varphi} + b^2 \cdot \varphi} \tag{5.8}$$

Lockett [13] showed that this correlation predicts capacities for structured packings in cryogenic air distillation and derived generalized values for the parameters for Y type packings (45°) with large specific packing area. A refinement can be made by using two parameter sets, one specific for low-flow parameters {a,b} and another for high-flow parameters {A,B}. The capacity of many packings can be predicted within several percent with this method over three or more orders of magnitude in flow parameter (see Figure 5.2). The parameter values for this graph are listed in Table 5.5 for various standard sheet and gauze packings fitted to the

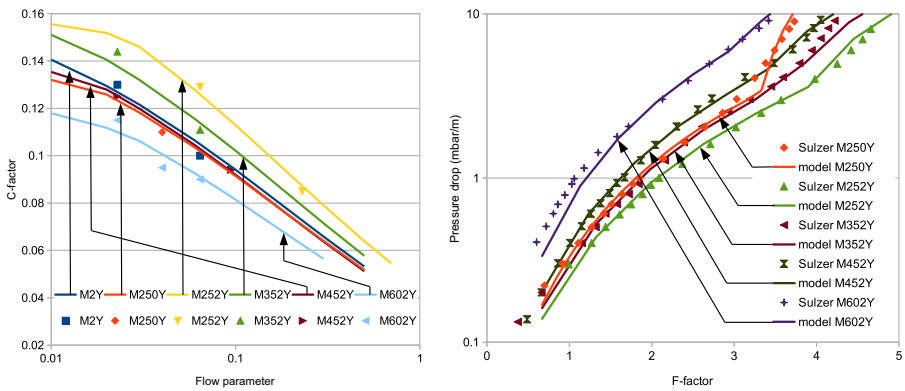

FIGURE 5.2

Capacities (left) and pressure drops (right) of various standard and high-capacity structured packings modeled using the two parameter Wallis capacity model and the pressure drop model of Kooijman et al. [17]. Points were extracted from the Sulzer brochure [11]; model parameters are from Table 5.5 and Ref. [17].

Table 5.5 Capacity and Pressure Drop Model Parameters for Various Standard Structured Packings

Parameter	M2Y	M250Y	M252Y	M352Y	M452Y	M602Y	BX	BX+
a	0.155	0.14	0.165	0.165	0.155	0.135	0.19	0.17
b	−0.5	−0.3	−0.3	−0.45	−0.7	−0.7	−1.9	−0.45
A	0.175	0.17	0.21	0.19	0.155	0.155	0.19	0.2
B	−1.15	−1.15	−1.15	−1.15	−1.2	−1.2	−1.9	−1.15
f_{pack}		0.25	0.2	0.2	0.25	0.45		
C_{load}		0.0047	0.0057	0.0057	0.0057	0.0057		
C_p		0.01	0.003	0.003	0.002	0.002		

Parameters a, b, A, and B are for the Wallis model, whereas and f_{pack}, C_{load}, and C_p are for the Kooijman et al. model [17].

chlorobenzene/EB data at two pressures [11]. Table 5.5 also includes model parameters for the Kooijman et al. pressure drop model [17], fitted to the 100 mbar pressure drop data, also shown in Figure 5.2. Both these models were used for the rate-based simulations discussed later in this chapter.

There is no agreement in the literature on how capacity factors should be corrected for variations in system properties. Some vendors do, others do not; for example, the Norton method as described by Strigle [18] has two corrections:

$$C_{V,\varphi,\sigma} = C_V \mathrm{MAX}\left[1.05, \left(\frac{\sigma}{20}\right)^{0.16} \cdot \left(\frac{\eta_L}{0.2}\right)^{-0.11}\right] \tag{5.9}$$

where C_V is the function of the flow parameter, and liquid viscosity is in cP and surface tension is in dyn/cm. Note that the use of the maximum function makes the capacities for air–water, the most common test system, only 5% higher than for generic type hydrocarbon systems.

5.1.3.3 Foaming

Normally, liquid drainage from the froth on a distillation tray causes films between bubbles to thin. Eventually films rupture, which leads to bubble coalescence. However, the mass transfer taking place on the tray can create a surface tension gradient and a force that opposes this gravity-driven process, significantly increasing the foaming of froths. Foaming decreases capacity as it hinders disengagement of the phases. Though the extent of foaminess as well as the severity in which the foaming actually affects capacity are difficult to predict from chemical composition and process conditions, the effect tends to be reproducible. As such it is often lumped into a so called system or foaming factor, often derived from pilot plant data, sometimes from actual plant test-runs. A knowledge of system factors are often part of a licensees trade-secret to be able to offer competitive plant designs. Hence, system factors are not widely published, something that has hindered the scientific process of predicting these factors for new processes. Foamings also tends to be hardware dependent; for example, the use of sieve large (19 mm) holes has been reported to suppress foam height on trays [19].

Lockett [13] and Kister [14] have compiled list of system factors for common trayed column applications (see Table 5.4). Though the foaming tendency of fluids tends to be suppressed inside packings, by no means are packings unaffected by foaming and their capacity also is affected. For packings, however, there are no published lists of system factors, but instead there exist recommended design pressure drops [14]; these are listed in Table 5.4.

Assuming a pressure drop model and an average design fraction of flood, these design pressure drops may easily be converted into system factors for packings. When this is done, it can be observed that all the system factors for packings are higher than those for trays. This confirms the general observations that packings are less affected by foaming. When both system factors were compared for the same systems, a simple relationship was derived (see Eqn (5.10)) that could help

to guide the designer in case there is no test-run data available for packings but there is for trays.

$$SF_{packing} = SF_{trays}^{0.7} \tag{5.10}$$

Table 5.4 shows that there is a standard deviation of 0.1 on the power in the above relationship. Thus, a conservative design can be made by using a power of 0.8. Nevertheless, it would be desirable if more data would be available.

When the propensity to foaming becomes so large that stable foams are formed, it may become necessary to use antifoaming agents (also known as defoamers, foam inhibitors, foam suppressants, and foam control agents). Although used in low concentrations, defoamers are the largest single category of process aid used in the chemical industry [20]. Traditionally, defoamers were single component liquids or homogenous solutions of vegetable or mineral oils, but nowadays hydrophobic solids are the most effective ingredients. Modern defoamers are complex, formulated specialty chemicals whose exact composition often is proprietary. The four most common liquid-phase components found in defoamers are hydrocarbons, polyethers, silicones, and fluorcarbons. Frequently, they are tailored to very specific applications, such as the polymerization inhibition of one specific compound in a process. Since the defoaming effect can have a very large impact on performance, defoamer cost is driven by plant savings and *not* by by manufacturing cost. Of course, in distillation one of the most important properties of the defoamer is its thermal stability and its low fouling propensity in heat exchangers, the reasons why polydimethylsiloxane (PDMS) is the most important silicon defoamer in the petrochemical industry. However, in aqueous systems, the effectiveness of PDMS depends on the addition of solid hydrophobic silica. Many defoamers require surface-active materials or emulsifiers and often a carrier component is added for ease of dosing the defoamer. The defoamer market is large and highly specialized with a very large diversity in manufacturers. Table 5.6 lists some significant defoamer suppliers together with their associated trade names.

5.1.3.4 Fouling and scaling

Fouling is a broad term that encompasses several different phenomena:

- Polymerization
- Sedimentation/precipitation/crystallization
- Chemical reaction/corrosion
- Evaporation/removal of solvents

The complexity of the fouling mechanism increases when two or more of these phenomena occur simultaneously, e.g. in an ethylene caustic tower. Factors that assist fouling are residence time, stagnant zones, sharp transitions, entrainment, and emulsion issues. Fouling and scaling are not static: they tend to get worse over time. If the fouling is localized in the liquid phase, an inhibitor can be utilized. Type and selection of inhibitors is highly process dependent; for example, to prevent

Table 5.6 Commercial Defoamer Examples

Supplier	Trade Names
Air Products and Chemicals	Surfynol
Akzo Nobel Chemicals	Propomeen
BASF	Mazu, Pluronic
Calgene Chemical	Calgene antifoam
Dow Corning	Dow Corning antifoam
General Electric	AF
Henkel	Foamaster
Huntsman	Jeffox
Rhone-Poulenc	FleetCol, Foamex
Taylor Chemical	Taylor antifoam

Adapted from [20].

fouling in distillation of the ethylbenzene-styrene, various styrene polymerization inhibitors are available on the market (e.g. Nufarm's AHM series® and Nalco's Prism® polymerization inhibitors contains dinitro-alkyl-phenols whereas Chemtura Naugard® consists of an alkylated aromatic diamine). Each type of inhibitor features different properties and application depending on the intended use of the chemicals produced; the polymerization process of monomer produced might determinate which polymerization inhibitors can be used.

In many applications, fouling results from the evaporation of volatile components. For example, in refinery vacuum and de-asphaltene oil towers, placing the process on recirculation without the addition of fresh feed can initiate fouling as volatile components that solvate the asphaltene components are being removed. Entrainment of short residue in vacuum columns containing heavy metals needs to be caught on a guard bed above the column inlet. If the wash bed is not fully wetted, the entrained residue will not be immediately removed and thus will cause the bed to coke up due to high temperature cracking and drastically shorten the 4- to 5-year turnaround cycle of these units. Wetting requires a minimum film thickness of the liquid running over the column internals.

Sedimentation is the accumulation of solids that are deposited in/on low velocity areas in the process equipment and block mass transfer surface area lowering a column's performance. Suspended solids can include salts, metal oxides/sulfides (i.e. corrosion products), catalyst fines, fermentation products, ashes, and coke fines. Precipitation and crystallization of dissolved salts often occur as the result of water evaporating but, for example, ammonia salt deposition can also occur directly from the gas phase. Sometimes the deposits formed do not adhere strongly to the surface and are self limiting the thicker the deposits become. Sedimentation fouling is strongly affected by velocity and less so by temperature, but when a deposit bakes on a surface it can become very difficult to remove. It is often effective to ensure

minimum velocities are maintained over trays as well as in downcomers and in liquid distributors, to prevent sedimentation. As such, it is better to use fewer but bigger slots or slits than many smaller openings. Stagnant zones are to be avoided wherever possible. Other solutions are periodic cleaning by means of water washing via auxiliary nozzles/devices. Corrosion control is often essential to limit sedimentation fouling. Corrosion products may be inherent to the process, e.g. iron sulphides in the Rectisol™ process to remove H_2S. Corrosion can be prevented by the combined use of the right materials, corrosion inhibitors (i.e. injection of caustic to neutralize acids in crude oil), and process conditions (i.e. operating the styrene distillation columns below a certain temperature).

Precipitation and crystallization can occur when process fluids become supersaturated. Certain salts, such as calcium sulfate, are less soluble in warm water than in cold; if such a stream encounters a wall above the salt saturation, it will crystallize on the surface. Particular attention needs to be taken with salt solutions in evaporators, mixing of streams with different compositions, variations in pH (affects solubility of CO_2), and temperature (if a dissolved wax is cooled it can solidify).

Scaling of distillation trays with calcium carbonate can happen in any columns fed with live steam or where water is being evaporated. Deposits tend to concentrate on the bottom where the vapor flow converges to the openings in the trays [21–23] and is material dependent. Plugging of openings is more pronounced for openings smaller than 1 in; hence, for trays in very fouling applications, either large hole, dual flow grid or bar trays, shed decks, and baffle trays are used. In refineries, wash beds are installed with very large channel packings made from smooth metal sheets to promote liquid rundown. There is some conflicting evidence that plugging of trays can be prevented if movable devices are deployed in the range where continuous movement is expected [22,23].

Despite the significant long-term effect of fouling and scaling on the performance of column internals, the topic is largely undocumented, probably because its occurrence is strongly dependent on the process and process conditions, sometimes even on the exact local feed-stock and materials and equipment used.

5.1.4 Distillation efficiency in industrial columns

As discussed in Section 5.1.2, the distillation efficiency plays an important role in setting the overall height of industrial columns. There are various ways of defining efficiency, but in industry the overall efficiency is the type used most often. It can be related to Murphree stage efficiencies that can be used in column simulation. Overall efficiency data has been collected over the years in pilot columns built for developing new chemical processes. Frequently, this information is available to the design engineer in the form of tables as function of type of hardware, system, and operating conditions. Often the type of hardware is determined by the system and process; for example, trays are typically applied in crude refinery columns because of their insensitivity towards fouling, accessibility for inspection, and cleaning as well as ease of repair after steam explosions. Similarly, structured packings are used where low

pressure drop per theoretical stage is key, such as in vacuum distillation or in the cryogenic distillation of argon. There remains a dependence on the type of tray and the layout, but because columns are made for the typical industrial range of plant capacities, these layouts are typically fixed as well, in which case a constant design tray efficiency can be assigned. This common practice became well established because efficiencies do not differ much between sieve trays and floating or fixed valve trays.

5.1.4.1 Packings

For packings, the distillation efficiency is expressed as the HETP, sometimes referred as the HETS because of the inconsistent use of the word "plate" for a "stage". For random packings, the typical size of the packings in industrial columns ranges from 1.5 to 3 in (38−76 mm). The larger the packing, the higher the HETP but also the higher the vapor handling capacity. Larger packing elements are also less susceptible to fouling and to deposits of solids. Over many years, several "generations" of random packings have been developed, where newer generations have higher liquid handling capacities and lower pressure drops. They can be typified by more open structures that have a higher void fraction. For columns of diameter less than 1 m, 1-in packings are also used in industry in order to maintain a ratio of column diameter to packing diameter that is larger than 10. This helps to limit maldistribution of liquid and vapor in the bed. Random packings made of plastic are more resistant to corrosion than metal packings; consequently, plastic packing is widely used in aqueous applications, especially for saline solutions. However, to realize a similar bed height with both plastic and metal packings, plastic packing must be thicker than the corresponding metal packing; hence, the void fraction is less, lowering capacity and requiring separate flood curves to be used in the design of columns with plastic rings.

There is one more degree of freedom in the design of a column fitted with structured packing: in addition to the materials (sheet metal, plastic, carbon, or gauze) and packing specific area, there is also a choice of angle (45 or 60°) the packing makes with the horizontal (i.e. "Y" or "X"). Although there are many structured packing vendors, the initial line of packings from Sulzer Chemtech, the BX wire gauze packing as well as their sheet metal Mellapak series, has become an industry standard. Vendors mainly differ in using different element heights. As a rule of thumb, the HETP (in m) of standard Sulzer Mellapak sheet metal packings [11] can be estimated by Eqn (5.11).

$$\mathrm{HETP} = 12\left[\frac{\cos(\theta)}{\cos(45^\circ)}\right]^{3/2} \cdot \frac{1}{a_p^{0.7}} \tag{5.11}$$

where a_p is the specific packing area ($\geq$170 m^2/m^3) and θ the packing corrugations angle with the vertical. This formula includes a contingency for stripping factors. For gauze BX packing, the constant 12 can be replaced by a value of 8−10. Note that packing efficiency increases with pressure; hence, application of the rule of thumb

at very low pressures requires a correction. For design purposes, most vendors report their packing HETP at low pressure (e.g. 100 mbar) and have their testing carried out in one of the independent test facilities (e.g. Fractionation Research Institute, Stillwater, OK or Separation Research Program at University of Austin, TX) to gain acceptance by the industry. Even when tested, licensors and operating companies remain somewhat reluctant towards using new suppliers/packings.

In 1999 Sulzer introduced a new type, the HC "Plus" series [11]. Initially offered only for Mellapak 250Y and marketed as M252Y, they now cover the full range from 200 to 500 m^2/m^3. Because these HC packings provided easy debottlenecking of existing plants, they became very popular in many revamps. Other vendors have followed quickly with different type of hardware innovations that improve capacity [24], such as Koch-Glitsch HC Flexipac [25,26] and Montz MN series [27]. These high-capacity packings each have different combinations of HETP and capacity such that they cannot be interchanged.

Because the HETP and capacity vary so strongly with packing size and materials, company design guides usually tabulate values for HETPs of a generic hydrocarbon system. Usually, these tabled values include unspecified safety factors. Because randomly packed beds show higher variations in HETP, their safety factors are often higher, e.g. 20% instead of 10% that typically is used for structured beds. Standard practice is to use process-specific system correction factors to convert tabulated values for use in design. For example, the HETPs of aqueous systems are often taken to be 10−20% higher. The first packing vendor to publish such a method was Norton [18]; they presented a relationship between HETP and the system physical properties:

$$\text{HETP} = B_{\text{packings}} \left[\frac{\eta_L^{0.213}}{\sigma^{0.187}} \right] \tag{5.12}$$

where the HETP is in feet, surface tension σ in dyn/cm ($4 < \sigma < 33$), and liquid viscosity η_L in cP ($0.08 < \eta_L < 0.83$). The packings constant B_{packings} can be approximated by $d_p/10$, where d_p is the packing diameter in mm. For small rings, the scaling factor is slightly less favorable, i.e. for $d_p < 30$ mm use 8 instead of 10. Note that this HETP does not include a contingency for operating conditions. Norton used the relationship between H_{og} and HETP for this; with Eqn (186) in chapter B1-C5, the above Eqn (5.12) becomes:

$$\text{HETP} = B_{\text{packings}} \left[\frac{\eta_L^{0.213}}{\sigma^{0.187}} \right] \cdot \ln\left(\frac{S}{S-1} \right) \tag{5.13}$$

where the stripping factor S is defined as $mV/L \approx KV/L$. The variation in manufactured random packings leads some companies to work with a single packing supplier so as to lower the cost of determining HETPs for each type and size of packing. Frequently, the system correction factors also can be derived only for a specific packing series. This implies that the design engineer often does not have complete freedom to choose a packing type; longstanding collaborations between companies and packing vendors in certain chemical areas are a result.

For more accurate predictions of the packing efficiency, various mass transfer correlations (MTCs) have been developed, as discussed in Chapter 3 of Volume 1.

Some recommended MTCs for predicting the performance of packings in industrial columns are

- Billet and Schultes (1999) [28] for random packing
- Bravo et al. (1985) and Rocha et al. (1996) [29] for structured sheet metal packings
- Brunazzi et al. (1995) [30] for gauze metal packings

Billet and Schultes developed a correction for the effect of the surface tension gradient. The latter induces Marangoni forces that can negatively impact the performance of packings [31–33]. The proposed correlation proportionally decreases the interfacial area with increasing surface tension gradient. However, it has been experimentally observed that HETPs decrease at most by 20–30% [34]. Therefore, we recommend bounding the Marangoni correction. In principle, the same correction can be added to other MTC models.

The second part of this chapter shows how these correlations can be used for industrial design. It must be noted that these published correlations do not yet properly predict the loss in packing efficiency at higher pressures [35] and care must be exercised when applying packings at pressures above 10 bar gauge. The mechanism behind this loss in efficiency is unclear: it could be liquid backmixing due to the lowered surface tension/density difference, vapor backmixing [36], or both. Furthermore, MTCs assume that the packings are sufficiently wetted, which is not always the case. The Glitsch rule [14] for CMR #1.5 random packing can be used to determine the minimum wetting rate that ensures mass transfer (0.3 USgal/min/ft^2 and roughly double this value for aqueous systems). For structured packing [14] refers to a minimum flow, which translates to a film minimum thickness of 0.1 mm for hydrocarbon and 0.2 mm for aqueous systems. Sometimes it is possible to select a high-capacity packing to avoid incomplete wetting of the packing. When wetting is not complete, the interfacial area can be assumed to be proportional to the fraction of actual superficial liquid velocity over the minimum wetting velocity. However, most published MTC models don't include such a correction.

Proper distributor design is essential for large industrial scale columns with packed beds. Poor performance of packed columns almost always is caused by the improper design or installation of the liquid distributor. Therefore, it is now industry standard to quality test all liquid distributors prior to installation to ensure that proper operation in the field can be met. Each distributor also requires a manhole for inspection and possible leveling and cleaning. High-quality distributors are essential to fully exploit the mass transfer performance of the packing for beds of more than a few stages and specific packing areas larger than 150 m^2/m^3. These can be pan distributors (when also functioning as collectors), but for very large columns it is preferable to use channel distributors which can be more straightforward to support and level when equipped with individual channels (for industrial-scale columns, levelness within 5–10 mm is necessary). They are also less sensitive to temperature excursions and enforce a

higher degree of mixing of the liquid in between beds; it is essential to mix liquids in between tall beds with many equilibrium stages, e.g. in the pure argon columns of air separation plants. Flow variations in the liquid distribution are less than 5% for high quality distributors over the whole operating range. In columns up to several meters, one central trough suffices to predistribute liquid over the channels; however, for columns exceeding 5 m for high liquid loads, multiple troughs will be necessary. For columns up to 9 m in diameter, often one circular trough or two interconnected troughs suffices for predistribution. For very high liquid flows, it may be necessary to construct a channel with overflows within the trough, to effectively create multiple predistributors. Liquid is piped into these troughs via pipes that are submerged into the liquid level. To further dampen the liquid momentum and to catch solids, pipes are placed in special parting boxes that are filled with packing. The troughs and channels discharge liquid via holes and/or overflows.

The holes in the channels discharge liquid over the packing and their size and number determine the actual distribution. For standard 250 m^2/m^3 structured packing, recommended drip-point densities are $\geq 80/m^2$; for 350 m^2/m^3 packing, $\geq 120/m^2$; for 500 m^2/m^3 packing, $\geq 160/m^2$; and for higher, $\geq 200/m^2$. This actually will still imply some packing height at the top of the bed is lost as to acquire fully irrigated packing. In structured packing, this will probably be limited to one element, but in random packings this will be a certain number of rings diameters (in the order of 10−20). To not lose bed height for irrigation, vendors recommend drip-point densities that are a good deal (50%) higher than the values above. However, this can pose problems with plugging of the inherently smaller distributor holes, which is an inherent operational risk.

Holes that are large (≥ 10 mm) can be placed in the bottom of the channels to prevent the buildup of solids in the distributor. Placement of holes in the side of the channels reduces the liquid gradient effect in the channel at low flows. The liquid can be guided down via a small pipe; however, when the liquid discharges onto splash plates, a two- to three-fold larger distribution density is created, which can be useful for low-flow distributors where the holes would become too small. Holes below 10 mm typically require filters in the liquid feed and reflux lines to the column, using a mesh that is two to three times smaller than the holes to catch solid debris; otherwise, a high-quality distribution is quickly lost. Each gutter requires a drain hole in the bottom of the channel. Attention must be paid to distributors with very small holes (≤ 4 mm) where the drain holes become larger than the holes for distribution (to ensure they are not plugged).

As liquid discharge is proportional to the square root of the liquid height above the holes, the height of liquid above the hole is proportional to the height at minimum flow and the square of the overall liquid turn-down ratio (maximum over minimum flow). In practice, this limits the turn-down ratio to ≤ 3 to be able to fit the distributor channels through typical 24-in (0.61 m) manholes. Flows in the troughs and channels are subject to a maximum velocity to prevent the buildup of a liquid gradient, as the liquid discharge is proportional to the square root of the liquid head above the hole. Typically, designs can use a safe ≤ 0.3 m/s value to

make maximum use of the distributor height. Higher velocities can be allowed but inherently will require more distributor height (for the same turn-down ratio).

Note that the relative largest differences due to liquid gradient occur at the minimum liquid flow. The recommend minimum liquid head is 25 mm. Liquid discharge from the holes is proportional to the hole discharge coefficient, C_D [37]. The latter is a function of the liquid head above the hole, liquid viscosity, and the contraction coefficient (depends on the size and shape of the holes and the thickness of the downcomer materials). For 4-mm holes, C_D changes from values of 0.85 at liquid heads of 30 mm to values of to 0.7 at heads of 250 mm or more. Larger holes and high viscosity can reduce the value C_D by 5% and requires careful assessment by the column internals vendor.

5.1.4.2 Trays

The development of correlations of tray efficiencies for industrial distillation columns coincided with the rapid growth of the (petro)chemical industry in the period of 1950−1970. During this period, many new processes were developed, most employing distillation for separating the products. Industrial plant design required first testing in small laboratory-scale columns with subsequent careful scale-up to full-size columns (see Chapter 10), which was a time-intensive process. Therefore, there was a strong incentive to develop methods for estimating distillation tray efficiencies.

One of the oldest and still popular methods is that of O'Connell [38], who correlated the overall tray efficiency of operating industrial columns with the product of the relative volatility (α) and the liquid viscosity (η_L). The original correlation was graphical. Various equations have been proposed to represent the correlation, one of which is shown in Eqn (5.14)'[3].

$$E_{OC} = 50.3 \cdot (\alpha \cdot \eta_L)^{-0.226} \tag{5.14}$$

with liquid viscosity expressed in cP and the overall column efficiency in percent. The attractive aspect of this correlation is its simplicity and that it does not contain any equipment design parameters. As such, no tray layout is required to determine column height, which facilitated the evaluation of different process configurations. However, O'Connell himself noted that his correlation, which was based on distillation column data, did not work well for typical absorbers and strippers. For those cases, he developed a separate correlation that accounts for the large vapor and liquid flows in said columns. It should be emphasized that when designing columns for new systems or different operating ranges, the design engineer must choose which, if any, of these correlation to apply. This complicates the use of the O'Connell method for industrial design.

The absence of any equipment or process data reduces the accuracy of the O'Connell method. It is evident that the overall tray efficiencies estimated with this correlation are valid only for some "average" tray layout, as deviations of up to 30% are visible in O'Connell's graphs. For example, trays with long liquid flow paths build up a liquid composition gradient over the tray and have efficiencies

that can easily be 10−20% higher than the efficiency of trays with shorter flow paths. For this reason, tray efficiency can exceed 100%. This effect became obvious because industrial trays have significantly higher efficiencies than those measured in small-scale Oldershaw laboratory columns and led to the development of models to convert "point" efficiencies to "overall tray" efficiencies by correcting for the staging of the liquid along the liquid flow path. An example is the correlation of Gautreaux and O'Connell [39], which Lockhart and Leggett [40] translated into a tabular method for the flow path length (FPL) effect. Their method can be represented in Eqn (5.15):

$$E_{OC} = \left[1 + 0.43 \cdot \left(1 - e^{-0.65(FPL-0.9)}\right)\right] \cdot 50.3 \cdot (\alpha \cdot \eta_L)^{-0.226} \tag{5.15}$$

where the FPL is given in meters. (Note that a longer FPL increases the hydraulic gradient over the tray, which leads to more liquid backup in the downcomer and lowers capacity.)

Though overall tray efficiency models remain popular, more detailed efficiency models were developed using the two-film resistance model; see Chapters 5 and 10 of Volume 1 as well as Refs [13,14] for further discussion of this topic. Via the American Institute of Chemical Engineers (AIChE), the industry sponsored research at the Universities of Delaware and Michigan to develop consistent tray efficiency methods that could be used over a whole range of operating conditions, for both distillation and absorption. This resulted in the AIChE Bubble Tray Design Manual [41]. The model includes tray layout parameters such as weir height and FPL and is much more accurate than the O'Connell method: on the normal operating range of trays the average deviations is 10%. The method has a slight negative bias (−3%) and is therefore conservative.

Figure 5.3 shows some typical results from efficiency models where it can be seen that the choice of vapor flow and liquid flow model is key to the correct prediction of the efficiency. Also note that both the point efficiency as well as the liquid flow model depend on the FPLs. Care should be exercised in combining correlations, as not all combinations are meaningful. Because the method was developed to fit the performance of typical industrial trays, care must also be taken when extrapolating to trays with low weirs or small holes.

Note that the AIChE (1958) model does *not* predict the typical fall-off in tray efficiency at low vapor loadings (due to weeping or dumping) or close to flood (due to liquid entrainment) as shown by the experimental points in Figure 5.3. Several methods have been developed to correct tray efficiencies for these effects, but in column design these have limited practical value. However, the short circuiting or bypassing of some liquid on the tray does affect the design tray efficiency. Examples of such bypass occur on industrial trays that:

- have too few holes (e.g. on ill-designed trays or when during a revamp the active area was blanketed off in a too radical a manner).
- have high liquid capacity such that the bottom of the dowcomer of the tray above sits close or overlaps the downcomer of the current tray.

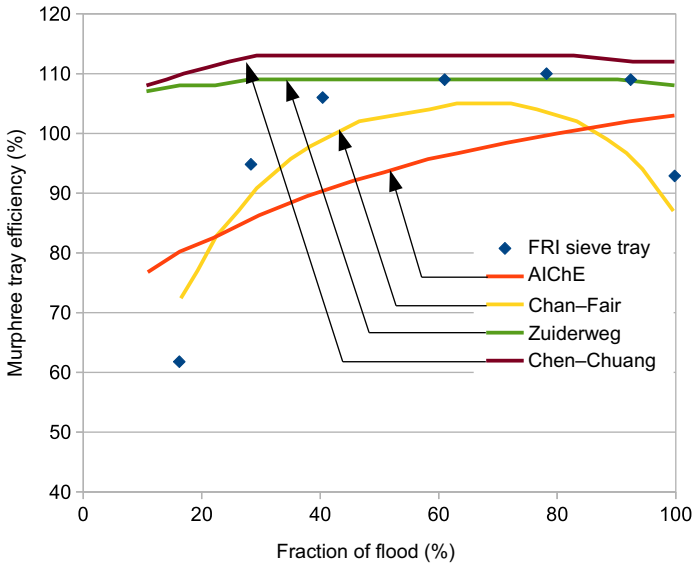

FIGURE 5.3

Sieve tray efficiencies for *i*-butane/*n*-butane operating at 11.38 bar from FRI (blue points) and mass transfer coefficient model predictions: Chan and Fair (yellow line), AIChE 1958 (orange line), Zuiderweg (green line), and Chen and Chuang (brown line). Trays have 14% hole area [42].

- consist of separate contacting and separating decks, where not all liquid flows over the complete contacting tray as some of it is entrained to the separator deck above (e.g. Shell ConSep tray).

Typically, these losses are avoidable except for the last case, where the efficiency must be derated for the lesser degree of staging in the liquid.

A special note must be given to the direction of the flow paths over the tray, also known as the different "Lewis" flow cases. If the tray designs are such that the liquid flow is parallel and in the same direction on all trays, additional staging can also occur in the vapor. This is the case in, for example, columns with circular flow paths. However, such tray designs have not found much application in bulk separation processes. Finally, when multiple liquid phases exist on the tray, such as a hydrocarbon phase and water, the tray efficiency can be much lower than is predicted by any of the known methods. For these type of operations, practical operating experience is required.

In practice, a new design for an existing industrial process is made with tray efficiency data derived from previously operated plants. This historical data may be adapted when tray layout parameters differ from before, e.g. for longer FPLs, increased weir heights, or smaller holes. For operations under different vapor and liquid loadings, it is common for design engineers to scale the efficiencies in the

same manner as scaling packing HETPs, i.e. with the ratio of $\ln\left(\frac{S}{S-1}\right)$. For entirely different systems where no experimental data exists, designers frequently fell back on the O'Connell correlation. In the second part of this chapter, you will see that use of MTCs and rate-based column simulation [43] can provide an excellent alternative.

5.2 Industrial distillation examples

In this second part, we will illustrate specific aspects of distillation column design in existing industrial (petro-) chemical processes. There are many different chemical industries, ranging from basic inorganic chemicals such as industrial gases, elements, alkalis and chlorine, acids, ammonia and fertilizers, to chemicals derived from gas and petroleum (e.g. aromatics), to organics derived from agricultural sources, to synthetics, plastics, and pharmaceuticals. Of these, the inorganic chemicals and petroleum chemicals are produced in bulk. In the case of petrochemicals, significant value is added over that of crude oil at the cost of process energy and capital to invest (see Figure 5.4). The margin of producing chemicals tends to be significantly higher than those for producing fuels but are cyclic, typically caused by oversupply but also by environmental regulations.

Here we will focus on the production of monomers of common plastics such as polyethylene (PE), polypropylene (PP), polystyrene (PS), acrylonitrile-butadiene-styrene (ABS), and polyethylene terephthalate (PET). Distillation is key in the production processes of the monomers; ethylene, propylene, styrene, and

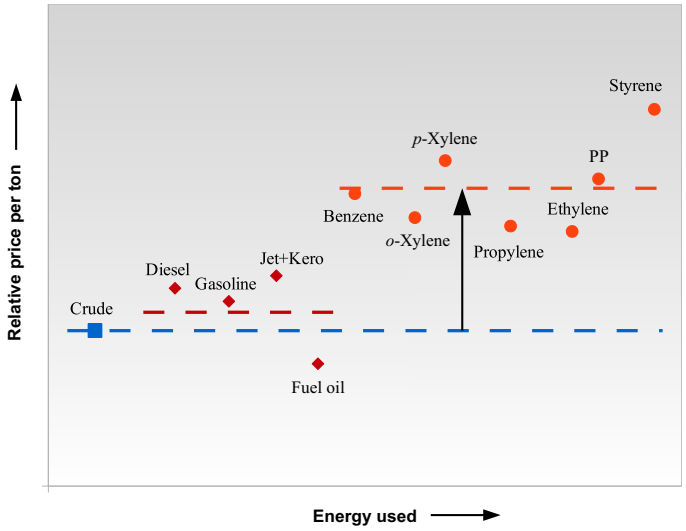

FIGURE 5.4 Added Value of Various Fuels and Petrochemicals in Relation to Crude Oil

ethylene-glycol are all bulk commodities [43] derived mainly from oil and gas. For example, acrylonitrile in ABS is a synthetic monomer produced from propylene and ammonia; butadiene is a petroleum hydrocarbon obtained from the C_4 fraction of steam cracking; and styrene is made by dehydrogenation of EB obtained from reacting ethylene with benzene. PET is made by the esterification of terephthalic acid with ethylene glycol (EG) or by transesterification reaction between EG and dimethyl terephthalate with methanol as a byproduct. The terephthalic acid in turn is made from p-xylene, and the EG is made from direct oxidation of ethylene. All these chemicals are either directly refined from oil (e.g. benzene) or by means of cracking natural gas (NG) or oil fractions, such as steam cracking of liquified petroleum gas for ethylene.

These industrial chemicals processes illustrate many of the general distillation line-ups of products separations as discussed in the first part of this chapter. Production in bulk quantities call for high-capacity tray and packing internals to make use of economies of scale and encounter design difficulties such as sizing pasteurization sections for high-purity products, liquid entrainment, foaming, as well as wetting and Marangoni losses on packings. All columns discussed in this chapter were simulated using the ChemSep rate-based column simulation software [44].

5.2.1 Ethylene and propylene production

A significant part of global olefin production derives from steam cracking of naphtha, gas oil, NG condensates, or from ethane that has been separated from NG. Such plants are designed to produce large quantities of ethylene, propylene, and butadienes, as well as aromatics (see Figure 5.5). The distillation columns in these plants are very large due to the low relative volatility of the alkane/alkylene mixtures that require large reflux ratios. To reduce the large separation costs, recent designs almost always use heat-pumped systems with additional interreboilers operating at lower pressures that reduce the column shell thickness (and thus cost) and increase relative volatility (lower reflux ratio). These columns are frequently equipped with high-capacity trays such as those from UOP or Shell that provide 20−30% higher capacities and further reduce cost. Licensors of this technology are many, including Technip/Shaw (with formerly independent players KTI and Stone & Webster), Linde, CB&I (formerly Lummus), and KBR (Kelogg, Brown, & Root). Typical modern cracker plants have from 5 to 15 modular furnaces [43], reaching capacities of up to 1.5 Mtpa ethylene, 500,000 tpa propylene, and 100,000 tpa butadiene (when fed on NG condensates).

The crackers consist of a hot section where feedstock is cracked in a short-residence-time furnace under the addition of steam. The hot gases are quenched, first using oil that recovers fuel oil, and then with water where aromatics are recovered. The light C2/3/4 olefins gases are compressed and washed in a caustic tower and sent to the cold box of the plant. A straight-run distillation train includes a demethanizer and a deethanizer, from which the tops is sent to an ethylene-ethane (EE) splitter. The ethane is recycled to the furnace to optimize ethylene yield. The bottom of the

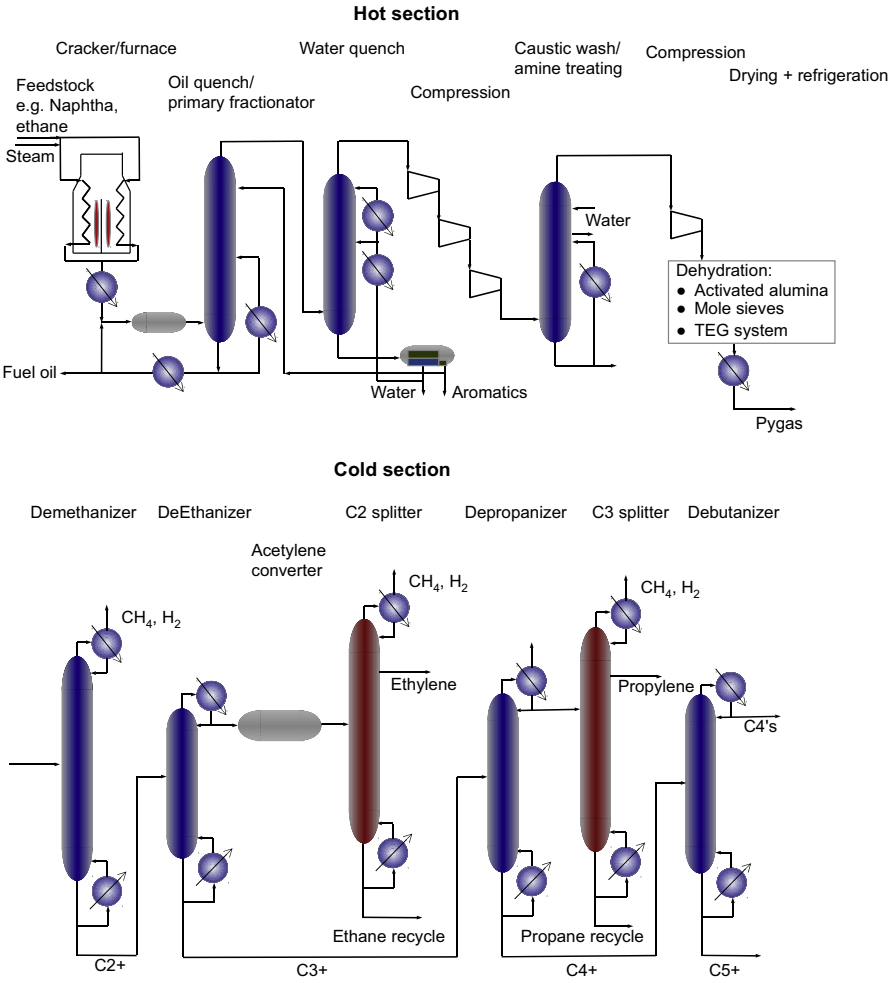

FIGURE 5.5 Typical Hot and Cold Section of a Naphtha Steam Cracker

Crackers of natural gas and condensates do not produce fuel oil or aromatics and have a simpler hot section lineup. Depending on the feedstock composition, it might be advantageous to employ a prefractionation step before the cold section that is not selective for C3 compounds. Highlighted are the C2 and C3 splitter.

deethanizer feeds a depropanizer where the overhead is sent to a propylene-propane splitter and the bottom is sent to a debutanizer. Again, propane is recycled to the furnace to optimize the propylene yield.

For feedstocks containing significant amounts of higher olefins, Stone and Webster developed an alternative lineup in which the majority of the C3 compounds are separated from the lighter gases first by means of a high-pressure depropanizer.

These C3s are then sent to a debutanizer where the overhead is sent to a propylene-propane splitter. The overhead of the high-pressure depropanizer are sent to a prefractionator, separating mostly methane with some C2 compounds over the top from mostly C2 compounds with some propylene and propane in the bottoms. The top product is sent to a demethanizer recovering ethylene and ethane with a very sharp removal of methane. The bottoms is sent to the EE splitter. The C2 stream containing some C3s is separated in a deethanizer with a sharp separation into C2s (sent to the C2 splitter) and C3s (sent to the C3 splitter). When the columns are arranged appropriately, it can be seen that this resembles a Petlyuk arrangement (although by performing the separations at different pressures, it is possible to take advantage of heat integration to come a more optimal scheme from an energy use point of view than the direct distillation train).

5.2.1.1 High-capacity trays for high-flow parameter trays

Tray design for PP splitters is characterized by their extremely large liquid handling capacity. Because of the separation is done at elevated pressures (to operate the condenser at ambient conditions), the vapor-to-liquid density ratio is much larger than in normal distillation columns. Furthermore, because the boiling points of these lower alkanes and alkenes are so close that large reflux ratios are required. The result is that the parameter that determines the hydraulic tray design, the flow parameter, is relatively large. Such trays must handle large flows of liquid with a relatively low density. In addition, the high vapor-to-liquid density ratio results in a low driving force for vapor disengagement in the downcomers. As such, the entrance to the downcomers can choke with the bubbly froth and must be sized appropriately.

High Capacity (HC) trays for high flow parameters now are available from various companies. Standard Oil patented a type of "hanging" downcomer tray in 1930 [45]; the capacity enhancement aspect of this design was overlooked. Shell and Union Carbide (now UOP) developed truncated downcomer trays in the 1960s and 1970s where, driven by the hydrocarbon revolution, they sought ways to scale-up distillation columns to very large column diameters [46,47]. It was recognized that by truncating the downcomers, the area below the downcomers could be used to provide additional active bubbling area. This lowers the effective vapor loading and provides higher jet-flood capacities on a cross-sectional area basis [46]. Figure 5.6 shows the Multi-Downcomer™ (MD) tray from UOP. Significantly more weir length can be created on an MD tray compared to a conventional tray with multiple downcomers with segmental weirs. Longer weirs lower the liquid height over weir, which translates into a lower wet tray pressure drop and hence more capacity. This effect increases with diameter. Zuiderweg [46] claims a 35% difference for 4-m diameter trays. At low liquid loadings, these truncated downcomers can be equipped with seal pans, but at high liquid loadings the pressure loss is such that only dynamically sealed downcomers can be used. When the bottom of such a downcomer is too open and drains too fast or when the liquid level is unstable, the downcomer will unseal and vapor will rise up the downcomers. This

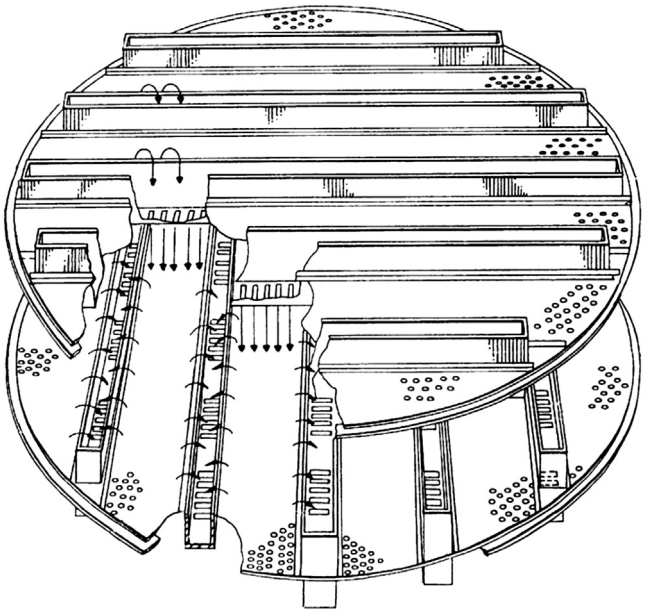

FIGURE 5.6 UOP Multiple-Downcomer™ Trays (US6390454)

results in a loss of separation. For these reasons, truncated downcomers require careful hydraulic design. For further reading on both Shell and UOP tray technology, see Refs [48–60].

Truncating the downcomers is just one way of increasing tray capacity. The following steps can be applied for any trays to increase capacity [45]:

- Increase tray-spacing: This increases the jet-flood and entrainment limits, typically with the square root of the tray-spacing (though at spacings larger than 1 m this benefit disappears).
- Sloping the downcomers: This tapers the downcomers and enlarges the tray area, effectively achieving a similar increase in tray bubbling area.
- Enlarging the hole area: This lowers the hole vapor velocity and reduces dry tray pressure drop, which helps to reduce backup limitations of the tray. However, this also lowers the liquid height and above a certain open area a loss of tray efficiency is observed. FRI reported a drop of 15% in the efficiency of an *i*-butane/*n*-butane system when changing from an 8% to a 14% open area tray [42].
- Lengthening the downcomer weir: This lowers the liquid height over weir (typically computed from the Francis weir correlation) and, consequently, the liquid height on the tray and also the wet tray pressure drop. Typically the downcomer are swept back or arced, but other arrangements can also be designed. Examples are the Koch-Glitsch Superfrac [61], which can be applied with up to 8 passes, and the Sulzer MVG Tray [62].

- Lowering or removing the weir: This further lowers the liquid height on the tray. However, lowering the weir height reduces the tray efficiency and heightens the risk of maldistribution due to tray unlevelness. Great care must be exercised when designing trays with weirs less than 1 in! Typically, this can only be done when the froth is very stable and small holes are used, such as in cryogenic air separation (see Chapter B3-C6).
- Using special downcomer devices, such as antijump baffles that enhance froth collapse and increases the downcomer capacity. Such downcomers can be made smaller, which will accommodate more tray bubbling area and, thus, increase jet-flood capacity.
- Using smaller holes and special bubbling devices, such as the MVG fixed valves, invented by Nutter [63,64]. These fixed valves, now also available from other vendors, direct the vapor sideways instead of up, and incur lower liquid entrainment and froth expansion. At low-flow parameters, these devices are shown to add up to 15−20% extra vapor capacity; however, at higher flow parameters, the advantage shrinks to 5% or less. Use of very small holes requires thin trays.
- Use of directional valves/slots to increase liquid velocity. This lowers the froth height and increases the flow of liquid over the tray.

By 2000, all these methods were being applied by all tray vendors, in different combinations. For example, UOP developed its Enhanced Capacity Multiple Downcomer™ (ECMD) trays with directional slots and antijump baffles in the early 1990s. In applications where many stages are needed, e.g. for EE and PP splitters and for the cryogenic separation of air, the optimal capacity is at low tray spacings. It has been reported that UOP uses tray spacings as low as 10 in (254 mm) [45]. Shell/Sulzer trays also have been deployed down to 12 in (305 mm) spacings [58,59]. Air separation trays without weirs have been installed at tray spacings as little as 6 in (152 mm)! Note that these are relative clean services where the reduced accessibility of the trays is acceptable.

5.2.1.2 Ethylene-ethane splitter

The EE splitter is a typical example where the column pressure is determined by the temperature of the condenser, which in turn depends on the mode of refrigeration and the chosen heat integration of the plant. The number of stages required to obtain polymer-grade ethylene (99.95 wt%) increases with top pressure/temperature due to the decreasing relative volatility, from approximately 60 stages at 4 bar/−75 °C, to 75 at 8 bar /−57 °C, up to 120 stages at 20 bar/−30 °C. Of course, higher temperatures require less refrigeration and are often preferred.

The EE splitter is a typical example of an industrial distillation column where a pasteurization section is used to obtain a very high purity product, 99.95% and higher, to eliminate the presence of a light boiling point compound, in this case methane. The pasteurization sections strip the light components from the product. Because the stripping factors are higher on these trays, their tray efficiencies are

reduced. The product is drawn several stages below the condenser, depending on the amount of light-ends and their concentration build-up. These trays must accommodate higher liquid loading, while also facing a higher foaming tendency due to the larger boiling point differences in the liquid. Therefore, to make optimum use of the column diameter, the trays in the pasteurization section are typically mounted at higher tray spacings than are the trays in the main rectification section.

Shakur [54,54a] described an EE-splitter revamp with ECMD trays of UOP, spaced at 15 in (381 mm) above, and at 13.3 in (338 mm) below the feeds (see Figure 5.7). A test-run was performed after the revamp where the number of theoretical stages were determined by matching compositions and the reflux rate with equilibrium simulations. Table 5.7 lists their test run simulation data; the reported reflux rate corresponds to a reflux ratio of 4.96. The back-calculated overall tray efficiency was 73% without mentioning which thermodynamic model was employed.

Urlic et al. [55] recommended the use of the SRK equation of state with a binary interaction parameter (BIP) of 0.0152. Using this value, the tray efficiency as assessed by UOP can be reproduced (Figure 5.7). Because no specific feed concentrations and locations were provided, it was assumed the two feeds differed by 10 mol% in concentration, and they were fed to the optimal feed stages.

When employing a rate-based model for the EE-splitter trays, the AIChE 1958 MTC model is recommended (see Volume 1, Chapter 3). However, that correlation requires the FPL of the liquid over these ECMD tray. Given the circular liquid flow over the tray, assignment of a FPL is not straightforward. It was approximated by averaging the flows in a quarter of rectangular unit cell that represents the tray (see Figure 5.8). Length L is the distance in between two downcomers. The outflow from the downcomers is assumed evenly (but blocked for the parts where the downcomers on two adjacent trays overlap).

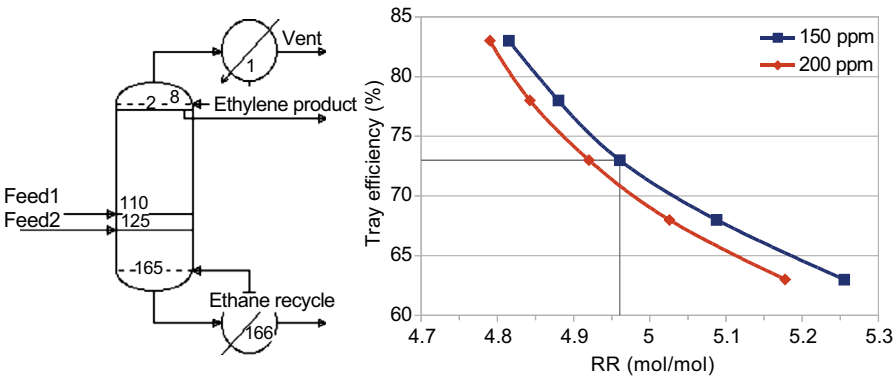

FIGURE 5.7

Ethylene-ethane splitter equilibrium simulation configuration after Shakur et al. [54] and determination of the tray efficiency on the basis of the measured molar reflux ratio (RR) and ethane content in the ethylene product.

Table 5.7 Plant Data of Ethylene-Ethane Splitter as per Shakur et al. [54] as Simulated by UOP and by Means of a Rate-Based Column Simulation

Data of December 8, 1997	Design	Data	Simulation	Rate-Based Simulation
Feed stream 1 rate (kg/h)	37,021	33,820	33,820	33,821
Feed stream 2 rate (kg/h)	112,220	110,055	115,007	115,000
Side draw rate (kg/h)	96,044	90,709	90,485	90,485
Side draw ethane (mol ppm)	261	150	150	137
Bottom stream rate (kg/h)	52,932	60,414	58,006	58,089
Bottom stream ethylene (mol%)	1	0.25	0.25	0.24
External reflux rate (kg/h)	434,597	445,233	445,596	445,575
Reflux temperature (°C)	−35	−31	−30.7	−32.3
Reflux pressure (bar)	18.7		19.36	19.36
Bottom temperature (°C)	−7.1	−6.5	−7.2	−7.2
Top pressure (bar)	19.6	19.6	19.6	19.6
Main condenser duty (GJ/h)	146.4		143.4	149
Reboiler duty (GJ/h)	94.3		92.5	119
Tray efficiency (%)			73	73

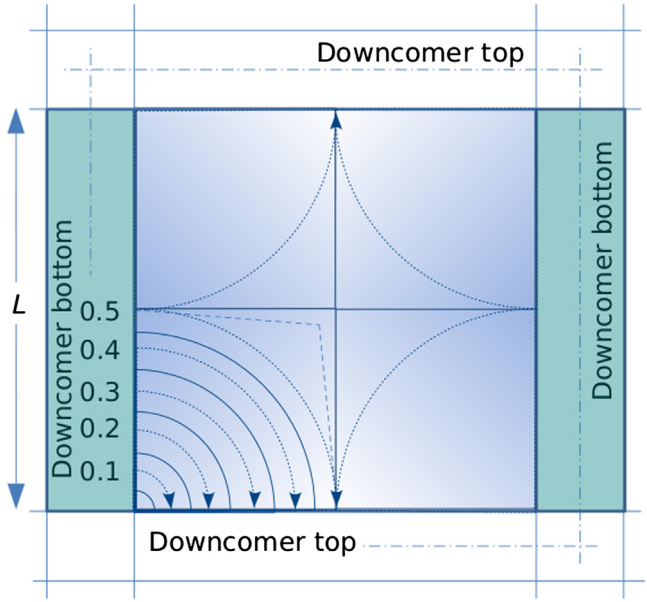

FIGURE 5.8 Unit Cell for Modeling a Tray with Multiple Downcomers

Dashed lines indicate the somewhat circular average flow path. Outflow is from the vertical downcomers from the tray above to the horizontal downcomers on the tray below. There is no direct flow from one downcomer into the next below as the bottom of the downcomers are closed where the downcomers overlap.

Flow paths are assumed to be circular except for the flow halfway the downcomer, as that flow path was averaged between a circular and a somewhat rectangular path. The "average" FPL over the square unit cell can then be expressed as fraction of L, namely as $0.21L$. When the trays are also perforated below the downcomers, the total FPL is then computed by adding an additional one quarter of the downcomer width. Note that though the circular path of the liquid reduces the effective FPL, it enhances the tray deck capacity. Scaling the capacity with the ratio of effective FPLs per active area leads to 15−20% extra capacity. However, the increase in capacity goes at the expense of some loss in tray efficiency (because of the smaller flow paths).

The downcomers on MD trays are typically 0.7−1 m apart, a balance between creating sufficiently long FPLs to maintain tray efficiency and not creating dead zones. For the EE splitter discussed here, this means each tray has five parallel downcomers. Using the downcomer velocity by Glitsch, the downcomers area is set to 10% of the cross-sectional area for liquid handling capacity, and the FPL is then determined to circa 200 mm. Using a typical value for the open area (10%), weir height (50 mm), and downcomer depth (85% of the tray spacing), a rate-based simulation with the AIChE model can be run (care must be taken to use the proper flow models for the liquid and vapor phase). The back-calculated tray efficiency for the EE splitter test run, 73%, was thus matched (see Figure 5.9). The efficiencies below and above the feed are roughly equal. The lower tray efficiency in the pasteurization section was caused by using equal weir heights. If they are

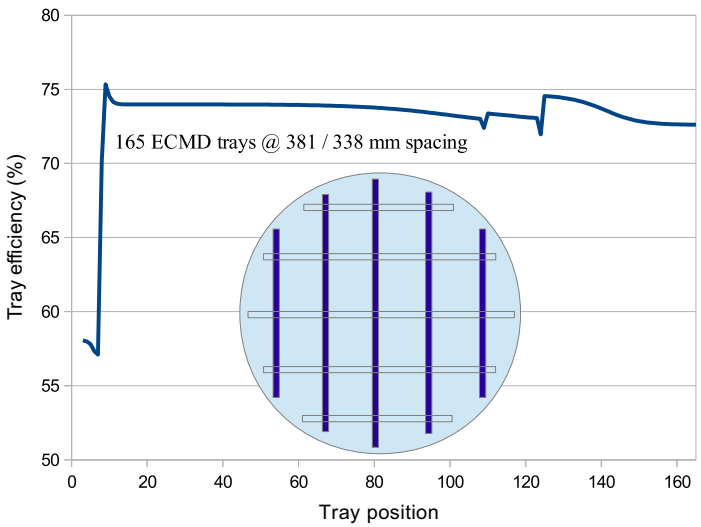

FIGURE 5.9 Back-Calculated Tray Efficiencies with the AIChE 1958 MTC Model for the Ethylene-Ethane Splitter Using UOP Enhanced Capacity Multiple Downcomer™ Trays

Blue boxes indicate the placing of the downcomers on these trays; open boxes indicate the position of the downcomers on the tray above.

increased, the tray efficiency can be kept constant in the whole column. Clearly, a rate-based simulation tool can give detailed insight into the actual required number of stages and required weir heights depending on type of light gas and concentrations. The simulated estimated capacity was at 93% in the main section (by jet flood) and 95% in the pasteurization section (by downcomer chocking).

Note that for proper design of the downcomer, it is necessary to have a correct estimate of the liquid density. Use of standard cubic equation of state will lead to an overestimate of the density and result in designing downcomers that are too small. The actual density difference is about 363 kg/m^3, which means the downcomer velocities must be de-rated slightly, as discussed in Section 5.1. This limits the downcomer capacity of the trays, mostly in the pasteurization section.

5.2.1.3 Propylene-propane splitter

To achieve high (>99%) recoveries of propylene (with a polymer grade product purity of 99.5 wt%), PP splitters may need more than 150 equilibrium stages. Operation at high pressure (20 bar) lowers the relative volatility and hence requires more stages and reflux than operation at low pressure (10 bar). As a result, the columns become so tall that they are frequently split into two column shells. When built as single-column units, they can exceed more than 100 m in height and are amongst the tallest pieces of equipment to be found in bulk chemical plants. The high energy requirements mean that modern PP splitters are VRCs operated at lower pressures, where the vapor overhead is compressed and condensed against liquid lower in the column. Often, these are further optimized in cost and energy usage by using one or more additional side reboilers. This permits the column below the side reboiler to be smaller in diameter because of the lower vapor loading, lowering cost.

As with the EE splitter, the economic upstream removal of components lighter than propylene, here mainly ethane, is such that a pasteurization section and associated vent are necessary to attain the required purity. Other components in the feed are boiling at higher temperatures and leave the column via the bottoms: MethylAcetylene (MA), Propadiene (PD), butadiene, and *iso*- and normal-butane (*i*C4, *n*C4). The amounts of these components present in the feed are dependent on the feed-stock and whether or not there is an upstream MA/PD hydrogenation reactor. MA and PD can build up in concentration in the stripping section of the PP splitter when present in higher quantities in the feed. When this happens, the precise interactions between MA, PD, and propylene cannot be assumed to be ideal. Although propane-propylene is close to ideal and the BIP for equations of state is small, the precise value is important to match the performance of the PP splitter. The parameter is actually temperature dependent, making the relative volatility a function of both pressure and location in the column. The API handbook [65] mentions a value of 0.0073 for the SRK equation of state whereas the reported value at −40 C is higher, 0.0144 [66]. Mathias [97] reviews the temperature dependence of the propane-propylene relative volatility as reported in literature. For operation at ambient temperatures the SRK-BIP will be around 0.008 to 0.010.

Summers et al. [67,68] discussed the 1992 revamping of a high-pressure, two-column C3 splitter with a combined 250 segmental four-pass valve trays. A total of 325 ECMD replacement trays were aimed at providing 40% extra production capacity. This revamp lasted 32 days and required replacement of the tray support rings (as MD trays require 360° rings). Subsequent analysis of the column operation by UOP and Chevron, the owner, resulted in an assessed tray efficiency of 74.2% using UOP's proprietary VLE model and the column operated at 93% of the design point. From the figures provided by Summers, it can be seen that UOP assessed the trays in the main column section to operate at 92% of downcomer backup flood and the trays below the feed to operate at 93% of the maximum liquid load. The ECMD trays were mounted at very low tray spacings of 343 mm in the main part of the column and 381 mm below the feed, where the highest internal flows occurred. To maintain a high efficiency in the pasteurization section, the weir height was raised to 102 mm and hence the tray spacing is largest in this section, namely 457 mm. Table 5.8 summarizes the tray layouts. A picture in the article indicates that the trays were not perforated below the downcomers (this shortens the FPL).

No test-run feed compositions or details on the thermodynamic model were given. The component feed flow rates as listed in Table 5.9 were reconstructed from a mass balance and the reported operating data as well as feed flow rates for the UOP design case specifications. Using this feed, the BIP value for the SRK EOS could be found by matching the UOP simulation results: With a value of 0.0087 and using the reported overall tray efficiency of 74.2%, both the top and bottom specifications as simulated by UOP could be matched almost exactly (see Table 5.10).

From the given tray layout, the FPL was estimated to be 155 mm using the method described in Section 5.2.1.2 for the EE splitter. A rate-based simulation

Table 5.8 ECMD Tray Layout of Propylene-Propane Splitter as per Summers et al. [30,31]

EDMD Trays	
Number of trays	12 / 220 / 93
Column diameter (m)	5.5
Tray spacing (mm)	457 / 343 / 381
Number of downcomers	6
Outlet weir length (m)	50.6
Downcomer width (mm)	178 / 165 / 178
Bubbling area (%)	81
Downcomer area (%)	19 / 17.7 / 19
Hole diameter (mm)	4.763
Outlet weir height (mm)	102 / 51 / 64
Tray thickness (mm)	2.667
Ring width (mm)	89

Table 5.9 Feed of the Propylene-Propane Splitter as per Summers et al. [67,68]

Feed Rates	kmol/h
Ethane	0.28
Propylene	985.66
Propane	334.30
Methylacetylene	1.63
Propadiene	1.63
Butadiene	1.04
Iso-butane	1.36
Normal-butane	2.00

Back-calculated from a mass balance of the operating data for November 22, 1994, but using the design point concentrations for methylacetylene, propadiene, and butadiene. The feed that entered the bottom column on tray 233 is fully vaporized.

was setup assuming a free area of 10%. The result is shown in Figure 5.10, from which it can be seen that the different weir heights result in equal tray efficiencies for all the trays in both columns. The averaged back-calculated tray efficiency is 2% higher than that determined from the simulations by UOP. Note this higher tray efficiency provides a close match of the propane content in the propylene product (see Table 5.10). The tray efficiency of MD trays can be improved by using different arrangements where liquid flow over each tray occurs in the same direction obtaining Lewis case I, such as on the UOP Parallel Flow Multi-Downcomer™ (PFMD) trays [69]. Zhu and others [70] have been developing multiple downcomer trays with high tray efficiencies by employing flow directors (to obtain more uniform liquid residence times) and anti-entrainment devices underneath the trays.

5.2.2 Ethylene oxide and ethylene glycol production

EO is produced by vapor-phase oxidation of ethylene with air or with pure oxygen (typically >99.9%) at temperatures of 200−270 °C, typically over silver-based catalysts. As ethylene and EO both can be fully oxidized to carbon dioxide (CO_2) and water, reactants are diluted with methane and the conversion of ethylene per pass is limited. Reactants are recycled after the produced EO and CO_2 are removed by two absorbers [71,72]. As EO will be oxidized faster than ethylene, it needs to be fully removed by absorbing it in water. The EO is recovered in a stripper column, its overhead being condensed and subsequently steam stripped to remove light gases. Removal of CO_2 is necessary as it lowers the selectivity for EO when present in too high a concentration. To moderate the reaction, ethylene dichloride can be used [73,74]. The use of air instead of oxygen requires a much larger gas purge and about 1.5 times more catalyst. The use of oxygen is preferred as the process

Table 5.10 Propylene-Propane Splitter Operating Data as per Summers et al. [67,68] as Simulated by UOP and by Means of Equilibrium and Rate-Based Column Simulations Using the SRK Equation of State

Data of December 8, 1997	Data	Simulation UOP	Simulation Equation-Based	Simulation Rate-Based
Feed stream rate (kg/h)	54,476.4	56,608.3	56,608.3	56,608.3
Feed pressure (bar)	19.7		19.7	19.7
Feed temperature (°C)	48.2		49.4	49.3
Feed propylene (wt%)		73.12	73.27	73.27
Tray 2 temperature (°C)	44.7		43.7	
Condenser pressure (bar)			18.3	18.3
Tray 2 pressure (bar)	18.3	18.3	18.3	18.3
Tray 164 pressure (bar)	19.4			
Tray 325 pressure (bar)	20	20.1	20	20
Vent temperature (°C)	40.4			
Vent rate (kg/h)	362.9	362.9	361.1	361.1
Reflux temperature (°C)	42.9	42.9	42.8	42.8
Reflux rate (kg/h)	683,520.0	684,285.1	684,255.6	684,255.6
Reflux ratio (RR) (–)	16.56	16.58	16.58	16.58
Condenser duty (MW)		55.71	56.27	56.27
Product rate (kg/h)	41,277.6	41,277.6	41,278.5	41,278.1
Propane in product (mol%)	0.396	0.415	0.415	0.397
Ethane in product (ppm mol)	22	22	22	21
Propylene recovery (%)		99.06	99.09	99.11
Reboiler duty (MW)		51.35	51.87	51.87
Bottom stream rate (kg/h)	14,968.8		14,969.3	14,969.7
Propylene in bottom stream (mol%)	0.19	0.18	0.18	0.13
*i*C4 in bottom stream (mol%)	0.4		0.4	0.4
*n*C4 in bottom stream (mol%)	0.6		0.6	0.6
Mass balance closure (%)	3.3			
Tray efficiency (calc.) (%)		74.2	74.2	76.2

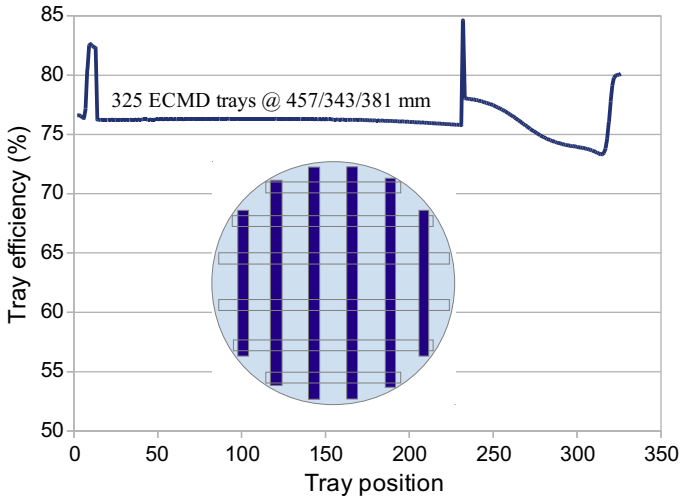

FIGURE 5.10 Back-Calculated Tray Efficiencies with the AIChE 1958 MTC Model for the Propylene-Propane Splitter Using UOP Enhanced Capacity Multiple Downcomer™ Trays

Blue boxes indicate the placing of the downcomers on these trays; open boxes indicate the position of the downcomers on the tray above.

economics are driven by EO selectivity and catalyst cost. Selectivity is dependent on the type of catalyst and moderator employed, as well as the ethylene to oxygen ratio (typically 3–4). Selectivity has increased from ~65% in the early 1950s to current 85–90% values. Catalyst lifespan is 2–3 years, during which the ethylene conversion decreases by approximately 3–4% per year due to deactivation [73]. EO processes are licensed by the various companies that also sell catalyst. The largest three licensors are Dow, Scientific Design Company (a subsidiary of SABIC & Süd-Chemie), and Shell Global Solutions.

About two thirds of the global EO produced [75] is converted into EGs, in which the excess heat available from the EO process is used in the EG process. About half of the monoethylene-glycol (MEG) produced is used for making polyester fibers (for clothing), a quarter is used for making PET, and a little over 10% is used as antifreeze agent. Other EO derivatives are ethylene amines, glycol ethers, and ethoxylates. Ethylene amines are made by reacting EO with ammonia to make mono-, di- and triethylene amines (MEA, DEA, and TEA). These are excellent solvents for removal of carbon dioxide from industrial gases.

MEG can also react with EO to form di- and triethylene glycols (DEG and TEG). Hence, the hydration of EO must be done with an excess of water (5× or more by mass) to minimize the formation of the higher glycols. This also helps to control the reaction temperature of this strongly exothermic reaction. The hydration reaction can be done without catalyst at elevated temperature (170 °C) and pressure (35 bar), or alternatively, catalytically at lower temperatures (100 °C) with an ion-exchanger giving a

higher selectivity towards MEG (~97% vs ~90%) and reducing the required excess of water. Typical EO conversion rates are high (>98%).

The global MEG market grew annually by 6–7% in the 2006–2010 period when demand for fiber-grade MEG outpaced that of higher glycols. Hence, a process that produces only MEG was developed by Shell Global Solutions and Mitsubishi Chemicals [76,77], where EO is first reacted with CO_2 to ethylene carbonate (EC). EC is subsequently hydrolyzed to MEG and CO_2, which is recycled. This "Omega" process [78,79] has a 99.5% selectivity for MEG. The first plants started up in 2008/2009 with capacities ranging from 400 to 750 kta. The new process features a 10% lower cost and produces less waste water. Nevertheless, demand for the standard glycol process remains because DEG and TEG are valuable byproducts (they are used for drying NG because of their high boiling points and hygroscopic nature).

The separation train of the standard glycols process illustrates the use of various distillation techniques in chemical processes; hence, it is selected for discussion. The combined EO/EG plant can have up to 20 columns, but here we will only discuss the details of four columns in the glycols lineup of a typical industrial-size MEG plant (i.e. 500 kt MEG per year, designed at 75% of flood and 91% production availability). These columns are highlighted in Figure 5.11.

The columns operate over a wide range of pressures, from 20 bar to deep vacuum (10 mbar). As water/glycol mixtures are highly nonideal, this puts quite a demand on the thermodynamic and property models (particularly the surface tension needs to be modeled properly to determine the effect of the Marangoni forces on the mass transfer). Equations of state that employ excess Gibbs mixing models, such as the predictive SRK (PSRK), can be used (see Figure 5.12). Glycols are hygroscopic in nature, and as such the trace removal of water needs special care.

The ratio of MEG/DEG/TEG is determined by the reactor conditions, the selected water dilution, and the MEG content of the condensate/steam recycle to the reactor. The typical DEG/MEG mass ratio varies from 1/10 to 1/12, and the TEG/MEG mass ratio varies from 1/150 to 1/200, respectively. Using a dilution factor of 5.4 by mass for the 500 kta MEG plant, 41.8 kta DEG, 2.5 kta TEG, and 0.16 kta higher EGs are produced.

The excess water needs to be removed again. This is done by three- or four-stage multiple-effect concentrators distilling off the bulk of the water. The first concentrator is reboiled using steam generated in the EO reactor; the others are reboiled by condensing the overhead water vapors of the previous concentrator. The overhead condensate water of the concentrators is recycled. The final water removal occurs in a mild vacuum dehydration column operating at 200 mbar. The MEG is then separated from the higher glycols in an MEG purification column operating at the same pressure that is equipped with a pasteurization section to obtain the required 99.9%wt purity [85].

To control the product impurities of MEG and DEG independently at different process rates, crude glycol is produced first in a dehydrator. This is distilled in a column with a pasteurization section to control water content by means of the overhead

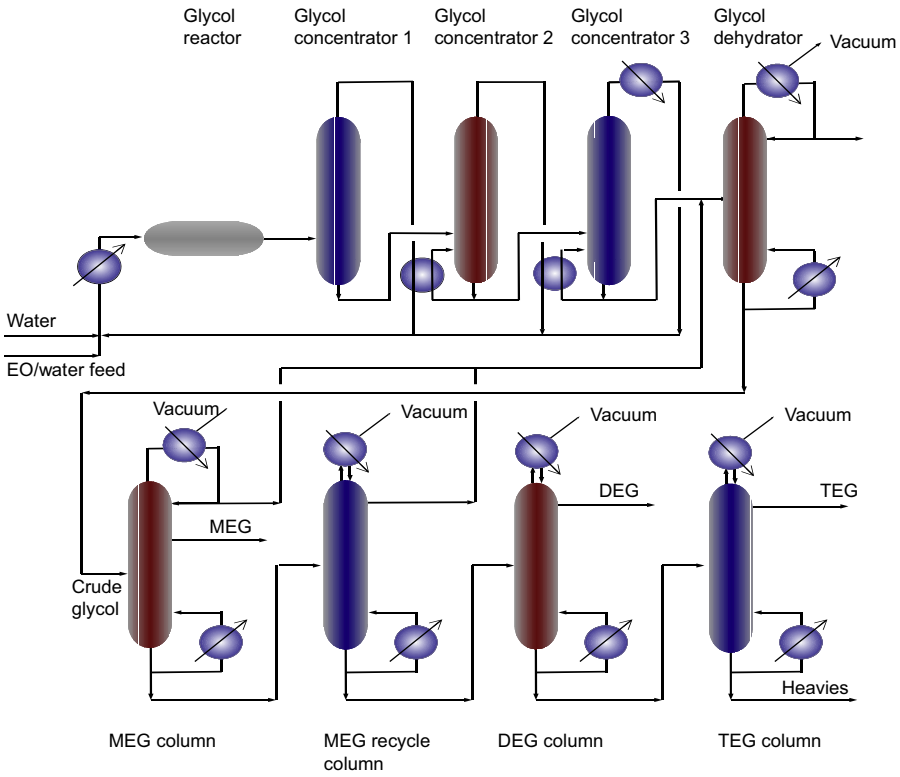

FIGURE 5.11 Process Flow Diagram of an Ethylene-Glycol Plant [80–82]

EO, ethylene oxide; MEG, monoethylene-glycol; DEG; diethylene-glycol; TEG, triethylene-glycol. Columns highlighted in red are the discussed in the text.

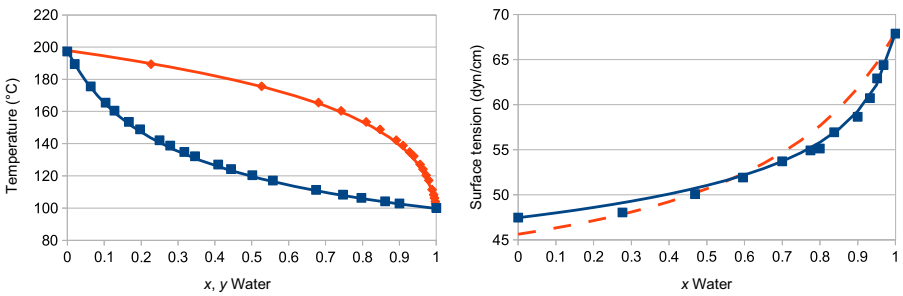

FIGURE 5.12

Left: VLE data for MEG-Water at 1 bar [83] modeled with the PSRK method. Right: Surface tension of MEG-Water at 50 °C [84] modeled with a mole fraction weighted average of the component surface tension with a ninth power (blue) or Winterfeld-Scriven-Davis (dashed orange).

rate, and of DEG by means of the reflux ratio. The MEG content in the higher glycols can be controlled in the separate MEG recycle column that operates at 100 mbar so as to lower the reboiler temperature. The overheads of both columns are recycled to the dehydrator. Subsequently, the bottoms is separated into DEG and TEG products at purities of 99.5%wt and 99%wt, respectively. The DEG and TEG columns must operate under deep vacuum (in order to run the reboilers using medium pressure steam). Because of the high viscosities, they employ falling film reboilers. By integrating the condensers and reflux vessels in the top of the columns, the lowest operating pressures are obtained.

The various recycles in an EG plant and the operation under vacuum means that all of the columns are in the 2- to 5-m range (except for the TEG column). Hence, high-capacity internals can be advantageous. Operating under vacuum also means that some column inlets can exhibit very high velocities. Specialized inlet devices such as Shell Schoepentoeters™ can be applied to promote adequate vapor distribution and minimize liquid entrainment to the bed above. Furthermore, the vacuum columns require high area packings, which require liquid distributors with high-quality distribution and large drip-point densities. This means some distributors have holes as small as 3 mm. To prevent plugging of these small holes, all feeds and reflux returns of the vacuum columns are to be equipped with filters with sufficiently small meshes.

5.2.2.1 Glycol concentrators

Heat integration between the condensers and reboilers of the concentrator columns is necessary in order to economically evaporate the large excess of water in the reactor effluent. For this reason, these columns operate at different pressures. Actual operating pressures are dependent on the chosen type of heat integration [86] and column shell cost optimization. Each concentrator distills off roughly the same fraction of the overall water content. The concentrators need to evaporate roughly three quarters of the mass of the process flow in the form of water (as steam). Design of the concentrators is determined by the maximum fraction of evaporation that the reboilers can deliver, and the available temperature difference. The concentrators tend to be similar in design except for the increasing column diameter, reflecting the decrease in vapor densities. At least three but often four concentrators are used. For a three-stage train, the first concentrator can operate at e.g. 14 bar, the second at 9 bar and the third at 4 bar. A four-stage train requires a higher starting pressure.

The concentrators are trayed as packing exhibits lower efficiencies at higher pressures. One tray below and 8−10 trays above the feed suffice to lower the overhead MEG contents to less than 0.1%. As the overhead is recycled to the reactor, the MEG concentration must be kept low so as to prevent MEG reacting into higher glycols. Each feed flashes to a lower pressure but remains mainly liquid. The trays below the feed encounter large liquid loadings whereas the trays above the feed have a rather small L/V ratio (and hence low flow parameter). Consequently, the trays operate in different regimes: the top trays have low liquid loadings and operate

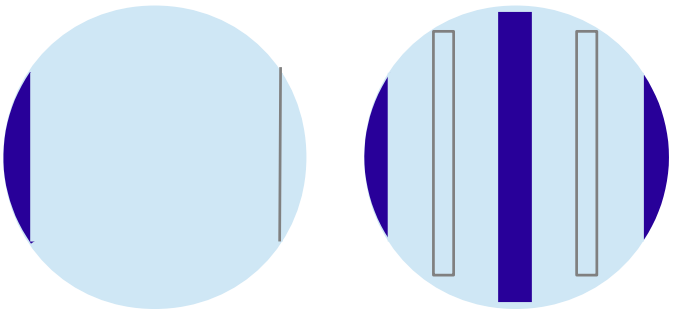

FIGURE 5.13

Layout of the one-pass trays in the rectification section (left) and the four-pass trays in the stripping section (right) for the 3.5-m diameter second concentrator in a three-stage train operating at 9 bar. The different weir loading causes the downcomer area to change from 3.3% (left) to 10% (right). Standard weir heights (2 in or approx. 5cm) and tray spacings (2 ft or approx. 61 cm) are used for both layouts. The free area ratios are 11.7% (left) and 10.5% (right), respectively.

in the spray regime, whereas the bottom trays have higher liquid loadings and operate in the froth regime. To accommodate the higher liquid loading, more weir length and more downcomer area is required. As such, the number of flow passes change from one in the rectifying section to four in the stripping section; see Figure 5.13 for a 9 bar concentrator column in a 500-kta MEG plant.

Simulation of such a concentrator column using the AIChE model predicts a 73–75% Murphree tray efficiency for the trays. This value may be higher than the efficiency observed in tests [87] due to the larger FPL applied here. Glycol concentrators are moderately foaming and the system factor is 0.85 (from Table 5.4). As the column diameter is determined by the trays below the feed, the use of high-capacity trays with truncated downcomers would decrease the column diameter by the percentage of one downcomers, about 10% (see Table 5.11). As the first concentrators

Table 5.11 Dimensions of the Highlighted Columns in Figure 5.11 of a 500-kta MEG Plant Designed at 75%, with Standard and HC Internals, as well as Projected Cost Savings

	Standard Internals		High Capacity Internals		
Column	Diameter (m)	Heights (m)	Diameter (m)	Heights (m)	Cost Savings (%)
Concentrator 2	3.9	8.4 / 1.2	3.6	6.3 / 1.2	5
Dehydrator	4.4	4.8 / 3	4	4 / 3	13
MEG purification	4.2	1 / 4 / 1.5	3.9	1 / 4 / 1.5	10
DEG	2.4	1.5 / 1.5			

operate at elevated pressure, reducing the column diameter helps to reduce cost. However, the sump of the concentrator must accommodate sufficient holdup time for the reboilers; as such, they are often designed with larger diameter sumps than their trayed column sections. This lowers the cost-benefit of applying high-capacity internals. Also note that the trays above the feed have sufficient weir loading such that no special care needs to be accounted for liquid maldistribution due to low liquid height over the weir at turn-down. High-capacity trays have a larger ratio of weir length to downcomer area and as such need picketing of the weirs.

5.2.2.2 Glycol dehydration column

The dehydration column operates under a mild vacuum (200 mbar) and is equipped with structured packing. Its rectification section sees only a small liquid reflux and the packing is close to the minimum wetting rate. At normal flows, the liquid film thickness should be sufficient to guarantee full wetting and mass transfer. This is the case when using high-capacity Mellapak Plus M252Y, where wetting rates are at 125% of the minimum wetting rate. This means that when the MEG section operates at reduced throughput (e.g. when the plant maximizes the EO output), the top section can operate below the minimum wetting rate. However, when the column operates at less than 80% of the nominal capacity, de-wetting will occur and the HETP will start to increase, as indicated by Figure 5.14. Hence the height of the

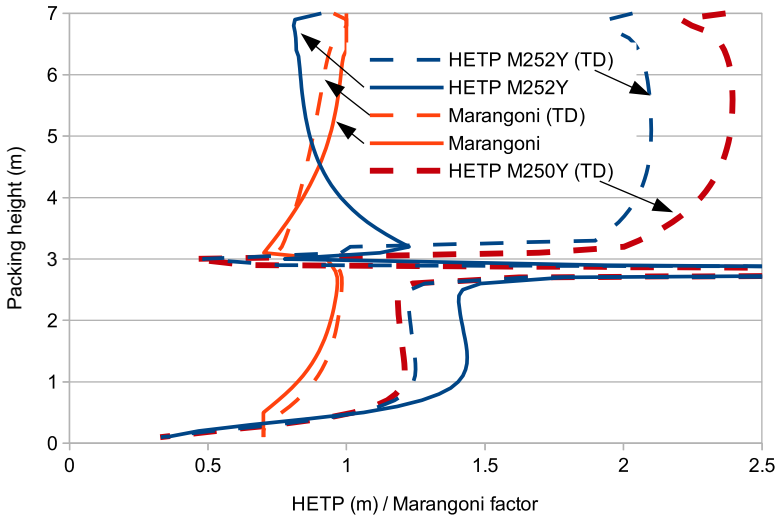

FIGURE 5.14

Predicted glycol dehydrator height equivalent to a theoretical plate (HETP) (blue) and Marangoni (orange) correction factors at normal flow rates (solid) and at 50% turn-down flow rates (dashed) for Mellapak Plus 252Y at a column diameter of 3.4 m. The 50% turn-down case for Mellapak 250 Y at a column diameter of 3.7 m is shown as a thick red dashed line. The higher diameter translates to a loss of HETP due to de-rating of the interfacial area as a result of de-wetting.

rectification section is set to 4 m to maintain an overhead MEG concentration of 0.1% while operating at 50% throughput (at the same reflux ratio). When regular Mellapak 250Y would be used, a larger column diameter is needed and the HETP will further deteriorate due to the lower wetting of the packing, requiring an additional 0.8 m bed height to obtain the same separation. Figure 5.14 shows the Marangoni correction factor for the mass transfer and the HETP as simulated using the Bravo-Rocha-Fair (1985) MTC model with the Marangoni correction from Billet and Schultes (1999). The stripping section of the column determines the water content. The water content should be less than 1%wt in order for the pasteurization section of the MEG column to operate properly. For design of the packing diameters of the dehydrator, a system factor of $0.85^{0.7} = 0.89$ was used, as per Table 5.4.

5.2.2.3 MEG purification column

Figure 5.15 shows the predicted compositions and HETPs for the MEG purification column equipped with Mellapak Plus 252Y as listed in Table 5.11 using the same MTC models as for the dehydration column. As can be seen from this figure, water builds up in the pasteurization section and also below the feed from the dehydrator. The HETP in this section is significantly increased as a result of the nonideal water–MEG interaction. Although the actual MEG product purity specification is 99.9%wt [85], the control of the column must be set at a higher value to ensure the specification is met. Some margin must be added for control and additional design safety. Design can be set for a 99.94% purity.

In the section, between the feed and the product draw, the DEG is removed and the water content remains practically constant and normal HETP values are obtained. Product is withdrawn where the concentration of water and DEG are about equal. Rate-based simulation shows that 4-m packing is needed to obtain the allowed 0.05 wt% DEG as per specification. Just below the feed from the dehydrator, there is a buildup of water that is removed. The pasteurization section is also seeing some minor Marangoni effect, but this is not significant.

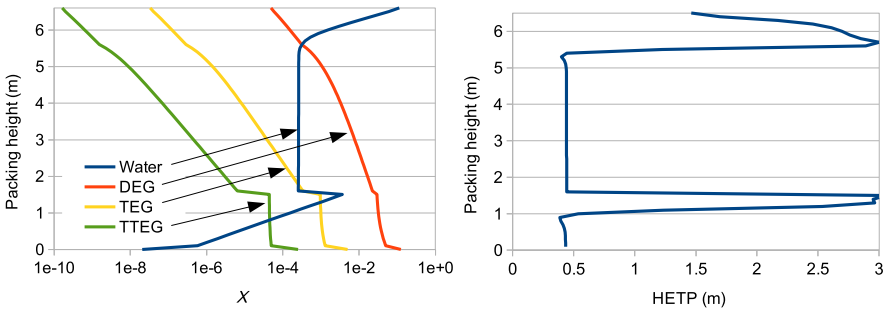

FIGURE 5.15

Predicted compositions (left) and HETP (right) for the monoethylene-glycol purification column using Mellapak Plus 252Y. HETP, height equivalent to a theoretical plate; DEG; diethylene-glycol; TEG, triethylene-glycol; TTEG, tetraethylene-glycol.

The bed height in the bottom stripping section determines the size of the MEG recycle. In order to keep this recycle less than 25% of the total MEG flow through the plant, a 2-m bed height suffices. Of course, actual plant designs may employ larger safety margins resulting in higher bed heights. Furthermore, Table 5.11 indicates the column diameter can be reduced significantly when high-capacity M252Y packing is used compared to the regular M250Y. For determination of the column diameter, a system factor of 1 was used. Note that Strigle [18] mentions an overall HETP of 1 m for the separation of MEG from DEG and TEG using IMTP #40 random packing at 70 mbar. Figure 5.15 shows that high-capacity structured packings provide much higher separation efficiencies.

5.2.2.4 DEG column

The DEG purity is mainly determined by the MEG content of the feed, i.e. by the control of the MEG recycle bottom temperature. For control purposes, the purity is set at 99.6%wt DEG. Design with 99.7%wt at 10 mbar gives a minimum of eight stages plus condenser and reboiler with feed in the middle, relatively independent of the reflux ratio. As the DEG and TEG separation is at deep vacuum, the most economic packing at these pressures is a gauze packing such as Sulzer BX. Gauze packings feature a higher efficiency than the sheet metal packings; by using an angle of 60° to the horizontal, a lower pressure drop per equilibrium stage is obtained. The gauze material also has a much lower minimum wetting rate, which in this case increases turndown. However, because gauze packings contain about 5 times more metal per cubic meter, they are also more costly. Gauze packing requires high drip-point type distributors; in this case, distributors with slash plates are needed as the liquid loadings are so low that otherwise the drip-point diameters would become impracticably small.

The left side of Figure 5.16 shows that the HETP for BX packing increases with pressure and that it is a rather strong function of the vapor velocity: Gauze packings require different MTC models than sheet metal. The packing has a design HETP of 0.25 m as the BX packing floods consistently at this HETP. As one layer of BX packing is 17 cm in height, six layers per bed are required. With so few stages in the column, a precautionary extra layer of packing is added to each bed. In addition, because liquid does not easily spread over gauze packings, it is typical to install also one or two additional layers of packing. Of course, the top packing layers are only partially wetted, and this must be accounted for in a column simulation. Thus, the DEG column has typically two beds of eight or nine layers, i.e. up to 1.53 m per bed. The right side of Figure 5.16 shows the simulated HETP for the DEG column with BX packing. The F factor varies from 2 in the bottom to 3 in the top, and the column has a pressure drop of 11 mbar at nominal capacity. The HETP is mainly determined by the stripping factor of DEG that is constant in the rectification section but varies by almost a factor of 5 in the stripping section. The minimum reflux ratio is about 0.4 determined by the feed pinch. Typically, an overdesign of factor 2 is used in sizing the DEG column diameter, to provide capability to produce more DEG if so desired.

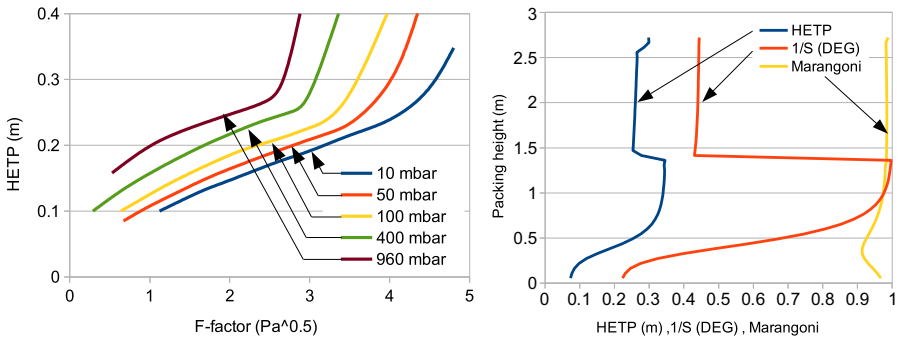

FIGURE 5.16

Left: height equivalent to a theoretical plate (HETP) of the Sulzer BX packing for a chlorobenzene/ethylbenzene at various pressures as function of the F-factor [11]. Right: HETP (blue) from the Brunazzi 1995 MTC model with Marangoni correction (yellow) for the diethylene-glycol (DEG) column with two beds of eight layers back calculated from a rate-based column model.

5.2.3 Aromatics and the production of styrene

Aromatics are the precursors of many common plastics; as such the global aromatics market grew at an average rate of about 3.5% per year over the past decade [88]. Typical sources are pyrolysis gas from napththa crackers (72%), reformate (24%) from refinery catalytic naphtha reforming/platformers, and coke oven gas (4%). The main licensors are Uhde and UOP [89].

The benzene content of gasoline is regulated to a maximum of 1%; hence, most benzene must be removed from the fuel pool. Over half of the global benzene produced is reacted with ethylene to form EB, which is further cracked to produce styrene for PS used in disposable utensils, DVD cases, food containers, packaging materials, etc. Roughly one fifth of the benzene produced is reacted with propylene to make cumene, which is used to produce acetone and phenol, and with these *bis*phenol-A, a precursor for polyester fibers or with phosgene for polycarbonate (used in soda bottles). Benzene is dehydrogenated to cyclohexane (14%) for making nylon used in the manufacture of fabrics and carpets, 7% is used to make nitrobenzenes, and 4% is alkylated with normal-alkanes for making detergents.

Toluene is widely used as solvent. It is also used to make nitrotoluene which is applied in explosives and dyes. Toluene is also reacted to toluene diisocyanate for polyuthane foams. However, since 1990, the demand for toluene grew about 1% less compared to the demand for benzene and xylenes. Hence, market prices have made it more attractive to convert toluene into xylenes and benzene by means of dehydroalkylation and disproportionation, such that as much as 22% of global demand for benzene is met in this way [88].

Orthoxylene is used for making phthalic anhydride for use in alkyl resins and methyl acrylate. Paraxylene is used to make terephthalic acid for use in PET

polyester. The demand for paraxylene has increased to the point that currently most metaxylene and a large fraction of orthoxylene is isomerized into paraxylene, which now forms over 90% of the xylene global market.

5.2.3.1 Xylene production

A large fraction of the global xylene production stems from severely continuous catalytic reformed hydrotreated naphtha. The debutanized reformate is split into a light fraction from which benzene, toluene, and xylenes are separated from the paraffins by means of extraction (e.g. Uhde Morphylane™ or UOP sulfolane process) and separated by a direct distillation train.

Because the market demand for benzene and specifically for paraxylene has outpaced the demand for toluene, many of the aromatics production plants have been maximized for xylene make over the years. Figure 5.17 shows how this can be done: toluene, EB, and trimethyl benzenes (TMBs) are converted to benzene and xylenes by means of disproportionation and transalkylation (e.g. using the Tatoray process), *p*-xylene is selectively removed (e.g. with UOP Parex™ continuous adsorption or with Sulzer chemtech suspention crystalization [90]), and finally the undesired xylenes are isomerized (e.g. with UOP Isomar™). Note that

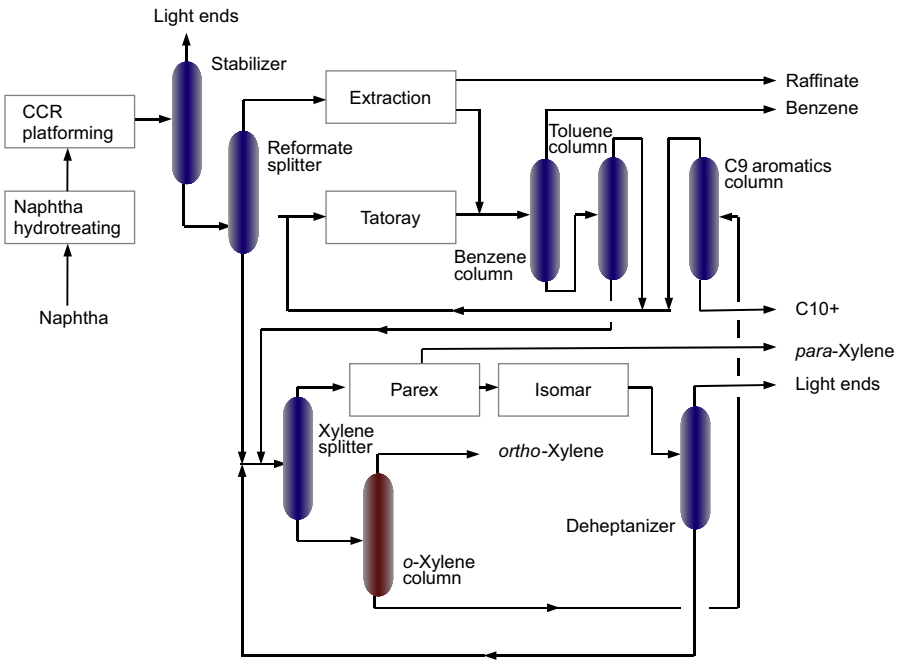

FIGURE 5.17 Integrated UOP Aromatics Complex for Maximized Xylene Production [44,46]

Clay treaters have been omitted. The highlighted orthoxylene column is discussed in more detail.

high-severity reforming ensures that the heavy C8+ part of the reformate consists almost completely of aromatic compounds and can directly be sent to the xylene splitter after clay treating.

The shift towards production of paraxylene significantly aided the advance of adsorption and crystallization technologies. For example, UOP reports >30% higher capacities for its Parex adsorbent over the past two decades [91]. If light naphtha is available cheaply or local benzene demand is sufficiently high, the yield can also be maximized for benzene by using a hydrodealkylation (HDA) unit that converts the toluene and TMBs selectively into benzene. To efficiently produce high-purity 99.9 wt% paraxylene, a Parex unit must be supplied with a xylene stream with low TMB concentration; otherwise, these C9 aromatics build up in the desorbent circulation loop. Typical recoveries are 99.7% per pass. The raffinate with <1 wt% paraxylene is sent to an isomerization reactor. Its effluent is sent to a deheptanizer where the xylenes in the bottom are recycled back to the xylene splitter, effectively converting all meta- into ortho- and paraxylene. The overhead is recycled to the platformer stabilizer for extra recovery of benzene.

Distillation is the main source of energy consumption in an aromatics complex, and there are many opportunities for energy optimization through heat integration. This can be done by raising operating pressures of columns such that condensing their distillates can be used as reboil heat for other columns. For example, the xylene splitter overhead can drive the desorbent recovery reboilers in a Parex unit, whereas the xylene splitter bottoms can reboil the Isomar deheptanizer.

Because of lower market demand, only about half of the aromatics plants are configured to produce both para- and orthoxylene. The orthoxylene is produced in an additional high purity orthoxylene distillation column that sits downstream of the xylene splitter. The splitter cut point must be lowered such that a targeted amount of orthoxylene enters the C9+ bottoms stream. If the plant has a Tatoray (or HDA) conversion unit, the TMBs in the bottoms of the orthoxylene column are distilled and sent for conversion; otherwise, they may be blended in the gasoline or fuel oil pool, together with the heavier components.

Most of the columns in Figure 5.17 were traditionally designed as trayed columns because of the potential for fouling. However, fouling can be prevented with proper treating and injection of inhibitors. When the flow parameter is less than 0.1, it can become interesting to use a high-capacity structured packing such as Sulzer M252Y, Koch-Glitsch Flexipac 250Y, or Montz B1-250MN for revamping existing aromatics columns. The much lower pressure drop over the structured packing lowers the reboiler temperature, increasing the temperature driving force in the reboiler. This can help to make available additional capacity in the various heat-integrated aromatic complexes.

Here we will discuss such a revamp for the orthoxylene column in an aromatics complex as described by Sulzer [92], which produced a 98.5% pure orthoxylene containing less than 0.3% cumene, at 7.5 t/h from a total xylene feed of 17.3 t/h. The tray efficiency was reported as 75%. No details were given on the exact feed compositions, tray and state, or tray layout and only approximate *o*-xylene and cumene

Table 5.12 Feed Flows for a 2-m Orthoxylene Column Equipped with 80 Two-pass Valve Trays, Which was Revamped for More Capacity; Tray Spacing 600 mm; Pressure Drop 650 mbar

Component	Flow (t/h)
m- and *p*-xylene	0.04
o-Xylene	7.7
C9 paraffins	0.04
Cumene	0.15
n-Propyl benzene	0.15
m-Ethyl toluene	1
Trimethyl benzene	0.02
p and *o*-ethylbenzene	1
4-Ethyl *o*-xylene	1.5
p-diethyl benzene	2.4
Tetramethyl benzene	3.3
Total	17.3

concentrations were provided, as well as a mass balance. Using typical feed compositions for orthoxylene columns, a detailed composition was created, as shown in Table 5.12. For the purpose of this discussion, it was assumed that the tray layout and the feed location were optimized (i.e. feed entering at saturation on tray 67). From the reported vapor density, the top pressure was determined as 1.4 bar.

The reported reboiler duty was 4.8 MW at 210 °C. Using this value, the reported tray efficiency of 75% could be reproduced using a rate-based column simulation using the AIChE model with the predictive SRK equation of state (to account for the activity of the various components) assuming standard 2-in Glitsch V1 type of floating valves with a bubbling free area 23.5% and downcomers area of 9.1%. The simulation shows the valve trays operating at 80% limited by jet-flood in the rectification section of the column. The McCabe-Thiele diagram is shown in Figure 5.18.

The column was revamped using six beds of Mellapak 252Y for a total height of 36.7 m. It was assumed that these beds were of roughly equal height. After the revamp, the feed was increased by 33% (to a value of 23 t/h) and a 98.5% orthoxylene could be produced at 10 t/h. The bottoms contained less than 1.5% orthoxylene. The column pressure drop was reduced to 0.1 bar. The reboiler duty required to reach the same cumene specification of <0.3% was now just 5.7MW at 198 °C, 10% less per ton of processed feed. Most importantly, it was about 12 °C lower in temperature, which avoided the need for installation of new heat exchangers. Sulzer reported operation of 79% of flood in the top and 90% in the bottom of the bed with pressure drops per meter bed of 2.7 and 5.4 mbar, respectively.

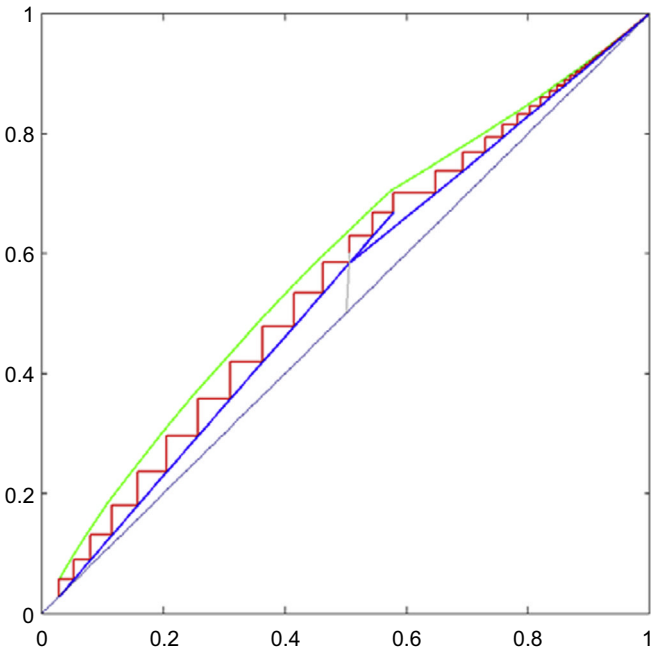

FIGURE 5.18 Lumped McCabe–Thiele Diagram for the 2-m Valve Tray Column

The key components are orthoxylene and cumene. Lumped mole fractions are used of o-Xylene and Cumene. Lumping is done by means of y1/(y1 + y2) for the vertical axis and x1/(x1 + x2) for the horizontal axis.

Rate-based simulation matched these numbers very closely (i.e. 79% and 87% using the Wallis correlation as discussed in Section 5.1.3.2). The back-calculated HETP was about 460 mm. Note that this is about 10% higher than the normal HETP for Mellapak 250Y. The conclusion is that for this ortho-xylene column high capacity packings can provide more interesting revamp options than high-capacity trays due to their low pressure drops.

5.2.3.2 Ethylbenzene and styrene production

Styrene is manufactured by dehydrogenation of EB obtained from reacting ethylene with benzene, as shown in Figure 5.19. In both processes, reactants and products are separated by means of distillation. Because styrene can polymerize and rapidly foul the column internals, it is very crucial that the right type of inhibitor is added to both reactor effluents in appropriate quantities. In both processes, the light compounds are separated from the reactor effluents first. Also, both reactions have undesired heavy byproducts. The trans-alkylation capability of the EB catalyst is used to react most of the di- and triethyl-benzenes back to EB, although some heavy "flux oil" is produced. Integration of an aromatics complex with HDA can be advantageous since

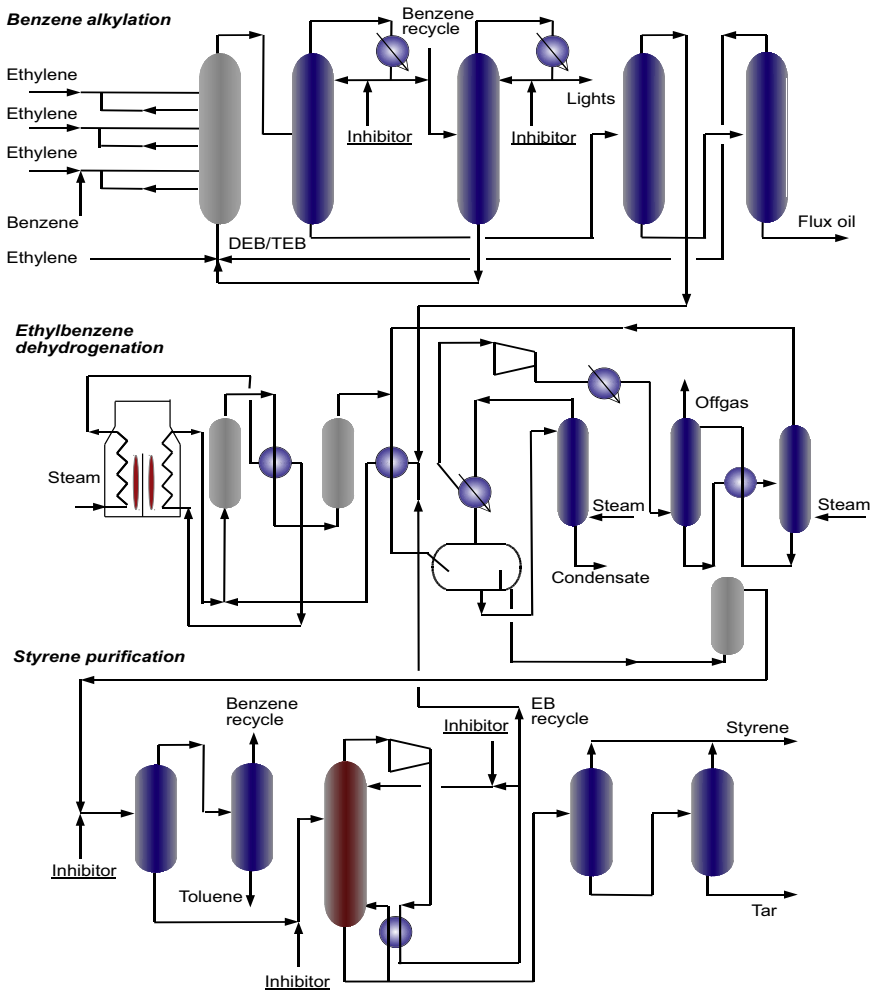

FIGURE 5.19 Ethylbenzene (EB) and Styrene Plant [93]

Highlighted is the ethylbenzene/styrene splitter with vapor recompression column, which is investigated in more detail in the text. DEB, diethylbenzene; TEB, triethylbenzene.

the dehydrogenation of EB also produces benzene and toluene. Conversion in the dehydrogenation reactor has improved from 45 wt% styrene yield just after World War II to up to 60 wt% in 2003.

Both EB and styrene recovery is by means of distillation, with the largest being the vacuum column separating styrene from its precursor EB with typical column diameters of 8–9 m. This column consumes about 75% of all energy in the process and hence is designed as a vapor recompression system in modern plants. The low

boiling point difference and the low specification of 100 ppm EB in polymer-grade styrene require a large number of stages, of the order of 100, and a high reflux ratio, in the range of 6−8. Styrene polymerizes rapidly at temperatures above 100 °C; therefore, the column must be operated under vacuum.

In the early days of styrene production, this separation had to be done in two separate column shells, each equipped with 70−75 bubble trays in total to maintain a bottom temperature that was sufficiently low. A bottom purity of 2000 wt ppm EB was obtained. The top vacuum had to be below 85 mbar as the total column pressure drop was around 500 mbar. The styrene in the overhead (3.6 wt%) was recycled the reactor together with the EB. A significant improvement came with the introduction of low-pressure drop trays by Linde [2] that had half the pressure drop of earlier designs (230 mbar). This allowed the distillation to take place in a single column shell but required a top vacuum of 65 mbar. The styrene loss overhead was reduced slightly (with concentration at 3.0 wt%).

A step change in performance occurred in the 1970s when columns could be equipped with sheet metal packings, such as M250Y. The lower pressure drop of the packing allowed over 90 theoretical stages in a single column with the pressure drop reduced to only 40 mbar! As a result, the EB specification became an order of magnitude lower, 150 ppm wt, and the styrene recycle rate was cut in half (with the top vacuum pressure at 100 mbar). These improvements in capacity, purity, and yield were so great that practically all columns with trays have been phased out. Note that the styrene purity is increased in the finishing columns. This increases the styrene concentration from 99 to 99.9 wt% styrene. Care needs to be taken in the design of these columns due to the high potential for polymerization. Thus, these columns also operate under vacuum, at 100−150 mbar top pressure and typically 6−9 m in diameter. Bottom styrene monomer (SM) concentrations depend on the internals, but typically are 30−50 wt% SM.

High-capacity structured packing allow styrene manufacturers to add significant extra capacity to their existing columns (as longs as the existing piping and auxiliary equipment permitted the expansion). The lower pressure drop of the new types of packing also lowers the demands on the top vacuum requirements in order to maintain a bottom temperature no higher than 100 °C.

Here we will consider the revamp of a typical 200 kta EB/ST column of 6 m diameter equipped with Mellapak 250Y. The column is over 60 m tall and operates at a reflux ratio of 8.1, a top pressure of 106 mbar [94], and a 40 mbar pressure drop resulting in a bottom temperature of 88 °C. The column feed consists of 60%wt styrene, 35%wt EB, and 5%wt tars, simulated as DEB. The column has two beds above the feed of 5.8 m height each, and four beds below the feed of 7.4 m each. The column produces styrene with 150 ppm EB and the overhead contains 1.55 wt% SM. However, polymer manufacturers are requesting styrene with a more stringent EB impurity levels down to 10 ppm.

Though the new specification can be reached by increasing the reflux ratio, this would severely impact the profitability of the plant and hence is not an option. Jongmans [95] indicated that future purity specifications might decrease even more,

possibly to as low as 1 ppm wt EB. This makes it worthwhile investigating what (high-capacity) packing revamp options are possible for producing styrene at the new specification while operating at the same throughput so as to maintain profitability. Since the revamp will require significant investments, it is desirable to simultaneously add capacity during the revamp. Of course, lowering the EB concentration in styrene by an order of magnitude is a drastic step and will requires many additional stages. The revamp focuses on installing new packing with lower HETP, i.e. with packings that have higher specific areas. Regular M350Y or M500Y have lower capacities but also significantly higher pressure drops than the current M250Y and cause too high bottom operating pressure and thus temperature. If the existing column shell is to be reused only high-capacity packings can be considered.

Figure 5.20 shows that the HETP (back calculated from a rate-based model of the column) of the M250Y packing varies between 340 and 410 mm, as function of the stripping factor of styrene. The highest vapor loading occurs in the top (at a C-factor of 0.071) and the maximum useful capacity there (MUC) is 57%.

From Figure 5.10, it can be seen that M602Y will be too close to flood at this C-factor. Hence, the packings with higher capacity and equivalent or better HETP are Mellpak Plus M252Y, M352Y, and M452Y. Table 5.13 lists these options and Figure 5.21 shows the computed HETPs for the various internals using the Bravo-Rocha-Fair (1985) MTC, the Wallis capacity, and the Kooijman et al. pressure drop models (parameters from Table 5.4). It can be seen that only M452Y will add a significantly higher number of stages, such that the new 10 ppm wt

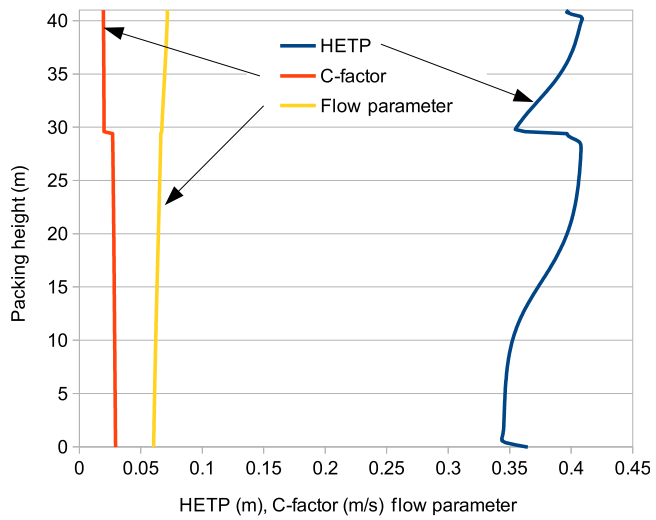

FIGURE 5.20

Rate-based back-computed height equivalent to a theoretical plate (HETP) (blue line) in a 6-m diameter EB/ST column with 41.2 m M250Y packing operating at a top pressure of 106 mbar and reflux ratio of 8. Also plotted are the C-factor and the flow parameter.

Table 5.13 Revamp Options for EB/ST Columns [94] Using Sulzer Mellapak Plus Packings for a 6-m Diameter Column with a 41.2-m Bed Height, Operating at 106 mbar Top Pressure

Packing	M250Y	M250Y	M252Y (A)	M352Y (B)	M452Y (C1)	M452Y (C2)
MUC (–)	Actual	0.567	0.645	0.655	0.862	0.693
Capacity increase (%)		0	40	29	58	36
SM capacity (kta)	198	198	277	256	312	269
Reflux ratio	8.1	8	8	8	8	7.25
SM top (wt%)	1.55	1.55	1.92	1.37	0.62	1.59
EB bottom (ppm wt)	150	150	150	150	150	10
Bottom pressure (bar)	146	146	169	172	169	150
Bottom temperature (°C)	88	85	89	90	89	86
HETP average (m)		0.38	0.40	0.36	0.30	0.28
Number of stages (–)		109	103	115	138	145

MUC, maximum useful capacity; SM, styrene monomer; EB, ethylbenzene; HETP, height equivalent to a theoretical plate.

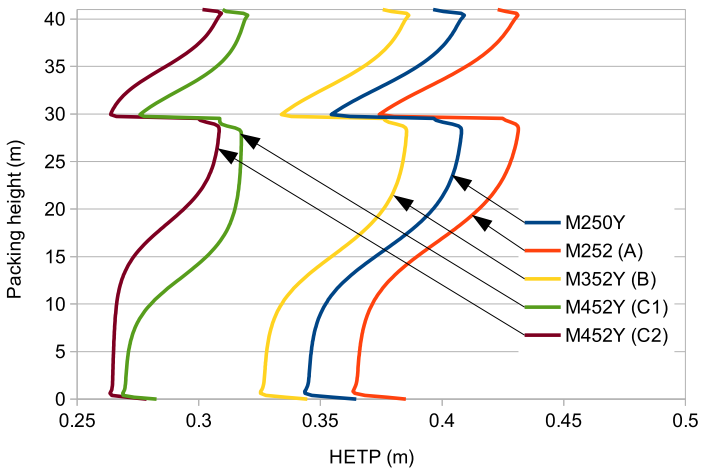

FIGURE 5.21 Height Equivalent to a Theoretical Plates (HETPs) for Various Packings Estimated with a Rate-Based Model Using the Bravo-Rocha-Fair (1985) Model

The reflux ratio is 8 and the bottoms EB concentration 150 ppm wt, except for the revamp option with M452Y that uses the new bottom specification of 10 ppm wt EB in styrene.

specification can be met while adding 36% more capacity. In conclusion, high-capacity packings with specific packing areas higher than 250 m^2/m^3 represent yet another step-change in styrene production.

5.3 Conclusion

Distillation is still the key separation technology in commercial production of chemical bulk commodities. Competitive plant design requires catalysts with the highest conversion/selectivity as well as the most efficient product separations. The use of high-capacity/efficiency distillation column internals has become well established and provides the most economic solutions: by combining sections with different types and sizes of internals, the most compact designs with highest capacity are obtained. The process engineer can make use of detailed (rate-based) simulations for this kind of optimization, and balance the required column flexibility against capital/operation expenditures. Similarly, unused capacity in existing plants can be unlocked by revamping those distillation column sections that limit the total plant production, either by capacity, theoretical stage count, or pressure drop (and hence, in temperature). Of course, this is contingent on the knowledge of the correct, process specific system factors and accurate hydraulic and mass transfer models. Despite the maturity of distillation as a technology, the continuous development of (high capacity/efficiency) trays and packings over the past decade has enabled old process plants to significantly expand capacity and brought "new" products to the market with increased purity. It is expected that more innovations, such as trayed devices using centrifugal forces [96], will further enhance the capabilities of distillation columns in the future.

References

[1] J.M. Douglas, Conceptual Design of Chemical Processes, McGraw-Hill, 1988.
[2] C.J. King, Separation Processes, second ed., Mcgraw-Hill, 1980.
[3] J.D. Seader, E.J. Henley, Separation Process Principles, second ed., Willey, NY, 2006.
[4] T. Hobler, Mass Transfer and Absorbers, Pergamon Press, Oxford, 1966.
[5] T.K. Sherwood, R.L. Piford, Absorption and Extraction, second ed., McGraw-Hill, New York, 1952.
[6] E.Y. Kenig, L. Kucka, A. Gorak, Rigorous modeling of reactive absorption processes, Chem. Eng. Technol. 26 (2003) 631.
[7] A.J. Bruma, US Patent 2,295,256, 1942.
[8] J.G. Stichlmair, J.R. Fair, Distillation, Principles and Practices, Wiley, 1998.
[9] A.A. Shenvi, V.H. Shah, R. Agrawal, New multicomponent distillation configurations with simultaneous heat and mass integration, AIChE J. 59 (2013) 272.
[10] V.H. Shah, R. Agrawal, Are all thermal coupling links between multicomponent distillation columns useful from an energy perspective? Ind. Eng. Chem. Res. 50 (2011) 1770−1777.

[11] Sulzer brochure, Structured Packings. Accessed from: https://www.sulzer.com/en/-/media/Documents/ProductsAndServices/Separation_Technology/Structured_Packings/Brochures/Structured_Packings.pdf.
[12] M.J. Lockett, J.F. Billingham, "The Effect of Maldistribution on Separation in Packed Distillation Columns", Distillation & Absorption, Baden-Baden, Germany, 2002, 2.2-2.
[13] M.J. Lockett, Distillation Tray Fundamentals, Cambridge University Press, 1986.
[14] H.Z. Kister, Distillation Design, McGraw-Hill, 1992.
[15] D.R. Summers, Tray Capacity Limitations at Low Surface Tension, AIChE Spring Meeting, San Antonio (TX), paper 130c, May 1, 2013.
[16] G.B. Wallis, One-dimensional Two-phase Flow, McGraw-Hill, NY, 1969.
[17] H.A. Kooijman, K.R. Krishnamurthy, M.W. Biddulph, "A New Pressure Drop Model for Structured Packing", Distillation & Absorption, Baden-Baden, Germany, 2002. pp. 6−15.
[18] R.F. Strigle, Packed Tower Design and Applications, Random and Structured Packings, second ed., Gulf Publish. Company, Houston, 1994.
[19] M.R. Resertarits, J.L. Navarre, D.R. Monkelbaan, C.W.A. Hangx, R.M.A. Van den Akker, Trays inhibit foaming, Hydrocarbon Process. 71 (March 1992) 61−64.
[20] Defoamers, Kirk-Otmer Encyclopedia of Chemical Technology, John Wiley & Sons.
[21] A. Zhou, Z. Zhang, Fouling rate of calcium carbonate on the surface of sieve trays, Ind. Eng. Chem. Res. 49 (2010) 870−875.
[22] D. Grosserichter, J. Stichlmair, Fouling Resistance of Different Column Internals, AIChE Meeting paper 306c, San Francisco, November 2003.
[23] D. Grosserichter, J. Stichlmair, Kristallisationsfouling in Bodenkolonnen, Chem. Ing. Technik. 1−2 (2004) 106−110.
[24] P. Bender, A. Moll, Modification to structured packings to increase their capacity, Chem. Eng. Res. Des. 81 (2003) 58−67.
[25] Koch-Glitsch brochure, FLEXIPAC HC High Capacity Structured Packing. Accessed 2013 from: http://www.koch-glitsch.com/masstransfer/pages/FLEXIPAC_HC.aspx.
[26] A. Zakeri, A. Einbu, H.F. Svendsen, Experimental investigation of pressure drop in structured packings, Chem. Eng. Sci. 73 (2012) 285−298.
[27] Ž. Olujić, B. Kaibel, H. Jansen, T. Rietfort, E. Zich, Fractionation Research Inc. Test data and modeling of a high-performance structured packing, Ind. Eng. Chem. Res. 52 (2013) 4888−4894.
[28] R. Billet, M. Schultes, Prediction of mass transfer column with dumped and arranged packings, Trans. Inst. Chem. Eng. 77 (Part A) (1999) 498.
[29] J.A. Rocha, J.L. Bravo, J.R. Fair, Distillation columns containing structured packings: a comprehensive model for their performance. 2. Mass-transfer models, Ind. Eng. Chem. Res. 35 (1996) 1660.
[30] E. Brunazzi, G. Nardini, A. Paglianti, L. Potarca, Interfacial area of Mellapark packing: absorption of 1,1,1-Trichloro-ethane by Genesorb 300, Chem. Eng. Technol. 18 (1995) 248.
[31] M.M. Dribika, M.W. Biddulph, Surface tension effects on a large rectangular tray with small diameter holes, Ind. Eng. Chem. Res. 26 (1987) 1489−1494.
[32] P.L.T. Brian, J.E. Vivian, S.T. Mayr, Cellular convection in desorbing surface tension − lowering solutes from water, Ind. Eng. Chem. Fundam. 10 (1971) 75.

[33] L.-M. Yu, A.-W. Zeng, K.T. Yu, Effect of interfacial velocity fluctuations on the enhancement of the mass-transfer process in falling-film flow, Ind. Eng. Chem. Res. 45 (2006) 1201−1210.
[34] R.C. Francis, J.C. Berg, The effect of surfactant on a packed distillation column, Chem. Eng. Sci. 22 (1967) 685.
[35] C.W. Fitz Jr., A. Shariat, J.G. Kunesh, Performance of structured packing in a commercial scale column at pressures of 0.02 to 27.6 bar, Inst. Chem. Eng. Symp. Ser. 142 (1997) 829.
[36] J.L. Nooijen, K.A. Kusters, J.J.B. Pek, The performance of packing in high pressure distillation applications, Inst. Chem. Eng. Symp. Ser. 142 (1997) 885.
[37] M. Schultes, W. Grosshans, S. Müller, Modern Liquid Distributor and Redistributor Design by Raschig, AIChE Meeting, November 2003.
[38] H.E. O'Connell, Trans. AIChE 42 (1946) 741.
[39] M.F. Gautreaux, H.E. O'Connell, Effect of length of liquid path on plate efficiency, Chem. Eng. Prog. 51 (1955) 232.
[40] F.J. Lockhart, C.W. Leggett, Advances in petroleum chemistry and refining, in: K.A. Kobe, J.J. McKetta (Eds.), Interscience, vol. 1, 1958, pp. 323−326.
[41] AIChE Bubble Tray Design Manual: Prediction of Fractionation Efficiency, AIChE, New York, 1958.
[42] T. Yanagi, M. Sakata, Performance of a commercial scale 14% hole area sieve tray, Ind. Eng. Chem. Process Des. Dev. 21 (1982) 712−717.
[43] R. Taylor, R. Krishna, H. Kooijman, Real-world modeling of distillation, Chem. Eng. Prog. (July 2003) 28−39.
[44] ChemSep, http://www.chemsep.org.
[45] A.W. Sloley, Should you switch to high capacity trays, Chem. Eng. Prog. 95 (January 1999) 23−35.
[46] F.J. Zuiderweg, J.H. de Groot, B. Meeboer, D. van der Meer, Scaling up distillation plates, Inst. Chem. Eng. Symp. Ser. 32 (1969) 5.78.
[47] W. Bruckert, US Patent 3,410,540 Vapor−Liquid Contact System and Method, 1968.
[48] R.J. Miller, D.R. Monkelbaan, M.R. Resertarits, US Patent 5,209,875, 1991.
[49] N.F. Urbanski, Z. Xu, US Patent Application 6,390,454 B1, 2002.
[50] M.R. Resertarits, US Patent 5,098,615, 1992.
[51] M.S.M. Shakur, J. Agnello, K.J. Richardson, N.F. Urbanski, US Patent Application 6,783,120, 2004.
[52] B.H. Bosmans, US Patent Application 6,902,154, 2005.
[53] B.H. Bosmans, US Patent Application 6,494,440, 2002.
[54] M.S.M. Shakur, R.E. Tucker, K.J. Richardson, M.R. Sobczyk, R.D. Prickett, C. Polito, S.E. Harper, Increase C2 splitter capacity with ECMD trays and high flux tubing, Ethylene Producers Conference, March 18, 1999.
[54a] S.E. Harper, W. Malaty, Chevron Port Arthur Ethylene Expansion Meets Objectives, Oil & Gas Journal 97 (9) (1999) 49−51.
[55] L. Urlic, S. Bottini, E.A. Brignole, J.A. Romagnoli, Thermodynamic tuning in separation simulation and design, Comput. Chem. Eng. 15 (7) (1991) 471−479.
[56] S. Kurukchi, J. Gondolfe, A.J.D. Prestes, S. Peter, P. McGuire, C2 Splitter Retrofit and Performance, PTQ Spring, 2003, pp. 93−97.
[57] P. McGuire, UOP MD™ and ECMD™ Trays, 6th Olefin Plant Seminar, Sao Paulo, Brazil, October 1−3, 2003.

[58] D.R. Summers, R. Alario, J. Broz, High Performance Trays Increase Column Efficiency and Capacity, AIChE Meeting, April 2, 2003 paper 7fm.
[59] A. Bernard, W. de Villiers, D.R. Summers, Improve product ethylene separation, Hydrocarbon Process. (April 2009) 61–69.
[60] D.R. Summers, R. Alario, J. Broz, High performance trays increase column efficiency and capacity, AIChE Meeting, April 2, 2003 paper 7fm.
[61] Koch-Glitsch Superfrac, online material accessed 2013 from: http://www.koch-glitsch.com/masstransfer/pages/SUPERFRAC_multi-pass_DC.aspx.
[62] M. Wehrli, M. Fischer, M. Pilling, "The MVG Tray with Truncated Downcomers, Recent Progress", Distillation & Absorption, Baden-Baden, Germany, 2002, pp. 6–8.
[63] D.E. Nutter, The MVG tray at FRI, Trans. Inst. Chem. Eng. 77 (Part A) (September 1999) 493.
[64] I.E. Nutter, US Patent 3,463,464, 1969.
[65] Technical Data Book – Petroleum Refining, seventh ed., American Petroleum Institute, 1977.
[66] H. Knapp, R. Döring, L. Öllrich, U. Plöcker, J.M. Prausnitz, DECHEMA Chem. Data Ser. VI (1982) 654,. Fit for Propylene-Propane data from M. Hirata, T. Hakuta, T. Onda, Int. Chem. Eng. 8 (1968) 175.
[67] D.R. Summers, P.J. McGuire, M.R. Resetarits, C.E. Graves, S.E. Harpter, S.J. Angelino, Enhanced Capacity Multiple Downcomer (ECMD) Trays debottleneck C3 Splitter, Spring AIChE Meeting, March 22, 1995.
[68] D.R. Summers, P.J. McGuire, M.R. Resetarits, C.E. Graves, S.E. Harpter, S.J. Angelino, High-capacity trays debottleneck Texas C3 splitter, Oil Gas J. (November 1995) 45.
[69] Z. Xu, D.R. Monkelbaan, B.J. Nowak, R.J. Miller, US Patent Application 2007 0126134 A1.
[70] L. Zhu, X. Yu, K. Yao, L. Wang, K. Wei, W. Wang, Promotions for further improvements in multiple downcomer tray performance, Ind. Eng. Chem. Res. 43 (2004) 6484–6489.
[71] US Patent 3,745,092 Recovery and Purification of Ethylene Oxide by Distillation and Absorption, 1973.
[72] US Patent Application US 7,598,406 B2 Production of Ethylene Oxide, 2009.
[73] M.R. Rahimpour, M. Shayanmehr, M. Nazari, Modeling and simulation of an industrial ethylene oxide (EO) reactor using artificial neural networks (ANN), Ind. Eng. Chem. Res. 50 (2011) 6044–6052.
[74] US Patent 4,012,425 Ethylene Oxide Process, 1977.
[75] Ethylene Oxide/Ethylene Glycol, 2009. Nexant, Accessed 2013 from: http://www.chemsystems.com/about/cs/news/items/PERP%200809_8_EO_EG.cfm.
[76] US Patent 5,763,691 Ethylene Glycol Process, 1998.
[77] US Patent 6,080,897 Method for Producing Monoethylene Glycol, 2000.
[78] Shell's Omega MEG Process Kicks off in South Korea, August 12, 2008, ICIS.com. Accessed from: http://www.icis.com/Articles/2008/08/18/9148176/shells-omega-meg-process-kicks-off-in-south-korea.html.
[79] OMEGA Process, Wikipedia. Accessed from: http://en.wikipedia.org/wiki/OMEGA_process.
[80] US Patent 4,822,926 Ethylene Oxide/Glycols Recovery Process, 1989.

[81] K.P. Struijk, J.A. Talman, Gekatalyseerde omzetting van etheenoxide naar monoethyleenglycol, TU Delft, 1993. Appendix 13. Accessed from: http://repository.tudelft.nl/view/ir/uuid%3Ab936da1b-5c5d-4ac6-9233-fc412620e82c/.
[82] L.Y. Garcia-Chavez, B. Schuur, A.B. De Haan, Conceptual process design and economic analysis of a process based on liquid−liquid extraction for the recovery of glycols from aqueous streams, Ind. Eng. Chem. Res. 52 (2013) 4902−4910.
[83] N. Kamihama, H. Matsuda, K. Kurihara, K. Tochigi, S. Oba, Isobaric vapor−liquid equilibria for ethanol + water + ethylene glycol and its constituent three binary systems, J. Chem. Eng. Data 57 (2012) 339.
[84] N.G. Tsierkezos, I.E. Molinou, Thermodynamic properties of water + ethylene glycol at 283.15, 293.15, 303.15, and 313.15 K, J. Chem. Eng. Data 43 (1998) 989.
[85] MEG (Monoethylene glycol), Sabic. Accessed from: http://www.sabic.com/corporate/en/productsandservices/chemicals/meg.aspx.
[86] US Patent 3,875,019 Recovery of Ethylene Glycol by Plural Stage Distillation Using Vapor Compression as an Energy Source, 1975.
[87] J.A. Garcia, J.R. Fair, A fundamental model for the prediction of distillation sieve tray efficiency. 1. Database development, Ind. Eng. Chem. Res. 39 (2000) 1809.
[88] Uhde brochure, Aromatics. Accessed 2013 from: http://www.thyssenkrupp-uhde.de/fileadmin/documents/brochures/uhde_brochures_pdf_en_16.pdf.
[89] J.A. Johnson, Base aromatics production processes, in: R.A. Meyers (Ed.), Handbook of Petroleum Refining Processes, Part 2, McGraw-Hill, NY, 2004.
[90] Sulzer brochure, Suspension_Crystallization_Technology. Accessed from: http://www.sulzer.com/en/-/media/Documents/ProductsAndServices/Separation_Technology/Crystallization/Brochures/Suspension_Crystallization_Technology.pdf.
[91] P. Wantanachaisaeng, K. O'Neil, Capturing Opportunities for Para-xylene Production, UOP, 2009.
[92] L. Ghelfi, "Improve Refinery Profitability", Sulzer chemtech, EFCE WP Meeting Distillation & Absorption, September 16, 2004. Huelva, Spain.
[93] Sulzer brochure, Separation Technology for the Chemical Process Industry. Accessed from: http://www.sulzer.com/en/-/media/Documents/ProductsAndServices/Process_Technology/Processes_and_Applications/Brochures/Separation_Technology_for_the_Chemical_Process_Industry.pdf.
[94] L. Spiegel, Improving Styrene Separation Using Mellapak Plus, EFCE Working Party Meeting, Helsinki, Finland, June 5, 2003.
[95] M. Jongmans, E. Hermens, M. Raijmakers, J.I.W. Maassen, B. Schuur, A.B. de Haan, Conceptual process design of extractive distillation processes for ethylbenzene/styrene separation, Chem. Eng. Res. Des. 90 (2012) 2086−2100.
[96] P. Wilkinson, E. Vos, G. Konijn, H. Kooijman, G. Mosca, L. Tonon, Distillation trays that operate beyond the limits of gravity by using centrifugal separation, Inst. Chem. Eng. Symp. Ser. 152 (2006) 327−335.
[97] P.M. Mathias, Sensitivity of Process Design to Phase Equilibrium - A new Perturbation Method Based Upon the Margules Equation, J. Chem. Eng. Data 59 (4) (2014) 1006−1015.

This page intentionally left blank

CHAPTER

Air Distillation

6

Anton Moll

Engineering Services, Linde Engineering Division, Pullach, Germany

CHAPTER OUTLINE

Distillation: Operation and Applications. http://dx.doi.org/10.1016/B978-0-12-386876-3.00006-5

6.1 Introduction

The topic of this chapter is air distillation, in which air as feed stock is separated into its main components of nitrogen, oxygen, argon, and the other noble gases contained in air. This separation is the most important distillation process taking place under cryogenic conditions.

Oxygen, nitrogen, and argon are used for many applications in manufacturing, chemicals, metallurgy, electronics, food, health care, glass, pulp and paper, enhanced oil recovery, and others. The cold of liquid nitrogen (LIN) is used for freezing purposes. There is also a wide field of applications for the other noble gases (krypton, xenon, neon, and helium), such as in lamps, lasers, insulation gas, and filling gas for plasma displays.

The worldwide demand for these gases is increasing by about 7.8% per year, according to a forecast for 2005 to 2010 [1]. This is a result of continuously decreasing production costs and new applications.

In Figure 6.1, it is shown how the O_2 production capacities of plants that have been annually ordered with Linde have increased over the years since 1903.

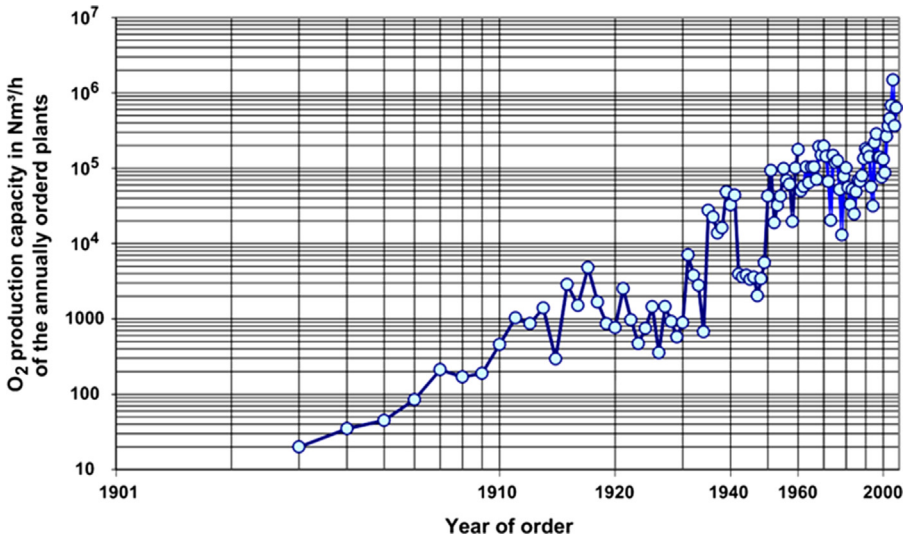

FIGURE 6.1

Annually ordered oxygen production capacity from Linde.

6.2 Process

6.2.1 Air composition

Air is a mixture of many different gases, but 99.962 mol% of it is nitrogen, oxygen, and the noble gas argon (Figure 6.2). The components of dry clean air are the same all over the world. Water vapor content varies according to atmospheric conditions, from approximately 0.5 up to 3 mol%.

The concentration of carbon dioxide of approximately 380 ppm CO_2 has been increasing continuously by about 1 ppm per year. This also depends slightly on the particular season and the region. Traces of hydrocarbons are not shown in the table of dry clean air composition because their proportion depends on industrial and civil emitters in the region. Methane has by far the highest concentration of these hydrocarbons, with 0.17 up to 10 ppm. The sum of the other hydrocarbons (C_2H_2, C_2H_4, C_2H_6, C_3H_6, C_3H_8, n-C_4H_{10}, oil, acetone, and methanol) is generally lower than 10 ppm. The boiling points of the hydrocarbons are higher than the boiling point of oxygen (CH_4: 111.7 K).

All noble gases (Ar, Kr, Xe, He, and Ne) are produced by the distillation of air, with the exception of radon. On a commercial scale, helium is mainly recovered from natural gas sources. More than 90% of world's oxygen and nitrogen production is done by the cryogenic distillation of air. Alternative methods are the recovery from air by membrane separation and by pressure swing adsorption. These production processes are advantageous for small quantities and lower purities of gaseous nitrogen and oxygen due to their lower investment costs.

The operating costs of the separation units are mainly determined by their energy consumption. Cryogenic air distillation has the least energy consumption of the three processes described. In contemporary air separation units, this energy consumption is about two or three times higher than the minimum theoretical separation

Air component		Content	Boiling-point [K]
Nitrogen	N_2	78.08%	77.3
Oxygen	O_2	20.95%	90.2
Argon	Ar	0.932%	87.3
Carbon dioxide	CO_2	0.038%	194.7 (1)
Neon	Ne	18.2×10^{-4}%	27.1
Helium	He	5.2×10^{-4}%	4.2
Krypton	Kr	1.138×10^{-4}%	119.8
Hydrogen	H_2	0.5×10^{-4}%	20.4
Nitrous oxide	N_2O	0.31×10^{-4}%	184.7
Carbon monoxide	CO	0.1×10^{-4}%	81.6
Xenon	Xe	0.086×10^{-4}%	165.1

FIGURE 6.2

Composition table of dry clean air and boiling point ((1) sublimation point) of the components at 1.013 bar.

work for the production of pure nitrogen (99.9999%, 8 bar). For 1 Nm^3, nitrogen this energy consumption is 0.15−0.25 kWh. For the production of oxygen (99.5%, unpressurized), it is about 0.35 kWh [2].

6.2.2 History

The basic requirement for the distillation of air was the possibility to liquefy it on an industrial scale. At 1 bar pressure, this liquefaction occurs at a temperature below 81.6 K. Even though some scientists had liquefied atmospheric gases successfully in small amounts before, Carl von Linde opened the door to cryogenic applications in 1895 when he successfully liquefied air on a continuous basis using the Joule-Thomson effect.

By the expansion of the air, it is cooled down by 0.25 K per bar pressure decrease. Because this cooling effect increases with decreasing temperature, air can be liquefied by countercooling it against previously expanded cold gas. In the first experiment, the cooling cycle was operated between 65 bar and 22 bar. With 400 Nm^3 air in the cycle, about 3 Nm^3/h of liquid was produced. The oxygen content in this liquid was about 70% due to the fact that the vapor pressure of oxygen is lower than the vapor pressure of nitrogen with only part of the air being liquefied [3].

In 1902, Carl von Linde produced pure oxygen by distilling the liquid air introduced on the column top and boiling off the liquid oxygen in the column sump by a reboiler heated by condensing air. The first column was filled with glass spheres. The nitrogen-rich waste gas still had a content of 7% oxygen.

In 1908, the Linde double-column process was developed [4] to improve efficiency and to get pure nitrogen as well as oxygen. The low pressure column and the pressure column are thermally coupled via a condenser-reboiler unit. This unit, named main condenser, is still the key element of each air separation plant.

6.2.3 Process for an air separation unit with gaseous products

There are various types of different ASU processes optimized to fulfil the customer's needs regarding capital and operating costs. Some of the more important are described, for example, by Schwenk [2]. In this chapter, only a basic plant for the production of gaseous oxygen (GOX), nitrogen, and liquid argon is described to demonstrate the special requirements for column design.

As also depicted in Figure 6.3, each cryogenic air separation unit consists of a warm part and a cold part, the latter of which is housed in an insulating container named the "coldbox". The warm part consists of an air filter, compression, precooling, drying, and prepurification of the air in molecular sieve adsorbers. The cold part contains the expansion turbine, the main heat exchanger, the subcooler, and the distillation columns with condensers.

Air is filtered and compressed in a multistage turbo compressor to about 5.5 bar with interstage cooling. In the direct contact air cooler (DCAC), the roughly 373 K

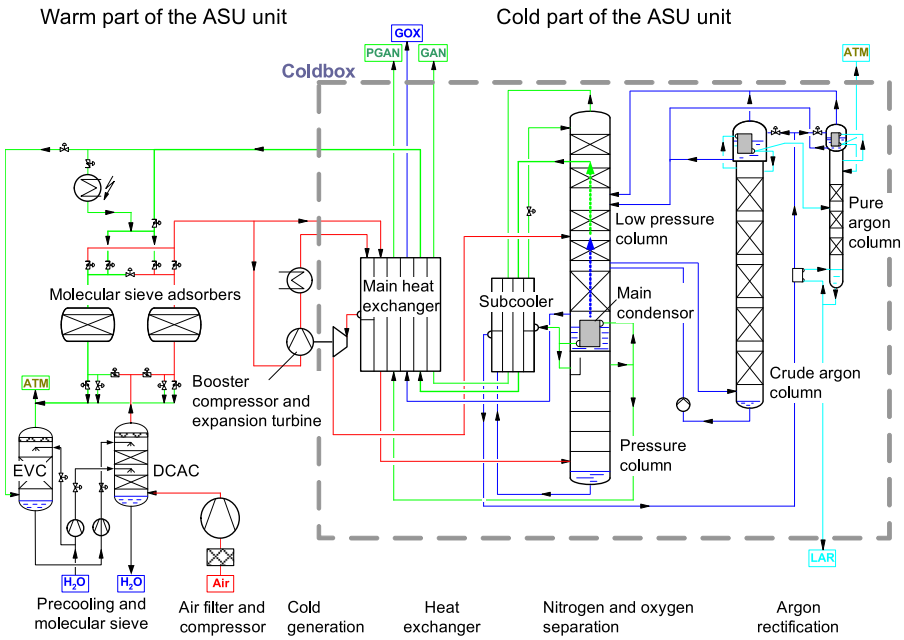

FIGURE 6.3 Flow Diagram of an Air Separation Unit for the Production of Gaseous Nitrogen, Oxygen, and Liquid Argon.

hot air from the compressor is cooled down with cooling water and chilled process water to about 283 K. The chilled water is supplied by the evaporation cooler (EVC).

This direct cooling of the air reduces the moisture and also removes possible traces of SO_2, NO_2, NH_3, Cl_2, and HCl in the air by washing with water. The remaining humidity and the carbon dioxide are almost completely removed in one of the two zeolitic molecular sieve adsorbers downstream of the DCAC. This is essential because these two components would desublimate at the required cryogenic temperatures and the snow formed would block the free area for gas flow. Most of the hydrocarbons are at least partly retained. In particular, the most dangerous acetylenes, dienes and C4+ hydrocarbons, are completely eliminated.

The air flow is divided into two parts after the molecular sieve adsorber. The main portion of the compressed air is cooled down close to the dew point at 98 K in the main heat exchanger in countercurrent flow to the cold products and is fed to the bottom of the pressure column. The second portion, about 10% of the total air, is boosted in pressure to about 9 bar, partly cooled with cooling water and in the main heat exchanger, and expanded via the turbine into the low-pressure column. The cold production of this turbine is sufficient to compensate for the heat losses of the main heat exchanger, the heat flux into the coldbox, and provides the necessary refrigeration to compensate the liquid argon production.

6.2.3.1 Pressure column

In the pressure column, the air is separated into the more volatile nitrogen at the top of this column and an oxygen-enriched liquid in the sump. The condensing high-purity nitrogen vapor at the column top delivers the heat that is necessary to evaporate the liquid oxygen in the sump of the low-pressure column. The working principle of the main condenser is further explained below.

A small amount of the gas with the noncondensing volatile components hydrogen, helium, and neon is vented from the condenser reflux line to the atmosphere (not shown in the flow diagram). About 60% of the total gas flow to the condenser is required as reflux in the pressure column. With typically 45 theoretical trays, the O_2 content of the air feed is then depleted to about 1 ppm at the top. Pressurized gaseous nitrogen can be taken out as a product at the top. The rest of the liquefied nitrogen is withdrawn, subcooled, and fed to the top of the low-pressure column, where it is needed as reflux.

The oxygen-enriched liquid from the pressure column sump is subcooled, throttled down in pressure, and fed to the middle of the low-pressure column. On the way to the low-pressure column, the sensible heat of the stream is used to heat the sump of the pure argon column and a part of the liquid stream is evaporated in the main condenser on top of the crude argon and the pure argon column, thus providing the necessary reflux for these columns.

6.2.3.2 Low-pressure column

The low-pressure column (LPC) is operated at nearly atmospheric pressure and separates the three main air components into high-purity oxygen and nitrogen, while a side cut stream with an oxygen-argon gas mixture is the feed for the crude argon column.

The least volatile component oxygen is enriched up to more than 99.5% in the sump. The even less volatile hydrocarbons and the noble gases krypton and xenon are concentrated in the sump also. For bigger plants, a further enrichment column for the production of Kr and Xe can be installed here.

The GOX product is withdrawn shortly above the reboiler. To avoid a dangerous accumulation of hydrocarbons in the condenser, a small amount of liquid has to be drained to keep their concentration far below the solubility and explosion limit. About half of the total 70−80 theoretical trays in the LPC are necessary to separate the argon from the oxygen.

Argon accumulates in the middle of the column and forms a big bulge. Here, an oxygen-rich gas with about 7−12% argon and less than 100 ppm nitrogen is withdrawn as feed for the crude argon column. It is important that the nitrogen content in this stream should be low because this component behaves as a noncondensable in the crude argon condenser.

The most volatile component, nitrogen, is enriched at the top. In the upper part of the LP column, about 8−20 theoretical trays below the top, a waste gas with about 0.5% O_2 is withdrawn. Due to this reduction in ascending vapor, the resulting stripping factor in the so called gaseous nitrogen product (GAN) section on top of the

column is lower than 1. Thus, the oxygen content in the gas is further reduced to a value lower than 1 ppm. The GAN is taken from the top of the low-pressure column.

The gaseous products and the waste gas are first used to cool the liquid streams from the HP to the LP column and then warmed to environmental temperature in the main heat exchanger, thereby cooling down the incoming feed air. A part of the waste gas is subsequently used to regenerate the second of the two molecular sieve adsorbers, which are alternately in adsorption or regeneration mode. After the depressurization phase to ambient pressure, the regeneration period includes a heating period with waste gas heated up to about 473 K and a cooling period with waste gas, followed by the pressure build-up phase.

The rest of the waste gas is fed to the EVC, where the dry gas saturates with water. The required evaporation heat is withdrawn from the water and cools it down to about 282 K. This chilled water is fed to the top of the DCAC.

6.2.3.3 Crude and pure argon column

In the crude argon column, the more volatile argon is separated almost completely from the oxygen [5]. The oxygen content in the crude argon at the top of the column is lower than 1 ppm. The small amount of nitrogen of less than 100 ppm in the feed is enriched to about 0.3% N_2 in the crude argon at the top of the column.

Due to the tight equilibrium between oxygen and argon, only 3–4% of the gas to the crude argon condenser can be taken out as crude argon product. This forms the feed for the pure argon column. The rest (about 96%) is condensed and forms the reflux. A pump is required to propel the liquid from the sump of this column back to the top of the oxygen section of the LP column. The column is explained in more detail in the section demonstrating the use of structured packing. In the pure argon column, the nitrogen is removed in the stripping section and released to the atmosphere, while the pure liquid argon is taken from the sump of the pure argon column as product.

6.2.3.4 Heat transfer between pressure and low-pressure column in the main condenser

All main parts of the air separation unit now have been introduced. We return to the key element of the plant—the condenser-reboiler unit, linking the pressure and the low-pressure column. Due to the heat of the condensing nitrogen on the pressure side of the unit, pure oxygen on the low-pressure side is evaporated. For these almost pure components, the temperatures depend only on the pressure of the condensing nitrogen and the boiling oxygen.

The pressure, and thus the temperature of the oxygen bath, is fixed by the pressure in the atmosphere and the sum of the pressure losses for the gas from the oxygen bath through the low-pressure column and the waste gas path to the atmosphere.

Figure 6.4 shows how the pressures of the low-pressure column and of the pressure column are connected by the mean temperature difference of the main condenser. The pressure in the oxygen bath in the sump of the low-pressure column is shown on the left vertical axis and the corresponding temperature on the right side.

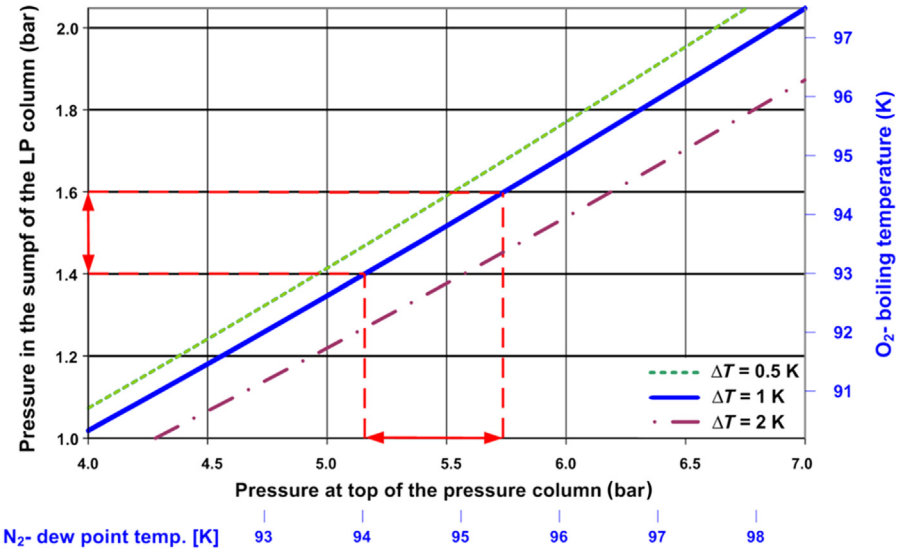

FIGURE 6.4

Dependence of the pressure in the pressure column from the pressure in the low-pressure column at 0.5, 1, and 2 K temperature difference of the main condenser. A certain pressure reduction on the low-pressure side saves about threefold of the value on the pressure side.

The typical mean temperature difference ΔT of the main condenser is 1 K. Adding this temperature difference to the temperature of the oxygen bath gives us the temperature of the condensing nitrogen and therefore the pressure on the top of the pressure column, which is shown on the x-axis. This pressure plus the pressure drop from the compressor to the condenser defines the necessary pressure p_2 for the main air compressor.

If a structured packing instead of trays is used in the LPC, the pressure drop in the LPC is reduced at least by 0.2 bar. This pressure drop in the oxygen bath decreases the bubbling temperature and thus also the temperature of the condensing nitrogen. According to Figure 6.4, the pressure in the pressure column reduces from about 5.74 to 5.16 bar. This pressure reduction is almost threefold the value of the pressure reduction on the low-pressure side.

A pressure reduction of 0.1 bar reduces the energy consumption for the air compression by 1% because the required energy E is proportional to the logarithm of the ratio between outlet pressure p_2 and the atmospheric pressure p_1.

$$E \propto \ln\left(\frac{p_2}{p_1}\right) \tag{6.1}$$

By using packing instead of trays in the low-pressure column, the energy consumption of the compressor is therefore reduced by 6%.

In addition to the temperature difference of 1 K (solid blue line), the relations for a temperature difference of 0.5 and 2 K are also plotted in Figure 6.4. This shows a similar large impact of the temperature difference ΔT, at which the main condenser operates, to the necessary pressure p_2.

The mean temperature difference ΔT of about 1 K can be achieved by the use of brazed aluminum plate-fin heat exchangers (BAHX). Normally, the BAHX block has been designed according to the thermosiphon principle as a bath condenser. The open-ended vertical fins of the boiling oxygen side are submerged to at least 80% in the oxygen bath. With respect to the hydrocarbon safety, a high degree of submersion is necessary to avoid the precipitation of a solid or liquid hydrocarbon phase by evaporating the oxygen almost to dryness in the plate-fin heat exchanger passages.

The liquid head of the oxygen bath increases the pressure of the boiling liquid and is a significant factor for the plant operation. For example, 1-m liquid bath height causes an increase of the pressure at the lower side of the block by 0.112 bar. This has led to the use of downward boiling exchangers. The liquid oxygen is evenly distributed at the top of the passages and evaporates out of the falling film. For safety reasons, the block has to be designed in such a way that a two-phase mixture leaves the bottom side of all passages to avoid complete vaporization. The excess liquid is recycled to the top. To reduce the high liquid head of the BAHX block, it is also possible to use a number of different shorter blocks. This is done in the so-called cascade condenser [6]. Different configurations of the main condenser are shown in Figure 6.5.

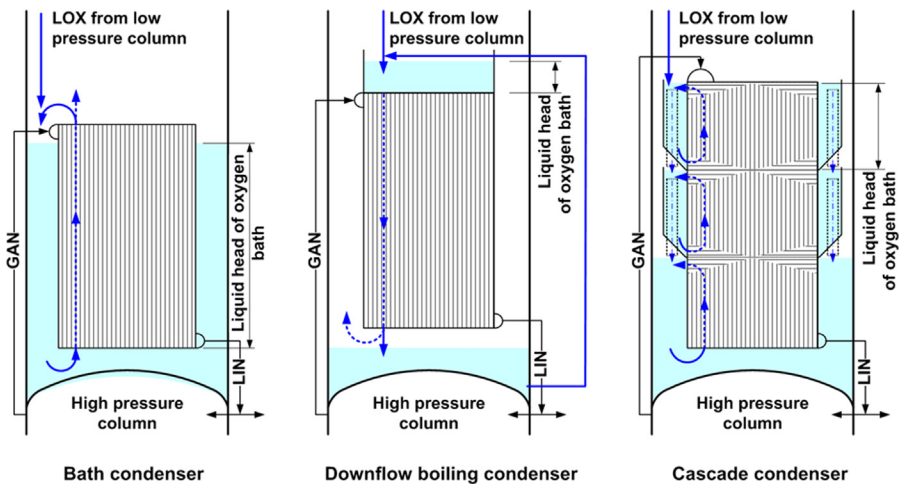

FIGURE 6.5

Different configurations of the main condenser. The liquid head of the oxygen bath influences the pressure and thus the temperature of the evaporating oxygen.

The passages of several BAHX blocks for evaporating the liquid oxygen, at the one side, are stacked on top of each other, while the passages for condensing the nitrogen, on the other side, are undivided over the total height. Each oxygen circulation section works according to the thermosiphon principle, where the liquid enters the block through lateral openings at the bottom side of the block and the two-phase mixture leaves it at the top side. These openings are connected to each other by a lateral pocket, where the liquid that is not evaporated falls back to the bottom opening. Excess liquid is guided by an overflow pipe to the section below. The height of this overflow pipe ensures that the passages of the block are completely flooded.

This principle is repeated several times. The last block is submerged in the sump oxygen bath.

6.2.4 Constraints for the column design

The optimum plant design is a design where the sum of the operating expenditure and the capital expenditure achieves a minimum. The operating expenditure depends on the energy valuation of the customer.

6.2.4.1 Minimizing the pressure drop

Because the operating costs of the air separating units are mainly determined by their energy consumption, it follows that all column internals, at least on the low-pressure side of the condenser, should be selected and designed with the minimum possible pressure drop.

6.2.4.2 Minimum possible height for the internals

The columns are operated in the temperature range between 80 and 100 K. To minimize the cryogenic losses, which have to be compensated by performing additional work, all cold parts are arranged inside a "coldbox". This is a container made up of a steel frame work with sheets and filled with insulating material (i.e. perlite). Perlite is a free-flowing granular material with low density and very low heat conductivity.

The height of the double column with the low-pressure column on top of the pressure column defines the necessary height of the coldbox. Typical values for the height of the pressure column are 9–18 m, about 4–10 m for the main condenser unit, and 20–40 m for the LP column. The lower values are reached with sieve trays while the use of structured packing requires more height. The height of the columns has to be minimized because each additional meter height causes high additional costs for the cold box.

If it is possible, the coldbox is assembled completely in a workshop and transported as a "packaged unit" to the erection site. This saves time and money of construction work. The possible dimensions for such a transportable unit (e.g. $41 \times 4.2 \times 3.7$ m) depend on the transportation route from the fabrication shop to the erection site. The weight of such a unit is also a matter of consideration. Photographs of a transportable packaged unit containing the pressure column, main condenser, the low-pressure column, and a coldbox assembly of a site-erected ASU are shown in Figures 6.6 and 6.7.

FIGURE 6.6 Photograph of a Transportable Packaged Unit Containing the Pressure Column, Main Condenser, and the Low-Pressure Column.

The heat exchangers are in a separate box.

FIGURE 6.7 Coldbox Assembly of a Site-Erected Air Separation Unit.

Typically, packaged plants are standardized small and medium ASUs for the production of 1000 Nm^3/h oxygen up to 20,000. If a packaged unit would exceed the transport limitations, then only submodules are shop-assembled, delivered to the erection site, and assembled there. After erection has been completed and the first functional tests have been carried out, the coldbox is filled with perlite.

6.2.4.3 No accessibility to the internals due to the cold box installation

After filling with perlite, all units inside the coldbox are generally not accessible for more than another 30 years—the typical operational life of an ASU. It is therefore not common practice to use removable column internals.

All internals are installed in the column in a horizontal position in the workshop (see photograph in Figure 6.8). The different sections and the dished heads are welded together after completion of mounting. The columns are not generally equipped with manholes.

Installing the internals in a workshop facilitates the fulfilment of the required high standards of fabrication. The tolerances for the internals are tighter than usual.

It is very expensive and time consuming if a nonperforming column has to be corrected because the perlite has to be removed and access to the internals in the

FIGURE 6.8

View into a workshop for assembling the column internals into the lying shell sections.

vessel is difficult. Therefore, only a proven design is applied for the columns. A revamp of an ASU column to increase the capacity is very rare.

6.2.4.4 Safety requirements

The installation of the internals is done under clean-room conditions. All parts have to be free from oil and grease because oxygen can react heavily with hydrocarbons. The released heat by such a reaction can ignite metal in the immediate vicinity.

All parts are designed in a way that no liquid pools can remain in the column internals or connecting pipes after a shutdown of the plant, because the last evaporating liquid drop of this pool can have a high concentration of oxygen and hydrocarbons as the least volatile components.

6.3 Column internals

After describing the constraints, the next topic is a general description of the ASU column internals used by Linde. The internals of competitors may differ because they have developed different engineering solutions for the given task. One competitor used for example parallel flow slotted sieve trays [7] and another one slotted trays of the Kühni-tray type [8].

Despite the higher pressure drop of sieve trays compared to packing, these trays are still in use, especially in pressure columns of packaged plants or where energy consumption is not a major design factor. The advantage of columns with trays is that they have an overall lower height. Also, the aluminum required for trays and their internals is only approximately 15% of that of an equivalent column fitted out with packing.

6.3.1 Sieve trays

The Linde sieve trays have developed continually over the last 110 years when ASUs were first built. In the first 10 years, lens-like dual-flow trays were used. The picture in Figure 6.10 shows a 100-mm diameter column of this type. The tray space alternates between 12 and 24 mm. Until the early 1930s, one-path sieve trays have been used followed by the Linde circular flow trays invented by Hellmuth Hausen. The circular liquid flow on the trays with one (see sketch in Figure 6.9), two (see photograph in Figure 6.10), or three downcomers has the same direction of rotational flow on all trays.

This design, with a parallel liquid flow on successive trays, compares with the Lewis Case II conditions [9] providing a higher tray efficiency compared to conventional cross-flow trays. Recorded measurements show section tray efficiencies up to 120%. Flow conditions according to Lewis Case II are also achieved by a tray design according to Kühni and with parallel-flow sieve trays.

Because the fabrication costs for circular flow trays are high, they were replaced by Linde in 1965 by the current one-, two-, and four-path cross-flow sieve trays.

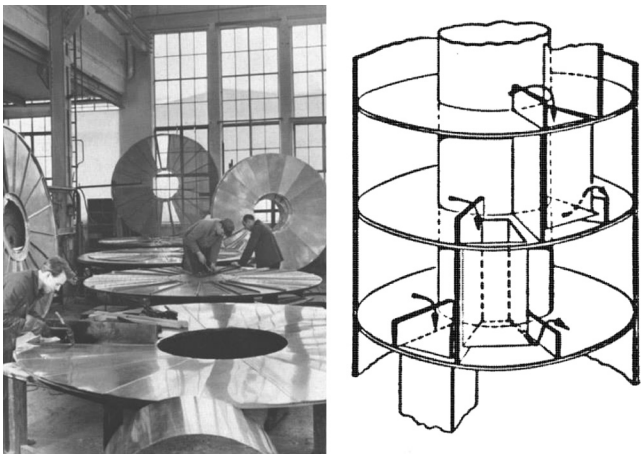

FIGURE 6.9 Preassembly of Circular Flow Trays in the Early 1960s and Principal Sketch Showing the Liquid Flow From Tray to Tray.

FIGURE 6.10

Lens-like dual-flow tray in one of the first air distillation columns.

Some competitors still used the circular flow trays or their equivalents until very recently because of their higher efficiency compared to cross-flow trays.

This design change was also accompanied by a change in material. Up to that time, trays were fabricated from brass and the shells and pipes from copper. Since then, the much-cheaper aluminum has been used. For the required low temperatures, the use of austenitic steel is also possible.

The essential parts of the trays have stayed the same, even today. The sieve hole diameter and the sieve sheet thickness are in the range of 1 mm. This is possible

because there are no fouling substances in the liquid to be distilled. There is no corrosion or polymerization. The open sieve areas range from 5 to 17%. Also, the small outlet weir heights of 5−10 mm and the small tray spaces from 60 to 300 mm have been the same for almost 100 years. A photograph of the installation of a four-path sieve tray in a column of 4.9 m diameter is shown in Figure 6.11.

Because pressure drop plays such an important role, the weir height has to be as low as possible. Due to the low liquid level, the dry tray pressure drop can also be lower than usual to prevent excessive weeping of the trays. The pressure drop of a typical ASU sieve tray for a typical operation range of 60−100% is about 3 mbar. With small outlet weir heights of 5−10 mm at column diameters up to 6 m in diameter, high evenness and horizontal tolerances have to be upheld when installing the trays.

Because of the sheet thickness of only 1 mm, the stiffness of the tray is weak and a supporting bolt construction is necessary to achieve the required accurate, even, and horizontal location of the trays. A sketch and three-dimensional view of the tray support construction is shown in Figure 6.12.

H-type beams are placed below the bottom tray for fixing the supporting bolt construction. All sieve tray parts are riveted together and can glide on the support rings fastened to column wall. This gliding connection is essential because, during the cooling down and warming up of the plant, there are large temperature

FIGURE 6.11 Photograph of the Installation of a Four-Path Sieve Tray in a Column that is 4.9 m in Diameter.

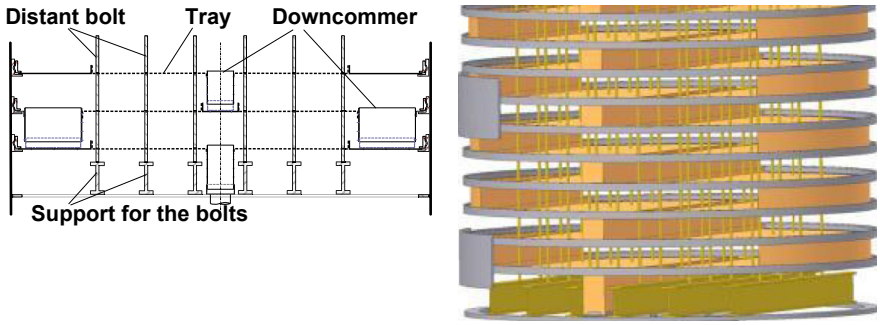

FIGURE 6.12

Sketch (left) and three-dimensional view (right) of the tray support construction with beams at the bottom and bolts between the trays.

differences between the tray and the column shell. The contraction of aluminum is 2 mm/m for a temperature change of 100 K.

This has also to be considered in the design of the coldbox. For example, during cooling down of about 200 K, a 30-m long column or pipe shrinks by 120 mm.

6.3.1.1 Comparison to conventional trays

Table 6.1 compares the essential dimensions of an ASU sieve tray with conventional sieve trays.

6.3.1.2 Tolerances

According to a literature survey from Angermeier cited in Lockett and Augustyniak [10], the maximum degree of out-of-levelness (high to low point) for a tray is in general a function of the column diameter D_C. The most stringent allowance is $\Delta = 1.5 + 0.007\ D_C$ (mm) and the least stringent allowance is $\Delta = 4.8 + 0.012\ D_C$ (mm). According to the Linde standard, the allowance (see Figure 6.13) for diameters smaller than 3000 mm is $\Delta = 0.001\ D_C$ (mm) and for bigger diameters is $\Delta = 3$ (mm).

The main differences in permitted deviation from the horizontality also reflect the different sensitivities of the separation processes and tray designs.

Table 6.1 Cryogenic ASU Sieve Trays Compared to Conventional Sieve Trays

	Cryogenic	Conventional
Tray fastening	Immovable	Removable
Tray support	Supported by bolts	Self-supporting
Hole diameter	0.9–1.1 mm	5–19 mm
Tray thickness	1 mm	2–3 mm
Outlet weir height	5–10 mm	25–50 mm
Tray space	60–250 mm	350–900 mm

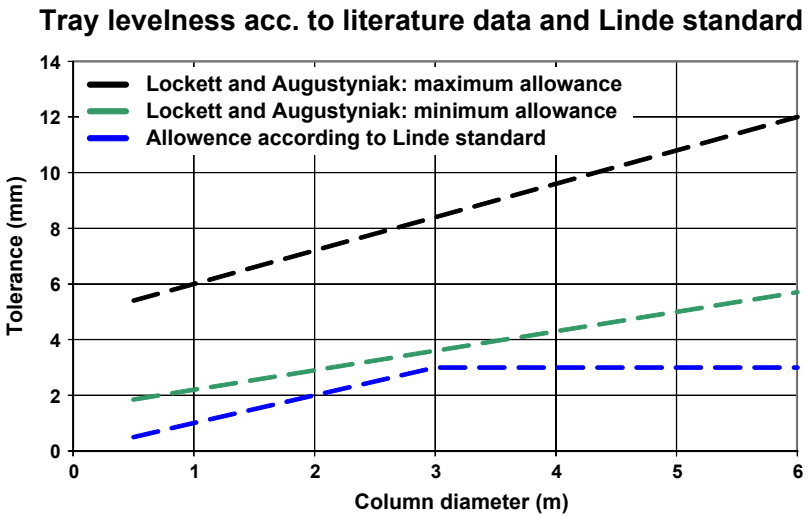

FIGURE 6.13

Comparison of common tray levelness tolerances with the allowance according to the Linde standard.

6.3.1.3 Hydraulic design

The recognized relations and rules for the calculation of the dry and wet pressure drops, downcomer, and jet flooding are valid also for the ASU sieve trays [11]. The small hole size of the sieves produces small bubbles and therefore creates a higher mass transfer area than normal; it also allows a higher gas throughput compared to bigger holes.

Designing the trays for a low pressure drop is important. The required dry pressure drop depends on the load range of the trays and their clear liquid height. A minimum clear liquid height of about 15 mm is necessary to achieve full efficiency. Because the weir load and thus the clear liquid height increases proportionally to the column diameter, the number of flow paths is increased as soon as the flow path reaches a certain length to minimize the wet pressure drop.

A reduction of the clear liquid height also is possible by using "pushing" slots in the sieve tray deck. The transferred gas momentum to the liquid reduces the liquid residence time and therefore the liquid height [12]. This measure is not presently used by Linde.

6.3.1.3.1 High specific mass transfer area

The section tray efficiency of ASU sieve trays ranges from 65% to more than 90%. Tests with weir heights higher than 10 mm showed only a poor improvement in efficiency accompanied by higher wet pressure drops. These efficiencies are reached with clear liquid heights h_{cl} in the range of only 15−20 mm. The main reason

assumed for this is the high mass transfer area probably created by the small sieve holes.

With tray design for packaged plants, with tray spacing of about 100−120 mm, the number of theoretical trays reached at the same active column height is about 1.5 times higher than that with a 750Y packing. If we assume that the two-phase layer on the trays fills 70% (void fraction $\varepsilon = 0.3$) of the available tray space, then the resulting specific surface area a of the two phase layer is in the range of 1600 m^2/m^3 (=1.5 × 750/70%). The diagram in Figure 6.14 shows the specific surface area as a function of the Sauter diameter. Therefore the Sauter diameter d_S of the bubbles is in the range of 2.6 mm (cf. Eqn (6.2)).

$$d_S = 6 \cdot \frac{(1-\varepsilon)}{a} \tag{6.2}$$

According to Stichlmair [13], the stable bubble diameter d_{bubble} for this system is about 2.6 mm (using Eqn (6.3)), which is in good agreement with the value above.

$$d_{\text{bubble}} = \sqrt{\frac{6 \cdot \sigma}{(\rho_L - \rho_V) \cdot g}} \tag{6.3}$$

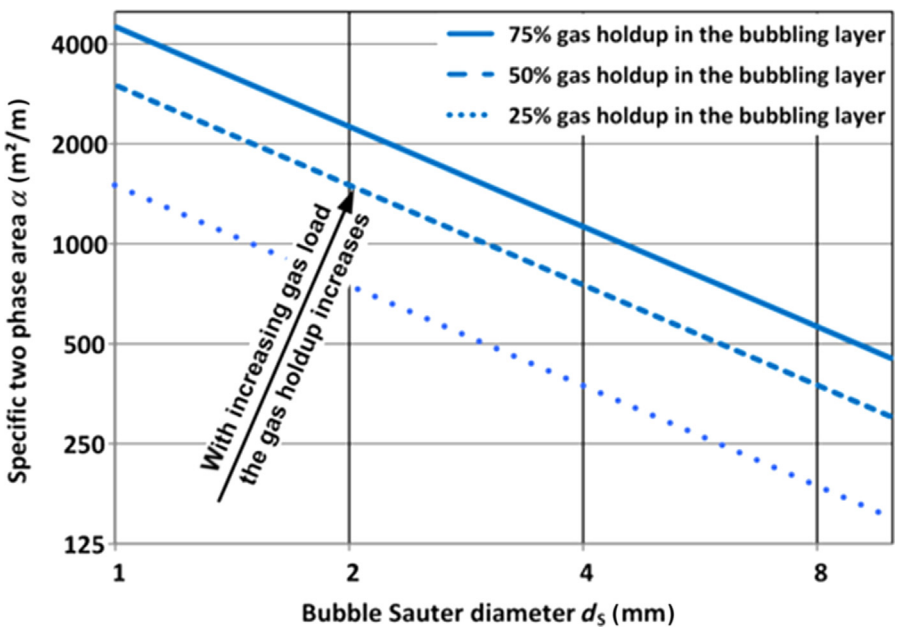

FIGURE 6.14

Specific surface area as a function of the Sauter diameter.

Haselden and Thorogood [14] investigated the bubble formation for a typical ASU sieve plate with 1-mm hole diameter and 10% open area. They found a very high bubble formation frequency of about 150−160 bubbles per second at a vapor velocity through the holes of about 5 m/s. The bubble diameters observed a few millimeters above the sieve plate have a diameter of about 1.8 mm and grow rapidly to a diameter of about 3.5 mm in the observed cellular foam (see "foaming" further below) and to about 5 mm in the bubbling dispersion. The bubble size increases with increasing height above the sieve plate.

It is debatable whether the small Sauter diameter could be reached using big holes within the relatively low liquid level. The small-hole diameter influences the two-phase layer, which can also be concluded from the following observation.

6.3.1.3.2 High gas throughput

It is known that small sieve holes allow a higher gas throughput than bigger ones at the same conditions [15]. According to this publication, the advantage in capacity of 1-mm holes compared to 5-mm holes is about 13%.

To demonstrate this effect, the gas capacity of ASU pressure columns with 250-mm tray space (TS) has been compared with the gas capacity of C2 splitters from Linde ethylene plants with 350-mm tray space for the guaranteed values. The sieve hole diameter d_h of the C2 splitters is 5 mm.

According to Kirschbaum [16], the gas capacity increases proportional to the square root of the tray space (TS). At the same conditions, a tray space of 350 mm compared to 250 mm thus allows an 18% higher gas load. The gas capacity difference between a column with $TS = 350/d_h = 5$ mm to one with $TS = 250/d_h = 1$ mm should therefore have the ratio 118:113%.

The viscosity and the surface tension of the two systems are comparable. The different densities are regarded in the capacity diagram (see Figure 6.15) in which the Souders−Brown factor based on the bubbling area (y-axis) is shown as a function of the flow parameter.

Regarding the scatter between the individual designs of the two column types, there is no significant difference in the gas load.

6.3.1.3.3 High downcomer capacity

At high liquid loads, the required tray space is defined by the clear liquid backup in the downcomer and the gas holdup in the liquid. The liquid backup in the downcomer is defined by the pressure difference between the trays, the liquid backup into the downcomer from the next tray, and the flow resistance, mainly caused by the flow restriction at the outlet gap.

The first two factors cannot be modified by the downcomer design. The flow resistance can be reduced by increasing the outlet gap below the level of the next tray with the use of a rounded lip, further reducing flow resistance. Figure 6.16 shows the use of these two features in the circular flow trays. This costly downcomer design shaped like a trumpet funnel was formerly used at column diameters above 1.2 m.

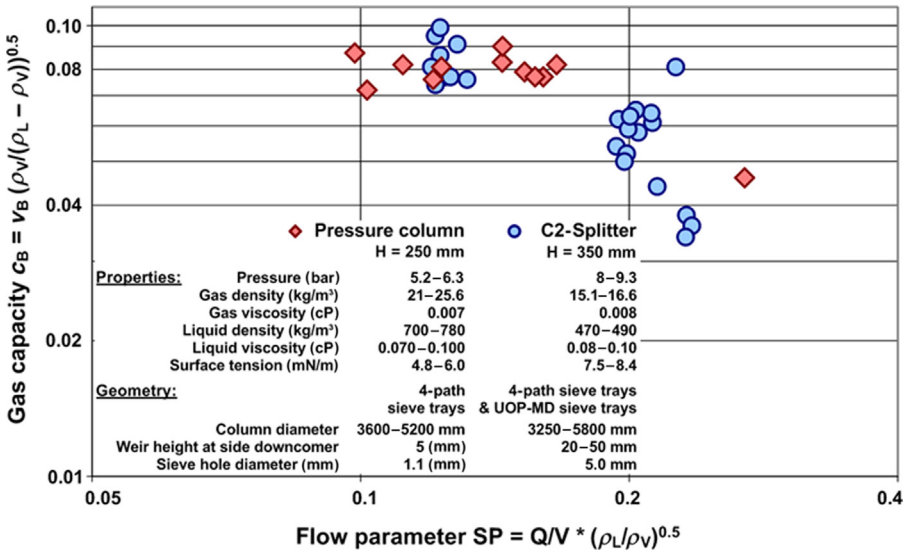

FIGURE 6.15

Comparison of the capacity of pressure columns with hole diameters of 1.1 mm with the capacity of C2 splitters with 5-mm hole diameter. At high-flow parameters, the necessary tray space is defined by the liquid load and not by the gas load.

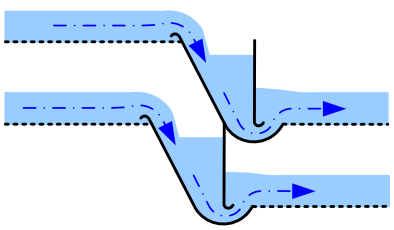

FIGURE 6.16

Advanced downcomer design for high liquid loads used in circular flow trays.

The deepened inlet pan to increase the outlet gap was seldom used with the conventional cross-flow trays because an expensive additional welding seam below the tray support ring was necessary. However, because the deepened pan is an integrated part of the even inlet plate, this design is used often. This patented solution [17] is shown in Figure 6.17. It allows higher liquid loads and reduces the required tray spacing.

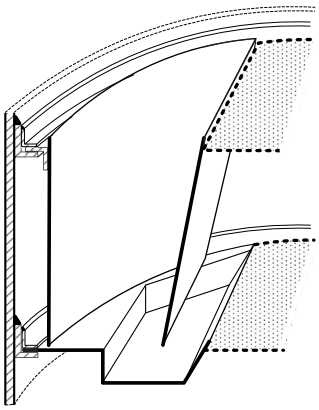

FIGURE 6.17

Patented deepened pan integrated in the inlet plate. This solution does not require additional welding at the column wall.

6.3.1.4 Load range of the sieve trays

The typical load range of the ASU sieve trays is about 70−100%, according to the load range of the air compressor. If two compressors are used, a load range of more than 1:2 is also possible, but with a somewhat higher dry tray pressure drop.

In general, the efficiency of the column sections decline slightly with decreasing load. If the load is reduced from the maximum guaranteed load to about 50%, a relative efficiency reduction of about 15−20% is expected and should be considered during the process calculation for the turndown cases. The cause of this reduction is probably the reduced mass transfer area due to a lower froth height and a higher froth density.

Columns with bigger diameters and with decreasing load show sometimes a stronger decline in the section tray efficiency than expected. This is almost certainly caused by trays out of level. The influence of tilted trays on efficiency can also be observed with some coldboxes, which show a day-and-night effect. Due to the heat of the sun, the side of the box facing the sun is heated up and expands, thus bending the box and also the columns connected to it. A sensitive section is the GAN section at the top of the LP column, which is characterized by a low liquid load.

6.3.1.5 Sensitivity to tilted trays

The influence on efficiency depends on the direction of the tilt. Trays tilted in the direction of the liquid flow are less harmful than trays tilted perpendicular to the flow direction [10]. A tilted tray perpendicular to the direction of liquid flow causes a much bigger liquid flow on the lower side because the flow is proportional to the crest height to the power of 1.5. Systematically tilted trays of this type can seriously influence efficiency.

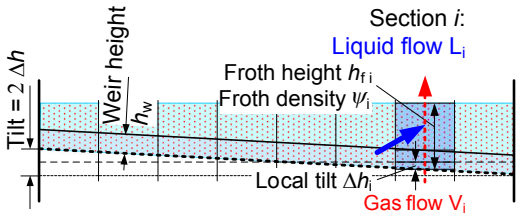

FIGURE 6.18

Trays tilted perpendicular to the liquid flow direction and divided in parallel sections stacked one above the other.

To investigate the sensitivity of column efficiency on tilted trays in the GAN section of the LP column, this section is divided in J parallel column sections, as shown in Figure 6.18. This is a valid approximation because the lateral mixing of the vapor and liquid is limited, especially at large column diameters and small tray spacing. The liquid and vapor flow L_i and V_i for each section i of the tray can be calculated. The deviation of the local L_i/V_i from the regular L/V depends on the local tilt and also on the column load.

Assuming no mixing of gas and liquid between the different sections, it is possible to calculate the depletion of the less volatile component y with the local L_i/V_i for N_t theoretical trays using the Kremser equation:

$$N_t = \ln(y_{top}/y_{bottom})/\ln(k/(L/V))$$

The sum of $y_{top,i} \times V_i/\sum(V_i)$ gives the concentration $y_{top,\ tilt}$ reached with the tilted trays. To reach this concentration $y_{top,\ tilt}$ with the regular L/V, the necessary theoretical trays are $N_{t,tilt} = \ln(y_{top,\ tilt}/y_{bottom})/\ln(kV/L)$.

This calculation has been made for the above-mentioned GAN section, where L/V is 0.431 and the component equilibrium factor k for oxygen in nitrogen is $k = 0.29$. The section should realize 19 theoretical trays.

In the example, the calculations for the local liquid and vapor flows L_i and V_i were carried out with Collwell's equations for clear liquid height h_{cl} and froth density ψ [18] and Stichlmair's equation for the dry tray pressure drop [13]. The dry tray pressure drop at position i $\Delta p_{dt,i}$ plus the wet pressure drop at i is equal to the total pressure drop of the tray.

6.3.1.5.1 Maldistribution increases with decreasing load

According to Colwell's equation, the liquid flow L_i is proportional to the froth crest height over the weir to the power 1.5. The relative throughput differences between the high and the low side increase with decreasing load because the froth height h_f is falling while the tilt remains the same.

The relative gas and liquid flows have been calculated for the above-mentioned GAN section, assuming a tilt of 4.5 mm for 60%, 80%, and 100% load, as plotted in Figure 6.19.

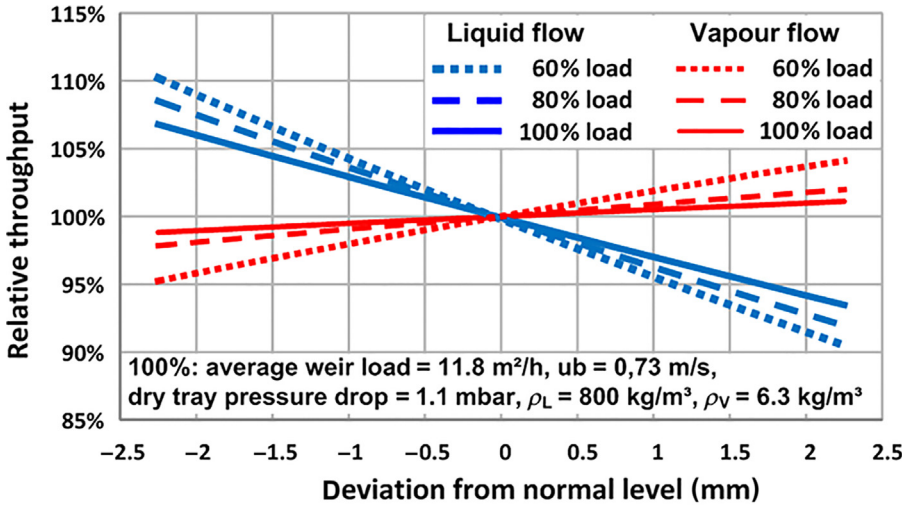

FIGURE 6.19

Relative liquid and vapor flow as a function of the position for a tray 4.5 mm tilted perpendicular to the liquid flow direction. With decreasing load, the maldistribution increases.

The effect of the deviation of the local L_i/V_i from the regular L/V to the efficiency of the section is plotted in Figure 6.19 as a function of the column load as solid blue line. According to this calculation, the relative efficiency of the 4.5-mm tilted trays at 100% load is about 95% of even trays. At 60% load, the relative efficiency drops to about 84% compared to even trays.

The calculation does not consider any weeping, which will further reduce the efficiency.

6.3.1.5.2 Measures to reduce the sensitivity to tilted trays

A common measure to reduce the sensitivity of the efficiency to tilted trays is the use of a higher dry tray pressure drop Δp_{dt} [10]. The previous calculations have been repeated with a 1 mbar per tray higher dry tray pressure drop at 100% load. The green dashed line indicates the resulting relative efficiency. The efficiency decline with reduced load is somewhat smaller.

The large liquid maldistribution is not changed by using a higher dry tray pressure drop. This can be done by increasing the weir load by reducing the weir length by use of a picked fence weir. At a given tilt, the resulting crest height is higher and the differences in the relative liquid throughput are therefore reduced. By reducing the outlet weir height to 0 mm for a picked fence weir with 50% effective weir length, it is possible to keep a similar wet pressure drop.

This measure reduces the deviation of the relative liquid throughput at 60% load to a level comparable to the curve at 100% load of the normal weir (cf. Figure 6.20).

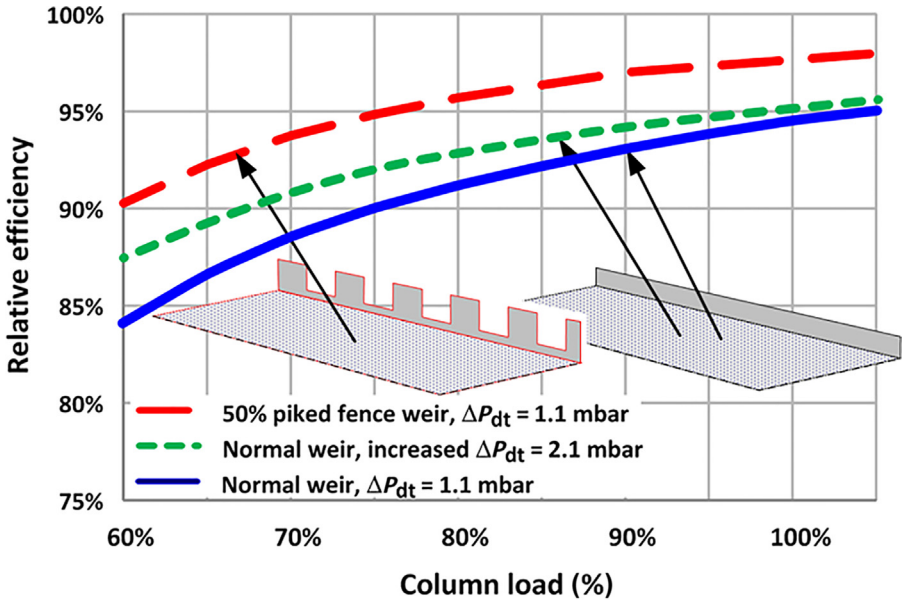

FIGURE 6.20

Relative efficiency of the gaseous nitrogen product section as function of the column load for a tray 4.5 mm tilted perpendicular to the liquid flow direction. The efficiency of the normal tray with a regular weir load of 11.8 m^2/h and 1.1 mbar dry tray pressure drop is shown as solid blue line. The short dashed green line shows the relative efficiency of a normal tray with a 1 mbar additional higher dry tray pressure drop and the dashed red line the efficiency of a tray using a 50% picked fence weir. (For interpretation of the references to color in this figure legend, the reader is referred to the online version of this book.)

The resulting relative efficiency is plotted as a red dashed line. The use of a picked fence weir with a lower weir height achieves the most reduction in the sensitivity to tilted weirs.

6.3.1.6 Foaming system

According to Zuiderweg and Harmens [19], the cryogenic distillation of N_2 and O_2 and also N_2 and Ar represent "positive" systems. A positive system is defined as one in which surface tension increases with increasing boiling point. Positive systems can produce foam at a large surface tension gradient from tray to tray because during the bubble formation on the tray the heavier component condenses preferably, forming a film with a higher surface tension compared to the bulk liquid. The higher surface tension "gives rise to unbalanced forces which result in concentration at the interface, drawing fresh liquid into the film. The thickness of the film will then be increased, coalescence opposed and the foam stabilized." [20].

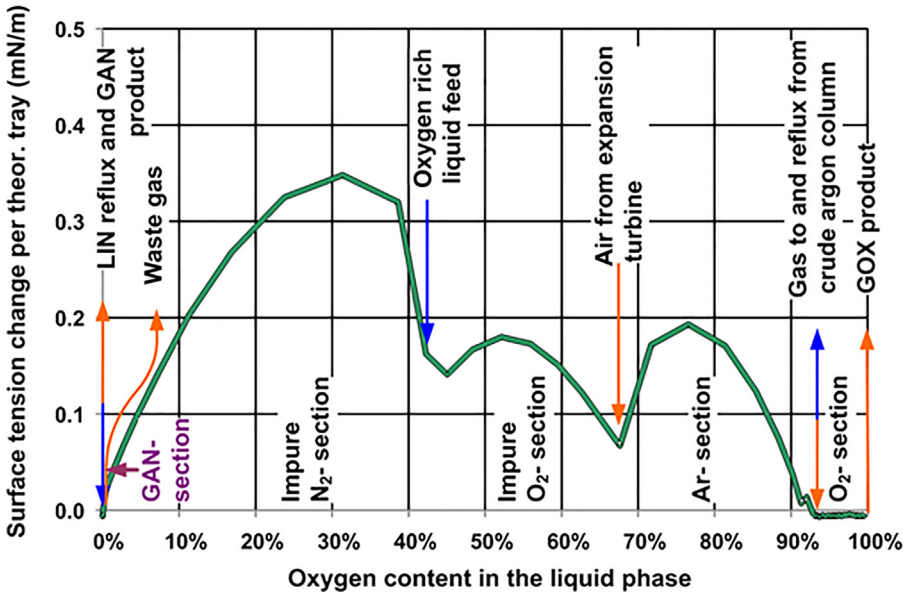

FIGURE 6.21

Typical surface tension gradient in the low-pressure column as a function of the liquid O_2 concentration. The position of the oxygen rich liquid feed can influence the gradient noticeably.

In a N_2−Ar−O_2 mixture, the formation of foam related to composition of the liquid caused by the so-called Marangoni effect and the influence of the foam height to the mass transfer has been investigated by G. Linde [21], R. Brown [20], Haselden and Thorogood, and others. The biggest surface tension gradient from tray to tray occurs in the LPC in a region of concentration of about 40% O_2 (cf. Figure 6.21). To avoid a capacity bottleneck, the tray design has to consider this phenomenon, especially at the feed point of the oxygen rich liquid.

The photographs in Figures 6.22 and 6.23 are taken of a 200-mm small sieve tray column distilling liquid air. The tray space is 120 mm. The pictures show the occurrence of the foaming system on the tray (right side) and the flow of the foam into the downcomer (above).

6.3.2 Structured packing

At the end of the 1980s, structured packing started to replace trays on the low-pressure side of the condenser, with large benefits with regard to the energy consumption of the air compressor. The pressure drop per theoretical tray decreased dramatically from about 4 to 0.5 mbar.

FIGURE 6.22

Flow of a foamy liquid into the downcomer of an air distillation test column with 200-mm diameter and 120-mm tray space.

FIGURE 6.23

Formation of foam on the tray of an air distillation test column with 200-mm diameter and 120-mm tray space.

The use of structured packing also permitted the production of pure argon solely by means of rectification [5]. The argon bath condenser is cooled with oxygen-enriched liquid taken from the sump of the pressure column and, at a pressure of about 1.5 bar, has a bubbling temperature of about 86.5 K depending on the resulting oxygen content in the bath. The dew point of pure argon at a temperature 2.0 K lower (temperature difference of the condenser) has a pressure of about 1.2 bar. At a pressure of 1.5 bar for the transfer of the gas to the crude argon column, the available pressure drop is only about 300 mbar. About 200 theoretical trays are required to remove the oxygen content in the crude argon to below 1 ppm O_2. This is easily possible with structured packing but impossible with trays because trays would cause about 800 mbar pressure drop.

Prior to the use of packing, distillation with trays allowed only a purification of the crude argon to about 1% O_2 and 0.3% N_2 impurities. The oxygen was then totally removed by catalytic combustion with hydrogen to water. The water was removed by absorption. After the removal of the oxygen, the gas was cooled down again and the nitrogen was distilled out of the argon in the pure argon column.

6.3.2.1 Common packing types in air separation

Due to height constraints, the packing types for ASU applications have a higher specific surface area than commonly used in noncryogenic applications. About 80% of the total ASU packing volume is of the type 750Y. The types 500Y, 500X, 350Y, and 350X are also in use. In the case that the column diameter is restricted due to transport limitations, coarser packing types (e.g. 250Y and 250X) are possible. For applications in packaged units, a dense packing 1200Y packing is also available to maintain the column's height restriction. A sketch of a packing sheet is shown in Figure 6.24.

In Figure 6.25 a photo of a Sulzer M750Y (top) is shown in comparison to a Linde A750Y (below). The Linde packing is characterized by a bigger corrugation radius. For the same wave height, this results in an increased surface area.

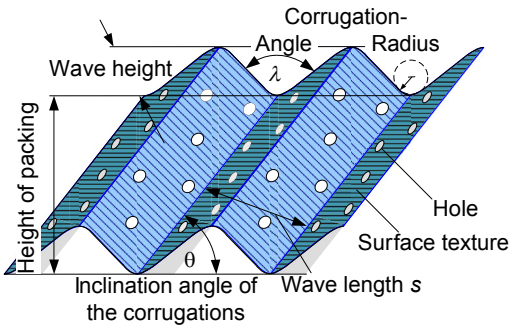

FIGURE 6.24 Sketch of a Packing Sheet.

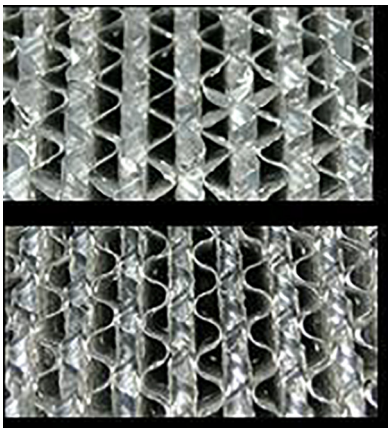

FIGURE 6.25 Photograph of a Sulzer M750Y (top) and a Linde A750Y (below).

Normal packing material is aluminum with sheet thicknesses of 0.1−0.15 mm. For the use in the range of higher oxygen concentrations in the bottom part of the LP column, the sheet thickness is increased to 0.2 mm due to the flammability increase with lower aluminum sheet thickness, higher oxygen concentration, and higher pressure [22]. In the oxygen section, copper packing is also in use. Copper does not propagate a combustion [23].

Some of the tier companies produce their own structured packing and column internals. Linde has manufactured its own structured packing and all the necessary internals since the beginning of the 1990s. The necessary height for some commonly used internals for structured packing does not reflect the impact of the height on the coldbox costs.

6.3.3 Use of structured packing demonstrated in the crude argon column

Difficulties initially arose with the use of structured packing in the crude argon column. The use of structured packing in this column is more challenging than in the other ASU columns. The rectification of the almost pure binary mixture O_2-Ar can be best visualized in the McCabe−Thiele diagram shown in Figure 6.26. In this diagram, the more volatile component Ar (plus traces of N_2) of the vapor (y-axis) and of the liquid (x-axis) leaving the equilibrium stage is plotted. These points form the working line L/V. The red line shows the equilibrium curve. Between both lines, the theoretical stages are drawn as a staircase.

At the argon transition, a gas with about 90% O_2, 10% Ar, and 10−100 ppm N_2 enters the crude argon column. At the top of the column, the crude argon gas contains argon with less than 1 ppm O_2 and about 0.3% N_2. The 200 trays of the crude

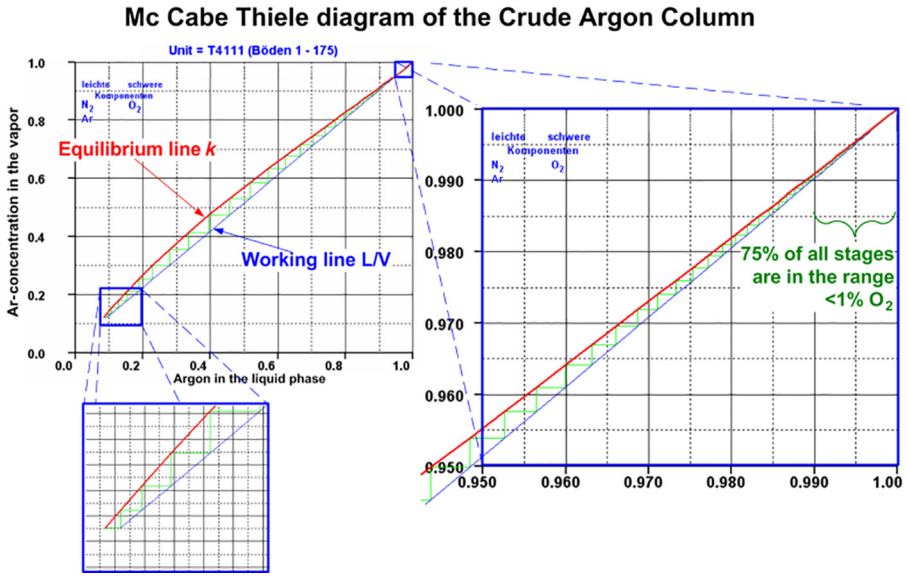

FIGURE 6.26 McCabe–Thiele Diagram for a Crude Argon Column.

argon column are arranged between five and eight beds packed with a 750Y packing. Others use even 10 or more beds for this separation [24].

Because each additional redistribution unit increases the column height, there is the desire to minimize the number of beds without affecting the efficiency of the packing. The required number of packed beds depends on column diameter, the type of packing, and segment design.

6.3.3.1 High sensitivity to maldistribution

As shown in the McCabe–Thiele diagram (see Figure 6.26), the stripping factor $S = k \times \text{V/L}$ is constant for about the upper 175 theoretical trays since the equilibrium line k and the working line L/V form straight lines.

The Kremser equation can be applied here to demonstrate the sensitivity of this system to maldistribution. A packed bed with 30 theoretical trays is divided in the middle. One half gets 3% less and the other gets 3% more liquid than average flow. The ascending vapor is divided equally between these sections with an average L/V of 0.96. The component equilibrium factor k for oxygen in argon is about 0.905. The vapor concentration flowing to the bottom of the bed is $y_{\text{bottom}} = 1000$ ppm O_2. According to the Kremser equation, the gas exiting the two halves contains, separately, 425 and 70 ppm O_2 (Table 6.2). This is mixed to a combined concentration of 247 ppm O_2. A sketch to illustrate the efficiency calculation is depicted in Figure 6.27.

If no maldistribution occurs, only 23.6 theoretical trays are necessary to reduce from 1000 to 247 ppm O_2. The relative bed efficiency is thus 78.9% (=23.6/30).

Table 6.2 Effect of Liquid Maldistribution

	Without Maldistribution	With Liquid Maldistribution	
	0%	−3%	3%
Liquid (L)	96%	46.56%	49.44%
Gas (V)	100%	50%	50%
L/V	0.9600	0.9312	0.9888
$y_{top} = (k/(L/V))^{N\_t} \times y_{bottom}$	170.34	424.78	70.18

The 3% maldistribution results in an efficiency loss of 21%. With increasing liquid maldistribution, the efficiency decreases rapidly. This is plotted as solid black line in Figure 6.28 for the given k value 0.905 and the L/V of 0.96. The liquid maldistribution is plotted on the x-axis.

The efficiency of separation also depends on the number of theoretical stages in one packed bed. With increasing stages per bed, the efficiency at a given maldistribution decreases steadily. This is shown (dashed blue lines) within the diagram for equal conditions to each of the two bed halves for 1%, 3%, and 5% liquid maldistribution. The x-axis for these lines is plotted on top of the diagram.

That this system is truly so sensitive to maldistribution was demonstrated in the first packed crude argon column, designed in 1988. This crude argon column, with a diameter of 1125 mm, was equipped with commercially available packing and internals. The internals of this column were installed on site through the vessel manholes. At this time, no filter box at the inlet into the distributor was commonly employed. Despite the washing procedure used to remove oil and grease from the packing, there

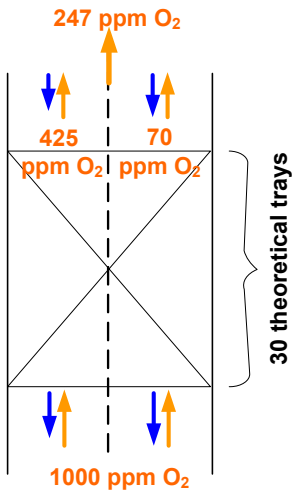

FIGURE 6.27 Sketch to Illustrate the Efficiency Calculation.

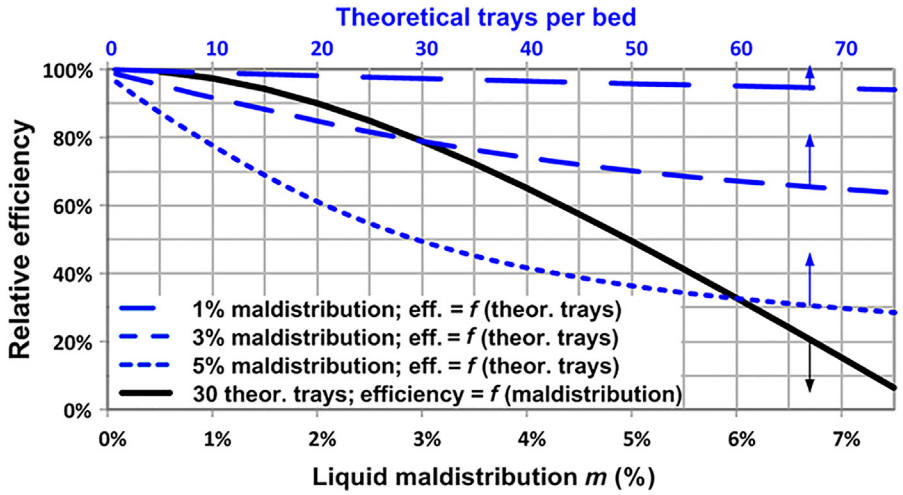

FIGURE 6.28

Relative efficiency of a bed with 30 theoretical trays in the crude argon column as function of the liquid maldistribution in the bed halves (bottom *x* axis) and at 3% maldistribution as a function of the theoretical trays.

must have been aluminum swarf attached to the packing. During startup, this material was washed down from the packing and collectors into the liquid distributor below. The distributor at the top, below the condenser, was clean.

The particles obstructed a section of the 3-mm distributor holes, mainly those situated at the end of the arm channels. Refer to the photograph in Figure 6.29. The effect of these blocked holes could be observed by the efficiency of the different beds. The lower red line in the diagram on the right side shows the oxygen concentration measured at the column feed and also above each packed bed. Because the striping factor is constant for all the upper beds, the gradient of the curve is according to the Kremser equation directly proportional to the packing efficiency (N_t/h_{bed} (m) = $(\ln(y_{top}/y_{bottom})/\ln(S))/h_{bed}$). The more holes that are blocked, the worse the efficiency of the bed becomes. The second bed from the top achieved only 50% of the efficiency it was able to achieve subsequently. The blue line in the graph plots the measured oxygen concentration after installation of the filter boxes and cleaning of the distributor holes. The smaller remaining differences in the slope of the curve can be mainly attributed to differences in the installation quality of the segmented packing layers in the different beds.

6.3.3.2 Using the crude argon column as a test facility

Because the stripping factor in the upper beds of the crude argon column is the same, these beds are ideal for testing the efficiency of different packing types and different bed modifications (bed height and packing segmentation) under

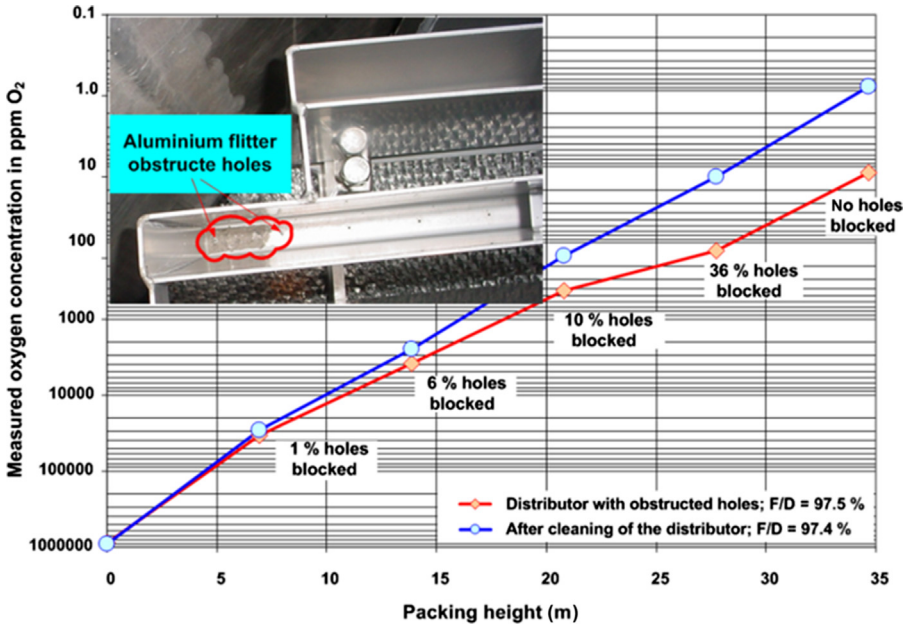

FIGURE 6.29

Measured concentration profile in the first crude argon column with partially obstructed holes in four of the five liquid distributors (red line) and after cleaning the liquid distributors (blue line). (For interpretation of the references to color in this figure legend, the reader is referred to the online version of this book.)

identical circumstances (column diameter, load, and reflux). The relative efficiency of the tested bed A to bed B is directly proportional to the concentration ratio $y_{\text{bottom A}}/y_{\text{top A}}$ to $y_{\text{bottom B}}/y_{\text{top B}}$. Two examples of such tests are mentioned in the Chapter 6.3.3.3.3 "Inhomogeneity of the packed bed". The only disadvantage in this test procedure is that the time to obtain experimental results after posing a question is overall about 12 months or even more.

6.3.3.3 Causes for maldistribution in a packed bed

The following sections discuss what causes maldistribution and how it can be reduced.

6.3.3.3.1 Quality of the liquid distributor

An evident reason for maldistribution is a bad liquid distribution caused by blocked distributor holes as described above, an imbalanced arrangement of the holes, or out of levelness of the distributor, just to mention the main causes. To distribute the liquid, a patented distributor [25] with rectangular pipes is used. The liquid enters the distributor through a central inlet pot with an integrated filter device. In this central pot, the collected liquid is completely mixed.

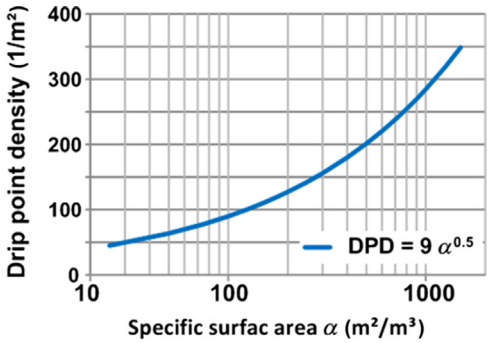

FIGURE 6.30

Applied drip point density for liquid distributors as a function of the specific surface area of the packing.

A predistribution system within the main channels, rectangular to the pipes, ensures that each pipe gets the correct amount of liquid. The main channels are closed on the top side to reduce the liquid inventory of the distributor. The liquid holdup increases proportionally to the square of the load range in commonly used channel distributors, as shown above in the example for the first packed crude argon column. In the pipe distributor, the liquid holdup is much smaller and the level varies only in the main channels and in the mixing pot.

The drip point density depends upon the packing density; for 750Y packing; it adds up to about 250 per m^2 (see Figure 6.30).

Each liquid distributor is tested with water before it is installed in the column shell in the workshop. The normal distribution quality in terms of standard deviation is in the range of 0.5−1% at full load and about 1−2% at 50% partial load. Each measured sampling point collects about 1−3% of all drip points. A photograph of a pipe distributor is depicted in Figure 6.31.

6.3.3.3.2 Liquid collectors, two-phase liquid and gas feeds

To minimize the height necessary for collecting the downflow of liquid, the packing bed support is integrated into the collector. This also allows a good gas distribution to the bottom side of the bed. The central collector trough is connected to the bed support beams. All parts are made of extruded aluminum profiles (see Figures 6.32 and 6.33).

Liquid and two-phase feeds are fed into the central collector trough. For large columns, instead of one central collector trough, an H-shaped trough can be used.

6.3.3.3.3 Inhomogeneity of the packed bed

An important cause of maldistribution is the packing and the packed bed itself. It is well known that the extent of liquid maldistribution grows with increasing bed height caused by zones of the packing, where its homogeneity is interrupted.

FIGURE 6.31 Photograph of a Pipe Distributor.

Column diameter is 5800 mm.

Such a zone is the outer circumference of the packing layer toward the column wall; another zone is the horizontal plane between two adjacent packing layers rotated by 90°. Because the lower and upper side of the packing elements are not perfectly even, there may be gaps between the layers.

At larger diameters, the longer segmental packing strips are divided for fabrication and installation reasons. The resulting gap is also a zone where noticeable maldistribution occurs. The gaps have to be minimized with regard to their size and number. A filling of the gaps reduces maldistribution and results in better efficiency. This was tested in an early crude argon column with a diameter of 3300 mm. During installation of the packing on site, it was reported that there were large gaps, up to 20 mm, at the junctions of the packing segment strips. It was decided to fill the gaps in the remaining uninstalled beds with small 10-mm random packing elements.

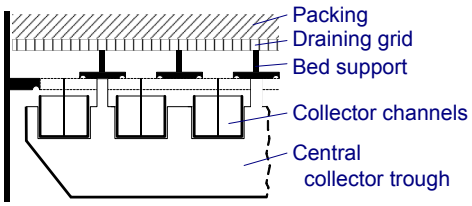

FIGURE 6.32 Principal Sketch of the Bed Supporting Liquid Collector.

FIGURE 6.33

View to the bottom side of the liquid collector with the central collector trough. Through the central hole in the trough, feeding the liquid distributor, the packing, the draining grid, and the support beams are visible.

The measured oxygen concentration profile proved the much improved performance of the beds with filled gaps. Tests in another column of 1120-mm diameter with packing beds made from divided segmented layers, and from one disc layers without gaps, verified the conclusion that unfilled gaps produce severe maldistribution.

The picture in Figure 6.34 shows a segmented packing layer from the mid-1990s with filled gaps. With accurate manufacturing of the packing elements and by

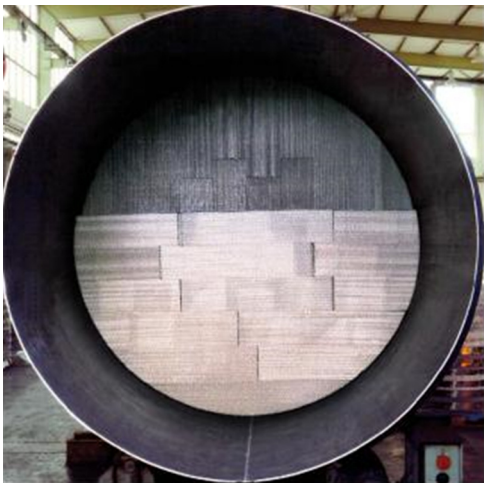

FIGURE 6.34 Photograph (c. mid-1990s) of a Shop-Mounted Packed-Column Section with Filled Gaps at the Junction of the Segmented Packing Stripes.

FIGURE 6.35 Photograph (c. 2002) of a Shop-Mounted Packed-Column Section with Segmented Packing Stripes and Reduced Gaps at the Junction of the Divided Elements.

careful installation of the elements, it is possible to reduce the size of the gaps to such an extent that it is not possible or necessary to fill them. The picture in Figure 6.35 shows such a packing layer. The efficiency of a packed bed consisting of layers produced and installed in such a way is the same as the efficiency of one made from disc layers.

The negative effect of the gaps can be avoided by also using disc layers for large-column diameters. Some competitors use them up to more than 4-m column diameter [26]. For handling such huge disc layers, with a weight of approximately 100 kg, special collars are necessary. The installation is carried out in the workshop into the vertically standing column shell.

6.3.3.3.4 Le Chatelier's principle

Inhomogeneity causes maldistribution because Le Chatelier's principle of least resistance applies. The specific pressure drop changes in the area where an inhomogeneity creates a liquid maldistribution. The bigger the maldistribution, the lower the resulting pressure drop in distillation applications.

Besides the packing itself (corrugation and crimp angle, surface texture and perforations), and the packed bed geometry, the system to be distilled and the column load also influence the development of maldistribution [27]. For explanation, some calculations have been done regarding a packing element of the area A divided equally into area A_1 and A_2. The gas load $V$and liquid load L of area A represent the average load of the column. The pressure drop calculations are done with the Linde in-house model Pack9, but similar results are obtained with other calculation tools also.

If the mean irrigation rate L/A in one-half A_1 is increased by $m\%$ of L and in the other half A_2 decreased by $m\%$ of L, then the specific gas load V/A changes in A_1 by $n\%$ of V and in A_2 by $-n\%$ of V, to a point where the pressure drop in both halves is the same. In Figure 6.36, the relative pressure drop—that is, the calculated pressure drop with maldistribution divided by the pressure drop without maldistribution—is shown as a function of the liquid maldistribution m. The slope of the pressure drop curve decreases with increasing m. Independent of the level of maldistribution m reached, the pressure drop gain grows further with additional liquid maldistribution.

For the crude argon system, two different column loads (50 and 75% of flooding) are plotted and compared with the pressure column system and the top (GAN-) and bottom (O_2-) section of an LPC. According to this diagram, the crude argon column is less disposed to form maldistribution than the other systems examined, but the sensitivity of the efficiency to maldistribution is by far higher.

The next diagram explores what happens when the maldistributed liquid portion mL is not added to a halved area A_1. The area A is split in unequal parts from a large portion A_1 with 75% of A to 50%, 25% and a very small portion of A_1 with only 10% of A. A_1 is the side, where the maldistributed share m of the liquid increases the irrigation rate. The relative pressure drop $\Delta p/\Delta p_{m=0}$ is shown as a function of the liquid maldistribution m and the resulting gas maldistribution n (negative numbers) is presented additionally.

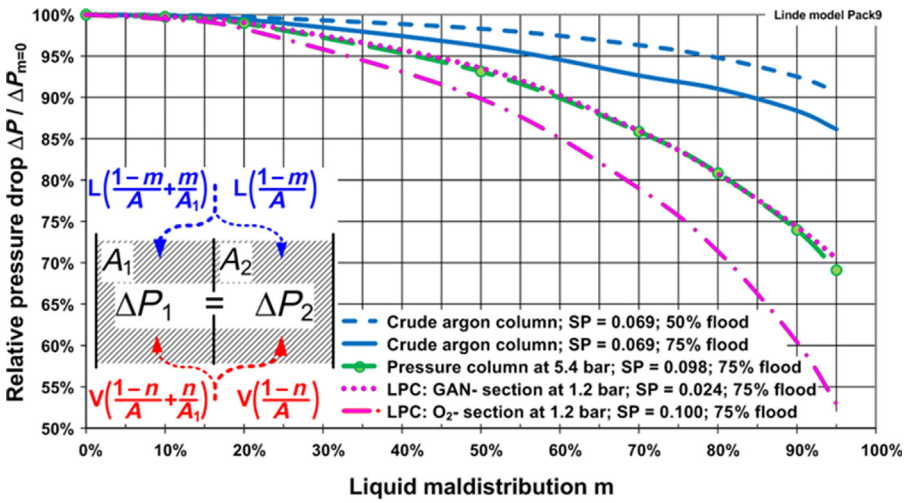

FIGURE 6.36

Relative pressure drop gain as a function of the liquid maldistribution for different sections of air separation unit columns.

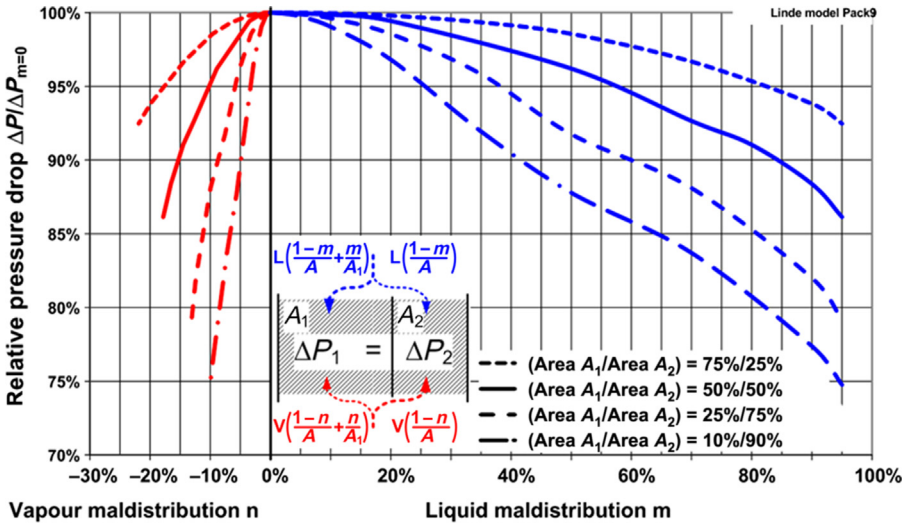

FIGURE 6.37

Relative pressure drop gain for a crude argon column for a liquid maldistribution m added to area A_1 unequal to area A_2.

The more the irrigation rate is concentrated in the smaller area, the more the resulting pressure drop reduces. The calculations are done for a crude argon system with an $L/V = 0.97$ and at 75% flood. The gas flow for the case $A_1/A_2 = 10\%/90\%$ with $m = 90\%$ and $n = -9.2\%$ is reduced to 16.7% $(=(1-n)/A + n/A_1)$ and the liquid flow increases to 910% $(=(1-m)/A + m/A_1)$; (see also Figure 6.37).

The conclusion is therefore that, over the packing cross-section, the homogeneous liquid and vapor distribution represents an unstable equilibrium. Once maldistribution is created within the packed bed, the required pressure drop reduces. Correcting the maldistribution would require energy; therefore, the maldistribution persists.

6.3.3.4 Maldistribution model and the importance of the radial mixing

In the initial use of structured packing in crude argon columns the measured efficiency of the same 750Y packing varied significantly from column to column, depending on the column diameter, the bed height, the segmentation of the packed layers and in a smaller extent from bed to bed. The measured height equivalent of one theoretical plate (HETP) ranged from 140 up to more than 350 mm.

To understand this behavior, a two-dimensional maldistribution model was developed (see Figure 6.38). According to a proposal by Zuiderweg [28], the packed bed is divided into small cells. The cell dimensions represent the basic HETP; this is the efficiency of the packing without maldistribution. Each cell interacts with the adjacent neighboring cells and the equilibrium of the vapor and liquid phase leaving each cell is reached.

A basic HETP of 120 mm for this system has been assumed based on measurements in a test column of 265-mm diameter. The interaction with the adjacent neighboring cells is simulated by split factors for the liquid and the vapor phase. These split factors define the portion of vapor and liquid phase flowing to the neighboring cells left and right of the adjacent top and bottom cells. The development of maldistribution within the bed is produced by adjusted factors for the cells at the column wall and at segmentation gaps.

With this simple model, it is possible to calculate with satisfactory accuracy the measured efficiencies. It is possible to characterize each packing by its basic HETP and the split factors for the gas and liquid phase. These split factors are a measure for the radial mixing of the phases.

One important conclusion from this model is that measurements in smaller columns reflect strongly the basic HETP. The ability of the packing to mix the phases sufficiently to compensate the developing maldistribution within the bed is not measured. Packing A and B performed the same in small columns with beds made up of one-disc layers.

In addition, the importance of the mixing of the gas and liquid phases is shown. By improving the surface texture of the packing sheets, it is possible to enhance the liquid and also the vapor mixing by generating small vapor vortices near the liquid surface. The result of more than 25 years packing development is summarized in this diagram.

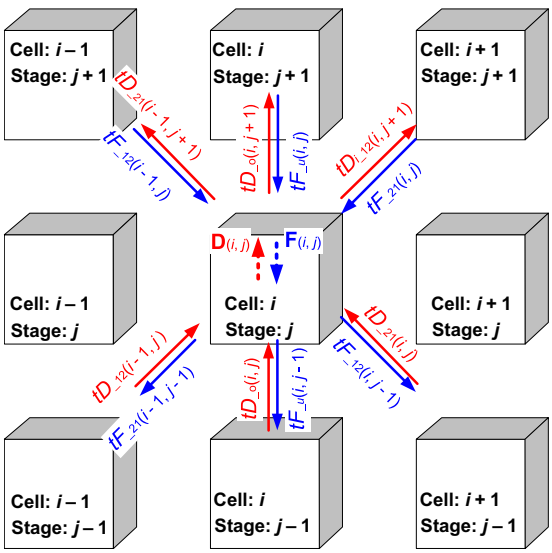

FIGURE 6.38 Sketch of a Simple Maldistribution Model.

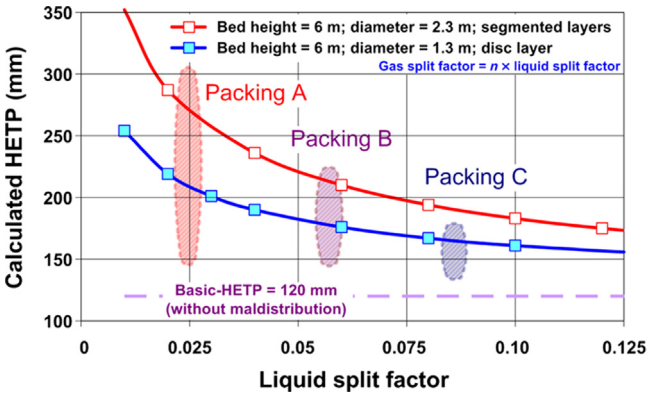

FIGURE 6.39

Calculated height equivalent of one theoretical plate (HETP) with a two-dimensional maldistribution model as a function of the liquid split factor for a packed bed. The shaded areas show the range of the measured HETPs for three generations of the A750Y packing. The packing generations differ from each other by the packing bed installation, the segmentation, and their surface texture.

The current design and the installation practices for the packed beds produce much less maldistribution. The packing structure itself tolerates a certain amount of maldistribution by good mixing of the phases. Naturally, the low HETP values for the packing C generation shown in Figure 6.39 can also be achieved by a major reduction of the applied bed height, thus reducing the sensitivity to maldistribution but the redistributors required for the additional necessary beds would have increased the column height by some meters.

6.4 Conclusion

Since its beginnings more than 110 years ago, the technology of air distillation has been continuously developing and thus changing. This is also valid in the application of sieve trays and structured packing in air distillation columns. Some of the main aspects of this continuous improvement process in the application of trays and packing were described in this chapter.

References

[1] H.-W. Häring, Industrial Gases Processing, Wiley-VCH Verlag GmbH & Co. KGaA, Weinheim, 2008.

[2] D. Schwenk, Industrial gases processing, in: H.-W. Häring (Ed.), Industrial Gases Processing, WILEY-VCH Verlag GmbH, Weinheim, 2008, p. 9 ff.

[3] H. Hausen, H. Linde, Tieftemperaturtechnik, Springer Verlag, Berlin, Heidelberg, New York, Tokyo, 1985.
[4] C. v. Linde, Verfahren und Vorrichtung zur Herstellung von reinem Sauerstoff und reinem Stickstoff durch Rektifikation athmospärischer Luft. DE 203814 DE, November 5, 1908.
[5] W. Rohde, H. Corduan, Argon Purification. EP 377117 B2, US 5019145 EP, US, 1988.
[6] K.H. Schweigert, et al., US 6748763 B2; EP 1287302 B1 US, EP, 2004.
[7] M.J. Lockett, J.D. Augustyniak, Parallel-flow slotted sieve tray efficiency, Gas Sep. Purif. 6 (4) (1992) 215, p. 215 ff.
[8] Jean Aucher, DE950190 Germany, 1954.
[9] W.K. Lewis, Rectification of binary mixtures, Ind. Eng. Chem. 28 (1936) 399 (vol. 1).
[10] M.J. Lockett, J.D. Augustyniak, On tilted trays, Trans. IChemE 69 (Part A) (March 1991) 99−107.
[11] M.J. Lockett, Distillation Tray Fundamentals. s.l, Cambridge University Press, 1986.
[12] D.W. Weiler, M.J. Lockett, The design and performance of parallel flow slotted sieve trays, Symp. Ser. 94 (1985) 141−155.
[13] J. Stichlmair, Grundlagen der Dimansionierung des Gas/Flüssigkeit- Kontaktapparats Bodenkolonne, Verlag Chemie, Weinheim, New York, 1978.
[14] G.G. Haselden, R.M. Thorogood, Point efficiency in the distillation of the oxygen−nitrogen−argon system, Trans. Inst. Chem. Eng. 42 (1964) T81−T100.
[15] H. Kreis, M. Raab, Industrial application of sieve trays with hole diameters from 1 to 25 mm with and without downcomers, 3. Int. Symp. Ser. 56 (1979) 63−83.
[16] E. Kirschbaum, Destillier- und Rektifiziertechnik, Springer-Verlag, Berlin, 1960.
[17] S. Hieringer, A. Moll, US 7552915 B2; EP 1704906 B1 US, EP, 2006.
[18] C.J. Colwell, Clear liquid height and froth density on sieve trays, Ind. Eng. Chem. Process Des. Dev. 20 (1981) 298−307.
[19] F.J. Zuiderweg, A. Harmens, Chem. Eng. Sci. 9 (1958) 59.
[20] B.R. Brown, Factors Affecting the Plate Efficiency of a Sieve Plate Distillation Column for the Separation of Liquid Oxygen/Nitrogen Mixtures. University of London: (Thesis), 1961.
[21] G. Linde, Chem. Ing. Tech. 27 (1955) 661.
[22] EIGA/CGA, G-4.8. Safe Use of Aluminum Structured Packing for Oxygen Distillation, 1993.
[23] B.R. Dunbobbin, B.L. Werley, J.G. Hansel, Structured packings for use in oxygen service: flammability considerations, Plant/Oper. Prog. 10 (1) (1991) 45−51.
[24] M.J. Lockett, J.F. Billingham, The effect of maldistribution on separation on packed distillation columns, Trans. IChemE 81 (Part A) (2003) 131 ff.
[25] H. Kreis, A. Moll, K.H. Stiegler, US 5501079; EP 607887 B2 US, EP, 1994.
[26] J.-Y. Lehman, DE 43 06 235 B4 Germany, 1993.
[27] M. Duss, A new method to predict the susceptibility to form maldistribution in packed columns base on pressure drop correlations, Symp. Ser. 152 (2006) 418 ff.
[28] F.J. Zuiderweg, P.J. Hoek, L. Lahm, The effect of liquid distribution and redistribution on the separating efficiency of packed columns, I. Chem. E. Symp. Ser. 104 (1987) A217−A231.

This page intentionally left blank

CHAPTER

Distillation of Specialty Chemicals

7

Gerit Niggemann, Armin Rix, Ralf Meier
Evonik Industries AG, Hanau/Marl, Germany

CHAPTER OUTLINE

7.1 Introduction

Special chemistry products are typically designed and produced for specialized markets and applications. In the final product they are often a minor ingredient by volume but are essential for its performance and function. Production rates range from several hundred tons per year in fine chemicals such as pharma intermediates, and up to some 100,000 tons/year in large-volume specialties such as monomers, comonomers, and polymers. Product specifications often require rather high purity

Distillation: Operation and Applications. http://dx.doi.org/10.1016/B978-0-12-386876-3.00007-7

and tight control of contaminants or by-products down to the part per million or part per billion. Secondary qualities such as viscosity, color number, flavor or (absence of) odor may also be specified.

Most specialty chemicals are multifunctional molecules with low vapor pressure and limited thermal stability. Their high reactivity often calls for rather gentle operating conditions in process equipment and may require the use of stabilizers for storage and transport. They are produced in a complex multistep synthesis. Therefore, recovery is the second most important objective for separation besides purity. Because the physical properties of specialty chemicals often differ widely from those of test mixtures, predicting separation efficiencies is not straightforward, and catalog efficiencies cannot be directly applied.

Specialty chemicals often are not marketed as simple feedstock for further production but as solutions tailored for a customer's specific applications. A product's life cycle may, as a consequence, be rather short, and time to market may be the deciding parameter in process development. Separations often have to be designed before accurate or even preliminary phase equilibrium and physical property data are available. The design of separation processes is then based on scale-up from laboratory or pilot plant experiments, experience from similar processes already in operation, and common sense. Internals cannot always be selected solely from hydraulic considerations; often a close match to the pilot plant setup is desired or existing equipment is to be reused to save investment or time to market. Other important factors influencing the selection and design of internals are resistance against foaming or fouling and easy access for cleaning.

To allow for fast reaction to changes in demand, specialty chemicals processes often are designed for high flexibility, that is, high turndown ratios and fast product changeover. Continuous processes are favored because of their lower residence times and higher recovery of products.

7.2 Distillation at low liquid load

Many specialty chemicals and their intermediates are complex molecules with a high molecular weight, low vapor pressure, and high reactivity. To achieve tight product specifications in distillation, many separation stages are required, even in systems with medium relative volatility. To avoid thermal degradation, columns often are operated at the lowest feasible pressure, and total pressure drop is specified to limit bottoms pressure. In some cases, tower diameter and internals are primarily designed to meet this pressure drop, not for a certain safety distance to flooding.

To meet the objective of low-pressure drop in vacuum distillation, the obvious choice of internal is structured packing. In deep vacuum operation, liquid loads may be low enough to approach the lower operating limit imposed by dewetting of the packing accompanied by a severe drop in separation efficiency. In strongly fouling or aqueous systems, the use of packing often is discouraged, and trays are

preferable. In tray columns operating at low liquid loads, the hydraulic condition known as tray blowing may occur in the spray regime and greatly reduce the efficiency of the tray.

7.2.1 Minimum liquid load in packed columns

To illustrate the hydraulics of low liquid load in deep vacuum operation, consider a simplified example: the rectification section of a column in which unreacted starting material is to be separated from a specialty monomer with a high molecular weight, very low vapor pressure, and high reactivity. The separation requires 30 theoretical stages; to minimize fouling risk, the column operates at an absolute top pressure of 1000 Pa. With an allowable pressure drop limited to 1000 Pa, or 33 Pa per theoretical stage, only structured packing is a viable option. Liquid and vapor rates are 1000 and 3000 kg/h, respectively. Vapor and liquid densities ρ_V and ρ_L are 0.05 and 760 kg/m^3 at the top and 0.1 and 780 kg/m^3 at the bottom, respectively. Liquid viscosity η_L and surface tension σ are constant at 0.65 cP and 30 mN/m, respectively, throughout the column. Hydraulics for different packings is designed using Sulcol [1]. For simplicity, catalog height equivalent of theoretical plate (HETP) values based on standard test systems are used, and diameter is chosen to meet the pressure drop specification. Results are summarized in Table 7.1.

For all metal sheet packings, flooding factors around 40% result to meet the pressure drop criterion. Column diameter increases with larger specific surface area, but bed depth decreases because of lower HETP values. Total volume for sheet metal packings is about 20 m^3. At F-factors around 2.0 Pa$^{0.5}$, there is little difference between conventional and high-capacity packing. For gauze packing, however, both diameter and bed depth are lower. Apart from savings in packing volume, gauze packing has the highest liquid load and F-factor of all packings and has the best wettability for organics. Therefore, gauze packing often is the first choice in deep vacuum specialty chemical applications. However, many designers do not use gauze packing if fouling is possible. For this reason, 350.Y packing with a specific surface of 350 m^2/m^3 is chosen. Liquid load is 0.68 m^3/m^2 h at 100% design and 0.34 m^3/m^2 h at 50% turndown. At such low liquid loads the design of internals

Table 7.1 Hydraulic Results for an Example Column for a 1000-Pa Pressure Drop

Packing Type	HETP (m)	Diameter (m)	Packing Volume (m^3)	Liquid Load (m^3/m^{2}h)	F-factor (Pa$^{0.5}$)	Flooding Factor (%)
250.Y	0.40	1.540	22.7	0.71	2.00	37
350.Y	0.28	1.575	16.8	0.68	1.91	41
500.Y	0.25	1.745	18.1	0.55	1.56	42
750.Y	0.20	1.975	18.5	0.43	1.22	40
BX	0.20	1.420	9.7	0.83	2.35	38
BX plus	0.20	1.285	7.8	0.99	2.87	52

should focus on creating enough effective area for mass transfer by ensuring sufficient wetting of the packing. It should be noted that pressure drop correlations may show considerable relative error at low flooding factors. Furthermore, pressure drop of nonseparating internals has to be considered.

The minimum liquid load in packed towers has been investigated by Schmidt [2]. In experiments with metal and ceramic Raschig and Pall rings, the point where further reduction of the irrigation rate starts to decrease efficiency was identified. Schmidt correlated his experimental results by:

$$u_{\mathrm{L,min}} = 7.7 \cdot 10^{-6} \cdot \frac{\mathrm{Ca}^{2/9}}{\sqrt{1 - \frac{F}{F_{\max}}}} \cdot \sqrt{\frac{g}{a_{\mathrm{P}}}} \quad \text{where} \quad \mathrm{Ca} = \frac{\rho_{\mathrm{L}} \cdot \sigma^3}{\eta_{\mathrm{L}} \cdot g} \tag{7.1}$$

with a mean error of 22%. Here, $u_{\mathrm{L,min}}$ is the liquid velocity in meters per second, Ca is the capillary or falling film number, F and $F_{\max}$ are F-factors at design and flooding, a_{p} is the specific packing area in meters squared per meters cubed, and g is the acceleration due to gravity. All physical properties have to be entered in the international system of units. If the influence of the liquid–solid contact angle θ is taken into account, the correlation reads:

$$u_{\mathrm{L,min}} = 1.25 \cdot 10^{-4} \cdot \frac{\mathrm{Ca}^{2/9} \cdot (1 - \cos\theta)^{2/3}}{\sqrt{1 - \frac{F}{F_{\max}}}} \cdot \sqrt{\frac{g}{a_{\mathrm{P}}}} \tag{7.2}$$

and relative error is decreased to 8%.

Equation (7.2) is reduced to Eqn (7.1) for a contact angle of 10.3°; complete wetting is predicted for 0°, and minimum liquid load becomes zero. Equation (7.2) is of both practical and theoretical interest because it gives an approach to estimating systems with low wettability.

Other researchers have pointed out the importance of the contact angle for liquid wetting in packing as well. In the effective area model of Shi and Mersmann [3], the contact angle is used to model the number and width of rivulets flowing down a packing. They also give a diagram to estimate the contact angle of liquids on different materials based on their surface tension. They point out that the measurement of contact angles less than 25° is often inaccurate and recommend the use of a minimum contact angle of 25°. Figure 7.1 shows results for the example column obtained from Eqn (7.2) using a contact angle of 25° for different packing sizes. With a higher packing surface area, the minimum liquid load decreases. This is in contradiction to models for complete wetting in falling film evaporators [4]. In distillation, however, we are mostly interested in developing enough effective area, not in complete wetting. Equation (7.1) (see the curve for $\theta = 10.3°$) predicts a minimum liquid rate of about 1 m^3/m^2 h. Furthermore, the packing rating results from Table 7.1 are shown as data points. All liquid loads are smaller than the results predicted by Eqn (7.1). According to Schmidt's model, all sheet metal packings listed in Table 7.1 can be expected to suffer from dewetting and reduced efficiency because of underirrigation. Practical experience shows, however, that columns operating

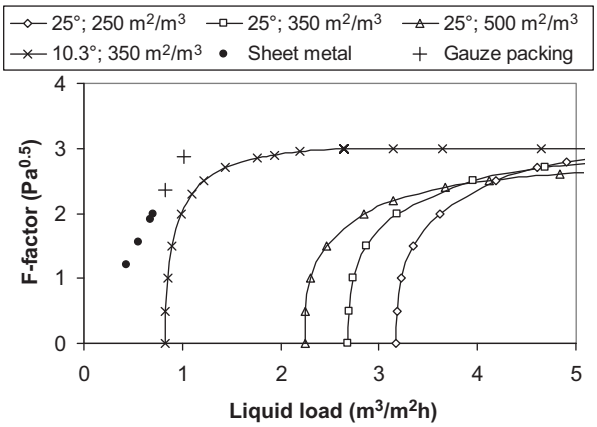

FIGURE 7.1 Minimum Liquid Load for Packed Columns as Function of Specific Area and Contact Angle.

All designs for gauze packing (crosses) and sheet metal packing (solid dots) from Table 7.1 are shown lie outside the calculated operating range.

satisfactorily at very low liquid loads of less than 0.2 m^3/m^2 h in organic mixtures and less than 1 m^3/m^2 h in aqueous mixtures can be designed. In these applications, special attention has to be given to the design of liquid distributors and their interaction with other internals such as bed limiters, liquid collectors, packing supports, and feed inlets.

Both Eqns (7.1) and (7.2) are easily evaluated and they are very useful for determining the range of liquid loads, where separation efficiency may suffer from underirrigation and special attention has to be paid to the design of internals. The model, however, as never been tested or reevaluated for structured or modern random packing and is not applicable to gauze packing. For aqueous systems with contact angles around 60°, the model predicts minimum liquid loads in the range of 15 m^3/m^2 h. However, there is positive practical experience with appropriately designed columns running at considerably lower liquid loads.

The importance of the contact angle for wetting was first described by Hartley and Murgatroyd [5]. As Simon and Hsu [6] showed, the minimum flow rate for complete wetting shows hysteresis: The flow rates required to initially achieve total wetting are higher than those required to prevent dewetting of an originally wetted wall. The authors account for this hysteresis by assigning different contact angles for increasing and decreasing flow. This is in accordance with the industrial practice of starting up columns with flow rates as high as are practical to ensure initial wetting. Measuring contact angles under distillation conditions is difficult for several reasons. The highly textured surface of structured packing reduces the contact angle compared to one measured on a flat plate [7]. That packing microstructure can reduce the effective contact angle has been shown both by experiments [8] and computational fluid dynamics (CFD) simulations [9]. Furthermore, contact angles

measured under vapor–liquid equilibrium (VLE) conditions are smaller than those obtained under atmospheric conditions and depend on surface structure and mixture composition [10]. Recent detailed studies of a liquid flow down inclined textured and smooth plates have shown that the surface texture not only improves liquid spreading but also improves liquid-side mass transfer [11].

A practical example from the experience of the author of this chapter shows the importance of wetting for separation. In a column equipped with sheet metal packing separating an aqueous system at liquid loads less than 3 m^3/m^2 h, separation efficiency continuously deteriorated over time. While column diagnostics provided noisy scan lines, no clear evidence for severe maldistribution, fouling, or mechanical damage of internals was found. Closer inspection of the process fluids revealed that the liquid phase contained trace amounts of a hydrophobic component with an extremely low solubility. It was suspected that this component partially covered the packing material, increasing the contact angle and causing progressive dewetting of the packing. The problem was solved without opening the column: a hot steam-out run supposedly removed the troublesome component.

Plastic packing is another well-known application where surface properties that change over time may cause considerable variations in separation efficiency. After start-up, the packing surface may require several weeks of operation to reach its final surface activity and wettability. Treatment of plastic packing with a hot caustic may increase its surface energy and considerably improve liquid wetting and separation efficiency in aqueous service [12].

Liquid viscosity can be quite high in some distillation columns. Increasing liquid viscosity will considerably reduce the separation efficiency of packings [13].

7.2.2 Design of liquid distributors

In liquid distributors, metering orifices in the bottom or side wall of troughs are evenly distributed across the column section. The flow from the orifices is driven by gravity and follows Torricelli's equation:

$$u_L = N_{drip}\frac{\pi}{4}D_O^2 \cdot C_O\sqrt{2gh} \tag{7.3}$$

where u_L is the liquid load in meters per second, N_{drip} is the number of drip points per square meter, D_O is the orifice diameter, C_O is the orifice coefficient, and h is the height of liquid over the metering orifice. Low liquid loads result in very small values of either overflow height, orifice diameter, or drip point density. A general overview of distributor design is given by Schultes et al. [14]. Standard distributors are designed for liquid loads of 2–80 m^3/m^2 h. The velocity in distributor troughs should be limited to less than 0.5 m/s, liquid overflow height over metering orifices should be higher than 30 mm (at turndown), and liquid velocity in the individual channels should be less than 0.3 m/s to avoid a hydraulic gradient.

Figure 7.2 shows the orifice diameter calculated from Eqn (7.3) for an orifice coefficient of 0.7 and different drip point densities as a function of the liquid

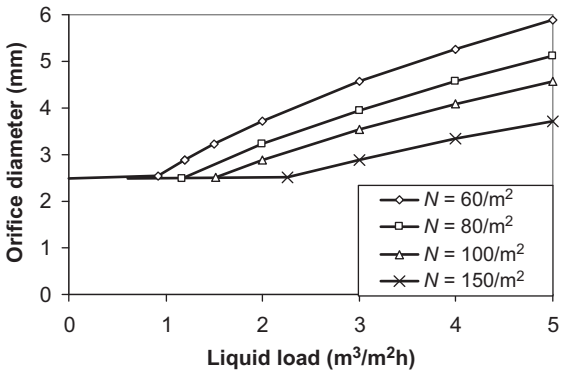

FIGURE 7.2

Orifice diameter calculated from Eqn (7.3) for a constant overflow height of 75 mm for different drip point densities.

load. An overflow height of 75 mm is chosen. This is considered a minimum value to ensure distribution quality over the column's cross-section by compensating imperfect leveling of distributor troughs and allow some amount of turndown. A minimum orifice diameter of 2.5 mm is chosen to provide some resistance against fouling or plugging.

It is clear from Figure 7.2 that some compromise has to be made for the low liquid load of the example column described above. The first option is to reduce the density of primary drip points and the use of flow multiplying devices, which split the flow from a single metering orifice into a certain number of equal flows. This allows a more robust design by using larger metering orifices and/or greater overflow heights. Several proprietary devices are available on the market. As an example, Figure 7.3 shows photographs of a commercial product, the "Type S" distributor fabricated by Montz. In Figure 7.3(a), an overview of the distributor arms and the flow multipliers at a rather high liquid load is shown. In Figure 7.3(b), the mechanism of flow division is visible: Liquid from a primary metering orifice flows into a tube with sealed bottom, which has several lateral orifices. In each orifice, a wire spring draws liquid from the pool inside the tube using the capillary effect. In this way, the liquid stream is divided literally drop by drop. Similar devices are available from other companies but are omitted here for the sake of brevity.

A second option is the use of line distributors [15]. Here, the metering orifices are in the side walls of the troughs and discharge against a baffle. On the baffle, the individual liquid jets spread in the form of parabolas. When the orifices are properly spaced, the parabolas connect and form a continuous liquid film, which is discharged onto the packing. With line distributors, the number of metering orifices per unit area can be cut almost in half. The number of drip points is replaced by the number of distributing lines per meter column diameter, and a proper orientation angle of distributor to packing should be chosen [15]. Another advantage of line distributors is that the baffles may be streamlined for low-pressure drop and liquid entrainment.

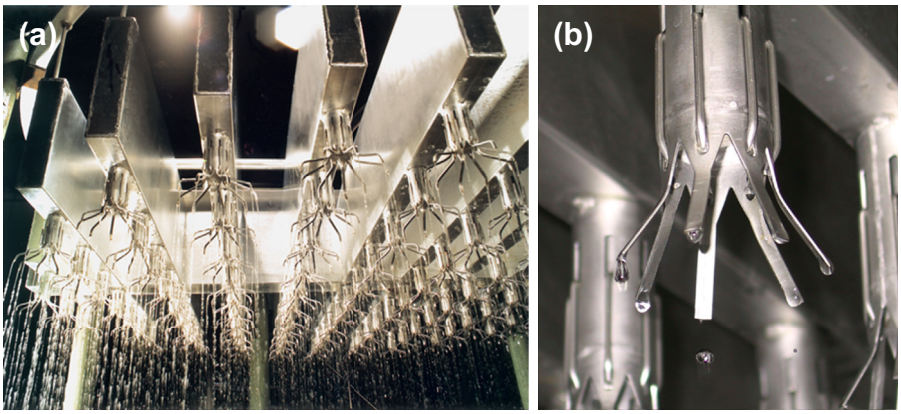

FIGURE 7.3

"Type S" distributor fabricated by Montz *(Photo courtesy of Julius Montz GmbH, www.montz.de.)*. Wire springs divide the liquid flow into the primary drip tube (a) into seven equal flows utilizing the capillary effect (b).

A third option is to relax some of the design rules mentioned above. In addition to using flow multipliers or line distributors, the minimum liquid overflow height can be reduced to very small values. To ensure sufficient distribution quality, the distributors need to be manufactured using the highest quality standards. This mostly concerns the diameter, position, and exact form of the metering orifices. The design must allow for lateral mixing either by communicating channels between the distributor troughs or in the parting box. At low overflow heights, the distributor design must allow the individual troughs to be perfectly leveled inside the column. Installation must be done by an experienced team, and tight quality control during installation is required. There is positive industrial experience with distributors with flow deviations of less than 5% at overflow heights of only 25 mm. It is obvious that every single distributor is to be water-tested, even if several distributors are of the same design.

Independent of distributor type and load, a uniform distribution of drip points over the column area is required. Moore and Rukovena [16] provide a simple geometric model to calculate a distribution quality rating. Each drip point is represented by a circle with an area proportional to the flow rate from the drip point. Areas of overlap and areas not covered by circles are detrimental to the distribution quality. Large areas with no irrigation (e.g. under large gas risers in pan-type distributors) should be avoided. According to this method, a triangular pitch is best, with a maximum quality of 95%, followed by a quadratic one, with a maximum quality of 90% (see Figure 7.4).

Besides its simplicity and the convincing geometric argumentation, the merit of the Moore/Rukovena method primarily lies in discovering under- or overirrigated areas. Liquid maldistribution studies conducted at FRI [17] clearly show that randomly dispersed, small-scale deviations in liquid load are compensated by the

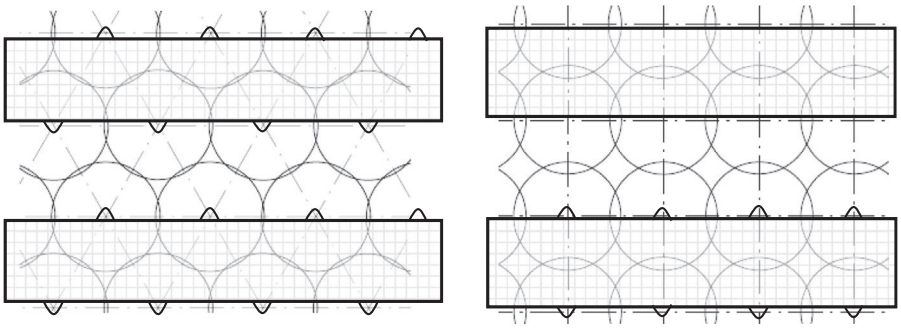

FIGURE 7.4

Triangular (left) and quadratic (right) drip point patterns with distributor troughs with lateral drip tubes.

self-distribution properties of the packing. Initial maldistribution on a larger scale, however, cannot be compensated for by the radial spreading effect of the packing and leads to a loss of separation efficiency. Billingham et al. [18] investigated the effect of maldistribution with a zone-stage model and defined a suitable cell size that may serve as a measure to discern small- from large-scale. For structured packing, the cell size is equivalent to the HETP value. On the basis of these considerations, it is doubtful whether there is really a difference in quality between triangular and quadratic drip point patterns.

In modern computer-aided designs, drip point patterns are automatically generated. For mechanical constrictions, distributor troughs must be terminated some way off the column wall. Here, automatically generated designs will most likely produce underirrigated zones. A simple way of accounting for this is reported by Nutter and Hale [19]. Figure 7.5 shows the sketch of a pan-type distributor. The radius used to create the drip point pattern must be reduced by the width of the support ring to avoid collisions. The column cross-section is divided into three concentric zones of equal area, and the number of actual drip points in each zone is counted by hand. In large columns the counting can be limited to a 60° wedge, as indicated. In many cases, the number of drip points in the outer zone near the column wall will be lower than in the two inner zones (see the areas marked by clouds). Here, additional drip points may be easily defined by human intervention. The regularity of the pattern can be maintained only if the gas risers do not interrupt it. For 100 drip points/m^2, the pitch of the drip points is 100 mm and the gas risers need to be rather slim, say, less than 80 mm. Large gas risers covering one or more rows of drip points are to be avoided.

Nonseparating internals such as distributors, chimney trays, and chevron collectors may contribute significantly to the total pressure drop in a packed bed. In these internals, the vapor flow undergoes contraction and expansion losses. The dry loss coefficient for contraction and expansion without pressure recovery is given by:

$$\xi_{\mathrm{dry}} = 2.5 \cdot (1 - \upsilon) \tag{7.4}$$

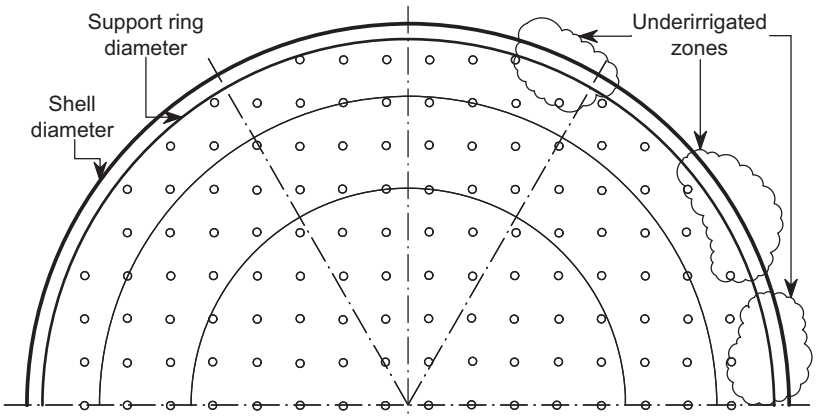

FIGURE 7.5 Sketch of a Pan-Type Distributor with Support Ring.

Underirrigated areas are marked by clouds. This illustrates a regular drip point pattern; slim gas risers are not shown.

where v is the fraction of free area left for vapor flow; the vapor velocity in the constricted area is to be used. While the definition of free area is straightforward in distributors or chimney trays, the geometry of chevron collectors is not standardized. Figure 7.6 shows experimental data for two chevrons with 60° and 80° vane inclination [20]. Clearly, there is a two-phase flow effect on the pressure drop. Quite independent of liquid load, wet pressure drop is almost 50% higher. The key variable in minimizing pressure drop is the free area in the internals' most constricted cross section. Furthermore, the form of riser hats and liquid catching hooks can be streamlined.

7.2.3 Spray regime operation

At low liquid and high gas load, structured or random packing is the preferred solution from a purely hydraulic standpoint. Other considerations such as fouling, insufficient wetting, or formation of a second liquid phase in aqueous systems may be in favor of the application of trays. Last but not least, trays may have the lowest cost and implicate the most economical internal. Trays with low liquid load often are encountered in the rectifying sections of low-pressure columns, such as methanol-water separation, in ethanol plants, in backwash sections of absorption and extractive distillation towers, in reaction columns, and in the separation of wide-boiling mixtures at a low reflux ratio.

At low liquid load, high entrainment can be generated at rather low F-factors. While counter-current operation is still possible, efficiencies may decrease to a point where the separation task can no longer be met. The tray is not able to maintain a continuous liquid layer, holdup drops, and the tray may appear to be "blown

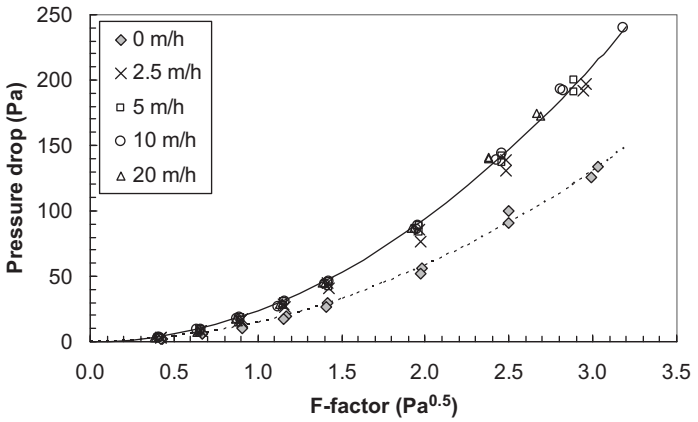

FIGURE 7.6

Pressure drop of a chevron-type collector; the dotted line indicates the dry pressure drop and the solid line indicates the wet pressure drop [20].

dry" of liquid. At the transition into the spray regime, vapor becomes the continuous phase, while liquid is dispersed in droplets, which may be thrown directly into the downcomer. Loss of the downcomer seal is also possible. This hydraulic condition is often called "tray blowing" [21].

To overcome the loss of efficiency in the spray regime, de-entrainment devices were suggested as early as 1950. With regard to bubble cap trays, Kirschbaum [22] observed the formation of a fine spray even at medium gas loads and investigated the effect of impingement plates under the gas risers and of layers of random packing fixed in the intertray space. Impingement plates moved the efficiency curve to higher values, while the typical drop of efficiency with increasing gas load persisted. With random packing, however, good de-entrainment was achieved, tray capacity was increased, and efficiency was constantly high in the whole range. Since then, many trayed columns operating in the spray regime have been successfully revamped with structured packing as a de-entrainment device. A systematic study of methanol-water separation is presented by Yang et al. [23]. A layer of structured packing was fastened directly under the valve trays of a pilot column. Useful capacity was increased by about 10%. The trays, however, were probably not operating in the spray regime because the column was run at total reflux.

At low liquid load, maldistribution is severe and tray efficiency may be impaired. As a consequence, a minimum weir overflow height of 5 mm, corresponding to a minimum weir load of about 2 m^3/m/h, often is specified [24]. This is, however, in conflict with another rule of thumb requiring a weir length of at least 55% of the column diameter to prevent maldistribution caused by severe constriction of the liquid flow path.

The safest way to design trays for low liquid load is to avoid the spray regime altogether. Lockett [25] proposed the following correlation for the transition from the froth to the spray regime on sieve trays:

$$\frac{h_{cl}}{d_h} = 2.78 \cdot \sqrt{\frac{\rho_V}{\rho_L}} \cdot u_h \tag{7.5}$$

where h_{cl} is the clear liquid height on the tray, d_h is the hole diameter, and u_h is the hole velocity.

According to Summers and Sloley [21], valve trays produce less entrainment at low liquid load than sieve trays because the vapor enters the tray in a horizontal direction. To account for industrial data and for valve trays, Summers and Sloley rearranged this equation and defined the spray factor:

$$\text{Spray Factor} = K \cdot \sqrt{\frac{\rho_L}{\rho_V}} \cdot \frac{h_{cl}}{d_h \cdot u_h} \tag{7.6}$$

Consistent with Lockett's model, the minimum spray factor is 2.78, where the constant K is 1.0 for sieve trays and 2.5 for fixed and moving valve trays. To move tray operation from the spray to the froth regime, one can decrease the hole velocity by increasing the open area or increasing the weir height. These modifications will increase the weeping rate of the tray, where loss of liquid by leaking is already a problem at low liquid load. Another option is to decrease the hole diameter. However, the most effective way to increase the spray factor is by reducing the weir length using picket fence weirs. Summers and Sloley [21] give several examples of radical picketing, one of which is blocking up to 90% of the original weir length in several tower revamps.

In one example from the author's experience, the backwash section of an absorber was operated and performed adequately for more than 20 years. To account for the extremely low liquid rate, V-notch weirs were originally designed. During a shutdown, extensive welding work was performed on the column shell. Upon start-up, entrainment caused a loss of solvent into the gas stream and created a wastewater problem. Close inspection revealed that after welding, the column shell was slightly tilted and the trays were no longer level. To solve the problem, the V-notch weirs were replaced by picket fence weirs with 97% blocking, and inlet weirs were designed to ensure the downcomer seal. The height of the pickets was about half the tray spacing to allow for droplet removal. After the revamp, the column again achieved its original efficiency. To avoid extensive constriction of the liquid flow path, a gap should always be left between the column wall and the first pickets.

Besides weeping, the performance of trays at low liquid load can be impaired by leakage. During installation, the trays should be carefully inspected. In practice, problems have been encountered because tolerances in tower diameter, roundness, and tray parts added up to create large gaps through which liquid leaked from the tray.

7.3 Reactive distillation

In special chemistry, many processes involve multistep synthesis, where high recovery and the minimization of recycle streams is especially important. Furthermore, there are many reasonably fast equilibrium-controlled reaction systems such as etherifications, esterifications, or condensations that are suitable for reactive distillation. Reactive distillation, therefore, is of great importance in special chemistry. Some practical aspects and applications in special chemistry are outlined here. For general information see Chapter 8 [26].

7.3.1 Overview

Reactive distillation is the field of process intensification that has received the most research interest in recent years. The basic idea of reactive distillation is simple enough. By combining reaction and separation in a single vessel/unit operation, considerable savings in investment may be possible. Conversion and even selectivity may be higher than in conventional reactors, and heat of reaction can be used for separation to reduce energy requirements. If there were a proven way to meet all or even most of these objectives, one would expect to see reactive distillation as a standard in most chemical processes. In reality, achieving this in the same design is almost impossible, and reactive distillation is far from being a standard in process industries. However, even if only one or two of the advantages, such as increased conversion or selectivity, is reliably met, reactive distillation may be a powerful technology to improve a process' economic performance by reducing recycle or by-product streams.

On the other hand, the drawbacks of this type of process intensification are obvious. Most importantly, the degrees of freedom are lower than in a conventional reaction/separation system, which gives less flexibility to counteract errors in process design or inaccuracy in VLE and kinetic data. First of all, system pressure has to be selected to ensure that reaction rates are fast enough for the reaction volume that is realizable inside a column. This pressure is not necessarily the one that enables most economical separation. The reflux ratio often is determined by reaction, not by separation requirements, and energy demand may even be increased. As in conventional reactors, homogenous and heterogeneous catalysis show fundamental differences.

7.3.2 Heterogeneous catalysis

In heterogeneously catalyzed reactive distillation, the catalyst is fixed in internals designed to give free access to liquid. Typical hardware is described in Chapter 8 [26] for additional information see Krishna [27]. While novel ideas like the immobilization of catalyst in containers on a distillation tray or in downcomers have been patented and are reported in the literature, the only hardware proven in industrial practice is reactive packing, such as Katapak by Sulzer [28] and

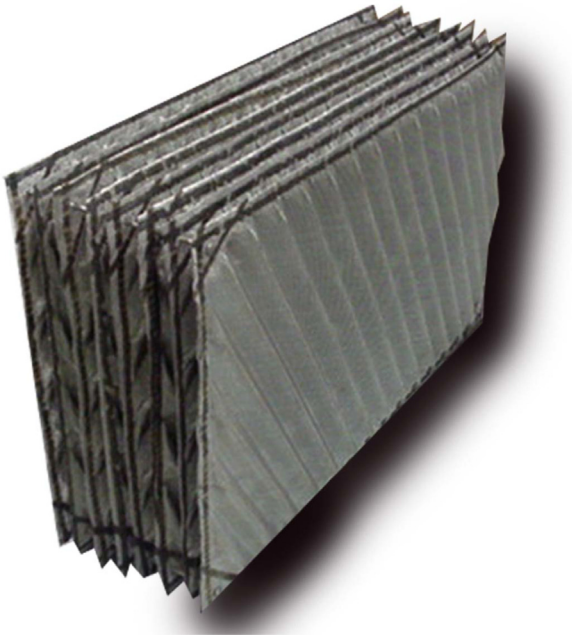

FIGURE 7.7

In KataMax catalytic packing, the catalyst is seal-welded in corrugated metal gauze sheets in thin layers.

Photo courtesy of Koch-Glitsch, LP, www.koch-glitsch.com.

KataMax by Koch-Glitsch [29]. These packings are commercially available and can be purchased filled with proprietary catalysts supplied by the user. They consist of envelopes of wire gauze sheets of different geometric shapes in which catalyst is sealed by welding. The typical thickness of catalyst layers is 3−15 mm. Because of capillary forces, the liquid phase preferentially flows through the catalyst bed, while mass transfer takes place on the surface of the envelopes. Figure 7.7 shows a block of KataMax packing supplied for a world-scale plant.

Currently, there is no modeling technique that allows direct design from kinetic and VLE data alone. Laboratory experiments are indispensable. Scale-up, however, is complicated by the fact that basic design parameters such as free area for vapor flow, catalyst holdup, and specific area differ between laboratory and industrial versions of catalytic packing. In applications where a certain conversion or selectivity must be guaranteed, even pilot plant experiments may be imperative to ensure safe scale-up [30]. Catalyst holdup in commercial packings ranges from 25% to 40%, and hydraulic capacity is therefore lower than in distillation. A thorough investigation of flow regimes and hydraulics in Katapak SP is given by Behrens et al. [31] and Moritz and Hasse [32].

In conventional distillation, mainly the product specification of key components must be met; errors in the prediction of the concentration profile are often of little consequence. The usual design margin on the number of stages will help to counteract inaccuracies. In heterogeneously catalyzed reactive distillation, however, the location of catalyst inside the column is fixed and excellent VLE data is required to reliably compute the concentration profiles of all reaction partners—especially of middle boilers—in order to provide correct input for kinetic rate models. A further design challenge arises from the fact that the amount of catalyst is fixed. In conventional fixed-bed reactors, catalyst deactivation is compensated for by adjusting temperature. In heterogeneous reactive distillation, column pressure must be increased to achieve the same result. Internals, reboiling, and condensing systems must be designed for an operating range wide enough to accommodate the expected variations in feed composition, feed flow rate (turndown ratio), and catalyst activity while maintaining separation performance.

Catalytic distillation internals are expensive. On the one hand, the raw materials themselves, such as stainless steel wire gauze and catalyst, are costly. On the other hand, there is an immense amount of work to be done by hand, like welding seals on the literally kilometers of catalyst envelope per cubic meter of packing, filling defined amounts of catalyst into each envelope, and so on. To replace spent catalyst, the packing must generally be exchanged completely. Besides the high cost, the manufacture and transport of replacement packing may last several months because of limited manufacturing capacities. Therefore, the packing must be protected from catalyst poisons by careful operation of upstream units and tight control of the temperature profile in the reactive zone to maximize the catalyst's lifetime, which should be long enough for the time span between two planned plant shutdowns.

Also, tight quality control is essential in all phases of material procurement, packing manufacture, installation, and operation. Catalyst can be damaged or deactivated by environmental influences or mishandling during manufacture or transport. All welded seals must be tight enough to keep the catalyst in the reaction zone—leakage from the packing and migration to a separation zone may cause a reverse reaction or by-product formation. In many applications, ion exchange resins are applied as catalyst. The resin is shipped in a water-saturated form and will shrink during operation, which in turn will change its hydraulic parameters. As one researcher wisely put it, "That kind of packing is alive!" [33].

Designing a new heterogeneously catalyzed reactive distillation process is a challenging task. Derivation of basic data of sufficient quality and laboratory and/or pilot plant experiments accompanied by careful modeling and scale-up work requires considerable time and financial effort. It is therefore not really surprising that most processes are developed and marketed by licensors, who can distribute the development cost among several customers.

The leading application is the synthesis of fuel ethers such as methyl tertiary butyl ether (MTBE), ethyl tertiary butyl ether, and tert-amyl methyl ether [33]. Most licensed MTBE processes consist of a fixed-bed reactor system where isobutylene reacts selectively with methanol to form MTBE using a debutanizer column and an extraction of azeotropic methanol from the columns' distillate stream with water. Regenerated washing water is recycled to the extractor and methanol is recycled to the reaction section. Isobutylene conversions of around 95% are possible in these processes. To considerably increase conversion of isobutylene and arrive at a raffinate-2 stream with an isobutylene concentration sufficiently low to allow the production of high-purity 1-butene, the Hüls process incorporates a second reaction stage with a high stoichiometric excess of methanol followed by a second distillation step.

In reactive distillation, however, a catalytic packing is placed in the rectifying section of the debutanizer to increase conversion. High-boiling MTBE is efficiently removed from the reaction zone by distillation, while the azeotrope of C_4 and methanol supplies excess methanol to the catalytic zone. High conversions are achieved in a one-stage process [34]. Important licensors are UOP and CDTECH (CBI Lummus Chemical Research & Licensing).

Further heterogeneously catalyzed reactive distillation processes available for licensing include high-purity isobutylene, selective hydrogenations, hydrodesulfurization, alkylation, and cumene [35] as well as synthesis of methyl, ethyl, and butylacetate and hydrolysis of methylactate [36].

7.3.3 Homogeneous catalysis

In homogeneous reactive distillation, catalysts have to be removed from the product stream in an additional separation step, where the catalyst (usually an acid or a base) often cannot be recycled. The process, however, offers several decisive advantages. Most important, catalyst concentration in the reaction zone can be adjusted to the required conversion or production rate by adjusting its flow rate. Extra capacity is often easily accessible with a higher concentration of catalyst, albeit at the price of lower selectivity. If the production rate is reduced, lower concentration of catalyst and lower conversion may increase the selectivity. Because of this higher flexibility, the quality of VLE and kinetic data used for design need not be quite as high as in heterogeneous systems.

Furthermore, modifications of standard internals, for which many established suppliers are active in the market, may be used.

- For very fast reactions, the residence time on structured packing may be sufficient. Here, close attention should be paid to the holdup in liquid collectors and distributors [37]. The holdup of these nonseparating internals may be the equivalent of several meters of packing. Reactions will continue without simultaneous separation.
- In most systems, reactions are slower and trays are the preferred internal. The holdup on the active area of sieve and valve trays is similar; however,

higher dry pressure drop will cause higher holdup in the downcomers of valve trays.
- Bubble cap trays are frequently used as reaction trays. They can be manufactured and installed to be liquid tight and are therefore ideal candidates in low liquid load systems and for extreme turndown requirements.
- For very high residence times, sieve trays or bubble cap trays with large weir heights or even nonaerated chimney-type residence time trays have been proposed [38].

The most important design objectives for reaction trays are residence time (i.e. holdup), residence time distribution, and separation efficiency. These parameters must be carefully optimized to ensure stable operation at varying loads. In-house designs exist for many proprietary processes and are optimized for the specific process requirements. The open literature on reaction trays is rather scarce.

Whenever large residence times are required, the obvious solution is trays with a high weir height. Designing trays with a high weir height, however, is not without pitfalls. Established design correlations for tray design given in Chapter 2 were developed and validated for trays with weir heights typical for distillation (i.e. lower than ~75 mm). Their extrapolation to large weir heights should, therefore, be done with due caution. Experimental validation using operational data from similarly industrial sized trays is strongly recommended.

First, estimating holdup on reactive distillation trays with large weir height is a challenging task. Holdup may be computed from models for clear liquid height, which, however, is mainly modeled to account for wet pressure drop. While a certain holdup is required to achieve sufficient separation efficiency on distillation trays, its exact value is of little consequence for the tray's performance. At high F-factors, sieve tray holdup is only slightly dependent on weir height [25].

On reactive distillation trays, however, holdup is the key variable, and weir heights up to 500 mm and more have been reported [39]. No published model for clear liquid height may be safely extrapolated that far. Holdup data on sieve trays with weir heights up to 100 mm were reported by Krishna et al. [40]. Tray holdup increases with liquid load and weir height, whereas a larger gas load increases the tray aeration factor and decreases the holdup. At very high gas loads, holdup may even be independent of weir height. A holdup of active area times half the weir height may serve as a first rough estimate for moderate F-factors. Furthermore, the caps on bubble cap trays designed for high gas load may occupy up to 40% of the active area. Inside the caps there will be mostly gas, so that the holdup is further reduced. When existing reaction trays are to be evaluated, the holdup is best computed from pressure drop data. A large volume of liquid may be accumulated in the downcomers of reaction trays. There is no literature on the effect of evaporation due to the heat of reaction in downcomers.

To separate reaction products, reactive distillation trays need sufficient separation efficiency. Murphree tray efficiency increases with weir height, but little gain can be expected above 50 mm. On the other hand, liquid back-mixing will be

stronger on trays with high weirs. Therefore, tray efficiencies should not be expected to be higher than point efficiency. In a theoretical paper Fisher and Rochelle [41] investigated the effect of reactions on tray efficiency. Reactions may dominate the axial concentration profile on the tray so that their Murphree efficiency may differ from distillation trays by an order of magnitude. To overcome these shortcomings, the authors recommend using a rate-based model. Most commercial rate-based models, however, do not evaluate the liquid concentration profile on trays.

The stability of sieve trays with weir heights from 300 to 900 mm was investigated by Haug [39]. At low loads, uneven gas distribution was observed, and the area of preferred aeration moved around the tray in a rotating pattern. At higher gas loads, when all sieve holes were active, stable operation was achieved and weeping was much reduced. A minimum hole F-factor of 14 $Pa^{0.5}$ or a dry pressure drop of about 2 mbar showed stable operation, independent of weir height or hole size. A safety factor of two is recommended for the design hole F-factor. Reaction trays carry a considerable weight. Mechanical stability is important because flexing, sagging, or unevenness of the tray may influence gas distribution. A CFD study of reactive trays with weir heights up to 100 mm found three-dimensional flow patterns very similar to the ones described by Haug [40]. F-factors in holes did not quite reach the stability criterion given by Haug. No information on residence time distribution was given. However, the simulation revealed recirculation in roll cells perpendicular and parallel to the main flow direction, while a large part of the liquid feed flowed directly to the downcomer along the tray axis. Residence time distribution will be rather broad on reaction trays without guiding elements. On the other hand, Haug [39] reported that baffling may even worsen gas distribution at low gas load, where gas may break through on one side of a baffle, while weeping occurs on the other side.

Many of the problems in the design of reaction trays with high weirs outlined above can be avoided by performing reaction and distillation on separate trays. Large residence time for a reaction can be provided on chimney-type trays, where the gas bypasses the liquid and the liquid holdup is not diminished by bubbling action. To achieve separation, conventional sieve or valve trays are placed in an alternating arrangement. The amount of reaction and separation necessary in a specific application can be realized by optimizing the number and weir height of reaction and distillation trays. Dörhöfer [38] describes a detailed investigation of this approach using five different tray geometries for the synthesis of methylacetate. While a column with only reactive trays generated a higher conversion per unit holdup than a column with residence time trays, its total conversion was lower. Doubling the weir height of reactive distillation trays increased conversion by about 10%. Slow reactions were investigated by reducing the flow rate of the catalyst. In this case, an alternating pattern of reaction and separation trays showed the highest conversion.

For the successful application of residence time trays as reactive column internals, several critical design issues need to be addressed. At low liquid flow rates, leaking of trays must be prevented. The layout of gas chimneys should be chosen to prevent vapor maldistribution or premature flooding in the trays above. The

hydraulic gradient on the tray should be considered when selecting the height of gas risers. As chimney trays offer little resistance for liquid flow, residence time distributions can be expected to be rather broad. Furthermore, there is no information in the literature on the effect of bubbling caused by exothermal reactions.

The concept of side-reactors is closely related to reactive distillation. A side-stream is withdrawn from the column, fed to a conventional reactor, and in most cases returned to the stage below the draw [42]. To increase conversion, it may be advantageous to run the reactor at a temperature different from the column temperature. With one reactor, one or two heat exchangers, and two return pumps, side-reactors call for considerable investment and plot space. Furthermore, a side-reactor will give not more than one equilibrium stage for reaction. If more than one side-reactor is required to achieve the desired conversion, the economic feasibility of the concept will be questionable.

The design of reactive distillation columns is much more complex than the design of conventional columns. The most important design objective is to create the residence time required to ensure sufficient conversion, not to minimize investment by approaching a certain safety factor from flooding.

7.4 Fouling

Fouling is a major problem in industrial plants producing specialty chemicals. Fouling is the undesired formation and accumulation of deposits on surfaces (see Figure 7.8). It is a main factor for malfunction of vapor–liquid separation towers [43]. Deposits decrease the free cross-sectional area for vapor and liquid flow, which in turn increases gas velocity and pressure drop. A simultaneous loss of capacity and separation efficiency is observed. If deposition continues further, the tower is ultimately flooded. Fouling in reboilers and condensers may force changes in column

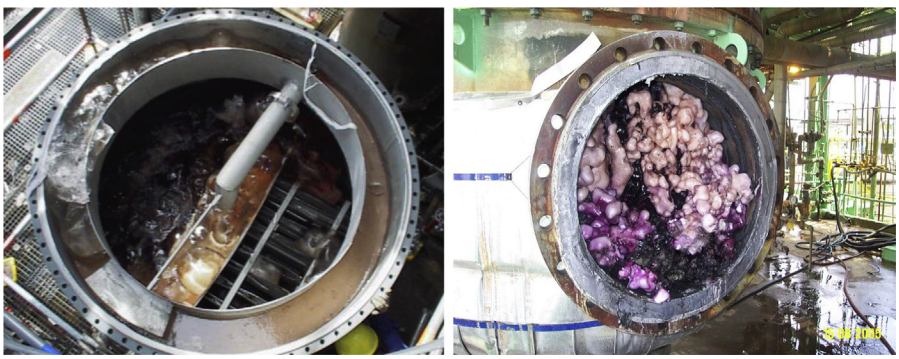

FIGURE 7.8

Severe fouling in liquid distributor (left) and man hole (right).

pressure to enable continued operation. To cope with fouling issues, plants are oversized, which leads to increased investment costs.

The mechanisms of fouling are still poorly understood. Fouling is a battle of adhesion and removal forces on surfaces and can hardly be predicted or calculated quantitatively. While fouling in heat exchangers has been studied extensively (e.g. [44]), little information is available on vapor−liquid separation systems.

Deposits on surfaces are based on chemical, physical, or biological mechanisms. According to Epstein [45], fouling mechanisms are classified as follows:

- Particulate or sedimentation fouling describes deposits of suspended solids, such as salts, metal oxides, catalyst particles, coke fines, or denaturated proteins. These suspended solids can settle out on surfaces. Sedimentation fouling is strongly influenced by changes of flow direction and velocity, which occur at sharp transitions and corners.
- In crystallization fouling, soluble substances begin to crystallize in a liquid when process conditions become supersaturated. Supersaturation is caused by the evaporation of solvents, cooling below/heating above the solubility limit, or a variation of pH. Crystallization usually starts at nucleation sites (active points) such as scratches or existing nuclei [46].
- In reaction fouling, a chemical reaction or corrosion occurs in the liquid phase or at the gas-liquid interface and causes deposition of solids, as slightly soluble products deposit on surfaces; (e.g. polymerization of monomers) [47].

In chemical plants, several fouling phenomena may occur in parallel or consecutively; they may influence each other and cannot be considered separately. If, for example, corrosion occurs, the increased surface roughness may promote other fouling mechanisms, whereas unstable corrosion layers may lead to particle fouling.

The economic impact of fouling is definitely not negligible. Fouling is responsible for increased pressure drop, reduced capacity, and frequent, often unscheduled downtime for cleaning. Additional costs comprise disposition of fouling wastes and replacement of plugged internals.

Many columns used in the chemical and petrochemical industries are prone to fouling [48]. Examples in specialty chemicals include columns in acrylonitrile production [49], beer stills in ethanol plants [50], separations of diolefins and specialty monomers, as well as downstream processing of bio-based feedstocks.

Different approaches exist to fight fouling in gas−liquid separation towers. Particulate fouling may be reduced by filtering solids before they enter the column [51]. If the solids cannot be separated, the internals have to be designed to cope with fouling. If the solids are created in the tower, possible approaches to avoid fouling are changing the operating conditions (pressure, temperature, pH) and the application of stabilizers to suppress polymerization accompanied by proper design of the column internals.

Mass transfer equipment can be designed to tolerate a certain degree of fouling if the governing fouling mechanisms have been identified. In any case, proper cleaning

strategies for fouled internals need to be derived and considered in the design of the hardware.

7.4.1 General considerations

Fouling is a complex interplay of the chemical system, material of construction, operating conditions (including pressure, temperature as well as vapor and liquid loads), and the specific geometry of the given internal. If a chemical system is prone to fouling, no design will ever be able to completely avoid it. Any strategy to minimize the effects of fouling therefore must consider the following elements:

- Avoid stagnant zones and fluid accumulation traps, which increase the local residence time and may result in the precipitation of solids and the build-up of polymers [52]. Typical stagnant zones in towers are in the corners of the tray decks, in downcomers, or inside manways.
- Backmixing and recirculation on column internals and in downcomers result in a broad distribution of residence time and favor the formation of by-products. In particular, by-products with higher molecular weights may precipitate and cause fouling problems.
- Sharp transitions and corners are areas where polymers and solids can be deposited, seed, and grow. Designs with a reduced number of edges and corners (macroscopic design) and smooth surfaces (microscopic design) contribute to increased fouling resistance [46]. Sharp flow changes may cause dewetting and lead to dry spots, which favor undesired polymerization reactions.
- Fouling reaction rates may be reduced by careful selection of operating conditions. Lower pressure and temperature generally are beneficial in reducing polymerization fouling, although they may promote crystallization fouling.
- Additives can help to suppress certain fouling mechanisms.

Internals selection in fouling services is always a tradeoff between fouling resistance and efficiency. Fouling-resistant internals such as grid packings or dual flow trays often show low separation efficiency. Trays are generally preferred when a pressure drop is not a concern. In many temperature-sensitive systems, however, pressure drop is critical and there is no alternative to structured packing. Selection of operating conditions is a key factor in avoiding fouling. Care must be taken to avoid undesired condensation on cold piping or heat exchanger surfaces.

A practical example shows the importance of operating conditions and process design to solve a fouling problem. In a trayed column, polymerization caused a significant increase of pressure drop and forced regular cleaning shutdowns. Polymer analytics showed that the deposits were polymers of a middle boiling component. Process simulation revealed that this middle boiler could accumulate only in the fouled column section because it contained too many separation stages. Reducing the number of trays and adjusting the reflux ratio helped to push the middle boiler into the overhead product and solved the fouling problem.

7.4.2 Antifouling agents

Polymerization fouling mostly follows radical mechanisms. To start polymerization fouling, both monomers and radical starters must be present at the same time. Consequently, additives to suppress fouling aim at removing the radical starters and can be grouped into antioxidants and radical catchers [53,54].

A problem-solving strategy for the successful application of additives therefore must answer the following questions:

- Where does the polymer deposit?
- What is the chemical composition of the polymer?
- Where do process conditions favor polymerization?
- Where are catalytically active sites?
- Where are the monomers formed and how does their concentration develop along the downstream units?
- Where is polymerization likely to start and/or where do starter molecules come into play?

Once these questions are answered by careful analysis of the process and the compounds involved, the selection of a suitable additive can be tackled. Inhibitor selection requires chemical expertise as well as knowledge about processes including fluid dynamics, operational experience, and reaction kinetics. Selection of antifouling agents is dependent on the kind of reaction to be suppressed, but the problem-solving process needs to cover further important points. Once a suitable additive is identified, it may be beneficial to test its performance in a lab. This may give valuable information on its effect on downstream operations. Within the process, the most effective location for injection must be determined. Note that most additives are high boilers and will leave a column with the bottoms product. An increasing concentration of additive will further inhibit the reaction at higher cost. Typically, some 5 to 500 wppm in the process stream gives the best cost-to-performance ratio.

Classical additives include derivatives of hydroquinone, which are applied in acrylic acid or (meth-)acrylic monomer production [53,55]. Hydroquinone, however, is mutagen and toxic, calls for elaborate procedures to ensure safe handling, and requires oxygen in the process fluid to be effective [56]. Hydroquinone monomethyl ether also requires oxygen for stabilization, but it is far less critical and therefore is used to stabilize acrylic acid during storage [55]. Parabenzoquinone is used in the production process of vinyl acetate [56]. Phenothiazine-based additives act as antipolymerants in acrylic acid or (meth-)acrylic monomer production [54,55]. A new family of additive working both as an antipolymerant and an antioxidant has recently been successfully applied in various processes including ethylene, butadiene, and styrene monomers and in the production of acrylonitrile, (meth-)acrylates, and vinyl acetate [57] (see Figure 7.9). In some cases, these additives also are able to remove preexisting insoluble deposits.

FIGURE 7.9

Valve tray after 8 months of operation without additive (left) and after 15 months of operation with additive (right).

At room temperature, most additives are solids and need to be dissolved for proper injection into the process stream. Reliable and safe application technology is required.

7.4.3 Trays

In fouling service, trays offer important advantages. They are more accessible and robust for cleaning, for example, by hydroblasting. Therefore, trays are preferred whenever the process conditions tolerate their higher pressure drop. Some general design guidelines can be derived:

- Elimination of inlet weirs prevents the accumulation of solids.
- Sloped downcomers minimize residence time and avoid stagnant zones.
- Push valves and bubble promoters cause fast aeration at the downcomer exit and can be designed to induce plug flow and reduce stagnant zones [48].
- The lateral vapor release of fixed valves can cause a sweep effect.
- Stepped and sloped outlet weirs enable the transport of solids from the active area. Sloped outlet weirs are less resistant to fouling but have higher flexibility compared to stepped weirs [48].
- Eletropolishing of surfaces is recommended because smooth surfaces shed deposits more easily.

To complement the points above, it is worth having a closer look on individual tray types. *Sieve trays* show limited resistance to fouling [58]. Fouling often starts at the lower edge of the hole because of high gas velocity in combination with low liquid flow rates, resulting in the concentration of high boilers and the formation of deposits. Weeping causes a washing effect [59], and large hole diameters are highly beneficial [58]. However, sieve trays did not rank high in an experimental study of crystallization fouling that compared many tray and packing types [46].

In *dual flow trays*, liquid and vapor pass through the same holes as countercurrents or in an alternating fashion. This exploits the self-cleaning effects mentioned above. There are no downcomers and weirs, and the inherently strong weeping of liquid reduces the formation of dry spots and deposits. The washing effect of weeping liquid is maximized and may even flush solids from the underside of the tray. However, once fouling occurs, it reduces the hole size and causes liquid backup on the tray. In severe fouling, service trays with open areas of up to 50% are used. The efficiency of dual flow trays is low because there is little holdup and basically complete backmixing. Shed decks, disc and donut trays, and baffle trays show the highest resistance to fouling at the lowest efficiency.

On *valve trays*, fixed and moveable valves are used. If they are operated at partial opening, movable valves can have a self-cleaning effect [46]. In practice, a wide operating range has to be covered, and fixed valves have been used to successfully revamp sieve and moveable valve trays [49,50]. The suitability of moveable valves in fouling service is unclear, and conflicting recommendations can be found in the literature [60,52].

7.4.4 Packings and liquid distributors

In quenching columns and in petrochemical plants, use of large-size random packing or grid packing is well established. In special chemistry, the use of packings in fouling services is generally restricted to applications where a pressure drop is crucial. In spite of its obvious drawbacks and conflicting recommendations [61], structured packing is preferred over random packing because it offers the lowest pressure drop per theoretical stage and achieves the lowest bottoms temperature for a given number of stages.

Distributor design must be adapted to improve resistance to fouling. Sedimentation should be prevented by avoiding low flow velocities and high residence times. Therefore, larger orifices, lower drip point density, ground holes, and high lateral velocities in troughs are advantageous. Ground holes are preferred over lateral holes to avoid sedimentation in the troughs and allow the passage of small particles. The use of pan-type distributors is discouraged, whereas V-notch distributors have been successfully applied even in severely fouling services [52]. In all designs, simplicity is beneficial, following the simple rule: “If it’s not in the tower, it cannot contribute to fouling.”

Besides loss of production and cleaning cost, fouling in structured packing may cause a safety risk if the deposits are pyrophoric or easily ignited. Once a fouling layer is ignited, for example, by hot work during turnarounds, it can ignite the packing metal, which can be a combustion fuel itself. The combustibility of structured packing is high because of its high surface-to-volume ratio; the thin material does not dissipate the heat [62]. Fouling layers may form unnoticed because structured packing is hard to inspect and to clean. At least 56 incidents of structured packing fires have been reported. They occurred mostly in turnarounds, when the columns

were open to atmosphere and hot work was done [63]. An excellent overview of packing fires is given by the Design Practices Committee of FRI [62].

7.5 Aqueous systems

7.5.1 Aqueous systems: properties and efficiencies

Water is omnipresent in specialty chemicals process plants. Water is present at least at trace levels in both petrochemical and green feedstocks, and it frequently is a by-product in esterification, condensation, and oxidation reactions. Water has extraordinary properties including high enthalpy of vaporization and heat capacity. It is chemically inert, nontoxic, not inflammable, and shows good solubility for many functionalized molecules. These properties make water an excellent solvent in many reactions and an excellent cooling medium in quenching towers. In modern processes for the production of propylene oxide [64], hydrogen peroxide is used as an oxidation agent and water is a by-product, which is separated by distillation.

The thermodynamic properties of water-organic mixtures are not ideal. Activity coefficients are often large enough to cause splitting in two liquid phases. If water forms heteroazeotropes, it may be removed in condensate drums equipped with water boots or in intermediate decanters. Marangoni instabilities caused by the strong dependence of surface tension on concentration may cause film rupture, spray formation, and foaming in columns [65]. As an example, Figure 7.10 shows the strong increase of surface tension in water-alcohol mixtures as a function of water concentration at 298 K and 323 K [66]. Note the strong effect of 200 ppm of surfactant at 298 K at water concentrations above 70 mol% [67]. Other physical properties show

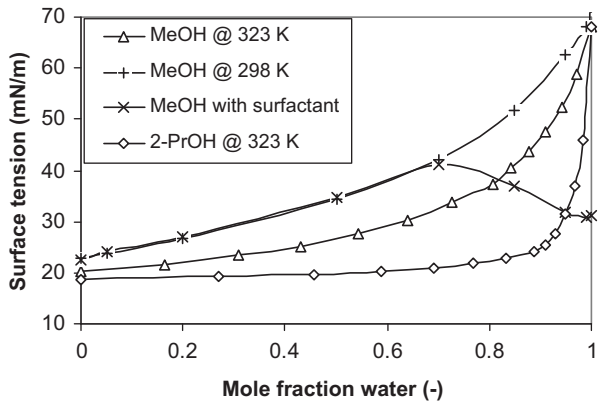

FIGURE 7.10

Surface tension of aqueous mixtures: methanol with surfactant, methanol at 298 and 323 K, and 2-propanol at 323 K.

similar nonideal mixture effects, making modeling of aqueous mixtures quite demanding.

The separation efficiency in aqueous mixtures has been the subject of many studies (see e.g. [23,68–73]). It depends on water concentration and can differ greatly from efficiencies measured in standard test systems. In packed columns, efficiency is expressed in terms of the HETP. From two-film theory, it follows that:

$$\mathrm{HETP} = (h_{\mathrm{VTU}} + \lambda h_{\mathrm{LTU}}) \frac{\ln(\lambda)}{\lambda - 1} \tag{7.7}$$

where λ is the ratio of the slopes of the equilibrium line m and the operating line L/V and h_{VTU} and h_{LTU} are the heights of vapor and liquid-side transfer units, defined by the respective superficial velocities (meters/second) mass-transfer coefficients (meters/second), and the effective area (meters squared/meters cubed):

$$\lambda = \frac{m}{\mathrm{L/V}}; \quad H_{\mathrm{V}} = \frac{u_{\mathrm{V}}}{k_{\mathrm{V}} a_{\mathrm{e}}} \quad H_{\mathrm{L}} = \frac{u_{\mathrm{L}}}{k_{\mathrm{L}} a_{\mathrm{e}}} \tag{7.8}$$

Figure 7.11 shows the effect of nonideal VLE data on HETP. In Figure 7.11(a), the slope of the equilibrium line of methanol-water at 1 bar (10^5 Pa) is compared to an ideal mixture of relative volatility $\alpha = 1.1$. In the limiting cases of low boiler concentrations of 0 and 1, the slope has the values α and $1/\alpha$. For the ideal mixture, the slope changes from 1.1 to 0.91, whereas it changes from 7.6 to 0.77 in an aqueous system. HETP values are computed for both systems, assuming constant values of $h_{\mathrm{VTU}} = 250$ mm and $h_{\mathrm{LTU}} = 80$ mm. As Figure 7.11(b) shows, the HETP of the ideal

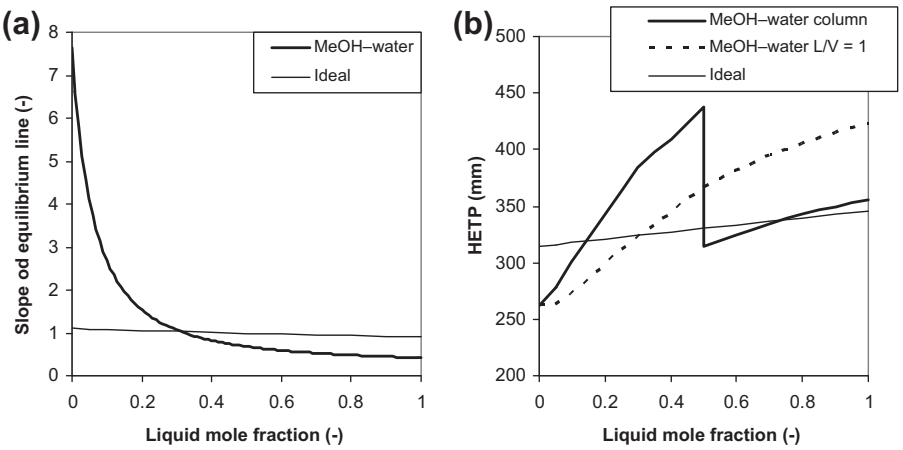

FIGURE 7.11

Slope m of the equilibrium line and height equivalent of theoretical plate (HETP) resulting for constant heights of liquid and vapor transfer units. Infinite reflux is assumed in both cases. In addition, the methanol–water case is evaluated with values for the operating line L/V typical in a distillation column (1.8 in the stripping and 0.56 in the rectifying section).

system is constant, whereas it changes from 260 up to 440 mm in the aqueous system.

There is currently no widely accepted model to predict packing efficiency [24]. In the example shown above, the only difference between the HETP curves is the nonideal VLE of methanol-water and the reflux ratio. In reality, the mass transfer coefficients and, most importantly, the effective area are functions of packing type, operating variables, and mixture properties (e.g. densities, diffusivities, viscosities, and surface tension). As shown in Figure 7.10, all properties in aqueous systems are strong nonlinear functions of mixture composition. The difficulties in predicting the mixing rules increase still further the margin of error inherent in HETP models. These uncertainties also affect the predictive power of mass-transfer models. Similar arguments can be made for predicting tray efficiency. In trays, however, vapor and liquid phases are well mixed before entering each stage, interphase area is effectively created in the froth, and maldistribution and wettability are not an issue. Therefore, trays often are preferred in aqueous systems, even if the pressure drop per theoretical stage can be an order of magnitude higher than in packings. Recently, however, a new hybrid of gauze and sheet metal packing has been marketed with custom-made distributors specifically designed for low liquid load in aqueous applications [74].

7.5.2 Quenching towers

Many reactions in special chemistry are conducted at elevated temperature (e.g. oxidation reactions). If the products are very reactive then fast cooling, condensation/absorption, and dilution in an inert solvent is essential. A typical example of a quenching column is shown in Figure 7.12. Hot gas is fed to the bottom of the column and contacted with a water-rich pump-around in a packed bed. In the bed, the hot gas is cooled to saturation temperature by intimate contact with and evaporation of the cooling liquid. In many cases several pump-arounds with different cooling media such as air, water, or brine are applied to improve separation and utility cost. In the upper part there is often a further absorption section at a substantially lower liquid load. The bottom product contains the reaction product in aqueous solution and is removed for further downstream treatment.

Liquid load is generally rather high at 20–80 m^3/m^2 h. In older designs, simple, fouling-resistant trays such as baffle trays were specified. These can be revamped with random and structured packing to reduce pressure drop or increase capacity [75–79].

In our example, hot nitrogen is fed to the quenching column at 493 K and cooled by a pump-around of water cooled to 291 K in an external heat exchanger (see Figure 7.12). Simulation results show the shortcomings of equilibrium-based models, where the gas temperature reaches equilibrium in the first stage. Rate-based models, on the other hand, are able to account for heat transfer kinetics, model the real gas temperature profile in column, and give information on required packing height. The F-factor in the rate-based model closely follows gas temperature and

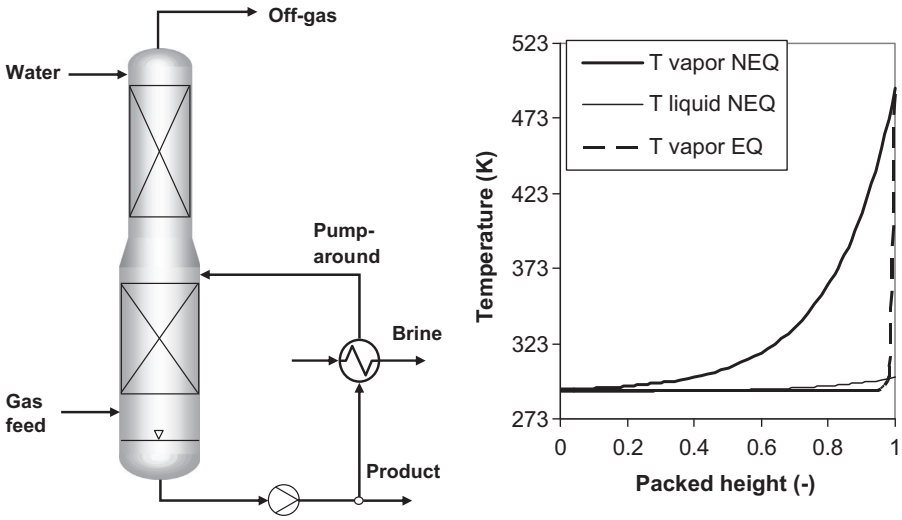

FIGURE 7.12

Flowsheet of a typical quenching column (left) and gas and liquid temperatures (right) calculated by rate-based (no equilibrium (NEQ)) and equilibrium (EQ) models.

decreases as water evaporates into the gas stream. In the equilibrium model the maximum F-factor is seen only in the vapor flow entering lowest stage. If a spray were modeled, complete desuperheating would have already occured when the vapor flow enters. Consequently, the flooding factor calculated with the rate-based profiles for a given packing is about 10% higher. However, even results from rate-based models must be handled with care because there is no proven way of predicting heat transfer coefficients and effective area in aqueous systems.

7.5.3 Foaming in columns

If foaming occurs in fractionation towers, their capacity and efficiency can be reduced considerably. Foam is stabilized in surface tension-positive systems, where the surface tension increases as the liquid flows down the column [68]. A number of foaming indices have been defined based on this observation, all of which incorporate the surface tension gradient $d\sigma/dx$ along the column axis [80]. Prediction of surface tension gradients, however, is anything but easy or reliable: As the data in Figure 7.11 shows, even small concentrations of possibly unknown active surface components may even change its sign. Systems in which the formation of a second liquid phase is imminent have a very high foaming tendency (Ross-type foaming). Once the second liquid phase occurs, it works as a defoaming agent [81]. Foaming frequently occurs in some services, whereas is not observed in others. In the overview given by Kister [60], absorbers using aqueous solutions of high-boiling solvents and extractive distillation columns rank highest.

Once foam appears, it forms a third phase in the column, with considerable flow resistance. Its presence reduces the free area for vapor flow. Pressure drop and backmixing are increased, while efficiency is reduced.

At low shear-stress, foam deforms elastically like a solid. Once a certain yield stress is reached, bubbles rearrange and foam flows like a liquid—albeit one of very low density. Liquid holdup in foams decreases over time (drainage) and bubbles coalesce (coarsening) by sudden film rupture [82]. These processes are fundamentally different in absorption and distillation. Because of the limited solubility of inert gases in liquid films, coarsening is slower and foaming occurs more often in absorption service. In special chemistry distillation, foaming problems mainly arise from small particles in the feed and surface active agents, whose concentration may change over time as catalysts are deactivated or may accumulate over time if they are middle boilers. The effects of foaming generally increase with vapor load. Foaming can be detected by sudden changes and large fluctuations in pressure drop and by suddenly decreasing separation efficiency.

The most important countermeasure is the early detection of the foaming tendency during process design. A number of test cells are known. In the Bikerman test, the liquid is aerated by nitrogen and the height of the foam layer is related to the gas flow rate. The test is simple but of limited use for process industries [83]. First, foaming in liquid nitrogen systems is very different from foaming in vapor–liquid distillation systems. Furthermore, foam coarsening can be expected to be slower in process equipment, where a constant supply of fresh liquid is available as reflux. These observations have led to the development of new test cells, in which packing elements can be placed under constant irrigation, while vapor can be supplied by either heating the process liquid or using an inert gas [83,84].

Foaming is not really predictable. It may be caused by minor amounts of surface active agents, which can be present in one plant but absent in another [85]. Furthermore, it may originate in different locations inside the column, for example, in the reboiler circuit, at the distributor in the packings, or on the trays. It is highly recommended to closely inspect pilot plant data. However, these data often are of limited use because liquid and gas loads generally do not reach the values of industrial plants.

Once a potential foaming problem is identified, the only known design strategy is the application of system factors, which are fitted to industrial data for certain systems. For a number of accepted values, see the compilation by Lockett [80]. They are used to de-rate allowable jet flood and downcomer flooding factors but give no insight into the consequences of foaming inside the column, such as changes in pressure drop. Downcomer rating equations proven in hydrocarbon systems often give rather small downcomer sizes in aqueous systems. Great care should be applied here if surface active traces are suspected in the feed. Oversizing small downcomers will only marginally increase total cost but may give some safety against foaming.

There is no clear ranking of which internals are best suited to cope with foaming. Some experts prefer random packing. Structured packing, however, may give the best tradeoff between capacity and efficiency. Some experts recommend

unperforated packing. In trays, larger open areas, larger perforations, and lower hole gas velocities may be of advantage [86].

Defoaming agents will be able to solve most foaming problems. Besides continuing cost, defoamers contaminate the bottoms product, and an additional process step may be required to remove them. Defoamers must be carefully selected in laboratory tests.

In a practical example from the author's experience, Ross-type foaming occurred when a small aqueous flow rate was fed on a tray separating an organic mixture. Although the overall mass balance predicted complete solubility, the point-wise feed via a single nozzle caused a local concentration range near the liquid–liquid phase split. The problem was solved by properly mixing the feed with internal reflux before feeding it on the tray.

7.5.4 Three-phase systems

As long as water is homogeneously dissolved in the organic liquid phase, its presence is of little consequence [87]. Many separations in special chemistry even exploit the tendency of water to form (hetero)azeotropes. Hydrocarbons such as hexane or toluene often are used as entrainers to remove water from aqueous solutions. In some cases, it is beneficial to withdraw the liquid from a column, cool it, force a liquid–liquid phase split in a decanter, remove the aqueous phase, and recycle the organic phase. Furthermore, water may be useful to reduce the boiling point of temperature-sensitive components in deep vacuum columns [87]. The foaming tendency of mixtures nearing the liquid–liquid phase split has already been noted [81] and shown experimentally [88].

On trays, the violent vapor–liquid action ensures efficient interaction of both liquid phases and tray design can follow the usual path [89]. In another study, mass transfer rates were somewhat decreased because of liquid–liquid mass transfer resistance [90].

If heterogeneous water falls to the hot bottom of a vacuum column, it may evaporate rather explosively. Strong oscillations in pressure drop and premature flooding have been reported as a consequence [87]. In one well-documented case even plate damage resulted [91].

In packed towers, the situation is much more complex. Recently, great progress in closing the knowledge gap has been made; see the overview given by Chen et al. [92]. Compared to two-phase operation, the existence of a second liquid phase may increase or decrease mass transfer efficiency or even leave it constant. Individual effective areas for the two liquid phases may be increased or decreased. This mainly depends on the flow characteristics on the packing; for example, one liquid phase may overflow the other and shield it from contact with the gas phase. Mass transfer coefficients and correlations for effective areas are given by Chen et al. [92], and a detailed investigation of three-phase flow on inclined plates by experiments and CFD simulation is given by Hoffmann et al. [93].

In an industrial case study, the design of a column equipped with random packing is reported by Harrison [94]. Pressure drop could be well described with two-phase models, and HETP exceeded expectations by about 40%. If one phase preferentially wets the packing, the residence time of the nonwetting phase may be reduced because of lower relative holdup. Because of the apparent problem of equally distributing each of two liquid phases, avoiding redistribution and going for longer packed beds is suggested. If redistribution cannot be avoided, the use of ground holes is discouraged because they offer no chance to build up an independent layer of heavy phase necessary for its forced distribution. A special distributor design with individual overflow slots for both phases and reduced drip point density is presented.

A further industrial case study is presented by Meier et al. [95]. In spite of the difficulties in parameterization, the use of rate-based models is suggested to plan pilot plant experiments that in turn can be used to tune the model. To facilitate scale-up, using the same packing in experiments and in the technical scale is recommended. Calculating pressure drop using a modified Stichlmair approach [96] and considering a higher liquid holdup, which consists of the addition of both individual liquid streams, shows a good agreement with measurements on a technical scale column (see Figure 7.13).

Distributor design is closely investigated. It has been shown that the liquid phases will probably not completely separate in the distributor troughs and a cloudy layer will be present. Therefore, a three-stage design offers the chance to distribute the heavy and light phases through the lower and upper orifices, whereas the cloudy layer may flow through the middle orifice. Figure 7.14(a) shows a photograph of a four-stage distributor.

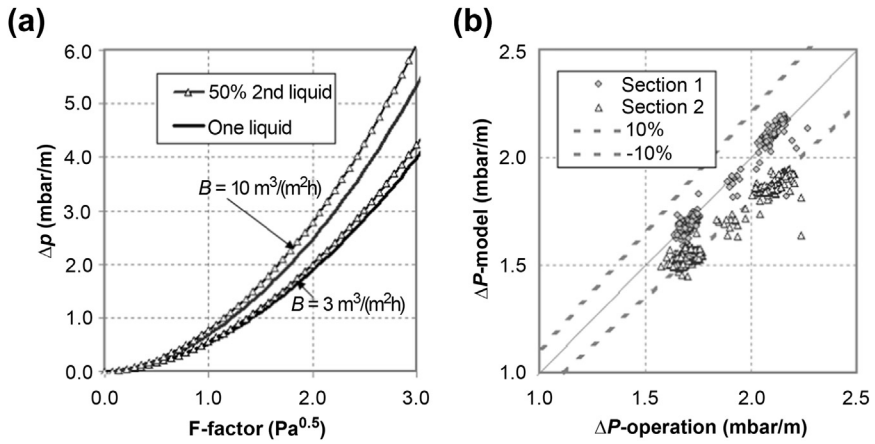

FIGURE 7.13 Pressure Drop Calculations of a Gauze Packing (500 m^2/m^3) Using a Modified Stichmair Approach [95].

(a) Comparison with one or two liquids. (b) Comparison of the model with plant data.

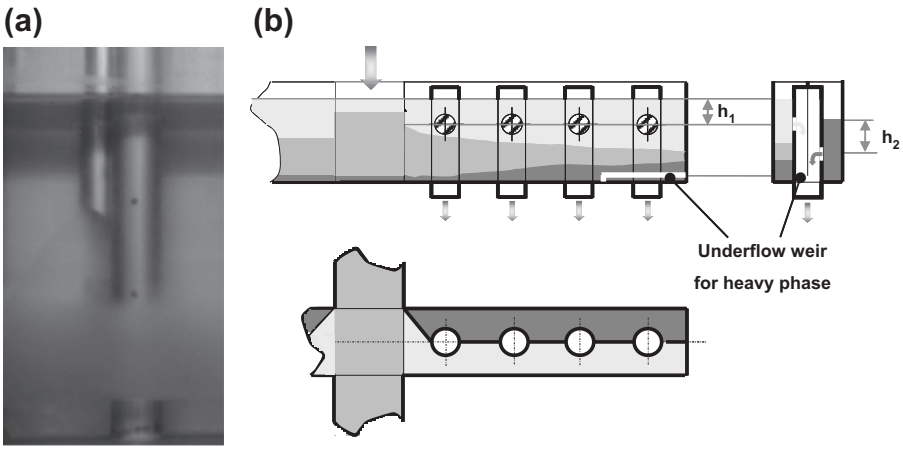

FIGURE 7.14 Distributors for Three-Phase Columns.

(a) Photograph of a four-stage drip tube. Two orifices are in the light phase. (b) Distributor with targeted phase separation and independent distribution [97].

A distributor specially designed for two liquid phases is presented in Ref. [97] (see Figure 7.14(b)). Mixed-phase liquid is distributed to the troughs through a parting box with low residence time. In the individual troughs, residence time is large enough to separate the heavy and light phases from the cloudy layer. Heavy phase flows through an underflow weir to one side of the trough and flows to the packing via its own designated orifices. The light phase stays on the other side of the trough and flows through dedicated orifices. The height and size of orifices can be individually designed according to the required flow rates and residence times.

7.6 Modeling, simulation, and scale-up: a conclusion

Many specialty chemicals are rather complex molecules and have a comparatively short life cycle. Time to market is often one of the most important aspects, and process development must then be performed based on minimal information and data. Variable costs are often dominated by raw materials, and overall process yield has the greatest effect on process economics.

Column configuration (number of stages, feed location, and reflux ratio) can be determined using simulations with equilibrium models. VLE data are available in the literature and data banks, can be estimated, or must be collected experimentally to ensure sufficient accuracy. The next design step is concerned with the physical dimensions (diameter and height). Here, parameters such as allowable pressure drop, flooding factor, load range, and efficiency come into play. To estimate efficiency, industrial data from similar separation problems are valuable. Different models for HETP or tray efficiency are published and may also be used in

rate-based models to challenge the results from equilibrium models. Additional information about transport properties and mass transfer area is required.

As has been illustrated in the previous sections, the well-known methods for distillation hydraulics and efficiency offer a sound basis for column design. However, we have shown that many designs in special chemistry are outside of the established parameter ranges of these models. Examples are extremely low liquid loads and fouling or foaming systems, where efficiency and capacity may change over time, and reactive distillation, where the accurate prediction of the concentration profiles and holdup is crucial. Furthermore, product specifications often include very high purities, down to the parts per million or parts per billion level, or secondary qualities such as viscosity, color (number), flavor, or (absence of) odor. Despite the high standard of commercial simulation tools, some uncertainties remain in any theoretical design, and laboratory-scale experiments are of decisive importance to ensure a reliable result. Experiments, however, are time consuming and cost intensive. Modifications of laboratory equipment should therefore be largely excluded by carefully designing the experimental setup using the best available model. Experimental data should in turn be used to validate and continuously improve the model. The outlined interplay of modeling and experiment is most beneficial to speed up process design.

In laboratory experiments, standardized hardware is used. The column diameter is to be as small as possible to reduce the quantity of feed material required. On the other hand, diameters should be 50 mm or larger to limit wall effects [98−100]. Heat loss causes condensation and increases the local reflux ratio as the liquid travels down the column, whereas efficiency is impaired by wall flow. Vacuum tightness is important to limit the loss of light boilers to the vacuum system and because oxygen in the invading air may promote polymerization or product degradation.

Column internals should provide constant efficiency independent of load. For vacuum operation, excellent results have been obtained with Rombopak, a lamella-type packing, which is quite similar to sheet metal packing [98−100]. As an alternative, gauze laboratory packing with surface areas up to 1000 m^2/m^3 is available from different vendors. Gauze laboratory packing offers more theoretical stages than Rombopak, which reduces column height. Its efficiency is, however, more dependent on liquid and vapor load. All laboratory packings are delicate structures requiring careful handling and installation to avoid damage. Bubble caps offer a large turndown ratio and can be operated at extremely low liquid loads. Separation efficiency of these internals is calibrated with test systems in terms of HETP or tray efficiency.

To run the experiment, the available hardware needs to be adapted to the specific requirements of the separation at hand. The exact setup of the laboratory hardware is determined by simulation using the best model and VLE data. Feed material should be as close to as possible to real case because synthetic feed mixtures have a different trace component spectrum. Furthermore, it is often difficult to provide feed material in sufficient quantities for a test distillation run. In early development stages, often no pure substances are available for, for instance, vapor pressure measurements.

Regarding the operation of laboratory columns, time to steady state may generally be rather long. Arrival at steady-state conditions needs to be carefully and critically evaluated since very high concentrations of especially middle boilers in multicomponent mixtures can build up inside the column. In one example from the authors' experience, a miniplant column (diameter 50 mm; 10 m structured packing) did not reach steady-state conditions after 4 days of operation, although the temperature profile was constant. A middle-boiling component with a concentration of a few parts per million in the feed accumulated to more than 10 w% inside the column. Therefore constant operation is beneficial.

Another important result of a laboratory experiment is the real separation efficiency, which may differ widely from the one measured in test systems. The real HETP or tray efficiency can be estimated with reasonable accuracy by simulating the experiment and fitting the number of stages. Because product purity in specialty chemicals is typically very high, efficiency data cannot be estimated from product purities alone but requires sampling and fitting of temperature and composition profiles along the column. A simulation model validated by this procedure may be used with some confidence to further optimize process and column design. For further details concerning scale-up, see [101] (Book on Distillation (Book 2), Equipment and Processes).

Distillation in specialty chemistry covers all operating ranges, from deep vacuum to high pressure, and from extremely low to rather high liquid loads. The dynamic markets demand fast changes in both product purity and quantity, which force frequent revamps of existing plants. Almost all internals available on the market are used, from gauze packing to high-capacity trays. In many cases, however, standard solutions do not meet the strict requirements, and tailor-made designs are essential. To summarize, specialty chemistry is an exciting field, offering a wide variety of challenging problems for creative distillation designers.

References

[1] Sulcol 3.0, http://www.sulzer.com/de/Resources/Online-Tools/Sulcol.

[2] R. Schmidt, The lower capacity limit of packed columns, IChemE Symp. Ser. 56 2 (1979) 3.1/1−3.1/14.

[3] M.G. Shi, A. Mersmann, Effective interfacial area in packed columns, Ger. Chem. Eng. 8 (1985) 87−96.

[4] K.R. Morison, Q.A.G. Worth, N.P. O'Dea, Minimum wetting and distribution rates in falling film evaporators, Trans. IChemE Part C Food Bioproducts Process. 84 (2006) 302−310.

[5] D.E. Hartley, W. Murgatroyd, Criteria for the break-up of thin liquid layers lowing isothermally over solid surfaces, Int. J. Heat Mass Transfer 7 (1964) 1003−1015.

[6] F.F. Simon, Y.Y. Hsu, Effect of Contact Angle Hysteresis on Moving Liquid Film Integrity, NASA TM X-68071, 1972, www.nasa.gov.

[7] J. Bico, U. Thiele, D. Quéré, Wetting of textured surfaces, Colloids Surf. A Physicochem. Eng. Asp. 206 (2002) 41–46.
[8] E.M.A. Nicolaiewsky, F.W. Tavares, K. Rajagopal, J.R. Fair, Liquid film flow and area generation in structured packed columns, Powder Technol. 104 (1999) 84–94.
[9] P. Valluri, O.K. Matar, G.F. Hewitt, M.A. Mendes, Thin film flow over packings at moderate Reynolds numbers, Chem. Eng. Sci. 60 (2005) 1965–1975.
[10] X.C. Zhou, X.G. Yuan, L.T. Fan, A.W. Zeng, K.T. Yu, M. Klabassi, et al., Experimental study on contact angle of ethanol and *n*-propanol aqueous solutions on metal surfaces, in: A.B. de Haan, H. Kooijman, A. Gorak (Eds.), Distillation and Absorption, 2010, pp. 359–364.
[11] M. Kohrt, I. Ausner, G. Wozny, J.-U. Repke, Texture influence on liquid-side mass-transfer, Chem. Eng. Res. Des. 89 (2011) 1405–1413.
[12] K.J. Hüttinger, H. Rudi, Hydrophilic PVDF random packing, Chem. Ing. Tech. 55 (11) (1983) 867–869 (in German).
[13] S. Böcker, G. Ronge, Distillation of viscous systems, Chem. Eng. Technol. 28 (2005) 25–28.
[14] M. Schultes, W. Grosshans, S. Müller, M. Rink, All the mod cons Part 1, Hydrocarbon Eng. (January 2009).
[15] L. Spiegel, A new method to assess liquid distributor quality, Chem. Eng. Process. 45 (2006) 1011–1017.
[16] F. Moore, F. Rukovena, Liquid and Gas Distribution in Packed Towers, CPP Edition, Europe, August 1987, 11–15.
[17] J.G. Kunesh, L.L. Lahm, T. Yanagi, Controlled maldistribution studies on random packing at a commercial scale, IChemE Symp. Ser. 104 (1987) A233–244.
[18] J.F. Billingham, D.P. Bonaquist, M.J. Lockett, Characterization of the performance of packed column liquid distributors, IChemE Symp. Ser. 104 (1997) 841–851.
[19] D.E. Nutter, A. Hale, Liquid distribution for optimum packing performance, Chem. Eng. Prog. (January 1990) 30–35.
[20] A. Rix, Z. Olujic, Pressure drop of internals for packed columns, Chem. Eng. Process. 47 (2008) 1520–1529.
[21] D.R. Summers, A.W. Sloley, Tray Design at Low Liquid Load Conditions, AIChE Spring Meeting, Orlando, 2006.
[22] E. Kirschbaum, Destillier- und Rektifiziertechnik, second ed., Springer Verlag, Berlin, 1950.
[23] N.S. Yang, K.T. Chuang, A. Afacan, M.R. Resetarits, M.J. Binkley, Improving the efficiency and capacity of methanol-water distillation trays, Ind. Eng. Chem. Res. 42 (2003) 6601–6606.
[24] J.G. Stichlmair, J.R. Fair, Distillation. Principles and Practice, Wiley-VCH, New York, 1998.
[25] M.J. Lockett, The froth to spray transition on sieve trays, Trans. IChemE 59 (1981) 26–34.
[26] T. Keller, Reactive Distillation, in: Górak (Ed.), Distillation: Equipment and Processes, (Chapter 8), Elsevier, Amsterdam, 2014, pp. 305–355.
[27] R. Krishna, Hardware selection and design aspects for reactive distillation columns, in: K. Sundmacher, A. Kienle (Eds.), Reactive Distillation, 2003, pp. 169–189.
[28] P. Moritz, Scale-up der Reaktivdestillation mit Sulzer Katapak-S, Shaker-Verlag, Aachen, 2002 (in German).

[29] J.L. deGarmo, V.N. Parulekar, V. Pinjala, Consider reactive distillation, Chem. Eng. Prog. 88 (3) (1992) 43–50.
[30] T. Frey, F. Nierlich, T. Pöpken, D. Reusch, J. Stichlmair, Application of reactive distillation and strategies in process design, in: K. Sundmacher, A. Kienle (Eds.), Reactive Distillation, 2003, pp. 49–61.
[31] M. Behrens, Z. Olujic, P.J. Jansens, Combining reaction with distillation hydrodynamic and mass transfer characteristics of modular structured packings, Chem. Eng. Res. Des. 84 (2006) 381–389.
[32] P. Moritz, H. Hasse, Fluid dynamics in reactive distillation packing Katapak®-s, Chem. Eng. Sci. 54 (1999) 1367–1374.
[33] Z. Olujic, Personal communication, 2002.
[34] M. Winterberg, E. Schulte-Körne, U. Peters, F. Nierlich, Methyl *tert*-butyl-ether, in: Ullmann's Encyclopedia of Industrial Chemistry, 2012.
[35] G.R. Gildert, K. Rock, T. McGuirk, Advances in Process Technology through Catalytic Distillation, http://www.cdtech.com/updates/publications.
[36] C. von Scala, L. Götze, P. Moritz, Acetate technology using reactive distillation, Sulzer Tech. Rev. 3 (2001) 12–15.
[37] T. Keller, A. Górak, Modelling of homogeneously catalysed reactive distillation processes in packed columns: experimental model validation, Comp. Chem. Eng. 48 (2013) 74–88.
[38] T. Dörhöfer, Gestaltung und Effektivität von Bodenkolonnen für die Reaktivdestillation, Verlag Dr. Hut, München, 2006 (in German).
[39] H.F. Haug, Stability of sieve trays with high overflow weirs, Chem. Eng. Sci. 31 (1976) 295–307.
[40] R. Krishna, J.M. van Baten, J. Ellenberger, A.P. Higler, R. Taylor, Chem. Eng. Res. Des. 77 (1999) 639–646.
[41] K.S. Fisher, G.T. Rochelle, Effect of mixing on efficiencies for reactive tray contactors, AIChE J. 48 (2002) 2537–2544.
[42] R. Baur, R. Krishna, Distillation column with reactive pump arounds: an alternative to reactive distillation, Chem. Eng. Process. 43 (2004) 435–445.
[43] H. Kister, What Caused Tower Malfunctions in the Last 50 Years? Distillation & Absorption, Baden-Baden, 2002.
[44] L.F. Bott, Fouling of Heat Exchangers, Elsevier, Dordrecht, 1995.
[45] N. Epstein, Thinking about heat transfer fouling: a 55 matrix, Heat Transfer Eng. 4 (1983) 43.
[46] D. Großerichter, Fouling in Boden- und Packungskolonnen für Gas-Flüssig-Systeme, (dissertation), Shaker-verlag, Aachen, 2004.
[47] A.P. Watkinson, D.I. Wilson, Chemical reaction fouling: a review, Exp. Therm. Fluid Sci. 14 (1997) 361–374.
[48] G. Mosca, E. Tacchini, J. Chandrakant, De-bottlenecking an ACN Heads & Dry Column with VG AF (V-grid Anti Fouling) Trays, AIChE Annual Meeting, San Francisco, 2006.
[49] G. Mosca, E. Tacchini, Keep the trays clean–a step ahead in distillation technology, Sulzer Tech. Rev. 3+4 (2005) 22–25.
[50] D. Summers, Experiences in Severe Fouling Service, AIChE Spring Meeting, New Orleans, 2008.
[51] A.W. Sloley, G.R. Martin, Subdue solids in towers, Chem. Eng. Progr 91 (1995) 64–73.

[52] K. Kolmetz, A.W. Sloley, T.M. Zygula, W.K. Ng, P.W. Faesseler, Design guidelines for distillation columns in fouling service, in: The 16th Ethylene Producers Conference, New Orleans, 2004.
[53] W. Kurze, F. Raschig, Antioxidantien, in: Ullmann's Encyclopedia of Technica Chemistry, vol. 8, VCH, Weinheim, 1975, pp. 19–45.
[54] U. Hörlein, Phenothiazin, in: Ullmann's Encyclopedia of Technica Chemistry, vol. 8, VCH, Weinheim, 1975, pp. 259–268.
[55] H. Becker, Polymerisationsinhibierung von (meth-)acrylaten–stabilisator- und sauerstoffverbrauch, (Dissertation), 2003.
[56] D.A. Foster, A.R. Syrinek, J.P. Street, F. Hisbergues, Tackling fouling in vinyl monomer manufacture, Pet. Technol. Q. (Summer 2003).
[57] SiYProTM–performance additives, simplify your process with our antifoulants for monomer production, brochure, http://www.siypro.com/sites/dc/Downloadcenter/Evonik/Product/SiYPro/081201_SiYPro_DINA4_H2_E_final.pdf.
[58] H.Z. Kister, Distillation Design, McGraw-Hill, New York, 1992.
[59] G.X. Chen, A. Afacan, K.T. Chuang, Fouling of sieve trays, Chem. Eng. Comm. 131 (1995) 97–114.
[60] H.Z. Kister, Distillation Operation, McGraw Hill, New York, 1990.
[61] R. Hauser, J. Richardson, Prevent plugging in stripping columns, Hydrocarbon Process. (September 2000) 95–98.
[62] Design Practices Committee, Fractionation Research Inc, Causes and prevention of packing fires, Chem. Eng. (July 2007) 34–42.
[63] M.K. O'Connor Process Safety Center, Best Practice in Prevention and Suppression of Metal Packing Fires, August 2003. http://kolmetz.com/pdf/articles/MetalFires.pdf.
[64] Propylene oxide: the Evonik-Uhde HPPO technology, ThyssenKrupp Uhde Technical bulletin, http://www.thyssenkrupp-uhde.de/en/publications/brochures.html.
[65] S.J. Proctor, M.W. Biddulph, K.R. Krishnamurthy, Effects of Marangoni surface tension forces on modern distillation packings, AIChE J. 44 (1998) 831–835.
[66] G. Vázqez, E. Alvarez, J.M. Navaza, Surface tension of alcohol + water from 20 °C to 50 °C, J. Chem. Eng. Data 40 (1995) 611–614.
[67] G.X. Chen, T.J. Cai, K.T. Chuang, A. Afacan, Foaming effect on random packing performance, Chem. Eng. Res. Des. 85 (A2) (2007) 278–282.
[68] F.J. Zuiderweg, A. Harmens, The influence of surface phenomena on the performance of distillation columns, Chem. Eng. Sci. 9 (1958) 89–103.
[69] M.J. Lockett, I.S. Ahmed, Tray and point efficiencies from a 0.6 meter diameter distillation column, Chem. Eng. Res. Des. 61 (1983) 110–118.
[70] T.D. Koshy, F. Rukovena, Reflux and surface tension effects on distillation, Hydrocarbon Process. (May 1986) 64–66.
[71] S.R. Syeda, A. Afacan, K.T. Chuang, Effect of surface tension gradient on froth stabilization and tray efficiency, Chem. Eng. Res. Des. 82 (A6) (2004) 762–769.
[72] M. Caraucán, A. Pfenning, Efficiency in the distillation of aqueous systems, in: International Conference on Distillation and Absorption, Baden-Baden, 2002.
[73] M.W. Biddulph, M.A. Kalbasi, Distillation efficiencies for methanol/1-propanol/water, Ind. Eng. Chem. Res. 27 (1988) 2127–2135.
[74] J. Rauber, A new system solution for challenging separation processes, Sulzer Tech. Rev. 1 (2012) 19.
[75] L. Spiegel, P. Bomio, R. Hunkeler, Direct heat and mass transfer in structured packings, Chem. Eng. Process. 35 (1996) 479–485.

[76] J.G. Kunesh, Direct-contact heat transfer from a liquid spray into a condensing vapor, Ind. Eng. Chem. Res. 32 (1993) 2387−2389.
[77] J.F. Mackowiak, A. Górak, E.Y. Kenig, Modelling of combined direct-contact condensation and reactive absorption in packed columns, Chem. Eng. J. 146 (2009) 362−369.
[78] R.F. Strigle, T. Nakano, Increasing efficiency in direct contact heat transfer, Plant/Operations Prog. 6 (4) (October 1987) 208−210.
[79] T.J. Cai, J.G. Kunesh, Heat Transfer Performance of Large Structured Packing, AIChE Spring Meeting, Houston, 1999.
[80] M.J. Lockett, Distillation Tray Fundamentals, Cambridge University Press, Cambridge, 1986.
[81] S. Ross, G. Nishioka, Foaminess of binary and ternary solutions, J. Phys. Chem. 79 (1975) 1561−1565.
[82] D. Weaire, S. Hutzler, The Physics of Foam, Clarendon Press, London, 1999.
[83] G. Senger, G. Wozny, Impact of Foam to Column Operation, Technical Transactions, Cracow University of Technology Publishing House, 2012.
[84] G. Senger, Systematische Untersuchung von Schaum in Packungskolonnen, VDI-Fortschritt-Berichte, Düsseldorf, 2012.
[85] R. Thiele, O. Brettschneider, J.-U. Repke, H. Thielert, G. Wozny, Experimental investigations of foaming in a packed tower for sour water stripping, Ind. Eng. Chem. Res. 42 (2003) 1426−1432.
[86] M.R. Resetarits, J.L. Navarre, D.R. Monkelbaan, G.W.A. Hangx, R.M.A. van den Akker, Trays inhibit foaming, Hydrocarbon Process. (March 1992).
[87] J.L. Bravo, A.F. Seibert, J.R. Fair, The effects of free water on the performance of packed towers in vacuum service, Ind. Eng. Chem. Res. 40 (2001) 6181−6184.
[88] B. Davies, Z. Ali, K.E. Porter, Distillation of systems containing two liquid phases, AIChE J. 33 (1) (1987) 161−163.
[89] C.C. Herron, B.K. Kruelskie, J.R. Fair, Hydrodynamics and mass transfer on three-phase distillation trays, AIChE J. 34 (8) (1988) 1267−1274.
[90] H.R. Mortaheb, H. Kosuge, K. Asano, Hydrodynamics and mass transfer in heterogenous distillation with sieve tray column, Chem. Eng. J. 88 (2002) 59−69.
[91] K. Hallenberger, M. Vetter, Plate damage as a result of delayed boiling, in: International Conference on Distillation and Absorption, Baden-Baden, 2002.
[92] L. Chen, J.-U. Repke, G. Wozny, S. Wang, Exploring the essence of three phase distillation: substantial mass transfer computation, Ind. Eng. Chem. Res. 49 (2010) 822−837.
[93] A. Hoffmann, I. Ausner, J.-U. Repke, G. Wozny, Detailed investigation of multiphase (gas-liquid and gas-liquid-liquid) flow behaviour on inclined plates, Chem. Eng. Res. Des. 84 (A2) (2006) 147−154.
[94] M.E. Harrison, Consider three-phase distillation in packed columns, Chem. Eng. Prog. 86 (11) (1990) 80−85.
[95] R. Meier, J. Leistner, A. Kobus, Three-phase distillation in packed columns: guidelines for devolpement, design and scale-up, in: International Conference on Distillation and Absorption, London, IChemE Symposium Series, 152, 2006, pp. 267−273.
[96] M. Siegert, Dreiphasenrektifikation in Packungskolonnen, in: Fortschritt Bericht VDI, Reihe, 3, VDI-Verlag, Düsseldorf, 1999, 586.
[97] WO 2007/033960 A1.
[98] L. Deibele, R. Goedecke, H. Schoenmakers, Investigations into the scale-up of laboratory distillation columns, IChemE Symp. Ser. 142 (1997) 1021−1030.

[99] R. Meier, G. Ruffert, J. Spriewald, F. Heimann, A. Kobus, R. Proplesch, et al., Scale-up von Destillationskolonnen: Kolonnendurchmesser 50 mm—eine unüberwindbare Grenze, Fachausschuss Thermische Zerlegung von Gas- und Fluessigkeitsgemischen, Weimar, April 2003.

[100] R. Goedecke, A. Alig, Comparative Investigations on the Direct Sale up of Packed Columns from Labatory Scale, AIChE Spring Meeting, Atlanta, 1994.

[101] H. Schoenmakers, L. Spiegel, Laboratory Distillation and Scale-up, in: Górak, et al. (Eds.), Distillation: Equipment and Processes, (Chapter 10), Elsevier, Amsterdam, 2014, pp. 319—339.

This page intentionally left blank

CHAPTER

Distillation in Bioprocessing

8

Philip Lutze

Department of Biochemical and Chemical Engineering, Laboratory of Fluid Separations, TU Dortmund University, Dortmund, Germany

CHAPTER OUTLINE

Distillation: Operation and Applications. http://dx.doi.org/10.1016/B978-0-12-386876-3.00008-9

8.1 Introduction

Several crucial global challenges, such as a general shortage of material resources (energy and water specifically), increasing food demand, environmental pollution, and aging societies are drivers for the increasing interest in biotechnology. Biotechnology is an interdisciplinary research field between biology (microbiology, molecular biology, genetics, bioinformatics), chemistry (biochemistry, classical chemistry), and engineering (process engineering, apparatus engineering). Biotechnology deals with the development of biocatalysis (enzymes to carry out a reaction that is performed inside or outside of a cell) and biocatalytic reaction routes, the development of biobased processes using biobased raw materials, and the design of bioproducts [1]. It is accompanied by research focusing on the development of biobased processes using biobased raw materials based on nonbiocatalytic processing steps. Both technologies are captured within this chapter using the term *bioprocesses*. Biotechnology in general has applications in major industrial sectors such as health care, crop production, and agriculture; in the use of crops/plants as biobased raw materials for industrial production processes of bulk and specialty chemicals, such as biodegradable polymers; or as biofuels and waste/environment treatment. Biotechnology can therefore be classified into several different application areas (Table 8.1).

Biotechnology enables the production from biobased, renewable raw materials instead of oil or gas [1]. Besides the ecological advantages, biotechnology allows the production of novel products [2]—that is, products with very specific properties or products that cannot be produced by conventional chemical processing only. The reason for that is the high selectivity of biotechnological catalysts called enzymes. Enzymes are capable of using a wide array of substrate molecules, even complex ones, and are still able to produce the desired product with a high selectivity [1,2]. Especially in enantio- and regioselective catalysis, enzymes can be applied to selectively react only with one enantiomer. One example of those specific products is antibodies [2]. Some of the advantages of biotechnological processing are listed in Table 8.2.

Bioprocesses can be divided into three stages (Figure 8.1): upstream, transformation, and downstream [2]. In upstream processing, the substrate is processed in order

Table 8.1 Classification of Biotechnology Into Application Areas [1]

Classes	Application Area
Blue technology	Marine and aquatic applications
Green biotechnology	Agricultural (plant and forest) processes
Grey biotechnology	Waste treatment
Red biotechnology	Medical and pharmaceutical processes
White (industrial) biotechnology	Chemical, food, and textile processing

Table 8.2 Advantages of Biotechnological Processes

	White Biotechnology	
Red Biotechnology	**Biobased Raw Materials**	**Biological Catalysts (e.g. organisms, enzyme, cells)**
Biobased raw materials	Renewable feedstock	Highly selective (also towards chiral components)
New (tunable) products	Nontoxic/nonhazardous components	Efficient
	Locally produced raw materials (strengthen of agricultural sector)	Low waste
	Use of waste	Mild conditions
		Low energy consumption
		New products
		New reaction pathways

to bring the substrate into the state in which it is available for the subsequent transformation step. In the transformation step, the substrates are transformed into products by using biocatalysis (biotechnological process) and/or chemical catalysis (biobased processes). Within biocatalysts, it can be distinguished between enzymes either in solution or heterogeneously activated on a support or present in a cell. In some cases, the biotechnological transformation may also be coupled with a chemical transformation. Afterwards, in the downstream processing, the remaining substrates and the catalysts (enzymes, cells) are separated from the product(s); purification of the products into their final form and concentration also are performed, which is (from a separation task point-of-view) not different from conventional processing.

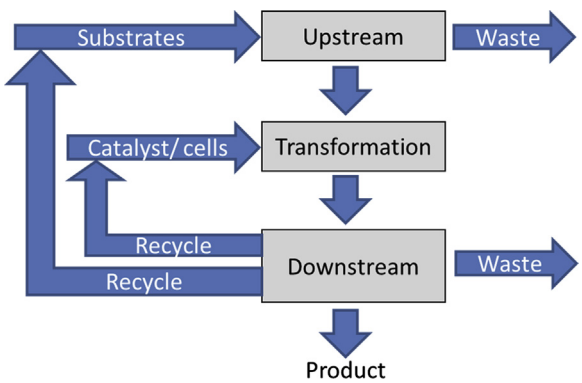

FIGURE 8.1 Processing Steps of Bioprocesses

Even though the main focus of bioprocesses is either on the development of the product or on accelerating/enhancing the reaction step, downstream processing plays a crucial role when developing efficient and economic processes [1,2]. Distillation is an important unit operation within downstream processing of bioprocesses. However, it does not have such a dominant role as in chemical processes [2], for reasons including the temperature sensitivity of the biological products (e.g. antibodies, vitamins), the molecular sizes of the components leading to high viscosities, and the high temperatures necessary for distillation.

In this chapter, the characteristics, challenges, and bottlenecks for application technologies and application areas of distillation systems within bioprocesses are highlighted. The main application areas of distillation systems are in the biobased processes as well as white and red biotechnology, which will be the main focus in the next section. The challenges for distillation systems vary largely between biobased processes and white in comparison to red biotechnology; hence, those two areas are characterized in context to the application of distillation systems in Sections 8.2 and 8.3. Based on those, the application of distillation, including hybrid and advanced distillation systems (Section 8.4) and reactive distillation (Section 8.5) within white and red biotechnology are discussed in detail before an outlook is given in the final section (Section 8.6).

8.2 White biotechnology and biobased processes

The interest of the industry in the use of biobased chemicals is steadily increasing as a result of the limitation of oil reserves, increasing costs due to an increasing effort for the exploitation of oil, and also increasing costs [1] and shortages due to political reasons. The costs for the production of one barrel of oil already vary from $4 to 5 per barrel in Saudi Arabia [3] to $70 per barrel for the extraction of oil shale [4]. It is assumed that approximately 5% of the total energy content of the oil is used for the production of oil, which was much lower compared to the first oil produced (around 1%) [3].

Therefore, the use of biomass as a feedstock for the production of fuels and chemicals becomes more attractive in terms of costs but also potentially leads to an independent locally producible raw material for the chemical industry. Also, residues from agricultural and food processing have been considered as raw materials for transformation into a wide range of chemical compounds (see Figure 8.2). As a result of the transition from an oil-based to a biomass-based chemical industry, technologies and processes need to be developed for the transformation of renewable resources into valuable chemical products [5]. White biotechnology uses microbiological systems, while biobased processes use chemical-catalytic or noncatalytic steps for the production of chemicals such as fine and bulk chemicals, solvents, polymers and polymer precursors, vitamins, pigments, food additives, and fuels, as well as the transformation into usable energy. Biocatalysis uses enzymes as catalysts to initiate or accelerate chemical reactions. These

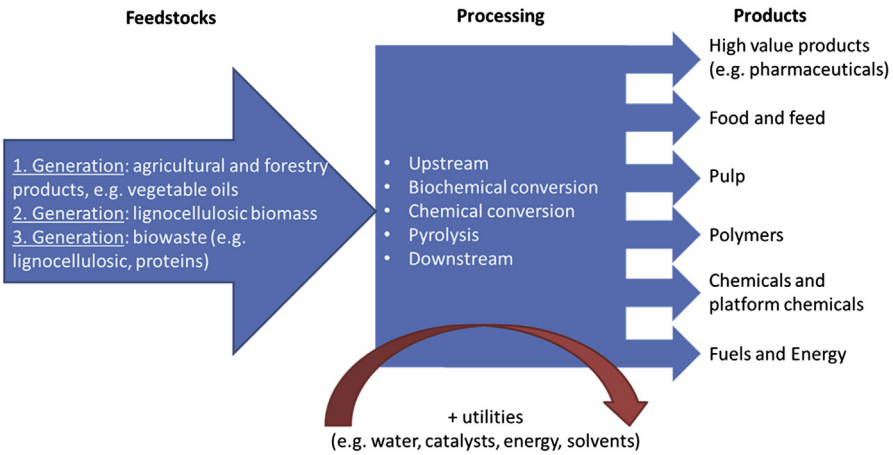

FIGURE 8.2 The Biorefinery Concept: from Multiple Feedstocks to Multiple Products by Integrated Processes

reactions often occur at mild conditions and often in diluted systems [1]. The enzymes are either isolated or delivered within a (not-growing) cell. Isolated enzymes can be provided in solution, acting as a homogenous catalyst, or immobilized (e.g. resins). Fermentation is the transformation of renewable resources such as sugars (e.g. glucose or fructose), plant materials (e.g. cellulose) or plant- or animal-derived oils into valuable products by using living (growing) microorganisms such as bacteria, fungi, or cell cultures.

Biorefinery systems focus on waste minimization and resource-efficient economies from biogenic raw materials in their highest form into multiple products (see Figure 8.2). Biorefineries combine necessary technologies and processes between multiple biogenic raw materials and multiple products that are industrial intermediates and final products of the chemical, pharmaceutical, and food industries as well as fuels [1,5]. In literature different biorefinery concepts starting with different biobased raw materials have been proposed which are summarized in an excellent review paper [6]. Those raw materials include, besides others, agricultural products such as seeds of different plants, whole plants (lignocellulosic materials) as well biological waste (e.g. cooking oil).

In 2004, the US Department of Energy published a report on biobased products in an attempt to highlight the needs for future research [7]. Within this report, a list of so-called platform chemicals, which represent a set of molecular structures that can be produced via biorefineries, was identified [7]. Biobased platform chemicals are supposed to lead to a small number of basic building blocks, like they are used nowadays in the classic chemical industry. This list has been revised and extended by Bozell and Petersen [8] using an additional set of criteria to select the platform chemicals, which also takes the research progress made in the years between those two studies into the account. The original set of criteria are based on factors such as

known processing, economics, industrial viability, size of markets, and the structure of the molecule [7]. The updated set contains the following nine criteria:

1. The attention of the compound in literature
2. The applicability to multiple products
3. The potential as a direct substitute of a chemical compound
4. The applicability to high-volume products
5. The strength as a platform chemical for flexible production
6. The scale-up ability
7. The establishment of the biobased compound already as a commercial product/intermediate/commodity
8. The use as a primary building block within the biorefinery concept
9. The establishment of a commercial production from renewable resources [8]

For example, (bio)ethanol has been added as one important product within the production of biofuels based on the second set of criteria because research and economics has been already widely addressed to establish several potential production routes. A full list of these biobased platform chemicals is given in Table 8.3.

Using renewable agricultural crops or their residues as preferred starting materials, the technology consequently has an overall beneficial effect on greenhouse

Table 8.3 Biobased Platform Chemicals [7,8]

Werpy and Petersen (Department of Energy), 2004 [7]	Bozell and Petersen, 2010 [8]
2,5-Furan dicarboxylic acid	Furan (e.g. furfural, hydroxyl-methyl-furfural (HMF), 2,5-Furan dicarboxylic acid (FDCA))
3-Hydroxypropionic acid	Hydroxypropionic acid/aldehyde
	Biohydrocarbons (e.g. isoprene)
Aspartic acid	
	Ethanol
Itaconic acid	
	Lactic acid
Levulinic Acid	
3-Hydroxybutyrolactone	
Glycerol and Derivatives	
Glucaric acid	
Glutamic acid	
Succinic, fumaric and malic acid	Succinic acid
Sorbitol	
Xylitol/arabinitol	Xylitol

gas emissions and global climate change, while at the same time supporting the (local) agricultural sector, the basic provider of these materials [1,2]. The general opinion that biotechnological processes are slower and more costly than the conventional petrochemical route is a myth. There are many examples in the literature in which (white) biotechnological processes outcompete conventional ones in process performance such as reaction rates, conversion, and especially selectivity leading to improved product purity, overall energy input, and waste generation [1].

8.2.1 Characteristics of white biotechnological processing and biobased processes

Even though conditions and process characteristics of white biotechnological and biobased processes vary within chemical processes, some general statements can be made, including the following:

- Diluted systems: Often, biotechnological transformation using isolated enzymes or microorganisms take place at relatively low concentrations of substrate and achieved products in order to handle the high viscosity and the low solubility of these components in the solvent (often, water is used as solvent).
- Low product concentrations after transformation step: Most biotechnological transformations are inhibited by substrate or product inhibition, leading to a low concentration of product(s).
- Mild conditions: Most microorganisms or biocatalysts are sensitive to temperature. That leads on the one hand to lower energy input but also limits the operating window.
- Large set of impurities from biobased raw materials: Biobased raw materials are never as pure as chemicals if an extensive (but costly) upstreaming is not performed.
- Sensitive biocatalysts/microorganisms: The biological catalysts are sensitive to stress, meaning that during startup high concentrations, too little or too much oxygen/substrate or too much shear in the reactor can cause the irreversible death of the catalysts.
- Batch processing: Biocatalytic transformations and especially fermentations are still often investigated/performed at the industrial scale in batch or semibatch processes.

8.2.2 Issues/challenges for distillation systems within white biotechnology and biobased processing

Based on the characteristics, the following issues and challenges for downstream processing with a focus on distillation systems are present:

- Diluted systems: Large flow-rates within the separation steps are necessary to purify the product from the reaction broth. The energy demand using distillation systems may potentially be high.

- Low product concentrations after transformation step: Several separation steps are necessary to purify the product from the reaction broth. The energy demand using distillation systems may potentially be high.
- Mild conditions: The mild conditions limit the operating window for integration of the biocatalytic reaction step with a distillation.
- Large set of impurities from biobased raw materials: The large set of potential impurities may cause (1) a large set of separation units in case those impurities are critical for the product or (2) the impurities within the product may cause difficulties in its subsequent application in further reactions. For example, in a subsequent chemical reaction of this product, the chemical catalysts (which may not be as selective as the biocatalyst) may produce a set of esters in an esterification reaction from a set of alcohols produced in a previous fermentation step. That may lead to the production of compounds that deactivate the catalyst or to the occurrence of additional azeotropes, which will increase the effort in downstream processing.
- Sensitive biocatalysts: Biocatalysts are sensitive to shear, temperature, and concentrations of present components in the system. This may limit the operating window for integration of reaction steps or the direct integration of the reaction step with a distillation.
- Batch processing: The integration of a batch with continuous production, such as batchwise fermentations and continuous downstreaming, may still be a challenge due to the complex scheduling problem. Batch distillation systems for bulk chemicals would lead to the additional necessity of large storage tanks as well as large pumping costs. Sophisticated heat integration between batch and continuous systems is still unsolved.

In addition, the high viscosity of the large biobased components (e.g. glucose) may limit the applicability or at least the operating window for distillation systems. Another issue is that the investigation of thermodynamics for large (bio)molecules is still ongoing, which limits the predictive design of distillation systems for biobased processes.

8.2.3 General application of distillation systems within white biotechnology and biobased processing

Currently, distillation systems are used within white biotechnology mostly for the following:

- Purification of the product: Similar to the chemical processing, such as in the separation of alcohol and water (see Section 8.4).
- Solvent or substrate recovery, such as glucose recycling (see Sections 8.4 and 8.5).
- Coupled with the reaction for purification of the product and driving of the reaction in biobased process systems (see Section 8.5.1) or biotechnological systems (see Section 8.5.2) within a reactive distillation column.

8.3 Red biotechnology

Red biotechnology aims at the development of products to be applied in or which are related to medical purposes [2]. Therefore, red biotechnology is also often defined as medical biotechnology. The main research focus is the development of biological or biobased products (such as antibodies) and related technologies for their production as well as the development or genetic modification of microorganisms, animals, or plants to produce medical products [2]. Compared to white biotechnology, red biotechnology is more product-driven than process-driven.

The general processing within red biotechnology has six main tasks starting from the preparation of the raw materials (pretreatment) and ending with the purification of the targeted product (see Table 8.4, Ref. [2]). In each task, the concentration and/or the quality profile of the product is increased. A generalized overview of concentration and quality profiles of the products throughout the process is exemplified for the production of an antibiotic in Table 8.4. These tasks are achieved sequentially in batch, semibatch, or continuous operation or integrating different operating modes within one process [2]. In the first task, the raw materials are prepared to fit the reaction conditions. That includes processing steps, such as the milling and dissolving of, for example, solid raw materials. In the second task, the actual reaction step is performed, usually a fermentation step in which the product is formed. Subsequently, in the third task, the removal of insoluble materials is performed. Those can be present in the reaction due to the formation of insoluble side products because solubility boundaries have been crossed, the presence of solid components from raw materials, or the microorganisms themselves. Here, usually, physical separations such as filtration and centrifugation are used. In the isolation, purification, and polishing tasks, the product is removed and purified into its desired state and concentration. Firstly, in the isolation task, the product is isolated from all other components with large differences in separation properties, such as boiling point, solubility, etc. In the fifth task, the product is purified by separation from the remaining components. In the last task, the product is brought into its final state, mostly solid or crystalline form, and the desired concentration.

Table 8.4 Generalized Processing Within Red Biotechnology Exemplified for the Production of an Antibiotic [2]

	Product Characteristics	
Step	**Concentration (g/l)**	**Quality (%)**
1. Pretreatment		
2. Harvest broth	0.1–5	0.1–1.0
3. Removal of insolubles	1.0–5	0.2–2.0
4. Isolation	5–50	1–10
5. Purification	50–200	50–80
6. Polishing	50–2002	90–100

8.3.1 Characteristics of bioseparations within red biotechnology

Conditions and process characteristics of red biotechnological processes compared to processes within white biotechnology have some similarities but also large differences. Some generalized characteristics of downstream processing of red biotechnology are:

- Highly purified ("clean") products are necessary: The application of products from red biotechnology is medical and the quality of the product is the main driver, including the tracking of impurities.
- Large molecules and similar molecules: After transformation, it is not often scarce that the products produced are large molecules that potentially lead to low solubility in the solvents and high viscosities of the fluid streams. Additionally, higher boiling and melting points of large molecules as well as similar side products (e.g. in chiral components) complicates downstream processing.
- Temperature-sensitive products: Most products are sensitive towards temperature, which may cause products to degrade.
- Flexible and multiproduct units leading to batch processing: Biocatalytic transformations and especially fermentations are still performed at industrial scale in batch or semibatch processes.
- Diluted systems: Often, biotechnological transformation using isolated enzymes or microorganisms take place at relatively low concentrations of substrate and achieved products in order to handle the high viscosity and the low solubility of these components in the solvent (often, water is used as solvent).
- Low product concentrations after transformation step: Most biotechnological transformations are inhibited by substrate or product inhibition, leading to a low concentration of product(s).
- Mild conditions: Most microorganisms or biocatalysts are sensitive to temperature, which leads to lower energy input but also limits the operating window.
- Sensitive: Biocatalysts are sensitive to shear, temperature, and concentrations of present components in the system. This may limit the operating window for integration of reaction steps or an integration of the reaction step with a distillation.

8.3.2 Issues/challenges for distillation systems within red biotechnology

Based on the characteristics of red biotechnological processing, the following issues and challenges for downstream processing with a focus on distillation systems are identified:

- Highly purified ("clean") products are necessary: High purity is necessary, which may not be achieved by distillation systems. Coupled with the necessity of obtaining solid or crystalline product crystallization, this is often the last purification step coupled with chromatography. Furthermore, purity and recovery is more important than productivity because products are of high value.

- Large molecules and similar molecules: The similarity of the properties for separation of remaining components by relative volatility in the last separation steps (e.g. purification) are coupled with the large boiling points of most products limits the use of distillation systems.
- Temperature-sensitive products: The temperature sensitivity limits the application of distillation columns that may have locally hot spots. Therefore, the use of more complex and more expensive distillation systems, such as falling film evaporators as well as operating under a vacuum, may be necessary.
- Flexible and multiproduct units leading to batch processing: Integration of batches with continuous production may still be a challenge due to the complex scheduling problem.
- Diluted systems: The energy demand associated with using distillation systems may potentially be high, but also large temperature differences between the top and bottom of the columns may need to be established, which may raise difficulties for temperature-sensitive products.
- Low product concentrations after transformation step: Several separation steps are necessary to purify the product from the reaction broth. The energy demand using distillation systems may potentially be high.
- Mild conditions: The mild conditions limit the operating window for integration of the reaction step with distillation.
- Sensitive biocatalysts: This may limit the operating window for integration of the reaction step with a distillation.

Similar to white biotechnology, a big challenge is that the investigation of thermodynamics for large biomolecules is still ongoing, which limits the predictive design of distillation systems for biobased processes.

8.3.3 General application of distillation systems within red biotechnology

Currently, distillation systems are used within red biotechnology mostly for solvent or substrate recovery (e.g. glucose recycle, see Sections 8.4 and 8.5). A limited application of distillation systems within red biotechnology is the purification of the product (see also Chapter 7) due to the high boiling points and high similarity of the components to separate. One example in which distillation is used for product purification is the purification of 3-omega fatty acids (see Section 8.4.1).

8.4 Conventional, hybrid and advanced nonreactive distillation processes

Within this chapter, some examples of conventional as well as advanced (nonreactive) distillation processing are given to exemplify its applications within biobased as well as white and red biotechnological processes.

8.4.1 Conventional distillation

The main application of conventional distillation within bioprocesses is the purification of the product and solvent or substrate recovery (see Section 8.2 and 8.3). For each of those, examples are given, from which two are explained in more detail—the production of bioethanol and the production of esters from carboxylic acids.

The fermentation broth producing bioethanol from sugar consists of, besides water and ethanol, carbon dioxide, solid particles, aldehydes, ethers, and other alcohols ("fusel oils") [9]. In a conventional process flowsheet [9], the fermentation broth is introduced into a beer stripper, which is a combination of distillation and stripping. The bottom product consists of all heavy boiler and solid particles, which can be directly used for the production of animal food. Gaseous (i.e. carbon dioxide) as well as light-boiling components leave the beer stripper at the top. An almost binary mixture of ethanol/water and other streams containing alcohol components are taken from the column at several side-draws. The mixture of ethanol and water can only be purified up to the azeotropic concentration within one column. Hence, different technologies [9–11] have been investigated, including heteroazeotropic and extractive distillation, two-pressure column arrangements, distillation-adsorption, or membranes as single stand-alone or in combination with distillation (see Section 8.4.2).

For the extractive distillation configuration [9], the side-stream of ethanol/water is mixed with a solvent and afterwards separated in a distillation column (Figure 8.3). At the bottom of this column, the purified ethanol is obtained, while at the top a mixture of solvent, ethanol, and water is fed to a decanter in which two phases occur. One phase consists mostly of the solvent and is recycled back to the column, while the other phase consists mostly of ethanol and water and is fed to a second distillation column. In the second distillation column, water is obtained at the bottom and the azeotropic concentration at the top is recycled back to the first column. However, this technology is expensive and highly energy consuming [10]. More details on different processes for the production of bioethanol, including distillation systems, are given by Huang et al. [11]. The separation of bioethanol by distillation coupled with a membrane is explained in Section 8.4.2.

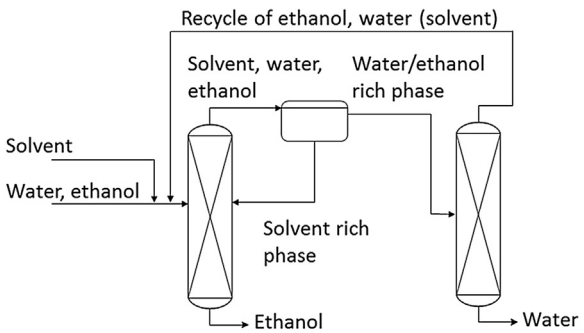

FIGURE 8.3 Simplified Extractive Distillation Process for the Separation of Bioethanol

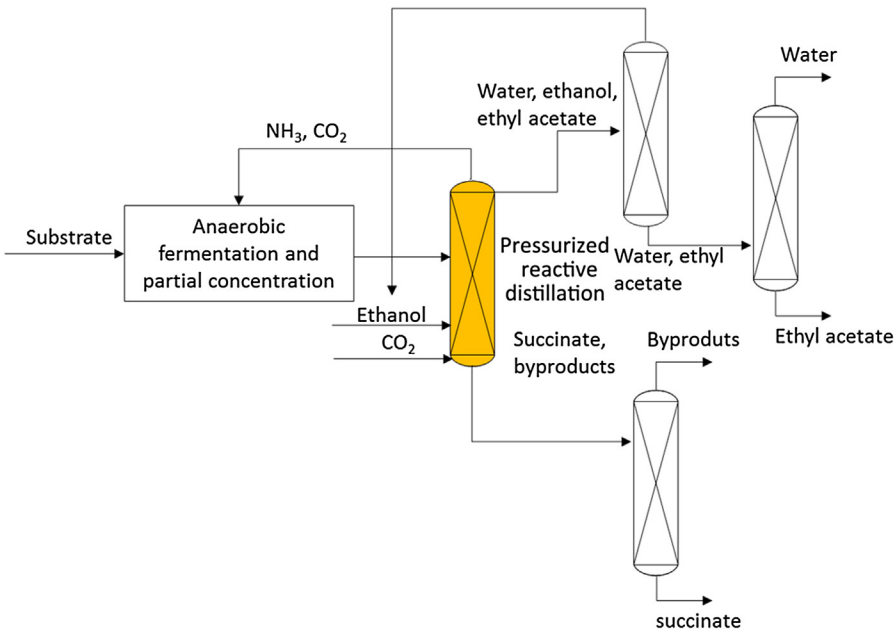

FIGURE 8.4 Production of Esters of Carboxylic Acids from Fermentation Broths [12]

Another example of conventional distillation in bioprocesses can be found in the production of esters of carboxylic acids from fermentation broths (see Figure 8.4) [12]. In a fermentation, diammonium succinate is formed from sugar, which is the feed for the following esterification reaction to produce the desired esters. Within this process, distillation is used for the concentration of diammonium succinate from the fermentation broth by vacuum distillation to achieve a concentration of 20−60 wt%. This stream is fed to a reactive distillation (see also Section 8.5.1) for the ester product formation, such as diethyl succinate, using ethanol as additional reactant. Two top streams exit, one noncondensable and the other condensable. In a subsequent separation of the condensable top stream, the product ethyl acetate is separated from ethanol and water, which are recycled back to the reactive distillation column. Furthermore, the obtained diethyl succinate is purified from the bottom stream of the reactive distillation using conventional distillation.

Even though distillation is mostly used for solvent recovery within red biotechnology [2], some examples are known in which distillation is used for purification. One example is in the production of 3-omega fatty acids [13,14]. Because omega-3 ethyl esters are used as active pharmaceutical ingredients (API), they have to be purified to high concentrations (>90%) and it has to be ensured that no contamination of the product with undesired compounds occurs. The API is a highly purified pharmaceutical preparation of eicosapentaenoic acid (EPA) and docosahexaenoic acid (DHA) ethyl esters chemically modified from fatty acids. Starting from oil of

biotechnological modified plants or marine oil, the products are formed via chemical or chemo-enzymatic esterification processes [13,14]. The purification process includes several steps incorporating vacuum (molecular) distillation, urea complexation reactions, chromatography, and others to produce the final product [13]. The first distillation process takes place directly after the product is formed. Under vacuum, the mixture is distilled in a multieffect evaporator to achieve a concentration of the omega-3 fatty acid of around 50−70%. Further purification is achieved by chromatographic steps.

8.4.2 Hybrid and advanced distillation

Hybrid separations are the external integration of two different unit operations for the same separation task [15]. That allows using each unit operation in that operating window in which it outperforms all others. Additionally, occurring synergies allow the crossing of thermodynamic boundaries of a single unit operation (e.g. azeotropes) by another unit operation that is based on a different separation principle. Also, cost savings can be achieved [15]. Hybrid distillation is the coupling of a distillation with one other unit. More details on hybrid processing can be found in the chapter: Hybrid distillation. Within bioprocesses, hybrid distillations have been investigated mostly for the separation of alcohol-water mixtures in which feed and product concentration are on different sides of the occurring azeotrope at one pressure. An example is hybrid processing in the production of bioethanol, in which a coupling of distillation with vapor permeation and pervaporation together with adsorption (Figure 8.5) has shown large benefits in energy as well as total costs savings compared to the conventional hetereoazeotropic distillation process (see Figure 8.3) [10]. The first industrial application of a hybrid process including pervaporation and distillation has been installed with a membrane area of 2100 m^2 in Betheniville in 1988 [16]. Dijkstra et al. [17] proposed a combination of distillation, pervaporation/vapor permeation, and adsorption for the dehydration of ethanol. Distillation is used for separation of water and ethanol up to the azeotropic

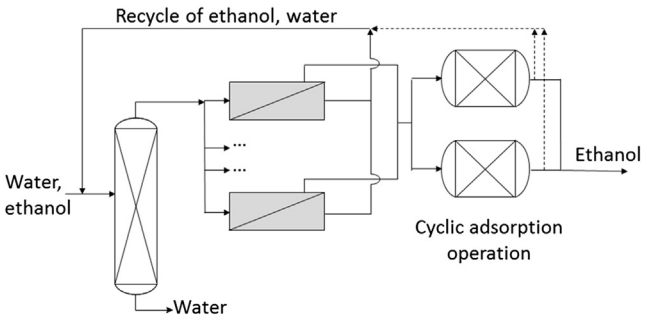

FIGURE 8.5 Integrated Process Incorporating Distillation, Vapor Permeation, and Pressure Swing Adsorption for the Dehydration of Ethanol [10]

concentration. The azeotropic concentration is afterwards purified to 99 wt% by using membrane operations. That allows an economic operation of the system because only a relatively small membrane area compared to a single stand-alone membrane unit/cascade is necessary. Adsorption may be used to dehydrate the mixture to its final product specification.

Besides hybrid distillation processes, advanced distillation systems have also been investigated within bioprocessing including:

- Membrane distillation: Advantages are the separation at relatively mild conditions and the provision of large and defined interfacial areas. Membrane distillation is often used in the production of juices or in production of pharmaceuticals from biological raw materials. Another example is the integration of batch fermentation with membrane distillation for in situ product removal. Udriot et al. [18] studied the anaerobic batch cultivation of *Kluyveromyces fragilis* on a feed medium containing glucose, in which fermentation ethanol is produced to inhibit growth and further product formation. The in situ removal of ethanol by membrane distillation resulted in an 87% increase in ethanol productivity [18]. Detailed information of this technology is given in Chapter 9.
- Heat-integrated distillation column: Heat-integrated distillation allows heat supply/removal necessary for evaporation and condensation within rectifying and stripping section or top and bottom, respectively, to be integrated within the same unit operation. It potentially offers energy and hence operating cost savings as well as savings in capital costs. Examples can be found for the production of hydroxyl-methyl-furfural (HMF) from fructose (discussed within this section) or the production of biodiesel (discussed in Section 8.5.3).
- Dividing wall columns: Within dividing wall columns, multiproduct columns can be realized by vertical arrangement of sectors with no phase change occurring. They allow savings in capital as well as operating costs. An example for the biotechnological process sector is the production of biodiesel (see Section 8.5.3).

As an example, the application of a heat-integrated distillation column for the production of HMF from fructose is discussed elsewhere [19]. HMF can be produced from fructose by the following reaction scheme consisting of four reactions [20]. Fructose is converted in the main reaction to produce HMF and water from Eqn (8.1):

$$C_6H_{12}O_6 \leftrightarrow C_6H_6O_3 + 3H_2O. \tag{8.1}$$

HMF is degraded in water to levulinic acid and formic acid in a side-reaction Eqn (8.2).

$$C_6H_6O_3 + 2H_2O \leftrightarrow C_5H_8O_3 + CH_2O_2 \tag{8.2}$$

In addition, two additional side-reactions are taking place to form humins, which are the degradation of fructose Eqn (8.3) and the degradation of HMF Eqn (8.4). Humins are undetermined insoluble polymers [21].

$$C_6H_{12}O_6 \leftrightarrow [C_6H_6O_3]_{\text{Humins.1}} + 3H_2O \tag{8.3}$$

$$C_6H_6O_3 \leftrightarrow [C_6H_6O_3]_{\text{Humins.2}} \tag{8.4}$$

Different process routes are discussed in academia and industry targeting to increase conversion, selectivity, and space-time-yield including the use of different catalysts, different solvents (water, dimethyl sulfoxide, ionic liquids) or mixture of solvents (e.g. water-acetone), and different technologies for the reaction as well as the subsequent product recovery [19,22]. An excellent review has been made by Boisen et al. [22]. Environmentally, water seems to be the ideal solvent. No commercial process is known so far, but the largest setup reported in the literature is the water-based process route by Rapp [21], in which fructose (25 wt% of fructose) is dissolved in water and fed to a reactor in which the reaction takes place for 2 h at a temperature of 413 K using oxalic acid as catalyst. The selectivity towards the main product is 55% and the conversion of fructose is 60%. The produced humins in the side reactions Eqns 8.3 and 8.4 are insoluble and can therefore easily be separated using a filter. All acids are neutralized by addition of a base (sodium hydroxide). The salt and afterwards the fructose are removed in a chromatography column requiring the addition of water. Subsequently, the water is evaporated and the HMF crystallized. The process flowsheet is given in Figure 8.6.

Lutze et al. used a systematic synthesis/design method for (bio)chemical processes to identify a better and intensified process flowsheet [19,23,24] for the HMF process using the water-based process route. Their method is based on the decomposition approach for synthesis/design [25] and divides the problem to be

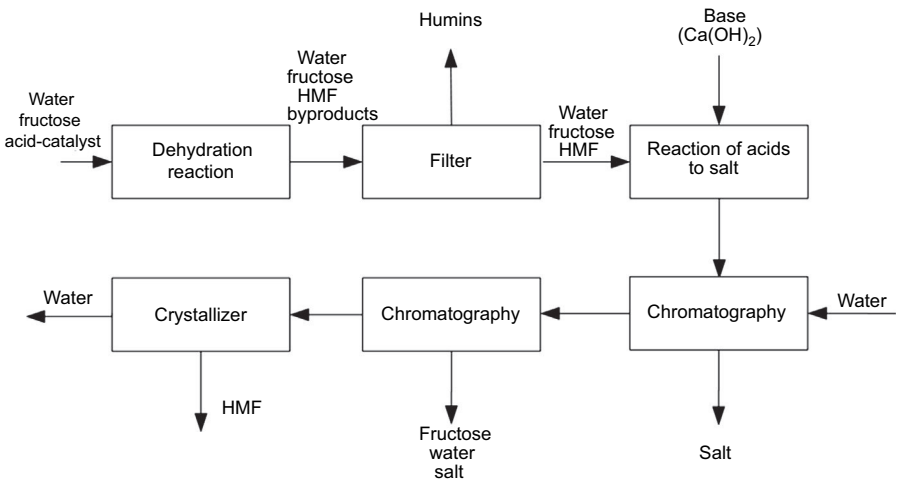

FIGURE 8.6 Simplified Production Route of Hydroxyl-methyl-furfural (HMF) from Fructose Through a Water-based Process Route [21]

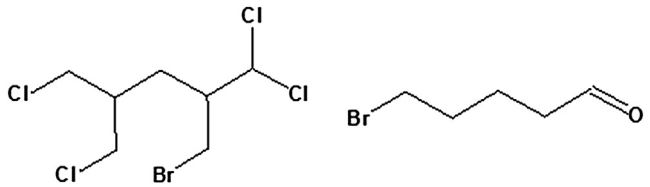

FIGURE 8.7 Potential Candidates for a High-Boiling Solvent $C_7H_{11}BrCl_4$ (a) and a Low-Boiling Solvent (b) [19]

solved into six steps. Applying their theoretical method, in total 1.2×10^6 different process configurations were generated based on 35 different technologies in the search space for synthesizing the process, from which only 1.1×10^5 of them are feasible. In a subsequent screening based on the evaluation using a set of performance criteria, they efficiently reduced the number of options to only 12 promising process candidates. In final optimization, their best solution is a microchannel reactive extractor in which the product HMF leaves with the solvent in one phase, while all side-products and the reaction medium (water) remain in the reaction phase. The ideal solvent is theoretically designed using computer-aided molecular design approaches and selected based on the performance as solvent and based on the boiling point temperature to later separate HMF/solvent from each other easily by its difference in relative volatility. The separation of a high boiling solvent from HMF as the light boiling component takes place in a heat-integrated distillation column. The solvent is recycled back to the reaction. By this process scheme, the operational costs can be reduced by a factor of 6.5 compared to the base case design by Rapp [21]. The main contributor to the cost is still the substrate fructose, followed by the operating costs for the reaction at a temperature of 453 K. One of the keys is the identification of potential new solvents with increased solvent power and desired boiling point (see Figure 8.7) by using computer-aided molecular design tools. The best option is using a high-boiling solvent compared to HMF because the light-boiling component (here HMF) having the smaller flow-rate can be efficiently vaporized in a heat-integrated distillation column.

8.5 Conventional, hybrid and advanced reactive distillation processes

The concept of reactive distillation (see also Volume 2, Chapter 8), which is the integration of reaction and distillation occur at the same time and place within one unit operation, has been investigated for several processes within bioprocessing. The concept of reactive distillation is one of the most important applications of the integrated reaction-separation concept as it can increase economics but also enables the production of products, which would have not been able to be produced in such a

simple arrangement [15,23]. Currently, two main topics are focused in research on reactive distillation (RD) in the frame of the development of a biobased chemical economy:

- The application of the reactive distillation concept for the further processing of platform chemicals and the purification of fermentation broth (Section 8.5.1).
- The use of enzymes as biocatalysts in the reactive section of the reactive distillation column (Section 8.5.2).

For bioprocesses, the following factors have been reported to be the main drivers for the investigation of reactive distillation using chemical catalysts (see Volume 2, Chapter 8, [15]):

- *Improved conversion*: By the removal of products from the reactive section, the chemical equilibrium of equilibrium-limited reactions is shifted towards the side of the products. Improved reactant conversions approaching 100% are achievable.
- *Circumventing/overcoming of azeotropes*: In the case of chemical systems that tend to form azeotropes, RD allows one to circumvent azeotropic mixtures by "reacting away" participating components.
- *Reduced side-product formation*: Consecutive reactions are reduced by the removal of products from the liquid reaction phase, thereby maintaining low product concentration.
- *Direct heat integration and avoidance of hot-spots*: In the case of exothermic reactions, the heat of reaction can directly be used to evaporate components, reducing the amount of total heat needed and avoiding the occurrence of hot-spots.
- *Capital savings*: Removal of components due to high conversions and circumvention of azeotropes, resulting in a simplified or eliminated separation system.
- *Decreased catalyst amount*: Reduced requirements of catalysts for a comparable conversion of the reactants.

Additionally, by the use of enzymatic catalysts within reactive distillation, two more drivers for the investigation have been reported:

- *Improved selectivity*: Circumvention of the formation of side-products by using selective catalysts, which not only increase conversion towards the targeted product and minimization of generated waste but also circumvent the formation of side-products, which may be part in nonideal behaviors, such as the formation of immiscibilities or azeotropes that complicate downstream processing.
- *Novel product formation:* The use of enzymes as highly selective components allows the separation of isomers as well as chiral molecules in a simple and more cost-efficient setup.

8.5.1 Reactive distillation using chemical catalysts

The current interest into the use of reactive distillation for the production of biochemical and biopolymers is exemplified by two large projects, one sponsored in the US, the other one in the European Union. From 2003 to 2006, the US Department of Energy sponsored a project (Award Number DE-FG36-04GO14249) that investigated the production of esters from different biobased organic acids (lactic acid, citric acid, succinic acid, and propionic acid) using reactive distillation processes. Organic acid esters are important building blocks for chemicals as well as biofuels, which can be made from corn or other renewable biomass carbohydrates [7,8]. The European Union sponsored a project called EuroBioref, in which as part of the project investigates the production of butyl-acrylate. In the last step of the process, butanol and acrylic acid, which can both be produced from renewable resources, react in a reactive distillation column to form butyl acrylate [26]. Within this chapter, some examples of reactive distillation for the production of biobased platform chemicals (Table 8.3) or products resulting from these components are discussed.

8.5.1.1 Succinic, fumaric, and malic acid

Succinic, fumaric, and malic acid are four-carbon diacids that are produced via similar biochemical paths [7]. These acids can be used as building blocks for the production of large commodity chemicals, such as 1,4-butanediol, tetra-hydrofuran, hydroxybutyrolacetone [7], or succinates [27,28]. Reactive distillation processes have been reported for the production of diethyl succinate from succinic acid [27] and the co-production of ethyl acetate and diethyl succinate from a feed mixture containing succinic acid and acetic acid coming from a biotechnological waste stream [28]. In both cases, an ion-exchange resin Amberlyst 70, immobilized in Katapak-SP11™ reactive packings, has been used in an experimental investigation in a pilot-scale reactive distillation column. Conversions of 100% for both acids and diethyl succinate purities of 98% have been achieved experimentally.

A general process for the direct production of esters of carboxylic acids from fermentation broths has been patented [12], specifically the production of succinic acids and its esters. Substrates for the fermentation are all kind of fermentable sugars or other fermentable waste products. The special feature of their process is the direct integration of fermentation of substrates to salts of succinic acid or dialkyl succinates and the esterification to succinate esters or diammonium succinates. Besides the fermenter, the key process step is the esterification of the salt of succinic acid under presence of an alcohol (such as ethanol and methanol) in the reactive distillation column in which CO_2 is used to catalyze the reaction. A heterogeneous catalyst would be incompatible to impurities from the fermentation broth, while a homogenous catalyst may have to be recovered and recycled. The heavy esters are obtained at the bottom of the column, while the light boiling esters as well as water and the alcohol leave the column at the top. The volatile ester such as ethyl acetate is separated from the alcohol/water mixtures in a vacuum distillation and obtained as a side-product. The gaseous ammonia and the CO_2 are recycled back to the fermenter

because CO_2 is required in the anaerobic fermentation while NH_3 is used as neutralizing agent. In subsequent steps, the obtained esters can be purified by conventional distillation and subsequent reactions to produce 1,4-butanediol, tetrahydrofuran, gamma-butyrolactone, or dialkyl maleates.

Liu et al. developed a process for the purification of 2,3-butanediol from fermentation broth [29]. After an extractive reaction, a hydrolysis of 1-2-propyl-1,3-dioxolane is performed in a reactive distillation column for the purification of 2,3-butanediol. In their theoretically investigated process, a bottom concentration of 15 mol% of 2,3 butanediol was obtained with a yield of 98.1%.

8.5.1.2 2,5-Furan dicarboxylic acid

2,5-Furan dicarboxylic acid (FDCA) belongs to the chemical group of furans and is biologically formed by an oxidative dehydration of glucose. It is supposed to be used as a replacement for terephthalic acid, which is a reactant for the production of polyesters such as polyethylene terephthalate and polybutylene terephthalate [7]. For the transformation of FDCA to esters, the use of heterogeneous catalyzed reactive distillation, which removes the co-product water in order to shift the equilibrium, has been patented [30]. Another six-carbon acid is citric acid. Here, reactive distillation has been investigated to produce triethyl citrate from citric acid [31]. In reactive distillation experiments in a pilot-scale column using an excess of ethanol, the technical feasibility of this process has been verified. A following theoretical investigation demonstrated the necessity of 60 stages to obtain a product (triethyl citrate) yield of approximately 98.5%.

8.5.1.3 3-Hydroxypropionic acid

3-Hydroxypropionic acid (3-HPA) is a three-carbon acid building block and can be used for the synthesis of 1,3-propanediol, acrylic acid, or acrylamide [7]. Kuppinger et al. investigated RD for the production of acrylic acid from 3-HPA [32] in which the equilibrium is shifted by the continuous removal of water. In their process, they proposed to run the dehydration of 3-HPA in a CO_2 atmosphere, which avoids the undesired decarboxylation reaction(s).

8.5.1.4 1,3-Propanediol

1,3-Propanediol is a coproduct of the fermentative synthesis of 3-HPA [33]. To separate it from the fermentation broth, a reactive extraction is performed first to form acetals of 1,3-propanediol. In the subsequent step, those acetals are hydrolyzed in a reactive distillation column to obtain 1,3-propanediol in a mixture with 2,3-butanediol, glycerol, and glycerol acetals at the bottom of the column [33]. Adams et al. [34] investigated a semicontinuous process for the dehydration of 1,3-propanediol using the solvent isobutyraldehyde. They proposed to use one multifunctional catalytic column to alternating perform the reactive extraction and the reactive distillation within one apparatus. The 1,3-propanediol broth solution is fed to the column for the reactive extraction in which it reacts with the solvent isobutyraldehyde to form 2-isopropyl-1,3-dioxane, which accumulates in the

organic phase. Afterward, in the RD column operation, the organic components are fed to the column, and 1,3-propanediol is formed by a reverse reaction and accumulates at the bottom of the column. In their theoretical study, product concentrations of 98 mol% are achieved.

8.5.1.5 Lactic acid

Lactic acid, also known as 2-hydroxypropionic acid, is a potential building block for polymers and is similar in its structure to 3-HPA. In addition, similar fermentation performance and yields compared to 3-HPA are reported [7]. The recovery of nonvolatile lactic acid from the fermentation broth is difficult due to the similarity of the boiling points. Hence, an esterification is performed to form an ester that can be separated more easily and afterwards recover the acid by back hydrolization. Asthana et al. [35] developed a process for the synthesis of ethyl lactate from lactic acid and ethanol using a heterogeneously catalyzed reactive distillation column. They performed pilot-scale experiments to demonstrate the technical feasibility of the ethyl lactate synthesis using reactive distillation technology. Gao et al. [36] performed experimental studies in a glass column and proposed the combination of an esterification reactor and a reactive distillation column, ending up with an increase in yield for ethyl lactate of 82% in comparison to the simple esterification reactor. Lunelli et al. [37] investigated the ethyl lactate process chain theoretically, including the fermenter and further downstream steps. The process was designed for full conversion of the raw materials (all unconverted raw materials are recovered and recycled back) and to achieve a product concentration of ethyl lactate of 99 mol%. Besides esterification with ethanol, also other alcohols such as *n*-butanol [38] and methanol [39,40] have been investigated. Kumar et al. [38] studied the esterification of lactic acid with *n*-butanol to form butyl lactate and water. Experimental studies in a batch and continuous reactive distillation column were performed achieving lactic acid conversions of 92% and 99.5%, respectively. This technology can be used either for the esterification of lactic acid, or, in combination with a subsequent hydrolysis, for the recovery of lactic acid from aqueous solution. The feasibility of the recovery of lactic acid by hydrolysis of ethyl lactate in a pilot-plant RD column was shown by Barve et al. [41]. They demonstrated that a purity of 99.85% for a lactic acid stream of 3.86 kg/h can be achieved using three subsequent RD columns without the use of a catalyst. Finally, an RD process for the production of acrylic acid and acrylic acid esters from lactic acid has been patented [42].

8.5.1.6 Levulinic acid

Levulinic acid may be a widely used building block for valuable components, such as methyltetradydrofuran, a potential fuel, delta-aminolevulinic acid, a herbicide, or acrylic acid [7]. Several RD processes have been investigated. For example, a reactive distillation column for the esterification of levulinic or pentanoic acid together with an alcohol has been investigated, in which the distillate is separated by exploiting a miscibility gap, using a decanter to remove the water and recycle the organic components to the column [43].

8.5.1.7 Glycerol

Biobased glycerol is already produced in large quantities because it is a side product in the production of biodiesel [7]. Glycerol is a potential building block for the production of triacetates, glycerol esters, 1,3-propanediol, glycerol carbonates, or propylene glycol [7]. Numerous studies on the use of glycerol in combination with the RD technology are available in literature; some of the recent studies are summarized within this section. Siricharnsakunchai et al. [44] investigated theoretically the esterification of glycerol from the biodiesel production and acetic acid to triacetin. They investigated and evaluated different process configurations and the effect of the methanol concentration in the mixed glycerol feed into account. The same reaction was theoretically and experimentally investigated by Hasabnis et al. [45] who performed steady-state experiments for model validation purposes and used the validated model to design an RD configuration for the production of highly pure triacetin. Luo et al. [46] investigated the synthesis of dichloropropanol from a consecutive two-step reaction from glycerol. Based on pilot-plant experiments, the authors proved the feasibility of the use of RD and theoretically achieved a glycerol conversion above 98 mol% and a product yield for dichloropropanol of around 93 mol%. Chiu et al. [47] experimentally investigated the synthesis of propylene glycol from glycerol within a batch and semibatch laboratory-scale RD setup using a copper-chromite catalyst. They achieved a glycerol conversion above 92% and a selectivity of around 90% and proposed the use of semibatch operation to increase the catalyst loading to glycerol ratio in the reaction. An experimental and theoretical study of an RD process for the indirect utilization of glycerol was reported for the heterogeneously catalyzed synthesis of *n*-butyl acrylate from acrylic acid and butanol [26]. One way of the biobased production of acrylic acid is via double dehydration and oxidation of glycerol [48]. Niesbach et al. [49] investigated the production of butyl-acrylate and analyzed the influence of impurities within both biobased feed stream. They demonstrated that a reactive distillation column system (see Figure 8.8) has the potential to replace the conventional process consisting of a reactor and several distillation steps.

8.5.1.8 Biodiesel

Biodiesel is an alternative diesel fuel. It is nontoxic, biodegradable, and has low emission profiles, which makes it an attractive alternative to classical fuels. Biodiesel mainly consists of monoalkyl esters obtained from different vegetable oils and more recently from used cooking oils or animal fats transesterified with an alcohol (mostly methanol or ethanol) [50]. The reaction is equilibrium limited and has been investigated using different chemical catalysts as well as biocatalysts. The equilibrium in the reaction as well as azeotropes in the system have led to the investigation of RD columns. Until now, only chemical catalysts have been investigated for RD in the production of biodiesel. Kiss et al. [51] developed a process for the production of biodiesel using the synthesis of fatty acid methyl ester (FAME) from fatty acids and methanol. They experimentally investigated the reaction of dodecanoic (lauric) acid with methanol, propanol, and 2-ethylhexanol and

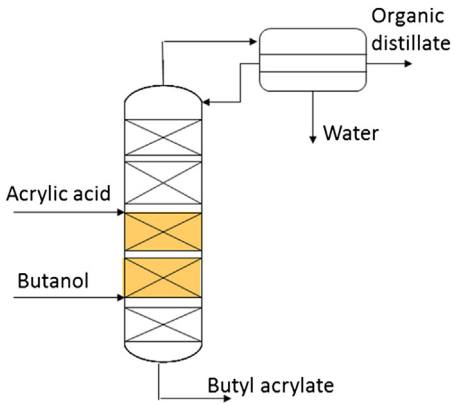

FIGURE 8.8 Reactive Distillation with Decanter at the Top for the Production of Butyl Acrylate [49]

determined kinetic data for these reaction schemes. They concluded that significant improvements, such as an increased productivity by a factor of 6−10, can be achieved. However, a reduction of the alcohol excess into the column is necessary for the economic use of reactive distillation compared to a conventional reactor-distillation setup. Mueanmas et al. [52] showed in a theoretical study that the use of palm oil for the biodiesel production in an RD is economically more promising due to the decreased stoichiometric feed ratio. He et al. [53] used canola oil as starting material and performed experiments in a continuous-flow laboratory-scale reactive distillation column. They demonstrated the feasibility of the reactive distillation technology for this reaction and could significantly reduce the excess of alcohol compared to the conventional process. Da Silva et al. [54] performed experiments for the synthesis of biodiesel from soybean oil and ethanol. They investigated different catalyst concentrations and molar feed ratios and obtained a reactant conversion of 98%. Noshadi et al. [55] studied the RD for the production of FAME from waste cooking oil using a heteropolyacid. They varied the total feed flow, the feed temperature, the reboiler duty, and the molar feed ratio of methanol to oil and obtained a FAME yield of around 94% by using a large excess of methanol. All of those studies showed that alcohol excess and energy costs are critical parameters for an economic production of biodiesel in an RD column. Hence, also advanced distillation systems have been studied for reactive distillation processes. which are discussed in detail in Section 8.5.3.

8.5.2 Biocatalytic reactive distillation using biocatalytic internals

Enzymes are capable of using a wide array of substrate molecules, even complex ones, and are still able to produce the desired product with a high selectivity [1,2]. Especially in enantio- and regioselective catalysis, enzymes can be applied

to selectively enable the reaction of one enantiomer, resulting in cost savings during the purification steps. Therefore, the use of enzymes within RD to use the synergies of both technologies has increased its research interest. In general, the enzyme can be introduced into the column homogeneously (meaning in solution), immobilized by bonding the enzyme on the surface of the column internal or immobilized by enclosure into envelops within packing structures, such as for Katapak© from Sulzer or others [56]. However, as enzymes are sensitive to higher temperatures, the use of enzymatic catalysis for reactive distillation processes is limited.

One of the first experimental studies of a biocatalytic reactive distillation column was published in 2003 for the synthesis of butyl butyrate using lipase as catalyst [57]. In order to avoid thermal denaturation of the enzymes, a vacuum of 15,000 Pa was applied in the column. The enzymes were immobilized on inverted pear bulbs. Heils et al. [58] studied the integration of enzymatic catalysts in a reactive distillation column for the transesterification of ethyl butyrate and *n*-butanol. Candida antarctica lipase B was immobilized in a newly developed silica-gel matrix that was applied as a stable coating onto commercially available packing and as granulate. The newly developed coating exhibits a large specific surface area, higher productivity compared to granulate, and good thermal stability. In experimental studies, the stability of enzymes as well as the catalyst leaching was tested in a batch-reactive distillation column operating at reduced pressure around 10,000 Pa. Each batch RD run lasts for approximately 6−8 h. The enzyme showed high stability within the runs. However, the enzyme leaching on the coated packing totaled a loss of around 30 wt% for four sequential runs with the same packing. However, after the fourth run, the catalysts leaching yielded losses of less than 2 wt%. A conversion of 98% of butanol has been achieved, which is beyond the equilibrium conversion.

8.5.3 Advanced reactive distillation systems

Similar to nonreactive distillation systems (see Section 8.4.2), advanced distillation systems have been investigated for reactive distillations. For example, the production of biodiesel has been investigated by several authors in order to establish thermally coupled reactive distillation systems or dividing wall column [59−61]. The application of reactive distillation for the production of biodiesel has been explained in Section 8.5.1. Instead of a classical reactive distillation column, Gomez-Castro et al. [59] studied theoretically the use of a Petlyuk reactive distillation column and a reactive thermally coupled direct sequence (RTCDS) for the supercritical methanol biodiesel production process in which methanol at supercritical conditions ($T = 623$ K, $p = 20$−50 MPa) is used as a catalyst (see Figure 8.9), which circumvents the formation of side-products and expensive catalyst recycling. The reactive Petlyuk column (Figure 8.9(a)) consists of the side separation column coupled with the reactive distillation column between middle and top section. The fatty acid feed (here oleic acid) is introduced at the top, while the methanol is fed to the reboiler of the reactive column. The reactive section is situated below the integration of the

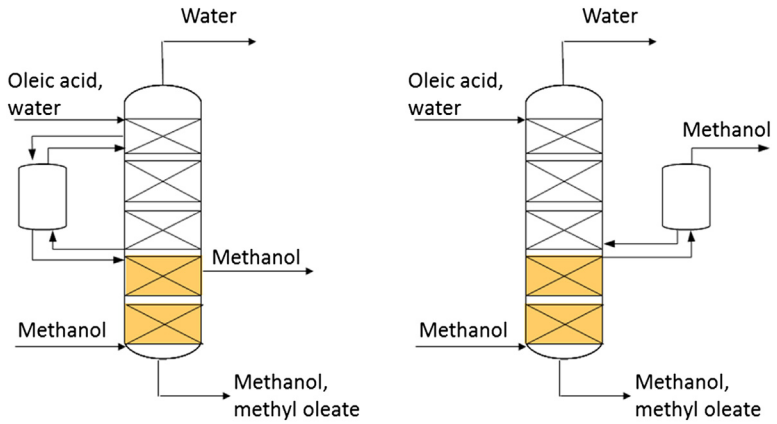

FIGURE 8.9 Thermally Coupled Reactive Distillation Systems: (a) Petlyuk Arrangement; (b) Direct Sequence (RTCDS) [59]

side-column and the side-draw removal of methanol (see Figure 8.9(a)). The product (methyl oleate) in a mixture with methanol is obtained at the bottom at the column and pumped for further purification to another distillation column. In the RTCDS arrangement (Figure 8.9(b)), the reactive distillation column looks the same. However, the methanol side-draw is now fed to a side distillation (rectifier) column to obtain methanol, which may be recycled back to the column. Through simulation studies, it was found that energy savings compared to a conventional biodiesel process using a conventional reactive distillation column are approximately 18.2%—for the Petlyuk reactive column around 30% and for the RTCDS around 54%. Additionally, the total costs have been reduced compared to a conventional biodiesel process using a conventional RD, which is approximately 12%, whereas RD in a Petlyuk arrangement saves approximately 14% and an RD in an RTCDS arrangement saves approximately 17% of the total cost [59].

A similar study has been made by Nguyen et al. [60] for the methyl dodecanoate (biodiesel) production from lauric acid using a solid catalyst. They also identified the RTCDS arrangements as the potentially most promising to achieve a maximal reduction of the energy consumption. They theoretically determined energy savings of around 21%.

Kiss et al. [61] proposed a reactive dividing-wall column (see Figure 8.10) for the production of fatty acid methyl esters (FAME). Their motivation has been that most biodiesel processes are using solid acid/base catalysts, which need a stoichiometric ratio of reactants to allow complete conversion of the fatty acid raw materials and, hence, the production of two highly pure products (water as byproduct and FAME). However, this stoichiometric ratio is difficult to maintain during operation, leading to impure products and recycling of reactants, which results in additional costs. Hence, their new reactive dividing wall column concept allows the use of only 15% excess of methanol to completely convert the fatty acids feedstock. FAMEs

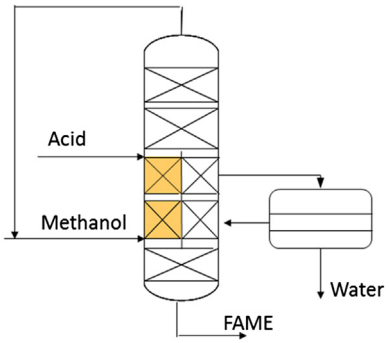

FIGURE 8.10 Reactive Dividing Wall Column for the Production of Fatty Acid Methyl Esters (FAME) [61]

are produced as pure bottom products, with water as side stream, while the methanol excess is recovered as top distillate and recycled. Their final processing scheme after optimization leads to an energy savings of around 25%, which is a much simpler process flowsheet because only one column is necessary, a more flexible plant concerning concentration and kind of fatty acid, and circumventing catalyst losses and neutralization steps.

8.6 Discussion and outlook

Due to the specific challenges occurring in bioprocessing, such as the handling of diluted systems with a low product concentration, flexible raw materials, or raw materials with a varying set of impurities, sensitive biocatalysts and integrated batch-continuous processing, the application of distillation systems has been limited. Despite those challenges, distillation systems are mostly used within biobased processes and white biotechnology mostly for purification of the product, as well as solvent or substrate recovery. Besides, distillation coupled with the reaction for purification of the product and driving of the reaction in nonbiotechnological catalyzed systems or biotechnological catalysts within a reactive distillation column has been reported. Within red biotechnology, distillation has been mostly and solely applied for solvent or substrate recovery and only very limitedly for the purification of the targeted product.

The application of intensified distillation systems, such as reactive distillation, thermally coupled reactive distillation systems, and reactive dividing wall columns, shows great benefits to achieving an economic process, energy savings, and a more flexible process. In particular, the latter is a big advantage when handling biobased raw materials. Also, hybrid processing plays an important role within implementation of economic bioprocesses. The coupling with membrane systems seems especially promising because often water is used as a solvent for the biotechnological transformation steps or occurs in subsequent reactions (e.g. esterifications), which

have to be separated from the products afterwards, often forming azeotropes that can be overcome by using membranes. Further application of advanced or intensified distillation systems will be promising when continuing to develop the concept of biorefineries away from single product systems to multiple product systems [1,5,6]. Also, the integration of biobased raw materials into existing conventional plants will further push those intensified systems or hybrid processing. However, challenges to implement distillation systems into biotechnological processes remain with respect to operating conditions such as handling solid systems (e.g. enzymes, cells) and highly viscous systems. This will require the development of new distillation systems, such as Higee distillation, which could fill in this gap for specific cases [15].

Another interesting concept is the integration enzymatic catalysts into reactive distillation because it allows exploiting the high selectivity of the enzymatic reaction leading to the potential production of new products. Also, the reaction may be exploited as an additional separation step within a reactive distillation, which allows/enables the separation of enantiomers/isomers or other close boiling components by reacting one of those selectively away and therefore enables the production of totally new products. However, matching operating windows between reaction and distillation is the main challenge. Controlling and circumventing enzyme leaching, the development of stable (especially for temperature) enzymes, and sufficient reaction rates will be key issues to be tackled for the implementation. Here, besides metabolic and protein engineering of the catalyst, also new energy forms may be beneficial. Ultrasound, for example, has been reported to increase enzymatic reactions by several factors.

Last but not least, the development of thermodynamic data and models for the description of systems containing biocomponents [62], as well as development of synthesis/design tools, are crucial to support the quick implementation of those systems. The latter one should track biobased impurities and allow the safe and reliable design of distillation as well as intensified process systems. In addition, tools to design and optimize the energy integration between batch and continuous operations are necessary.

Acknowledgments

The author would like to thank Dipl. Ing. Alexander Niesbach and Dipl. Ing. Sebastian Heitmann for their support.

References

[1] W. Soetaert, E.J. Vandamme, Industrial Biotechnology-Sustainable Growth and Economic Sucess, first ed., Wiley-VCH Verlag GmbH & Co., Weinheim, 2010.

[2] P.A. Belter, E.L. Cussler, W.-S. Hu, Bioseparations: Downstream Processing for Biotechnology, first ed., Wiley, 1988.

[3] M. Kircher, Biofuels Bioprod. Biorefin. 6 (2012) 240.
[4] International Energy Agency (IEA), Key World Energy Statistics, 2011.
[5] B. Kamm, Angew. Chem. 119 (2007) 5146.
[6] B. Kamm, M. Kamm, Chem. Biochem. Eng. Q. 18 (1) (2004) 1.
[7] US Department of Energy, in: T. Werpy, G. Petersen (Eds.), Report: Top Value Chemicals from Biomass, 2004.
[8] J.J. Bozell, G.R. Petersen, Green Chem. 12 (2010) 539.
[9] N. Kosaric, Z. Duvnjak, A. Farkas, H. Sahm, S. Bringer-Meyer, O. Goebel, et al., Ethanol, in: Ullmann's Encyclopedia of Industrial Chemistry, Wiley-VCH Verlag, 2002.
[10] T. Roth, P. Kreis, A. Gorak, Chem. Eng. Res. Des. (2013), http://dx.doi.org/10.1016/j.cherd.2013.01.016.
[11] H.-J. Huang, S. Ramaswamy, U.W. Tschirner, B.V. Ramarao, Separation and purification processes for lignocellulose-to-bioalcohol production, in: K. Waldron (Ed.), Bioalcohol Production: Biochemical Conversion of Lignocellulosic Biomass, Woodhead Publishing Ltd, 2010, pp. 246–277.
[12] D.D. Dunuwila, Patent CA2657666A1, 2009.
[13] H. Breivik, G.G. Haraldsson, B. Kristinsson, J. Am. Oil Chem. Soc. 74 (11) (1997) 1425.
[14] A. Halldorsson, C.D. Magnusson, G.G. Haraldsson, Tetrahedron 59 (2003) 9104.
[15] P. Lutze, A. Gorak, Chem. Eng. Res. Des. (2013) (accepted).
[16] T. Melin, R. Rautenbach, Membranverfahren, third ed., Springer-Verlag, Berlin, 2007.
[17] M. Dijkstra, T. Brinkmann, K. Ebert, K. Ohlrogge, Patent DE10333049B3, 2004.
[18] H. Udriot, S. Ampuero, I.W. Marison, W. von Stockar, Biotechnol. Lett. 11 (7) (1989) 509.
[19] P. Lutze, An Innovative Synthesis Methodology for Process Intensification, J&R Frydenberg A/S, 2012, ISBN 978-87-92481-67-2.
[20] B.F.M. Kuster, H.M.G. Temmink, Carbohydr. Res. 54 (1977) 185.
[21] K.M. Rapp, Patent US4740650, 1988.
[22] A. Boisen, T.B. Christensen, W. Fu, Y.Y. Gorbanev, T.S. Hansen, J.S. Jensen, et al., Chem. Eng. Res. Des. 87 (2009) 1318.
[23] P. Lutze, R. Gani, J.M. Woodley, Chem. Eng. Process 49 (2010) 547.
[24] P. Lutze, A. Roman-Martinez, J.M. Woodley, R. Gani, Comput. Chem. Eng. 36 (2012) 189.
[25] A.T. Karunanithi, L.E.K. Achenie, R. Gani, Ind. Eng. Chem. Res. 44 (2005) 4785.
[26] A. Niesbach, J. Daniels, B. Schröter, P. Lutze, A. Gorak, Chem. Eng. Sci. 88 (2013) 95.
[27] A. Orjuela, A. Kolah, X. Hong, C.T. Lira, D.J. Miller, Sep. Purif. Technol. 88 (2012) 151.
[28] A. Orjuela, A. Kolah, C.T. Lira, D.J. Miller, Ind. Eng. Chem. Res. 50 (2011) 9209.
[29] J. Liu, J. Zhu, Y. Wu, Y. Li, Chem. Reac. Eng. Technol. 51 (2012).
[30] O. Franke, O. Richter, Patent EP2481733 A1, 2012.
[31] A.K. Kolah, N.S. Asthana, D.T. Vu, C.T. Lira, D.J. Miller, Ind. Eng. Chem. Res. 47 (2008) 1017.
[32] F.F. Kuppinger, A. Hengstermann, G. Stochniol, G. Bub, J. Mosler, A. Sabbagh, Patent US 20110105791, 2011.
[33] J. Hao, F. Xu, H. Liu, D. Liu, Chem. Technol. Biotechnol. 81 (1) (2006) 102.
[34] T.A. Adams II, W.D. Seider, Chem. Eng. Res. Des. 87 (3) (2009) 245.
[35] N. Asthana, A. Kolah, D.T. Vu, C.T. Lira, D.J. Miller, Org. Proc. Res. Dev. 9 (2005) 599.
[36] J. Gao, X.M. Zhao, L.Y. Zhou, Z.H. Huang, Trans. IChemE part A, Chem. Eng. Res. Des. 85 (2007) 525.

[37] B.H. Lunelli, E.R. Morais, M.R.W. Maciel, R. Filho, Chem. Eng. Trans. 24 (2011) 823.
[38] R. Kumar, S.M. Mahajani, Ind. Eng. Chem. Res. 46 (21) (2007) 6873.
[39] R. Kumar, H. Nanavati, S.B. Noronja, S.M. Mahajani, J. Chem. Technol. Biotechnol. 81 (11) (2006) 1767.
[40] M. Liu, S.-T. Jian, L.-J. Pan, S.-Z. Luo, Chem. Eng. Res. Des. 89 (11) (2011) 2199.
[41] P.P. Barve, I. Rahman, B.D. Kulkarni, Org. Process Res. Dev. 13 (3) (2009) 573.
[42] C. Ozmeral, J.P. Glas, R. Dasari, S. Tanielyan, R. Bhagat, M.R. Kasireddy, Patent WO2012033845, 2012.
[43] H. Dirkzwager, L. Petrus, P. Poveda-Martinez, Patent WO2007099071, 2007.
[44] P. Siricharnsakunchai, L. Simasatikul, A. Soottitantawat, A. Arpornwichanop, Comput. Aided Chem. Eng. PSE 2010 (2012) 170.
[45] A. Hasabnis, S. Mahajani, Ind. Eng. Chem. Res. 49 (2010) 9058.
[46] Z.-H. Luo, X.-Z. You, J. Zhong, Ind. Eng. Chem. Res. 48 (24) (2009) 10779.
[47] C.-W. Chiu, M.A. Dasari, G.J. Suppes, W.R. Sutterlin, AIChE J. 52 (10) (2006) 3543.
[48] J. Deleplanque, J.-L. Dubois, J.-F. Devaux, W. Ueda, Catal. Today 157 (1−4) (2010) 351.
[49] A. Niesbach, R. Fuhrmeister, T. Keller, P. Lutze, A. Górak, Ind. Eng. Chem. Res. 51 (2012) 16444.
[50] G. Knothe, Top. Catal. 53 (2010) 714.
[51] A.A. Kiss, A.C. Dimian, G. Rothenberg, Energy Fuels 22 (2008) 598.
[52] C. Mueanmas, K. Prasertsit, C. Tongurai, Int. J. Chem. React. Eng. 8 (2010) A141.
[53] B.B. He, A.P. Singh, J.C. Thompson, Trans. ASABE 49 (1) (2006) 107.
[54] Nde L. da Silva, C.M. Santander, C.B. Batistella, R.M. Filho, M.R. Maciel, Appl. Biochem. Biotechnol. 16 (2010) 245.
[55] I. Noshadi, N.A.S. Amin, R.S. Parnas, Fuel 94 (2012) 156.
[56] A. Górak, L.U. Kreul, Patent DE 19701045 A1, 1998.
[57] A.L. Paiva, F.X. Malcata, Biotechnol. Tech. 8 (1994) 629.
[58] R. Heils, A. Sont, P. Bubenheim, A. Liese, I. Smirnova, Ind. Eng. Chem. Res. 51 (2012) 11482.
[59] F.I. Gomez-Castro, V. Rico-Ramirez, J.G. Segovia-Hernandez, S. Hernandez-Castro, Chem. Eng. Res. Des. 89 (2011) 480.
[60] N. Nguyen, Y. Demirel, Energy 36 (2011) 4838.
[61] A.A. Kiss, J.G. Segovia-Hernandez, C.S. Bildea, E.Y. Mair-Galindo, S. Hernandez, Fuel 95 (2012) 352.
[62] C. Held, Measuring and modeling thermodynamic properties of biological solutions (Ph.D Thesis), Dr. Hut, 2012, ISBN: 3843903700.

This page intentionally left blank

CHAPTER

Special Distillation Applications

9

Eva Sørensen[1], **Koon Fung Lam**[1], **Daniel Sudhoff**[2]
Department of Chemical Engineering, UCL, London, UK[1],
Department of Biochemical and Chemical Engineering,
TU Dortmund University, Dortmund, Germany[2]

CHAPTER OUTLINE

Distillation: Operation and Applications. http://dx.doi.org/10.1016/B978-0-12-386876-3.00009-0

9.1 Short path distillation

Short path distillation is a technique that involves vaporized compounds traveling a short distance, only a few centimeters, from an evaporator surface to a condenser surface. The operation is normally performed at reduced pressure, down to 0.001 mbar. A pressure gradient from evaporator to condenser is thereby essentially avoided, and vapor molecules may travel between the evaporator and the condenser without colliding with other molecules. Short path distillation is therefore often referred to as *molecular distillation* as the process is based on the free transfer of molecules evaporated under high vacuum. Although the two terms are both used in the literature, only *short path distillation* will be used in this chapter. As the pressure is reduced, the heating temperature can be considerably lower than at standard pressure. In addition, the distillate only has to travel a short distance before condensing, hence the material is only exposed to elevated temperatures for a very short time. The technique is therefore often used for compounds that are unstable at high temperatures and that will degrade or denature if distilled at higher pressures, for biological material, or to purify very small amounts of compound. As the process does not involve the use of a solvent as in extractive distillation, the product material is not polluted and no further purification is needed.

Interest in the short path distillation process is increasing due to its applicability and advantages for the recovery, purification, and concentration of substances of high added value in industries such as cosmetics, food, pharmaceuticals, and petrochemicals. Examples of usage are separation of fat-soluble vitamins [1], grape seed oil deacidification [2], separation of free fatty acids from vegetable oil [3], purification of octacosanol extracts from transesterified rice bran wax [4], increasing citral concentration in lemongrass oil [5], and removing phthalates from sweet orange oil [6]. Furthermore, short path distillation can also be used for separation of waxes, fats, and natural oils [7], and for fish oils, petroleum residues, solvent removals, and many more.

9.1.1 Separation principle

In short path distillation, the separation is based on transfer of evaporated molecules from the free surface of the liquid feed, and not directly on differences in volatility as in conventional distillation, thus allowing components with similar boiling points to be separated. There are two main types of short path distillation units, *falling film*

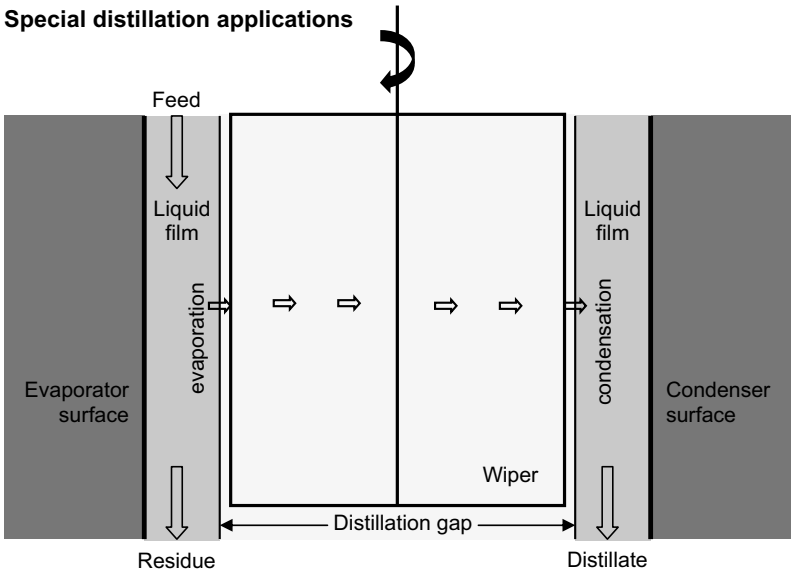

FIGURE 9.1 Short Path Distillation Principle

and *centrifugal*, and the separation principles are similar in both types as both use the principle of vacuum to enable the transfer of vapor molecules from the evaporator to the condenser. Furthermore, both modes introduce the liquid feed in the form of a thin liquid film that promotes heat and mass transfer effects. Falling film uses gravitational force to allow the liquid to be distributed as a thin film on a vertical evaporator surface, usually with the aid of a wiping system (see Figure 9.1). The wiping system mixes and distributes the liquid evenly across the entire surface of the evaporator [8]. The centrifugal units use centrifugal force, generated by a rotor, to promote the formation of the thin film. In both cases, two product streams are generated: the distillate stream, rich in the molecules that have evaporated from the evaporator to the condenser; and the residue stream, rich in the higher boiling molecules that have not.

9.1.2 Falling film short path distillation

Short path distillation in a falling film type apparatus consists of two vertical tubes, one inside the other, with one acting as an evaporator and the other as a condenser. The feed may be preheated before entering the evaporator, and the evaporator can therefore be both heated and unheated. For a heated evaporator, the distillation rate is faster, but the separation factor has in some cases been observed to decrease at higher temperatures when compared to an unheated evaporator [9].

The feed is introduced to the evaporator at the top of the unit, normally to the outer tube, with the condenser being the inner tube, but can also be to the inner

tube with the condenser being the outer tube. In the former case, a heating medium is placed on the outside of the tubes, sometimes using steam as high heat transfer coefficients may in some cases be required in order to achieve equally balanced heat transfer resistances. In the latter case, the outer tube would have a cooling jacket.

In both cases, the process fluid to be evaporated flows downward by gravity as a continuous phase, thus creating a film along the tube walls, progressing (or falling) downward. The liquid film partially evaporates as it flows, and the vapor molecules find a free path and diffuse through the distillation gap under high vacuum. To ensure efficient separation, the distillation gap should be smaller than the mean free path of the more volatile component but larger than that of the less volatile component. Once the vapor molecules find their way to the condenser, they condense back into liquid form. The condensed liquid, which consists mainly of the more volatile component and is therefore called the distillate, is collected at the bottom of the condenser tube. The residue, likewise, is collected at the bottom of the evaporator tube.

9.1.2.1 Falling film design and operation

A number of studies have been conducted to identify and characterize the key parameters that determine the performance of short path processes. The design of the unit, in particular the distance between the evaporator tube and the condenser tube (the distillation gap), clearly has an impact on the separation efficiency. The operating conditions, such as pressure, feed temperature, and condenser temperature, also have a major impact on the performance.

9.1.2.1.1 Configuration

Industrial falling film short path units are designed with the evaporator in the outer tube, normally heated by steam or hot oil, and with a condenser inserted inside with a cooling medium flowing through. Lutisan and Cvengroš [10] concluded, however, that having the evaporator in the inner tube and the condenser as the outer tube will result in higher separation efficiency for the same diameter. This is due to the fact that in a concave-surfaced evaporator (outer tube), the vapor molecules can "miss" the condenser and hit the evaporator on the other side instead. This can be avoided by having a fairly large diameter of the inner tube.

9.1.2.1.2 Distillation gap

Splashing, or physical transfer of liquid from the evaporator to the condenser, must be avoided as it leads to a reduction in the separation efficiency [11]. This problem is particularly acute when the gap between the evaporator and condenser is very small. To reduce this from happening, a sieve that acts as an entrainment separator can be placed in between the tubes in the distillation gap. Note that some reevaporation may occur on both sides of the sieve. The sieve stabilizes the distillate composition and reduces the effects of splashing [11]. Even though the composition of the distillate is improved, the distillation rate will, however, be reduced.

9.1.2.1.3 Operating conditions

Although boiling points are lower when the operating pressure is lower, there nevertheless exists an optimal operating pressure for each compound given by the Knudsen-Langmuir equation, which gives the maximum evaporation rate at a given operating temperature and evaporator surface area.

Kawala and Stephan [9] considered evaporation of a binary mixture of di-*n*-butyl-phthalate and di-*n*-butyl-sebacate in an unheated, nonwiped, falling film evaporator. They found that an increase in the inlet feed temperature increased the temperature and concentration gradients. Maximum gradient values were achieved at low feed rates. If the evaporator is heated, the distillation rate will be faster as the increased temperature increases the velocity of molecules which makes them move to the condenser more easily rather than accumulate in the distillation gap. However, the separation efficiency may decrease at high temperature. The authors proposed a general rule for designing a molecular evaporator under adiabatic conditions: if the separation efficiency is more important than the distillation rate, the diameter should be small and the height should be large and vice versa. Cvengroš et al. [12] investigated the effect of temperatures at the film surface along the length of the evaporator under steady state conditions and found that the temperature of the feed inlet has a considerable effect on the separation efficiency. They therefore recommended that the feed should be preheated to avoid the need for heating from the evaporator.

Hu et al. [13] considered the impact of the condenser temperature and confirmed that the lower the condenser temperature, the better the separation. Also, they found that greater evaporation efficiency is achieved when the ratio of condenser area to evaporator area is high.

9.1.2.2 Falling film behavior

Investigations have shown that the actual degree of separation achieved in a short path distillation process depends not only on the relative volatility of the components but also on the transport resistances in the liquid phase and their interaction with the intrinsic interfacial resistance to evaporation that exists because of kinetic-molecular constraints that become important at these low pressures and temperatures. When analyzing the performance of the unit, heat and mass transfer in the liquid film on the evaporator, as well as in the liquid film of condensed liquid on the condenser, must be considered, as must the transfer within the vapor phase between the two tubes, i.e. in the distillation gap [14].

9.1.2.2.1 Evaporator behavior

Bose and Palmer [1] considered separation of a binary mixture into a partial vacuum and found that separation factors approach thermodynamic and kinetic limits only at low temperatures and correspondingly low distillation rates. At higher temperatures, the separation factor decreased sharply to values that may be nearly half the theoretical maximum. The mass transfer resistance was more significant than the heat transfer resistance in determining the drastic decline in separation factor with increasing

temperature. However, because of the coupling between heat and mass transfer through the vapor pressure vs temperature relations, interfacial cooling helped to compensate for the deleterious effect of surface depletion. If interfacial cooling is ignored, separation factors may be underestimated by 25% or more.

9.1.2.2.2 Vapor phase behavior

The concept of collision factor to account for the possible collisions between molecules in the distillation gap was introduced by Burrows [15], who studied the mean free path in short path distillation. A collision between molecules can result in a molecule bouncing back to the evaporator, or alter its path so it cannot reach the condenser. Burrows also demonstrated that the arrangement of a curved surface reduces the effects of the collisions and hence results in higher separation efficiency. The vapor phase can thus be modeled by introducing a collision factor in the Langmuir-Knudsen evaporation equation [9].

Lutisan and Cvengroš [10] also studied the mean free path in the vapor phase. They noted that there are other factors that may affect the distillation rate other than just the collisions, making the kinetic theory of gas equation alone invalid. The reevaporation of molecules from the condenser, for instance, may also have an effect on the process efficiency, although Badin and Cvengroš [16] claimed that this effect is limited. Hu et al. [13] took into account molecular rotation in the vapor phase in their theoretical study, arguing that most of the compounds that are being separated by short path distillation are polyatomic, and orientation therefore has an impact. Also, when an inert gas is present, an accumulation of the inert gas near the condenser surface can cause the temperature and molecular density in the distillation gap to increase, thus cooling down the components becomes more difficult.

9.1.2.2.3 Condenser behavior

Badin and Cvengroš [16] found that the process can be severely disturbed if the temperature conditions of the condenser do not allow total condensation. The authors concluded that efficient condensation may be achieved by either lowering the distillation rate, installing side off-takes of the condensate, or lowering the temperature of the condenser with respect to the compounds' boiling points. Furthermore, in their experience, a temperature gradient of 60–80 °C between the evaporator and the condenser is required for total condensation to occur.

9.1.3 Wiped falling film short path distillation

A wiped falling film short path unit is similar in design to a *wiped falling film evaporator*, but where the short path unit has a condenser placed at the center upon which the vapor condenses, whilst the evaporator unit does not. In a standard falling film unit, temperature and concentration gradients exist in the liquid film, both axially and radially, causing lowered separation efficiency. The radial gradients are due to the heat that is added to the evaporator surface, the evaporation of vapor from the

liquid–vapor interphase, and the liquid velocity at the surface of the interphase being different than at the surface of the evaporator. The wiping system is therefore introduced to reduce the gradient and improve the separation efficiency. In a wiped film short path distillation unit, the liquid film is continuously mixed and evenly distributed across the entire surface of the evaporator by the action of the wiping blades, thereby ensuring sufficient liquid also at the lower part of the evaporator, which may be an issue for an unwiped unit. In addition, it is possible for wiped film short path distillation to treat liquids with quite high viscosities depending on the design of the blades. Wiper blade design is subject to much research amongst equipment providers, much like tray and packing internals for distillation column providers.

9.1.3.1 Wiped falling film behavior

Approximate and exact solutions for the calculation of evaporator film thickness were developed by Godau [17] taking into account the dependence of the thickness on the density, viscosity, and flow rate, however, he did not consider the influence of the action of the wiper blades. McKelvey and Sharps [18] studied the velocity profiles and the structure of the bow waves that were developed as a consequence of wiping on certain parameters. Komori et al. [19,20] went a step further and examined the flow structure and mixing mechanisms of the bow waves in detail, both theoretically and experimentally, using wiped film devices with limited blades. The degree of mixing in the area between the film and the bow waves was closely investigated.

Lutisan et al. [21] found that the flow regime of a wiped film short path distillation unit lies between the laminar and turbulent regimes. In the laminar case, the velocity distribution has a semiparabolic behavior for the temperature and concentration gradients. In the turbulent case, there is ideal mixing in the direction perpendicular to the flow without temperature and concentration gradients. The evaporation rate is much higher in the turbulent regime than in the laminar regime at the same evaporator surface temperature. This means smaller thermal decomposition rate and lower residence time. The flow regimes have limited effects on the separation efficiency.

Proper account of the flow regime is required to accurately predict the behavior of the system. Early models assume the flow regime to be laminar [1,9,22]. Nguyen et al. [23] took into account a wiped film short path unit with turbulent flows, building on the knowledge from Erdweg [24]. A relationship between the heating surface, the initial concentration, the overall throughput, and the concentration change inside the unit was established. Wang and Xu [25] used computational fluid dynamics (CFD) to investigate the effects of the liquid flow rate and the speed of the wiper on the film thickness and the liquid flow field.

9.1.4 Centrifugal short path distillation

In a centrifugal short path distillation unit, the liquid feed is either heated to the desired temperature prior to entering the system or heated within the unit. The

feed is pumped to the top and center of the evaporator, which is the centrifugal part of the system. The liquid, by centrifugal force, spreads evenly along the evaporator's surface into a thin film, approximately 0.1−1 mm depending on the viscosity, rotor speed, and flow rate. If the liquid is heated within the unit, then this is provided through the cone wall via steam or hot oil. Molecules evaporate from the thin liquid film and travel toward condenser tubes, through which a cooling medium is circulated, placed close to the evaporator surface where the molecules are cooled back into the liquid phase. The condensate is collected and becomes the distillate. The residue is also collected and removed.

9.1.4.1 Centrifugal short path behavior

The evaporation of molecules in a centrifugal unit is similar to the falling film unit in terms of evaporation and molecular transport across the distillation gap, but a centrifugal unit has an additional degree of freedom, in the rotor speed, which will also have an influence on the separation. Few authors have, however, considered centrifugal operation.

Kaplon et al. [22] proposed a mathematical model to simulate the temperature profile of the liquid film evaporating from the rotating disc under high vacuum. They identified a temperature drop across the path of the flow as the liquid evaporated from the surface of the rotating disc under high vacuum. This temperature gradient, from the center of the disc, was found to alter the evaporation rate.

Ishikawa et al. [26] investigated centrifugal short path distillation with reflux and found that the separation efficiency was enhanced by the addition of reflux operation, i.e. recycling back of some of the condensed liquid. With increasing reflux ratio, the distillate rate decreased while the efficiency increased. Chen et al. [27] simulated centrifugal short path distillation taking into account the two phases (liquid and vapor), and the interfacial transport between them, using a CFD model. They found that the interfacial transfer mechanism introduced was more accurate than the Langmuir evaporation theory for describing the mass transfer at the interface of centrifugal short path evaporators.

9.1.5 Comparison between falling film and centrifugal short path distillation

Batistella et al. [28] compared the performance of a falling film short path unit and a centrifugal short path unit for the recovery of vitamin E from vegetable oils using simulation models based on Kawala and Stephan [9] for the falling film unit and on Bhandarkar and Ferron [29] for the centrifugal unit. They found that the choice of unit depends on the separation problem. Products that could be damaged when exposed to heat for a long period of time should be distilled in a centrifugal unit since the residence time is much shorter than that of the falling film unit. On the other hand, products that are more sensitive at high temperatures should be handled by a falling film unit as the apparatus can reach the same concentration as the centrifugal unit but at lower temperatures.

Batistella et al. [30] compared the centrifugal and falling film unit in terms of reflux and using a cascade of units to separate fine chemicals. A cascade of units was considered to improve the separation power. The cascade may also have some reflux returned. It was concluded that the use of reflux improved the efficiency of the centrifugal unit; however, it was not convenient for a falling film unit.

9.1.6 Reactive short path distillation

Short path distillation may also be suitable for reactive separations as a hybrid unit combining a reactor and short path separator. In a reactive unit, the reaction occurs on the surface of the evaporator and one or more of the products, and possibly some of the reactants, are partially evaporated. Once evaporated, the separation occurs as in normal short path distillation by means of free path of molecules. This combination is particularly useful for equilibrium-limited reactions as the products of the reaction are continuously being removed from the reaction zone, thus increasing the yield. Also, the selectivity is higher through the suppression of undesired consecutive reactions [31], and thermal degradation of products is avoided as they are exposed to the heat only very briefly.

Reactive short path operation has been considered in both falling film [32,33] and centrifugal [5,34] short path distillation apparatus. Winter et al. [33] developed a reactive short path distillation unit for cracking of heavy oils and investigated its operation. Biller [32] developed a mathematical model of an industrial reactive short path unit based on thermally unstable reactants and products, and conducted a sensitivity study of the operating conditions and also considered control of the process. Tovar et al. [5] considered operation in a centrifugal unit to increase the citral concentration in lemongrass essential oil, without adding any extra components to the system, causing minimal thermal impact and reaching high quality for the essential oil extracted at the distillate stream. Finally, Tovar et al. [34] considered separation from high boiling petroleum fractions.

9.1.7 Summary and outlook

Short path distillation is a well-established process in industry for niche separations of unstable compounds, for biological material, and to separate very small amounts of product. The design is inherently simple, although great care must be taken in establishing the unit height, but more importantly, the diameter of the evaporator and the condenser to ensure that the conditions in the distillation gap are optimized to guarantee maximum separation efficiency. The operating pressure and evaporator and condenser temperatures, and rotor speed for centrifugal operation, must be chosen carefully to ensure that the feed is not damaged, but that the operation is nevertheless optimized both in terms of separation efficiency and in terms of separation rate.

More work is needed to better understand the behavior of these units, in particular, in terms of the liquid film resistance, the impact of wiping, as well as the

behavior in the vapor phase. Operation in centrifugal and reactive units has hardly been considered, and is therefore not well understood, and requires further consideration.

9.2 HiGee distillation

Distillation is a highly energy demanding unit operation, and numerous modes of energy, or process, intensification alternatives have been proposed and implemented over the years. Many of these are based either on the application of additional and alternative energy forms or on the manipulation of structural parameters [35]. Using high gravity fields rather than normal gravity for distillation addresses both approaches. The additional energy provided by the high centrifugal forces enables intense mass transfer and high capacities. Additionally, the transformation of a longitudinal geometry to a radial geometry leads to a compact and intensified device. High gravity fields have benefits over single gravity operation for certain applications as discussed below. This technology, applying high gravity ("high g"), is generally referred to as "HiGee" technology [36] and consists of packed beds that are rotated.

The main applications of rotating packed beds are as reactors for the production of nanoparticles or polymers [37], for absorption and stripping processes [38], as well as for degassing of liquids [39]. The most prominent industrial application is for reactive stripping in the production of hypochlorous acid [40].

Centrifugal separations have been commercially available in numerous liquid−liquid extraction applications for more than three decades, such as in extractive recovery of penicillin, the separation of caustic solutions and oils in the soap making process, in uranium extractions, and in many others. The application for vapor−liquid separations, i.e. distillation, is rather new [41,42], and not yet established in industry, although in China, zig-zag rotating beds are claimed to be applied for several hundred distillation processes [43]. Only very few industrial studies of rotating packed beds for distillation have been carried out, and only few results have been published [44,45]. Detailed information about these studies, or about the applications of zig-zag rotating beds, is, however, not available.

9.2.1 Separation principle

The idea of performing distillation in a high gravity environment rather than in a single gravity environment was first proposed by Ramshaw and Mallinson in 1981 [46]. In their patent, they suggest the application of a rotating packing with a large interfacial area for contacting a liquid with a second immiscible fluid, either liquid or vapor. The high gravity field is generated by the rotation of cylindrically shaped packings. These devices are therefore usually referred to as rotating packed beds (RPBs). The packing internals can be structured or random, as well as rings, comparable to tray columns [47].

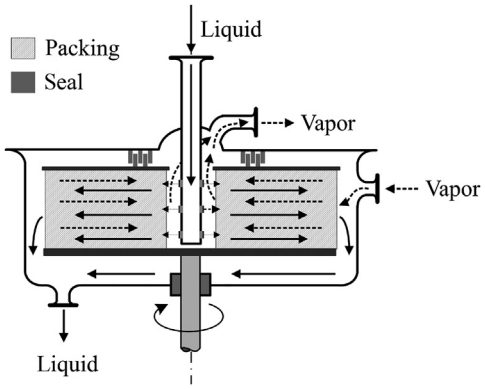

FIGURE 9.2 HiGee Distillation Principle

The basic principle of a rotating backed bed unit is illustrated in Figure 9.2. The cylindrical packing is mounted to a shaft and serves as a rotor. For countercurrent operation, which is essential for distillation, the liquid is introduced to the eye of the rotor through small nozzles. Entering the rotating packing, the liquid is accelerated toward the outer radius by the centrifugal forces and is collected at the casing. The vapor, or generally the lighter fluid, is introduced through the casing and flows due to an externally applied pressure toward the center of the rotor and is withdrawn there. The seals between the rotating and nonrotating parts are essential to avoid bypassing of liquid and vapor [47].

The characteristics of rotating packed bed units for distillation can be illustrated by an analogy to distillation columns as given in Figure 9.3. The overall orientation of the liquid and vapor flows in columns is vertical. In contrast, streams in rotating packed beds are generally horizontal. Taking one packing section in a column, its vertical height represents the separation efficiency and its radial diameter represents the capacity. In contrast, the radial length of the rotor in a rotating packed bed

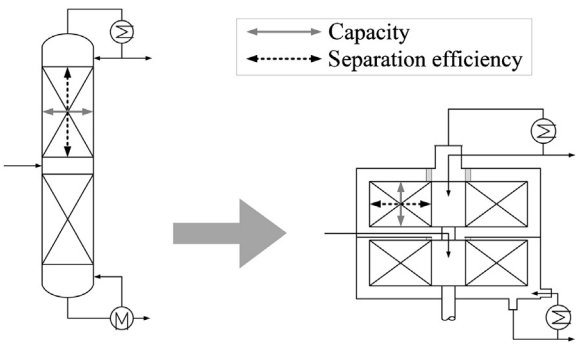

FIGURE 9.3 Transformation of Gravitational to Centrifugal Distillation

represents the separation efficiency, and the vertical height of one packing represents the capacity.

Whilst the feed to a distillation column can easily be introduced, in rotating packed beds the introduction of a liquid feed is rather complex. In units consisting of only one rotor, a feed pipe has to be located along the radial coordinate of a rotor. A good distribution of the feed over the cross-section of the rotor packing is therefore difficult. A further possibility is to attach two consecutive rotors to the same shaft. The liquid from the upper rotor is collected at the outer casing and redistributed to the eye of the lower rotor, while the vapor has to follow the countercurrent path from the eye of the lower rotor to the outer surrounding of the upper rotor. A liquid feed can easily be introduced to the eye of the lower rotor. Hereby a rectifying section in the upper, and stripping section in the lower, rotor is formed (Figure 9.3).

In addition to the design decision in terms of the particular geometry of rotating packed beds, the rotational speed provides an additional degree of freedom in terms of operation. This operating parameter is flexible and can be set up to 2500 rpm, generating a centrifugal force that exceeds the gravitational force by up to three orders of magnitude [43,47]. It should be noted that the centrifugal acceleration is a function not only of rotational speed but also of radius. At high rotational speeds and large radii, very high centrifugal factors are reached very quickly, assuring an intense mixing and an increased mass transfer. However, the radial dependency of the centrifugal acceleration generates an inhomogeneous centrifugal field in the packing, from a low centrifugal acceleration at the center, to a high centrifugal acceleration at the outer edge of the rotor. The liquid and vapor loads are, however, large at the center and small at large radii in the packing. This opposite behavior between loads and centrifugal force leads to varying separation efficiencies over the radius.

The fundamentals of mass transfer in rotating packed beds have yet to be fully explored and understood, and only a few investigations have been undertaken. The flow patterns inside a rotating packed bed are difficult to observe inside a rotating packing. Burns and Ramshaw observed three different types of liquid flows inside a structured packing [48]. At low centrifugal forces, a rivulet flow with severe liquid maldistribution occurred, whereas a droplet flow, and eventually a film flow, was observed with increasing rotational speeds.

In addition to the basic design of a rotating packed bed, alternative designs have been proposed in the literature, including integration of a reboiler and a condenser into the casing [49], different orientation of the rotors [50,51], and other types of packing [43].

9.2.2 Rotor design

Several different types of packing internals and rotor designs exist. In all, the applied centrifugal field is the basis, and the major flow direction is therefore radially.

For all rotor designs for distillation, the flow direction of the liquid is radially outward whilst the vapor flows radially inward [47]. A radial countercurrent flow

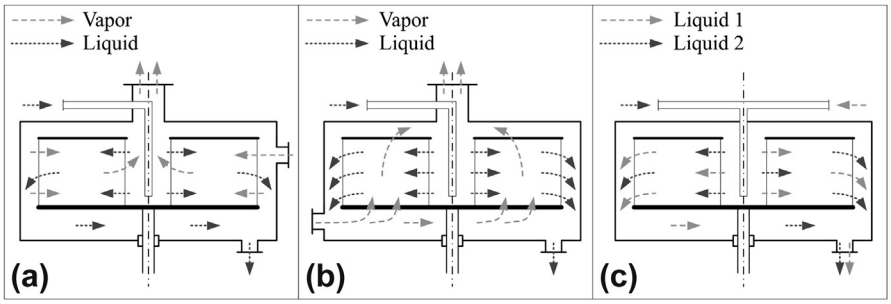

FIGURE 9.4 Flow Directions in Rotating Packed Beds

(a) countercurrent, (b) crosscurrent, and (c) cocurrent.

is thereby realized as indicated in Figure 9.4(a). Applications of rotating packed beds for mixing or reaction are, however, also carried out in cocurrent flow (Figure 9.4(c)) [52], whilst for absorption, crossflow rotors are also used (Figure 9.4(b)) [53].

Amongst the countercurrent flow designs, two different concepts exist. In the first concept, a cylindrically shaped packing is applied that can be compared to packed columns. As indicated in Figure 9.5 this packing can be either solid (Figure 9.5(a)) [45] or split (Figure 9.5(b)) [54]. The first is the most commonly used and easiest to build since it consists of a solid cylinder that is used as the rotor. Normally, metal wire mesh, glass spheres, or metal foams are applied [47]. The latter consist of multiple concentric rings of packing, mainly metal foams, with increasing diameter [54]. The packing rings are alternately attached to the rotors and may rotate in the same or opposite direction. Higher turbulences in the vapor phase are expected [55].

The second concept for countercurrent flow is a rotor with perforated concentric rings [43], comparable to sieve tray columns. A first version of this concept used a

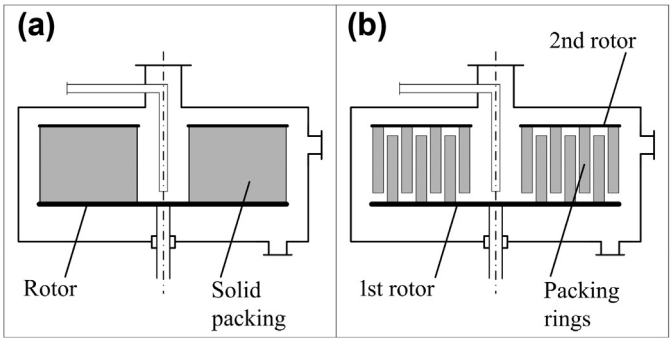

FIGURE 9.5 Rotating Packed Beds

(a) solid packing, and (b) split packing.

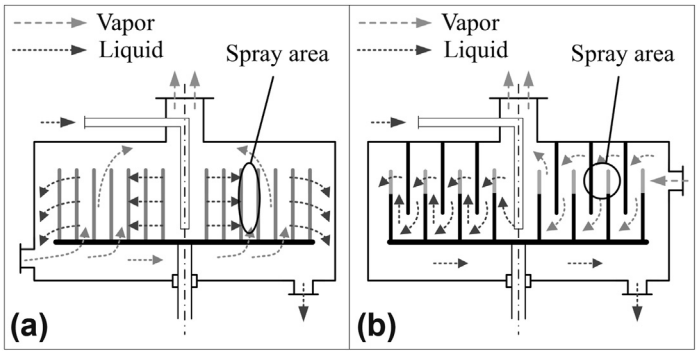

FIGURE 9.6 Countercurrent Flow Rotating Packed Beds

(a) concentric-ring rotating bed and (b) rotating zig-zag bed.

crosscurrent flow direction [56]. The liquid passes the perforated rings radially outward, while the vapor crosses the flow upward as shown in Figure 9.6(a). This so-called concentric-ring rotating bed (CRRB) is mainly used for stripping processes [56]. For distillation, a second version, the so-called rotating zig-zag bed (RZB) is employed (Figure 9.6(b)) [57]. The flow direction is not really countercurrent, since the liquid follows a rather zig-zag flow pattern. The rotating zig-zag bed has alternating stationary and rotating rings. The liquid is accelerated radially outward until it is stopped by the rotating rings. The ends of these rings are perforated to realize a spray or dropping of liquid from the end of the rings. The stationary rings stop the liquid and make sure it flows downward again before the next rotating rings [57]. Of the most commonly used designs, only the countercurrent flow rotating packed beds with solid or split packing, and zig-zag rotating beds, are used for distillation [47,57].

9.2.3 Summary and outlook

The exceptional geometric design of HiGee distillation, and the additional degree of freedom in the form of the rotational speed, have yet to be exploited by industry. However, potential fields of application for rotating packed beds for distillation exist. Primarily, the remarkable reduction in size and independence from the vertical orientation of columns offer new opportunities for implementation of rotating packed beds for distillation. A potential field of application is the retrofitting of existing plants with an integration of the plant design with mobile or modular applications.

Additionally, the high forces applied to the liquid can be utilized not only to increase the capacity but also to apply new packing materials with very large surface areas of more than 3000 m^2/m^3 [47], to treat sensitive media that require short residence times, also for reactive applications [40], and to handle mixtures with high viscosities [58]. The rotational speed can also be exploited as an additional degree

of freedom as it has a strong effect on the separation efficiency of rotating packed beds [59]. The separation efficiency in terms of number of theoretical stages reaches a maximum at a certain rotational speed offering a dynamic operating mode. In a certain window, the rotational speed can be varied to quickly react to changes in the feed composition or in the required purities of the products. Finally, offshore applications of distillation may also become feasible [39] as a HiGee unit is easier to operate when there is movement.

9.3 Microdistillation

Microchemical processing technology has been identified as a promising strategy to intensify chemical processes. By definition, such technology involves the design and fabrication of chemical processing equipment such as reactors, separators, and mixers, with at least one dimension less than 1 mm. Distillation is a common process for separating miscible fluid mixtures based on differences in volatility between components. The process involves mass transfer between a vapor and a liquid phase, and thus, it can potentially be intensified by microchemical processing technology. Separations at micro scale have been considered in an extensive review by Lam et al. [60]. When process fluid flows through channels at submillimeter level, heating and cooling becomes much more effective due to the significant increase in the surface area-to-volume ratio. The reduction of the dimension, e.g. depth of a liquid channel, also reduces the mass transfer distance for mass exchange between two distinct phases, including gas−liquid and liquid−liquid phase systems, resulting in significantly higher mass transfer.

9.3.1 Separation principle

A conventional distillation column operates by generating a vapor phase by heating a liquid holdup in the reboiler at the bottom of the column. The vapor flows upward and condenses in the condenser located at the top of the column, forming liquid product (distillate). Some of the liquid is removed as product and some is returned back to the column as liquid reflux. The liquid inside the column flows downward due to the gravitational force until it reaches the reboiler. In a microfluidic environment, however, this operation principle is not applicable as the extent of gravitational force is less significant whilst surface tension and viscosity dominates. This phenomenon is described by the dimensionless Bond number (Bo), which is a measure of the importance of surface tension forces compared to body forces. When the characteristic length is small, the Bo number becomes smaller, meaning that surface tension of the liquid dominates over gravitational force. Under such conditions, the direction of liquid flow inside the microchannel is disturbed, and a stable vapor−liquid interface is not achievable by simple miniaturization of conventional distillation.

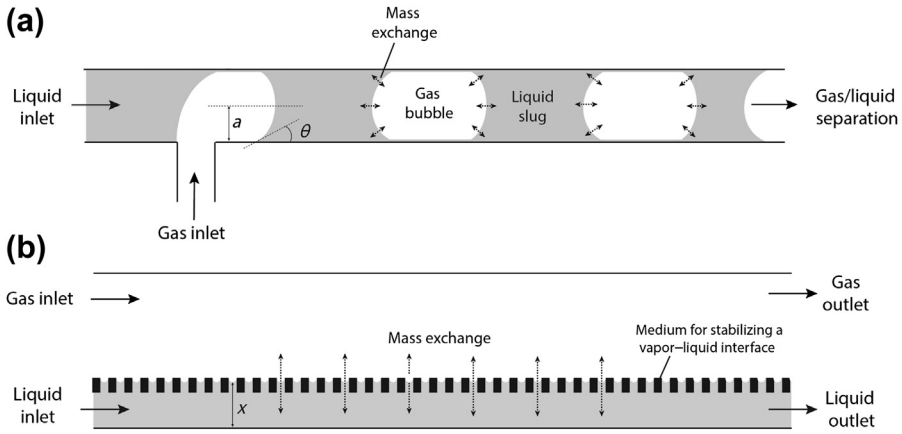

FIGURE 9.7 Microcontactors

(a) dispersed-phase and (b) continuous-phase.

9.3.2 Design of microdistillation

Two major approaches, based on a dispersed phase or on a continuous phase, have so far been adopted to overcome the challenge of a stable vapor–liquid interface. In dispersed-phase microcontactors, gas bubbles are induced by merging the streams of gas and liquid flows. The bubbles are separated by liquid slugs, whereas a liquid film also separates them from the wall, as shown in Figure 9.7(a). The mass exchange takes place at the surfaces of the bubble, followed by a subsequent step for the gas–liquid separation. In continuous-phase microcontactors, gas and liquid phases form two streams, which are fed separately in a liquid and a gas region of the microcontactor (Figure 9.7(b)). The two streams are brought to contact for mass exchange with a stable vapor–liquid interface that can be established by different means.

9.3.2.1 Dispersed phase

A dispersed-phase microdistillation system using nitrogen as carrier gas, which is used to create a gas–liquid boundary by forming bubbles or slugs, was demonstrated by Hartman et al. [61]. Their system consisted of two separate units: a silicon-based microchip for gas–liquid contact, and a subsequent gas–liquid separator. The silicon chip was fabricated using a conventional semiconductor processing technique with a microchannel pattern. The microchannel was of a serpentine shape with a gas and a liquid inlet for bringing the mixture and carrier gas together. By controlling the ratio of flow rates between the gas and liquid streams, dispersed and segmented flow of liquid and gas was achieved (Figure 9.8). When the silicon chip was heated, the liquid vaporized until the carrier gas was saturated with the vapor. The residence time for mass transfer was determined by adjusting the flow rates of the streams and the length of the serpentine microchannel. The outlet of the microchannel was connected to a gas–liquid separator that was used to separate

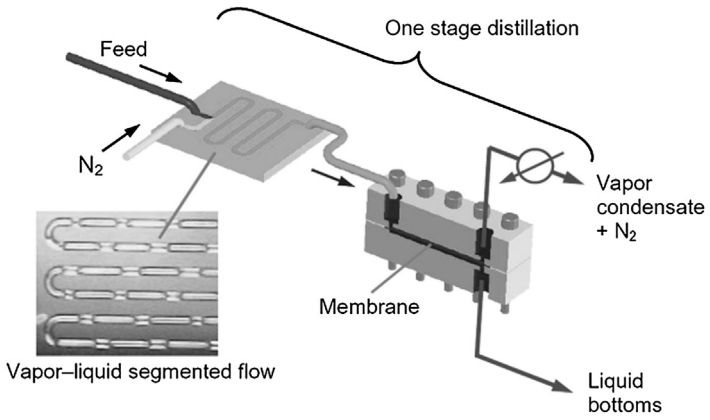

FIGURE 9.8 Schematic Diagram of the Microdistillation System Developed by Hartman et al. [61]

Reproduced from Ref. [61] with permission by the Royal Society of Chemistry.

the carrier gas bubbles saturated with the more volatile component from the remaining liquid that contained a higher fraction of less volatile component. The experimental results showed that this design was capable of separating equimolar mixtures of methanol/toluene and dichloromethane/toluene. The optimal separation performance was equivalent to a single equilibrium stage. The same research group also demonstrated the possibility of connecting this microdistillation system with a microreactor for chemical synthesis [62].

Another approach to creating the dispersed vapor−liquid contact was suggested by Boyd et al. [63]. In their conceptual design, a microchannel with a layer of gold nanoparticles was fabricated. By directing and focusing a laser beam onto the gold nanoparticles, heat was evolved in the localized region and the liquid mixture was vaporized. The vapor formed a gas bubble, and condensation took place at the region without laser exposure (Figure 9.9). This process is known as the bubble-assisted interphase mass-transfer (BAIM) method, which allows the separation to take place without the need for high temperatures, vacuum, or active cooling. However, there are limited quantitative results for its separation efficiency.

9.3.2.2 Continuous phase

Several strategies have been employed to establish a stable gas−liquid interface with continuous vapor and liquid flow at micro scale, in particular, falling film, carrier gas, vacuum, capillarity, and centrifugal force. These strategies will be considered in the following sections.

9.3.2.2.1 Falling film

Although gravitational force is less significant than surface tension for the liquid flow in a microdistillation device, operation of microdistillation based on gravity is still possible. For instance, Ziogas et al. [64] designed a vertically operated

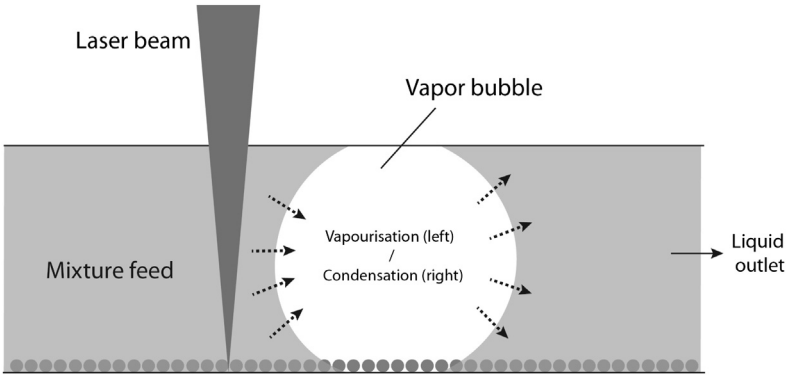

FIGURE 9.9 Conceptual Design of Microdistillation Based on the Bubble-Assisted Interphase Mass-Transfer Method Proposed by Boyd et al. [63]

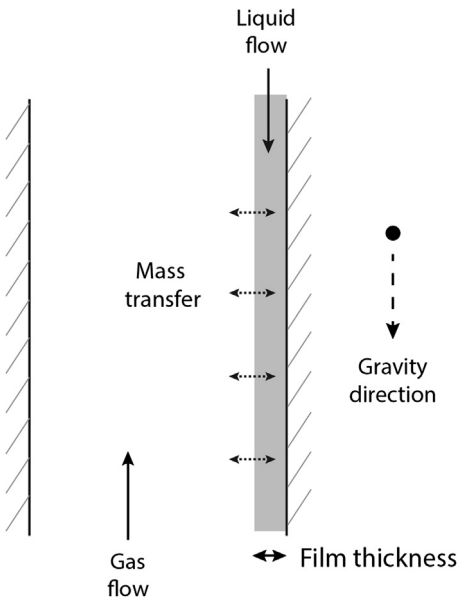

FIGURE 9.10 Operating Principle of the Microdistillation Apparatus Used by Ziogas et al. [64]

plate-type microdistillation device resembling a conventional distillation column (Figure 9.10). Liquid, including both feed and reflux, flowed continuously downward driven by gravity along the plate wall. The wall and plate structure facilitated the wettability of the liquid so a thin liquid film was formed, thus the configuration is also known as a *falling film microcontactor*. A temperature gradient was induced by controlling the temperature of the heating cartridge and the reflux from the

condenser. As the distance between the bubbling liquid layer and the vapor domain was small, the heat and mass transfer exchanges in the device were significantly enhanced. The device was employed for separation of mixtures of toluene/*o*-xylene, *i*-octane/*n*-octane, and *o*-xylene/*p*-xylene. A very low height equivalent to a theoretical plate (HETP) value of 1.08 cm was reported and demonstrated the process intensification achievable by miniaturization. It is worth noting, however, that the miniaturization is expected to reach a limit at the size where gravity is no longer able to drive the liquid flow.

9.3.2.2.2 Carrier gas

Wootton and de Mello [65] demonstrated a continuous purification of volatile liquids within microfluidic systems using a microdistillation chip with the aid of helium as a carrier gas. The chip consisted of three regions: evaporation, condensation, and carrier gas−liquid separation. The liquid mixture feed was partially vaporized in the evaporation region. The less volatile component remained in the liquid phase while the carrier gas was saturated with the more volatile component. The liquid was directed to a designated outlet by capillary action, while the gaseous flow guided by the carrier gas was diverted through the long condensation microchannel. The condensed liquid and carrier gas was finally separated by the carrier gas−liquid separation region based on capillarity, as shown in Figure 9.11. Equimolar mixtures of acetonitrile/dimethylformamide and dimethylformamide/toluene were separated, and the separation was equivalent to 0.72 theoretical plates. Although successful at achieving a separation, the major disadvantage of this system is the lack of reflux flowing back to the reboiler, limiting the separation performance to less than a single stage.

An alternative approach is to perform sweep gas membrane distillation (see Section 9.4) in microchannels. Adiche and Sundmacher [66] assembled a microseparator that consisted of two chambers separated by a microporous polymeric

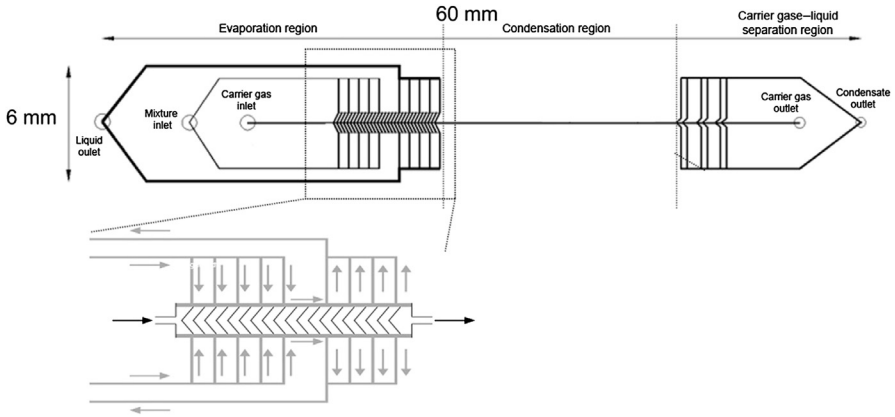

FIGURE 9.11 Continuous-Phase Microdistillation System Developed by Wootton and de Mello [65]

Reproduced from Ref. [65] with permission by the Royal Society of Chemistry.

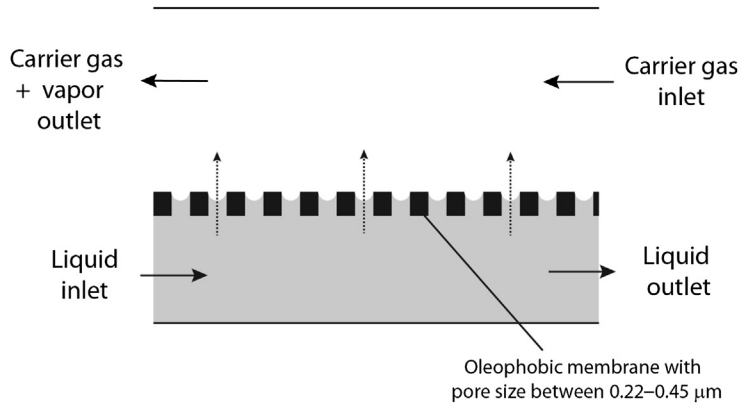

FIGURE 9.12 Operating Principle of the Microscale Sweep Gas Distillation System Developed by Adiche and Sundmacher [66]

oleophobic membrane. Its operating principle is illustrated in Figure 9.12. The liquid mixture was fed to one of the chambers, while the carrier gas (nitrogen) flowed through the other in a countercurrent mode. A stable liquid−vapor interface was established at the pores of the membrane due to capillary action induced by the small pore size, in the order of 0.22−0.45 μm. The capillary action can be described by the Young−Laplace equation. Since the small size of the pores induces a large pressure difference across the vapor and liquid phases, the interface between the two phases is stable. During the process, as the more volatile component vaporizes at a faster rate than the less volatile component, separation is achieved. The device was used for separation of a methanol/water mixture, and the highest separation factor (defined as $[x_p/(1-x_p)][(1-x_f)/x_f]$, where x_p and x_f are the compositions of the less volatile component in the permeate and the feed, respectively) was around five, which depended on the flow rates of the carrier gas and the feed, the composition of the feed, and the type of membrane used. The miniaturization of the sweep gas membrane distillation potentially leads to a reduction of the temperature and concentration polarization within the separation device. However, an external condensation effort is still required for separation of the more volatile component from the carrier gas.

On a similar principle, Ju et al. [67] designed a batch miniaturized distillation column for the separation of sulfurous acid (H_2SO_3) in the form of sulfur dioxide (SO_2) and water for SO_2 detection purposes. The system was comprised of a heated inlet reservoir, a cooled serpentine channel, and a cooled collection chamber. Nitrogen carrier gas was passed through the microchip, causing the vapor and gaseous SO_2 to flow in the cooled serpentine channel. The vapor condensed in the cooled serpentine channel, while SO_2 was driven by the carrier gas into the collection chamber filled with deionized water, where it was absorbed. Ninety-five percent of the SO_2 was removed from the sample in around 20 min. The major drawback of using

carrier gas for continuous microdistillation is that no reflux is circulated back to the microchannel. This limits the separation performance, and, in addition, an extra gas–liquid separator is required after the distillation process.

9.3.2.2.3 Vacuum

Instead of inducing vapor flow by applying positive pressure from a carrier gas, Zhang et al. [68,69] made use of vacuum to drive the flow of the vapor inside the microscale distillation system. A microporous PTFE membrane (0.1–0.2 μm pore) was sandwiched between a liquid and gas chamber in a multilayer configuration. In the operation, liquid flow was driven by a pump, and the gas chamber was connected to a vacuum pump. When the liquid vaporized, the vapor flow was driven by the vacuum and condensed before being discharged. As the pore size of the membrane was small, the pressure drop was kept strong to maintain a stable vapor–liquid interface along the membrane. The separation performance of the unit was tested using a methanol/water mixture. Its efficiency was optimized by tuning the temperature gradient that was controlled by the flow rate of cooling water. A maximum number of theoretical plates of 1.8 was achieved. Since no additional component (i.e. carrier gas) was added to the vapor stream, no extra separation step was required for the vacuum-driven microdistillation system.

9.3.2.2.4 Capillarity

Porous media can be employed to facilitate liquid flow within microdistillation devices by capillarity. Seok and Hwang [70] first designed a tubular microdistillation system, which they called *zero-gravity micro-distillation*, with glass fiber wick material as the porous medium. Figure 9.13 illustrates the operating principle. During the operation, a temperature gradient along the device was set. The feed was pumped into the system, and thus the glass fiber wick was wetted. At the heating region, the liquid in the wick vaporized and generated a higher vapor pressure. The vapor flowed toward the cooling region where condensation took place. The pressure gradient was therefore maintained along the device, and the vapor flowed continuously. On the other hand, as the liquid volume was reduced due to vaporization, as well as withdrawal as bottom product, the liquid feed, and part of the condensate from

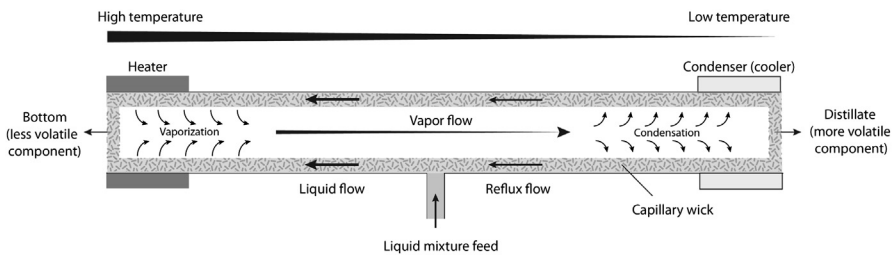

FIGURE 9.13 Operating Principle of the Zero-Gravity Microdistillation Device Designed by Seok and Hwang [70]

the cooling region, was drawn toward the heating region to replenish the liquid volume, forming a reflux in the distillation device.

As the porous medium induced strong capillary action, liquid breakthrough to the vapor channel was prevented even if the device was operated with a tilted angle or even vertically. Mass transfer took place at the liquid−vapor interface, leading to a separation based on vapor−liquid equilibrium. Seok and Hwang [70] found that their device was capable of separating a methanol/water mixture with a measured HETP value of 5−7 cm. Tonkovich et al. [71] designed a scalable microchannel distillation unit based on a similar principle with a woven stainless steel mesh as the wick material for liquid flow. The device was reported to have an HETP value of 0.83 cm for a hexane/cyclohexane separation. The system was applied as part of an integrated distillation-hydrosulfurization-steam reforming process for powering fuel cells for removal of sulfur content of a JP-8 fuel from 1300 to 329 ppm [72].

Similarly, Sundberg et al. [73] employed a flat microdistillation device using metal foams as the convective wick for the separation of an *n*-hexane/cyclohexane mixture. The metal foam (0.5−3.0 mm thick) was placed at the bottom of the chamber, resulting in a gas chamber thickness of 1.5−2 mm. At total reflux conditions, the minimum HETP value observed was 1.3 cm. The authors highlighted that the main challenges for the operation were the significant heat loss and lack of degasification. The same group further incorporated an external flat channel reboiler, a preheater, and a heat exchanger to allow independent control of heat input to the device and reflux [74].

Although the microdistillation designs discussed above are efficient, the capillary wicks are implemented into a prefabricated column, or case, in the assembly. This limits the designs to a millimeter level as it is technically challenging to put the wick material inside a submicron channel. To realize a true microscale distillation system, the wick, or the liquid conduit, has to be fabricated inside the microchannel, and vapor−liquid contact must be allowed. Figure 9.14 shows two different microdistillation designs with fabricated wicks for guiding the liquid flow via capillary action. Hibara et al. [75] designed a microdistillation device consisting of micro-nano combined structures at the condensation zone (Figure 9.14(a)). In their design, liquid condensate was formed when the saturated vapor was in contact with the micro-nano structures. To prevent backflow of the liquid, the liquid microchannel was fabricated shallower than the vapor channel. Separation of a 9 wt% ethanol/water mixture using the chip was demonstrated. The reported bottom stream consisted of 8.6 wt% ethanol, whilst the distillate contained 19 wt% ethanol. The performance was limited due to the lack of reflux.

A multistage microdistillation chip based on the heat-pipe principle applied by Seok and Hwang [70] was fabricated by Lam et al. [76]; however, the dimensions were further reduced down to submillimeter level. Instead of using foreign wick materials, the capillary action for liquid movement was induced by arrays of fabricated micropillars along the walls of the microchannel (Figure 9.14(b)). Liquid feed and condensate from the cooling region flowed within the domain of the micropillars, whilst the vapor from the heating region flowed at the center of the microchannel

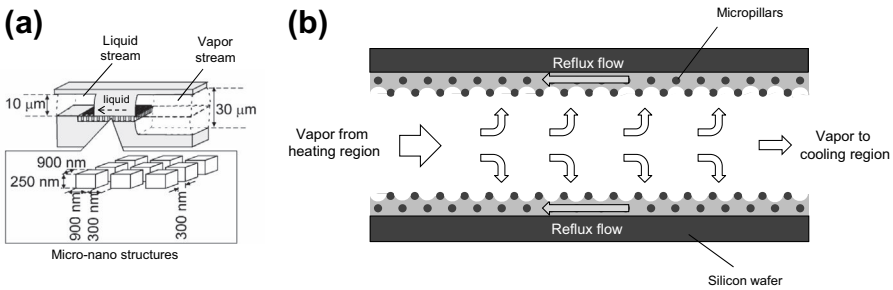

FIGURE 9.14 Microdistillation designs with built-in micro- and nano-structures

(a) Hibara et al. [75] and (b) Lam et al. [76].

Reproduced from Ref. [75] with permission by the Chemical Society of Japan.

countercurrently. The distillation chip was used for separation of various binary solutions including acetone/water and methanol/toluene mixtures achieving up to four theoretical stages. In a more detailed parametric study by the same authors, Lam et al. [77], it was found that the same chip is equivalent to at least 5.4 equilibrium stages estimated at total reflux conditions for an acetone/ethanol mixture. The separation performance was strongly affected by the operating conditions, including temperatures of heating and cooling, flow rates and concentration of feed, flow rates of bottom and of distillate. When the heating temperature was too high, too much liquid was vaporized and the microchannel was not capable of accommodating the excessive condensate, resulting in flooding. To better understand the actual working principle and operating window of the microdistillation chip, Förster et al. [78], conducted an in situ study using Raman spectroscopy of the same chip as used by Lam et al. [76,77] for the separation of a toluene/benzaldehyde mixture. Concentration profiles of the components were measured along the microchannel. It was found that the separation occurred within a limited section of the channel, the length of which was affected by the heating and cooling temperatures. This indicates that the chip can be further optimized. The separation performance was affected by the heating and cooling temperatures, mainly due to the various effects that the temperature profile has on the separation, i.e. not only on vapor–liquid equilibrium but also on surface tension and thus capillary forces, and thereby on liquid flow, unlike conventional distillation where liquid flow is governed by gravity.

9.3.2.2.5 Centrifugal force

Another way of maintaining the continuous contact between gas and liquid phases is based on the use of centrifugal forces and pressure gradient. MacInnes et al. [79] developed a rotating spiral microchannel distillation system in which the liquid flows along one side of the wall of a spiral microchannel (as illustrated in Figure 9.15) due to the effect of centrifugal acceleration occurring perpendicularly to the microchannel, which is applied to counter the capillary action of the liquid phase. The liquid film thickness could be controlled to as low as 50 μm depending

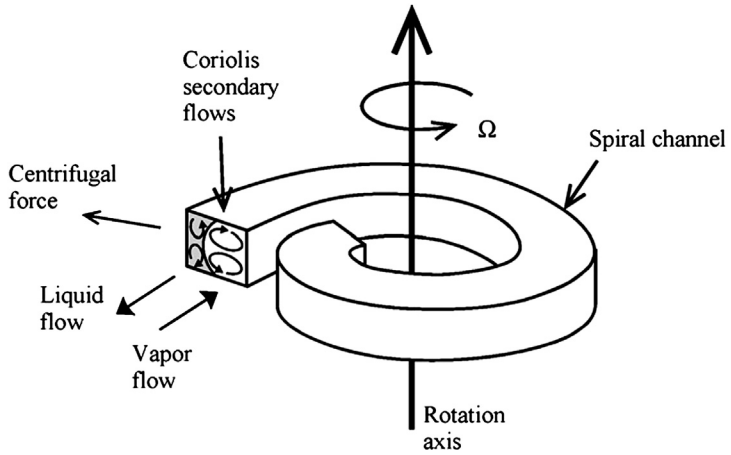

FIGURE 9.15 Rotating Spiral Microchannel Distillation System Developed by MacInnes et al. [79]

Reproduced from Ref. [79] with permission by Elsevier.

on the centrifugal force applied. As the vapor phase had a lower density than the liquid phase, the same effect acting on the vapor phase was much less significant. Coriolis forces were also important for internal mixing. When a temperature gradient was applied to the rotating spiral microchannel distillation system, more volatile components of the liquid phase along the wall preferentially vaporized while the remaining liquid flowed outward to the liquid outlet. The vapor phase flowed countercurrently to the center of the spiral system due to the pressure difference created by controlling the temperatures for condensation and boiling. The device achieved 6.6 theoretical stages (HETP value of 0.53 cm) for the separation of an equimolar 2,2-dimethylbutane/2-methyl-2-butene mixture, operating at 5000 rpm. The major disadvantage of this device was the complexities associated with the requirements of thermal control and its rotational assembly.

9.3.3 Summary and outlook

Over the last century, the petrochemical industry has been the main driver for the development of efficient separation methods, at an ever increasing complexity and scale. In the future, however, separation needs will also be driven by pharmaceutical, microelectronics, water, energy, and life sciences industries. Microseparation is well placed to serve many of these needs due to its small and flexible production scale and unique advantages offered by point of use and intensified operation, as the small scale provides enhanced mass and energy transfer, high flexibility, ease of control and safer operation.

There are various challenges facing separations at microscale, in particular in terms of hydrodynamics that are key to optimizing performance, and thus requires closer attention. A better understanding of vapor–liquid equilibrium at very small

scale, and the impact of surface tension on this, is also needed. Finally, different micro devices have been proposed that are based on various contacting principles, each with its own characteristics, and further characterization and understanding of these is also required. As our understanding and experience with microchannel separations matures, they will start to be integrated with other unit operations to achieve complex separations or multistep synthesis of chemicals.

9.4 Membrane distillation

Membrane distillation is a distillation process in which the liquid and gas phases are separated by a porous membrane, the pores of which are not wetted by the liquid phase. It is a thermally driven separation process whereby vapor molecules are transferred, or distilled, through a microporous nonwetted hydrophobic membrane. The driving force is the vapor pressure difference induced by the temperature difference between the two sides of the membrane pores, typically in the order of 5−20 K. (In other membrane processes, the driving force is the chemical potential difference through the membrane thickness.) Simultaneous mass and heat transfer thus occurs in membrane distillation.

Membrane distillation operates at a lower temperature than ordinary distillation, as well as at lower hydrostatic pressures than in other membrane-based processes, which makes membrane distillation a more advantageous operation, particularly as it also has less demanding membrane mechanical properties and a high rejection factor.

Although yet to be implemented industrially, the process has potential applications in various sectors, such as desalination, wastewater treatment, heavy metal removal, and in the food industry. The primary interest has so far been for water desalination. Most of the current membrane distillation applications are still in laboratory or small-scale pilot plant phase. The possibility of using renewable energy sources, such as waste heat, solar energy, or geothermal energy, may enable membrane distillation to be integrated with other processes, making it a more promising separation at an industrial scale.

Despite the hesitance from industry, membrane distillation is receiving considerably interest in the academic community with at least one textbook [80], a virtual special journal issue [81], and several review papers devoted to the topic [82,83]. This section will therefore just provide a summary of the main principles of the process.

9.4.1 Separation principle

In membrane distillation, only vapor molecules are transported across the membrane. As water is strongly polar, whilst the membrane is hydrophobic, the membrane is not wetted by the liquid due to the high surface tension. The liquid feed is kept in direct contact with one side of the membrane, but without penetrating

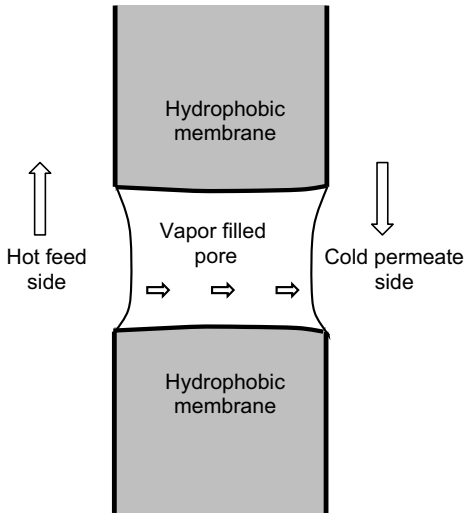

FIGURE 9.16 Membrane Distillation Principle

the dry pores, which is achieved by applying a pressure lower than the breakthrough pressure. (If the pressure is above the breakthrough pressure, then the membrane will nevertheless be wetted.) A vapor liquid interface is thereby formed at the entrance of each pore as illustrated in Figure 9.16.

Mass transfer in membrane distillation is controlled by three basic mechanisms: Knudsen diffusion, Poiseuille flow (viscous flow) and molecular diffusion [82]. The Knudsen number, defined as the ratio of the mean free path of transported molecules to the membrane pore size, is an indication of which mechanism is active inside the membrane pore. The mechanisms give rise to different types of resistance to mass transfer resulting from transfer of momentum to the supported membrane (viscous), collision of molecules with other molecules (molecular resistance), or with the membrane itself (Knudsen resistance). The resistance in the boundary layer is generally negligible, as is surface resistance as the surface area is small compared to the pore area. The thermal boundary layer, on the other hand, has been found to be the limiting step to mass transfer [83].

9.4.1.1 Membrane material

As for all membrane processes, the separation efficiency and the production rate depends strongly on the membrane material and the membrane properties. The membranes currently used in membrane distillation are hydrophobic and normally made from synthetic material such as PTFE, PVDF, or PP, with typical pore sizes in the order of 0.1−0.5 μm. Larger pore sizes will result in larger fluxes across the membrane, however, too large pore sizes can increase the possibility of wetting of the membrane. The best pore size will depend on the feed type [84]. The surface area available for evaporation increases with increasing membrane porosity, thus

promoting higher fluxes. Higher porosities also reduce the heat losses due to conduction through the membrane. The permeate flux is inversely proportional to membrane thickness, hence membranes tend be very thin, in the order of 10^{-6} m. Heat loss is, however, also inversely proportional to membrane thickness, consequently an optimum thickness has to be found [84].

9.4.1.2 Membrane modules

The membranes used in membrane distillation can be configured into different membrane modules: plate and frame, hollow fiber, tubular, and spiral wound. Plate and frame configurations with flat sheet membranes have been widely used at laboratory scale as they are easy to clean and to replace. Hollow fiber modules have also been used [83,85]. The main choice of membrane module depends on operating conditions and cost. Important criteria for performance include efficient control of temperature and concentration effects.

9.4.2 Membrane distillation configurations

There are four basic process configurations in membrane distillation: direct contact membrane distillation, sweep gas membrane distillation, vacuum membrane distillation, and air gap membrane distillation [80]. A schematic of each is shown in Figure 9.17. The most widely studied configuration is direct contact membrane distillation due to its simplicity and ease of application, and because the feed is liquid at ambient conditions. Two new configurations named vacuum-multi-effect membrane distillation (V-MEMD) and permeate gap membrane distillation have also been tried recently [81].

9.4.2.1 Direct contact membrane distillation

Direct contact membrane distillation (DCMD) is the most commonly considered configuration due to its simplicity (Figure 9.17(a)). In this configuration, the hot feed solution, which is maintained at atmospheric pressure at a temperature below its boiling point, is in direct contact with the hot membrane surface. The feed is circulated tangentially to the membrane surface by the use of circulating pumps within the membrane cell or stirred using magnetic stirrers [80]. The permeate side of the membrane is kept at a much lower temperature and is circulated by the same means, and this temperature difference induces a vapor pressure difference across the membrane. The vapor pressure difference causes evaporation of molecules from the hot feed side and moves them through the membrane pores as vapor. As the molecules exit the membrane pores into the permeate, they condense due to the lower temperature and pressure on the pervaporation side. The transmembrane pressure must be kept below the breakthrough pressure to prevent liquid entering the pores. A DCMD with liquid gap is a DCMD variant in which a stagnant cold liquid is kept in direct contact with the permeate side of the membrane. The main drawback of DCMD is the heat lost by conduction [82].

DCMD has similarities to conventional distillation, as evaporation and condensation occur at the vapor−liquid interface on the surfaces of the pores of the

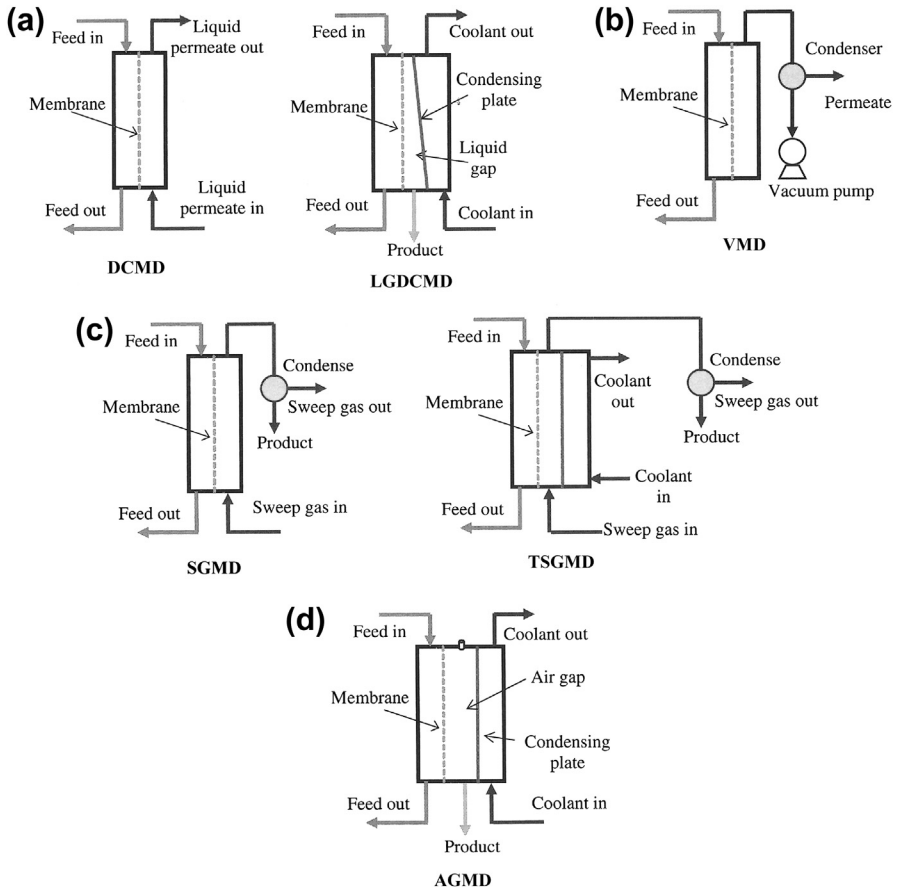

FIGURE 9.17 Membrane Distillation Process Configurations

(a) direct contact and direct contact with liquid gap, (b) vacuum, (c) sweep gas and thermostatic sweep gas, and (d) air gap.

Reproduced from Ref. [80] with permission by Elsevier.

membrane on the feed and permeate side, respectively. In addition, both methods require the supply of latent heat of evaporation to be supplied to the aqueous feed to create mass and heat fluxes.

9.4.2.2 Air gap membrane distillation

Air gap distillation (AGMD) is a slight variation of direct contact membrane distillation, where a stagnant air gap is placed between the membrane and the condensation surface, which is placed in the module (Figure 9.17(d)). The vapor molecules therefore move through both the membrane and the air gap before condensing. The air gap helps reduce the heat loss due to conduction, however, additional resistance is created that reduces the permeate flux.

AGMD is considered the most flexible configuration, showing great promise for the future of membrane distillation. It is also more adaptable to desalination of geothermal resources, with a lower energy requirement than DCMD [80].

9.4.2.3 Vacuum membrane distillation

Vacuum membrane distillation (VMD) involves the application of a low pressure or vacuum on the permeate side of the membrane module through the use of vacuum pumps (Figure 9.17(b)). This applied pressure is lower than the saturation pressure of the volatile feed molecules to be separated from the feed solution. Condensation takes place outside the membrane module at temperatures much lower than room temperature, at laboratory scale using nitrogen liquid filled condensers.

The VMD configuration is advantageous as there is a very low conductive heat loss across the membrane resulting from the application of a vacuum. There is also the benefit of reduced mass transfer resistance as diffusion is favored at the liquid–vapor interface. However, there is a disadvantage of increased risk of pore wetting. VMD is sometimes confused with pervaporation, however, pervaporation uses dense and selective membranes, which alter vapor–liquid equilibrium, whilst VMD uses porous and hydrophobic membranes, although these have a smaller pore size than other membranes used for distillation.

9.4.2.4 Sweep gas membrane distillation

As the name implies, sweep gas membrane distillation (SGMD) uses a cold inert gas to sweep the permeate side of the membrane carrying the vapor molecules (Figure 9.17(c)). Similar to AGMD, there is a gas barrier, this time sweep gas rather than air, but this barrier is not stationary as in AGMD which improves mass transfer. The condensation will take place outside the membrane module through the use of an external condenser. The main disadvantage of this configuration is that a small volume of permeate diffuses into a large sweep gas volume, thus requiring a large condenser [82].

In SGMD, the gas temperature, mass transport rate, and heat transfer rate change substantially during the course of the circulation of the inert sweep gas along the membrane module. Temperature change in the gas can be minimized with the use of a cold surface on the permeate side of the membrane. This addition is a cross between the AGMD and SGMD, called thermostatic sweeping gas membrane distillation (TSGMD).

9.4.3 Summary and outlook

Membrane distillation is a promising separation method for certain applications, in particular for water desalination. Although it is a thermally driven process, the heat required may be obtained from lower energy sources than those normally required in conventional distillation, in other words, waste energy, geothermal energy, or solar energy may be applied, enabling membrane distillation to be integrated with other processes, making it a more promising separation at an industrial scale.

9.5 Microwave-assisted distillation

A further possibility to intensify distillation processes is the addition of alternative energy in the form of microwaves to the interphase between the liquid and vapor. The local increase of the energy level thereby generated can positively influence the interphase concentrations [86]. The change in concentrations may lead to an enhanced separation of components, may be capable of crossing an azeotropic composition, or of reducing a large number of theoretical stages for very narrow boiling mixtures [87]. Although no successful installation of a microwave field to a distillation or reactive distillation column has yet been reported, several promising publications can be found. Fundamental research on the effect of microwaves on liquids showed a significant rise in boiling temperature of pure components due to superheating effects [86], and a positive disturbance of the vapor and liquid composition while superposing of a microwave field [88]. A few applications of microwave-assisted distillation of volatile components, such as essential oils from herbs prior to chromatographic analysis, have successfully been applied but only at microscale [89,90].

The application of a microwave field to reactive distillation for an enhancement of reaction rates has been proposed for the synthesis of *n*-propyl propionate [91]. The effect of the microwaves on the reaction rate was small and the positive effect on separation occurred solely due to local superheating of the liquid in a distillation head. The application of microwaves to enhance reaction rates has, however, been studied widely, suggesting that a transfer to reactive and nonreactive distillation is possible [87].

9.6 Conclusions

It is hoped that this chapter has shown some of the wide and wonderful range of distillation applications that exist beyond traditional distillation columns. Short path distillation is well established in industry for heat sensitive material, although little has been reported in the open literature on the precise behavior of these units and on recommendations for optimal design and operation. HiGee distillation is reported to be widely and successfully applied in China, yet no applications have been reported elsewhere. Given the compact nature of the HiGee units, and their flexible operation, several niche applications have nevertheless been proposed and may well appear in the not-too-distant future. Separation at microscale, in particular in horizontal units relying solely on capillary forces, is perhaps as far removed from traditional distillation columns as it is possible to come. Yet these microunits are highly efficient and may provide the separation power that is needed to turn the currently widely studied microreactors into a reality as complete microplants. Membrane distillation may also prove to be an efficient separation process in the future, in particular for desalination, to contribute toward the ever-increasing demands for clean drinking water.

References

[1] A. Bose, H.J. Palmer, Influence of heat and mass transfer resistances on the separation efficiency of molecular distillations, Ind. Eng. Chem. Res. Fund. 23 (4) (1984) 459–465.

[2] M. Martinello, G. Hecker, M.D. Carmen Pramparo, Grape seed oil deacidification by molecular distillation: analysis of operative variables influence using the response surface methodology, J. Food Eng. 81 (1) (2007) 60–64.

[3] P.F. Martins, C.B. Batistella, R. Maciel-Filho, M.R. Wolf-Maciel, Comparison of two different strategies for tocopherols enrichment using a molecular distillation process, Ind. Eng. Chem. Res. 45 (2) (2006) 753–758.

[4] F. Chen, Z. Wang, G. Zhao, X. Liao, T. Cai, L. Guo, X. Hu, Purification process of octacosanol extracts from rice bran wax by molecular distillation, J. Food Eng. 79 (1) (2007) 63–68.

[5] L.P. Tovar, G.M.F. Pinto, M.R. Wolf-Maciel, C.B. Batistella, R. MacIel-Filho, Short-path-distillation process of lemongrass essential oil: physicochemical characterization and assessment quality of the distillate and the residue products, Ind. Eng. Chem. Res. 50 (13) (2011) 8185–8194.

[6] Y. Xiong, Z. Zhao, L. Zhu, Y. Chen, H. Ji, D. Yang, Removal of three kinds of phthalates from sweet orange oil by molecular distillation, LWT – Food Sci. Technol. 53 (2) (2013) 487–491.

[7] L. Zuñiga Liñan, N.M.N. Lima, F. Manenti, M.R. Wolf Maciel, R.M. Filho, L.C. Medina, Experimental campaign, modeling, and sensitivity analysis for the molecular distillation of petroleum residues $673.15K^{+}$, Chem. Eng. Res. Des. 90 (2) (2012) 243–258.

[8] J. Cvengroš, S. Pollák, M. Micov, J. Lutišan, Film wiping in the molecular evaporator, Chem. Eng. J. 81 (1–3) (2001) 9–14.

[9] Z. Kawala, K. Stephan, Evaporation rate and separation factor of molecular distillation in a falling film apparatus, Chem. Eng. Technol. 12 (6) (1989) 406–413.

[10] J. Lutišan, J. Cvengroš, Mean free path of molecules on molecular distillation, Chem. Eng. J. Biochem. Eng. J. 56 (2) (1995) 39–50.

[11] J. Lutišan, M. Micov, J. Cvengroš, The influence of entrainment separation on the process of molecular distillation, Sep. Sci. Technol. 33 (1) (1998) 83–96.

[12] J. Cvengroš, J. Lutišan, M. Micov, Feed temperature influence on the efficiency of a molecular evaporator, Chem. Eng. J. 78 (1) (2000) 61–67.

[13] H. Hu, J. Huang, S. Wu, P. Yu, Simulation of vapor flow in short path distillation, Comput. Chem. Eng. 49 (2013) 127–135.

[14] M. Micov, J. Lutišan, J. Cvengroš, Balance equations for molecular distillation, Sep. Sci. Technol. 32 (18) (1997) 3051–3066.

[15] G. Burrows, Some aspect of molecular distillation, Trans. Inst. Chem. Eng. 32 (1) (1954) 23–34.

[16] V. Badin, J. Cvengroš, Model of temperature profiles during condensation in a film in a molecular evaporator, Chem. Eng. J. Biochem. Eng. J. 49 (3) (1992) 177–180.

[17] H.J. Godau, Flow processes in thin film evaporators, Int. Chem. Eng. 15 (3) (1975) 445–449.

[18] J.M. McKelvey, G.V. Sharpe, Fluid transport in thin film polymer processors, Polym. Eng. Sci. 19 (1) (1979) 652–659.

[19] S. Komori, K. Takata, Y. Murakami, Flow and mixing characteristics in an agitated thin film evaporator with vertically aligned blades, J. Chem. Eng. Jpn. 21 (1) (1988) 639–644.
[20] S. Komori, K. Takata, Y. Murakami, Mean free path of molecules on molecular distillation, J. Chem. Eng. Jpn. 22 (4) (1989) 346–351.
[21] J. Lutišan, J. Cvengroš, M. Micov, Heat and mass transfer in the evaporating film of a molecular evaporator, Chem. Eng. J. 85 (2–3) (2002) 225–234.
[22] J. Kaplon, Z. Kawala, A. Skoczylas, Evaporation rate of a liquid from the surface of a rotating disc in high vacuum, Chem. Eng. Sci. 41 (3) (1986) 519–522.
[23] A.-D. Nguyen, F. Le Goffic, Limits of wiped film short path distiller, Chem. Eng. Sci. 52 (16) (1997) 2661–2666.
[24] k.J. Erdweg, Molecular and short path distillation, Chem. Ind. 9 (1) (1983) 342–345.
[25] Y.-F. Wang, S.-L. Xu, Simulation of computational fluid dynamics for molecular distillation process, Huaxue Gongcheng/Chem. Eng. (China) 38 (1) (2010) 30–33.
[26] H. Ishikawa, M. Inuzuka, H. Mori, S. Hiraoka, I. Yamada, Distillation and Absorption Conference, Institution of Chemcial Engineers Symposium Series, 128, 1992.
[27] L.-J. Chen, H.-B. Dong, Q. Li, C.-C. Niu, A.-W. Zeng, Hydrodynamic and transport processes during centrifugal short path distillation, Chem. Eng. Technol. 36 (5) (2013) 851–862.
[28] C.B. Batistella, E.B. Moraes, R. Maciel Filho, M.R. Wolf Maciel, Molecular distillation rigorous modeling and simulation for recovering vitamin e from vegetal oils, Appl. Biochem. Biotechnol. Part A Enzym. Eng. Biotechnol. 98–100 (2002) 1187–1206.
[29] M. Bhandarkar, J.R. Ferron, Transport processes in thin liquid films during high vacuum distillation, Ind. Eng. Chem. Res. 27 (6) (1988) 1016–1024.
[30] C.B. Batistella, E.B. Moraes, M.R. WolfMaciel, Comparing centrifugal and falling film molecular stills using reflux and cascade for fine chemical separations, Comp. Chem. Eng. 23 (Suppl. 1) (1999) S767–S770.
[31] C. Noeres, E.Y. Kenig, A. Gorak, Modelling of reactive separation processes: reactive absorption and reactive distillation, Chem. Eng. Process. 42 (3) (2003) 157–178.
[32] N. Biller, Modelling and control of reactive short path distillation (Ph.D. thesis), UCL, UK, 2003.
[33] A. Winter, C.B. Batistella, M.R. Wolf Maciel, R. Maciel Filho, L.C. Medina, Development of intensified hybrid equipment: reactive molecular distiller, Chem. Eng. Trans. 17 (2009) 1633–1638.
[34] L.P. Tovar, A. Winter, M.R. Wolf-Maciel, R. Maciel-Filho, C.B. Batistella, L.C. Medina, Centrifugal reactive-molecular distillation from high-boiling-point petroleum fractions. 2. Recent experiments in pilot-scale for upgrading of a heavy feedstock, Ind. Eng. Chem. Res. 52 (2013) 7768–7783.
[35] A. Górak, A. Stankiewicz, Intensified reaction and separation systems, Annu. Rev. Chem. Biomol. Eng. 2 (2011) 431–451.
[36] R. Fowler, HiGee – a status report, Chem. Eng. (London) 456 (1989) 35–37.
[37] H. Zhao, L. Shao, J. Chen, High-gravity process intensification technology and application, Chem. Eng. J. 156 (3) (2010) 588–593.
[38] S.P. Singh, J.H. Wilson, R.M. Counce, J.F. Villiersfisher, H.L. Jennings, A.J. Lucero, G.D. Reed, R.A. Ashworth, M.G. Elliott, Removal of volatile organic-compounds from groundwater using a rotary air stripper, Ind. Eng. Chem. Res. 31 (2) (1992) 574–580.
[39] C. Ramshaw, Degassing of Liquids, US 4715869, USA, 1987.

[40] G.J. Quarderer, D.L. Trent, E.J. Steward, D. Tirtowidjojo, A.J. Mehta, C.A Tirtowidjojo, Method for Synthesis of Hypohalous Acid, US 6048513, USA, 2000.
[41] T. Kelleher, J.R. Fair, Distillation studies in a high-gravity contactor, Ind. Eng. Chem. Res. 35 (12) (1996) 4646−4655.
[42] C.C. Lin, T.J. Ho, W.T. Liu, Distillation in a rotating packed bed, J. Chem. Eng. Jpn. 35 (12) (2002) 1298−1304.
[43] G.Q. Wang, Z.C. Xu, J.B. Ji, Progress on HiGee distillation − introduction to a new device and its industrial applications, Chem. Eng. Res. Des. 89 (2011) 1434−1442.
[44] C. Ramshaw, 'HIGEE' distillation − an example of process intensification, Chem. Eng. (London) 389 (1983) 13−14.
[45] H. Short, New mass-transfer find is a matter of gravity, Chem. Eng. (London) 90 (4) (1983) 23−29.
[46] C. Ramshaw, R.H. Mallinson, Mass Transfer Process, US 4283255, USA, 1981.
[47] D.P. Rao, A. Bhowal, P.S. Goswami, Process intensification in rotating packed beds (HIGEE): an appraisal, Ind. Eng. Chem. Res. 43 (4) (2004) 1150−1162.
[48] J.R. Burns, C. Ramshaw, Process intensification: visual study of liquid maldistribution in rotating packed beds, Chem. Eng. Sci. 51 (8) (1996) 1347−1352.
[49] L. Agarwal, V. Pavani, D.P. Rao, N. Kaistha, Process intensification in HiGee absorption and distillation: design procedure and applications, Ind. Eng. Chem. Res. 49 (20) (2010) 10046−10058.
[50] A. Chandra, P.S. Goswami, D.P. Rao, Characteristics of flow in a rotating packed bed (HIGEE) with split packing, Ind. Eng. Chem. Res. 44 (11) (2005) 4051−4060.
[51] G.W. Chu, X. Gao, Y. Luo, H.K. Zou, L. Shao, J. Chen, Distillation studies in a two-stage counter-current rotating packed bed, Sep. Purif. Technol. 102 (2013) 62−66.
[52] Y.G. Jin, S.Y. Li, P. Li, P. Tian, Y.N. Zhang, X. Li, Numerical simulation and experiment on pressure drop of a co-current rotating packed bed, J. China Coal Soc. (China) 35 (8) (2008) 1369−1373.
[53] F. Guo, C. Zheng, K. Guo, Y.D. Feng, N.C. Gardner, Hydrodynamics and mass transfer in crossflow rotating packed bed, Chem. Eng. Sci. 52 (21−22) (1997) 3853−3859.
[54] A. Mondal, A. Pramanik, A. Bhowal, S. Datta, Distillation studies in rotating packed bed with split packing, Chem. Eng. Res. Des. 90 (4) (2011) 453−457.
[55] M.K. Shivhare, D.P. Rao, N. Kaistha, Mass transfer studies on split-packing and single-block packing rotating packed beds, Chem. Eng. Process. Proc. Int. 71 (2013) 115−124.
[56] G.Q. Wang, Y.Q. Jiao, Z.C. Xu, J.B. Ji, Hydrodynamic Performance of Crossflow Concentric-Ring Rotating Bed, AIChE Annual Meeting Conference Proceedings, Philadelphia, USA, 2008a.
[57] G.Q. Wang, O.G. Xu, Z.C. Xu, J.B. Ji, New HIGEE-rotating zigzag bed and its mass transfer performance, Ind. Eng. Chem. Res. 47 (22) (2008b) 8840−8846.
[58] Y.S. Chen, C.C. Lin, H.S. Liu, Mass transfer in a rotating packed bed with viscous Newtonian and non-Newtonian fluids, Ind. Eng. Chem. Res. 44 (4) (2005) 1043−1051.
[59] Y. Luo, G.W. Chu, H.K. Zou, Y. Xiang, L. Shao, J. Chen, Characteristics of a two-stage counter-current rotating packed bed for continuous distillation, Chem. Eng. Process. 52 (2012) 55−62.
[60] K.F. Lam, E. Sorensen, A. Gavriilidis, Review on gas-liquid separations in microchannel devices, Chem. Eng. Res. Des. 91 (10) (2013) 1941−1953.
[61] R.L. Hartman, H.R. Sahoo, B.C. Yen, K.F. Jensen, Distillation in microchemical systems using capillary forces and segmented flow, Lab Chip 9 (2009) 1843−1849.

[62] R.L. Hartman, J.R. Naber, S.L. Buchwald, K.F. Jensen, Multistep microchemical synthesis enabled by microfluidic distillation, Angew. Chem. Int. Ed. 49 (2010) 899–903.
[63] D.A. Boyd, J.R. Adleman, D.G. Goodwin, D. Psaltis, Chemical separations by bubble-assisted interphase mass-transfer, Anal. Chem. 80 (2008) 2452–2456.
[64] A. Ziogas, V. Cominos, G. Kolb, H.-J. Kost, B. Werner, V. Hessel, Development of a microrectification apparatus for analytical and preparative applications, Chem. Eng. Technol. 35 (2012) 58–71.
[65] R.C.R. Wootton, A.J. deMello, Continuous laminar evaporation: micron-scale distillation, Chem. Commun. (2004) 266–267.
[66] C. Adiche, K. Sundmacher, Experimental investigation on a membrane distillation based micro-separator, Chem. Eng. Process. 49 (2010) 425–434.
[67] W.-J. Ju, L.-M. Fu, R.-J. Yang, C.–L. Lee, Distillation and detection of SO_2 using a microfluidic chip, Lab Chip 12 (2012) 622–626.
[68] Y. Zhang, S. Kato, T. Anazawa, Vacuum membrane distillation on a microfluidic chip, Chem. Commun. (2009) 2750–2752.
[69] Y. Zhang, S. Kato, T. Anazawa, Vacuum membrane distillation by microchip with temperature gradient, Lab Chip 10 (2010) 899–908.
[70] D.R. Seok, S.-T. Hwang, Zero-gravity distillation utilizing the heat pipe principle (micro-distillation), AIChE J. 31 (1985) 2059–2065.
[71] A.L. Tonkovich, K. Jarosch, R. Arora, L. Silva, S. Perry, J. McDaniel, F. Daly, B. Litt, Methanol production FPSO plant concept using multiple microchannel unit operations, Chem. Eng. J. 135 (2008) S2–S8.
[72] X. Huang, D.A. King, F. Zhang, V.S. Stenkamp, W.E. TeGrotenhuis, B.Q. Roberts, D.K. King, Hydrodesulfurization of JP-8 fuel and its microchannel distillate using steam reformate, Catal. Today 136 (2008) 291–300.
[73] A. Sundberg, P. Uusi-Kyyny, V. Alopaeus, Novel micro-distillation column for process development, Chem. Eng. Res. Des. 87 (2009) 705–710.
[74] A. Sundberg, P. Uusi-Kyyny, K. Jakobsson, V. Alopaeus, Control of reflux and reboil flowrates for milli and micro distillation, Chem. Eng. Res. Des. 91 (2013) 753–760.
[75] A. Hibara, K. Toshin, T. Tsukahara, K. Mawatari, T. Kitamori, Microfluidic distillation utilizing micro–nano combined structure, Chem. Lett. 37 (2008) 1064–1065.
[76] K.F. Lam, E. Cao, E. Sorensen, A. Gavriilidis, Development of multistage distillation in a microfluidic chip, Lab Chip 11 (2011a) 1311–1317.
[77] K.F. Lam, E. Sorensen, A. Gavriilidis, Towards an understanding of the effects of operating conditions on separation by microfluidic distillation, Chem. Eng. Sci. 66 (2011b) 2098–2106.
[78] M. Foerster, K.F. Lam, E. Sorensen, A. Gavriilidis, In situ monitoring of microfluidic distillation, Chem. Eng. J. 227 (2013) 13–21.
[79] J.M. MacInnes, J. Ortiz-Osorio, P.J. Jordan, G.H. Priestman, R.W.K. Allen, Experimental demonstration of rotating spiral microchannel distillation, Chem. Eng. J. 159 (2010) 159–169.
[80] M. Khayet, T. Matsuura, Membrane Distillation Principles and Applications, Elsevier, 2011.
[81] E. Drioli, F. Macedonio, A. Aamer, Membrane distillation: basic aspects and applications, J. Membr. Sci. (2014). Virtual Special Issue, http://www.journals.elsevier.com/journal-of-membrane-science/virtual-special-issues/membrane-distillation-basic-aspects-and-applications/ (accessed 22.03.14).

[82] A. Alkhudhiri, N. Darwish, N. Hilal, Membrane distillation: a comprehensive review, Desalination 287 (1) (2012) 2−18.
[83] E. Curcio, E. Drioli, Membrane distillation processes and related operations − a review, Sep. Purif. Rev. 34 (1) (2005) 35−86.
[84] P. Onsekizoglu, Membrane distillation: principle, advances, limitations and future prospects in food industry, in: S. Zereshki (Ed.), Distillation: Advances from Modelling to Applications, InTech, 2012, pp. 233−266.
[85] M. Gryta, Concentration of saline wastewater from the production of heparin, Desalination 129 (1) (2000) 35−44.
[86] F. Chemat, E. Esveld, Microwave super-heated boiling of organic liquids: origin, effect and application, Chem. Eng. Technol. 24 (7) (2001) 735−744.
[87] M. Nüchter, B. Ondruschka, W. Bonrath, A. Gum, Microwave assisted synthesis − a critical technology overview, Green Chem. 6 (3) (2004) 128−141.
[88] X. Gao, X. Li, J. Zhang, J. Sun, H. Li, Influence of a microwave irradiation field on vapor-liquid equilibrium, Chem. Eng. Sci. 90 (2013) 213−220.
[89] C. Deng, Y. Mao, F. Hu, X. Zhang, Development of gas chromatography-mass spectrometry following microwave distillation and simultaneous headspace single-drop microextraction for fast determination of volatile fraction in Chinese herb, J. Chromatogr. A 1152 (1−2) (2007) 193−198.
[90] N. Sahraoui, M.A. Vian, I. Bornard, C. Boutekedjiret, F. Chemat, Improved microwave steam distillation apparatus for isolation of essential oils. Comparison with conventional steam distillation, J. Chromatogr. A 1210 (2) (2008) 229−233.
[91] E. Altman, G.D. Stefanidis, T. van Gerven, A. Stankiewicz, Microwave-promoted synthesis of n-propyl propionate using homogeneous zinc triflate catalyst, Ind. Eng. Chem. Res. 51 (4) (2012) 1612−1619.

This page intentionally left blank

CHAPTER

New Separating Agents for Distillation

10

Wolfgang Arlt
University Erlangen-Nuremberg, Erlangen, Germany

CHAPTER OUTLINE

10.1 Introduction

The distillative purification of narrow boiling or azeotropic mixtures is hardly or even not possible in a single distillation column. This is especially true for enantiomeric mixtures, where even enantomeric additives do not show a change of separation factor. But diastereomers can be separated by suitable additives [1]. Common textbooks [2–4] recommend using pressure swing distillation, azeotropic distillation, or extractive distillation to achieve the required product purity. In general,

Distillation: Operation and Applications. http://dx.doi.org/10.1016/B978-0-12-386876-3.00010-7

the engineer should avoid adding one more component into the process because it costs money and may cause traces in the desired product. This is an important advantage of pressure swing distillation. In the field of extractive distillation, an additional separating agent (entrainer) is used to overcome the poor separation factor because pressure swing distillation (or, better, temperature swing distillation) is applicable in only rare cases. From the standpoint of thermodynamics, there are two main criteria in the process development of such systems.

1. The additional separating agent (entrainer) should be able to enhance the separation factor to facilitate a complete separation of the desired product.
2. The regeneration of the entrainer should be as easy as possible and consume minimal energy.

According to the shift of the phase equilibrium, a list of possible entrainers for typical narrow boiling or azeotropic mixtures can be found in Ref. [2], which describes what has been done to date. Almost all of the listed compounds have the same magnitude of vapor pressures compared to the mixtures to be separated. Therefore, the thermal regeneration of the entrainer is costly. To overcome the regeneration problem, classes of substances with low volatility should be taken into account. The listed entrainers cannot be used for a new separation problem, and thus a predictive tool for tailor-made entrainers is necessary.

Ionic liquids (ILs) and hyperbranched polymers (HyPols) are proven to be effective entrainers in extractive distillation [5,6]. They fulfill the second criterion and therefore allow a straightforward regeneration step [7]. In addition, both substance classes can be tailored to the specific needs of a process [8]. Thus, such entrainers can be optimized with regard to the first criterion.

In this chapter, a suitable strategy for the selection of an entrainer is presented. After a short introduction to the basics of equilibrium thermodynamics and materials, methods for experimental [9,10] and computational [8,11] screening are explained. Further, the applicability of the methods is demonstrated by means of selected examples.

10.2 Fundamentals

This section briefly introduces the fundamentals necessary for understanding thermodynamics and experimental methods. First, the basic concepts of vapor–liquid phase equilibria (VLE) are presented. Based on that, the applications of headspace gas chromatography (HS-GC), inverse gas chromatography (IGC), and the predictive tool conductor-like screening model for real solvents (COSMO-RS) are introduced with regard to extractive distillation.

10.2.1 Vapor–liquid phase equilibrium

The thermodynamic basics of distillation can be easily derived from equilibrium thermodynamics. Equation (10.1) states the conditions of an equilibrium between

a vapor phase V and a liquid phase L. The thermodynamic equilibrium is reached when the temperatures T, the pressures p are constant in both phases, and the fugacities f of the component i are the same.

$$\begin{aligned} T^{\mathrm{V}} &= T^{\mathrm{L}} \\ p^{\mathrm{V}} &= p^{\mathrm{L}} \\ f_i^{\mathrm{V}} &= f_i^{\mathrm{L}} \end{aligned} \tag{10.1}$$

The fugacities can be calculated by Eqns (10.2) and (10.3). In the simplest case, the fugacity of component i in the vapor phase is given by its molar fraction y_i and the system pressure p. In the simplest case, the liquid phase fugacity of component i is given by the liquid molar fraction x_i, the activity coefficient γ_i, and the vapor pressure $p_{0,i}^{\mathrm{LV}}$. A complete derivation can be found in Refs [12,13].

$$f_i^{\mathrm{V}} = y_i \cdot p \tag{10.2}$$

$$f_i^{\mathrm{L}} = x_i \cdot \gamma_i \cdot p_{0,i}^{\mathrm{LV}} \tag{10.3}$$

An important quantity for distillation is the phase ratio K_i. It shows the distribution of a single component i between the vapor and liquid phase. By using Eqns (10.2) and (10.3), it can be expanded to Eqn (10.4).

$$K_i = \frac{y_i}{x_i} = \frac{\gamma_i \cdot p_{0,i}^{\mathrm{LV}}}{p} \tag{10.4}$$

The separation of two components i and j is expressed by the separation factor α_{ij}, which can be applied to only binary mixtures.

$$\alpha_{ij} = \frac{K_i}{K_j} = \frac{\gamma_i \cdot p_{0,i}^{\mathrm{LV}}}{\gamma_j \cdot p_{0,j}^{\mathrm{LV}}} \tag{10.5}$$

For $\alpha_{ij} \approx 1$, a distillative separation is not possible. Because the vapor pressures are pure component properties and depend only on temperature, a separation factor of unity can be changed only by a shift of the activity coefficients. This shift can be achieved by the addition of a third component, the entrainer. The activity coefficient is a function of the concentration, temperature, and pressure. It is related to the free excess energy G^{E} as a partial molar quantity (see Eqn (10.6)). The free energy consists of two terms (Eqn (10.7)): the enthalpy and the entropy [13].

$$\left(\frac{\partial G^{\mathrm{E}}}{\partial n_i}\right)_{T,P,n_{j\neq i}} = RT \ln(\gamma_i) \tag{10.6}$$

$$\Delta G^{\mathrm{E}} = \Delta H^{\mathrm{E}} - T\Delta S^{\mathrm{E}} \tag{10.7}$$

In Eqn (10.7), H^{E} is the excess enthalpy and S^{E} is the excess entropy.

So, a change of the free energy and thus of the activity coefficient can be done by changing the enthalpy or the entropy of the mixture. ILs mainly address intermolecular

forces and thus enthalpy. HyPols have a remarkable entropy effect because of their molecular size and the end groups of HyPols have an additional enthalpy effect. Note that the entropy of mixtures is not a strong function of temperature, but the influence of the entropy toward the free energy is an expression whereby the entropy is multiplied by T; therefore entropy becomes more and more important at different temperatures.

The activity coefficient is a liquid phase property; therefore the entrainer should preferentially stay in the liquid phase at what is equal to a small or negligible vapor pressure compared to the components i and j.

10.2.2 Headspace gas chromatography

The activity coefficients can be determined experimentally by HS-GC [14]. Using the headspace sampler, a ternary mixture of entrainer and the two components to be separated can be measured by one experiment. From the HC-GS analysis, the separation factor can be obtained directly.

Figure 10.1 shows the schematic setup of an HS-GC measurement.

A liquid sample is prepared in a headspace vial. During the equilibration in the temperature bath, the VLE is reached. A small mass balance is required to calculate the liquid concentration after forming a vapor phase. Thus, the molar fractions in the gas phase change according to the selectivity and capacity of the entrainer. After equilibration, a sample is drawn from the vapor space and analyzed in a standard gas chromatograph. The execution and evaluation of the single experiments can be found in Refs [10,15–17]. The data set is the corrected liquid concentration,

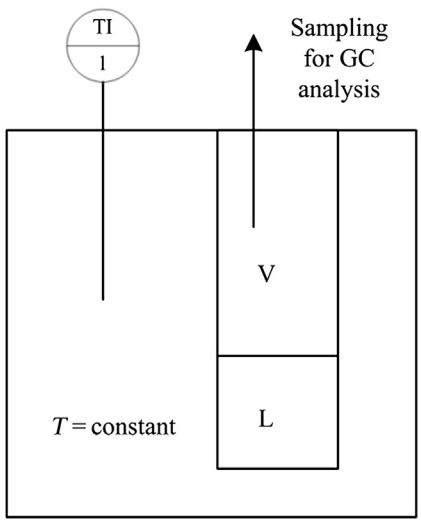

FIGURE 10.1 Schematic Setup of A Headspace Gas Chromatography (GC) Measurement

V, vapor; L, liquid; TI, temperature indicator; PI, pressure indicator.

measured vapor phase concentration, and temperature. These data do not allow for a consistency test (except the area test, because system pressure cancels), but the total pressure can be calculated by standard thermodynamics. The experimental effort can be reduced by the so-called express screening method, cf. Ref. [18].

10.2.3 Inverse gas chromatography

The activity coefficients of volatile components at an infinite dilution can be obtained by IGC [19]. The setup is shown schematically in Figure 10.2. A small amount of the sample (low-boiling component) is injected into the mobile phase, which consists of an inert carrier gas. The mobile phase (inert carrier gas plus the sample) pass through the column, where the sample interacts with the stationary phase. The column consists of porous particles coated with the high-boiling liquid, which acts as stationary phase (e.g. IL or HyPol). The VLE between the mobile and stationary phase is established. Because of the interactions between the sample and the high-boiling component, the low-boiling component is retained and the resulting retention time is measured. The IGC apparatus is placed in an oven to control the temperature.

The activity coefficient at an infinite dilution of the low-boiling component i in the high-boiling liquid can be calculated according to Eqn (10.8). The retention volume of component i, V_R, and the temperature are obtained from the IGC measurement.

$$\gamma_i^{\infty} = \frac{n^{L}_{\text{High-boiler}} RT}{V_R \, p^{LV}_{0,i}} \cdot \exp\left(- \frac{B_{11} p^{LV}_{0,i}}{RT} \right) \tag{10.8}$$

In Eqn (10.8), $n^{L}_{\text{High-boiler}}$ is the amount of the high-boiling component on the porous support and B_{11} is the second virial coefficient of component 1 at system temperature, if needed.

The derivation of the equation and further information are given elsewhere [19,20]. This method returns the separation factor at an infinite dilution when the measured activity coefficients are inserted into Eqn (10.5). While the amount of entrainer in the liquid phase is dominant, it is far away from the finite dilution of

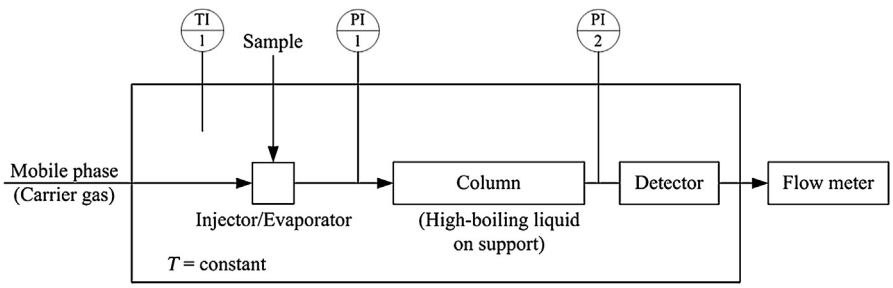

FIGURE 10.2 Principle Setup of Inverse Gas Chromatography

the mixture to be separated. It is my experience that a ranking of possible entrainers by separation factor at an infinite dilution holds also for finite concentrations. To know the separation factor at the right concentration of the entrainer, HS-GC must be performed.

10.2.4 Conductor-like screening model for real solvents

The COSMO-RS can be used to predict thermodynamic properties (e.g. activity coefficients). The only necessary input information is the molecular structure of the involved components. The underlying COSMO approach [21] calculates the screening charge of the respective substances in an ideal conductor. The model extension COSMO-RS [22] uses statistical thermodynamics to calculate the chemical potential (and thus all properties that can be derived from the chemical potential) of a mixture. The applicability in chemical engineering was shown recently [23–25]. To achieve reliable results, a conformational search should be performed [26].

10.2.4.1 Specific aspects of COSMO-RS calculations for ILs

ILs consist of cations and anions. These ions are treated individually during the building of the molecular structure and the calculation of the screening charge density. For a COSMO-RS calculation, the IL is synthesized in silico. This can be done either by an equimolar mixture of cation and anion or by the creation of a metafile [27]. The first option is preferred [28]. The benefit is that all combinations of anions and cations from a database can be used as possible ILs. Since the ions are treated individually in the COSMO-RS calculation, the resulting activity coefficient $\gamma_i^{\mathrm{COSMO-RS}}$ is converted into the experimental activity coefficient γ_i^{exp} according to Eqn (10.9).

$$\gamma_i^{\mathrm{exp}} = \gamma_i^{\mathrm{COSMO-RS}} \cdot \frac{x_i^{\mathrm{COSMO-RS}}}{x_i^{\mathrm{exp}}} \tag{10.9}$$

The activity coefficient of component i at infinite dilution in a univalent IL can be calculated using the simplified Eqn (10.10).

$$\gamma_i^{\mathrm{exp}} = \gamma_i^{\mathrm{COSMO-RS}} \cdot 0.5 \tag{10.10}$$

10.2.4.2 Specific aspects of COSMO-RS calculations for HyPols

HyPols are macromolecules that have basic building blocks (cf. Figure 10.3). Because of the polydispersity and size of the molecules, it is not possible to calculate the screening charge density of the entire polymer. However, it is possible to calculate the screening charge density of single building blocks (or multiple building blocks) and synthesize the polymer using metafiles [27,31]. The use of larger fragments (multiple building blocks) for the calculation of the screening charge density leads to more accurate results. Thus, the selectivity and capacity of different functional groups can be tested without the need for a time-consuming chemical synthesis.

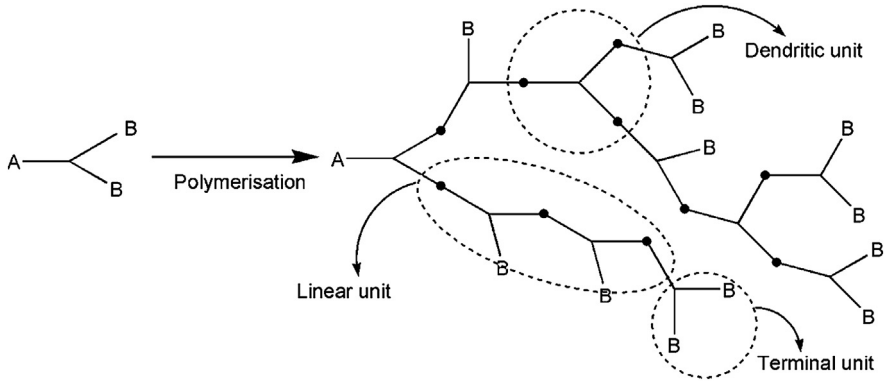

FIGURE 10.3 Schematic Structure of A Hyperbranched Polymer [29,30]

10.2.5 Process setup

The common setup of the distillation process is slightly extended for extractive distillation. Figure 10.4 shows a possible flowsheet for an extractive distillation process using an entrainer E with negligible vapor pressure ($p_{0,E}^{LV} \rightarrow 0$).

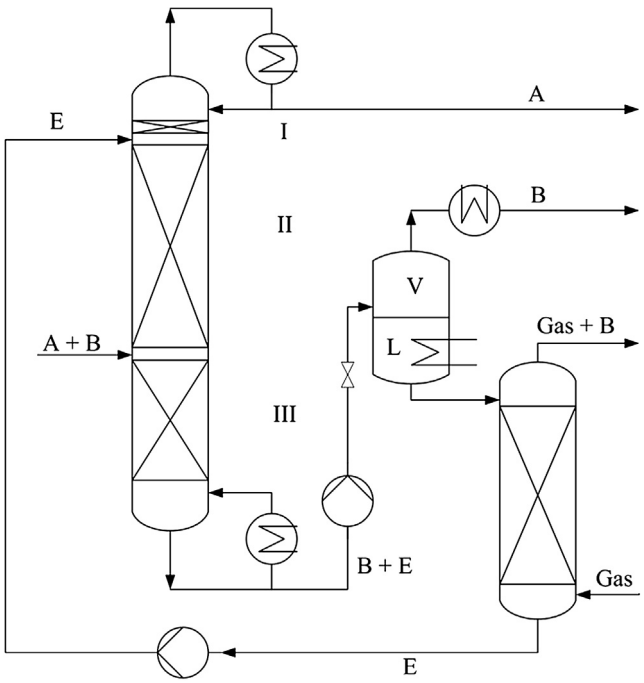

FIGURE 10.4 Possible Process Flowsheet for An Extractive Distillation and the Subsequent Entrainer Recovery Units Using An Entrainer with Negligible Vapor Pressure

A, component A; B, component B; E, entrainer; V, vapor; L, liquid [7].

The distillation column is fed with the components A and B, which either are narrow boiling or have an azeotropic point. The entrainer E is added above the feed and close to the top to ensure a long distance for action in the liquid phase. The distillation column can be divided into three parts (I–III) with different separation tasks: The stages above the entrainer (I) are used to separate the low-boiling component A from the entrainer E ($\alpha_{A,E} \gg \alpha_{A,B\,(E)}$). If $p_{0,E}^{LV}$ is negligible (as in this case), the height of part I approaches zero. Besides thermodynamics, the entrainment of liquid drops to the distillate should be considered. In part II, component A is separated from component B (the separation is provoked by the entrainer E), resulting in an enrichment of component A. In the lower part of the column (III), components A and B are separated (the separation is provoked by the entrainer) and component B is enriched. The entrainer E is separated from component B in a recovery unit. The recovery process shown in Figure 10.4 is designed for an entrainer with $p_{0,E}^{LV} \to 0$. The combination of a flash unit (operating under vacuum) and a stripper is energetically the most favorable solution. The entrainer is returned to the distillation column. Its purity is essential for the purity of the distillate.

The influence of an entrainer with negligible vapor pressure on the VLE of an azeotropic mixture is shown in Figure 10.5. The azeotropic point disappears after the addition of the entrainer.

From this exemplary setup, the thermodynamic needs for the choice of entrainer can be deduced easily. The following criteria should be fulfilled:

1. The entrainer should break the azeotrope to achieve a complete separation between components A and B. Namely, above the stage of entrainer insertion,

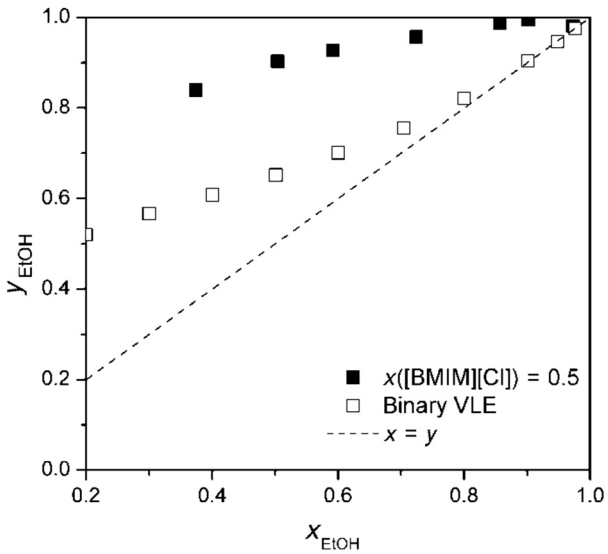

FIGURE 10.5 Influence of the Entrainer [BMIM][Cl] (50 mol%) on the Vapor Liquid Equilibrium (VLE) of Ethanol (EtOH)–Water at 363.15 K

Pseudobinary data are taken from Ref. [32] and binary data are taken from Ref. [29].

no component B should be present. At the bottom of the column, no component A should be present.
2. The separation of components A and the entrainer should be easy to minimize the installation of trays above where the entrainer is inserted at the top of the column. Entrainment of the distillate by the entrainer should be avoided.
3. The separation of component B and the entrainer should be easy to keep the regeneration unit simple. Also, a leaching of the entrainer should be avoided. Component B should be removed quantitatively from the entrainer recycle.

All these requirements can be satisfied by HyPols and ILs. The tailored structure of both solute classes allows the first prerequisite to be fulfilled. For items 2 and 3, the negligible vapor pressures of both solute classes are beneficial. Thus, both the separation of component A and the entrainer at the top of the column and the regeneration of the entrainer can be realized.

10.3 Solvent families

This section gives a short introduction to HyPols and ILs. Further detailed information is provided in several reviews [30,33–36].

10.3.1 Hyperbranched polymers

HyPols consist of one or more building units that have one center group A and two or more terminal groups B. Figure 10.3 shows an example of the synthesis and structure of a HyPol.

During the polymerization, three types of units arise:

1. Dendritic units: all terminal groups B are polymerized
2. Linear units: not all terminal groups B are polymerized
3. Terminal units: no terminal group is polymerized

It is not necessary to convert all terminal groups in the center of the molecule, so the synthesis is straight forward and easy [37]. The thermodynamic characteristics of the polymer mainly are influenced by the chemical structure of the terminal groups and by the degree of polymerization [9,34]. In comparison to linear polymers, HyPols mostly have low melting points [38–40], good thermal stabilities [41], and remarkably high selectivities and capacities [9].

10.3.2 Ionic liquids

ILs are salts with a melting point below 373 K [33]. They consist of asymmetric organic cations and inorganic or organic anions.

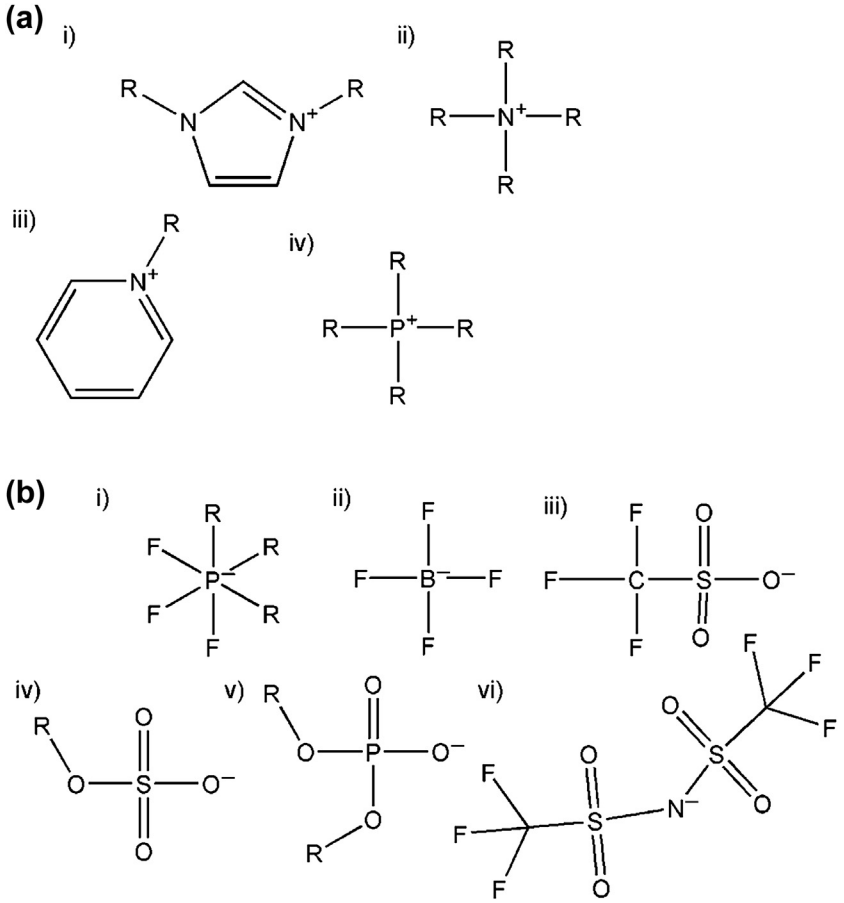

FIGURE 10.6 Typical Ion Families in Ionic Liquids

(a) Cations (b) Anions.

Figure 10.6 shows the typical ion structures of ILs. All residues *R* can be replaced by various chemical groups (e.g. alkyl chains, hydroxyl groups, and amino groups). Thus the number of possible ILs is about 10^{18} [42]. ILs are less corrosive in comparison to inorganic salts [43]. By tailoring the residues *R* to the specific process, the capacities and selectivities can be optimized [8,15,18].

10.4 Separation examples

This section gives several examples of entrainer selection for different mixtures to be separated. All these binary mixtures exhibit separation factors near one or azeotropic

behavior. To quantify the capability of a possible entrainer, the separation efficiency β can be used.

$$\beta = \frac{(\alpha_{ij})_{\text{with entrainer}}}{(\alpha_{ij})_{\text{binary}}} \tag{10.11}$$

In Eqn (10.11), $(\alpha_{ij})_{\text{binary}}$ is the value that is obtained from Eqn (10.5); $(\alpha_{ij})_{\text{with entrainer}}$ is a pseudo-binary value that is defined for a fixed molar amount of a specific entrainer. High values of β indicate a good entrainer.

10.4.1 Ethanol–water

The VLE of the binary mixture ethanol–water is well characterized. Figure 10.7 shows the equilibrium data from two sources from the literature [44,45] in a y–x plot. At an ethanol molar fraction of 0.9, the angle bisector is cut by the VLE data. According to Eqn (10.5), the separation factor is one, and therefore an azeotropic point is reached.

10.4.1.1 Utilization of ILs

The effect of a salt on the VLE of an azeotropic mixture was already identified by Kirschbaum [46], who reported the apparent disappearance of the azeotropic point after the addition of a salt to an ethanol–water mixture. The vapor pressure of water

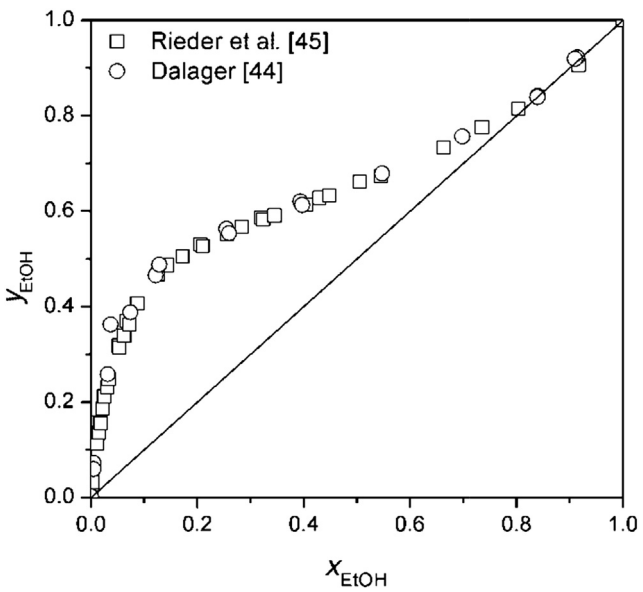

FIGURE 10.7 Vapor Liquid Equilibrium of the Binary Mixture Ethanol (EtOH)–Water at 10^5 Pa [44,45]

decreases because of the attractive interactions of water and the salt calcium chloride ($\gamma_{water} < 1$). The disadvantage of the approach was that the entrainer was solid (and therefore had to stay in the still at the bottom of the column) and poorly miscible in the mixture. So, as ILs that are liquid at room temperature appeared, it was obvious to use them in the sense of Kirschbaum, i.e. for breaking azeotropic behavior.

A water-soluble ionic liquid mostly influences the contribution of enthalpy and subsequently the activity coefficient (cf. Eqn (10.7)). The possible interactions via hydrogen bonding (via −C−H···F− in the presented example −) between the anion $[BF_4]^-$ and water molecules are depicted in Figure 10.8 as the water−$[BF_4]^-$−water complex, as suggested by Wang et al. [47]. According to quantum chemical calculations [47], water and $[BF_4]^-$ could also form the complex water−$[BF_4]^-$.

The influence of ILs on the VLE of ethanol−water mixtures was investigated by Jork et al. [32], and the resulting separation factors of ethanol−water mixtures containing different quantities of ILs—$(\alpha_{EtOH,Water})_{with\ IL}$—are plotted in Figure 10.9. All three ILs break the behavior of the azeotropic system at concentrations higher than 30 mol% ($x(IL) > 0.3$) because of their strong attractive interactions with the water molecules (consider the molecular weight of the mixture to be separated and of the entrainer). There is an upper limit for the separation factor because—on the molecular level, if all molecules of the mixture are surrounded by IL—more IL molecules have no beneficial effect.

Most suitable entrainers are ILs with a imidazolium cation with a short alkyl chain, since the separation factor of ethanol−water mixtures containing [EMIM][BF_4] is slightly higher than that of mixtures containing [BMIM][BF_4]. However, a more pronounced effect on the separation factor can be realized by an exchange of the anion.

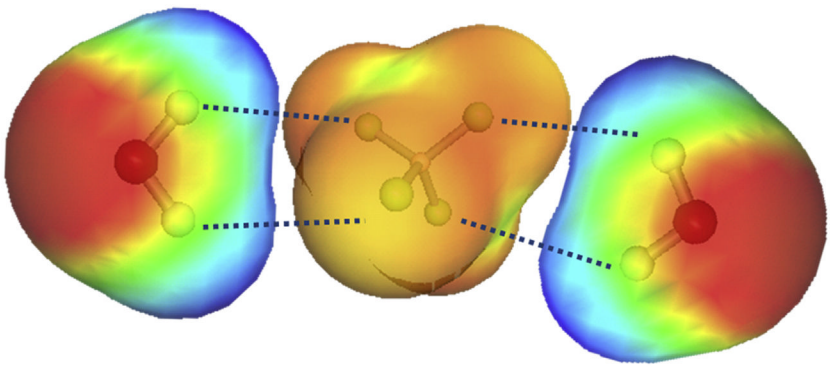

FIGURE 10.8 Schematic Drawing of the Possible Interactions of the Anion $[BF_4]^-$ with Two Water Molecules as Proposed by Wang et al. [47]

Screening charge densities on the surface by the conductor-like screening model are shown for each molecule. Red indicates positive surface charges and screens negative partial charges of atoms. Blue indicates positive partial charges of atoms. (For interpretation of the references to color in this figure legend, the reader is referred to the online version of this book.)

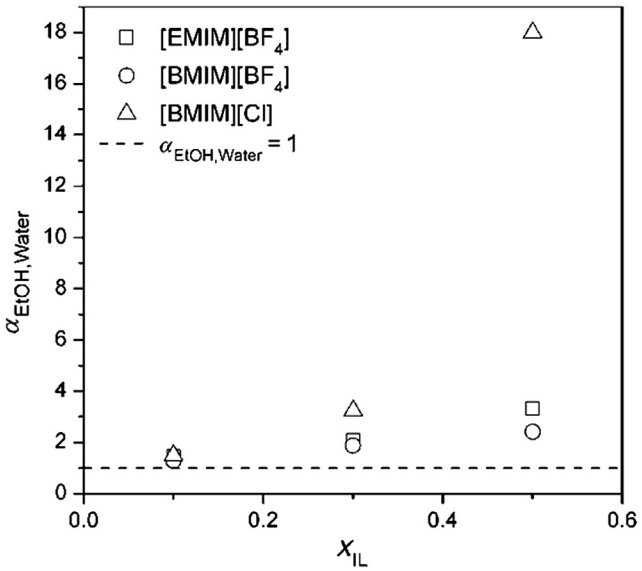

FIGURE 10.9 Separation Factors from Vapor Liquid Phase Equilibria Data at *x*(Ethanol) ≈ 0.9 of Ethanol (EtOH)–Water Mixtures Containing Imidazolium-Based Ionic Liquids at 363.15 K [32]

Extractive distillations using HyPols or ILs are energetically superior to conventional processes because the low vapor pressure allows for a broad range of entrainer recovery options. The process shown in Figure 10.4, using hyperbranched polyglycerol as the entrainer, saves 19% process energy, and the [EMIM][BF_4] process saves 24% compared to the conventional process (recovery of the entrainer 1,2-ethanediol in a vacuum distillation column) [48]. The entrainers used were not optimized before.

10.4.1.2 Utilization of HyPols

In aqueous polymer solutions, the extent of hydrogen bond formation is the major factor influencing the solvent activity, as observed by Seiler [29].

The influence of the hyperbranched polyesteramid Hybrane S1200, the hyperbranched polyglycerol PG1, and the linear analogue of PG1 (LPG) on the ethanol–water separation factors is compared with that of the conventional entrainer 1,2-ethanediol. The separation factors calculated from VLE data of ternary ethanol–water–polymer mixtures are plotted versus the pseudo-binary liquid ethanol molar fraction in Figure 10.10. The results are taken from Ref. [29].

The polymer concentration in an ethanol–water mixture can be increased up to 80 wt% (for Hybrane S1200) at 363.15 K without the formation of two liquid phases. Both HyPols and the linear polymer are able to break the azeotrope at polymer concentrations higher than 40 wt%. Hybrane S1200, PG1, and LPG shift the separation factor of the ethanol–water mixture to be higher than the value of one,

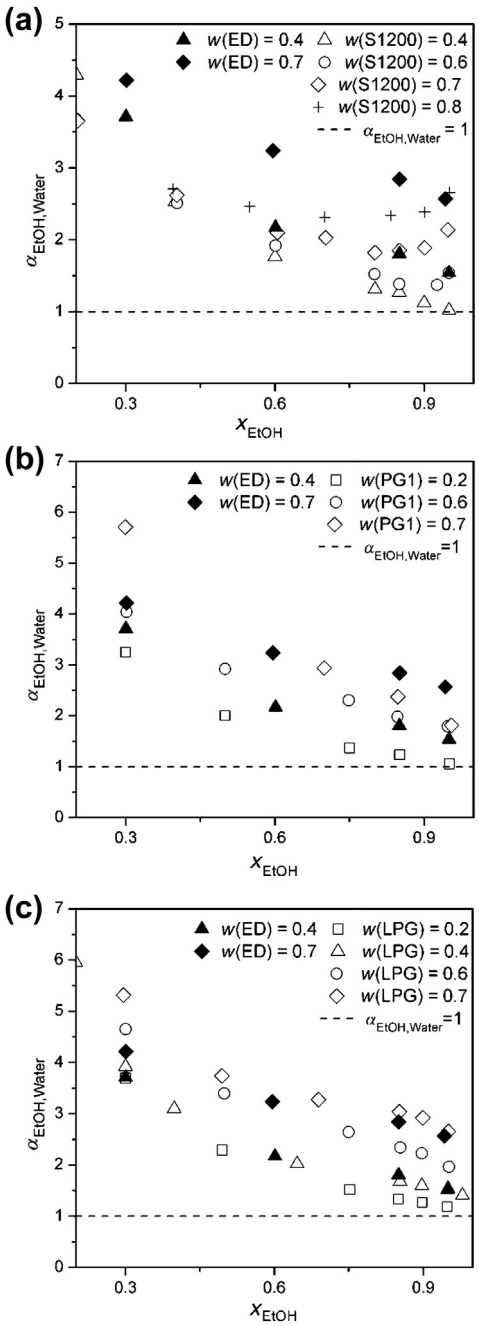

FIGURE 10.10 Separation Factors from Vapor Liquid Phase Equilibria Data of Ethanol (EtOH)—Water Mixtures Containing Polymers and the Conventional Entrainer 1,2-ethanediol (ED) at 363.15 K

(a) The hyperbranched polyesteramide Hybrane S1200. (b) Hyperbranched polyglycerol (PG1). (c) Linear polyglycerol analogue of PG1 (LPG) [29].

and the order of magnitude is comparable with that of 1,2-ethanediol (cf. Figure 10.10), whereas that of ILs is higher (cf. Figure 10.9). The higher the quantity of the entrainer, the stronger the influence on the separation factor. Large deviations of the separation factor from one means that a smaller number of stages or a lower reflux ratio are required to separate the azeotropic system by extractive rectification.

In the case of PG1 (cf. Figure 10.10(b)), an increase in the entrainer concentration from 60 to 70 wt% does not lead to a further increase in the separation factor at a pseudo-binary liquid ethanol molar fraction of 0.95. All available water molecules are already bound by hydrogen to PG1 at 60 wt% of PG1, so that a higher entrainer concentration results in a constant separation factor.

Seiler [29] concluded that the interactions between solvent molecules and polymer functionalities have a major impact on the VLE of aqueous polymer solutions and not the degree of branching. However, HyPols are more promising entrainers than LPGs since LPGs have a significantly higher solution and viscosity when melted compared to HyPols [29].

An a priori evaluation of suitable entrainers can be done using COSMO-RS. As an example, the influence of the hyperbranched polyesteramide Hybrane S1200 on the phase behavior of the ethanol–water system was predicted and compared with experimental data. The predicted and measured pseudobinary VLE of the ternary systems, as well as the VLE of the binary system, are plotted in Figure 10.11. In agreement with the experimental data, COSMO-RS predicts a break of the azeotrope by the addition of 80 wt% Hybrane S1200. But the suitability of Hybrane S1200 as the entrainer is underestimated by COSMO-RS.

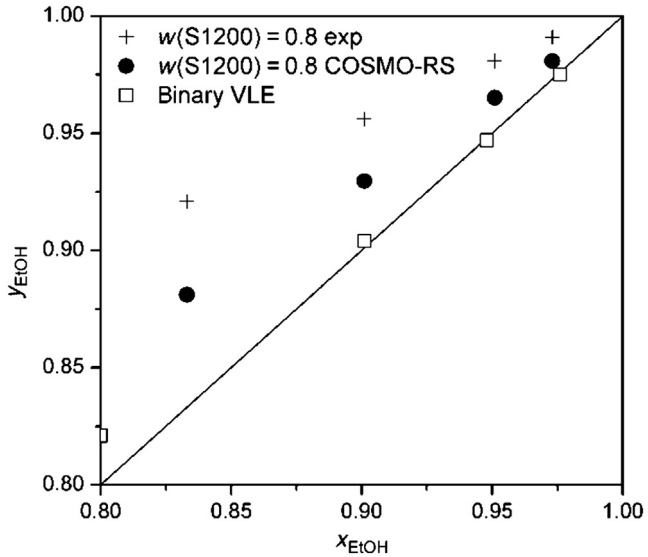

FIGURE 10.11 Comparison of Experimental [29] and Predicted Vapor Liquid Equilibrium Data of the Ternary Mixture Ethanol (EtOH)–Water Hyperbranched Polyesteramide (Hybrane S1200) at 363.15 K [49]

10.4.2 Chloromethane-isobutane

Because chloromethane shows an azeotropic behavior with lower alkanes, one challenging task during the synthesis of methyl chlorosilanes is the recovery of the main reactant chloromethane from the synthesis product mixture. Chloromethane and the lower, branched alkane isobutane demonstrate a maximum pressure azeotrope at x(chloromethane) $\approx$ 0.8 at 327 K [18].

Since the low-boiler chloromethane is more highly polarizable than the high-boiler isobutane, chloromethane experiences stronger solvation in ionic liquids compared to isobutane. Hence, the entrainer used here should fulfill additional criteria compared to the entrainer selected in the ethanol–water case. It should convert the low-boiler chloromethane in a high-boiling substance, resulting in a separation factor smaller than unity. And the separation factor should be as low as possible over the whole concentration range of the low-boiler chloromethane. The suitability of various ILs as entrainers was evaluated by performing express screening using HS-GC (cf. Section 10.2.2). The effect of different cations on the separation factor $\alpha_{CH_3Cl,i-butane}$ and on the solubility of the chloromethane/isobutane mixture in the respective IL is shown in Figure 10.12. The ILs are based on the bis(trifluoromethylsulfonyl)imide $[Tf_2N]^-$ anion. The results are taken from Ref. [18].

Small separation factors are achieved by shortening the alkyl chain length of the imidazolium-based cation, but the solubility decreases simultaneously.

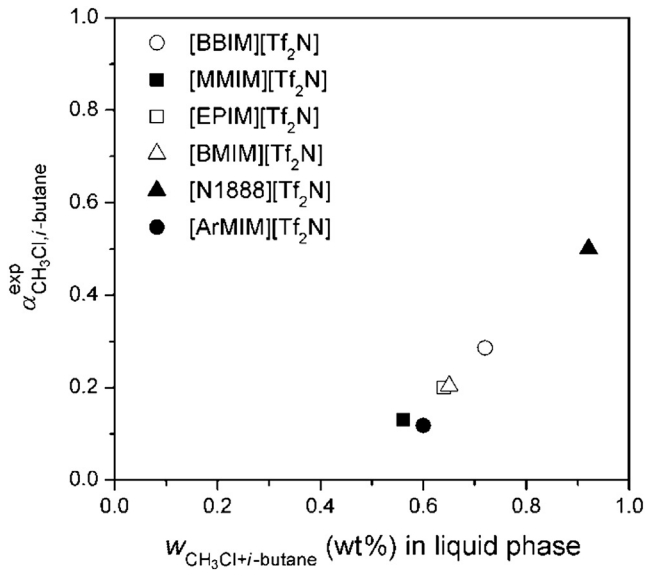

FIGURE 10.12

Separation factors of chloromethane (CH_3Cl)–isobutane (*i*-butane) mixtures containing ionic liquids with the bis(trifluoromethylsulfonyl)imide anion, $[Tf_2N]^-$, at room temperature and at a weight fraction of CH_3Cl in the initial gas mixture of w(chloromethane) = 0.7027 [18].

Besides the experimental screening, a screening of the imidazolium-based ILs using COSMO-RS was performed by Mokrushin et al. [18] and compared with the experimental results. At room temperature and low pressures, the solubility of gases in ILs is very low and approaches the Henry constant. Hence, the separation factor can be estimated with the help of Henry constants $H_{i,\mathrm{IL}}$ and fugacity coefficients φ_i:

$$\alpha_{\mathrm{CH_3Cl},i-\mathrm{butane}} = \frac{H_{\mathrm{CH_3Cl,IL}} \cdot \varphi_{\mathrm{CH_3Cl}}}{H_{i-\mathrm{butane,IL}} \cdot \varphi_{i-\mathrm{butane}}}, \tag{10.12}$$

$$\text{with} \quad H_{i,\mathrm{IL}} = \gamma_i^{\infty} \cdot \varphi_{0,i}^{\mathrm{LV}} \cdot p_{0,i}^{\mathrm{LV}}. \tag{10.13}$$

The fugacity coefficients were taken from the virial equation of state. Since the Poynting factor was set to 1, it is not shown in the equation 10.13. The limiting activity coefficient γ_i^{∞} of chloromethane and isobutane was predicted with the help of COSMO-RS. More details can be found in Refs [12,13].

A parity plot of experimental and predicted data is depicted in Figure 10.13. The general trend of the experimental values is represented by the predicted values, proving the potential of COSMO-RS as a preliminary screening tool.

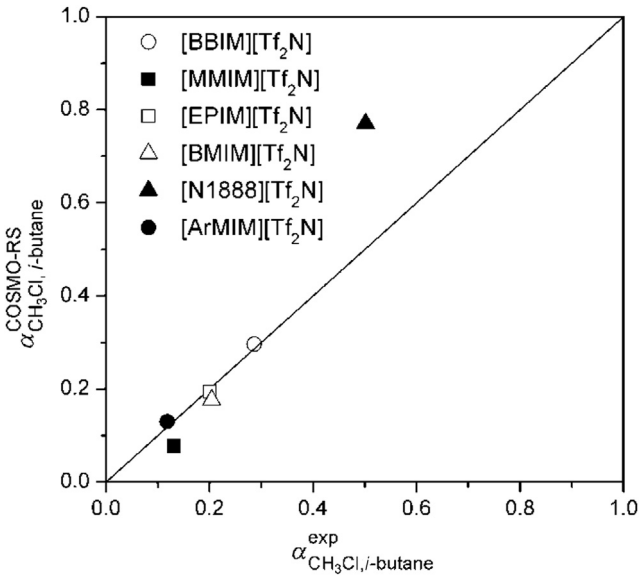

FIGURE 10.13

Comparison of experimental and predicted separation factors of chloromethane (CH_3Cl)—isobutane (*i*-butane) mixtures containing imidazolium-based ionic liquids at room temperature and at w(chloromethane) = 0.7027 in the initial gas mixture [18].
COSMO-RS, conductor-like screening model for real solvents.

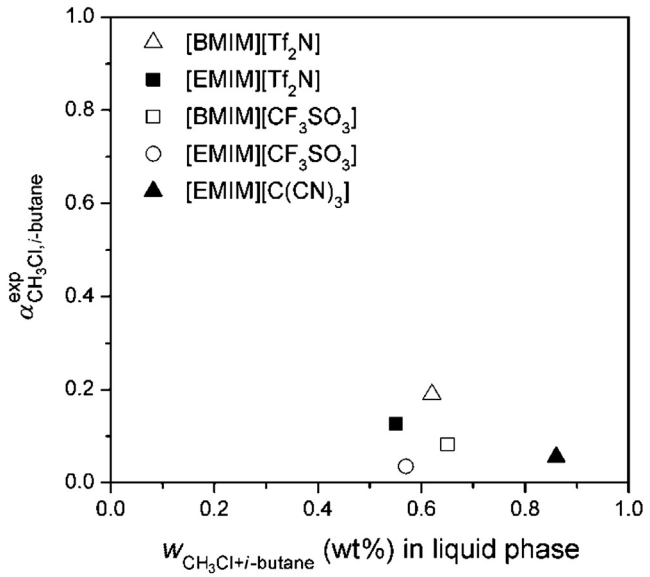

FIGURE 10.14

Separation factors of chloromethane (CH_3Cl)—isobutane (*i*-butane) mixtures containing imidazolium-based ionic liquids at room temperature and at w(chloromethane) = 0.7183 in the initial gas mixture [18].

The effect of the anion on the entrainer's performance also is evaluated by means of the HS-GC screening method, and the observed separation factors and solubilities of the chloromethane/isobutane mixture in the respective ILs are presented in Figure 10.14 [18]. From a thermodynamic point of view, ILs containing the trifluoromethanesulfonate $[CF_3SO_3]^-$ or tricyanomethanide $[C(CN)_3]^-$ anion are best suited for applications as extractive solvents compared to the corresponding ILs based on the bis(trifluoromethylsulfonyl)imide $[Tf_2N]^-$ anion. Moreover, their costs are lower [18].

After the screening and selection of the best-suited IL, the next step is the study of the performance of the IL at temperatures and pressures that are close to the operating conditions of a possible separation process.

10.4.3 Propane—propene

The VLE data of the binary mixture of propane and propene taken from Ref. [50] is shown in Figure 10.15. The binary mixture shows close-boiling behavior.

As the low-boiler propene is preferably dissolved by an IL compared to propane, the entrainer should fulfill the same tasks as in the case of chloromethane—isobutane (cf. Section 10.4.2). It should convert the low-boiler propene into a high-boiling

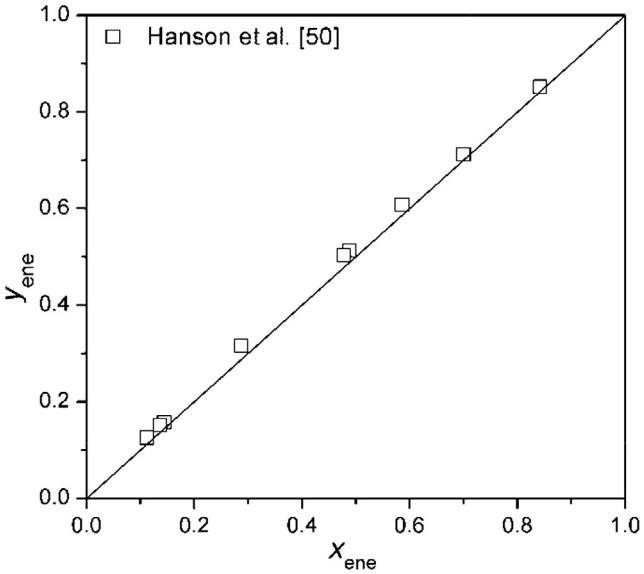

FIGURE 10.15 Vapor Liquid Equilibrium of the Binary Mixture Propane–Propene (ene) at $22 \cdot 10^5$ Pa [50]

substance (i.e. one with a low separation factor) and provide a high solubility. The suitability of various ILs as entrainers was investigated by means of an express screening method (cf. Section 10.2.2). Since the number of ILs investigated in this study (23 in total) is high, an express screening method is important to save time and money. The results are taken from Ref. [15].

The results of the express screening method are shown in Figure 10.16. In general, selectivity decreases, whereas capacity increases. The IL no. 14 [N1888] [Tf_2N], for example, shows a very high solubility of the gases, but the separation factor is also high (cf. Figure 10.16(a)). A high separation factor leads to a low separation ability in this case.

As already observed in the case of chloromethane–isobutane, the shortening of the alkyl chain length of the imidazolium-based cation leads to higher separation ability and, simultaneously, to a lower capacity (cf. Figure 10.16(a)). The insertion of carbon–nitrogen functional groups in the ILs enhances the separation ability of the ILs but only slightly changes the capacity (cf. Figure 10.16(b)). For example, the separation factor of IL no. 18 [OMIM][$C(CN)_3$] is lower than that of IL no. 15 [OMIM][Tf_2N], but the capacity is almost the same. However, the effect is stronger for ILs with the carbon–nitrogen group in the anion.

From a thermodynamic point of view, IL no. 23 [EMIM][$B(CN)_4$] is the most promising entrainer.

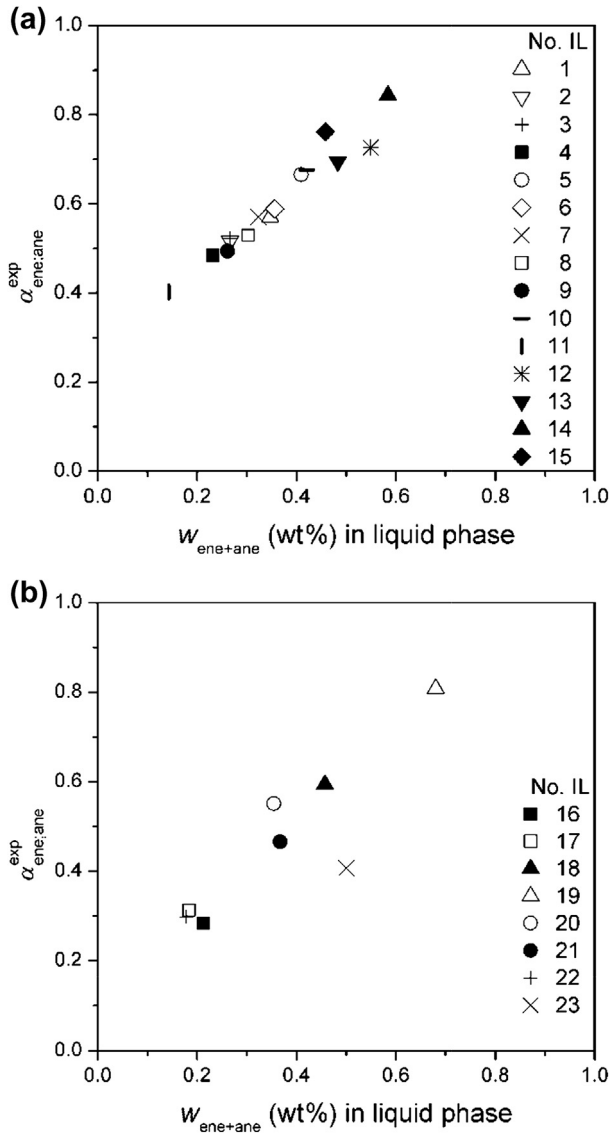

FIGURE 10.16

Separation factors of propane (ane)—propylene (ene) mixtures containing ionic liquids (ILs) at ambient temperature and low pressure: (a) ILs without carbon—nitrogen (CN) functional groups; (b) ILs with CN functional groups [15]. The numbers represent the following ILs: 1. [BMIM][Tf_2N], 2. [PMIM][Tf_2N], 3. [EMIM][Tf_2N], 4. [MMIM][Tf_2N], 5. [BBIM][Tf_2N], 6. [PBIM][Tf_2N], 7. [EBIM][Tf_2N], 8. [EPIM][Tf_2N], 9. [ArMIM][Tf_2N], 10. [BMIM][$OctSO_4$], 11. [EMIM][$EtSO_4$], 12. [BBIM][$(BuO)_2PO_2$], 13. [EBIM][$(BuO)_2PO_2$], 14. [N1888][Tf_2N], 15. [OMIM][Tf_2N], 16. [BMIM][DCA], 17. [EMIM][DCA], 18. [OMIM][$C(CN)_3$], 19. [C_6CN-OIM][Tf_2N], 20. [C_6CN-MIM][Tf_2N], 21. [EMIM][$C(CN)_3$], 22. [C_6CN-MIM][$C(CN)_3$], 23. [EMIM][$B(CN)_4$].

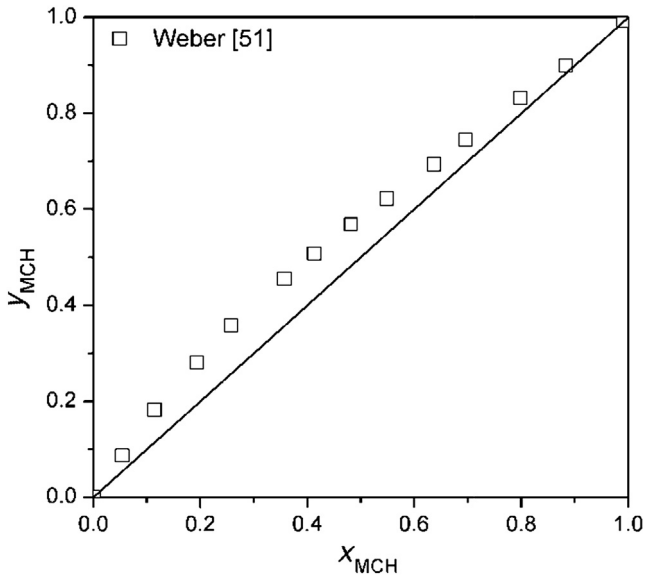

FIGURE 10.17 Vapor Liquid Equilibrium of the Binary Mixture Methylcyclohexane (MCH)–Toluene at 400 mmHg (53,329 Pa) [51]

10.4.4 Methylcyclohexane–toluene

The mixture methylcyclohexane–toluene was used as a nonaqueous test system by Jork et al. [8]. The equilibrium data taken from Ref. [51] is depicted in Figure 10.17 in a y–x plot. The aromatic system shows close-boiling behavior.

The selectivity β^{∞} and capacity $C^{\infty}_{\text{toluene, IL}}$ of ILs can be optimized at an infinite dilution using COSMO-RS. The screening parameters at an infinite dilution of the component are defined according to Eqns (10.14) and (10.15). The limiting activity coefficient $\gamma^{\infty}_{\text{toluene,IL}}$ is used to estimate the capacity and selectivity.

$$C^{\infty}_{\text{toluene,IL}} = 1/\gamma^{\infty}_{\text{toluene,IL}} \tag{10.14}$$

$$\beta^{\infty} = \gamma^{\infty}_{\text{MCH,IL}}/\gamma^{\infty}_{\text{toluene,IL}} \tag{10.15}$$

The ILs were tailor-made by Jork et al. [8] with respect to the ion combination and the degree of substitution and alkyl chain length of the cation. The predicted influence of the alkyl chain length of the imidazolium cation on the separation efficiency and on the IL capacity by means of COSMO-RS is shown in Figure 10.18. Since capacity and selectivity in this nonaqueous system show opposite trends, an optimum must be found. Further details regarding the optimization are published in Ref. [8].

According to the COSMO-RS predictions, the resulting best-suited IL is $[C_8\text{Chin}][NTf_2]$; it shows a high capacity combined with very good selectivity (cf. Table 10.1).

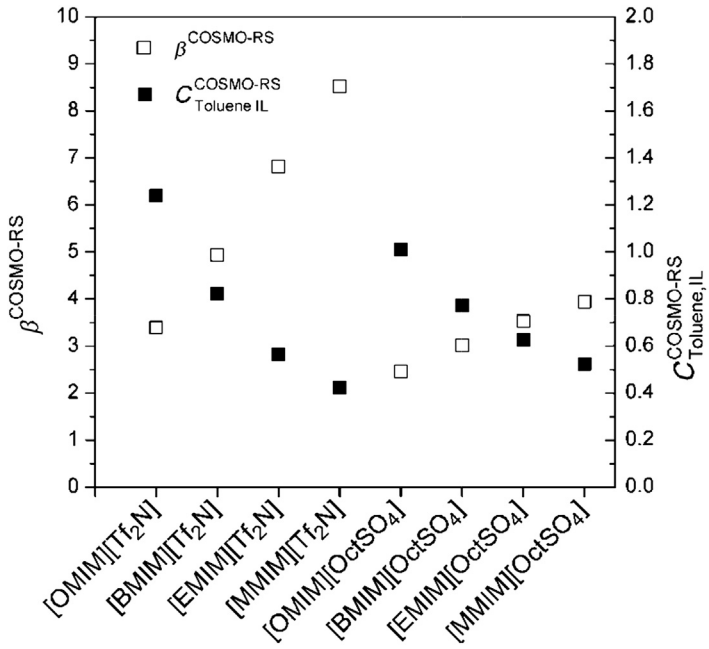

FIGURE 10.18

Conductor-like screening model for real solvents (COSMO-RS)—predicted effect of the alkyl chain length of the imidazolium cation on the separation efficiency of methylcyclohexane (MCH)—toluene infinitely diluted in ionic liquid (IL) and on the IL capacity at 373.15 K [8].

The screening of the ILs was performed at infinite dilution of the solutes in the respective IL. In the following section, the suitability of selected ILs at a finite dilution is investigated. Separation factors of the binary mixture methylcyclohexane—toluene and of the methylcyclohexane—toluene mixtures containing ILs—as predicted by COSMO-RS and experiments—are compared in Figure 10.19. The separation factors are calculated from VLE data according to Eqn (10.5). As shown in Figure 10.19, the trend is qualitatively correctly predicted.

Table 10.1 Predicted Separation Efficiencies and Capacities of Methylcyclohexane–Toluene Infinitely Diluted in Four Different Ionic Liquids at 373.15 K Using the Conductor-like Screening Model for Real Solvents [8]

Ionic Liquid	Separation Efficiencies β^{∞}	Capacities $C^{\infty}_{toluene,IL}$
$[C_8Chin][NTf_2]$	3.24	1.52
$[C_8Chin][BBB]$	3.12	1.37
ECOENG™ 500	2.45	0.93
$[BMIM][NTf_2]$	4.93	0.82

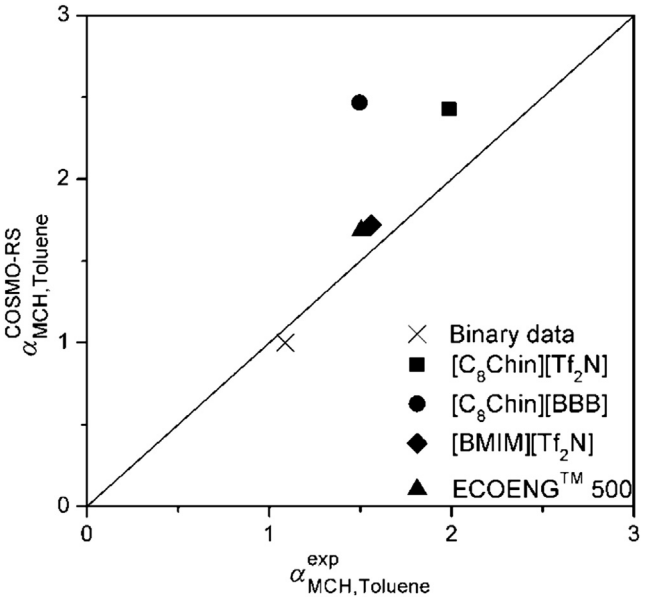

FIGURE 10.19

Comparison of experimental and predicted separation factors from vapor liquid phase equilibria data of the binary mixture methylcyclohexane (MCH)—toluene and of MCH—toluene mixtures containing ionic liquid ($x_{IL} = 0.3$) at 373.15 K [8].

According to the predicted and experimental data, all selected ILs are suitable entrainers. However, the separation factor of $[C_8Chin][BBB]$ is overestimated by COSMO-RS.

The example demonstrates that screening ILs and selecting the best-suited entrainer by means of COSMO-RS minimizes the experimental effort, saving time and money. However, the COSMO-RS predictions for the most promising ILs at finite dilutions should be confirmed by experiments.

10.5 Conclusions

ILs and HyPols are promising entrainers for extractive distillation because they possess high selectivities and capacities and a negligible vapor pressure.

This chapter has shown that ILs and HyPols are able to break the behavior of an azeotropic system and they can be tailor-made for specific applications. These findings have been made using three examples: an aqueous azeotropic system, a nonaqueous narrow-boiling system, and a nonaqueous azeotropic system in which the low boiler is converted to a high boiler by the IL entrainer. Furthermore, IL entrainers can be tailored using the thermodynamic COSMO-RS (theoretical screening) and/or the HS-GC method (experimental screening).

The economic feasibility of extractive distillations using an IL as an entrainer is higher than that of processes using a conventional entrainer; alternative regeneration processes lead to lower investment and operating costs [52]. Besides the thermodynamic optimization, other properties such as costs, availability, long-term stability, toxicity, storage, and corrosion must be taken into account.

Acknowledgment

The author thanks E. Hopmann and A. Buchele for their help in preparing the manuscript.

References

[1] D. Arlt, U. Schwartz, H.W. Brandt, W. Arlt, A. Nickel, Separation of Diastereomers by Extractive Distillation, DE Patent No. 3613975.
[2] J.G. Stichlmair, J.R. Fair, Distillation: Principles and Practice, John Wiley & Sons, New York, 1998.
[3] J. Gmehling, A. Brehm, in: M. Baerns (Ed.), Grundoperationen, Thieme Georg Verlag, Stuttgart, 2001.
[4] K. Sattler, Thermische Trennverfahren: Grundlagen, Auslegung, Apparate, second ed., Wiley-VCH, Weinheim, 1995.
[5] W. Arlt, M. Seiler, C. Jork, T. Schneider, Ionic Liquids as Selective Additives for the Separation of Close-Boiling or Azeotropic Mixtures, WO Patent No. 02/074718 A2, 2002.
[6] W. Arlt, M. Seiler, G. Sadowski, H. Frey, H. Kautz, R. Muelhaupt, Hyper-Branched Polymers as Selective Solvents for the Separation of Azeotropic Mixtures or Mixtures Having Very Similar Boiling Points, DE Patent No. 10160518.8, 2003.
[7] Y.A. Beste, H. Schoenmakers, W. Arlt, M. Seiler, C. Jork, Recycling of Ionic Liquids with Extractive Distillation, DE Patent No. 10336555, 2003.
[8] C. Jork, C. Kristen, D. Pieraccini, A. Stark, C. Chiappe, Y.A. Beste, et al., Tailor-made ionic liquids, J. Chem. Thermodyn. 37 (2005) 537–558.
[9] M. Seiler, D. Kohler, W. Arlt, Hyperbranched polymers: new selective solvents for extractive distillation and solvent extraction, Sep. Purif. Technol. 29 (2002) 245–263.
[10] M. Seiler, W. Arlt, H. Kautz, H. Frey, Experimental data and theoretical considerations on vapor-liquid and liquid-liquid equilibria of hyperbranched polyglycerol and PVA solutions, Fluid Phase Equilib. 201 (2002) 359–379.
[11] I. Clausen, W. Arlt, A priori calculation of phase equilibria for thermal separation processes using COSMO-RS, Chem. Eng. Technol. 25 (2002) 254–258.
[12] J.M. Prausnitz, R.N. Lichtenthaler, E. Gomes de Azevedo, Molecular Thermodynamics of Fluid-Phase Equilibria, third ed., Prentice Hall, New Jersey, 1998.
[13] J. Gmehling, B. Kolbe, Thermodynamik, second ed., VCH Verlagsgesellschaft mbH, Weinheim, 2012.
[14] H. Hachenbach, K. Beringer, Die Headspace-Gaschromatographie als Analysen- und Meßmethode, Springer Verlag, Berlin, 2000.
[15] V. Mokrushin, D. Assenbaum, N. Paape, D. Gerhard, L. Mokrushina, P. Wasserscheid, et al., Ionic liquids for propene-propane separation, Chem. Eng. Technol. 33 (2010) 63–73.

[16] H.M. Petri, B.A. Wolf, Concentration-dependent thermodynamic interaction parameters for polymer solutions: quick and reliable determination via normal gas chromatography, Macromolecules 27 (1994) 2714−2718.
[17] C.B. Castells, D.I. Eikens, P.W. Carr, Headspace gas chromatographic measurements of limiting activity coefficients of eleven alkanes in organic solvents at 25 °C, J. Chem. Eng. Data 45 (2000) 369−375.
[18] V. Mokrushin, L. Mokrushina, W. Arlt, D. Assenbaum, P. Wasserscheid, M. Petri, et al., Ionic liquids for chloromethane/isobutane distillative separation: express screening, Chem. Eng. Technol. 33 (2010) 993−997.
[19] G. Sadowski, L.V. Mokrushina, W. Arlt, Finite and infinite dilution activity coefficients in polycarbonate systems, Fluid Phase Equilib. 139 (1997) 391−403.
[20] C. Jork, Optimization of ionic liquids as selective entrainers in chemical engineering (thesis), University Erlangen-Nuremberg, 2006.
[21] A. Klamt, G. Schüürmann, COSMO: a new approach to dielectric screening in solvents with explicit expressions for the screening energy and its gradient, J. Chem. Soc. Perkin Trans. 2 (1993) 799−805.
[22] A. Klamt, Conductor-like screening model for real solvents: a new approach to the quantitative calculation of solvation phenomena, J. Phys. Chem. 99 (1995) 2224−2235.
[23] S. Maassen, H. Knapp, W. Arlt, Determination and correlation of Henry's law coefficients, activity coefficients and distribution coefficients for environmental use, Fluid Phase Equilib. 116 (1996) 354−360.
[24] S. Maassen, W. Arlt, A. Klamt, Prediction of gas solubilities and partition coefficients on the basis of molecular orbital calculations (COSMO) with regard to the influence of solvents, Chem. Ing. Tech. 67 (1995) 476−479.
[25] A. Klamt, F. Eckert, W. Arlt, COSMO-RS: an alternative to simulation for calculating thermodynamic properties of liquid mixtures, Annu. Rev. Chem. Biomol. Eng. 1 (2010) 101−122.
[26] M. Buggert, C. Cadena, L. Mokrushina, I. Smirnova, E.J. Maginn, W. Arlt, COSMO-RS calculations of partition coefficients: different tools for conformational search, Chem. Eng. Technol. 32 (2009) 977−986.
[27] F. Eckert, COSMOtherm Users Manual. COSMOlogic, 2008.
[28] M. Diedenhofen, A. Klamt, COSMO-RS as a tool for property prediction of IL mixtures. a review, Fluid Phase Equilib. 294 (2010) 31−38.
[29] M. Seiler, Phase Behavior and New Applications of Hyperbranched Polymers in the Field of Chemical Engineering (thesis), University Erlangen-Nuremberg, 2004.
[30] A. Hult, M. Johansson, E. Malmstrom, Hyperbranched polymers, Adv. Polym. Sci. 143 (1999) 1−34.
[31] K.U. Goss, Predicting equilibrium sorption of neutral organic chemicals into various polymeric sorbents with COSMO-RS, Anal. Chem. (Washington, DC, U.S.) 83 (2011) 5304−5308.
[32] C. Jork, M. Seiler, Y.A. Beste, W. Arlt, Influence of ionic liquids on the phase behavior of aqueous azeotropic systems, J. Chem. Eng. Data 49 (2004) 852−857.
[33] P. Wasserscheid, T. Welton, Ionic Liquids in Synthesis, 2, Wiley-VCH Verlag GmbH & Co. KGaA, Weinheim, 2007.
[34] B. Voit, New developments in hyperbranched polymers, J. Polym. Sci. Part A: Polym. Chem. 38 (2000) 2505−2525.
[35] A. Sunder, J. Heinemann, H. Frey, Controlling the growth of polymer trees: concepts and perspectives for hyperbranched polymers, Chem. Eur. J. 6 (2000) 2499−2506.

[36] M. Seiler, Dendritic polymers—interdisciplinary research and emerging applications from unique structural properties, Chem. Eng. Technol. 25 (2002) 237–253.
[37] M. Seiler, J. Rolker, W. Arlt, Phase behavior and thermodynamic phenomena of hyperbranched polymer solutions, Macromolecules 36 (2003) 2085–2092.
[38] Y.H. Kim, Hyperbranched polymers 10 years after, J. Polym. Sci. Part A: Polym. Chem. 36 (1998) 1685–1698.
[39] T.H. Mourey, S.R. Turner, M. Rubinstein, J.M.J. Frechet, C.J. Hawker, K.L. Wooley, Unique behavior of dendritic macromolecules: intrinsic viscosity of polyether dendrimers, Macromolecules 25 (1992) 2401–2406.
[40] K.L. Wooley, J.M.J. Frechet, C.J. Hawker, Influence of shape on the reactivity and properties of dendritic, hyperbranched and linear aromatic polyesters, Polymer 35 (1994) 4489–4495.
[41] Y.H. Kim, O.W. Webster, Hyperbranched polyphenylenes, Macromolecules 25 (1992) 5561–5572.
[42] J.D. Holbrey, K.R. Seddon, Ionic liquids, Clean Technol. Environ. Policy 1 (1999) 223–236.
[43] C.M. Gordon, New developments in catalysis using ionic liquids, Appl. Catal., A 222 (2001) 101–117.
[44] P. Dalager, Vapor-liquid equilibriums of binary systems of water with methanol and ethanol at extreme dilution of the alcohols, J. Chem. Eng. Data 14 (1969) 298–301.
[45] R.M. Rieder, A.R. Thompson, Vapor-liquid equilibria measured by a Gillespie still. Ethyl alcohol-water system, J. Ind. Eng. Chem. (Washington, D.C.) 41 (1949) 2905–2908.
[46] E. Kirschbaum, Destillier- und Rektifiziertechnik, fourth ed., Springer-Verlag, Berlin, Heidelberg, New York, 1969.
[47] Y. Wang, H. Li, S. Han, A theoretical investigation of the interactions between water molecules and ionic liquids, J. Phys. Chem. B 110 (2006) 24646–24651.
[48] M. Seiler, C. Jork, W. Arlt, Phase behavior of highly selective nonvolatile liquids with a designable property profile and new uses in thermal process engineering, Chem. Ing. Tech. 76 (2004) 735–744.
[49] J. Voelkl, W. Arlt, Predicting thermodynamic properties of hyperbranched polymers, in: 25th European Symposium on Applied Thermodynamics. Saint Petersburg, Russia, 2011.
[50] G.H. Hanson, R.J. Hogan, W.T. Nelson, M.R. Cines, Propane-propylene system-vapor-liquid equilibrium relationships, J. Ind. Eng. Chem. (Washington, D.C.) 44 (1952) 604–609.
[51] J.H. Weber, Vapor-liquid equilibria for system methylcyclohexanetoluene at subatmospheric pressures, J. Ind. Eng. Chem. (Washington, D.C.) 47 (1955) 454–457.
[52] Y. Beste, M. Eggersmann, H. Schoenmakers, Extractive distillation with ionic liquids, Chem. Ing. Tech. 77 (2005) 1800–1808.

Index

Note: Page numbers followed by "f" indicate figures; "t", tables; "b", boxes.

A

B

C

D

E

F

G

H

I

M

N

O

P

Q

R

S

T

U

V

W

X

Z